



# NEXT GENERATION PATHOLOGY

107. JAHRESTAGUNG  
DER DEUTSCHEN  
GESELLSCHAFT  
FÜR PATHOLOGIE

München  
23. - 25. Mai  
2024



## ABSTRACTBAND

# **Abstractband**



## **107. Jahrestagung der Deutschen Gesellschaft für Pathologie e.V. 23. – 25. Mai 2024, München**

### **„Next Generation Pathology“**

#### **Schwerpunkte der Jahrestagung**

- Molekulare Pathologie
- Personalisierte Medizin
- Computational Pathology
- Vergleichende Pathologie
- Aus- und Weiterbildung
- Gemeinsame Sitzungen mit anderen Fachgesellschaften
- AG Sitzungen zu allen Teilbereichen der Pathologie

#### **Vorsitzender der Fachgesellschaft**

Prof. Dr. med. Gustavo Baretton, Dresden

#### **Tagungspräsident**

Prof. Dr. med. Wilko Weichert, München (posthum)

#### **Organisationsteam der TU München**

Prof. Dr. Carolin Mogler  
PD Dr. Katja Steiger  
Dipl.-Biol. Nicole Pfarr  
PD Dr. Dr. Kristina Schwamborn  
Dr. Karin von Schwarzenberg  
Prof. Dr. Peter Schöffler

#### **Herausgeberin, Lektorat und Copyright**

Deutsche Gesellschaft für Pathologie e.V.  
Geschäftsstelle  
Robert-Koch-Platz 9  
10115 Berlin  
geschaefsstelle@pathologie-dgp.de

#### **Veranstaltungsorganisation**

Kongress- und Kulturmanagement GmbH (KUKM)  
Weimar

[Klicken Sie auf den Beitragstitel, um direkt zum ausgewählten Abstract zu gelangen.](#)

## Inhaltsverzeichnis

<b>Keynote 1: Mass Spectrometry based Spatial Biology in Molecular Pathology</b> .....	<b>14</b>
Mass spectrometry based Spatial Biology in Molecular Pathology .....	14
<b>Keynote 4: Beyond Angiogenesis: Vascular Control of Tumor Progression and Metastasis</b> .....	<b>14</b>
Beyond Angiogenesis: Vascular Control of Tumor Progression and Metastasis .....	14
<b>Molecular Pathology 1 - Data Analysis</b> .....	<b>15</b>
Classification, Interpretation and Reporting of Somatic Sequence Variants in Cancer..	15
Utilizing mutational signatures from whole genome sequencing in cancer .....	15
Definition of quality parameters for diagnostic reporting of WES in FFPE tissue specimens .....	15
<b>Personalisierte Medizin 2- Personalized medicine at the interface with pathology...</b>	<b>16</b>
The precision medicine in Spain. How we are implanting the digital and molecular diagnosis .....	16
Personalized medicine at the interface with pathology - Uro-Oncology .....	16
Molecular pathology and molecular imaging - similarities and differences .....	17
Integrating proteomics into diagnostic molecular pathology reports to support molecular tumor board decisions. ....	17
<b>Biobanking 1: Network Structures</b> .....	<b>18</b>
National autopsy registry and network (NAREG & NATON).....	18
Evidence-based guideline for tissue handling and biobanking in Japan .....	19
<b>Personalisierte Medizin 1</b> .....	<b>20</b>
Mass Spectrometry-based Proteomic Characterization of Undifferentiated Small Round Cell Sarcomas with EWSR1- and CIC-Translocations Point to Diverging Tumor Biology and Reveal Distinct Diagnostic Markers .....	20
Using Mass Spectrometry Imaging to predict patient's treatment response from transurothelial bladder resections .....	20
Tumor Specificity by Quantitative Proteomics in the ADC Age.....	21
Spatial Transcriptomic Analysis of T-Cells in Colorectal Carcinoma and Identification of an HLA-A*02:01-Restricted EBV and Tumor Cross-Reactive T-Cell Receptor.....	22
Oncogenic role of ACSL5 (acyl-CoA synthetase long-chain family member 5) and its clinical implications in colorectal carcinoma.....	23
Dissecting the spatial heterogeneity of molecular subtypes in muscle-invasive urothelial bladder cancer using spatial transcriptomics .....	24
A novel TROP2 complex affects the cytoskeleton architecture and mechanobiology in colorectal cancer .....	25
<b>Neuroendocrine Tumours</b> .....	<b>26</b>
Diagnostic and prognostic biomarkers for pancreatic neuroendocrine neoplasms .....	26
Neuroendocrine Neoplasms of the Gastrointestinal Tract .....	26
Diagnostic issues in neuroendocrine neoplasms of the lung .....	26
Activated mTOR signaling promotes the expression of the mitochondrial biogenesis regulator PGC1 $\alpha$ in pancreatic neuroendocrine tumors (panNETs) .....	27
<b>Advances in Computational Pathology 1</b> .....	<b>27</b>
Built to Last? Reproducibility and Reusability of Deep Learning Algorithms in Computational Pathology.....	27
The transition to digital pathology in routine diagnostics. Milestones and open questions. ....	28
Using AI in Digital Pathology – Opportunities and Regulatory Challenges .....	28
Enhancing Prostate Cancer Diagnosis: AI-Driven Virtual Biopsy for Optimal Targeted Biopsy Approach and Gleason Grading Strategy .....	28



Histopathology-based prediction of pathway activities for targeted therapies in HNSCC .....	29
<b>Personalisierte Medizin 3 - Stand der personalisierten Medizin.....</b>	<b>30</b>
Molecular Tumorboard beyond Genomics - ADCs advancing .....	30
NECTIN4 Amplification is Frequent in Solid Tumors and Predicts Enfortumab Vedotin Response in Metastatic Urothelial Cancer.....	31
Proteomic Profiling of IDH-wildtype Glioblastoma Tissue reveals prognostic Subtypes with matching Proteomic Patterns in Serum .....	32
<b>Molecular Pathology 2 - Technologien .....</b>	<b>33</b>
DNA basierte Techniken in der molekularpathologischen Diagnostik - State of the Art und Ausblick .....	33
RNA-based techniques for precision medicine .....	33
Pilot study for diagnostic whole-genome sequencing from routine formalin-fixed, paraffin-embedded specimens (FFPE) using Ultrashar and DNA repair. ....	34
Integrated Genomic and Epigenetic Analysis of Matched Primary and Metastatic Highly Malignant Osteosarcoma.....	34
<b>Animal Models in Human Research 1 .....</b>	<b>36</b>
The benefits of comparative genomics in understanding bladder cancer .....	36
From bearded dragons to horses: Special features of selected spontaneous skin tumors in various animal species (Von Bartagame bis Pferd: Besonderheiten ausgewählter spontaner Hauttumore bei verschiedenen Tierarten) .....	37
Comparative Study of Feline and Human Intestinal Carcinomas.....	37
Comparative digital estrogen receptor alpha (ER $\alpha$ ) expression analysis in benign and malignant prostate tissue of men and dogs .....	38
<b>Biobanking 2: Wichtige Themen im Biobanking .....</b>	<b>39</b>
Quality assured biobanking according to DIN EN ISO 20387 - curse or blessing?.....	39
Hybrid financing of biobanking structures - focus on tissue biobanking.....	39
Integrated biobanking - A key role for the quality of biosamples.....	40
Multimodal evaluation of an organotypic slice culture platform for cell renal cell carcinoma .....	40
Patient-derived colon tumor organoids fuse and build ring structures in floating collagen I matrix.....	41
<b>ESP - The European Perspective of Pathology – Where will we be in 2030 .....</b>	<b>42</b>
ESP 2030 - The challenges and strategy .....	42
The changing world of further education and training in European Pathology .....	42
Computational pathology – pitfalls and potential .....	42
<b>Proteomics 1: Proteomics in Personalized Medicine .....</b>	<b>43</b>
(Phospho)Proteomics for Personalized Precision Oncology.....	43
Deep Proteomics and Integrated Multiomics of Primary and Metastatic Colorectal Adenocarcinoma Uncovers Novel Proteomic Subtypes and Therapeutic Targets.....	43
Proteomic Profiling of Malignant Melanoma reveals Expression of Checkpoint Ligand Galectin-9 correlates with Response to Immune Checkpoint Inhibitors. ....	44
<b>Advances in Computational Pathology 2 .....</b>	<b>45</b>
AI for breast cancer diagnostics 2.0 .....	45
The Use of Spatial Omics in Head & Neck Cancer.....	46
Automated image analysis of HE-stained slides can partially predict immunohistochemical staining and subtyping of pancreatic ductal adenocarcinoma ....	46
Artificial Intelligence-Enriched Classification of Intrahepatic Cholangiocarcinoma.....	47
<b>Molecular Pathology 3 - International .....</b>	<b>48</b>
Current status and future development of precision oncology in Europe.....	48
Validation of Whole Genome Sequencing and first experiences after its introduction in the diagnostic routine of molecular pathology.....	48

<b>Proteomics 2: Mass Spectrometry Imaging in Pathology</b> .....	<b>49</b>
MALDI Mass Spectrometry Imaging - A New Method in Pathology? .....	49
Raman spectroscopic features of metastatic colorectal cancer .....	49
Multiplexed Immunohistochemistry with Matrix-assisted Laser Desorption/ Ionization Mass Spectrometry Imaging for Subtyping of Lung Tumors .....	50
<b>Animal Models in Human Research 2</b> .....	<b>51</b>
Centers for experimental animal pathology still occupy a small but valuable niche in translational medicine – time for change? .....	51
Hydrodynamic models of cholangiocarcinoma for molecular studies and therapeutic interventions .....	51
Animal models for pancreatic cancer and its precursor lesions .....	52
Tenascin C deficiency impairs regeneration after cerulein-induced acute pancreatitis ..	52
Investigation of Sporadic Congenital Portosystemic Shunts in Mice .....	53
<b>Autopsy</b> .....	<b>53</b>
Next-generation postmortems: what are we waiting for? .....	53
Comparative analysis of microsatellite instability and standard mismatch repair protein deficiency tests in a large cancer cohort.....	54
COVID-19 shows a milder presentation in cancer patients: experience from a large tertiary center autopsy series.....	55
Reconstructing 3D histological structures using machine learning (AI) algorithms .....	55
Detection of pancreatic adenocarcinoma by Stimulated Raman Scattering scanning microscopy with convolutional artificial neural network on unstained tissue sections ....	56
Evaluation of diagnostic accuracy of state of the art post-mortem imaging compared to clinical hospital autopsy .....	57
<b>Rising Stars</b> .....	<b>58</b>
"Predictive and prognostic biomarkers on solid tumors with focus on lung carcinoma" .	58
New technologies in tumor pathology .....	58
<b>Junges Forum 1: How to do....?</b> .....	<b>59</b>
How to do...Molekularpathologie .....	59
Dermatopathology for pathologists – don't panic. Advices for beginners. ....	59
How to do... Knochentumoren .....	60
<b>AG Gynäko- und Mammathologie 1</b> .....	<b>60</b>
Analysis of DNA methylation patterns in HRR genes and its correlation with the homologous repair deficiency (HRD).....	60
Unintentional Off-label Use of PARP Inhibitors in Low-Grade Serous Ovarian Carcinoma: A Potential First Case and Call for Further Investigation .....	61
Correlation and prognostic differences of L1CAM and tumor budding in endometrial carcinoma .....	62
Interaction of FAP-positive activated fibroblasts and the immune microenvironment of endometriosis .....	62
<b>AG Gynäko- und Mammathologie 2</b> .....	<b>63</b>
Breast Cancer Subtyping and Omission of Radiotherapy.....	63
Prediction of response to neoadjuvant chemotherapy from histopathological slides and clinical data using a transformer-based AI approach.....	64
Qualitative assessment of histomorphological regression patterns in lymph node metastases in breast cancer patients after NAST – a combined analysis of 373 tumors from neoadjuvant clinical trials.....	65
Aberrant p53 immunohistochemical staining patterns correlate with differential variant effects of TP53 mutations observed by targeted sequencing (NGS) in HR+HER2- invasive breast carcinoma (NST).....	65
The breast cancer tumor microenvironment in women living with HIV shows an altered CD276/B3-H7 expression and T cell infiltration .....	66

<b>Fortbildungsveranstaltung der AG Zytopathologie .....</b>	<b>67</b>
From Cellular Findings to Patient Management in Gynecologic Cytology .....	67
Experiences from the First Cycle of Co-Testing Cytology/HPV and with Digital Cytology .....	68
<b>AG Hämatopathologie 1 .....</b>	<b>68</b>
High expression of ADAM family members is associated with progressive disease and proliferation signaling in MM. ....	68
Neuropilin-2 in mesenchymal stromal cells as a druggable target in myelofibrosis .....	69
Altered IFN-gamma signaling remodels the bone marrow tumor microenvironment in MPN and is associated with disease progression.....	70
Histomorphological Spectrum of Nodal Marginal Zone Lymphoma .....	70
Improving the diagnosis, therapy and understanding of severe blood diseases with AI .....	71
FDC network in human lymph nodes: structure and function based on 3D confocal microscopy .....	72
The three-dimensional landscape of reactive and neoplastic human lymph nodes .....	73
CD70/CD27 Signaling Promotes the Expansion of Clonal Plasma Cells in Multiple Myeloma and Is a Promising Therapeutic Target in Advanced Disease.....	73
<b>AG Hämatopathologie 2 .....</b>	<b>74</b>
The Tumor Genome of the future - from a bioinformatics perspective.....	74
Targeted panel sequencing for refining B cell lymphoma diagnosis: A real-life, reference center experience .....	74
In-depth molecular profiling of predominantly diffuse follicular lymphoma.....	75
Targeted genomic sequencing of Epstein-Barr virus-positive inflammatory follicular dendritic cell sarcomas in comparison to classic follicular dendritic cell sarcomas .....	76
<b>AG Herz-, Gefäß-, Nieren- und Transplantationspathologie .....</b>	<b>76</b>
Cardiac transplantation: the role of pathology .....	76
A podocentric view on glomerular disease .....	77
High CD163 <sup>+</sup> macrophage densities in pre-implantation renal biopsies - precisely quantified and localized by convoluted neural networks (CNNs) - are predictive for delayed graft function (DGF) .....	77
The role of MIF-2 (D-DT) in kidney fibrosis.....	78
<b>AG Uro-pathologie 1 .....</b>	<b>78</b>
Revision of Patient-derived Kidney Organoids for Disease Modelling .....	78
Assessing the risk to develop a growing teratoma syndrome based on molecular and epigenetic subtyping as well as novel secreted biomarkers .....	80
Ultra-high resolution imaging of prostate cancer using synchrotron-based virtual histology .....	81
Long term treatment with darolutamide increases neddylation of the androgen receptor .....	81
Molecular subtypes of urothelial muscle-invasive bladder cancer – assessing immune cell infiltration and survival.....	82
ELOC-mutated renal cell carcinoma - a new player in the differential diagnosis of renal neoplasms .....	83
Immunohistochemical ERG positivity in primary prostate cancer is associated with decreased PSMA expression, and lower visibility in corresponding [68Ga]Ga-PSMA-11 PET scans .....	83
Tumor infiltrating B cells are an independent prognostic factor in penile cancer .....	84
CoreQuest: Determining Tumor content in prostate biopsies .....	85
<b>AG Uro-pathologie 2 .....</b>	<b>85</b>
The Divine Comedy of Prostate Cancer .....	85
Proteogenomic Integration Underlines the Stability and Relevance of Proteomic Subtypes in Urothelial Bladder Cancer.....	86

Transcription factor GRHL1 is a key regulator of early differentiation processes during squamous bladder cancer development.....	86
Acetylation of Lysine 619 abolishes AR-V7 signalling .....	87
Whole-organ mapping bladder cancers reveal heterogeneous expression patterns of TROP2 and NECTIN-4, varying according to distinct subtypes of urothelial bladder cancer.....	88
<b>AG Kopf-Hals-Pathologie .....</b>	<b>89</b>
Tumor budding and lymphovascular invasion help to identify high-risk p16-positive oropharyngeal squamous cell carcinomas.....	89
CD103+ tissue-resident T-cells accumulate in head and neck squamous cell carcinomas of patients responding to anti-PD1 therapy. ....	89
Expanding the spectrum of low-grade sinonasal adenocarcinoma with biphasic seromucinous differentiation and activating HRAS/AKT1 mutations .....	90
<b>AG Knochen-, Gelenk- und Weichgewebspathologie.....</b>	<b>91</b>
Prognostic factors in the diagnosis of Sarcomas from the perspective of a Reference Center (CSUR) .....	91
microRNA profiling in combination with whole exome sequencing reveals insights into long-term recurrence patterns in chordoma.....	91
Proteomic and N-Glycan in-situ Characterization of Small Blue Round Cell Tumors ....	93
Do BAF complexes regulate the differentiation status in synovial sarcoma?.....	93
CDK inhibitors reduce TBXT gene expression in chordoma cell lines .....	94
TFCP2 - a potential regulator of TBXT expression in chordoma .....	95
<b>AG Dermatopathologie.....</b>	<b>96</b>
Genitaler Lichen sclerosus - eine weiße Gefahr? .....	96
Giant Dermatofibroma with associated basal cell carcinoma: A case report of a rare collision.....	96
<b>AG Geschichte und Ethik der Pathologie .....</b>	<b>97</b>
Translational Biomedical Research at the Institute of Veterinary Pathology (LMU Munich).....	97
Die Siegfried Oberndorfer Präparate-Lehrsammlung - Von der Magazinsammlung zum Museum.....	97
Survey on working and training conditions and professional satisfaction of residents in surgical pathology.....	98
Lost Journals – forgotten journals and series of books in pathology .....	98
<b>AG Thoraxpathologie 1 .....</b>	<b>99</b>
Extensive Autoptic Morphomolecular Characterization of a Metastatic Small Cell Lung Cancer with Promising Response to SSTR-directed Peptide Receptor Radionuclide Therapy .....	99
Is the association of small cell lung carcinoma with ectopic Cushing's syndrome as frequent as suggested in the literature?.....	100
Predictive biomarkers for checkpoint inhibitor therapy in NSCLC: KRAS/TP53 co-mutations and brain metastasis-specific PD-L1 expression – two real-world cohort analyses .....	100
One-Carbon-Metabolismus in Karzinomen der Lunge.....	101
The growth-inhibitory role of bile acids in non-small cell lung cancer cells in the presence of PD-L1 and the clinical implication .....	102
Upregulation of Serpin B13 in squamous cell carcinomas of the lung predicts favorable prognosis .....	103
<b>AG Thoraxpathologie 2 .....</b>	<b>103</b>
Pathologic diagnosis of lung cancer: my approach to selected topics .....	103
Computational pathology platform for lung cancer: development and validation of diagnostic and prognostic algorithms .....	104

Pleural manifestation of a spindle cell tumor with prominent vascular pattern: A rare manifestation of Dermatofibrosarcoma protuberans, a diagnostic pitfall .....	104
<b>AG Molekularpathologie 1</b> .....	<b>105</b>
MCPIP1 is a novel regulator of necroptotic cell death in colorectal cancer .....	105
Amyloid typing by mass spectrometry .....	106
<b>AG Molekularpathologie 2</b> .....	<b>106</b>
Implementation of plasma-based ESR1 mutation testing for breast cancer patients in Germany - a harmonization study.....	106
Conclusions from the QuIP MSI ring trial 2023 for practical application in MSI diagnostics.....	107
Dissecting the Methylomes of Non-Small Cell Lung Cancer with high and low PD-L1 expression .....	108
Multimodel, AI-based, data-integrated cell-omics derived cell niches advance UICC staging system in non-small cell lung cancer patients. ....	109
Implementation and Optimization of a Single Cell DNA Sequencing Assay for Reconstructing the Clonal Evolution of Tumors from FFPE Samples.....	109
P-PROFILER: Homologous recombination deficiency in pancreatic ductal adenocarcinoma .....	110
<b>AG Molekularpathologie 3</b> .....	<b>111</b>
Resistance testing of Helicobacter pylori: Analysis of gyrase B is essential to detect the whole spectrum of resistance mutations against Levofloxacin .....	111
Automation of molecular pathology NGS dataflow, processing and reporting .....	112
Long term effect of choline-deficient high fat diet and correlation of carbohydrate response element binding protein (ChREBP) to NAFLD-mediated hepatocarcinogenesis .....	112
MSI: colorectal cancer and beyond-The complexity of specific biomarkers within genome wide NGS .....	113
Up-date of molecular pathology diagnostics for the Molecular Tumorboard in Freiburg .....	114
Histomorphological and molecular analysis of pancreatic neuroendocrine tumours....	115
<b>AG Kinder- und Fetalpathologie 1</b> .....	<b>115</b>
Differentialdiagnosen der Molenschwangerschaft .....	115
Post-mortem trio genome sequencing in families with children or adolescents with an unexplained cause of death - initial results and outlook .....	116
Placenta pathology in COVID-19-pregnancies – an update .....	116
<b>AG Kinder- und Fetalpathologie 2</b> .....	<b>117</b>
The role of fluorescence confocal microscopy in evaluation of vitality in pediatric tumor specimens and tumor cell isolation.....	117
Congenital gastrointestinal malformations: Pathological perspectives and diagnostics .....	118
Single-Shot Cardioplegia: Del Nido or HTK solution?.....	118
Fetal autopsy in comparison to prenatal diagnostics .....	119
Viral Myocarditis in Childhood .....	120
<b>AG Informatik, digitale Pathologie und Biobanking 2</b> .....	<b>120</b>
Key Steps when Implementing New Diagnostic Technologies in Routine Practice ....	120
Lessons learned from 10+ years using Digital Pathology .....	121
Automatic Detection of Esophageal Cancer in Whole Slide Image .....	121
Morphometry of tissue architecture distortion and inflammatory environments in IBD-associated crypt branching.....	122
Learning by doing: Iterative development of software and a seminar format to teach computational pathology in interdisciplinary teams.....	123
Identification of relevant tumor tissue structures and corresponding metastasis over	

deep learning of annotated $\mu$ CT data .....	125
<b>AG Informatik, digitale Pathologie und Biobanking 1 .....</b>	<b>127</b>
Why we need clinical trials to validate AI-assays: a proposal .....	127
Empowering minimally invasive postmortems with modular standard operating procedures to qualify for scientific demands .....	127
Low-resource finetuning of foundation models beats state-of-the-art in histopathology .....	128
Tissue Concepts: Supervised Foundation Models for Resource-Efficient, Robust Deep Learning in Pathology .....	131
Surface microscopic techniques for distortion-free digital pathology .....	132
Visualizing histopathological images through Activation Atlases: a tool for enhancing model explainability and discovering novel features with AI .....	133
<b>AG Gastroenteropathologie 1 .....</b>	<b>134</b>
Immunohistochemical In-situ Protein Expression Analysis for Anti-Claudin-18.2 Therapies - Which is the Correct Antibody? .....	134
Investigating Unconfirmed HER2 Status.....	135
Low microsatellite instability – a distinct instability type in gastric cancer? .....	135
The clinical importance of the locoregional host anti-tumour immune reaction in patients with oesophagogastric cancer .....	136
<b>AG Gastroenteropathologie 2.....</b>	<b>137</b>
Sacituzumab govitecan represents a novel therapeutic approach in cholangiocarcinoma .....	137
The Clinical and Biological Dichotomy of Early-Onset Pancreatic Cancer: A Matched Case Study .....	138
Subtyping of PanNETs by transcription factors, hormones, histology and patient outcome.....	139
PITX2 as a Sensitive and Specific Marker of Midgut Neuroendocrine Tumors: Results from a Cohort of 1157 Primary Neuroendocrine Neoplasms .....	140
Deciphering histological growth patterns in colorectal carcinoma liver metastasis: insights from single-cell RNA sequencing and spatial transcriptomics .....	141
<b>AG Gastroenteropathologie 3.....</b>	<b>142</b>
Why liver metastases of colon cancer don't all look the same: gene expression analysis of colorectal carcinoma liver metastases with different patterns of infiltration.....	142
Stroma AReactive Invasion Front Areas (SARIFA) and the plasmin/plasminogen system in gastric and colorectal cancer .....	142
Linking H&E-Based Histopathological Indicators of Tumor-Adipocyte Interaction SARIFA and TAF to Gene-Expression Based Consensus Molecular (CMS), Pathway- Derived (PDS) and Immune Subtyping in Colorectal Cancer .....	143
Single cell quantitative analysis of H&E tumor slides for survival prediction in colorectal cancer.....	144
Investigation of intratumoral heterogeneity as influencing factor in the development of therapy resistance in rectal carcinoma .....	145
Fast track development and multi-institutional clinical validation of the AI algorithm for detection of lymph node metastasis in colorectal cancer.....	145
<b>Poster Computational Pathology 1 .....</b>	<b>146</b>
AI-based Anomaly Detection for Clinical-Grade Histopathological Diagnostics.....	146
Mediating diverging expectations for AI-based applications in pathology: Providing best practice AI recommendations for pathologies .....	147
Scanner Contest: Comparison of Whole Slide Scanners in Digital Pathology .....	148
AI Model Transferability: Using NoisyEnsembles to Overcome Domain Differences Without Prior Knowledge .....	149
RudolfV: A Foundation Model by Pathologists for Pathologists .....	149

Development and clinical validation of a digital pathology algorithm for stroma-tumor ratio quantification in lung adenocarcinoma.....	151
Stable Diffusion for generation of synthetic histopathological image data of clear cell renal cell carcinoma (ccRCC).....	151
Contribution of specific cell types to the development of Barrett's esophagus and carcinoma via germline genetic risk.....	152
Utilizing AI to employ microvasculature as new diagnostic marker for routine pathological diagnostics in interstitial lung disease.....	154
Diff-ST: Staining Translation between HE and IHC by Diffusion Models.....	154
<b>Poster Computational Pathology 2 .....</b>	<b>156</b>
AI-based detection of oral squamous cell carcinoma with Raman histology .....	156
Quantitative Continuous Scoring of IHC assays using computational pathology allows superior patient selection for biomarker-informed cancer treatments .....	156
From CLL to Richter syndrome: at the interface of Boolean network modeling and experimental readouts .....	157
AI-based stroma-tumor ratio quantification algorithm: comprehensive evaluation of prognostic role in primary colorectal cancer .....	158
Computer-aided claudin-18.2 assessment in gastric cancer .....	158
Automated Locoregional Antigen Determination as a Prerequisite for CAR T-Cell Therapy Target Selection .....	159
Continuous AI-supported surveillance of IHC assay performance for sustainable staining quality.....	160
What you can learn from Pokémon for nephropathology: About the creation of diagnostic decision trees based on different types of knowledge graphs. ....	161
Gene expression prediction for patient stratification in muscle invasive bladder cancer .....	162
AI-based identification of lung carcinoma with Stimulated Raman Histology.....	162
A biomathematical approach to separate nodal marginal zone B-cell lymphoma from nodal diffuse large B-cell lymphoma on the basis of H&E-morphology. ....	163
<b>Poster Personalisierte (Krebs-)Medizin 1 .....</b>	<b>165</b>
Tumor budding of pancreatic ductal adenocarcinoma in a chorioallantoic membrane model - potential pitfall in the evaluation.....	165
A noisy NFκB-A20-RIPK3 circuit controls necroptosis kinetics in fibrosarcoma .....	166
αβ6-Integrin expression in gynaecological and urogenital cancer entities: Eligibility as a theranostic target.....	166
Establishment of an organotypic tissue slice culture for intrahepatic cholangiocarcinoma .....	167
Biological Makeup of Pancreatic Ductal Adenocarcinoma Predicts Prognosis and Indicates Treatment Response.....	168
Modeling Immunotherapies in Live 3D Human cancer tissue Bioreactors.....	169
Trop-2 expression in solid tumors - a molecular tumorboard experience .....	169
The Novel HSF1 Inhibitor NXP800 Possesses Antineoplastic Activity in Human Hepatocellular Carcinoma .....	170
<b>Poster Personalisierte (Krebs-)Medizin 2 .....</b>	<b>171</b>
Proteomic characterisation of pancreatic ductal adenocarcinoma (PDAC) by MALDI-TOF with regard to protein expression profiles, biological subtypes and clinical outcomes.....	171
Cytokine profiling in cerebrospinal fluid after intraoperative radiation of primary and secondary brain tumors .....	171
Inter-Observer Agreement Assessment in Estimating Tumor-Infiltrating Lymphocytes and Tumor-Stroma Ratio .....	172
Beyond the norm - unforeseen outcomes in brain autopsies.....	173

Spinning disk confocal multiplex immunofluorescence for simultaneous assessment of tissue organization and subcellular protein quantification.....	174
Peptide-Level Batch Normalization Reduces Variance in Multiplexed Clinical Proteomics .....	174
Proteomic and immunopeptidomic landscape of non-small cell lung cancer .....	175
<b>Poster Vergleichende Pathologie .....</b>	<b>176</b>
In-depth histological evaluation and comparison of mouse models for cholangiocarcinoma studies .....	176
miRNA profiling in intestinal tumors of dogs – a comparison of FFPE tissue and liquid biopsy .....	177
Spatial transcriptomics reveal multiple clusters in murine pancreatic preneoplastic lesions .....	177
$\beta$ 6-integrin expression in genetically engineered mouse models: mouse versus human .....	178
Subtyping of murine pancreatic ductal adenocarcinoma (mPDAC) .....	179
Pathology Skills Lab: Tumor models in pathology teaching .....	180
<b>Poster Gynäko- und Mammopathologie .....</b>	<b>180</b>
An Extremely Rare Differential Diagnosis – Metaplastic Papillary Tumour of the Fallopian Tube .....	180
Expression of circular LSD1 RNAs and LSD1 protein in endometrial cancer .....	182
Prostate specific membrane Antigen (PSMA) expression in Endometrial carcinoma and its metastases .....	183
Predictive biomarkers in uterine cervical cancer - Immunohistochemical analyzation of Her2, Tissue factor, Folatreceptor alpha, Trop2, CDH6, Nectin4 and cMet in cervical cancer.....	183
Trop-2 expression in carcinoma of the uterine cervix - a possible target for the treatment approach with antibody drug conjugates (ADC) .....	184
Prognostic impact of peritumoral stromal response in surgically treated carcinoma of the uterine cervix .....	185
Anti-HPV16/18-E6 (Clones: C1P5, BF7), Anti-HPV18-E7 (Clone: 8E2) and Anti-HPV (Clone: K1H8) Antibodies are Not Suited to Replace the Anti-p16 Antibody in Routine HPV Diagnostics.....	186
Incidental Diagnosis of Lymphangioliomyomatosis (LAM) in Gynecological Surgery - A Case Series .....	186
A node in the male breast. Case report of an unusual tumor manifestation. ....	187
<b>Poster Hämatopathologie .....</b>	<b>189</b>
The Pathogenesis of Pathological Splenic Rupture in Diffuse Large B-Cell Lymphoma – Enzymatic Degeneration of the Splenic Capsule? .....	189
Deep Learning (DL) based artificial intelligence (AI) algorithm for diagnostic and prognostic usage in myeloproliferative neoplasm (MPN).....	190
The challenge of spatially mapping the mononuclear phagocytic system in B-cell lymphoma.....	191
Reduction of intra-cellular ROS levels by NOX inhibitors or BHA attenuates cell survival and JAK/STAT signaling in classical Hodgkin's lymphoma. ....	192
<b>Poster Herz-, Gefäß-, Nieren- und Transplantationspathologie.....</b>	<b>192</b>
Representative clinical case with Nutcracker syndrome (NCS) favoring transposition of superior mesenteric artery (SMA) onto the infrarenal aorta .....	192
Aneurysm of the internal jugular vein – case report on a rare entity .....	193
TGF $\beta$ induced mechanosignaling controls the transcriptome and microenvironmental composition of proximal tubules in chronic kidney disease.....	194
Sustainable Benchmarking of deep learning models for computational pathology .....	195
Two Cases of Lymphofollicular Myocarditis – a Specific Entity? .....	195



Arrhythmogenic Cardiomyopathy and/or Oxymetazoline Abuse as a Putative Cause for Myocardial Fibrofatty Replacement and Sudden Cardiac Death .....	196
Role of ANXA4 as a modifier in VHL-dependent ccRCC .....	197
A new mouse model of glomerular thrombotic microangiopathy .....	197
Effectiveness of Combined Lipoprotein Apheresis and PCSK9 Inhibitor Therapy: A Comprehensive Analysis in the Context of Cardiovascular Risk Reduction .....	198
<b>Poster Uropathologie .....</b>	<b>199</b>
Real world data on the prevalence of BRCA1/2 and HRR gene mutations in patients with prostate cancer. ....	199
Androgen receptor non-genomic signaling as potential androgen sensitizer in castration resistant prostate cancer cells .....	199
Expression profiles of co-inhibitory receptors in non-urothelial neoplasms of the urinary bladder.....	200
Heterogeneity of PSMA-Expression in Primary Prostate Cancer .....	201
Selective embedding of prostatectomy specimen - is “more” really “better” .....	202
The coding Toll-like Receptor 4 polymorphism rs4986790 does not influence the risk for penile cancer development in Caucasians .....	202
Investigating novel treatment options:Inhibition of cullin 1, 4 and 5 reduces viability of testicular germ cell tumour cell lines.....	203
Immunohistochemical validation of potential prognostic biomarkers for prostate cancer .....	204
Proteomic signatures in sporadic progressive and localized clear cell renal cell carcinoma .....	205
The non-clear cell renal cell carcinoma subtype composition of a European cohort- Results from reference pathology of the SUNNIFORECAST study.....	206
<b>Poster Thoraxpathologie.....</b>	<b>207</b>
Long-term cryopreservation and revitalization of human PCLS.....	207
Machine-learning based BAL cytology of lung transplant patients.....	207
Correlation of pulmonary ultrasound features with histopathology in conventional and minimally invasive postmortems .....	208
mRNA expression analysis of explanted decellularized allogenic cardiovascular heart valves .....	209
<b>Poster Molekularpathologie I.....</b>	<b>210</b>
Cloud-based software for visualization and data analysis of Visium-measured tissue cohorts.....	210
TU-SIMPL - our solution for a digitalized molecular pathology lab .....	211
Rapid simultaneous detection of 16 pathogenic NRAS mutations in advanced colorectal cancer specimens.....	212
The BMP/TGF- $\beta$ Signaling in the Development of Dedifferentiated Chondrosarcoma .....	212
The role of ChREBP deletion in hepatocellular carcinoma pathogenesis in high-fat diet mouse model .....	214
Entity specific prediction of single-nucleotide variants in carcinomas of the bladder and urinary tract.....	215
Exploring Tumor Evolution in Advanced Colorectal Cancer: Comprehensive Genomic Profiling Using Tissue and Liquid Biopsy in a Research Autopsy Case .....	216
Tumor heterogeneity analysis of malignant melanoma .....	216
Comprehensive genomic instability testing: Empowering analysis beyond conventional boundaries.....	217
Tumours with low level of MSI, ERBB2- and/or MET-amplification reveal more patients who can benefit from targeted therapies.....	218
Classification of cancer types using RNA-seq data from cancer panel TSO500 .....	219
<b>Poster Molekularpathologie II.....</b>	<b>220</b>

Single-cell multi-omic detection of DNA methylation and histone modifications reconstructs the dynamics of epigenetic maintenance .....	220
Is the Prediction of the TP53 Mutation Status By Immunohistochemistry in Breast Carcinoma With a Wild-Type Pattern Really Feasible in the Individual Case? .....	220
The diagnostic value of ACSL1, ACSL4 and ACSL5 and the clinical application of ACSL inhibitor in non-small cell lung cancer .....	221
Fast-track analysis of lung cancer samples - implementation and evaluation of a customized Easy®PGX assay in routine diagnostics .....	222
Catching Proteomic Intratumoral Heterogeneity in Breast Cancer - A Miniaturized Low Input Proteomic Approach with a Microfluidic System .....	223
Understanding the Impact of Macrophages on Lung Transplant Outcomes .....	224
The next generation of cell death research: enhancing immunotherapy .....	225
Tumor heterogeneity of glioblastoma analyzed via SpatialOMx and HiPLEX-IHC .....	225
Molecular detection of Severe Acute Respiratory Syndrome Coronavirus 2 (SARS-CoV-2) by mass spectrometry in formalin-fixed paraffin embedded (FFPE) post-mortem tissue specimens .....	226
The transcription factor CREB1 is a regulator of IKK2 expression .....	227
Longitudinal transcriptomic profiling of dystrophin-deficient satellite cells .....	228
2NA FISH: a novel spatial transcriptomics tool for therapy decisions based on mRNA diagnostics in the tissue context .....	228
<b>Poster Kinder- und Fetalpathologie .....</b>	<b>229</b>
Comparison of neonatal autopsy findings with prenatal diagnoses .....	229
Congenital diarrhea, severe metabolic acidosis and retinal dystrophy: Syndromic Microvillus Inclusion Disease caused by homozygous Syntaxin 3 mutation .....	230
Life-threatening hemorrhage of congenital hemangioma in unborn infant at 32 weeks of gestation .....	230
<b>Poster Informatik, digitale Pathologie und Biobanking .....</b>	<b>231</b>
Retrospective Analysis of Rare, Triple-Negative Breast Carcinomas with Low Malignant Potential Utilizing the Forschungsdatenportal Gesundheit (FDPG) .....	231
Digitalization of Histopathological Routine Diagnostics - Do's and Don'ts .....	232
Quantitative tissue analysis with easily customizable AI-based segmentation .....	233
A Systematic Review of Machine Learning-Based Tumor-Infiltrating Lymphocytes Analysis in Colorectal Cancer: Overview of Techniques, Performance Metrics, and Clinical Outcomes.....	234
Decoding pan-cancer treatment outcomes using multimodal real-world data and explainable artificial intelligence .....	236
AI-driven analysis for real-time detection of morphologic characteristics in unstained microscopic cell culture images .....	236
Puzzling in pathology: Post-operative tissue reconstruction .....	237
A versatile and non-proprietary multiplex immunohistochemistry approach for tissue-based spatial phenotyping .....	238
<b>Poster Gastroenteropathologie I .....</b>	<b>239</b>
Structured evaluation of histopathological findings for future research puposes using the example of chronic inflammatory bowel disease .....	239
Prospective multicenter observational study on the impact of intestinal anastomosis onto early postoperative and long-term oncological outcome in resection of colon cancer (CA) .....	240
Prospective multicenter observational study including propensity score analysis on the impact of multivisceral resection of advanced colon and rectal cancer onto outcome characterized by morbidity, mortality and survival .....	240
Intraabdominal inflammation indicated by diverticulitis of the sigmoid colon under immunosuppressive medication after previous lung transplantation.....	241

Detection of oncofetal matrix proteins in collagenous colitis.....	242
Neuroendocrine differentiation in conventional adenocarcinomas and adenoneuroendocrine carcinomas of the colorectum .....	243
The role of the host: Stroma Areactive Invasion Front Areas (SARIFA) - concordance in double carcinoma of the colon and rectum.....	244
Morpho-proteomic analyses differentiate between crohn's disease and ulcerative colitis in routine diagnostic colon stage biopsies .....	245
Proteomic Insights into Treatment Response in Crohn's Disease Patients .....	245
Mesenteries as a novel ex vivo co-culture model to study peritoneal metastasis .....	246
Disseminated spread of a well-differentiated neuroendocrine tumor in the small bowel potentially associated with a HOXB13 G84E mutation .....	247
Mass spectrometry imaging of a large cohort of rare intrahepatic cholangiocarcinoma deploying tissue micro arrays .....	248
Strawberry Notch 1 is essential in hepatocellular carcinoma and cholangiocarcinoma .....	248
<b>Poster Gastroenteropathologie II .....</b>	<b>249</b>
Methylprednisolon-induced liver injury - a case series .....	249
Sister Mary Joseph nodule (SMJN): clinicopathological analysis in a cohort of ten patients.....	250
Investigating the significance of CEACAM6 in GBC and clinical relevance .....	250
Pathogenetic, Prognostic, and Therapeutic Role of Fucosylation in Intrahepatic Cholangiocarcinoma .....	251
Analysis of neoplastic steatogenesis in hepatocellular neoplasia in relation to Wnt/CTNNB1 status .....	252
Three-Dimensional and Molecular Characterization of the Human Ductular Reaction in Liver Cirrhosis.....	252
An often-unrecognized side effect in dialysis patients and its histological detection using a special stain.....	253
Expression of fibroblast activation protein (FAP) in neuroendocrine tumours of ileum and lung.....	254
Characterization of neuroendocrine differentiation in conventional pancreatic ductal adenocarcinomas .....	255
Improved survival of mouse colon precision cut tissue slices (cPCTS) using Air liquid cultivation.....	256
Invasive Fungal Disease in Chronic Liver Transplant Failure – an Underestimated Burden.....	256
Multimodal and site-specific differentiation dynamics of type 2 conventional dendritic cells in liver damage and cholestasis .....	257
STAT1 and STAT3 are associated with increased Inflammation in Hepatocellular Carcinoma .....	258
<b>Poster Gastroenteropathologie III .....</b>	<b>259</b>
Helicobacter pylori recurrence: clinico-pathological evaluation of molecular analysis in FFPE specimens of 968 patients.....	259
Combining gene expression analysis of gastric cancer cell lines and tumor specimens of the VARIANZ study to identify biomarkers for anti-HER therapies .....	260
Familial Mediterranean Fever (FMF) - an exotic but rising differential diagnosis of “unclear abdominal illness” in Germany due to increasing migration over the last decade, a Late-Onset-Case.....	261
Characterization of Septins as proteins of the nucleoskeleton in cancer cells.....	261
Gene expression analysis of gastric cancer cell lines reveals modulation of PD-L1 expression by HER inhibitors.....	262
Successful pancreatic cancer operation annihilated by port infection: A case report ..	263

Mechanisms of local adipose tissue-tumour crosstalk in pancreatic cancer .....	264
Screening for putative actionable targets reveals dynamic changes of PD-L1 expression throughout IPN-associated cholangiocarcinogenesis .....	264
Tumor regression grading in neoadjuvantly treated ductal adenocarcinoma of the Pancreas – Proposal of a new grading scheme .....	265
Deciphering Intra-Tumoral Heterogeneity and Metastatic Processes in Pancreatic Ductal Adenocarcinoma Using In Situ Sequencing .....	266
Pancreatic ductal adenocarcinoma (PDAC) has distinct morphological subtypes with different characteristics and prognostic values .....	267
Mucinous Cystic Neoplasms of the Pancreas and Liver share a similar DNA methylation profile with mucinous ovarian tumors .....	267
Lysyl oxidase-like 2-associated immunomodulation in pancreatic ductal adenocarcinoma .....	269

Amount of abstracts: 339

# Keynote 1: Mass Spectrometry based Spatial Biology in Molecular Pathology

KN01

## ***Mass spectrometry based Spatial Biology in Molecular Pathology***

R. M. Heeren

Maastricht University, Maastricht MultiModal Molecular Imaging Institute, M4i, Maastricht, The Netherlands

Molecular analytical technologies in the field of spatial biology are rapidly evolving. New innovative technologies improve sensitivity, resolution, content and throughput at an ever increasing speed. Mass spectrometry is undergoing a revolution in spatial biology. Innovative “omics” & imaging technologies, push the limits of single cell information. It is making a broad impact in molecular pathology. Contextual local metabolomics drives various applications. This lecture will focus on developments in innovative analytical imaging MS and its role in molecular pathology. It allows sensitive and selective molecular microscopy in the spatial study of distribution of molecules in cells and tissue. New insights in the spatial and molecular complexity of cellular metabolism help us to contextualize cellular function in health and disease. Innovations in mass spectrometry based chemical microscopes have now firmly established themselves in translational molecular research. One key aspect of translational success is the ability to obtain this molecular information on thousands of molecules on a process relevant timescale. Modern mass microscopes can now rapidly acquire images of metabolites, lipids, polymers, peptides and proteins, depending on the spatial resolution chosen. Combined this offers a truly precision multi-omics molecular pathology approach that reveals contextual molecular complexity of cellular phenotypes. The possibilities of high throughput targeted and untargeted MSI are seemingly endless, and will revolutionize the way we deal with spatial biology in the future.

# Keynote 4: Beyond Angiogenesis: Vascular Control of Tumor Progression and Metastasis

KN04

## ***Beyond Angiogenesis: Vascular Control of Tumor Progression and Metastasis***

H. G. Augustin<sup>1,2</sup>

<sup>1</sup>European Center for Angioscience (ECAS), Medical Faculty Mannheim, Heidelberg University, Mannheim, Germany, <sup>2</sup>German Cancer Research Center, Heidelberg, Germany

The molecular analysis of tumor vessel interactions during tumor progression and metastasis has primarily focused on the study of tumor cell-derived angiogenic and lymphangiogenic signals with the purpose to exploit such factors as therapeutic targets. Angiogenic factors activate endothelial cells in nearby blood and lymphatic capillaries to sprout towards the tumor. Tumor angiogenesis thereby not only nourishes the growing tumor, but access to the blood and lymphatic vasculatures enables cells from the primary tumor to enter the circulation to eventually form metastases at distant sites. The complex cellular interactions between tumor cells and endothelial cells have in this context mostly been studied from a tumor cell-centric perspective, i.e., the tumor cells send signals to which endothelial cells merely respond. Yet, the past decade has witnessed a fundamental change of paradigm with the discovery that the vascular endothelium does not just respond to exogenous cytokines, but exerts active ‘*angiocrine*’ gatekeeper roles controlling their microenvironment in an instructive manner. We have applied the concepts of angiocrine signaling towards the study of tumor progression and metastasis. Employing novel surgical preclinical metastasis models that better mimic tumor progression and the response to therapy as it occurs in humans, we have molecularly dissected vascular endothelial cells in progressing primary tumors as well as in the pre-metastatic and metastatic niches. These experiments were on the one hand aimed at establishing the systems map of endothelial transcriptomic changes during tumor progression and metastasis and on the other hand to identify and validate novel therapeutic targets. This presentation will review recent advances in the field of tumor microenvironment research and present novel angiocrine signaling mechanisms as promising targets of future mechanism-driven anti-metastatic therapy.

# Molecular Pathology 1 - Data Analysis

DGP01.02

## ***Classification, Interpretation and Reporting of Somatic Sequence Variants in Cancer***

P. Horak

Nationales Centrum für Tumorerkrankungen Heidelberg, Translationale Medizinische Onkologie, Heidelberg, Germany

With the adoption of next-generation sequencing in routine oncological practice, the accurate and prompt classification, interpretation, and reporting of somatic variants have become essential for effective patient management. The reporting of somatic tumor profiles is vital in the treatment of cancer patients, as it aids in the selection and prioritization of therapeutic strategies based on prognostic and predictive biomarkers. Harmonized methods for interpreting genomic profiles are crucial to assist physicians in their clinical decision-making and to optimize the therapeutic outcomes from available cancer treatments. Interpretation of variants typically focuses on the biological or clinical classification of mutations. Several professional societies have issued guidelines for the biological and clinical classification of germline and somatic biomarkers, as well as for their subsequent clinical interpretation and reporting. These guidelines have achieved broad adoption in clinical oncology and molecular pathology, being integrated into knowledge databases, supporting clinical laboratory procedures, and enhancing commercial applications. Proper utilization of these standards not only facilitates the standardization and harmonization of molecular diagnostics but also advances clinical research, improves understanding of molecular disease mechanisms, and aids in designing future clinical trials.

DGP01.03

## ***Utilizing mutational signatures from whole genome sequencing in cancer***

G. C. Koh<sup>1</sup>, S. Nik-Zainal<sup>2</sup>

<sup>1</sup>Early Cancer Institute, University of Cambridge, Department of Medical Genetics, University of Cambridge, Cambridge, United Kingdom, <sup>2</sup>University of Cambridge, Early Cancer Institute, Cambridge, United Kingdom

In this talk, I will describe how our team has explored the extraordinary DNA graffiti that has been seen in human cancers, using a combination of big data computational approaches and systematic experimental methods. I will provide an account of how we have designed algorithms that could be used to interpret cancer genomes for clinical purposes and how we have taken steps towards clinical validation studies for some of these algorithms. I will end the talk with a real cancer WGS patient story.

DGP01.04

## ***Definition of quality parameters for diagnostic reporting of WES in FFPE tissue specimens***

S. Wolter<sup>1,2,3</sup>, U. Matysiak<sup>1,2,3</sup>, E. Adam<sup>1,2,3</sup>, M. Werner<sup>1,2,3,4</sup>, S. Lassmann<sup>1,2,3</sup>

<sup>1</sup>Institute for Surgical Pathology, Medical Center, University of Freiburg, Germany, Freiburg, Germany, <sup>2</sup>Comprehensive Cancer Center Freiburg, Medical Center, Freiburg, Germany, Freiburg, Germany, <sup>3</sup>Zentrum für Personalisierte Medizin, partner site Freiburg, Germany, Freiburg, Germany, <sup>4</sup>German Cancer Consortium (DKTK), partner site Freiburg, Germany, Freiburg, Germany

### **Background**

Whole Exome Sequencing (WES) of Formalin-fixed and Paraffin-Embedded (FFPE) tissue specimens has entered the analytic portfolio of molecular pathology diagnostics, including cases of molecular tumorboards (MTB). Here, we present experiences with the WES workflow in a daily routine diagnostic setting, identifying limitations and key technical quality parameters.

### **Methods**

FFPE tissue specimens of n=27 cases (e.g. carcinomas: colorectal, esophageal, cholangio; astrocytoma; sarcomas) were processed for WES in a “real-world” setting of individual case requests over a time period from Jan/2023 to Jan/2024. Library preparation (SSel XTHS2 + HS Human All Exon V8, Agilent) was with modifications of the manufacturer’s protocol. In 5 cases, reproducibility was assessed. WES libraries were sequenced (NextSeq550, Illumina) and data was analyzed using an automated in-house pipeline. A structured diagnostic report format was used for results. Coverage metrics were analyzed and SNV/InDel status was correlated to previous analyses, if applicable.

## Results

For the 27 cases, samples with a range of 25 to 90 % tumor cell content and 40 to 200 ng of DNA were subjected to the WES workflow. All cases yielded sequencing results. Limitations were seen in 3/27 cases due to mean target coverage (normal sample) and in 8/27 cases due to inhomogeneity of median target coverage (tumor and/or normal sample). For example, a previously identified *ATR* variant was not reproducible in a case with low quality samples (3 repeats). QC-parameters median target coverage (cut-off 100 x for tumor and normal) and median/mean target coverage ratio (cut-off 0.75) were defined as technically valid for diagnostic reporting. Filtering of artifacts and reporting of true positive somatic variants was improved by implementing a cut-off  $\geq 5$  variant supporting reads in targets with a mean target coverage  $< 100$  x. With these QC-parameters, the precision of SNV/InDel reporting was optimized, especially in FFPE samples of lower quality.

## Conclusion

The application of WES for routine diagnostic in (*per se* limited) FFPE tissue specimens requires continuous quality controls (histologically, technically) and plausibility checks throughout the wet- and dry-lab process. Thereby, key technical sequencing QC-parameters and cut-offs can improve validity of especially SNV/InDel calling and reporting.

# Personalisierte Medizin 2- Personalized medicine at the interface with pathology

DGP02.01

## ***The precision medicine in Spain. How we are implanting the digital and molecular diagnosis***

S. Ramon Y Cajal Agueras

Vall Hebron Institut de Recerca, Patologia Molecular Translacional, Barcelona, Spain

Everybody is talking about precision medicine but usually they do not realize that precision medicine has to be based on 3 pillars: 1. In a correct pathological diagnosis. 2. In precise tumor staging. 3. In the application of biomarkers associated with targeted therapy.

Therefore, for the first step to implement a correct precision medicine is to optimize the pathological diagnosis, which goes through the digitization of the images, which allow telepathology and the application of computational pathology algorithms to objectify the quantification of biomarkers in tissue sections. In relation to molecular studies, it is mandatory to study NGS in most lung, colon and melanoma tumors, as well as sarcomas and brain tumors for their differential diagnosis.

To implement NGS technology and extend it to the largest possible number of patients, it is essential to concentrate molecular studies in a few centers that can allow more experience for biologists and pathologists, and also optimize the cost per sample. In Spain, there is still a great inequality between the different autonomous communities regarding the implementation of digital pathology and NGS studies. Moreover, the quality control in the labs performing biomarkers is not yet mandatory. In Catalonia, by government decision, 5 pathological anatomy laboratories have been selected to carry out all the molecular sequencing studies of a community of almost 8 million inhabitants. The hospitals which depend on our Institution send us the samples and we return the molecular study in a week. The results obtained must be integrated into the pathological diagnosis of the referral hospital. Joint molecular committees are held weekly with the reference centers. This network concentration of pathological and molecular studies allows this molecular study to be extended to the entire population with a similar quality, regardless of their place of residence. I will present how we are working in Cataluña and data from Spain

DGP02.02

## ***Personalized medicine at the interface with pathology - Uro-Oncology***

M. Retz

Technische Universität München, Urologie, München, Germany

Metastatic prostate cancer and urothelial cancer are heterogeneous diseases. To date, however, treatment decisions are often based on the extent and symptom burden of the tumour, concomitant diseases and the patient's wishes. Molecular

pathology aspects are rarely taken into account. The increasing use of the next-generation sequencing (NGS) and the interdisciplinary tumorboard have led to a better understanding of the significance of molecular alterations for the development and spread of cancer in the urogenital system.

In metastatic urothelial cancer (mUC), Fibroblast Growth Factor Receptors (FGFRs) have recently emerged as a novel therapeutic target in cancer. In particular, FGFR3 genomic alterations are potent oncogenic drivers in bladder cancer and represent predictive biomarkers of response to FGFR inhibitors. Erdafitinib is a pan-fibroblast growth factor receptor (FGFR) inhibitor. In a phase-3 trial (THOR), Erdafitinib resulted in significantly longer overall survival than chemotherapy among patients with metastatic urothelial carcinoma and *FGFR* alterations after previous anti-PD-1 or anti-PD-L1 treatment. A compassionate use program for Erdafitinib is available in the EU and the EMA approval is expected soon. Finally, a molecular analysis of urothelial cancer should already be performed in the firstline therapy of mUC.

In metastatic castration resistant prostate cancer (mCRPC), Poly (ADP-ribose) polymerase (PARP) inhibitors have antitumor activity in advanced prostate cancer associated with loss of homologous recombination repair (HRR) function. About 20% of all patients with advanced prostate cancer present germline or tumor mutations in HRR-related genes, the most common being BRCA2, mutated in approximately 10% of all advanced prostate cancers. The TALAPRO-2 and PROpel trials both showed a marked benefit of PARPi in combination with an androgen receptor signaling inhibitor (ARSI), compared with an ARSI alone in both the homologous recombination repair (HRR)-mutated, as well as in the HRR-non-mutated subgroup. Nevertheless, patients with BRCA1/2 mutations have the highest tumor response with the combination PARPi and ARSi in comparison to patients with HRR+nonBRCA and HRR-. Although olaparib plus abiraterone and talazoparib plus enzalutamide are approved for allComers in mCRPC, the scientific data strongly supports a routine molecular testing in every mCRPC patient.

DGP02.03

### ***Molecular pathology and molecular imaging - similarities and differences***

W. Weber

Technische Universität München, Nuklearmedizin, München, Germany

Molecular pathology and molecular imaging are two distinct yet interconnected disciplines, both utilize molecular biology tools to diagnose diseases and elucidate the underlying mechanism, but their core methodologies, applications, and implications differ significantly.

Molecular imaging focuses on visualizing biological processes in vivo using imaging technologies. This field combines various disciplines including chemistry, physics, biology, computer technology, and engineering. Techniques such as positron emission tomography (PET), and single-photon emission computed tomography (SPECT) are commonly used, because they quantitatively assess the expression of proteins at nano- and picomolar concentrations in humans. These techniques allow for non-invasive, in-vivo imaging of the expression but also of the function of molecular pathways at the molecular level.

Fundamental limitations of molecular imaging include the limited spatial resolution of about 2 mm with modern systems and a very limited ability for multiplexed imaging, i.e. the imaging of multiple targets in one session. The latter limitation is partially offset by the ability of molecular imaging to image functional processes and not only determine expression level of a protein. For example, imaging with a radiolabeled glucose analog does not measure the expression levels of one molecule, such as a glucose transporter, but the activity of the whole metabolic process, which includes also multiple enzymes involved in the metabolism of glucose.

Overall, molecular imaging and molecular complement each other with molecular pathology providing multiplexed information at the cellular level and molecular imaging providing information at the organ and whole-body level as well as information about the functional state of a protein or pathway.

DGP02.05

### ***Integrating proteomics into diagnostic molecular pathology reports to support molecular tumor board decisions.***

M. Fahrner<sup>1,2</sup>, E.-P. Dopfer<sup>1</sup>, J. Thiery<sup>1</sup>, N. Pinter<sup>1</sup>, U. Matysiak<sup>1,3</sup>, S. Riemer Cysar<sup>1</sup>, U. Wlokka<sup>1</sup>, S. Laßmann<sup>1,3</sup>, M. Werner<sup>1,2,3</sup>, O. Schilling<sup>1,2</sup>

<sup>1</sup>Institute for Surgical Pathology, Medical Center – University of Freiburg, Faculty of Medicine, University of Freiburg, Freiburg, Germany, <sup>2</sup>German Cancer Consortium (DKTK) and Cancer Research Center (DKFZ), Freiburg, Germany, <sup>3</sup>Comprehensive Cancer



## Background

Molecular pathology predominantly depends on genomic and transcriptomic methods for thorough and sensitive molecular diagnostics. The ongoing advancements in quantitative mass spectrometry (MS)-based proteomics facilitate consistent and thorough examination of the proteome in diverse patient samples, such as body fluids and tissue specimens. Therefore we set out to incorporate clinical proteomics into molecular diagnostics, enhancing and broadening the current molecular diagnostic practices while offering additional biological insights.

## Methods

We applied automated MS-based quantitative proteomic workflows to perform reproducible and robust in-depth proteomics of formalin-fixed paraffin-embedded (FFPE) tissue from patients that were included in the molecular tumor board. All patients also received molecular diagnostic routines including Gene-Panel sequencing and RNA Fusion analysis. A key advancement was the development of a semi-automated Galaxy workflow. This workflow streamlines file uploads and generates comprehensive reports, emphasizing reproducibility and robustness in proteomic data handling.

## Results

With our robust, reproducible, and automated sample preparation approach, we routinely identify and quantify more than 5500 proteins in patient-derived FFPE samples. We acquired protein profiles from over 200 MTB patients and in many cases the proteomic analysis has contributed to the molecular pathology reports. In these cases, proteomics has provided additional insights into the underlying molecular mechanisms in the respective malignancies.

In addition to the full proteome approach, we've established a phosphoproteomic protocol for functional insights into pathways in selected MTB cases. Furthermore, we've developed a proteogenomic workflow integrating genomics and proteomics. Notable findings include detecting CDK4 and CDK6 in cases with CDKN2A loss-of-function mutation, supporting recommendations for CDK inhibition, and identifying ERK signaling in a patient with a BRAF-KIAA1549 fusion, providing evidence for the recommendation of MEK inhibition.

## Conclusion

Integrating proteomics into molecular diagnostics offers significant advantages, particularly in analyzing complex tumor cases, such as rare and recurrent/resistant malignancies. Our semi-automated Galaxy workflow further strengthens this integration by ensuring reproducible and robust data analysis, making it a valuable tool in the molecular pathology field.

# Biobanking 1: Network Structures

DGP03.01

## *National autopsy registry and network (NAREG & NATON)*

P. Boor

RWTH Aachen University, Institut für Pathologie, Aachen, Germany

### Questions/Background

Autopsies have long been considered the gold standard for quality assurance in the field of medicine, yet their potential for advancing fundamental research has often been neglected. The emergence of the COVID-19 pandemic highlighted the potential of autopsies in invaluable role autopsies can play in unraveling pathophysiological mechanisms, refining therapeutic approaches, and enhancing disease management strategies.

### Methods

This prompted the establishment of the German Registry for COVID-19 Autopsies (DeRegCOVID) in April 2020, followed by the formation of the DEFEAT PANDEMIcs consortium (2020-2021), which later transitioned into the National Autopsy Network (NATON). As of 2024, DeRegCOVID aims to expand into the National Autopsy Registry (NAREG) facilitating the analysis of cases beyond COVID-19. Over a period of three years, DeRegCOVID collected and analyzed autopsy data from COVID-19 deceased in Germany, serving as the largest national multicenter autopsy study. DeRegCOVID served and supported data analysis, research requests, and public communication, playing a vital role in informing policy changes and responding to health authorities, e.g., leading to an Amendment to the Infection Protection Act (IfSG) in 2021.

## Results

**NATON.** NATON serves as a data and method platform, enabling and supporting collaboration across pathology, neuropathology, and legal medicine. It facilitates the exchange of information between researchers, medical professionals, and pandemic management. Supported by the Network University Medicine (NUM), NATON has developed as a sustainable infrastructure for autopsy-based research. NATON is supported by all five societies of Pathology, Neuropathology and Forensic Medicine, the Robert-Koch-Institute (RKI), the Paul-Ehrlich-Institute (PEI) and the Bernhard Nocht Institute for Tropical Medicine (BNITM).

**NAREG.** Due to the achievements and potential, and serving as the electronic backbone of NATON, DeRegCOVID is in the process of evolving into NAREG. Its modular structure will enable addressing multiple (potentially all) use cases beyond COVID-19, serving and adapting to the needs of the researchers, e.g., the first use case addressing Borna-Virus encephalitis is being tackled in collaboration with the RKI and BNITM. First international centers joined the registry.

## Conclusion

The autopsy registry and network have promoted the importance of autopsy-derived data and biomaterials for understanding COVID-19 pathophysiology.

DGP03.04

## ***Evidence-based guideline for tissue handling and biobanking in Japan***

Y. Kanai

Keio University School of Medicine, Department of Pathology, Tokyo, Japan

The success of data-driven molecular pathological research for identification of disease biomarkers and therapeutic targets depends on the quality of pathological tissue specimens. In this context, the Japanese Society of Pathology (JSP) has developed guidelines on the handling of pathological tissue samples for genomic research ("The JSP Guidelines") (Ref. 1) based on an abundance of data from empirical analyses of tissue samples collected and stored under various conditions. Such tissue samples should be taken from appropriate sites within surgically resected specimens without disturbing routine pathological diagnostic procedures, avoiding any bleeding or necrotic foci where nucleic acid and protein may be degraded. They should also be collected as soon as possible after resection: at the latest within about 3 hours of storage at 4°C. Preferably, snap-frozen samples should be stored in liquid nitrogen until use. Attention should be paid to not only the sample storage conditions but also procedures for nucleic acid extraction. If genomic DNA is extracted from formalin-fixed paraffin-embedded tissue, 10% neutral buffered formalin should be used. Both inadequate fixation and overfixation should be avoided. By establishing these evidence-based guidelines, the JSP has played an important role in making Japanese researchers aware of the importance of specimen quality. It is hoped that for management of biobanks, pathologists, clinicians, clinical laboratory technicians and biobank staff will master the handling of pathological tissue samples based on the guidelines.

Currently, Japan has three major government-supported megabanks: the Biobank Japan, the Tohoku Medical Megabank Organization, and the National Centre Biobank Network. In addition, some university hospitals and general hospitals operate their own biobanks of various sizes, known as 'hospital-attached biobanks'. Biobank management in Japan faces a serious shortfall of funding. Moreover, since individual biobanks have their own methods for genomic analysis and database development, unification of the platform to achieve a true nationwide network of biobanks remains a distant goal. It is therefore imperative to maintain our commitment to these unique biobanks and pursue our current role of developing and maintaining research infrastructure to foster clinical breakthroughs through which personalized and preventive medicine can be achieved.

Literaturangaben:

[1] Kanai Y, Nishihara H, Miyagi Y, Tsuruyama T, Taguchi K, Katoh H, Takeuchi T, Gotoh M, Kuramoto J, Arai E, Ojima H, Shibuya A, Yoshida T, Akahane T, Kasajima R, Morita KI, Inazawa J, Sasaki T, Fukayama M, Oda Y., (2018), The Japanese Society of Pathology Guidelines on the handling of pathological tissue samples for genomic research: Standard operating procedures based on empirical analyses., *Pathol Int*, 68: 63-90, <https://onlinelibrary.wiley.com/doi/10.1111/pin.12631>

# Personalisierte Medizin 1

DGP04.01

## **Mass Spectrometry-based Proteomic Characterization of Undifferentiated Small Round Cell Sarcomas with EWSR1- and CIC-Translocations Point to Diverging Tumor Biology and Reveal Distinct Diagnostic Markers**

L. Schweizer<sup>1</sup>, S. Doll<sup>2</sup>, C. Bollwein<sup>3</sup>, K. Steiger<sup>3</sup>, N. Pfarr<sup>3</sup>, M. Walker<sup>3</sup>, K. Wörtler<sup>4</sup>, C. Knebel<sup>5</sup>, R. von Eisenhart-Rothe<sup>5</sup>, W. Hartmann<sup>6</sup>, W. Weichert<sup>3</sup>, M. Mann<sup>1</sup>, P.-H. Kuhn<sup>3</sup>, [K. Specht](#)<sup>3</sup>

<sup>1</sup>Max-Planck-Institute for Biochemistry, Martinsried, Germany, <sup>2</sup>OmicEra Diagnostics GmbH, Planegg, Germany, <sup>3</sup>Institute of Pathology, Technical University of Munich, Munich, Germany, <sup>4</sup>Klinikum rechts der Isar, Technical University of Munich, Musculoskeletal Radiology Section, Munich, Germany, <sup>5</sup>Klinikum rechts der Isar, Technical University of Munich, Department of Orthopaedic Surgery, Munich, Germany, <sup>6</sup>Gerhard-Domagk-Institute of Pathology, University Hospital Muenster, Münster, Germany

### **Background**

Undifferentiated small round cell sarcomas of bone and soft tissue (USRS) represent a group of clinically aggressive tumors with heterogenic genomic alterations sharing similar morphology.

Recently, in-depth proteomic analysis of formalin-fixed, paraffin-embedded (FFPE) tissues in a clinical setting has become feasible.

### **Methods**

A comparative large-scale proteomic analysis of USRS (n=45) with diverse genomic translocations was performed. Cases included classic Ewing sarcomas with *EWSR1-FLI1* fusions (n=24) or *EWSR1-ERG* – fusions (n=4), sarcomas with an *EWSR1* – rearrangement (n=3), *CIC-DUX4* fusion (n=8), *EWSR1-NFATC2* fusion (n=1), *BCOR-MAML3* fusion (n=1) as well as tumors classified as USRS with no genetic data available (n=4). Molecular characterization of selected cases was carried out using next-generation-sequencing (NGS) techniques. Proteins extracted from FFPE pretherapeutic tumor biopsies were analyzed qualitatively and quantitatively using shot gun mass spectrometry (MS). Immunohistochemistry was used to confirm and validate differential expression of selected protein markers identified by the MS-based approach in the study cohort and in an independent cohort of USRS (n=34 ).

### **Results**

More than 8000 protein groups were quantified using data-independent acquisition. Based on the proteomic data, unsupervised hierarchical cluster analysis allowed stratification of the 45 cases into distinct groups reflecting their molecular genotype. Protein signatures that significantly correlated with the different genomic translocations were identified and used to generate a heatmap of all 45 sarcomas with assignment of cases with unknown molecular genetic data to either the *EWSR1*- or *CIC*-rearranged groups. MS-based prediction of sarcoma subtypes was molecularly confirmed in three cases where NGS was technically feasible. Three protein markers identified by the proteomic study, BCL11B, Bach2, and ETS-1, highly expressed in either Ewing sarcoma or *CIC-DUX4*-associated sarcomas, were chosen for immunohistochemical confirmation of MS data. Differential expression of these markers in the two genetic groups were further validated in an independent cohort of USRS.

### **Conclusion**

Our results indicate that BCL11B, Bach2, and ETS-1 immunohistochemistry may help in the differential diagnosis of USRS. Furthermore, our results demonstrate that large scale studies of proteomes of tumor tissue are feasible, pointing towards diverging signaling pathways in the different USRS subgroups.

DGP04.02

## **Using Mass Spectrometry Imaging to predict patient's treatment response from transurothelial bladder resections**

J. Gonçalves, S. Chakraborty, E. Mayr, W. Weichert, N. Pfarr, [K. Schwamborn](#)

Technical University of Munich, Institute of Pathology, School of Medicine and Health, Munich, Germany

### **Background**

Urothelial bladder cancer demonstrates responsiveness to immune checkpoint inhibitor (ICI) treatment; however, monotherapy elicits a response in only a minority of patients. Consequently, combining ICI treatment with other

modalities such as radiation, along with molecular preselection of likely responders, presents potential avenues to optimize ICI treatment.

In this clinical study, the combination of radiation with ICI treatment in the neoadjuvant setting was explored as a therapeutic option for patients with muscle-invasive bladder cancer. Mass spectrometry imaging was employed to evaluate transurethral resection as well as cystectomy specimens from patients undergoing this treatment approach, aiming to identify molecular features that could predict treatment success. The outcomes were compared with DNA/RNA sequencing data.

## Methods

48 samples were affixed onto ITO glass slide and subjected to deparaffinization and rehydration. Subsequently, tryptic digestion was performed, followed by matrix application. Mass spectrometry proteomic data were recorded using a RapifleX MALDI-TOF mass spectrometer (Bruker). Afterward, tissue sections were stained with hematoxylin and eosin and scanned. Tumor regions were annotated, distinguishing between invasive and non-invasive carcinoma. Data analysis was conducted using SCiLS Lab. Responders were defined as patients with no residual viable tumor present in cystectomy specimens.

## Results

The mass spectrometry profile of invasive carcinomas from treatment responders exhibited a distinct profile from non-invasive. Collagen  $\alpha$ -2(I) chain and collagen  $\alpha$ -1(I) chain precursor showed higher expression in invasive carcinoma. For non-invasive carcinoma, overexpression of histones and keratin, type 2 cytoskeletal 7 (KRT7) was identified. However, a greater number of peptides from KRT7 was detected in the non-responder subgroup. A dedicated quantitative analysis is required to accurately determine the significance of KRT7 in tumor invasiveness. The feature with the highest expression in treatment responders was  $m/z$  1032.59, corresponding to Histone H3. Further investigation revealed that overexpression of histone H3 correlated with the histological annotations of the tumor region in responders.

## Conclusion

Although various techniques, including RNASeq data, methylome data, and proteomic data, provided a breadth of information, collectively, they suggest involvement of keratin and collagen-related pathways, and genes associated with histone methylation.

DGP04.03

## ***Tumor Specificity by Quantitative Proteomics in the ADC Age***

F. F. Dreßler<sup>1</sup>, F. Diedrichs<sup>1</sup>, D. Sabtan<sup>2</sup>, S. Hinrichs<sup>2</sup>, P. Mackedan<sup>2</sup>, M. Schlotfeldt<sup>2</sup>, M. Henning<sup>3</sup>, A. Merseburger<sup>3</sup>, A. Miernik<sup>4</sup>, R. Zubarev<sup>5</sup>, P. Wolf<sup>4</sup>, S. Perner<sup>2</sup>, D. Horst<sup>1</sup>, Á. Végvári<sup>5</sup>

<sup>1</sup>Charité - Universitätsmedizin Berlin, Institut für Pathologie, Berlin, Germany, <sup>2</sup>Universitätsklinikum Schleswig-Holstein, Campus Lübeck, Institut für Pathologie, Lübeck, Germany, <sup>3</sup>Universitätsklinikum Schleswig-Holstein, Campus Lübeck, Klinik für Urologie, Lübeck, Germany, <sup>4</sup>Universitätsklinikum Freiburg, Klinik für Urologie, Freiburg, Germany, <sup>5</sup>Karolinska Institutet, Division of Physiological Chemistry I, Department of Medical Biochemistry and Biophysics, Stockholm, Sweden

## Background

With the advent of Enfortumab Vedotin (EV) urothelial bladder cancer (UC) has emerged as one of the vanguards for the new class of antibody-drug conjugates (ADCs). After good initial response rates, growing evidence suggests that tumor specificity and target overexpression are heterogeneous. Despite being the only quantitative method for protein analysis, mass spectrometric proteomic studies are still lacking. We have previously analyzed the UC proteome and identified five proteomic subtypes. Leveraging the value of paired samples with healthy mucosa in our cohort, we have now investigated the tumor specificity of actual and potential ADC targets and made this data available via a custom web interface.

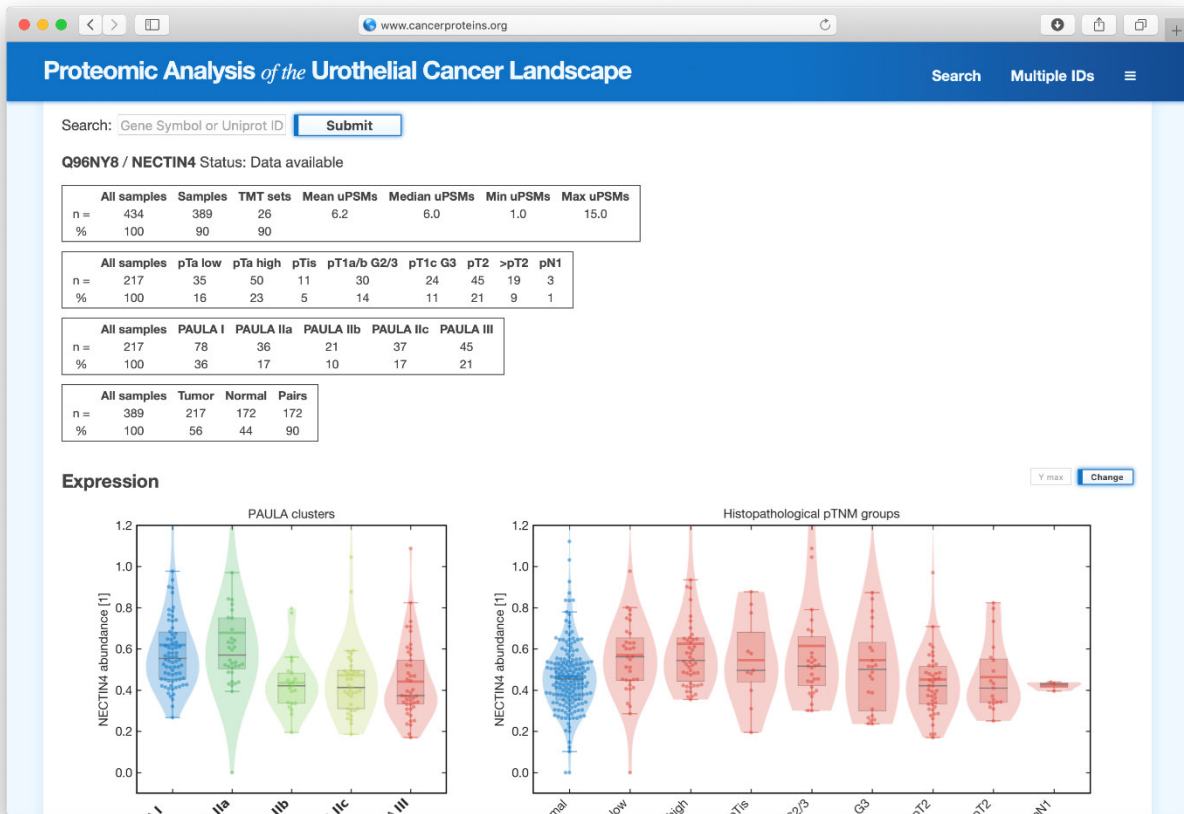
## Methods

We analyzed our PAULA cohort with 242 tumor as well as 193 paired healthy samples of adjacent normal mucosa and 9543 quantified proteins across the full range of UC from pT<sub>a</sub> low grade up to  $\geq$ pT<sub>3</sub> samples. Apart from differential expression analysis, we chose a single-sample approach with an individualized null distribution to quantify the rates of

per-patient over- or underexpression across subtypes and stages.

## Results

Even at the proteomic scale, no single protein showed universal overexpression. As an example, the EV target NECTIN4 was overexpressed in up to 31 % of the NMIBC samples but only in 4 % and 18 % in pT2 and  $\geq$ pT3 samples respectively. The maximum mean increase of the protein abundance compared to the healthy mucosa was 41 % in pTa high grade samples and only 21 % across all samples. EpCAM, the target of Opportuzumab Monatox, was not relevantly overexpressed or increased. CEACAM5 in turn, was overexpressed in 37 % of the basal-like high-risk samples. The complete dataset can be accessed directly at [cancerproteins.org](http://cancerproteins.org).



The web interface at [cancerproteins.org](http://cancerproteins.org)

## Conclusion

General overexpression of target proteins cannot be assumed in UC. Instead, patient-specific predictive testing is necessary and requires quantitative proteomics.

DGP04.04

## ***Spatial Transcriptomic Analysis of T-Cells in Colorectal Carcinoma and Identification of an HLA-A\*02:01-Restricted EBV and Tumor Cross-Reactive T-Cell Receptor***

S. Elezurtaj<sup>1</sup>, J. Franzen<sup>2</sup>, N. Genzel<sup>3</sup>, S. Schaper<sup>3</sup>, J. Liebeskind<sup>4</sup>, E. von der Wall<sup>1</sup>, A. Trinks<sup>1</sup>, B. Obermayer<sup>5</sup>, B. Hirsch<sup>1</sup>, M. Hummel<sup>1</sup>, A. Hauser<sup>6</sup>, H. Radbruch<sup>7</sup>, D. Kainmüller<sup>2</sup>, D. Horst<sup>1</sup>, N. Blüthgen<sup>1</sup>, M. Morkel<sup>1</sup>, V. Lennerz<sup>8</sup>, S. Hennig<sup>3</sup>, V. Seitz<sup>1</sup>

<sup>1</sup>Charité - Universitätsmedizin Berlin, Institut für Pathologie, Berlin, Germany, <sup>2</sup>Max-Delbrück-Centrum für Molekulare Medizin in der Helmholtz-Gemeinschaft (MDC), AG Biomedizinische Bildanalyse und HI Helmholtz Imaging, Berlin, Germany, <sup>3</sup>HS Diagnostik GmbH, Berlin, Germany, <sup>4</sup>Freie Universität Berlin, Institut für Immunologie, Berlin, Germany, <sup>5</sup>Berliner Institut für Medizinische Systembiologie (BIMSB), Berlin, Germany, <sup>6</sup>Deutsches Rheumaforschungszentrum (DRFZ), Institut der Leibniz-Gemeinschaft, AG Immundynamik, Berlin, Germany, <sup>7</sup>Charité - Universitätsmedizin Berlin, Institut für Neuropathologie, Berlin, Germany, <sup>8</sup>TheryCell GmbH, Berlin, Germany

## Background

Colorectal cancer (CRC) ranks third globally in cancer mortality, with emerging evidence highlighting T-cells' pivotal role in combating CRC. To deepen our understanding of T-cell responses in CRC, we analyzed T-cell infiltration, exhaustion markers, and tumor cell spatial distribution in CRC cases. Additionally, we explored the presence of tumor-associated tertiary lymphoid structures (TLS) and investigated the presence of a previously identified HLA-A\*02:01-restricted EBV cross-reactive, tumor-specific T-cell receptor (tsTCR), initially detected in lung carcinoma [1].

## Methods

We employed spatial transcriptomics and single cell sequencing via the 10x Genomics platform to study the T-cell distribution and phenotypes in eight CRC cases. Additionally, we characterized the TCR alpha and beta chains and connected our findings with patients' HLA types.

## Results

We observed distinct T-cell distribution patterns in the CRC cases. Specifically, two cases showed abundant TLSs near the tumor. One of these cases presented with a defective mismatch-repair phenotype (dMMR) whereas the other case displayed proficient mismatch-repair. Exhaustion markers were found to be expressed by T-cells at the T-cell/tumor-cell interface and HLA typing confirmed both cases as homozygous for HLA-A\*02:01. Further TCR profiling revealed that only these two, out of eight cases, contained a distinct HLA-A\*02:01-restricted, EBV cross-reactive, tumor-specific TCR previously identified in lung cancer [1]. EBER-in-situ-hybridization revealed only isolated lymphocytes with evidence of a latent EBV-infection in the tumor microenvironment and in normal mucosal lymphoid tissue.

## Conclusion

The occurrence of tsTCRs and exhaustion markers at the tumor cell front may offer insights into distinct T-cell immune responses in CRC. Cross-reactive tsTCRs to viral antigens may represent interesting targeted agents for tumor therapy.

Literaturangaben:

[1] Chiou, S.H., et al., (2021), Global analysis of shared T cell specificities in human non-small cell lung cancer enables HLA inference and antigen discovery, *Immunity*, 586-602, 54(3)

DGP04.05

## ***Oncogenic role of ACSL5 (acyl-CoA synthetase long-chain family member 5) and its clinical implications in colorectal carcinoma***

M. Nenkov<sup>1</sup>, Y. Ma<sup>1</sup>, M. Schmidt<sup>2</sup>, O. Huber<sup>2</sup>, A. Berndt<sup>1</sup>, K. M. Engel<sup>3</sup>, T. Kretzschmar<sup>4</sup>, C. Schulze<sup>5</sup>, N. Gaßler<sup>1</sup>, Y. Chen<sup>1</sup>

<sup>1</sup>Jena University Hospital, Section of Pathology, Institute of Forensic Medicine, Jena, Germany, <sup>2</sup>Jena University Hospital, Institute of Biochemistry II, Jena, Germany, <sup>3</sup>Faculty of Medicine, Leipzig University, Institute for Medical Physics and Biophysics, Leipzig, Germany, <sup>4</sup>Jena University Hospital, Department of Internal Medicine I, Division of Cardiology, Jena, Germany, <sup>5</sup>Jena University Hospital, Jena University Hospital, Germany, Department of Internal Medicine I, Division of Cardiology, Germany

## Background

Colorectal carcinoma (CRC) is the third most common cause of cancer-related death, with an increasing incidence among adults aged < 49 years. ACSL5, one of the ACSL family members, is predominantly expressed in the intestine and is deregulated in different cancers, including CRC. The implications of ACSL5, particularly the roles of its different isoforms, have not yet been clearly addressed in CRC.

## Methods

Immunohistochemistry on tissue microarrays containing 204 primary CRCs was used to evaluate the expression of ACSL family members and their clinical implications. Multiplex immunofluorescence was used to examine the spatial distribution of ACSL5 and  $\beta$ -catenin in normal colon mucosa and colorectal carcinoma tissue samples. 'Gain-of-function' ACSL5-CRC cell models were investigated for tumorigenic properties, oxygen consumption rates (The Cell Mito Stress) and lipidomic profiling (Mass Spectrometry).

## Results

Our data revealed that ACSL5 was highly expressed in the majority of primary colorectal carcinoma cases and that

higher ACSL5 expression was significantly associated with shorter patient survival ( $p = 0.0041$ ). Overexpression of different ACSL5 isoforms, including a (long), b (canonical, short), and x1 (exon 20 skipping), promoted colony formation, proliferation, migration, wound healing, and invasion, accompanied by metabolic reprogramming of CRC cells to upregulate oxidative phosphorylation, resulting in higher mitochondrial ATP production. Enhanced tumorigenic properties induced by ACSL5 overexpression are accompanied by enrichment in Wnt/ $\beta$ -catenin signalling and elevated levels of lipid metabolic regulators, such as ACSL3, ACSL4, and FASN. Lipid metabolic profiling showed changes in membrane lipid fractions, including phosphatidylcholine, phosphatidylethanolamine, phosphatidylinositol, and storage lipids such as triglycerides. Silencing of ACSL5 in HT-29 cells (HT-29-shACSL5) significantly reduced spheroid volume in 5-FU treated spheroids of HT-29-shACSL5. ACSL5 expression in primary CRCs was found to be significantly positively correlated with nuclear  $\beta$ -catenin (Pearson's  $R = 0.253$ ,  $p = 0.004$ ), ACSL3 (Pearson's  $R = 0.258$ ,  $p = 0.008$ ) and ACSL4 (Pearson's  $R = 0.301$ ,  $p = 0.001$ ) expressions.

## Conclusion

Based on our data, we conclude that ACSL5 has potential clinical implications as a prognostic marker in CRC patients. ACSL5 exerts oncogenic functions via metabolic reprogramming, accompanied by elevated Wnt/ $\beta$ -catenin signalling. Silencing of ACSL5 may sensitize CRC cells to 5-FU.

DGP04.06

## ***Dissecting the spatial heterogeneity of molecular subtypes in muscle-invasive urothelial bladder cancer using spatial transcriptomics***

C. Matek<sup>1,2</sup>, P. L. Strissel<sup>2,3</sup>, R. Strick<sup>2,3</sup>, D. Sikić<sup>2,4</sup>, B. Wullich<sup>2,4</sup>, A. Hartmann<sup>2,5</sup>, M. Eckstein<sup>2,5</sup>

<sup>1</sup>Pathologisches Institut Universitätsklinikum Erlangen, Erlangen, Germany, <sup>2</sup>Bayerisches Zentrum für Krebsforschung, Erlangen, Germany, <sup>3</sup>Universitätsklinikum Erlangen Frauenklinik, Erlangen, Germany, <sup>4</sup>Universitätsklinikum Erlangen Klinik für Urologie und Kinderurologie, Erlangen, Germany, <sup>5</sup>Universitätsklinikum Erlangen Pathologisches Institut, Erlangen, Germany

## Background

Bladder cancer represents the second most common genitourinary malignancy and, when advanced to a muscle-invasive stage, represents a therapeutic challenge associated with poor outcome [1]. In recent years, several techniques for molecular subtyping schemes have been developed based on gene expression profiling and are associated with different outcomes and therapy responses. However, these subtyping efforts were primarily based on the overall tumor tissue rather than on separate transcriptional compartments.

## Methods

Here, we used the Visium spatial transcriptomics workflow in order to analyse tissue sections from 16 samples of human muscle-invasive bladder cancer. Sequencing data were processed using the Space Ranger pipeline (version 2.1) [2] as well as the Seurat package (version 5.0.1) [3] to determine the molecular tumour subtype for each relevant spot according to 6 different recent transcriptomic molecular classifiers [4–8] and a consensus classifier [9].

## Results

We determined the spatial arrangement of transcription patterns within the tumor. This allowed assessing the contribution of different spatial compartments of the tissue sections to the overall subtype classification of individual cases. Our results suggest an important contribution of the tumour environment regarding the overall subtype classification. Specifically, we identified that one main contributing signal to the stroma-rich subtype originates from the surrounding stroma rather than the tumour cells. This suggests that this histological subtype reflects the configuration of the tumour environment rather than the composition of the tumour itself.

## Conclusion

Spatial transcriptomic methods are critical to obtain information on all relevant contributing tissue components in a detailed manner. Our results highlight the contribution of different tissue components rather than analyzing the total tumor tissue on a bulk level. Specifically, aspects of the tumour, associated fibrosis and inflammatory reactions can be distinguished. For muscle-invasive bladder cancer, results suggest that the stroma-rich subtype is mainly defined by the tumour environment rather than an intrinsic property of tumour cells themselves.

## Literaturangaben:

- [1] Lopez-Beltran A, Cookson MS, Guercio BJ, et al., (2024), Advances in diagnosis and treatment of bladder cancer, *BMJ*, e076743, 384, doi:10.1136/bmj-2023-076743
- [2] 10x Genomics, (2024), Space Ranger - Official 10x Genomics Support., <https://www.10xgenomics.com/support/software/space-ranger/latest>, 2024-02-25
- [3] Hao Y, Stuart T, Kowalski MH, et al., (2024), Dictionary learning for integrative, multimodal and scalable single-cell analysis., *Nat Biotechnol*, 293–304, 42, doi:10.1038/s41587-023-01767-y
- [4] Mo Q, Nikolos F, Chen F, et al., (2018), Prognostic Power of a Tumor Differentiation Gene Signature for Bladder Urothelial Carcinomas., *J Natl Cancer Inst*, 448–459, 110, doi:10.1093/jnci/djx243
- [5] Damrauer JS, Hoadley KA, Chism DD, et al., (2014), Intrinsic subtypes of high-grade bladder cancer reflect the hallmarks of breast cancer biology., *PNAS*, 3110–3115, 111, doi:10.1073/pnas.1318376111
- [6] Marzouka N-A-D, Eriksson P, Rovira C, et al., (2018), A validation and extended description of the Lund taxonomy for urothelial carcinoma using the TCGA cohort., *Sci Rep*, 3737, 8, doi:10.1038/s41598-018-22126-x
- [7] Rebouissou S, Bernard-Pierrot I, de Reyniès A, et al., (2014), EGFR as a potential therapeutic target for a subset of muscle-invasive bladder cancers presenting a basal-like phenotype., *Sci Transl Med*, 244ra91, 6, doi:10.1126/scitranslmed.3008970
- [8] Robertson AG, Kim J, Al-Ahmadie H et al., (2017), Comprehensive Molecular Characterization of Muscle-Invasive Bladder Cancer., *Cell*, 540–556, 171, doi:10.1016/j.cell.2017.09.007
- [9] Kamoun A, de Reyniès A, Allory Y, et al., (2020), A Consensus Molecular Classification of Muscle-invasive Bladder Cancer., *Eur Urol*, 420–433, 77, doi:10.1016/j.eururo.2019.09.006

DGP04.07

## ***A novel TROP2 complex affects the cytoskeleton architecture and mechanobiology in colorectal cancer***

K. Huebner<sup>1</sup>, A. Nursaitova<sup>1</sup>, A. Maiuthed<sup>2</sup>, B. Mrazkova<sup>3</sup>, D. Soteriu<sup>4</sup>, M. Kubankova<sup>4</sup>, M. Kraeter<sup>4</sup>, A. Battistella<sup>4</sup>, A. Gehring<sup>1</sup>, J. Knittel<sup>1</sup>, F. Gebhart<sup>1</sup>, K. Erlenbach-Wuensch<sup>5</sup>, J. Prochazka<sup>3</sup>, A. Hartmann<sup>5,6</sup>, R. Palmisano<sup>7</sup>, J. Guck<sup>4</sup>, R. Schneider-Stock<sup>1,6</sup>

<sup>1</sup>University Hospital, Friedrich-Alexander-University Erlangen-Nürnberg, Experimental Tumorpathology, Institute of Pathology, Erlangen, Germany, <sup>2</sup>Faculty of Pharmacy, Mahidol University., Department of Pharmacology, Bangkok, Thailand, <sup>3</sup>Czech Center for Phenogenomics, Institute of Molecular Genetics of the ASCR, Prague, Czech Republic, <sup>4</sup>Max Planck Institute for the Science of Light & Max-Planck-Zentrum für Physik und Medizin, Erlangen, Germany, <sup>5</sup>University Hospital, Friedrich-Alexander-University Erlangen-Nürnberg, Institute of Pathology, Erlangen, Germany, <sup>6</sup>Comprehensive Cancer Center Erlangen-EMN (CCC ER-EMN), Erlangen, Germany, <sup>7</sup>Friedrich Alexander University Erlangen-Nürnberg, OICE, Erlangen, Germany

### **Background**

Although metastasis significantly contributes to the majority of colon cancer (CC)-related deaths, its molecular mechanisms are still not yet fully deciphered. Cancer cell mechanobiology has greatly expanded our knowledge on cancer progression by linking the cells' mechanical properties to their metastatic potential.

As the cancer driver and cell surface glycoprotein TROP2, known to advance invasion and metastasis, has found its way to the clinics as a novel target for antibody-drug-conjugates, we aimed to evaluate its function on cell mechanical properties in CC.

### **Methods**

Real-time deformability cytometry (RT-DC) and atomic force microscopy (AFM) were used to determine cell stiffness in CC cell and organoid lines, chicken xenografts and human tumors. We modulated *TROP2* expression by overexpression and knockout (KO) experiments. Gene expression of YAP/TAZ target genes was measured. A combined TROP2 immunoprecipitation (IP)/mass spectrometry approach and proteomics analysis were performed to assess new TROP2 interaction partners. *In silico* results were validated by Co-IP and proximity ligation assays (PLA). The intracellular localization of TROP2 and its binding partners as well as their impact on the cytoskeleton architecture were assessed by confocal microscopy.

### **Results**

High levels of TROP2 in cell and organoids lines were associated with an increased cell stiffness, while decreasing *TROP2* expression resulted in more compliant cells. By TROP2-IP, ITGB5 and DIAPH1 were identified as new interaction partner that were validated by Co-IP and PLA. The triple complex TROP2-ITGB5-DIAPH1 only formed in stiff cells and was enriched at the perinuclear region. TROP2 binding to the cytoskeleton regulator DIAPH1 blocked DIAPH1 function followed by F-actin depolymerization and perinuclear microtubule condensation. The perinuclear localization of



both the triple complex and condensed microtubules affected nuclear mechanics and gene expression. Thus, stiff cells upregulated YAP/TAZ target genes in 2D and 3D models which could be reversed when perturbing cytoskeleton or complex dynamics.

### **Conclusion**

Our mechanistic approaches disclosed TROP2 as a crucial mediator of cell stiffness in CC. We identified a novel complex of TROP2, ITGB5, and DIAPH1 with an impact on the cytoskeleton and gene expression. Our results suggest that stiffness is associated with increased tumor aggressiveness and elevated metastatic potential in CC.

## **Neuroendocrine Tumours**

DGP05.01

### ***Diagnostic and prognostic biomarkers for pancreatic neuroendocrine neoplasms***

L. Brosens

Department of Pathology, UMC Utrecht, 3508 GA Utrecht, The Netherlands

Neuroendocrine neoplasms of the pancreas include well differentiated neuroendocrine tumors (pNET) and neuroendocrine carcinoma (NEC). Distinction between pNET and NEC is crucial as the prognosis and treatment of pNET and NEC differ greatly. Although distinction between pNET and NEC is straightforward in most cases, some cases cause significant diagnostic challenges. Several (surrogate) molecular markers can be very helpful to improve distinction between pNET and NEC in such challenging cases.

NEC is by definition a high-grade neoplasm and therefore not graded. pNETs, on the other hand, are subdivided in three grades based on mitotic activity and Ki67 proliferative activity. Although tumor grade is a key prognostic marker, it is not sufficient for optimal patient stratification and the disease course of pNET remains heterogenous and unpredictable. Therefore better prognostic biomarkers are needed to improve patient stratification and management of patient with a pNET.

In recent years molecular genetic analyses of pancreatic neuroendocrine neoplasms (NEC and pNET) have greatly increased our understanding of the molecular underpinnings of these neoplasm. In addition, epigenetic studies revealed insights in different pNET subtypes. This has led to several practically useful diagnostic and promising predictive biomarkers that can greatly refine diagnoses of pancreatic neuroendocrine neoplasms and improve patient stratification.

DGP05.02

### ***Neuroendocrine Neoplasms of the Gastrointestinal Tract***

M. Jesinghaus

Institut für Pathologie, Universitätsklinikum Marburg, Marburg, Germany

The gastrointestinal tract (GIT) is the main primary site of origin for Neuroendocrine Neoplasms (NENs), which encompass well-differentiated neuroendocrine tumors (NETs) and poorly differentiated neuroendocrine carcinomas (NECs) as their principal entities. Despite the metastatic potential of NETs, they frequently show long-term clinical courses and have a comparably favorable prognosis. In contrast, NECs are biologically highly aggressive neoplasms characterized by a markedly inferior prognosis compared to conventional carcinomas arising from the same primary site. This talk will address diagnostic approaches for GIT-NEN and also discuss prognostic implications as well as their molecular alterations underlying these neoplasms.

DGP05.03

### ***Diagnostic issues in neuroendocrine neoplasms of the lung***

A. Kasajima

TUM School of Medicine and Health, Department of Pathology, Munich, Germany

Bronchopulmonary neuroendocrine neoplasms (BP-NENs) account for approx. 30% of all NENs. Although BP-NENs and NENs of digestive organs share morphological and molecular features, they differ in terminology and classification. Neuroendocrine tumors (BP-NETs) have been classically termed as carcinoid and grouped into typical (TC) and atypical

carcinoid (AC) based on presence or absence of necrosis and mitotic count. In the most recent WHO classification for NENs of endocrine organs (WHO2022), neuroendocrine tumor (NET G1 and G2) are introduced as a synonym of TC and AC, respectively. However, Ki67 index, which defines the grade of NETs in digestive organs, is only discussed in description and not included into the criteria for classification of BP-NENs. In addition, well-differentiated NENs with high mitotic counts which correspond to a NET G3 in digestive organ system, are not defined. This talk discusses the role of Ki67 for a proper classification of BP-NETs/carcinoids.

DGP05.04

## ***Activated mTOR signaling promotes the expression of the mitochondrial biogenesis regulator PGC1 $\alpha$ in pancreatic neuroendocrine tumors (panNETs)***

J. Buchwaldt, D.-C. Wagner, M. Kloth, K. E. Tagscherer, W. Roth, N. Hartmann

University Medical Center Mainz , Johannes Gutenberg University Mainz, Institute of Pathology, Mainz, Germany

### **Background**

Since a considerable number of pancreatic neuroendocrine tumors (panNETs) exhibit mTOR activity, current therapy for advanced panNETs involves the use of mTOR inhibitors. There has been recent discussion regarding the potential benefits of combined treatment with inhibitors targeting cellular metabolism in patients. These are based on observations that mTOR signaling also impacts mitochondrial function and the expression of nuclear-encoded mitochondria-related genes. However, there remains limited understanding of the interplay between mTOR and mitochondria, particularly within panNETs. Therefore, the objective of this study was to identify proteins that link these two systems and to assess functional consequences of this relationship.

### **Methods**

We established a well-characterized cohort of 157 panNETs and determined the activity of the mTOR signaling by expression analysis of the phosphorylated ribosomal protein S6 in a tissue micro array (TMA). To dissect gene expression profiles induced by mTOR activity, RNA sequencing was performed on panNETs with and without mTOR pathway activity. The expression of the identified genes was subsequently examined using quantitative PCR. Functional consequences of the observed molecular alterations were assessed in cellular assays using BON1 and QGPT1 cells.

### **Results**

In total 34 cases out of 157 panNETs (22 %) showed activation of mTOR signaling. RNA sequencing revealed that the *PPARGC1A* gene is the top upregulated gene in panNETs with increased mTOR activity. *PPARGC1A* encodes the peroxisome proliferator-activated receptor gamma coactivator 1-alpha (PGC1 $\alpha$ ) protein, which has been described as a master regulator of mitochondrial biogenesis. This observation is supported by quantitative PCR, showing upregulation of the *PPARGC1A* gene expression up to 50% in cases with activated mTOR pathway in comparison to cases with no activation. Moreover, downregulation of *PPARGC1A* in panNET cell lines with high mTOR activity reduced cell proliferation.

### **Conclusion**

Taken together, 22 % of analyzed panNETs exhibit increased mTOR signaling and our results suggest that PGC1 $\alpha$  could be a new possible link between mTOR signaling and mitochondrial activity.

## **Advances in Computational Pathology 1**

DGP06.01

### ***Built to Last? Reproducibility and Reusability of Deep Learning Algorithms in Computational Pathology***

T. Peng

Helmholtz Center, Oberschleißheim, Germany

Recent advancements in computational pathology are driven by deep learning, but ensuring model reproducibility and reusability is challenging. This requires well-documented code, easy integration into workflows, and robust, generalizable models. Notably, few computational pathology algorithms have been reused by researchers or applied clinically. We

reviewed peer-reviewed articles on PubMed from January 2019 to March 2021 across five use cases: stain normalization, tissue type segmentation, cell-level feature evaluation, genetic alteration prediction, and grading/staging/prognostic inference. Only 25% (41 of 160 publications) made their code publicly available, with even fewer providing sufficient documentation and user guidance. To enhance reproducibility and reusability, we recommend involving clinicians early in the model development process to define relevant tasks and necessary modifications. We illustrate this workflow with a study predicting microsatellite instability (MSI) from colorectal cancer histology, as published in our recent Cancer Cell article (Wagner et al. Cancer Cell (2023)).

DGP06.02

### ***The transition to digital pathology in routine diagnostics. Milestones and open questions.***

P. Ströbel

Universitätsmedizin Göttingen, Institut für Pathologie, Göttingen, Germany

The transformation of a conventional workflow into a fully digital workflow (including, but not limited to, the use of whole slide imaging, WSI, or the application of AI algorithms) in pathology has many decisive advantages with the potential to change the way pathologists work, but it is also a fraud with obstacles and high costs. Since the financial benefits of this transformation will usually be slow and may be indirect, hospital administrations may vary to invest their money. A firm and realistic understanding of the expected outcome is crucial to calculate the costs and benefits and to lead a successful dialogue with the financial officers. Careful change management is important to convince the teams working with the technology and to avoid friction. Despite the great potential connected with digitalization, there are as yet no standard "plug-and-play" solutions available on the market that could satisfy all the requirements, making preparations in a multi-professional team including pathologists, vendors, and IT specialists mandatory. In this iterative contribution, we will reflect 3 years of experience with a fully digital workflow in an academic pathology institute with a highlight on milestones and future challenges.

DGP06.03

### ***Using AI in Digital Pathology – Opportunities and Regulatory Challenges***

K. Zatloukal

Medical University of Graz, Diagnostic & Research Institute of Pathology, Graz, Austria

Digital pathology not only allowed optimisation of diagnostic workflows but also opened the opportunity for using AI-based technologies for image analysis. This is on the one hand important for better quantification of certain features such as immunohistochemical staining, tumor cell context, number of mitoses etc. On the other hand there are an increasing number of AI models that can reproducibly recognize complex features, such as Gleason Scores or tumor-environment compositions. Any use of AI-assisted pathological diagnosis has to meet the requirements of the European regulation on in vitro Diagnostic Medical Devices (IVDR; EU 2017/746) and, in the future, the Artificial Intelligence Act (AI Act) that has been approved by the European Parliament on April 16th 2024. The challenge is that IVDR applies to all AI-based diagnostics but does not provide further guidance on how to demonstrate compliance as principles are well established for classical diagnostic tests but experience is lacking on how these principles shall be applied to innovative diagnostics such as an AI model. At the same time the AI Act will apply to essentially any use of AI including medical applications but does not provide further guidance on how the requirements should be met by AI-based medical devices. In any case disclosing information on the quality of the data used for training an AI model that at the end defines its performance as well as demonstration of causability and plausability of the results is essential.

DGP06.04

### ***Enhancing Prostate Cancer Diagnosis: AI-Driven Virtual Biopsy for Optimal Targeted Biopsy Approach and Gleason Grading Strategy***

C. Harder<sup>1</sup>, A. Prylukhin<sup>2</sup>, A. Quaas<sup>1</sup>, M.-L. Eich<sup>1,3</sup>, M. Tretiakova<sup>4</sup>, S. Klein<sup>1</sup>, A. Seper<sup>2,5</sup>, A. Heidenreich<sup>6,7</sup>, G. J. Netto<sup>8</sup>, W. Hulla<sup>2</sup>, R. Büttner<sup>1</sup>, K. Bozek<sup>9</sup>, Y. Tolkach<sup>1</sup>

<sup>1</sup>Universitätsklinik Köln, Pathologie, Köln, Germany, <sup>2</sup>Landeskrankenhaus Wiener Neustadt, Pathologie, Wien, Austria, <sup>3</sup>Charité – Universitätsmedizin Berlin, corporate member of Freie Universität Berlin, Humbolt-Universität zu Berlin and Berlin Institute of Health,, Institute of Pathology, Berlin, Germany, <sup>4</sup>University of Washington Medical Center, Department of Laboratory Medicine and Pathology,

Seattle, United States of America, <sup>5</sup>Danube Private Medical University, Krems, Austria, <sup>6</sup>Universitätsklinik Köln, Urologie, Uro-Onkologie, spezielle urologische und Roboter-assistierte Chirurgie, Köln, Germany, <sup>7</sup>Medizinische Universität Wien, Urologie, Wien, Austria, <sup>8</sup>Perelman School of Medicine at the University of Pennsylvania, Department of Pathology and Laboratory Medicine, Philadelphia, United States of America, <sup>9</sup>Universität Köln, Center for Molecular Medicine, Köln, Germany

## Background

An optimal approach to MRI fusion targeted prostate biopsy (PBx) remains unclear (number of cores, inter-core distance, Gleason grading (GG) principle). The aim of this study was to develop a precise pixel-wise segmentation diagnostic AI algorithm for tumor detection and GG as well as an algorithm for virtual prostate biopsy that are used together to systematically investigate and find an optimal approach to targeted PBx.

## Methods

Pixel-wise AI algorithms for tumor detection and GG were developed using a high-quality, manually annotated dataset (slides n=442) after fast-track annotation transfer into segmentation style. To this end, a virtual biopsy algorithm was developed that can perform random biopsies from tumor regions in whole-mount whole-slide images with pre-defined parameters. A cohort of 115 radical prostatectomy (RP) patient cases with clinically significant, MRI-visible tumors (n=121) was used for systematic studies of the optimal biopsy approach. Three expert genitourinary (GU) pathologists participated in the validation.

## Results

The tumor detection algorithm (aware version sensitivity/specificity 0.99/0.90, balanced version 0.97/0.97) and GG algorithm (quadratic kappa range vs pathologists 0.77-0.78) perform on par with expert GU pathologists. In total, 65,340 virtual biopsies were performed to study different biopsy approaches with the following results: 1) four biopsy cores is the optimal number for a targeted PBx, 2) cumulative GG strategy is superior to using maximal Gleason score for single cores, 3) controlling for minimal inter-core distance does not improve the predictive accuracy for the RP Gleason score, 4) Using tertiary Gleason pattern principle (for AI tool) in cumulative GG strategy might allow better predictions of final RP Gleason score. The AI algorithm (based on cumulative GG strategy) predicted the RP Gleason score of the tumor better than 2 of the 3 expert GU pathologists.

## Conclusion

In this study, using an original approach of virtual prostate biopsy on the real cohort of patient cases, we find the optimal approach to targeted PBx. We publicly release two large datasets with associated expert pathologists' GG and our virtual biopsy algorithm.

DGP06.05

## ***Histopathology-based prediction of pathway activities for targeted therapies in HNSCC***

J. Hense<sup>1,2</sup>, M. Jamshidi Idaji<sup>1,2</sup>, L. Ciernik<sup>1,2</sup>, J. Dippel<sup>1,2</sup>, O. Buchstab<sup>3</sup>, J. Hess<sup>4</sup>, K.-R. Müller<sup>1,2,5,6</sup>, F. Klauschen<sup>2,3,7,8</sup>, **A. Mock**<sup>3,7</sup>

<sup>1</sup>Technische Universität Berlin, Machine Learning Group, Berlin, Germany, <sup>2</sup>BIFOLD – Berlin Institute for the Foundations of Learning and Data, Berlin, Germany, <sup>3</sup>Pathologisches Institut, LMU München, München, Germany, <sup>4</sup>Heidelberg University Hospital, Section Experimental and Translational Head and Neck Oncology, Department of Otolaryngology, Head and Neck Surgery, Heidelberg, Germany, <sup>5</sup>Korea University, Anam-dong, Seongbuk-gu, Department of Artificial Intelligence, Seoul, Republic of Korea (South Korea), <sup>6</sup>Max Planck Institute for Informatics, Saarbrücken, Germany, <sup>7</sup>German Cancer Research Center (DKFZ) & German Cancer Consortium (DKTK), Munich Partner Site, München, Germany, <sup>8</sup>Institute of Pathology, Charité - Universitätsmedizin Berlin, Berlin, Germany

## Background

Systemic treatment options for recurrent and/or metastatic head and neck squamous cell carcinoma (HNSCC) remain limited. Novel therapeutic approaches are needed for patients progressing after or not eligible for chemotherapy, as well as for the majority of patients who do not profit from immunotherapy. While recent precision oncology trials could only show limited activity of novel anticancer agents targeting genetic alterations [Keam2024], transcriptome- and pathway activity-based biomarkers are a promising next frontier for drug development. However, RNA-seq is still not part of routine molecular pathology workup. To this end, we aimed to investigate if the activity of tumor-relevant pathways can be predicted from H&E-stained histopathology images.

## Methods

We collected whole-slide images from the TCGA HNSCC study for training and the CPTAC HNSCC project [Huang2021] as a hold-out test cohort. Excluding HPV-positive cases and slides with insufficient image quality led to cohort sizes of 390 slides from 370 patients (TCGA) and 207 slides from 94 patients (CPTAC). The PROGENy algorithm [Schubert2018] was used to calculate tumor-relevant pathway activities from matching RNA-seq data. We thresholded the pathway activations at 0.5 to binarize the prediction targets. The slides were tessellated at 20x magnification into patches of 340 x 340 pixels, which were preprocessed using background filters and Macenko stain normalization [Macenko2009]. We then obtained vector representations of the resulting patches from the deep pre-trained foundation model CTransPath [Wang2022]. We employed TransMIL [Shao2021], a transformer-based multiple-instance learning architecture, for aggregating the patch-level features to a slide-level feature vector, and added a linear head for predicting the binary score of each pathway activation. A 3-fold cross-validation (CV) scheme was used for training and validation.

## Results

The activities of the VEGF and JAK-STAT pathways on TCGA data could be reliably predicted (mean (standard deviation) validation AUROC of 0.77 (0.03), 0.71 (0.05), respectively). The mean (std) test AUROC on CPTAC data for VEGF, and JAK-STAT were 0.71 (0.02), 0.79 (0.02), respectively.

## Conclusion

The successful histopathology-based prediction of VEGF and JAK-STAT pathway activity might guide targeted treatment. We are currently validating the predictions by immunohistochemistry.

### Literaturangaben:

- [Huang2021] Huang C, Chen L, Savage SR, Egeuz RV, Dou Y, Li Y, da Veiga Leprevost F, Jaehnig EJ, Lei JT, Wen B, Schnaubelt M, Krug K, Song X, Cieřlik M, Chang HY, Wyczalkowski MA, Li K, Colaprico A, Li QK, Clark DJ, Hu Y, Cao L, Pan J, Wang Y, Cho KC, Shi Z, Liao Y, Jiang W, Anurag M, Ji J, Yoo S, Zhou DC, Liang WW, Wendl M, Vats P, Carr SA, Mani DR, Zhang Z, Qian J, Chen XS, Pico AR, Wang P, Chinnaiyan AM, Ketchum KA, Kinsinger CR, Robles AI, An E, Hiltke T, Mesri M, Thiagarajan M, Weaver AM, Sikora AG, Lu, (2021), Proteogenomic insights into the biology and treatment of HPV-negative head and neck squamous cell carcinoma, *Cancer Cell*, 361-379, 2021 Mar 8;39(3)
- [Keam2024] Keam B, Hong MH, Shin SH, Heo SG, Kim JE, Ahn HK, Lee YG, Park KU, Yun T, Lee KW, Kim SB, Lee SC, Kim MK, Cho SH, Oh SY, Park SG, Hwang S, Nam BH, Kim S, Kim HR, Yun HJ; KCSG TRIUMPH Investigators, (2024), Personalized Biomarker-Based Umbrella Trial for Patients With Recurrent or Metastatic Head and Neck Squamous Cell Carcinoma: KCSG HN 15-16 TRIUMPH Trial., *J Clin Oncol*, 507-517, 2024 Feb 10;42(5)
- [Macenko2009] Macenko M, Niethammer M, Marron JS, Borland D, Woosley JT, Guan X, Schmitt C, Thomas NE, (2009), A method for normalizing histology slides for quantitative analysis, 2009 IEEE International Symposium on Biomedical Imaging: From Nano to Macro, Boston, MA, USA, 1107-1110
- [Schubert2018] Schubert M, Klinger B, Klünemann M, Sieber A, Uhlitz F, Sauer S, Garnett MJ, Blüthgen N, Saez-Rodriguez J, (2018), Perturbation-response genes reveal signaling footprints in cancer gene expression, *Nat Commun*, 20, 2018 Jan 2;9(1)
- [Shao2021] Shao Z, Bian H, Chen Y, Wang Y, Zhang J, Wangyang J., (2021), Transmil: Transformer based correlated multiple instance learning for whole slide image classification, *Advances in neural information processing systems*, 2136-2147, 34
- [Wang2022] Wang X, Yang S, Zhang J, Wang M, Zhang J, Yang W, Huang J, (2022), Transformer-based unsupervised contrastive learning for histopathological image classification, *Medical image analysis*, 102559, 81

# Personalisierte Medizin 3 - Stand der personalisierten Medizin

DGP07.02

## ***Molecular Tumorboard beyond Genomics - ADCs advancing***

K. Utpatel

Universität Regensburg, Institut für Pathologie, Regensburg, Germany

### **Questions/Background**

In recent years, the discovery of distinct cancer biomarkers has prompted a reevaluation of how tumors are classified, moving beyond histology alone. Therapies are now being tailored to target specific molecular aberrations and immunologic markers in cancers. This shift has led to the adoption of multiple histology-agnostic therapies in clinical practice, treating patients irrespective of their tumor's original site. Biomarker analysis is currently focussing on genomic

data. In addition to this fundamental change in drug development, significant advancements have been made in approving various innovative antibody-drug conjugates (ADCs) for treating solid tumors by benefiting from engineering improvements in the conjugation process and the introduction of novel linkers and payloads, resulting in novel and efficient approaches of „targeted chemotherapy“. [1]

## Methods

The current landscape of approved ADC therapies and ongoing clinical trials in solid tumors has been analysed, particularly focussing on the necessity of accompanying biomarker analysis (companion diagnostics).

## Results

Her2, trophoblast cell-surface antigen 2 (Trop-2) and Nectin-4 are targets that have been studied intensively. The most advanced drug is trastuzumab deruxtecan, an anti-HER2 ADC, that has shown significant activity in HER2-overexpressing breast, gastric and colorectal cancer. Trop-2 and Nectin-4, among others, also hold promise for being potentially histology-agnostic in their application. Biomarker analysis is currently performed more often immunohistochemically than genomically and may not always be necessary.

## Conclusion

ADCs are the most important new group of substances in personalized cancer therapy. It appears that each drug has a different ideal biomarker. Based on the features of the ADC, the same biomarker may have divergent consequences. In some cancer types, indicators other than IHC expression may be useful in helping to choose patients profiting best from ADC therapy. Although often ignored in trials and drug approval, ADC target expression level often appears to affect drug efficacy. Thus, predictive biomarker research is required to improve the therapeutic value of ADCs and support clinical decision making.

Literaturangaben:

[1] Tarantino P, Carmagnani Pestana R, Corti C, Modi S, Bardia A, Tolaney SM, Cortes J, Soria JC, Curigliano G, (2022), Antibody-drug conjugates: Smart chemotherapy delivery across tumor histologies., CA: A Cancer Journal for Clinicians, 165-182, 2024-02-01

DGP07.04

## ***NECTIN4 Amplification is Frequent in Solid Tumors and Predicts Enfortumab Vedotin Response in Metastatic Urothelial Cancer***

M. Eckstein<sup>1</sup>, N. Ngoc<sup>2</sup>, GUARDIANS Studiengruppe<sup>1</sup>, BRIDGE Cosortium e.V.<sup>1</sup>, S. Zschäbitz<sup>3</sup>, O. Hahn<sup>4</sup>, F. Roghmann<sup>5</sup>, C. Schwab<sup>6</sup>, D. Nagy<sup>7</sup>, M. Toma<sup>7</sup>, G. Kristiansen<sup>7</sup>, M. Abbas<sup>8</sup>, M. Mayr<sup>9</sup>, D. Niedersüß-Beke<sup>10</sup>, P. Ivanyi<sup>11</sup>, D. Dietrich<sup>12</sup>, J. Saal<sup>13</sup>, M. Ritter<sup>14</sup>, G. Niegisch<sup>15</sup>, C. Kuppe<sup>16</sup>, T. Mokry<sup>17</sup>, J. Meeks<sup>18</sup>, S. Rausch<sup>19</sup>, K. Schlack<sup>20</sup>, F. Vera Badillo<sup>21</sup>, A. Nakauma-González<sup>22</sup>, K. Junker<sup>23</sup>, A. Hartmann<sup>1</sup>, V. Grünwald<sup>24</sup>, M. Hölzel<sup>2</sup>, N. Klümper<sup>14</sup>

<sup>1</sup>Universitätsklinikum Erlangen, Institut für Pathologie, Erlangen, Germany, <sup>2</sup>Universitätsklinikum Bonn, Institut für experimentelle Onkologie, Bonn, Germany, <sup>3</sup>NCT Heidelberg, Heidelberg, Germany, <sup>4</sup>Universitätsklinikum Göttingen, Klinik für Urologie und Kinderurologie, Göttingen, Germany, <sup>5</sup>Universität Bochum, Klinik für Urologie und Kinderurologie, Herne, Germany,

<sup>6</sup>Universitätsklinikum Heidelberg, Pathologisches Institut, Heidelberg, Germany, <sup>7</sup>Universitätsklinikum Bonn, Institut für Pathologie, Bonn, Germany, <sup>8</sup>Universitätsklinikum Münster, Institut für Pathologie, Bonn, Germany, <sup>9</sup>InnPath, Innsbruck, Austria,

<sup>10</sup>Wilhelminenspital, Wien, Austria, <sup>11</sup>Medizinische Hochschule Hannover, Klinik für Hämatologie und internistische Onkologie, Hannover, Germany, <sup>12</sup>Universitätsklinikum Bonn, HNO Klinik, Bonn, Germany, <sup>13</sup>Universitätsklinikum Bonn, Klinik für Hämatologie und internistische Onkologie, Bonn, Germany, <sup>14</sup>Universitätsklinikum Bonn, Klinik für Urologie und Kinderurologie, Bonn, Germany,

<sup>15</sup>Universitätsklinikum Düsseldorf, Klinik für Urologie und Kinderurologie, Düsseldorf, Germany, <sup>16</sup>Universitätsklinikum Aachen, Klinik für Nephrologie, Aachen, Germany, <sup>17</sup>Universitätsklinikum Heidelberg, Diagnostische Radiologie, Heidelberg, Germany, <sup>18</sup>Northwestern University, Department of Urology, Chicago, United States of America, <sup>19</sup>Universitätsklinikum Tübingen, Klinik für Urologie und Kinderurologie, Tübingen, Germany, <sup>20</sup>Universitätsklinikum Münster, Klinik für Urologie und Kinderurologie, Münster, Germany,

<sup>21</sup>Queen's University, Department of Medical Oncology, Kingston, Canada, <sup>22</sup>UMC Rotterdam, Department of Bioinformatics, Rotterdam, The Netherlands, <sup>23</sup>Universitätsklinikum Homburg, Klinik für Urologie und Kinderurologie, Homburg, Germany, <sup>24</sup>Universitätsklinikum Essen, Klinik für Urologie und Kinderurologie & Klinik für medizinische Onkologie, Essen, Germany

## Background

The anti-NECTIN4 antibody-drug conjugate (ADC) enfortumab vedotin (EV) is approved for patients with metastatic urothelial cancer (mUC). However, durable benefit is only achieved in a small, yet uncharacterized patient subset.

NECTIN4 is located on chromosome 1q23.3, and 1q23.3 gains represent frequent copy number variations (CNVs) in UC.

Here, we aimed to evaluate NECTIN4 amplifications as a genomic biomarker to predict EV response in mUC patients.

## Methods

We established a NECTIN4-specific fluorescence in-situ hybridization (FISH) assay to assess the predictive value of NECTIN4 CNVs in a multicenter EV-treated mUC patient cohort (mUC-EV, n=108). CNV were correlated with membranous NECTIN4 protein expression, EV treatment responses and outcomes. We also assessed the prognostic value of NECTIN4 CNVs measured in metastatic biopsies of non-EV treated mUC (mUC-non-EV, n=103). Further, we queried the The Cancer Genome Atlas (TCGA) datasets (10,712 patients across 32 cancer types) for NECTIN4 CNVs.

## Results

NECTIN4 amplifications are frequent genomic events in muscle-invasive bladder cancer (TCGA-BLCA: ~17%) and mUC (~26% in our mUC cohorts). In mUCEV, NECTIN4 amplification represents a stable genomic alteration during metastatic progression and associates with enhanced membranous NECTIN4 protein expression. 96% (27/28) of patients with NECTIN4 amplifications demonstrated objective responses to EV compared to 32% (24/74) in the non-amplified subgroup ( $P < 0.001$ ). In multivariable Cox analysis adjusted for age, sex and Bellmunt risk factors, NECTIN4 amplifications led to a 92% risk reduction for death (HR=0.08, 95%-CI 0.02–0.34;  $P < 0.001$ ). In the mUC-non-EV NECTIN4 amplifications were not associated with outcomes. The TCGA Pan-Cancer analysis demonstrated that NECTIN4 amplifications occur frequently in other cancers, e.g. in 5-10% of breast and lung cancers.

## Conclusion

NECTIN4 amplifications are genomic predictors of EV responses and long-term survival in mUC patients.

DGP07.05

## ***Proteomic Profiling of IDH-wildtype Glioblastoma Tissue reveals prognostic Subtypes with matching Proteomic Patterns in Serum***

T. Werner<sup>1,2,3</sup>, A. Schäfer<sup>4</sup>, M. Hennes<sup>1</sup>, M. Cosenza Contreras<sup>1</sup>, G. Espadas<sup>5</sup>, E. Sabido<sup>5</sup>, L. Cook<sup>4</sup>, A. Pagenstecher<sup>6</sup>, N. Pinter<sup>1</sup>, T. Feilen<sup>1</sup>, A. Grote<sup>4</sup>, C. Nimsky<sup>4</sup>, J. W. Bartsch<sup>4</sup>, O. Schilling<sup>1,7</sup>

<sup>1</sup>Institute for Surgical Pathology, University Medical Center Freiburg, Freiburg, Germany, <sup>2</sup>Faculty of Biology, University of Freiburg, Freiburg, Germany, <sup>3</sup>Spemann Graduate School of Biology and Medicine, University of Freiburg, Freiburg, Germany, <sup>4</sup>Department of Neurosurgery, Philipps University Marburg, Marburg, Germany, <sup>5</sup>Centre for Genomic Regulation (CRG), The Barcelona Institute for Science and Technology, Universitat Pompeu Fabra, Proteomics Unit, Barcelona, Spain, <sup>6</sup>Department of Neuropathology, Philipps University Marburg, Marburg, Germany, <sup>7</sup>German Cancer Consortium (DKTK) and German Cancer Research Center (DKFZ), Heidelberg, Germany

## Background

Glioblastoma multiforme (GBM) is the most prevalent primary brain cancer with a dismal 5-year survival rate below 10%. Despite multimodal first-line treatment through surgery and radiochemotherapy, nine out of ten patients will develop recurrences. Major challenges for GBM therapy are a lack of targeted treatment options and missing diagnostic markers for recurrent tumors.

## Methods

In this study, we present a GBM cohort including tissue and serum from 55 primary tumors and five matching recurrences. Utilizing mass-spectrometry based proteomics in data-independent acquisition mode, we detected 6300 proteins on average per sample.

## Results

Primary tumors were classified into four distinct subgroups through hierarchical clustering, which did not correspond to *EGFR* variant VIII expression, p53 accumulation, *ATRX* mutation or Ki67 levels. They included a neuronal cluster characterized by heightened mature neuron markers, an innate immunity cluster displaying increased protease expression, a mixed cluster, and a stem-cell cluster. Key influencers in clustering were identified as neurodevelopmental and inflammatory processes, with proteolytic activity escalating in tandem with inflammation levels. This pattern was confirmed and expanded in an analysis involving proteins with lower coverage. Patients in the neuronal cluster exhibited significantly prolonged survival compared to the stem-cell cluster.

In a patient-matched differential expression analysis, five recurrent tumors demonstrated significant alterations in protein

expression compared to their primary counterparts, underscoring the proteomic plasticity of recurrent tumors. Examining serum proteomes before and after surgery, using a depletion-based protocol, revealed patient-specific and stable proteome compositions despite a noticeable increase in inflammation markers post-surgery. This finding was consistent with an independent control cohort of serum from patients undergoing surgery for Meningioma (MNG). We identified several proteins that decreased in GBM serum after both initial and recurrent surgery, some of which remained unchanged in MNG serum. Furthermore, levels of circulating proteolytic products correlated with the proteolytic activity in the tissue, and one fragment of proteolysis-activated receptor 2 (PAR2) consistently decreased in abundance after the removal of inflamed tumors.

### **Conclusion**

We identified distinct tumor subgroups in a large GBM cohort, which may enable recurrence risk prediction and personalized therapies.

## **Molecular Pathology 2 - Technologien**

DGP08.01

### ***DNA basierte Techniken in der molekularpathologischen Diagnostik - State of the Art und Ausblick***

S. Merkelbach-Bruse

Universitätsklinikum Köln, Institut für Pathologie, Institut für Pathologie, Köln, Germany

Molekularbiologische Untersuchungsmethoden ermöglichen es, genetische Veränderungen in den Zellen zu identifizieren, die Krankheiten verursachen oder beeinflussen können. In meinem Vortrag möchte ich einen Überblick geben über die Anwendungen, Methoden, Vorteile und Herausforderungen der DNA-basierten molekularpathologischen Diagnostik.

Durch die Implementierung personalisierter Therapieoptionen hat der Einsatz von DNA-basierten Techniken in der Pathologie signifikant zugenommen. Hierbei wird nach genetischen Aberrationen gesucht, die für die Entstehung, die Progression und das Ansprechen auf Therapien bei verschiedenen Erkrankungen verantwortlich sind. Neben diesen onkologischen Fragestellungen wird aber auch ein breites Spektrum an Erregernachweisen in der molekularpathologischen Diagnostik abgedeckt.

Zu den Schlüsseltechniken der DNA-basierten Molekularpathologie gehören die Polymerase-Kettenreaktion (PCR), Sequenzierung (einschließlich Next-Generation-Sequencing, NGS) und Hybridisierung. Diese Technologien ermöglichen es, genetische Variationen wie Punktmutationen, Deletionen, Amplifikationen und Translokationen, aber auch fremdes Erbmateriale zu identifizieren. NGS von der Panel- bis hin zur Exomsequenzierung hat sich in den letzten Jahren als Technologie in der Fläche durchgesetzt, da es die gleichzeitige Untersuchung mehrerer Gene und die parallele Analyse vieler Patientenproben ermöglicht, was eine umfassende genetische Profilierung von Erkrankungen in einem einzigen Durchlauf erlaubt.

Eine der größten Herausforderungen wird zukünftig die immer umfassendere Analytik sein, die sich neben den Untersuchungen auf DNA-Ebene auch auf RNA- und Proteinanalytik erstrecken wird. Hierbei spielen insbesondere die Materialverfügbarkeit, Kosten und Dauer der Analysen eine Rolle. Die Eignung neuer Sequenziertechnologien wie der *long-read*-Sequenzierung für formalinfixiertes Ausgangsmaterial ist zur Zeit Gegenstand verschiedener Studien. Außerdem wird die Datenauswertung und – bereitstellung zunehmend anspruchsvoller und damit zeitintensiver, so dass auch der Bedarf nach speziell geschultem Personal steigen wird.

Durch fortlaufende Verbesserungen der Technologie und die Integration von künstlicher Intelligenz und maschinellem Lernen in der Datenanalyse kann die Molekularpathologische Diagnostik verbessert und weiter gefördert werden. Die Entwicklung kosteneffizienterer Methoden ist erforderlich, um die Verfügbarkeit dieser Technologien zu erweitern.

DGP08.02

### ***RNA-based techniques for precision medicine***

N. Pfarr

Technische Universität München, Institut für Pathologie, München, Germany

Currently the most common approach for therapy decisions is the analysis of the mutation status of cancer patients



alone. Nevertheless, a large set of patients do not receive a molecular diagnosis or a treatment recommendation. In addition to the DNA-based approach, RNA-based measurements can also be utilized for disease diagnosis, prognosis and treatment decision in cancer patients. Applying RNA sequencing (RNAseq) techniques allows the analysis of a wide area of RNA species, like mRNA, non-coding RNA, pathogen RNA, gene fusions transcripts, transcript isoforms and splice variants. Furthermore, gene expression analysis by quantification of known, pre-defined RNA species and analysis of rare RNA transcript variants within a sample, can be performed. In addition, genomic analysis on DNA level often reveals a high fraction of variants of unknown significance, therefore, implementing RNA sequencing (RNA-seq) as additional tool in the diagnostic approach might be helpful to complement genomic data with functional evidence. The implementation of RNA-based techniques in the field of precision medicine enables not only the prediction of gene fusions but also further therapeutically relevant insights into the functional impact of genomic alterations on the expression of the genes under investigation.

DGP08.04

### ***Pilot study for diagnostic whole-genome sequencing from routine formalin-fixed, paraffin-embedded specimens (FFPE) using Ultrashear and DNA repair.***

M. Hamdorf, P. Basitta, F. Hölscher, A.-L. Wulf, N. Pelusi, G. Kristansen, H. Schorle, V. Tischler  
Institut für Pathologie, Universitätsklinikum Bonn, Molekulare Pathologie, Bonn, Germany

#### **Background**

Formalin-fixed and paraffin-embedded (FFPE) samples represent the gold standard of pathology samples. This tissue source is a challenging candidate for whole-genome sequencing (WGS) of cancer patient samples due to the pretreatment of the tissue instead of using Fresh-frozen (FF) tissue as an optimal source for DNA. We performed and analyzed the suitability of FFPE tissues combined with DNA repair as a source of DNA for clinical WGS.

#### **Methods**

Following routine diagnostic protocols, we conducted a study using DNAs from matched healthy and tumor tissue from 12 cancer patients (24 samples). We performed the NEBNext Ultrashear FFPE DNA Library Prep Kit (NEB), which includes DNA repair and fragmentation of the DNA isolated from FFPE samples. The sequencing data was analysed applying our in-house bioinformatics pipeline. We compared somatic variants detected in FFPE-WGS, the coverage of the complete genome, and compared it to matching whole-exome and panel-NGS results performed from the same patients.

#### **Results**

Our results show a breadth of coverage of approximately 91 % (normal tissue) and 93 % (tumor tissue) with a read depth of 7.5-7.9x (normal tissue) and 25-47x (tumor tissue) at the genome level. The sequences showed no abnormal enrichment of FFPE-induced mutations and sequencing artifacts due to the efficient DNA repair step in the protocol. The comparison with targeted comprehensive next generation sequencing panels showed similar results with comparable variant allele fractions. The additional SNPs and genome modifications are currently under investigation. They will even display a broader range of regulatory mechanisms that work together to trigger tumor growth and survival.

#### **Conclusion**

WGS can be a great alternative to extensive panel-NGS sequencing. It allows enrichment analysis of promotor and regulatory regions, loss of miRNA binding sites, and mutations in the genes itself to understand the complete tumor pathway and its escape mechanisms to drugs.

DGP08.05

### ***Integrated Genomic and Epigenetic Analysis of Matched Primary and Metastatic Highly Malignant Osteosarcoma***

F. S. Karras, C. Schmidt, S. Franke, D. Jechorek, A. Roessner  
Otto-von-Guericke University Magdeburg, Institute of Pathology, Magdeburg, Germany

#### **Background**

The most prevalent osteosarcoma (OS) type is the highly malignant intramedullary OS, which has a high metastatic

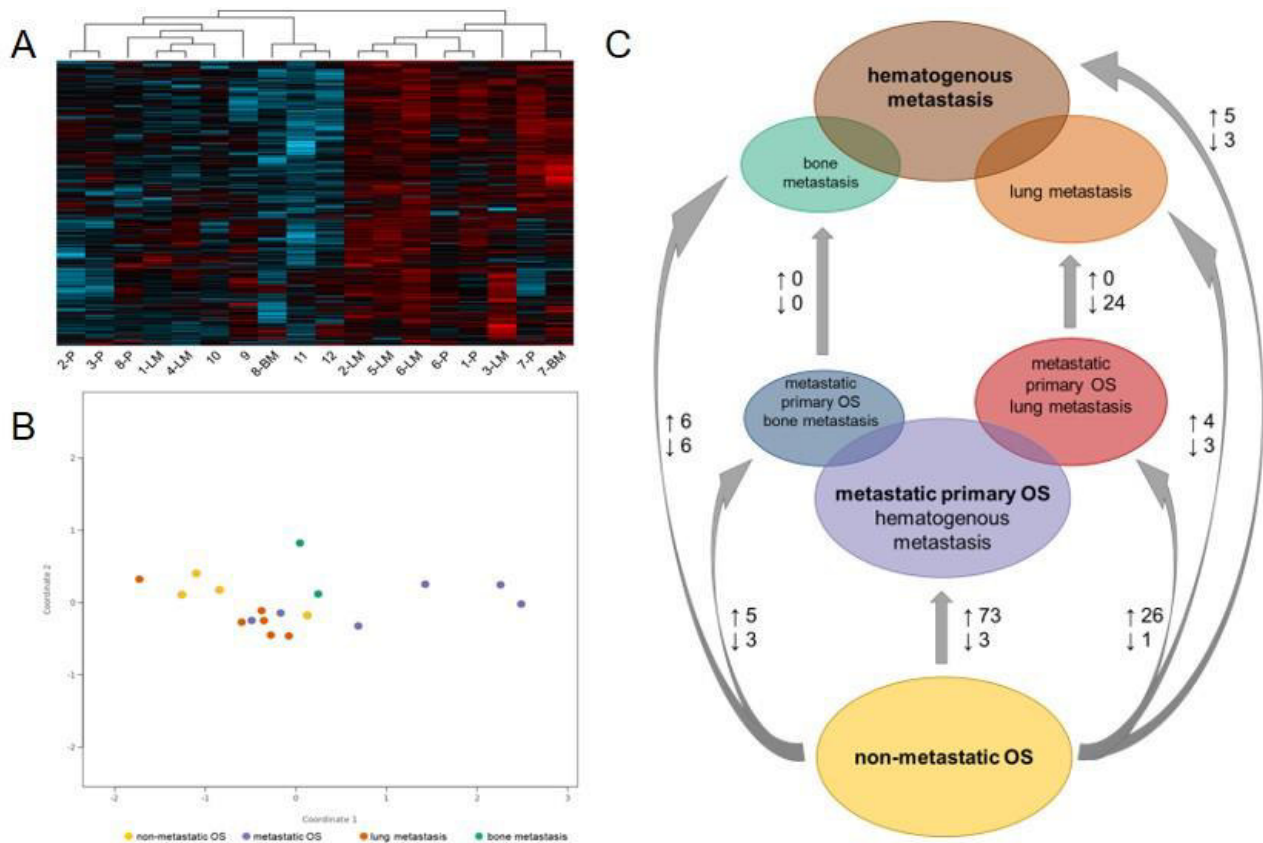
potential, whereby the lung is the main localization of metastases. In contrast to non-metastatic OS the prognosis of metastatic OS is poor with a 5-year survival rate of ~ 20 %. To improve the prognosis, a better knowledge of the OS biology is necessary. Besides genetic events, alterations in epigenetic control could play a role in OS metastasis. Therefore, we analyzed miRNA expression in paired samples of metastatic OS in comparison to non-metastatic OS. Additionally, we analyzed the mutational profile by whole exome sequencing (WES).

## Methods

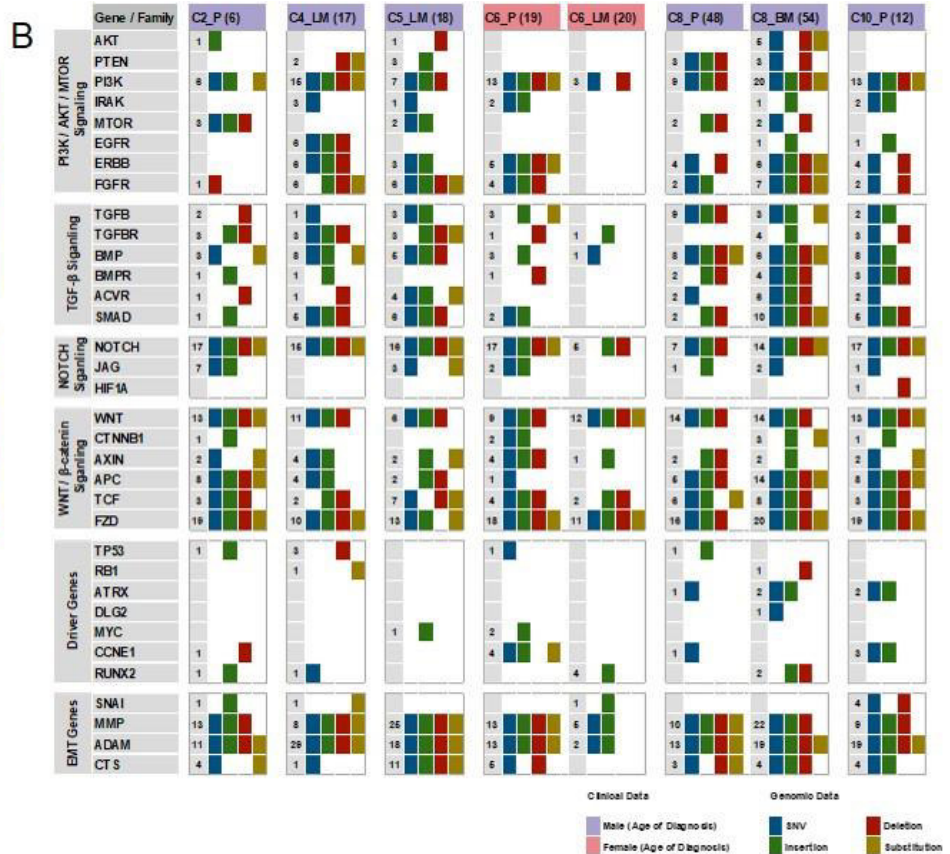
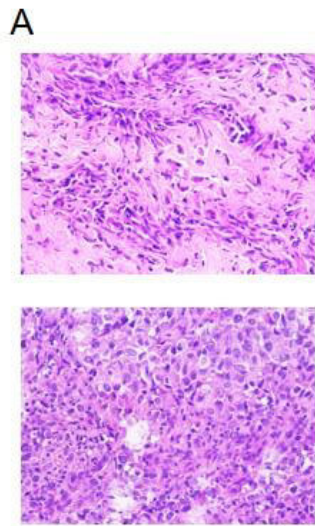
We investigated eight cases of metastatic OS and six cases of non-metastatic OS using FFPE tissue samples. Histologically all cases were conventional highly malignant OS (Fig. 2A). MiRNA expression was analyzed using the nCounter® MAX analysis system. The mutational profile of the DNA was analyzed by WES. To validate our findings, we performed immunohistochemical staining of different markers.

## Results

Unsupervised clustering analysis of miRNA expression revealed no distinct pattern between primary tumors and metastases (Fig. 1A,B). However, differential miRNA expression analysis revealed ten miRNAs, which were significantly upregulated in the primary tumors of lung metastases cases (Fig. 1C). However, the same ten miRNAs were significantly downregulated in the lung metastases, suggesting a possible role of these ten miRNAs in the metastasis process. Additionally, we identified mutations in the same pathways by WES, like TGF- $\beta$  and TP53 signaling (Fig. 2B).



MiRNA expression analysis. A) Unsupervised clustering analysis, B) multidimensional scaling plot and C) scheme of comparisons and significantly deregulated miRNAs.



A) Primary tumor (upper) and lung metastasis (lower) of case 6 showing high density of viable tumor cells (H&E, 400x)  
 B) Genomic alterations (P: primary, LM: lung metastasis, BM: bone metastasis)

### Conclusion

To our knowledge, we are the first analyzing paired samples of metastatic OS and non-metastatic OS, combining the analysis of miRNA expression and the mutational profile. We identified ten significantly deregulated miRNAs in the process of OS metastasis into the lung. Possibly, some of these miRNAs could lead to new target therapies for improving the prognosis of OS patients with disseminated tumors.

## Animal Models in Human Research 1

DGP09.01

### *The benefits of comparative genomics in understanding bladder cancer*

L. van der Weyden

Wellcome Sanger Institute, Experimental Cancer Genetics, Cambridge, United Kingdom

#### Background

Muscle-invasive bladder cancer (MIBC) in humans is highly aggressive and typically associated with poor prognosis. Whole-exome sequencing of human MIBC has revealed a high mutational rate, over 50 significantly mutated genes and numerous copy number alterations. Thus, strategies are needed to delineate key driver events. While both chemical carcinogen-induced and genetically engineered mouse models of MIBC share some histological and molecular similarities to human MIBC, spontaneously occurring urinary bladder UC in pet dogs and cats may offer distinct advantages as models of MIBC. In addition, cattle that graze on bracken fern (*Pteridium aquilinum*) can develop UC as a result of exposure to the carcinogen ptaquiloside, and thus may represent a relevant model of carcinogen-induced human MIBC.

#### Results

Whole-exome sequencing of domestic canine and feline UC, and comparative analysis with human MIBC revealed a lower mutational rate in animal cases and the absence of APOBEC mutational signatures. However, there was a convergence of driver genes (*TP53*, *FAT1*, *NRAS*, *ARID1A*, and *KDM6A*), along with common focally amplified and

deleted genes involved in regulation of chromatin remodelling and the cell cycle. In addition, mismatch repair deficiency was identified in a subset of canine and feline UCs, with biallelic inactivation of *MSH2*. Bovine UC showed a high mutational rate, and allowed identification of novel mutational signatures that were able to be recapitulated *in vitro* by exposure of a human urinary bladder UC cell line to bracken fern extracts or purified ptaquiloside.

## Conclusion

Cross-species comparative genomics can play an important role in understanding both human and animal UC.

## DGP09.03

### ***From bearded dragons to horses: Special features of selected spontaneous skin tumors in various animal species (Von Bartagame bis Pferd: Besonderheiten ausgewählter spontaner Hauttumore bei verschiedenen Tierarten)***

H. Aupperle-Lellbach<sup>1,2</sup>, K. O. Heckers<sup>1,3</sup>, J. Dietz<sup>1</sup>, U. Schwittlick<sup>1</sup>, I. Hoffmann<sup>1</sup>, C. Schandelmaier<sup>1</sup>, K. Jäger<sup>1</sup>, K. Steiger<sup>2</sup>, G. Loesenbeck<sup>1</sup>

<sup>1</sup>LABOKLIN GmbH & Co. KG, Pathologie, Bad Kissingen, Germany, <sup>2</sup>Institut für Pathologie, Technische Universität München, Comparative Experimental Pathology (CEP), München, Germany, <sup>3</sup>Tierarztpraxis Dr. K. Heckers, Kiel, Germany

Comparative oncology of spontaneous tumors in domestic and wild animals must consider differences in location, histology, prognosis, and treatment.

**Mast cell tumors (MCT)** are among the most common canine skin tumors but rare in other animal species. In dogs, mutation of exon 11 is of prognostic (worse) and therapeutic relevance (TK-inhibitors). Mutations in feline cutaneous MCT are found in exons 8+9 but are without prognostic or therapeutic relevance.

**Chromatophoromas** (melano-, irido-, erythro-, and xanthophoromas) are common pigment cell-derived neoplasms in various reptile species. Melanomas are rare in birds but common in rabbits. Canine oral and feline iridociliary melanomas are mostly aggressive. BRAF mutation is rare in canine melanomas, but RAS mutations are common in canine digital melanomas. Equine greys have a predisposition to multicentric melanomas.

**Soft tissue sarcomas (STS)** mainly occur on the limbs of dogs and are usually low-grade malignancies. Molecular genetic signatures of canine STS are still being studied. Feline fibrosarcomas may occur spontaneously or can be associated with injection/vaccination sites or viral infection (FeSV). Liposarcomas are common in guinea pigs. In contrast to dogs, STS are mostly locally aggressive and often metastasizing in snakes.

**Squamous cell carcinomas (SCC)** mainly occur in the oral/nasal region or at the ears of cats, African pygmy hedgehogs, and some avian species. In horses, SCC usually affects the eye or vulva/prepuce/penis. Especially in black-coated dogs, the toe is frequently affected by SCC. In black giant schnauzers, a genetic predisposition is associated with copy number variation of *KITLG*. SCC often appears in the preen gland of birds. Avipox virus infections can be a causative factor.

**Mammary tumors (MT)** in humans, rabbits, and cats are predominantly of epithelial origin, while complex and mixed MT are peculiarities in dogs. Hormone receptor expression and molecular genetic analyses play a minor role in the prognosis and therapy of canine and feline MT. The most common MT in rats is fibroadenoma, which can reach a considerable size.

**Conclusion:** There are impressive differences in the occurrence, histo-, and genotype of spontaneous skin tumors between the animal species. Transferring knowledge from one species to another seems tempting. However, comprehensive expert evaluation of the cases is crucial to avoid misleading conclusions in routine diagnostics and scientific settings.

## DGP09.04

### ***Comparative Study of Feline and Human Intestinal Carcinomas***

T. Groll<sup>1,2</sup>, C. Beutler<sup>1,2</sup>, U. Schwittlick<sup>3</sup>, N. Pfarr<sup>1</sup>, C. Mogler<sup>1,2</sup>, M. Jesinghaus<sup>4</sup>, H. Aupperle-Lellbach<sup>1,2,3</sup>, K. Steiger<sup>1,2</sup>

<sup>1</sup>Institute of Pathology, School of Medicine and Health, Technical University of Munich, Munich, Germany, <sup>2</sup>Institute of Pathology, School of Medicine and Health, Technical University of Munich, Comparative Experimental Pathology (CEP), Munich, Germany, <sup>3</sup>LABOKLIN GmbH & Co. KG, Bad Kissingen, Germany, <sup>4</sup>Institute of Pathology, University Hospital Marburg, Marburg, Germany

## Background

Comparative pathology aims at comparing and deciphering differences and similarities across species. Spontaneously

arising feline intestinal carcinomas show aggressive dissociative growth patterns and prognosis is bad. Small intestinal tumors occur as frequently as large intestinal carcinomas in cats. Our aim is to compare feline intestinal carcinomas with human colorectal carcinomas (CRC) in order to emphasize limitations and parallels, revealing possible future perspectives.

## Methods

A cohort of 88 feline intestinal carcinomas was evaluated histomorphologically (H.E.) regarding WHO-subtype, tumor budding (TB), and invasive features, e.g., metastasis. Furthermore, a tissue-micro array (TMA) of selected feline intestinal carcinomas was immunohistochemically evaluated regarding epithelial-mesenchymal transition (EMT, e.g., SLUG, TWIST), and microsatellite instability (MSI, i.e., MLH1, MSH2, MSH6, and PMS2). In 11 cases, the relevance of feline *CTNNB1* exon 2 ( $\beta$ -Catenin) was investigated by Sanger sequencing.

## Results

Feline intestinal carcinomas resembled human WHO-subtypes remarkably well. Based on the human WHO classification, feline subtypes included adenocarcinoma not otherwise specified (ANOS), serrated adenocarcinoma (SAC), mucinous adenocarcinoma (MAC), micropapillary adenocarcinoma (MPC), and signet ring cell carcinoma (SRCC). In general, feline intestinal carcinomas displayed a very aggressive phenotype and a strong tendency to EMT. Tumor budding was mostly high (Bd 3). Somatic missense mutations of feline *CTNNB1* were detected in 4 cases of feline colon tumors.

## Conclusion

Feline intestinal carcinomas morphologically mimic human late-stage CRC; however, prevalence of specific subtypes is different, and molecular and prognostic data is still lacking. We found that activated WNT-signaling seems to play a role for tumorigenesis in feline intestinal cancer, comparable to human CRC.

DGP09.05

## ***Comparative digital estrogen receptor alpha (ER $\alpha$ ) expression analysis in benign and malignant prostate tissue of men and dogs***

L. Aeschlimann<sup>1</sup>, J. Lothion-Roy<sup>2</sup>, N. Mongan<sup>2</sup>, L. Hiller<sup>1</sup>, S. Rottenberg<sup>1</sup>, S. de Brot<sup>1,2</sup>

<sup>1</sup>Institute of Animal Pathology, Vetsuisse Faculty, University of Bern, Bern, Switzerland, <sup>2</sup>Faculty of Medicine and Health Sciences, School of Veterinary Medicine and Science, University of Nottingham, Sutton Bonington, United Kingdom

## Background

The dog is the only animal that regularly and spontaneously develops prostate diseases, e.g. benign hyperplasia (BPH) and carcinoma (PCa), and is therefore considered a valuable model for comparative studies. Estrogens are important for normal prostate development and also play a role in prostatic carcinogenesis in men. Knowledge on ER $\alpha$  expression in benign and malignant canine prostate is limited, and it is unclear whether the expression between dogs and men is comparable at all. This study aimed to analyse and compare the level and spatial distribution of ER $\alpha$  expression in benign and malignant prostatic tissue of men (normal, hyperplasia, carcinoma) and dog [normal, hyperplasia, castration atrophy, premature, glandular carcinoma, urothelial carcinoma (UC)] by immunohistochemistry (IHC).

## Methods

A tissue microarray (TMA) containing formalin-fixed paraffin embedded (FFPE) prostatic tissue cores of men (n=160), and whole tissue sections of canine prostates (n=82) were included. IHC for ER $\alpha$  was performed using a monoclonal anti-human ER $\alpha$  antibody. Slides were scanned and digitally assessed for nuclear staining using a commercial software (Visiopharm, Horsholm, Denmark) for a fully quantitative and spatial deep-learning based digital analysis of ER $\alpha$  expression.

## Results

ER $\alpha$  expression was present in the stroma of benign and malignant tissues in both dog and men. Benign canine glandular epithelium in non-castrated dogs revealed very weak but consistent immunolabeling. In contrast, benign glandular tissue in men was invariably negative for ER $\alpha$ . Human and canine PCa epithelium remained unstained. The same was true for canine atrophic prostates and for premature prostates from puppies. In the latter, strong stromal

staining was seen, indicative of increased ER $\alpha$  expression compared to mature glands. Benign and malignant prostate urothelium of dogs was moderately to strongly ER $\alpha$  positive with regional heterogeneity.

### **Conclusion**

In both the human and canine prostate, ER $\alpha$  is expressed in the stroma of the benign and malignant gland, with highest levels in the premature canine gland. This confirms that estrogens are key for the prostate development. In both species, ER $\alpha$  expression is absent in malignant glandular epithelium. Given the lack of ER $\alpha$  in the premature as well as castration atrophic canine prostate, these tissue stages share the expression profile of cancer and might be relevant to study prostate oncogenesis of men and dogs.

## **Biobanking 2: Wichtige Themen im Biobanking**

DGP10.01

### ***Quality assured biobanking according to DIN EN ISO 20387 - curse or blessing?***

C. Kaufhold-Wedel<sup>1</sup>, P. Schirmacher<sup>2</sup>, A. Brobeil<sup>1,2</sup>

<sup>1</sup>Universitätsklinikum Heidelberg, Gewebekbank des NCT, Heidelberg, Germany, <sup>2</sup>Universitätsklinikum Heidelberg, Pathologisches Institut, Heidelberg, Germany

Gewebebiobanken sind wichtige Ressourcen- und Technologieplattformen der biomedizinischen Forschung, welche sich mit molekularer Pathogenese sowie Prävention, Diagnose und Behandlung von Krankheiten befassen.

Aufgrund ihrer zentralen Rolle bei der standardisierten Entnahme, Lagerung und Verteilung von menschlichem Gewebe und dessen Derivaten ist ein gelebtes Qualitätsmanagement eines der wichtigsten Maßnahmen, um eine umfassende Qualitätssicherung aller Biobankingprozesse zu erreichen und aufrechtzuerhalten. Dies fördert gleichzeitig Akzeptanz und Glaubwürdigkeit. Eine externe Qualitätssicherung von Biobanken kann durch eine Akkreditierung nach der Biobankennorm DIN EN ISO 20387 erreicht werden.

Die Gewebekbank des NCT wurde 2023 als erste deutsche Biobank nach DIN EN ISO 20387 akkreditiert. Wir präsentieren hier zum einen die Herausforderung und Chancen bei der Implementierung einer umfassenden Qualitätssicherung im Biobanking und zum anderen eine kritische Beleuchtung der Anwendung der Norm im alltäglichen Umgang mit biologischem Material und dem Nutzen für die Forschenden.

DGP10.02

### ***Hybrid financing of biobanking structures - focus on tissue biobanking***

K. Steiger<sup>1,2</sup>, C. Mogler<sup>3</sup>

<sup>1</sup>Institut für Pathologie, Technische Universität München, München, Germany, <sup>2</sup>BioTUM - Gewebe, TU München und Klinikum rechts der Isar, München, Germany, <sup>3</sup>Institut für Pathologie, Technische Universität München, München, Germany

Qualitätsgesichertes und strukturiertes Biobanking ist ein wesentlicher Baustein der translationalen Forschung in Deutschland, Europa und weltweit. Dabei decken Biobanken gemeinsam mit ihren lokalen Kooperationspartnern in der Regel die drei Säulen der Flüssig- und Gewebematerialsammlung sowie der Integration der Bioprobendaten ab.

Um eine akademische Biobank kontinuierlich betreiben zu können bietet sich eine hybride Finanzierungsstruktur an, welche neben einer Grundfinanzierung durch lokale Trägerinstitutionen auch aus drittmittelbasierten Projektförderungen und einer anteiligen fee-for-service Finanzierung bestehen. Bei der Ermittlung der notwendigen Grundfinanzierung sollte unbedingt ein wesentlicher Augenmerk auf die Sicherstellung der personellen Kontinuität der etablierten Biobankstrukturen gelegt werden, so dass diese unabhängig von Projektförderungen abgesichert ist.

Basierend auf einer Vollkostenrechnung für den Betrieb der Biobank, die den tatsächlichen Aufwand auf Personal-, Sachmittel-, Infrastruktur- und (Re-) investitionsebene berücksichtigt, können Kostenkataloge ermittelt und an die Nutzer transparent kommuniziert werden.

Für den Bereich des Gewebebiobankings sollte insbesondere bei subventionierten fee-for-service Kostenermittlungen bei prospektiv ungerichteten Sammlungen basierend auf einer broad consent Regelung die Rolle der einspeisenden Kliniken gesondert berücksichtigt werden.

Detaillierte Informationen zu hybriden Finanzierungsmodellen für Biobanken in Deutschland hat die Arbeitsgruppe Starterkit der German Biobanking Association erarbeitet.

## DGP10.03

### ***Integrated biobanking - A key role for the quality of biosamples***

A. Langer<sup>1,2</sup>, R. Claus<sup>3</sup>, S. Dintner<sup>2</sup>, B. Märkl<sup>2</sup>

<sup>1</sup>Medizinische Fakultät, Universität Augsburg, Augsburg Central BioBank, Augsburg, Germany, <sup>2</sup>Medizinische Fakultät, Universität Augsburg, Pathologie, Augsburg, Germany, <sup>3</sup>Medizinische Fakultät, Universität Augsburg, Hämatologie und Onkologie, Augsburg, Germany

Die Qualität von Bioproben ist von entscheidender Bedeutung für die Validität und Reproduzierbarkeit wissenschaftlicher Studien. Biobanken haben etablierte Prozesse und BoA\_Image\_Frames für die Verarbeitung verschiedener Arten von Bioproben, um Qualitätsschwankungen vorzubeugen. Allerdings haben eine Vielzahl an Parametern schon vor Ankunft in der Biobank maßgeblichen Einfluss auf die Proben.

Anhand von Beispielen soll verdeutlicht werden, wie gutes, integriertes Biobanking gelingen kann:

- 1) Die Augsburg Central BioBank beinhaltet ein Kollektiv mononukleärer Zellen von Patienten mit hämatologischen Neoplasien. Die langfristige Aufbewahrung dieser Proben ermöglicht es, in retrospektiven Studien potentiell wertvolle Erkenntnisse über Krankheitsverläufe und Behandlungsergebnisse zu gewinnen. Für die aufwendige Isolierung viabler, mononukleärer Zellen ist hier ein optimiertes Schnittstellenmanagement von besonderer Bedeutung.
- 2) Die Augsburger Longitudinale Plasmastudie (ALPS) führt bei Patienten mit metastasiertem Tumorleiden in bestimmten Abständen Liquid Biopsies durch. Die Plasmaproben werden hierfür in der Augsburg Central BioBank verarbeitet und gelagert. Für die Sequenzierung der zirkulierenden Tumor-DNA spielt dabei die Präanalytik eine essenzielle Rolle.

Biobanken leisten einen wichtigen Beitrag für die personalisierte Medizin durch die Bereitstellung geeigneter Bioproben und dazugehöriger Daten. Dies kann nur gelingen, wenn eine Bioprobe auch außerhalb des Wirkspektrums der Biobank - über den gesamten Lebenszyklus - nach gewissen BoA\_Image\_Frames bearbeitet wird und notwendige Informationen strukturiert zur Verfügung gestellt werden. Dabei ist eine effektive Zusammenarbeit zwischen Einsendern und Biobanken unerlässlich, um geeignete, hochwertige Proben zu erhalten.

## DGP10.04

### ***Multimodal evaluation of an organotypic slice culture platform for cell renal cell carcinoma***

M. Zirngibl<sup>1</sup>, A. Nägel<sup>2</sup>, G. Andreev<sup>2</sup>, M. Werner<sup>2</sup>, M. Grabbert<sup>1</sup>, M. Rogg<sup>2</sup>, C. Schell<sup>2</sup>

<sup>1</sup>Klinik für Urologie, Universitätsklinikum Freiburg, Freiburg, Germany, <sup>2</sup>Institut für Klinische Pathologie, Freiburg, Germany

#### **Background**

Clear cell renal cell carcinoma (ccRCC) is the most common subtype of kidney cancer. Although patients with early stage ccRCC have a rather good prognosis, progressive disease is associated with significantly worse outcome. Tyrosine kinase inhibitors (TKI) and immune checkpoint inhibitors (ICI) are the mainstay in the treatment of metastatic disease. However, interindividual heterogeneity in treatment response is a limiting factor. To date only a small number of studies have employed organotypic slice culture (OSC) approaches in the context of ccRCC. Here, we comprehensively characterized OSCs of ccRCC specimens and evaluated potential readout strategies to assess treatment effects.

#### **Methods**

ccRCC specimens were derived from cancer nephrectomies and organotypic slice cultures (OSC) were established employing air-liquid interface cultivation (n=20). Combination of inhibitors and compounds were applied in varying dosing schemes. Readouts included histology, immunohistochemistry, multiplex-immunofluorescence as well as RNA-sequencing.

#### **Results**

Thorough evaluation of ccRCC OSCs revealed a stable cultivation time up to 5 days ex vivo. Tumor cell as well as immune cell numbers remained at a stable level throughout this observational period (d0-d5). On the contrary, endothelial cells showed very early signs of single cell necrosis. Transcriptomic characterization of OSCs at different time points highlighted mainly cell-cycle associated gene signatures indicative of adaptive signaling during increasing

cultivation time. Cell type identification and quantification demonstrated significant inter- and intra-patient heterogeneity in terms of immune cell infiltration. Application of tyrosine kinase inhibitors (TKI) in combination with immune checkpoint inhibitors (ICI) showed differing immune response patterns in individual patient subsets.

## **Conclusion**

The comprehensive characterization of ccRCC OSCs demonstrated stable maintenance of inherent tumor features of individual patient specimens. Interestingly, also individual immunophenotypes were robust during the observational period and an accessible parameter for intervention experiments. As our treatment studies revealed heterogeneous response patterns, OSCs might serve as a versatile platform to study underlying mechanisms within the tissue context.

DGP10.05

## ***Patient-derived colon tumor organoids fuse and build ring structures in floating collagen I matrix***

D. Wimmers<sup>1</sup>, K. Huebner<sup>1</sup>, T. Dale<sup>2</sup>, A. Papargyriou<sup>3</sup>, M. Reichert<sup>3</sup>, A. Hartmann<sup>4,5</sup>, R. Schneider-Stock<sup>1,5</sup>

<sup>1</sup>University Hospital, Friedrich-Alexander-University Erlangen-Nürnberg, Experimental Tumorpathology, Institute of Pathology, Erlangen, Germany, <sup>2</sup>Cardiff University, European Cancer Stem Cell Research Institute (ECSCRI), Cardiff, United Kingdom, <sup>3</sup>Technical University of Munich, Klinik und Poliklinik für Innere Medizin II, Klinikum rechts der Isar, München, Germany, <sup>4</sup>University Hospital, Friedrich-Alexander-University Erlangen-Nürnberg, Institute of Pathology, Erlangen, Germany, <sup>5</sup>Comprehensive Cancer Center Erlangen-EMN (CCC ER-EMN), Erlangen, Germany

## **Background**

Intestinal organoids comprise the 3D architecture and organ-specific function of the originating tissue. So far, the extracellular matrix (ECM) mainly used for the cultivation of intestinal organoids is Matrigel, a gelatinous protein mixture with poorly defined ingredients. As its main components are collagen type IV and laminin it mimics the basal membrane, making it a suitable matrix to grow organoids of epithelial cells although not reflecting the stroma surrounding colorectal cancer (CRC) cells. Tumors are the results of their microenvironment and when it comes to CRC progression and invasiveness, the ECM and especially collagen plays a significant role. So far only a few efforts have been made to improve the ECM towards a more physiologically relevant matrix for studying organoid invasion.

## **Methods**

We tested the behavior of three exemplary patient derived CRC organoid lines with increasing tumor staging and metastasization when cultivated in a collagen type I matrix that is detached from the plate.

## **Results**

Embedded in a floating collagen (FC) gel organoids contract the matrix, align and fuse to form a macroscopic ring structure. Strikingly not only fusion of organoids to build a macroscopic ring structure appeared but also fusion of floating collagen matrices, when two FC matrices contact each other. Beyond this organoid-organoid and matrix-matrix interaction as well as the beginning of branch formation and invasion fronts with small tumor cell clusters were visible, an observation that has never been made before in CRC organoids cultivated in Matrigel. To better understand the morphological changes on a molecular level we defined four sets of genes (stemcell, differentiation, epithelial and mesenchymal markers) for qPCR analysis. It became clear that the formed macroscopic ring in the FC has a more stem cell like character compared to cultivation in Matrigel. When returned to Matrigel the organoids still showed a significant increase in stem cell markers but yet a clear shift towards differentiation became visible.

## **Conclusion**

Our new cultivation technique of patient derived CRC organoids in a detached collagen matrix can be used as an in-vitro model for cancer organization and matrix remodeling in order to allow CRC organoids utilize their full stemness potential.



# ESP - The European Perspective of Pathology – Where will we be in 2030

DGP12.01

## ***ESP 2030 - The challenges and strategy***

P. Schirmacher

Institute of Pathology, Heidelberg University Hospital, Heidelberg, Germany

European Pathology is facing many challenges. On one side the options for Pathology, such as new technologies (Computational Pathology, novel molecular technologies) are significant and the need for interdisciplinary activities (scientific platforms, interaction with other medical societies, guidelines, health politics) is immense, on the other side obstacles (shortage of resources; lack of skilled personnel, overregulation) threaten to limit the potential of our discipline. The European Society of Pathology is dedicated to actively tackle these upcoming challenges and performs a structured strategy process with the aim to identify the needs and priorities for European Pathology in the upcoming years and thus tailor future ESP activities. The basic principles of the ESP strategy 2030 will be outlined.

DGP12.03

## ***The changing world of further education and training in European Pathology***

C. Poullos

European Society of Pathology, Brussels, Belgium

The progress in Science and Technology is leading to new diagnostic methods, tumour classifications and biomarker testing. In parallel, modern Medicine requires an array of skills that include among others communication, management, inter-specialty teamwork, ethics and others. These lead to an increasing list of competencies that a Pathologist is required to have to effectively practice Medicine and Research.

Unquestionably, the basis of Pathology education is within the Residency Programmes. However, residency curricula cannot cover all required skills, either due to lack of time or lack of high level specialisation in the local community. Here is where international organisations have a role: to effectively supplement the national/local residency and post-residency training programmes.

The European Society of Pathology (ESP), the Leading Force of European Pathology, has established a Strategy for Education that covers all levels of expertise, from the first day in Pathology, up to the level of Expert.

- Updates on the latest developments in Pathology are being taught via the European Congress of Pathology (ECP), ESP webinars and via papers published in the Virchows Archiv.
- Diagnostic skills are honed via the multiple ESP courses.
- Advanced diagnostic training, communication and teamwork skills are being taught via the ESP Fellowship programmes (Giordano Fellowship and EMMP Scholarship) and specialised courses and workshops.
- Medical Leadership training is provided via the ESP Academy and the ESP Alumni Programme.
- Interdisciplinary training and skills for communicating with patients are provided via the collaboration with other Medical Societies and Organisations. An example for this is the EU funded INTERACT programme.

The success of the ESP Education is ensured by the energetic work of the many ESP Key Opinion Leaders and Experts who are from a diverse background covering all aspects of Modern Pathology. They accurately identify any educational needs and then effectively create/support educational programmes to cover them.

DGP12.04

## ***Computational pathology – pitfalls and potential***

A. Polonia

Ipatimup Institute of Molecular Pathology and Immunology of the University of Porto, Pathology, Porto, Portugal

A brief overview of digital pathology and computational pathology will be presented. Examples of computational pathology

tools will be shown along with an exploration of the associated problems that come with its use. In the end, two examples of real applications will be shown that are used on a daily basis in our pathology department.

## Proteomics 1: Proteomics in Personalized Medicine

DGP13.01

### ***(Phospho)Proteomics for Personalized Precision Oncology***

C. Jimenez

OncoProteomics Laboratory, VUmc-Cancer Center Amsterdam, VU University Medical Center, Amsterdam, The Netherlands

To better understand cancer in all its facets and work towards improved diagnostics and treatment, the OncoProteomics Laboratory focusses on the global analysis of the functional building blocks of life, *i.e.*, the proteins which activity and functions are highly deranged in cancer cells. Unbiased (phospho)protein profiling by mass spectrometry-based proteomics offers a means to measure the biochemical impact of cancer-related genomic abnormalities, and thereby can bridge the gap between cancer genome information and observed cancer phenotype. In the oncology context, where personalized treatment requires analysis of single samples, phosphoproteomics coupled to Integrative Inferred Kinase Activity (INKA) analysis has emerged as tool that can prioritize actionable kinases for targeted inhibition (1-4).

In the first part of my talk I will present a multi-laboratory collaborative cancer proteome profiling effort, The Pan-Cancer Proteome Atlas to better understand cancer biology and to identify core and cancer type enriched molecular therapeutic targets and biomarkers. This pan-cancer proteome landscape consists of a filtered dataset of 9663 proteins derived from 999 primary cancers representing 22 cancer types.

In the second part of my talk, I will present our on-going progress in the study of CRC, tALL and PDAC employing phosphoproteomics coupled to INKA analysis for target discovery and pinpointing personalized kinase inhibitor (combination) treatment in cancer.

Beekhof R, Henneman AA, Jimenez CR et al., INKA, an integrative data analysis pipeline for phosphoproteomic inference of active kinases. *Mol Syst Biol.* 2019 May 24;15(5):e8981.

Cordo' V, Jimenez CR, Meijerink JPP et al., Phosphoproteomic profiling of T cell acute lymphoblastic leukemia reveals targetable kinases and combination treatment strategies. *Nat Commun.* 2022 Feb 25;13(1):1048.

Vallés-Martí A, Jiménez CR et al. Phosphoproteomics guides effective low-dose drug combinations against pancreatic ductal adenocarcinoma. *Cell Rep.* 2023 Jun 1;42(6):112581.

Beekhof R, ... Trusolino L, Jimenez CR et al., Phosphoproteomics of patient-derived xenografts identifies targets and markers associated with sensitivity and resistance to EGFR blockade in colorectal cancer. *Sci Transl Med.* 2023 Aug 16;15(709):eabm3687.

DGP13.04

### ***Deep Proteomics and Integrated Multiomics of Primary and Metastatic Colorectal Adenocarcinoma Uncover Novel Proteomic Subtypes and Therapeutic Targets***

M. H. Roehrl

Beth Israel Deaconess Medical Center, Harvard Medical School, Pathology, Boston, United States of America

#### **Background**

Metastatic progression of colorectal adenocarcinoma (CRC) remains poorly understood and poses significant challenges for treatment. Deep multiomic characterization of both primary and metastatic CRC has not been done previously and promises new insights in disease biology, molecular subtypes, and metastatic progression.

#### **Methods**

We performed comprehensive multiomics analyses of primary CRC and liver metastases in a large cohort of over 250 patients using whole genome sequencing, RNA-seq, and deep quantitative proteomics by mass spectrometry.

#### **Results**

Unsupervised mass spectrometry-based proteomics of 135 primary and 123 metastatic CRCs uncovered distinct proteomic subtypes, three each for primary and metastatic CRCs, respectively. Integrated analyses revealed that

hypoxia, stemness, and immune signatures characterize these 6 subtypes. Hypoxic CRC harbors high epithelial-to-mesenchymal transition features and metabolic adaptation. CRC with a stemness signature shows high oncogenic pathway activation and alternative telomere lengthening (ALT) phenotype, especially in metastatic lesions. Tumor microenvironment analysis shows immune evasion via modulation of major histocompatibility complex (MHC) class I/II and antigen processing pathways.

## Conclusion

Distinct proteogenomic subtypes of colorectal cancer characterize primaries and metastases. A hypoxic signature was enriched in metastases along with metabolic reprogramming. A cancer stemness signature with ALT feature was elevated in metastases. Immune-cold cancer showed suppression of antigen presentation, especially in metastases. Our study characterizes both primary and metastatic CRCs at multiomic levels and provides a large and unique proteogenomics dataset for understanding disease subtypes, metastatic progression, and novel therapeutic targets.

DGP13.05

## ***Proteomic Profiling of Malignant Melanoma reveals Expression of Checkpoint Ligand Galectin-9 correlates with Response to Immune Checkpoint Inhibitors.***

F. Fusco<sup>1</sup>, M. Schliemann<sup>2</sup>, J. Weigel<sup>1</sup>, A. Schneider<sup>2</sup>, B. Kuster<sup>2</sup>, P.-H. Kuhn<sup>1,3</sup>

<sup>1</sup>Institut für Pathologie, Technische Universität München, München, Germany, <sup>2</sup>Leerstuhl für Proteomik und Bioanalytik, Technische Universität München, Freising, Germany, <sup>3</sup>Institut für Pathologie Kaufbeuren-Ravensburg, Kaufbeuren, Germany

## Background

In the last decade, Immune Checkpoint Inhibitors (ICI) demonstrated unprecedented efficacy against melanoma with, however, response rates limited to ca. 50%[1]. Concomitantly, accessible biomarkers of response (PDL1, TMB, TILs) have limited predictive value[2] and play therefore a minor role in therapeutic decisions, resulting in a non-selective use of ICIs with great costs in terms of treatment toxicity, missed consideration of alternative therapies, and healthcare economy.

In melanoma, proteomics has been already used to unravel molecular differences associated with mutational status and therapy response[3]. This study aims to further harness the power of mass-spectrometry to better define these differences and identify clinically useful predictors of ICI-response in order to optimize decisional approaches in the expanding context of targets and strategies against melanoma.

## Methods

Formalin-fixed, paraffin-embedded tissue (FFPE) of 155 Melanomas was analyzed using an optimized workflow for data-independent acquisition (DIA) of LC-MS. Proteins were bioinformatically quantified, the resulting protein levels were statistically analyzed and correlated with clinical data.

## Results

Our results, as highlighted by the comparison between pure, therapy-naive responders (R) and non-responders (NR), show a harmonious overlapping of the differentially expressed proteins with the ones described in other "-omics" studies [4], confirming interferon signaling, antigen presentation and TILs as hallmarks of immunogenically hot (R) vs cold (NR) tumors. Galectin9 was the only checkpoint ligand showing a differential expression in the two groups, with consistently high expression in R and low levels exclusively in NR.



efficiency and diagnostic accuracy. Such studies will be required for certification but are still mostly lacking in our field, making it difficult to assess the true potential of deep learning for pathology diagnostics.

DGP13.03

### ***The Use of Spatial Omics in Head & Neck Cancer***

C. Schürch

Universitätsklinikum Tübingen, Institut für Pathologie, Tübingen, Germany

Oral squamous cell carcinoma (OSCC) accounts for over 90% of head & neck cancers and around 2% of all cancers. OSCC has an aggressive nature, with 3-year recurrence rates of up to 30%; approximately 50% of patients die of the disease within 5 years. OSCC remains an understudied disease, and novel biomarkers are urgently needed to prognosticate patients at risk for adverse outcomes, to predict therapy responses, and as targets for novel (immuno-)therapies. The OSCC tumor microenvironment (TME) is typically characterized by marked inflammation and heavy immune cell infiltration, and the tumor cell-immune cell crosstalk plays an important role in tumor dedifferentiation and cancer progression. Single-cell spatial omics technologies have transformed our ability to study complex tumor tissues and are ideally suited to dissect tumor-immune interactions in OSCC. In this presentation, I will give an overview of single-cell spatial omics technologies and analysis techniques and highlight studies by us and others that employed these technologies to investigate the TME in OSCC.

DGP13.04

### ***Automated image analysis of HE-stained slides can partially predict immunohistochemical staining and subtyping of pancreatic ductal adenocarcinoma***

A. Muckenhuber<sup>\*1,2</sup>, M. Fischer<sup>\*3,4,5</sup>, K. Steiger<sup>6</sup>, P. Neher<sup>3,4,7</sup>, C. Ulrich<sup>3,4,8</sup>, S. Xiao<sup>3,9</sup>, S. D. Almeida<sup>3,5</sup>, M. Götz<sup>3,10</sup>, M. Nolden<sup>3,11</sup>, P. Schöffler<sup>12,13</sup>, R. Braren<sup>14</sup>, J. Kleesiek<sup>11,15</sup>, K. Maier-Hein<sup>3,5,9,11,16</sup>

<sup>1</sup>Institute of Pathology, Technical University of Munich, München, Germany, <sup>2</sup>German Cancer Research Consortium (DKTK), partner site Munich, München, Germany, <sup>3</sup>German Cancer Research Center (DKFZ), Division of Medical Image Computing, Heidelberg, Germany, <sup>4</sup>German Cancer Consortium (DKTK), partner site Heidelberg, Heidelberg, Germany, <sup>5</sup>Heidelberg University, Medical Faculty, Heidelberg, Germany, <sup>6</sup>Institut für Pathologie der TU München, Core Facility of Comparative Experimental Pathology, München, Germany, <sup>7</sup>Heidelberg University Hospital, Radiation Oncology, Pattern Analysis and Learning Group, Heidelberg, Germany, <sup>8</sup>National Center for Tumor Disease (NCT), Heidelberg, Germany, <sup>9</sup>Heidelberg University, Faculty of Mathematics and Computer Science, Heidelberg, Germany, <sup>10</sup>Ulm University Medical Centre, Clinic of Diagnostics and Interventional Radiology, Ulm, Germany, <sup>11</sup>Heidelberg University Hospital, Department of Radiation Oncology, Pattern Analysis and Learning Group, Heidelberg, Germany, <sup>12</sup>Technical University Munich, TUM School of Medicine and Health, Institute of Pathology, Munich, Germany, <sup>13</sup>Technical University Munich, TUM School of Computation, Information and Technology, München, Germany, <sup>14</sup>Technical University of Munich, Department of Diagnostic and Interventional Radiology, Faculty of Medicine, Munich, Germany, <sup>15</sup>University Medicine Essen, Institute for AI in Medicine (IKIM), Essen, Germany, <sup>16</sup>National Center for Tumor Diseases (NCT), Heidelberg, Germany

\*Contributed equally

#### **Background**

In our previously published works we have shown that immunohistochemical (IHC) subtyping of pancreatic ductal adenocarcinoma (PDAC) using the cytoskeletal protein KRT81 and the nuclear transcription factor HNF1A yields subgroups of PDAC of prognostic and possibly predictive importance [1, 2]. No clear cut connection between the IHC-derived subtypes and histomorphological characteristics could be observed [1]. This work tries to explore the question if an AI-based computational system might be able to predict the IHC staining results by recognizing morphological differences on HE-stained slides.

#### **Methods**

We have created a deep learning classification algorithm based on a multiple instance learning (MIL) approach using unpaired (consecutive) slides of tissue microarrays of 292 PDAC samples stained with HE, KRT81- and HNF1A-IHC. As ground, the pathologist-derived percentages and intensities of IHC stainings are used. The MIL approach first extracts abstract features from the image from multiple resolutions. A subsequent classifier is then trained to predict the respective PDAC subtype.

## Results

The algorithm trained directly on IHC-stained slides performed best (KRT81 AUC 0.94, HNF1A 0.71) and the algorithm trained on HE-stained slides but with IHC labels performed worst (KRT81 AUC 0.74, HNF1A 0.58) when tested against pathologist-derived staining results. Next, a deep learning approach was used to transfer HE-slides to the IHC domain creating in-silico stained IHC slides to help the algorithm extract the HE-features that are truly relevant. This drastically improved model performance (KRT81 AUC 0.91, HNF1A 0.68). Model-derived heat maps showed good correlation between algorithm-derived areas of interest and carcinoma areas annotated by pathologists.

## Conclusion

Our data shows that combining pathologist derived staining results, HE-stained and IHC-stained slides as input data for MIL-based deep learning algorithms can quite accurately predict certain IHC stainings based on HE-stained slides. Our data also indicates a possible limitation, as the HNF1A-prediction showed a much poorer performance compared to KRT81-prediction. This may reflect the biological reality that expression levels of a cytoskeletal protein lead to more reliable/recognizable changes in histomorphology compared to expression levels of a nuclear transcription factor with all its varied and co-regulated downstream effects.

Literaturangaben:

- [1] Muckenhuber, A., et al., (2018), Pancreatic Ductal Adenocarcinoma Subtyping Using the Biomarkers Hepatocyte Nuclear Factor-1A and Cytokeratin-81 Correlates with Outcome and Treatment Response., *Clin Cancer Res.*, 351-359, 2/24  
[2] Noll, E.M., et al., (2016), CYP3A5 mediates basal and acquired therapy resistance in different subtypes of pancreatic ductal adenocarcinoma., *Nat Med*, 278-287, 3/22

DGP13.05

## **Artificial Intelligence-Enriched Classification of Intrahepatic Cholangiocarcinoma**

T. Albrecht<sup>1</sup>, A. Roßberg<sup>1</sup>, B. K. Straub<sup>2</sup>, T. Gerber<sup>2</sup>, A. Vogel<sup>3</sup>, A. Saborowski<sup>4</sup>, F. Brinkmann<sup>1</sup>, A. Charbel<sup>1</sup>, J. Schreck<sup>1</sup>, B. C. Köhler<sup>5</sup>, A. Mehrabi<sup>6</sup>, S. Singer<sup>7</sup>, O. Neumann<sup>1</sup>, A. Stenzinger<sup>1</sup>, P. Schirmacher<sup>1</sup>, C.-A. Weis<sup>1</sup>, S. Roessler<sup>1</sup>, J. N. Kather<sup>8</sup>, B. Goeppert<sup>1</sup>  
<sup>1</sup>Heidelberg University Hospital, Institute of Pathology, Heidelberg, Germany, <sup>2</sup>Johannes Gutenberg University Medical Center, Institute of Pathology, Mainz, Germany, <sup>3</sup>Toronto General Hospital Medical Oncology, Division of Gastroenterology and Hepatology, Toronto, Canada, <sup>4</sup>Hannover Medical School, Department of Gastroenterology, Hepatology and Endocrinology, Hannover, Germany, <sup>5</sup>Heidelberg University Hospital, National Center for Tumor Diseases, Department of Medical Oncology, Heidelberg, Germany, <sup>6</sup>Heidelberg University Hospital, Department of General, Visceral and Transplantation Surgery, Heidelberg, Germany, <sup>7</sup>Eberhard-Karls University, Institute of Pathology and Neuropathology, Tübingen, Germany, <sup>8</sup>Medical Faculty Carl Gustav Carus, Technical University Dresden, Else Kroener Fresenius Center for Digital Health, Dresden, Germany

## Background

Intrahepatic cholangiocarcinoma (iCCA) has a poor prognosis, with recent advancements highlighting potential treatment targets such as alterations in isocitrate dehydrogenase (*IDH*) and fibroblast growth factor receptor (*FGFR*) genes. However, routine molecular sequencing is costly and not universally accessible. Moreover, the current surrogate marker, a histological small duct (SD) phenotype, depends on the expertise of pathologists. In order to streamline patient stratification for targeted therapy, we have developed an artificial intelligence-based algorithm capable of automatically classifying iCCA into small and large duct (LD) phenotypes.

## Methods

In this multicentre retrospective study, a deep learning model (CAST) was trained on a number of 852 060 H&E stained image tiles from 235 patients with iCCA who underwent surgical resection or biopsy at Heidelberg University Hospital. Model performance was assessed on a held-out internal test set (n=59) and two external test sets (n=231) from Mainz University Hospital and Hannover Medical School.

## Results

LD iCCA was associated with male gender, advanced tumor stages, and concurrent biliary precursor lesions. In the internal test set, CAST achieved an area under the receiver operating characteristic (AUROC) of 0.905 (95% CI 0.834-0.966). The model's generalization to external cohorts was effective, with an overall AUROC of 0.935 (95% CI 0.909-0.966), and it performed accurately in biopsy cases, yielding an external AUROC of 0.967 (95% CI 0.914-1.000). Gradient-based visualization techniques indicated that the model primarily based its decisions on the tumor epithelium.

Multivariate Cox regression analysis identified margin status ( $p=0.005$ ) and CAST-determined subtype ( $p=0.018$ ) as the most robust independent prognostic factors. CAST SD iCCA demonstrated a strong association with alterations in *IDH* and *FGFR* ( $p=0.024$ ), exclusive to this subtype.

### **Conclusion**

We present a universally applicable tool for histological classification of iCCA with predictive and prognostic implications, forming the basis for artificial intelligence-supported precision oncology.

## **Molecular Pathology 3 - International**

DGP15.01

### ***Current status and future development of precision oncology in Europe***

N. Normanno<sup>1,2</sup>

<sup>1</sup>Cell Biology and Biotherapy Unit, INT-Fondazione Pascale, Naples, Italy, <sup>2</sup>International Quality Network for Pathology (IQN Path), Luxemburg, Luxembourg

The approach to the diagnosis and treatment of tumors has changed radically in recent years with the advent of precision oncology. An increasing number of molecularly targeted drugs have become available for cancer patients. Over 30% of patients with advanced cancer can receive a biomarker-guided therapy. In this context, molecular tumor profiling is currently recommended for a relevant fraction of cancer patients. However, an investigation by the International Quality Network for Pathology (IQN Path) revealed that in several European countries access to biomarker tests is limited, in particular for next generation sequencing (NGS). This scenario requires immediate interventions to guarantee access for all patients to new therapies that require a molecular test and to favor the development of precision oncology. With the growth in target-based drugs being tested, the use of comprehensive genomic profiling (CGP) panels is increasingly relevant to facilitate the enrollment of advanced-stage patients in clinical trials. CGP panels can also provide information on tumor heterogeneity, including the presence of co-mutations, which allow for better stratification of patients and the development of more effective therapeutic strategies, also using real-world data. Finally, CGP testing can reveal the presence of possible germline mutations in genes associated with Hereditary Cancer Syndromes. The identification of families at increased risk of cancer facilitates the diagnosis of cancer in early stages as well as the implementation of preventive medicine strategies that can significantly reduce cancer mortality. Access to new sequencing technologies is therefore essential to promote the development of precision oncology in Europe.

DGP15.04

### ***Validation of Whole Genome Sequencing and first experiences after its introduction in the diagnostic routine of molecular pathology.***

R. Nienhold, C. Litchfield, M. Adamczyk, U. Wagner, M. Schmid, D. Seidl, D. Aguilera, M. Nowak, V. Kölzer, M. Zoche, J. Rüschoff, H. Moch, B. Sobottka

Universitätsspital Zürich, Institut für Pathologie und Molekularpathologie, Zürich, Switzerland

### **Background**

The continuous advancement of next-generation sequencing (NGS) has made whole genome sequencing (WGS) cost-effective and practical for clinical diagnostics. Although classical targeted NGS panels cover key markers of the most prevalent tumors, studies evaluating WGS in a clinical setting suggest improved off-label treatment options for patients with rare cancers or end-stage diseases. Therefore, the Department of Pathology and Molecular Pathology at the University Hospital Zürich aims to establish WGS for diagnostic purposes.

### **Methods**

Total nucleic acids were extracted from tumor tissue and matched-normal (blood) from 78 patients diagnosed with metastatic melanoma. WGS was performed with a target coverage of 60x for tumor and 30x for matched-normal. Tumor derived DNA was further analyzed with FoundationOne CDx, defining ground truth for WGS results. Bioinformatics analyses (variant calling and biomarker detection) was performed using DRAGEN (v3.9).

### **Results**

WGS identified 95% of single nucleotide variants ( $R=0.93$ ), 86% of multi nucleotide variants ( $R=0.92$ ), 88% of short indel

mutations ( $R^2=0.93$ ), 95% of amplifications with copy number  $\geq 6$  and 96% of homozygous deletions. Tumor mutation burden and estimated purity correlated  $R=0.98$  and  $R=0.67$ , respectively. The majority of missed alterations that were missed by WGS had a variant allele frequency below 10%. In two cases, TERT promoter mutations were missed due to significantly reduced coverage of this well-known GC-rich region. A total of 370 (26%) alterations identified by FoundationOne CDx were identified as germline alterations detected by WGS of control tissue. Annotation of variants using both commercial and public databases were utilized for variant prioritization and annotation. Results were summarized in an automated structured report. These reports may also be enriched by signatures and clinical actionability, such as treatments and studies.

### **Conclusion**

WGS can be used to identify established and emerging genetic biomarkers in a single assay in a diagnostic setting. Lower coverage in WGS may result in a lower sensitivity, when compared to targeted NGS. However, as the cost of sequencing continues to decline with the advent of higher throughput sequencers, we anticipate that coverage could be increased for the same cost per assay, thus improving the sensitivity. WGS in diagnostic guideline is expected to result in longer turnaround times, but may be counteracted by improving workflows and triggering molecular analysis earlier.

## **Proteomics 2: Mass Spectrometry Imaging in Pathology**

DGP16.03

### ***MALDI Mass Spectrometry Imaging - A New Method in Pathology?***

K. Schwamborn

Technische Universität München, Institut für Pathologie, München, Germany

Matrix assisted laser desorption ionization (MALDI) mass spectrometry imaging (MSI) combines the excellence in molecular characterization of mass spectrometry with microscopic imaging capabilities of stained tissue samples, enabling the precise location of different analyte classes (e.g., proteins, peptides, lipids, glycans) directly within intact tissue. In particular in the field of pathology, that can aid in tumor diagnosis, tumor subtyping, and biomarker identification. Since MALDI MSI goes far beyond microscopy and does not depend on target specific reagents such as antibodies, it is an ideal discovery tool. It can generate molecular maps of tissue sections that can elucidate the underlying biochemistry or provide information on how therapeutics or toxins influence the function or malfunction of an organ. Thus, it has the potential to overcome limitations of other approaches in the identification and routine diagnostic measurement of new marker molecules/profiles.

Different applications in the field of pathology/ oncology will be presented that highlight possible applications of MALDI MSI in Pathology. Combining MALDI MSI, histology, and statistical analysis allows for reliable and fast subtyping in a number of different tumor types while also conserving material that could be used for additional testing.

DGP16.04

### ***Raman spectroscopic features of metastatic colorectal cancer***

H. Deng

Zhejiang University School of Medicine, Department of Pathology, Hangzhou, China, People's Republic of

#### **Background**

Colorectal cancer has the third-highest morbidity and mortality worldwide, and metastasis accounts for the poor prognosis of patients and the majority of cancer-related deaths. Therefore, detecting metastatic cancer is an urgent need in clinic. Here we focused our sights on Raman spectroscopy, a noninvasive and label-free technique, to elucidate biochemical alterations in colorectal cancer patients with metastasis and distinguish differences between metastatic and nonmetastatic tumors.

#### **Methods**

We selected the patients cohorts diagnosed as colorectal cancer by pathologists, which were then divided into two groups depending on whether cancer metastasized (12 patients with metastatic, 13 without). Raman mapping of primary cancerous tissues of these patients was used to acquire spectra to reveal molecular features.



Labspec 6 was used for Raman spectral preprocessing. multivariate curve resolution-alternating least squares (MCR-ALS) analysis was performed on the preprocessed spectra to decompose the pure spectra of the mixed chemical components of the tissue specimen. Support vector machine (SVM) combined with principal component analysis (PCA) was used to develop a decision algorithm to identify the metastatic potential of colorectal cancer.

## Results

Performing MCR-ALS, we interpreted the spectral information to disclose significant changes in proteins and amino acids, polysaccharides (glycogen) and carotenes, and nucleic acid content, reflecting the distinguishability between two groups after quantitative analysis of spectral features assigning to key molecules. Moreover, SVM combined with PCA shows accuracy with 92.0% in distinguishing and predicting the metastasis of colorectal cancer.

## Conclusion

Combined with these results, our use of the tissue samples of clinical patients and Raman spectroscopy coupled with the classifier model provide the novel determination of biomolecular features in metastatic tumors, giving new insights into specific biochemical roles underlying metastasis of colorectal cancer. Our study illuminates a promising potential of the Raman spectroscopy for discerning alterations and predicting the metastasis of colorectal cancer at the biochemical level.

DGP16.05

## ***Multiplexed Immunohistochemistry with Matrix-assisted Laser Desorption/Ionization Mass Spectrometry Imaging for Subtyping of Lung Tumors***

J. Gonçalves, K. Schwamborn

Technical University of Munich, Institute of Pathology, School of Medicine and Health, Munich, Germany

## Background

Immunohistochemistry (IHC) is pivotal for pathologists assessing specific protein expressions linked to different tumor subtypes, supporting tumor classification. Yet, accurate diagnoses often demand multiple IHC stainings, and limited tissue (e.g., biopsies) can hinder a complete analysis, yielding inconclusive results. Multiplexed IHC overcomes this by using multiple primary antibodies, each targeting distinct proteins, visualized with unique labels. This study explores multiplexed IHC to differentiate lung tumor subtypes, providing a comprehensive approach to enhance diagnostic precision

## Methods

Building upon conventional diagnostic antibodies for lung cancer, we've pioneered a 10-plex panel (in collaboration with Ambergen Inc.) for simultaneous incubation on 4  $\mu\text{m}$  tissue sections. These antibodies feature photocleavable linkers that are detected with matrix-assisted laser desorption/ionization–mass spectrometry imaging, thereby retaining the spatial properties. Our methodology was applied to differentiate adenocarcinoma, squamous cell carcinoma, and neuroendocrine tumors in lung samples from 87 patients (archival samples) arranged in a tissue microarray. As a proof-of-concept, five biopsy samples were used to further validate the approach. Results were directly compared with the classical IHC utilizing serial sections.

## Results

Matrix-assisted laser desorption/ionization–mass spectrometry imaging (MALDI-MSI) successfully detected a curated panel of 10 antibodies concurrently incubated with lung cancer tissue. Despite the relatively low resolution of 20  $\mu\text{m}^2$ , this approach preserves the spatial distribution of proteins in situ, enabling correlation with hematoxylin and eosin staining (on the same tissue section) to enhance correlation with tissue morphology.

Another current limitation of the approach is the absence of quantification, particularly concerning the proliferation marker (Ki67), which is crucial for the comprehensive assessment of neuroendocrine tumors. However, based on our analysis and existing knowledge, we anticipate that quantification is feasible and will soon be accessible.

## Conclusion

MALDI-IHC and the presented workflow showcase high-plex spatial imaging of tissues using conventional MALDI

instruments, offering significant potential for complementary applications in multi-omic studies and advancing tools for personalized medicine. Moreover, it proves to be a valuable asset for the diagnostic assessment of lung tumors.

## Animal Models in Human Research 2

DGP17.01

### ***Centers for experimental animal pathology still occupy a small but valuable niche in translational medicine – time for change?***

T. Poth<sup>1</sup>, P. Schirmacher<sup>2</sup>

<sup>1</sup>Pathologisches Institut des Universitätsklinikums Heidelberg, Allgemeine Pathologie und Pathologische Anatomie; CMCP - Center for Model System and Comparative Pathology, Heidelberg, Germany, <sup>2</sup>Pathologisches Institut des Universitätsklinikums Heidelberg, Allgemeine Pathologie und Pathologische Anatomie, Heidelberg, Germany

Since CRISPR/Cas9 systems can be easily used to establish new genetically engineered mouse models, application of these models in the translational research field to explore predictive and therapeutic topics for human diseases is rising. Centers for comparative histopathology bridges the veterinary and human pathology fields and can combine optimally the technical, research, and diagnostic expertise for phenotyping, evaluation and interpretation of complex animal models in the context of human pathology. The expertise resulting of the close cooperation of both professional fields contribute substantially to meaningful study results.

In Germany, there are only two facilities pursuing such an integrative propose: the *Center for Model System and Comparative Pathology (CMCP)* in Heidelberg, and the core facility *Comparative Experimental Pathology (CEP)* in Munich. They provide essential prerequisites for high-quality, reproducible and sustainable research in the translational medicine and fulfills ideally the requirements for publications in top-class professional journals. Avoiding of repeat experiments reduces costs, decrease the number of used laboratory animals and contribute to the implementation of the 3R principle for animal welfare in the research field.

Facilities for experimental animal pathology provide high quality tissue processing that encompasses a broad spectrum of standard and specialized tissue-based technologies in a quality-controlled manner including immunohistochemistry according to individually established staining protocols. The histopathology platform enables animal model evaluation, phenotyping and scoring. To avoid misinterpretations, the existing expertise in veterinary pathology allows detecting of species-specific background lesions, individual spontaneous lesions as tumors, and infectious diseases. Further services include consulting in study planning, application of adequate methods, optimal preanalytics (organ trimming, fixation) as well as interpretation of results.

The importance of animal models reflecting human diseases will increase in future but the need for high quality animal tissue processing and animal model evaluation cannot be met by single facilities in a niche position. To cover the existing gap and the expectable rising demand in the German and European translational research landscape, further facilities for experimental animal pathology that are integrated in the human pathology environment should be established.

DGP17.02

### ***Hydrodynamic models of cholangiocarcinoma for molecular studies and therapeutic interventions***

D. F. Calvisi

University of Regensburg, Institut für Pathologie, Regensburg, Germany

Cholangiocarcinoma (CCA) is an aggressive neoplasm developing at any point along the biliary tree. The prognosis of CCA is dismal, its incidence is rising, and treatments' efficacy is limited or temporary. Therefore, generating preclinical models is imperative to elucidate the molecular pathogenesis of biliary tract tumors and to develop more specific and effective therapies. Among these models, the ones generated using the hydrodynamic gene delivery technology are constantly gaining consideration from the scientific community focusing on this tumor type. Hydrodynamic gene delivery is a flexible, reliable, and relatively inexpensive tool to generate preclinical murine models for liver cancer research by allowing the stable expression or deletion of the gene(s) of interest in mouse hepatocytes. Through this method, various features of CCA have been investigated and characterized in the last decade, including the oncogenic and tumor suppressive role of genes, the interplay of signaling cascades in tumor initiation and progression, the cell of origin of the

disease, the relevance of the tumor tissue microenvironment, the metastatic process, and the effectiveness of innovative therapeutic approaches.

DGP17.03

### ***Animal models for pancreatic cancer and its precursor lesions***

I. Esposito

Inst. für Pathologie Universitätsklinikum Düsseldorf, Düsseldorf, Germany

Genetically engineered mouse models (GEMMs) play a crucial role in studying pancreatic cancer and its precursor lesions due to their genetic similarity to humans and their ability to mimic the disease progression. These models are created by introducing specific genetic alterations into mice that recapitulate the genetic mutations found in human pancreatic cancer.

GEMMs allow researchers to investigate the molecular mechanisms underlying pancreatic cancer development, progression, and response to treatment in a controlled laboratory setting. By manipulating genes involved in key signaling pathways such as *KRAS*, *TP53*, and *SMAD4*, researchers can replicate the genetic landscape of pancreatic cancer observed in humans.

GEMMs enable researchers to study tumor development and biology, metastasis, and the tumor microenvironment, facilitating a deeper understanding of pancreatic cancer biology. Additionally, they are valuable tools for preclinical drug testing and the development of novel therapeutic strategies. Depending on the type of mutations, different kinetics of tumor development are observed, which can be exploited depending on the different research questions. The most relevant precursor lesions of pancreatic cancer, namely PanIN, IPMN and MCN, have been also successfully modelled, unraveling potential non-ductal pathways for ductal pancreatic carcinogenesis.

Overall, genetically engineered mouse models offer a powerful platform for advancing our understanding of pancreatic cancer and accelerating the development of new therapeutic interventions.

DGP17.04

### ***Tenascin C deficiency impairs regeneration after cerulein-induced acute pancreatitis.***

L. M. Rudroff, L. J. Häberle, F. Opitz, A. Yavas, I. Esposito

Universitätsklinikum Düsseldorf, Pathologie, Düsseldorf, Germany

#### **Background**

Tenascin C (TNC) is an extracellular matrix protein, which is expressed during tissue injury and contributes to its repair. It is further involved in the progression of different types of cancers, including pancreatic adenocarcinoma. While much is known about its role in carcinogenesis, the effects of TNC in pancreas inflammation and regeneration are yet to be discovered. The aim of this study was to analyze the role of TNC in regeneration following acute pancreatitis *in vivo*. A particular focus was set on acinar-ductal metaplasia, a process due to inflammatory stress, which is part of tissue repair, but also a vulnerable state with risk of dysplasia.

#### **Methods**

For this study, a genetically modified mouse model including TNC-Knockout (KO) and wildtype (WT) mice was used. To assess an acute pancreatitis, all mice were injected with cerulein (i.p. 8x100 µg/kg of body weight on two following days) and organs were removed at 3, 12, 24, 48 hours, 7 and 21 days. The severity of inflammation was determined on hematoxylin-eosin stained tissue using a semi-quantitative score including edema and immune cell infiltration.

Regeneration was examined via immunohistochemistry staining including markers for cell proliferation (Ki67), ADM formation (Amylase, CK19, Sox9), activation of pancreatic stellate cells ( $\alpha$ -SMA) and Integrin receptors (Integrin  $\beta$ 3 & Integrin  $\beta$ 6). The stained slides were analyzed semi-quantitatively or fully automatically with Aperio ImageScope, the respective analysis was adjusted to each specific staining. Statistical analyses were performed with GraphPad Prism.

#### **Results**

The severity of inflammation was similar in both WT and KO groups and tissue repair was completed by 7 days. However, TNC-KO showed a slightly delayed regeneration with persistent higher Ki67-Index and a reduced Sox9

expression. Results of quantitative analysis of ADM formation were similar in both groups, however, the KO group showed a slightly delayed decrease of ductal marker CK19. Further, ADM showed significantly higher expression of Integrin  $\beta 6$  compared to the overall tissue, without showing any difference between both genotypes. Inflammation also lead to activation of pancreatic stellate cells, although without formation of mature collagenous stroma.

### Conclusion

TNC deficiency slightly impairs pancreas regeneration after cerulein-induced pancreatitis. While this does not perceptibly affect morphological regeneration, it still underlines the importance of an intact stromal scaffold for tissue integrity.

DGP17.05

## ***Investigation of Sporadic Congenital Portosystemic Shunts in Mice***

S. Bobe<sup>1,2</sup>, D. M. Klump<sup>2</sup>, S. Hermann<sup>2</sup>, R. Erapaneedi<sup>2</sup>, F. Kiefer<sup>2</sup>

<sup>1</sup>University Hospital Münster, Gerhard-Domagk-Institute of Pathology, Münster, Germany, <sup>2</sup>University of Münster, European Institute for Molecular Imaging (EIMI), Münster, Germany

### Background

Congenital Portosystemic Venous Shunts (CPSS) are rare vascular malformations characterized by a connection between portal vein and systemic circulation allowing the intestinal blood to bypass the liver. Symptoms include encephalopathy and pulmonary hypertension. Furthermore, affected livers are predisposed to hepatic neoplasms. In this project, we identified C57Bl/6 mice exhibiting sporadic CPSS and investigated the hepatic (histo)pathology.

### Methods

Macroscopic imaging was performed using small animal computer tomography ( $\mu$ CT) on livers with vascular casts obtained by injection of the radiographic compound Microfil (Flow Tek, Inc.). Light sheet fluorescence microscopy was used to investigate the mesoscopic tissue architecture in immunostained and optically cleared liver samples, supplemented by microscopic evaluation using confocal laser scanning microscopy. Results were compared to literature on human CPSS.

### Results

While  $\mu$ CT scans revealed a vascular shunt between portal vein and *vena cava* in affected mice, microscopic and mesoscopic evaluation of the tissue architecture showed a disturbed portal organization with multiple enlarged arterial branches, scattered venous stubs, which lacked proper interconnections, and an extensive lymph vascular network surrounding portal tracts.

### Conclusion

Sporadic CPSS in mice exhibited histopathological features very similar to malformations observed in human individuals. Thus, the murine condition might serve as a promising disease model to further investigate the yet unidentified pathomechanism behind CPSS.

## **Autopsy**

DGP18.01

## ***Next-generation postmortems: what are we waiting for?***

G. Weirich<sup>1</sup>, K. Stock<sup>2</sup>, J. Slotta-Huspenina<sup>1,2,3</sup>

<sup>1</sup>Technical University Munich, School of Medicine, Institute of Pathology, München, Germany, <sup>2</sup>Technical University Munich, School of Medicine, Department of Nephrology, München, Germany, <sup>3</sup>Pathologie Starnberg MVZ GmbH, Starnberg, Germany

### Background

Precision medicine refers to the use of genetic and molecular information to identify specific disease subtypes and develop targeted therapies. This is especially relevant to cancer therapy. Surgical pathologists play an important role in defining cancer types, specifying tumour amount in a sample, and the amount of viable tumour before further analyses that rely on precision (genomics, proteomics). Tailored cancer therapies have produced unexpected treatment success rates, for instance, in melanomas. As new therapies may cause unwanted secondary changes that challenge disease

outcomes, efforts to monitor these changes are in demand. Boas Image-Frameized postmortem protocols, such as the imaging-guided minimally invasive tissue sampling (MITS) approach may help to fill this diagnostic gap.

## Methods

Based on our experience over the last two years, we present here the results of the newly established interdisciplinary ultrasound-guided MITS (US-MITS) at the University Hospital "Klinikum rechts der Isar. Organizational framework conditions (personnel and time expenditure) and tissue specificity and vitality were analyzed.

## Results

We carried out the US-MITS on 46 deceased COVID-19 patients and procured 3200 biopsies from various organs and sites. US-MITS was carried out between 90 and 180 minutes. Biopsies fulfilled precision requirements of specificity and viability in more than 90% of samples, such that they would comply with diagnostic, genomic, and proteomic requirements.

## Conclusion

US-MITS meets the contemporary requirements of precision medicine. Because of the speed, resource savings, and the power of scalability, US-MITS has the potential to shift postmortems into the next generation of analytic efforts devoted to stratifying diseases based on therapy-induced pathologic changes. To solve administrative, legal, and financial issues, the commitment of surgical pathologists is needed.

DGP18.02

## ***Comparative analysis of microsatellite instability and standard mismatch repair protein deficiency tests in a large cancer cohort***

A. Kiss, L. M. Nádorvári, J. Kulka, T. Barbai, E. Rásó, I. Kenessey, G. Lotz, J. Tímár

Semmelweis Universität Budapest, Department of Pathology, Forensic and Insurance Medicine, Budapest, Hungary

## Background

Mismatch repair deficiency (dMMR) and consequent microsatellite instability (MSI) is one of the most frequent genetic alterations of DNA repair systems of malignancies. It is most prevalent in gastrointestinal tract (colorectal, gastric, and esophageal) and endometrial cancers. Mismatched base pairing and frameshift mutations result finally in increased tumor mutational burden. dMMR/MSI test are required not only for Lynch syndrome but generally for malignancies as tumor-agnostic indication of immune checkpoint inhibitors. Most of the pathological guidelines consider MMR protein IHC assays as the gold standard test to identify cancers with dMMR and recommend molecular MSI tests only in special circumstances or to screen for Lynch syndrome.

## Material and methods

Large cancer patient cohort (n=1306) was tested for four MMR IHCs (MLH1 and PMS2 or MSH2 and MSH6). Further, parallel Pentaplex PCR tests (BAT-25, BAT-26, MONO-27, NR-21 and NR-24) were run in 703 cases at our pathology center after DNA extraction and followed by fragment analysis of the PCR products.

**Results:** The incidence of MSI-High molecular status in our cancer cohort was 12.1% and was very similar in the colorectal part of the cohort. Interestingly, the dMMR incidence was proved to be higher, 19.4 % in the colorectal part and was very similar, 20.3% in the entire cohort. High discrepancy rate (19.3%) was detected between the two diagnostic tests (dMMR versus MSI-High) which was independent of the tumor types. However, in case of proficient MMR the discrepancy rate for MSS (stability)/MSI-low was very low (2.0%). MSI PCR predictive value to MMR IHC was compared and statistical analysis indicated that MSI PCR has high specificity but low sensitivity, resulting in moderate positive and negative predictive values. Consequently, correlation of the two tests was low ( $\kappa < 0.7$ ). Low tumor percentage was excluded out of possible contributing factors responsible of poor performance. dMMR phenotypes were identified (classic versus non-classic or unusual) as possible contributors.

## Conclusion

Our data strongly support that preanalytical factors might strongly influence the results of MMR IHC and MSI PCR. It is open for discussion and further analysis whether the two test types are equally powerful markers of immunoncological therapies. Our observation might question the current dogma that dMMR phenotype and genetic MSI status are equal

predictive markers of the immunotherapies.

DGP18.03

### ***COVID-19 shows a milder presentation in cancer patients: experience from a large tertiary center autopsy series***

E. Kocsmar<sup>1</sup>, I. Kocsmar<sup>2</sup>, F. Elamin<sup>1</sup>, L. Papai<sup>1</sup>, A. Jakab<sup>1</sup>, T. Varkonyi<sup>1</sup>, T. Glasz<sup>1</sup>, G. Racz<sup>3</sup>, A. Pesti<sup>1</sup>, K. Danics<sup>1</sup>, A. Kiss<sup>1</sup>, G. Röst<sup>4,5</sup>, E. Belicza<sup>6</sup>, Z. Schaff<sup>1</sup>, G. Lotz<sup>1</sup>

<sup>1</sup>Semmelweis University, Department of Pathology, Forensic and Insurance Medicine, Budapest, Hungary, <sup>2</sup>Semmelweis University, Department of Urology, Budapest, Hungary, <sup>3</sup>Semmelweis University, Department of Pathology and Experimental Cancer Research, Budapest, Hungary, <sup>4</sup>University of Szeged, National Laboratory of Health Security, Szeged, Hungary, <sup>5</sup>Hungarian Centre of Excellence for Molecular Medicine, Szeged, Hungary, <sup>6</sup>Semmelweis University, Health Services Management Training Centre, Faculty of Health and Public Administration, Budapest, Hungary

#### **Introduction**

The severity of COVID-19 caused by SARS-CoV-2 varies in different subgroups of patients. Its outcome is strongly influenced by co-morbidities such as cancer, causing functional and compositional changes in the immune system during tumor progression.

Our aim was to investigate autopsy findings caused by SARS-CoV-2 infection and the role of COVID-19 in the fatal sequence leading to death in a large autopsy series.

#### **Methods**

We included a total of 2,641 adult patients who died during 2020-2022 and underwent a complete autopsy procedure at the Dept. of Pathology, Forensic and Insurance Medicine. Among the patient cohort, 539 patients were positive for SARS-CoV-2 by antemortem PCR or antigen rapid test, and 829 patients had suffered from malignant tumors. Overall, the cohort included 100 patients who simultaneously had cancer and SARS-CoV-2 infection. In total, 100 SARS-CoV-2 positive cancer patients were included in the study.

#### **Results**

A significantly lower number of cases of viral pneumonia with or without bacterial overinfection were detected in cancer patients than in non-cancer patients. In patients with cancer, SARS-CoV-2 positivity without viral disease was more common, but viral or bacterial pneumonia was also mainly present as a contributory disease or coexisting morbidity and was not involved directly in the fatal sequence leading to death.

Among SARS-CoV-2 positive cancer patients, non-metastatic disease and haematological malignancies were more common. In multivariable analyses, COVID-19 was more frequently included in the sequence leading to death in patients on active anticancer therapy, whereas antiviral treatment or length of hospitalization was not associated with the role of COVID-19 in death or the development of pneumonia. The role of SARS-CoV-2 infection and consequent pneumonia in death was significantly associated with wave of disease.

#### **Conclusion**

Based on the autopsy findings, COVID-19 showed a more balanced presentation across the pandemic waves and a milder overall course in cancer patients. This is presumably due in part to their weakened, immunosuppressed state, in which an early/mild viral disease can more easily lead to death from an underlying malignancy.

Foundations: K\_22 142604 grant of the National Research, Development and Innovation Office, and the ÚNKP-23-4-II-SE-24 New National Excellence Program of the Ministry for Culture And Innovation from the source of the National Research, Development and Innovation Fund.

DGP18.04

### ***Reconstructing 3D histological structures using machine learning (AI) algorithms***

E. Kontsek<sup>1</sup>, J. Baskay<sup>2,3</sup>, M. Kivovics<sup>4</sup>, D. Péntes<sup>4</sup>, O. Németh<sup>4</sup>, M. Szócska<sup>2</sup>, A. Kiss<sup>1</sup>, P. Pollner<sup>2,3</sup>

<sup>1</sup>Semmelweis University, Department of Pathology, Forensic and Insurance Medicine, Budapest, Hungary, <sup>2</sup>Semmelweis University, Data-Driven Health Division of National Laboratory for Health Security, Budapest, Hungary, <sup>3</sup>Eötvös Loránd University, Department of Biological Physics, Budapest, Hungary, <sup>4</sup>Semmelweis University, Department of Community Dentistry, Budapest, Hungary

## Questions/Background

### Introduction

Histomorphometry is currently the gold standard for bone micro-architectural examinations, but it relies on two-dimensional sections to deduce the spatial properties of structures. Micromorphometric parameters are calculated from these sections based on the assumption of a plate-like three-dimensional microarchitecture, resulting in the loss of three-dimensional structure due to the destructive nature of the classic histological processing.

### Materials and Methods

To overcome the limitation of histomorphometry and reconstruct the 3D architecture of bone core biopsy samples from 2D histological sections, bone core biopsy samples were decalcified and embedded in paraffin. Subsequently, 5 µm thick serial sections were stained with hematoxylin and eosin and scanned using a 3DHistech Panoramic® 1000 Digital Slide Scanner. The region of interest was preprocessed and oriented, and semantic segmentation of the bone, bone graft material, and soft tissue was performed. The faulty sections were filtered out using unsupervised filtering based on mutual information. The 3D reconstruction was created using ASIFT feature matching and homography.

### Results

Our method achieved an overall accuracy of 96% with an F-score of 0.967 for the segmentation of bone tissue. The filtering process accuracy was 89.7%, with a precision of 0.96 and a recall of 0.88.

### Discussion

This method enables the examination of tissue microarchitecture in 3D with an even higher resolution than microcomputed-tomography (micro-CT), without losing information on cellularity. However, the limitation of this procedure is its destructive nature, which precludes subsequent mechanical testing of the sample or any further secondary measurements. Furthermore, the number of histological sections that can be performed from a single sample is limited.

DGP18.05

## ***Detection of pancreatic adenocarcinoma by Stimulated Raman Scattering scanning microscopy with convolutional artificial neural network on unstained tissue sections***

É. Kocsmár<sup>1</sup>, K. Ócsai<sup>2</sup>, A. Biró<sup>1,2</sup>, V. Csajbók<sup>2</sup>, M. Veress<sup>2</sup>, Z. Mucsi<sup>2</sup>, B. Barkóczy<sup>2</sup>, K. Borka<sup>1</sup>, A. Pesti<sup>1</sup>, E. Kontsek<sup>1</sup>, A. Kiss<sup>1</sup>, B. Rózsa<sup>2</sup>, [G. Lotz](#)<sup>1</sup>

<sup>1</sup>Semmelweis University, Department of Pathology, Forensic and Insurance Medicine, Budapest, Hungary, <sup>2</sup>BrainVisionCenter Research Institute and Competence Centre, Budapest, Hungary

### Introduction

Stimulated Raman Scattering (SRS) scanning microscopy enables the unlabelled spectral fingerprinting of lipids, proteins and water in cells and tissues, allowing morphological examination and chemical composition analysis of unstained tissue samples. Furthermore, by training a convolutional artificial neural network on SRS images, the detection of malignant tumors can be also achieved.

### Methods

SRS imaging was performed on unstained sections of 49 pancreatic ductal adenocarcinomas at wavelengths of 2895 cm<sup>-1</sup> and 2950 cm<sup>-1</sup>. After hematoxylin-eosin staining, we determined the percentage of cancer cells and normal tissue components at the imaging site. 3256 SRS images were used to train a residual convolutional artificial neural network (ResNet-101), whose cancer detection ability was tested on 844 images.

### Results

The detection rate for individual non-tumorous tissue categories (including pancreatic exocrine and endocrine tissue, nervous tissue, lymphatic tissue, adipose tissue, connective tissue, smooth muscle, inflammatory infiltrate, chronic pancreatitis and mixed non-tumorous elements) ranged from 45% to 100%, with the overall detection rate of non-tumorous tissue reaching 86.3%. For images with more than 30% adenocarcinoma, the cancer detection rate was 98.4%, for tumor contents between 15% and 30% it was 100%, and for tumor percentages below this level it was 87.5-

92.0%. Overall, the cancer detection sensitivity was 97.7%, the specificity 86.3%, while the positive and negative predictive values were 90.6% and 96.6%, respectively, using convolutional artificial neural network.

## Conclusion

On deparaffinized, unstained sections of formalin-fixed paraffin-embedded specimens, SRS imaging with the convolutional artificial neural network identified the presence of pancreatic ductal adenocarcinoma with excellent results even when trained on a relatively small data set. Since the intra- and inter-institutional variability of unstained sections is much smaller than that of hematoxylin-eosin stained sections, their application to imaging with advanced microscopy techniques and to artificial intelligence training is promising.

The study was funded by the 2020-2.1.1.-ED-2022-00208 and K\_22 142604 grants of the National Research, Development and Innovation Office (Hungary), as well as the ÚNKP-23-4-II-SE-24 and 2023-2.1.2-KDP-2023-00016 grants of the Ministry for Culture and Innovation from the source of the National Research, Development and Innovation Fund.

DGP18.06

## ***Evaluation of diagnostic accuracy of state of the art post-mortem imaging compared to clinical hospital autopsy***

H. Hoppe<sup>1</sup>, I. Arnold<sup>2</sup>, N. Lange-Herr<sup>2</sup>, J. Klaus<sup>2</sup>, N. Schwendener<sup>2</sup>, J. Brünig<sup>2</sup>, B. Dislich<sup>3</sup>, M. Trippel<sup>3</sup>, Y. Banz<sup>3</sup>, W.-D. Zech<sup>2</sup>

<sup>1</sup>Lindenhofspital Bern, Radiologie, Bern, Switzerland, <sup>2</sup>Institut für Rechtsmedizin Bern, Universität Bern, Forensische Medizin und Bildgebung, Bern, Switzerland, <sup>3</sup>Institut für Gewebemedizin und Pathologie, Universität Bern, Klinische Pathologie, Bern, Switzerland

## Background

In the last decades, there has been a constant decline of non-forensic clinical hospital autopsy rates worldwide. Thus far, continuous efforts to highlight the importance of the clinical autopsy have unfortunately not influenced declining autopsy rates. In this context, the approach of post-mortem imaging has been proposed as a means to counteract this trend. Therefore, the goal of this study was to evaluate if state of the art post-mortem imaging (CT and MRI) can be used as a valid alternative to the classical clinical autopsy.

## Methods

Post-mortem imaging (whole-body CT and MRI) was conducted before clinical autopsy at the University of Bern, Switzerland, on n=120 deceased patients in a prospective study. Imaging findings were compared to autopsy findings (defined as the gold standard). Diagnostic accuracy (sensitivity, specificity, positive predictive value, negative predictive value) was calculated for causes of death and all autopsy findings for CT only, MRI only and a combined use of CT and MRI.

## Results

The overall sensitivity for the correct post-mortem imaging determination of the cause of death was 85 % for a combined use of CT and MRI (52 % CT only and 75 % MRI only). Even the combined use of CT and MRI could not visualize certain relevant autopsy findings such as those related to septic shock, certain tumor types (e.g. blood cancers), certain degenerative lesions (such as heart valve stenoses), and small findings in general. For specific causes of death and specific pathologic findings, post-mortem imaging showed high diagnostic accuracy. Such findings were for example acute myocardial infarction (MRI sensitivity 92 %, specificity 99 %), central and paracentral pulmonary embolism (MRI sensitivity 91 %, specificity 97 %), pneumonia (CT sensitivity 91 %, specificity 96 %), metastases (MRI sensitivity 92 %, specificity 100 %), aortic dissection (MRI sensitivity 86 %, specificity 100 %), and larger hemorrhages (MRI and CT sensitivity 92 %, specificity 100 %).

## Conclusion

Post-mortem CT and/or MRI cannot be used as a general alternative to the classical clinical hospital autopsy. However, if the goal of the post-mortem examination is to confirm or look for specific causes of death or a specific type of pathology, post-mortem imaging can be used as an alternative to autopsy. The combined use of CT and MRI may enhance diagnostic accuracy of some particular findings but the combined use is not always necessary nor useful.



# Rising Stars

DGP19.03

## ***"Predictive and prognostic biomarkers on solid tumors with focus on lung carcinoma"***

C. Kumpers

Institute of Pathology University Hospital Schleswig Holstein, Campus Luebeck, Lübeck, Germany

### **Background**

This cumulative habilitation thesis includes studies on predictive and prognostic biomarkers for solid malignancies, focusing on non-small cell lung cancer (NSCLC), with one original paper each dedicated to small cell lung cancer (SCLC) and malignant melanoma. These malignancies share a poor prognosis although, especially for melanoma and NSCLC, immense treatment advances have been achieved, significantly by anti-PD-1/PD-L1 immunotherapy. However, predictors of treatment response have still not been satisfactorily identified.

### **Methods**

Briefly summarising methods: Immunohistochemical/immunocytochemical analyses and transcriptome analyses.

### **Results**

In **original paper 1**, we surveyed immune cell infiltrate and tumoral PD-L1 expression of primary melanoma and melanoma metastases. The key finding was that in primary tumors, the quantity of immune cell infiltration, but not PD-L1 status, was associated with better OS.

In **original paper 2** we found that PD-L1-positive and PD-L1-negative NSCLC harboured significantly differentially regulated genes, most of which related to signaling cascades of tumor microenvironment. As the most interesting molecules we found STAT1 and KIT differentially expressed.

Determination of PD-L1 status has not been validated on cytologic specimens. With **original paper 3**, we aimed to address this issue and determined PD-L1 status on paired histologic and cytologic NSCLC specimens. We found a satisfying concordance rate after comparative analysis of 247 paired samples.

In **original paper 4** we investigated CDK7, a transcription-associated cyclin-dependent kinase that affects transcription.

In **original paper 5** we investigated TRIM11, a molecule involved in post-translational protein modification. We stated that high CDK7 and TRIM11 protein expression was significantly associated with shorter OS, respectively, suggesting CDK7 and TRIM11 as prognostic markers for NSCLC.

In **original paper 6** we assessed DLL3, discussed as a predictive marker for therapy with Rova-T, between paired pre- and post-therapeutic SCLC samples. In a large proportion, we found no stable DLL3 expression during course of therapy. Additionally, survival analysis showed differential results for pre- or post-therapy samples.

### **Conclusion**

This cumulative habilitation including 6 original papers is dedicated to malignant melanoma and SCLC in addition to NSCLC and attempts to contribute to the identification of new prognostic and predictive biomarkers in order to improve the prognosis of the corresponding patients.

DGP19.04

## ***New technologies in tumor pathology***

S. Foersch

University Medical Center Mainz, Institute of Pathology, Mainz, Germany

### **Background**

Die vorliegende Arbeit befasste sich mit innovativen Technologien in der modernen Krebsmedizin. Dabei lag der Fokus auf der Erforschung und Entwicklung von neuen Verfahren der feingeweblichen Diagnosestellung - insbesondere der Intravitalmikroskopie, der Molekularpathologie, sowie der digitalen Pathologie. Die genannten Ansätze kamen in grundlagenwissenschaftlichen, translationalen sowie klinischen Projekten zum Einsatz.

## Methods

Im ersten Studienabschnitt wurden neue mikroskopische Techniken, wie die konfokale Laserendomikroskopie oder die Multiphotonenmikroskopie dazu verwendet, gesunde Gewebsanteile sowie krankhafte Veränderungen intravital darzustellen. Hierbei gelang die Visualisierung *in vivo* mit und ohne Verwendung fluoreszierender Kontraststoffen. Darüber hinaus ermöglichte die Applikation markierter Antikörper eine molekular-gezielte mikroskopische Bildgebung während der laufenden Untersuchung. Dies könnte in Zukunft zum Beispiel dazu verwendet werden, Biopsien gezielter zu entnehmen und so das Komplikationsrisiko während eines endoskopischen oder interventionellen Eingriffs zu minimieren.

## Results

Der zweite Studienabschnitt griff die über die intravitale Mikroskopie gewonnenen tumorbiologischen Erkenntnisse auf und explorierte die Rolle verschiedener Schlüssel-moleküle im Tiermodell Entzündung-assoziiierter Tumore. Mit Hilfe moderner molekularpathologischer Verfahren konnte zum ersten Mal gezeigt werden, dass über die Inhibition eines bestimmten Zellmechanismus, welchen man z. B. aus der Altersforschung kennt, das Tumorwachstum gefördert wird. So konnte die Modulation zellulärer Seneszenz als ein Hauptgrund identifiziert werden, weswegen z. B. Entzündungs-assoziierte neoplastische Läsionen im Darm progredient werden können.

## Conclusion

Zur Untersuchung der tatsächlichen Relevanz für Patient\*innen mit bösartigen Tumorerkrankungen wurden in einem dritten Studienabschnitt verschiedene klinische Kohorten etabliert, um die Rolle Seneszenz-assoziierte Proteine, aber auch andere Moleküle als prognostische und prädiktive Biomarker zu evaluieren. Ein weiterer Fokus dieses letzten Studienabschnitts lag auf der digitalen Pathologie sowie der Implementierung von Verfahren der künstlichen Intelligenz (KI) und des maschinellen Lernens (ML) in der Tumorpathologie. Diese können nicht nur eine Unterstützung in der histopathologischen Routinediagnostik bieten, sondern alleine am Aussehen der Zellen und Gewebe unter dem Mikroskop eine Abschätzung zu Prognose und Therapieansprechen ermöglichen.

# Junges Forum 1: How to do....?

JuFo1.01

## ***How to do...Molekularpathologie***

A. Mock<sup>1,2</sup>

<sup>1</sup>Pathologisches Institut, LMU München, München, Germany, <sup>2</sup>German Cancer Research Center (DKFZ) & German Cancer Consortium (DKTK), Munich Partner Site, München, Germany

Dieser Vortrag im Rahmen des Jungen Forums richtet sich insbesondere an Patholog\*innen in Weiterbildung und soll Kernkonzepte und aktuelle Entwicklungen in der Molekularpathologie mit Schwerpunkt auf NGS vermitteln.

Im ersten Teil werden laborseitig verschiedene NGS-Verfahren gegenübergestellt (z.B. Panelsequenzierung vs. Exomsequenzierung vs. Ganzgenomsequenzierung).

Der zweite Teil beschäftigt sich mit der Interpretation molekularer Alterationen, insbesondere im Hinblick auf sog. Varianten unklarer Signifikanz (VUS). Außerdem sollen häufig verwendete Begrifflichkeiten in der Varianteninterpretation geklärt werden.

JuFo1.02

## ***Dermatopathology for pathologists – don't panic. Advices for beginners.***

E. Bierhoff

Heinz-Werner-Seifert-Institut, Dermatopathologie, Bonn, Germany

The spectrum of dermatopathology includes substantially non-neoplastic (mostly inflammatory) lesions as well as neoplastic diseases.

Inflammatory lesions are based on diagnostic algorithms including the pattern and composition of the infiltrate, reference to well-defined structures like epidermis, vascular structures, adnexa and soft-tissue. These changes are summarized in

major inflammatory patterns. Further criteria like interface-dermatitis, lichenoid, spongiforme or psoriasiforme dermatitis may help to narrow the differentials. Very important is the synopsis with the clinical informations. To know about clinical-dermatological basics is necessary and manageable. A close spectrum of differentials concerning inflammatory diseases is already a good job.

Neoplastic lesions first of all need a basic classification of differentiation (e.g. melanocytic, epithelial etc.). This already can be a challenge in individual cases. For further differentiation immunohistochemical analysis is necessary.

The lecture wants to encourage pathologists to face dermatopathology without fear or panic.

JuFo1.03

## **How to do... Knochentumoren**

T. F. Barth<sup>1</sup>, C. Mogler<sup>2</sup>

<sup>1</sup>Universitätsklinikum Ulm, Institut für Pathologie, Ulm, Germany, <sup>2</sup>Technische Universität München, München, Germany

Knochentumoren, ob benigne oder maligne, stellen immer eine Herausforderung für den Pathologen dar. Gründe dafür sind die verhältnismäßige Seltenheit im diagnostischen Alltag bei einer erheblichen Vielfältigkeit im morphologischen Erscheinungsbild. Die Biopsie kann die Heterogenität dieser Tumoren lediglich knopfartig abbilden. Hinzukommen technische Besonderheiten im Umgang mit der verknöcherten Biopsie, um zusätzliche Techniken wie die Immunhistologie oder auch molekularpathologische Untersuchungen anwenden zu können. Benigne Knochentumoren sind zwar dreimal so häufig im Vergleich zu den malignen Varianten, was vor dem Hintergrund von bis zu 60 Entitäten nach WHO, problematisch sein kann. Als Besonderheit hat die aktuelle WHO zudem bei den Knochentumoren, in Analogie zu den Weichteiltumoren, die Einteilung nach dem biologischen Verhalten (benigne-intermediär-maligne) übernommen und neue Entitäten aufgenommen (e.g. Osteochondromyxom) sowie Umbenennungen und Umgruppierungen vorgenommen (Chondrosarkom G1 zu atypischer kartilaginärer Tumor der langen Röhrenknochen). In dem Vortrag werden die Neuigkeiten der WHO vorgestellt, problemorientierte Lösungsvorschläge anhand von jeweiligen Fallbeispielen diskutiert umso den Pathologen in Ausbildung für das Thema zu sensibilisieren und zu erklären wieso es kaum einen anderen Bereich in der Pathologie gibt der eine so intensive Interaktion zwischen Radiologie und Chirurgie in der Planung, Durchführung, Versorgung und Interpretation des gewonnen Biopsats fordert.

Als weitere wertvolle Einrichtung in der Aus- und Fortbildung in der Diagnostik von Knochentumoren wird die Arbeitsgemeinschaft Knochentumoren (AGKT) von Ihrer Geschäftsführerin (Carolin Mogler) und ihrem aktuellen Vorsitzenden (Thomas F.E. Barth) vorgestellt. Die AGKT ist seit über 50 Jahren aktiv und trifft sich regelmäßig zweimal pro Jahr. Diskutiert werden in den Treffen Schnittpräparate, die den Mitgliedern verblindet virtuell vor den Sitzungen anhand von gescannten Schnitten zur Verfügung gestellt werden, um abschließend zusammen mit Radiologen, Orthopäden und Unfallchirurgen in intensiver Diskussion eine Konsensusdiagnose zu dem jeweiligen Fall zu finden. Die AGKT bietet folglich die einzigartige Möglichkeit sich an über 1000 dokumentierten Fällen mit Knochentumoren in Präsenztreffen, aber auch virtuell anhand von eingescannten Schnittpräparaten mit der entsprechenden Klinik und Bildgebung zu beschäftigen und permanent weiterzubilden.

## **AG Gynäko- und Mammopathologie 1**

AG01.02

### ***Analysis of DNA methylation patterns in HRR genes and its correlation with the homologous repair deficiency (HRD)***

S. Struckmann<sup>1</sup>, S. Bartels<sup>1</sup>, T.-W. Park-Simon<sup>2</sup>, H. Kreipe<sup>1</sup>, U. Lehmann<sup>1</sup>

<sup>1</sup>Institut für Pathologie, Medizinische Hochschule Hannover, Hannover, Germany, <sup>2</sup>Medizinische Hochschule Hannover, Gynäkologie, Hannover, Germany

#### **Background**

Deficiencies in DNA repair mechanisms have been linked to various malignancies. Mutations in homologous recombination repair (HRR) pathway genes can contribute to the development of high-grade serous ovarian, fallopian tube, and peritoneal carcinomas. Epigenetic alterations in the promoter region can result in gene silencing and represent an alternative to inactivation by mutation. Therefore, this projects aims to elucidate the contribution of epigenetic inactivation mechanisms to homologous recombination deficiency (HRD) in ovarian carcinomas.

## Methods

The promotor methylation status of three HRR genes (*BRCA1*, *BRCA2*, *RAD51C*) was examined in 123 formalin-fixed paraffin-embedded (FFPE) tumor tissue samples, primarily from ovarian cancer (107 ovarian carcinomas, 6 endometrial carcinomas, 3 mammary carcinomas, 7 others). DNA methylation levels were determined using pyrosequencing and next-generation sequencing (NGS). The amplicon-based NGS methylation panel examined the promotor regions of 7 genes (*BRCA1*, *BRCA2*, *RAD51C*, *ATM*, *CDH1*, *MLH1*, *MGMT*). HRD was examined employing SNP-array methodology (OncoScan™). All 123 tissue samples were evaluable and a GI-score (Genomic instability score) above 42 was defined as “HRD-positive”. In addition, the BRCA1/2 mutational status was known for 63 cases.

## Results

The OncoScan™ analysis revealed that 55 tumor samples have a defect in their HRR pathway. The DNA methylation analysis showed in 21 cases a *BRCA1* gene methylation and in 2 cases a *RAD51C* gene methylation (mean methylation of all CG sites >20% for *BRCA1*, >17% for *RAD51C*). Furthermore, 2 cases of *MLH1* methylation were found. All cases which exhibited high gene methylation showed a high HRD-score (> 42). Out of 55 HRD- positive tumors 24 (43.6%) showed a high methylation level suggesting epigenetic inactivation by DNA methylation as the underlying mechanism. However, some unmethylated samples also exhibited high GI-Scores, suggesting that HRD is also caused by factors other than DNA methylation.

## Conclusion

Our results show that in a substantial number of cases epigenetic inactivation seems to be the main defect underlying homologous recombination repair deficiency.

In future studies, the impact of gene methylation on mRNA expression levels and on the PARP inhibitor therapy needs to be evaluated.

AG01.03

## ***Unintentional Off-label Use of PARP Inhibitors in Low-Grade Serous Ovarian Carcinoma: A Potential First Case and Call for Further Investigation***

J. Lammer<sup>1</sup>, U. Schatz<sup>1</sup>, L. Rief<sup>1</sup>, H. Bronger<sup>1</sup>, M. Kiechle<sup>1</sup>, M.-L. Koppermann<sup>2</sup>, N. Pfarr<sup>2</sup>, C. Mogler<sup>2</sup>, E. Schmoeckel<sup>2</sup>

<sup>1</sup>Department of Gynecology and Center for Hereditary Breast and Ovarian Cancer, University Hospital rechts der Isar, Technical University of Munich (TUM), Munich, Germany, <sup>2</sup>Institute of Pathology, TUM School of Medicine and Health, Technical University of Munich (TUM), Munich, Germany

## Background

Low-grade ovarian cancers (LGOCs) represent a distinct clinical entity with unique challenges compared to their high-grade counterparts. While characterized by a more indolent course, LGOCs exhibit a high rate of recurrence, often requiring long-term management. Conventional chemotherapy demonstrates limited efficacy in LGOCs, with response rates ranging from 0% to 14%. This disparity likely stems from distinct molecular profiles compared to high-grade cancers, highlighting the need for targeted therapeutic strategies.

## Methods

This case presentation describes the inadvertent off-label use of PARP inhibitors for maintenance therapy in a now 76-year-old LGSC patient.

## Results

A 53-year-old female with initial diagnosis of FIGO III serous papillary ovarian carcinoma underwent debulking surgery and adjuvant carboplatin/paclitaxel. A late-onset recurrence was diagnosed 15 years post-diagnosis, necessitating surgical resection. An R1 resection outcome was achieved. No tumor tissue from either surgery was available for pathological evaluation at the time of presentation to our oncology clinic. Germline testing was negative for *BRCA1/2* mutations. The patient received carboplatin/gemcitabine/bevacizumab at recurrence, followed by carboplatin/pegylated liposomal doxorubicin upon relapse 3.5 years later. Subsequently, stable imaging findings led to maintenance therapy with olaparib, later switched to niraparib due to side effects. A single progressing skin metastasis prompted surgical resection and molecular analysis, revealing LGSC with a molecular profile consistent with LGSC but lacking targetable mutations. As of February 2024, the patient has achieved 3 years of oncologically stable disease on PARP inhibitor

therapy, representing a potential first case of LGSC responsive to this treatment.

### **Conclusion**

Unintended off-label use of PARP inhibitors for maintenance therapy in a patient with LGSC resulted in 3 years of disease stability, suggesting potential efficacy in this population with limited treatment options. Further investigation is warranted to validate this finding and explore its therapeutic potential.

AG01.04

### ***Correlation and prognostic differences of L1CAM and tumor budding in endometrial carcinoma***

C. Neppi<sup>1</sup>, A. Steege<sup>1</sup>, M. M. Anokhina<sup>1</sup>, F. Siegenthaler<sup>2</sup>, S. Imboden<sup>2</sup>, M. D. Mueller<sup>2</sup>, L. Christe<sup>3</sup>, K. Horny<sup>4</sup>, E. Ruchhaeberle<sup>5</sup>, T. Fehm<sup>5</sup>, T. T. Rau<sup>1</sup>

<sup>1</sup>Institut für Pathologie, Universitätsklinikum Düsseldorf, Düsseldorf, Germany, <sup>2</sup>Department für Gynäkologie und Geburtshilfe, Inselspital Bern, Bern, Switzerland, <sup>3</sup>Institut für Gewebemedizin und Pathologie; Universität Bern, Bern, Switzerland, <sup>4</sup>Institut für Medizinische Biometrie und Bioinformatik; Universitätsklinikum Düsseldorf, Düsseldorf, Germany, <sup>5</sup>Klinik für Gynäkologie und Geburtshilfe, Universitätsklinikum Düsseldorf, Düsseldorf, Germany

### **Background**

L1CAM has emerged as an unfavorable biomarker in endometrial carcinoma. In parallel, tumor budding showed evidence to prognostically stratify endometrial carcinoma. In colorectal cancer a link between L1CAM and Tumor budding has been suggested. With this study we want to transfer this correlation to endometrial carcinoma.

### **Methods**

Two cohorts were analyzed: 1) The TCGA cohort with N=468 accessible WSI of endometrial carcinomas and 2) An ngTMA cohort of N= 206 endometrial carcinoma treated with sentinel lymphonodectomy. In both cohorts, all conventional histological parameter have been updated to the current WHO classification. Stromal and intratumoral TIL evaluation, tumor budding, MELF pattern and a distinction between focal and extensive lymphangiosis were gathered. The TCGA cohort received an MSI status update via bio-informatics on the raw data substantially increasing the molecular subtype (previously N=213 cases). L1CAM immunohistochemistry with a cut-off of 10% for positivity was applied on the SLN cohort, whereas the median of L1CAM gene expression served as stratifier for the TCGA cohort. The SLN cohort was molecularly subtyped. Five year follow-up analysis was performed for recurrence-free and overall survival.

### **Results**

A performance screening of selected EMT markers in tumor budding versus no budding within the TCGA cohort revealed L1CAM as highly and significantly upregulated in tumor budding cases. This finding was validated applying L1CAM immunohistochemistry in the SLN cohort. In both cohorts, all conventional histopathological parameter as well as molecular subtyping showed the expected prognostic stratification. Tumor budding and L1CAM expression correlated positively (Spearman  $r=0.233$ ;  $p=0.001$ ), whereas correlations with iTILs and sTILs could not be found. In uni-variate analysis L1CAM outperformed tumor budding with log-rank test in overall survival with  $p=0.007$  versus  $p=0.118$ . In detailed morphological analysis, a substantial part of tumor buds expressed L1CAM.

### **Conclusion**

Tumor budding and L1CAM are functionally linked in endometrial carcinoma. However, L1CAM seems to better stratify endometrial carcinoma prognostically. A more detailed analysis within the molecular subgroups of the cohort is currently ongoing. From a functional perspective L1CAM might antecede tumor budding and contribute to the mechanism of epithelial-mesenchymal-transition (EMT) in endometrial carcinoma.

AG01.05

### ***Interaction of FAP-positive activated fibroblasts and the immune microenvironment of endometriosis***

F. Kellers<sup>1</sup>, U. Lützen<sup>2</sup>, F. Verburg<sup>3</sup>, A. Lebenatus<sup>4</sup>, K. Tesch<sup>4</sup>, V. Stoll<sup>1</sup>, C. Röcken<sup>1</sup>, D. Bauerschlag<sup>5</sup>, B. Konukiewitz<sup>1</sup>

<sup>1</sup>University Hospital Schleswig Holstein, Campus Kiel, Department of Pathology, Kiel, Germany, <sup>2</sup>University Hospital Schleswig Holstein, Campus Kiel, Department of Nuclear Medicine, Kiel, Germany, <sup>3</sup>Erasmus MC, Department of Radiology and Nuclear Medicine,

Rotterdam, The Netherlands, <sup>4</sup>University Hospital Schleswig-Holstein, Campus Kiel, Department Radiology and Neuroradiology, Kiel, Germany, <sup>5</sup>University Hospital Schleswig Holstein, Campus Kiel, Department of Obstetrics and Gynecology, Kiel, Germany

## Background

Endometriosis affects approx. 10 % of women and is defined by endometrium-like tissue growing outside of endometrium and myometrium, often associated with inflammation and fibrosis. Diagnosis is achieved through histology following surgical excision of lesions. The mechanisms underlying the symptoms such as chronic pain and infertility are not completely understood. In the context of endometriosis, activated fibroblasts as found in fibrosis-related pathologies and desmoplastic stroma of solid tumors have not yet been investigated but might contribute to symptoms and immune evasion of endometriotic lesions. They can be identified by expression of fibroblast activation protein (FAP). Moreover, FAP is traceable in PET/CT and thus comprises a potential target for non-invasive diagnostics of endometriosis.

## Methods

We investigated the expression of FAP and its effect on the microenvironment of endometriosis in 232 specimens of a cohort of n = 100 endometriosis patients. FAP expression and the abundance of immune cell subpopulations were detected via immunohistochemistry (IHC) followed by digitalisation of slides and digital image analysis. Tissue within a radius of 500 µm of heterotopic endometrial-like epithelium was analysed. Prussian blue staining for iron was used for age-dating of lesions. Eutopic endometrium and extralesional tissue served as controls. Prior to surgical removal of the lesions, selected patients received both a FAPI-PET/CT and an endometriosis MRI, the latter as an imaging reference method.

## Results

FAP expression was detectable by IHC in the stroma of endometriotic lesions of > 90 % of cases. Using QuPath[1] for digital image analysis, a histoscore (H-score) factoring in staining intensity as well as percentage of positive cells was calculated. Most samples showed marked expression of FAP in the environment of heterotopic endometrium-like tissue. The most intense FAP expression was found in ovarian endometriotic cysts (median H-score: 104). IHC analyses of various immune cell markers were conducted and correlated with FAP expression. FAPI PET/CT of selected cases revealed detectable lesions and was correlated with MRI and IHC results.

## Conclusion

FAP is expressed by activated fibroblasts in the environment of endometriotic lesions. Activated fibroblasts shape the microenvironment of endometriosis and might offer additional non-invasive diagnostic options which is further indicated by comparison of immunohistopathological and imaging results.

Literaturangaben:

[1] Bankhead P, Loughrey MB, Fernandez JA et al., (2017), QuPath: Open source software for digital pathology image analysis, Sci Rep, 16878, 7

# AG Gynäko- und Mammopathologie 2

AG01.06

## ***Breast Cancer Subtyping and Omission of Radiotherapy***

T. Nielsen

University of British Columbia, Department of Pathology & Laboratory Medicine, Vancouver, Canada

Two decades ago, genome-wide expression profiling highlighted the major intrinsic molecular subtypes of breast cancer. While these were not reliably distinguishable by histology, subsequent work developed immunohistochemical surrogates that have helped define the clinical features of Luminal A, Luminal B, HER2E and basal breast cancers. The Luminal A subtype (which can be detected by focussed gene panels including PAM50 as well as by IHC panels including Ki67) is now well-established as a low risk category that does not usually require chemotherapy. Whether this also means that adjuvant radiotherapy may be unnecessary has been an open question, which we addressed in the LUMINA prospective clinical trial. Using a Ki67-based definition of Luminal A, analytically-validated through the International Ki67 Working Group, women in this trial with small Luminal A tumors treated with hormone therapy and breast conserving surgery broke with standard of care by not getting adjuvant radiotherapy. As we reported in the New England Journal of Medicine

in August 2023, this has proven safe. Similar trials using gene expression profiling-based prognostic assays are currently underway; one recently reported early results that confirm our finding: women with low risk ER positive Luminal A type breast cancers, treated with endocrine therapy, do not need adjuvant radiation.

The broader concept that molecular subtypes have features recognizable by pathologists that can guide optimized therapy may also apply to triple negative breast cancers. The basal immune hot subtype of TNBC can be identified using methods developed by the International TIL Working Group, and as we just reported in JAMA (April 2024), early stage TNBC patients with lymphocytic infiltrates can have excellent prognosis even in the absence of chemotherapy. In addition, active research in my laboratory is assessing the more enigmatic mesenchymal subtype of TNBC, where mast cell infiltrates may support use of capecitabine-based chemotherapy.

In summary, while molecular genetic research continues to uncover new details about breast cancer biology, in many cases these result in features pathologists can detect using inexpensive methods that are sufficient to optimize breast cancer therapy for individual women with a high level of evidence.

AG01.07

## ***Prediction of response to neoadjuvant chemotherapy from histopathological slides and clinical data using a transformer-based AI approach***

S. Schulz<sup>1</sup>, M. Eckstein<sup>2</sup>, M. Jesinghaus<sup>3</sup>, C. Glasner<sup>1</sup>, F. Kellers<sup>4</sup>, A. Fernandez<sup>1</sup>, J. N. Kather<sup>5</sup>, D. Truhn<sup>6</sup>, S. Strobl<sup>1</sup>, D.-C. Wagner<sup>1</sup>, W. Roth<sup>1</sup>, C. Denkert<sup>3</sup>, S. Foersch<sup>1</sup>

<sup>1</sup>University Medical Center Mainz, Institute of Pathology, Mainz, Germany, <sup>2</sup>University Hospital Erlangen, Friedrich-Alexander-Universität Erlangen-Nürnberg, Institute of Pathology, Erlangen, Germany, <sup>3</sup>University Hospital Giessen-Marburg, Institute of Pathology, Marburg, Germany, <sup>4</sup>University Hospital of Schleswig Holstein, Campus Kiel, Department of Pathology, Kiel, Germany, <sup>5</sup>Medical Faculty Carl Gustav Carus, Technical University Dresden, Else Kroener Fresenius Center for Digital Health, Dresden, Germany, <sup>6</sup>University Hospital Aachen, Department of Diagnostic and Interventional Radiology, Aachen, Germany

### **Background**

Invasive breast cancer is the most common cancer entity in women with a lifetime prevalence of around 12%. Neoadjuvant chemotherapy can improve the long-term survival of patients and may allow for a de-escalation of surgical intervention towards breast-conserving procedures. Artificial intelligence (AI) methods can be used to develop novel predictive biomarkers for the response to neoadjuvant chemotherapy for breast cancer, which is particularly helpful for intermediate risk cases.

### **Methods**

Several cohorts are used as training, validation and true external test set to ensure generalization of the model. H&E-stained breast biopsy specimens are digitized, and tumor areas are annotated. The proportion of Ki67-positive tumor cells, Her2 status and tumor-infiltrating lymphocytes are determined. Other clinical baseline data such as clinical TNM stage and patient age are also used for an integrated training. Explainable AI methods such as activation maps and image tile markup are additionally deployed.

### **Results**

Preliminary results point to a good prediction capability of pCR, even for an out-of-the-box, end-to-end ViT model pretrained on image net. Features associated with therapy response can also be identified. Usage of a more sophisticated model, a multimodal approach, or an approach based on pathomic features could potentially further improve the prediction accuracy.

### **Conclusion**

In summary, a transformer-based AI approach may identify suitable candidates for NAC treatment, potentially offering a cost- and time-saving alternative to commercial molecular diagnostic multigene panel testing in future diagnostic pathways.

## **Qualitative assessment of histomorphological regression patterns in lymph node metastases in breast cancer patients after NAST – a combined analysis of 373 tumors from neoadjuvant clinical trials**

C. C. Westhoff<sup>1</sup>, B. Brune<sup>1</sup>, C. Solbach<sup>2</sup>, C. Hanusch<sup>3</sup>, M. Örum<sup>1,4</sup>, P. Jank<sup>1</sup>, V. Bjelic-Radicic<sup>5</sup>, M. Reinisch<sup>6</sup>, T. Link<sup>7</sup>, P. Klare<sup>8</sup>, M. Untch<sup>9</sup>, K. Lübke<sup>10</sup>, M. Gleitsmann<sup>1</sup>, K. Rhiem<sup>11</sup>, A. Hartkopf<sup>12</sup>, J. Huober<sup>13</sup>, V. Nekljudova<sup>14</sup>, B. Felder<sup>14</sup>, S. Loibl<sup>14</sup>, C. Denkert<sup>1</sup>

<sup>1</sup>Philipps-Universität Marburg und Universitätsklinikum Gießen und Marburg (UKGM) - Standort Marburg, Institut für Pathologie, Marburg, Germany, <sup>2</sup>Goethe University Frankfurt, University Hospital, Department of Gynecology and Obstetrics, Frankfurt, Germany, <sup>3</sup>Rotkreuzklinikum München, München, Germany, <sup>4</sup>Thoraxklinik Heidelberg, Pneumologie und Beatmungsmedizin, Heidelberg, Germany, <sup>5</sup>University Hospital Helios, University Witten Herdecke, Breast Unit, Wuppertal, Germany, <sup>6</sup>Evangel. Kliniken Essen-Mitte, Essen, Germany, <sup>7</sup>Medical Faculty and University Hospital Carl Gustav Carus, Technische Universität Dresden, Department of Gynecology and Obstetrics, Dresden, Germany, <sup>8</sup>MediOnko-Institut GbR Berlin, Berlin, Germany, <sup>9</sup>Helios Kliniken Berlin-Buch, Berlin, Germany, <sup>10</sup>DIAKOVERE Henriettenstift, Gynäkologie, Hannover, Germany, <sup>11</sup>Universitätsklinikum Köln, Zentrum Familiärer Brust- und Eierstockkrebs, Köln, Germany, <sup>12</sup>AGO Study Group and University Hospital Tübingen, Tübingen, Germany, <sup>13</sup>Kantonsspital St. Gallen, Brustzentrum, Departement Interdisziplinäre medizinische Dienste, St. Gallen, Switzerland, <sup>14</sup>German Breast Group, Neu-Isenburg, Germany

### **Background**

In the setting of neoadjuvant systemic therapy (NAST) of breast cancer (BC), adapting axillary surgery (AS) to response to de-escalate extent of local treatment is recommended. The majority of patients initially diagnosed with node-positive BC exhibit no evidence of residual disease in resected lymph nodes (ypN0). Implementing response to NAST in post-therapeutic AS decreases long-term morbidity among BC patients. The aim of this study is the evaluation of histomorphological regression patterns in post-NAST lymph nodes (LN) with software-assisted image analysis.

### **Methods**

A retrospective, exploratory analysis of patients from multicentric, randomized GBG/AGO trials (G3-4, G6-8) with ypN+ BC and differing NAST schemes was performed. 373 FFPE samples of LN from post-therapeutic AS were available including data for hormone receptor/HER2-status, disease-free survival (DFS) and overall survival (OS). QuPath software was trained on CKMNF-116 stained digitized slides and used to assess LN area, area of vital tumor cells, area of metastasis and proportion of vital tumor cells, fibrosis and necrosis. Proportion of stromal TILs in metastatic tissue was also assessed. Cutoff Finder analysis was performed for continuous parameters with respect to DFS/OS and parameters grouped accordingly. Data were explored for association with DFS, OS and baseline parameters.

### **Results**

Regarding molecular subtype, 256 out of 373 tumors were luminal/HER2-negative (HER2-) (68.6%), 60 HER2+ (16.1%) and 57 triple negative BC tumors (15.3%). Larger area of LN metastasis was significantly associated with worse DFS and OS, the optimal cutoff was 40 mm<sup>2</sup> with hazard ratio (HR) 1.513 [95% CI 1.1-2.079]  $p=0.011$  (DFS) and HR 1.748 [95% CI 1.209-2.528]  $p=0.003$  (OS) for > 40 mm<sup>2</sup> vs. ≤ 40 mm<sup>2</sup> in the overall cohort in univariate Cox regression analysis. Similar results were observed for luminal/HER2- (DFS: HR 1.803 [95% CI 1.196-2.716]  $p=0.005$ , OS: HR 2.054 [95% CI 1.256-3.36]  $p=0.004$ ) and HER2- tumors (DFS: HR 1.629 [95% CI 1.157-2.294]  $p=0.005$ , OS: HR 1.908 [95% CI 1.285-2.833]  $p=0.001$ ). In multivariate Cox regression analysis, larger area of LN metastasis was an independent prognostic factor in luminal/HER2- (DFS:  $p=0.007$ , OS:  $p=0.011$ ) and HER2- tumors (DFS:  $p=0.011$ , OS:  $p=0.005$ ). Similar results were seen for LN area.

### **Conclusion**

Tumor load in nodal metastasis after NACT is associated differentially with prognosis in molecular subtypes. Extent of regression parameters (fibrosis, necrosis) are not similarly relevant for prognosis.

## **Aberrant p53 immunohistochemical staining patterns correlate with differential variant effects of TP53 mutations observed by targeted sequencing (NGS) in HR+HER2- invasive breast carcinoma (NST)**

H. Armbruster<sup>1</sup>, I. Götting<sup>1</sup>, T. Schotte<sup>1</sup>, V. Bahlinger<sup>1</sup>, L.-L. Volmer<sup>2</sup>, D. Dannehl<sup>2</sup>, T. Engler<sup>2</sup>, A. Hartkopf<sup>2</sup>, S. Brucker<sup>2</sup>, I. Bonzheim<sup>1</sup>, F.



Fend<sup>1</sup>, A. Staebler<sup>1</sup>, I. Montes-Mojarro<sup>1</sup>

<sup>1</sup>Universitätsklinikum Tübingen, Pathologie, Tübingen, Germany, <sup>2</sup>Universitätsklinikum Tübingen, Universitäts-Frauenklinik, Tübingen, Germany

## Background

Recent studies have shown that *TP53* mutations are associated with endocrine resistance in hormone receptor positive, HER2 negative breast cancer (HR+HER2-BC). Therefore, a reliable evaluation method for aberrant p53 immunohistochemistry patterns (IHC) as a surrogate for *TP53* mutations is considered of great importance. Building upon a ternary algorithm recently described for gynecologic carcinomas, this study evaluates the suitability of p53 immunostaining as a viable screening tool for *TP53* mutations in early-stage, node-negative HR+HER2-BC (NST). Furthermore, it aims to characterize the histopathological and molecular profiles linked to these mutations.

## Methods

The cohort comprised 85 early-stage breast cancers (pT1-2, N0) diagnosed at our institution between 2010 and 2012, with available core biopsies and resection specimens. Targeted sequencing of *TP53* and *PIK3CA* was carried out using the Ion GeneStudio™ S5 System. IHC assessment of p53 (Novocastra, DO-7) was performed with aberrant staining defined as overexpression (OE), complete absence (CA) and cytoplasmic (CY).

## Results

Cases were categorized as follows: 85 cases; G1: 21, G2: 42, G3: 22. In total, *TP53* mutations were identified in 17 of 80 amplifiable cases (21.3%). Within G1, G2 and G3, *TP53* mutations were found in 0 (0%), 7 (17.9%) and 10 (45.5%) cases, respectively. *TP53*-mutated cases displayed greater nuclear pleomorphism and higher grade, compared to wild-type cases (p=.004). IHC accurately predicted *TP53* mutation in 88.2% of cases with a specificity of 100%. OE, CA and CY patterns were found in 68.8%, 31.3% and 0% of the mutated cases. This finding is consistent with our previous research, which showed an association between the occurrence of the rare CY pattern and the triple-negative subtype. Additionally, there was a notable level of agreement between missense mutations and OE identified by IHC, as well as between truncating mutations and CA (74.6% and 100% agreement, respectively). Mutations in the *PIK3CA* gene were identified in 43 of the 80 cases (53.8%). The frequencies in G1, G2 and G3 were 63.2%, 53.8% and 45.5%, respectively. Notably, there was an association between mutant *TP53* and wildtype *PIK3CA* (Chi-square test, p<0.02).

## Conclusion

Given the increasing clinical importance of *TP53* status in HR+HER2- BC in the context of endocrine resistance, the high concordance with abnormal p53 immunohistochemical staining patterns merits further investigation of p53 IHC as a reliable screening tool in larger case series.

AG01.10

## ***The breast cancer tumor microenvironment in women living with HIV shows an altered CD276/B3-H7 expression and T cell infiltration***

M. Bauer<sup>1</sup>, E. van den Berg<sup>2</sup>, I. dos-Santos-Silva<sup>3</sup>, C. Wickenhauser<sup>1</sup>, M. Joffe<sup>4</sup>, V. McCormack<sup>5</sup>, B. Seliger<sup>6</sup>, E. Kantelhardt<sup>7</sup>

<sup>1</sup>Universitätsmedizin Halle (Saale), Institut für Pathologie, Halle (Saale), Germany, <sup>2</sup>National Health Laboratory Service, Department of Anatomical Pathology, University of the Witwatersrand, Johannesburg, South Africa, <sup>3</sup>London School of Hygiene and Tropical Medicine (LSHTM), Department of Non-Communicable Disease Epidemiology, London, United Kingdom, <sup>4</sup>University of the Witwatersrand, Strengthening Oncology Services Research Unit, Faculty of Health Sciences, Johannesburg, South Africa, <sup>5</sup>International Agency for Research on Cancer (IARC/WHO), Environment and Lifestyle Epidemiology Branch, Lyon, France, <sup>6</sup>Medizinische Hochschule Brandenburg, Institut für Transnationale Immunologie, Brandenburg an der Havel, Germany, <sup>7</sup>Universitätsmedizin Halle (Saale), Global Health Working Group, Halle (Saale), Germany

## Background

There is a growing and ageing population of women living with HIV. The overall breast cancer (BC) related mortality of HIV positive BC patients is higher when compared to HIV negative BC patients. However, it is not known whether the HIV status influences the tumor microenvironment (TME) and if so, whether the altered TME mediates their poorer prognosis.

## Methods

Therefore, in this international, prospective, multicentre study with 296 black BC patients from South Africa and Namibia

was to analyse the TME in patients with known HIV status (HIV positive n=117, HIV negative n=179). Formalin-fixed, paraffin-embedded tumor specimens were analyzed by histomorphology, RNA expression, immunohistochemistry, and multispectral imaging.

### **Results**

HIV positive patients were younger and had more advanced clinical stage than HIV negative BC patients, while no differences in the proportion of hormone receptor and HER2 status were found. In the TME, significantly higher numbers of CD8+ T cells were demonstrated in HIV positive versus HIV negative patients, but the frequencies of CD8+ T cells in the TME did not correlate with CD4+ T cell numbers in the blood. Moreover, a significantly increased expression of CD276/B7-H3 and more pronounced IFN-gamma with higher pStat1 and ISG15 expression, aberrant spatial immune cell distribution and increased T cell exhaustion were found in HIV positive patients that were independent of age, stage, grading and IHC groups.

### **Conclusion**

In conclusion, the impaired T cell response in HIV positive BC patients with significantly increased CD276/B3-H7 and IFN-gamma signaling might contribute to inferior survival and could be used for targeted treatment.

## **Fortbildungsveranstaltung der AG Zytopathologie**

AG02.01

### ***From Cellular Findings to Patient Management in Gynecologic Cytology***

J. Schenck

Institut für Pathologie, Technische Universität München, München, Germany

#### **Hintergrund**

Seit das Zytologie-basierte Zervixkarzinom-Screening in Deutschland 1971 eingeführt wurde, gab es kontinuierlich Maßnahmen zur Qualitätsverbesserung. Seit 2015 werden die zytologischen Screening-Ergebnisse (Münchener Nomenklatur III) und die dazugehörigen histologischen Ergebnisse aller zytologischen Laboratorien als Jahresstatistik bundesweit zusammengeführt. 2020 wurde ein "organisiertes Screening" begonnen (oKFR), das u.a. eine zusätzliche HPV-Untersuchung (Ko-Test) ab dem 35. Lebensjahr im 3-jährigen Abstand inkludiert. Damit wurden für RVO-Patientinnen über 35 Jahre die Kombinationen aus Zytologie-Befund. und HPV-Test Grundlage des Patientenmanagements und teilweise als Algorithmen verpflichtend festgeschrieben (G-BA).

#### **Material und Methoden**

Die Betrachtung beginnt mit der Jahresstatistik von 2019 mit 17.609.082 Untersuchungen von 15.608.413 Frauen [1]. Um die Entwicklung ab 2020 darzustellen, wurden Jahresstatistiken der KV Bayern (2020 bis 2022) herangezogen. Diese Statistiken wurden als Feedback allen zytologischen Laboratorien zur Verfügung gestellt. Daten mit Bezug zu HPV-Ergebnissen liegen nicht vor.

#### **Ergebnisse**

Im Jahr 2019 waren ca. 97,5% der zytologischen Befunde unverdächtig. Nur in ca. 0,364% der Fälle ergaben sich nach der Münchener Nomenklatur III für das Patientenmanagement Maßnahmen, die über zytologische Kontrollen hinausgingen. In der Folgezeit ist die Anzahl der Untersuchungen sehr stark gesunken. Im Bereich von geringergradigen Veränderungen ist es durch HPV Ko-Tests und durch die von Algorithmen vorgegebenen Kolposkopien zu einem massiven Anstieg von Biopsien gekommen, wohingegen bis 2019 der Anteil von Biopsien bei II-p, IIID1 und IIID2 sehr niedrig war. Speziell histologische Ergebnisse mit CIN1 und CIN2 stiegen stark an, mit CIN3 weniger stark. Die Zahl der beim Screening gefundenen Malignome ist dagegen nicht gestiegen.

#### **Schlussfolgerungen**

Die Münchener Nomenklatur III ist seit 2015 voll implementiert, ihre risikoorientierten Empfehlungen wurden anscheinend gut befolgt. Das traditionelle Konzept, Läsionen bis zum Schweregrad einer Gruppe IIID2, einer mäßiggradigen Läsion, eine Gelegenheit zur spontanen Regression zu geben, hat offensichtlich die Anzahl von Biopsien bei nur marginalen Läsionen sehr niedrig gehalten. Wie ein Zervixkarzinom-Screening mit zusätzlicher HPV-Diagnostik ohne starke Überdiagnostik und Übertherapie durchgeführt werden kann, ist derzeit nicht absehbar.

Literaturangaben:

[1] Schenck, U., Hantschke-Zerbich, H., Woellner, F., Michel, F., (2023), Evaluations of the 2019 Annual Statistics Under the Cervical Cytology Quality Assurance Agreement 2019 Annual Statistics for Cervical Cytology from 15608413 Women, Thieme Verlag, Geburtshilfe Frauenheilk, Stuttgart

AG02.02

## ***Experiences from the First Cycle of Co-Testing Cytology/HPV and with Digital Cytology***

H. Ikenberg

CytoMol MVZ für Zytologie und Molekularbiologie, Frankfurt, Germany

Seit 2020 ist in der Zervixkarzinomprävention der GKV bei Frauen >35 Jahren statt jährlicher konventioneller Zytologie eine Co-Testung HPV/Zytologie (mit LBC als Option) der Boa\_Image\_Frame. Bei Auffälligkeiten wird nach vorgegebenen Algorithmen abgeklärt, welche bereits bei geringgradigen Veränderungen eine Kolposkopie vorsehen. In diesem Vortrag werden die zytologischen und histologischen Befunde eines großen Routinelabors in der primären Prävention 2020/21 mit denen aus 2018/19 verglichen. 2018/19 waren dies 650.600 (konventionelle) zytologische und 1.804 histologische Befunde, 2020/21 491.450 zytologische (alle LBC mit Computerassistenz [CAS] und HPV-Testung) und 7.156 histologische Befunde.

2020/21 gab es bezogen auf alle vorhergehenden Zytologien 5,2x mehr histologische Befunde als 2018/19, 10,6x mehr Biopsien, 3,8x mehr Konisationen und 1,2x mehr Hysterektomien. Besonders stark nahm die Abklärung niedriggradiger oder nur HPV-positiver Befunde zu. Mit der Co-Testung wurden 12,7x mehr CIN 1, 6,5x mehr CIN 2 und 3,2x mehr CIN 3 diagnostiziert. Biopsien ohne Dysplasie waren 7,6x häufiger als zuvor. Zervixkarzinome wurden 1,8x mehr und Endometriumkarzinome 0,7x weniger diagnostiziert.

Mit der Co-Testung wurden mehr CIN gefunden, aber die Zunahme der histologischen Befunde niederen Grades oder ohne Dysplasie war weit stärker als jene der CIN 3. Nicht therapiepflichtige Läsionen machten 2020/21 zusammen 94,4 % der Biopsieergebnisse aus. Der Einsatz von Progressionsmarkern könnte dieses Mißverhältnis reduzieren.

Bisher gibt es nur wenige Publikationen zu drei Systemen der digitalen Zytologie. Alle wenden Techniken der künstlichen Intelligenz auf Dünnschichtpräparaten der Zervix an. Mit der US-amerikanischen FDA-Zulassung des Genius™-Systems von Hologic (Berlin, Deutschland) zeichnet sich ab, daß dieses zum Boa\_Image\_Frame in der Zervixzytologie werden könnte. Neben dem Potential zu höherer Sensitivität und Spezifität ergibt sich hier die Möglichkeit zur ortsübergreifenden Kooperation. Die kürzere Screeningzeit wird durch einen höheren technischen Aufwand erkaufte.

Wir haben das Genius™-System in einer ersten Studie mit dem bisherigen Topstandard LBC mit CAS verglichen. 1994 Präparate, (mit 555 Histologien) aus dem ersten Jahr der Co-Testung wurden verblindet untersucht. Je nach Kriterien lag die Übereinstimmung zwischen 86,5% und 97,3%. Signifikant mehr Fälle höheren Schweregrades wurden gefunden. Erste Erfahrungen mit der Routineanwendung werden berichtet.

## **AG Hämatopathologie 1**

AG03.01

### ***High expression of ADAM family members is associated with progressive disease and proliferation signaling in MM.***

M. Evers<sup>1</sup>, T. Stühmer<sup>2</sup>, R. C. Bargou<sup>2</sup>, A. Rosenwald<sup>1</sup>, E. Leich<sup>1</sup>

<sup>1</sup>Institute of Pathology, University of Wuerzburg, Wuerzburg, Germany, <sup>2</sup>Comprehensive Cancer Center Mainfranken, University Hospital of Wuerzburg, Wuerzburg, Germany

#### **Background**

Multiple myeloma (MM) is an incurable hematological malignancy. Despite major advances in treatment, nearly all patients still eventually relapse, underlining the persisting need for novel therapeutic targets. We have previously shown that high gene expression (GE) of *ADAM8*, *9* and *15* are adverse prognostic markers in MM. This study therefore aimed to elucidate the functional role of these ADAMs in MM to examine their potential to serve as therapeutic targets in more detail.

## Methods

RNA sequencing (RNA-Seq) was performed for 73 primary MM samples. GE of *ADAM8*, *9* and *15* was compared between samples from patients with and without extramedullary disease (EMD) at time of biopsy using the Mann-Whitney U test. Using the same statistical test, MYC protein expression (previously determined by immunohistochemistry) was compared between samples with high and low expression of *ADAM8*, *9* and *15*, respectively. In the MMRF RNA-Seq dataset (CoMMpass IA15 cohort), expression of *ADAM8*, *9* and *15* was compared between baseline samples and samples obtained at a state of progressive disease from each respective patient (n=59) using the Wilcoxon test. siRNA knockdowns (kd) of *ADAM8*, *9* and *15* were performed in 5-7 human myeloma cell lines (HMCL) and the effect on downstream signaling assessed by western blotting and RNA-Seq. Differentially expressed genes (RNA-Seq) were analyzed using DESeq2 in R and gene set enrichment analysis (GSEA) using GSEA4.3.2 (Broad Institute).

## Results

*ADAM8*, *9* and *15* were upregulated in samples from patients with EMD compared to those with no EMD in our cohort. *ADAM8* and *ADAM15* were upregulated in samples taken at progressive disease compared to the baseline samples in the MMRF cohort. GSEA revealed an enrichment of several gene sets associated with proliferation signaling in *ADAM8/9/15*<sup>high</sup> samples in both cohorts and siRNA kd experiments. Commonly used proliferation markers were significantly upregulated in the *ADAM8/9/15*<sup>high</sup> samples in both RNA-Seq datasets. Furthermore, MYC protein expression was significantly higher in the *ADAM8*<sup>high</sup> and *ADAM15*<sup>high</sup> samples from our cohort. *ADAM8* siRNA kd downregulated IGF1R expression (4/5 HMCL) and activation (2/5) as well as pAKT levels (3/5). *ADAM9* kd reduced pmTOR (2/7) and ITGAV (3/7) expression. *ADAM15* kd reduced MYC expression (1/7 HMCL).

## Conclusion

*ADAM8*, *9* and *15* appear to play a role in MM progression and to regulate important proliferation signaling pathways, underlining their potential to serve as novel therapeutic targets in MM.

AG03.03

## ***Neuropilin-2 in mesenchymal stromal cells as a druggable target in myelofibrosis***

K. Vosbeck<sup>1</sup>, T. Mayr<sup>1</sup>, S. Förster<sup>1</sup>, O. Al-Adilee<sup>1</sup>, S. Bisht<sup>2</sup>, A. Sahu<sup>3</sup>, S. Nestic<sup>3</sup>, E.-M. Haddouti<sup>4</sup>, R.-M. Körber<sup>2</sup>, M. H. Muders<sup>1</sup>, A. Bunes<sup>3</sup>, F. Schildberg<sup>4</sup>, G. Kristiansen<sup>1</sup>, I. Gütgemann<sup>1</sup>

<sup>1</sup>Universitätsklinikum Bonn/Institute of Pathology, Bonn, Germany, <sup>2</sup>Universitätsklinikum Bonn/Department of Medicine III, Bonn, Germany, <sup>3</sup>Universitätsklinikum Bonn/Institute of Medical Biometry, Informatics and Epidemiology, Bonn, Germany,

<sup>4</sup>Universitätsklinikum Bonn/Clinic for Orthopedics and Trauma Surgery, Bonn, Germany

## Background

Progressive bone marrow (BM) fibrosis in myeloproliferative neoplasm (MPN), myelodysplastic syndromes (MDS), MPN/MDS overlap syndromes and acute myeloid leukemia (AML) is associated with poor prognosis and early treatment failure. Myelofibrosis is accompanied by reprogramming of multipotent bone marrow mesenchymal stromal cells (MSC) into osteoid and fibre-producing stromal cells. Neuropilin-2 (NRP2) inhibition is a clinically druggable target in pulmonary fibrosis.

## Methods

Histology, Immunohistochemistry, scRNAseq data analysis, murine transgenic and knockout models, CRISPR/Cas9 knockout in MC3T3E1 pre-osteoblasts, mineralization assays.

## Results

We demonstrate NRP2 and osteolineage marker NCAM1 (neural cell adhesion molecule 1) expression within the endosteal niche in normal bone marrow and aberrantly in MPN, MDS, MPN/MDS overlap syndromes and AML (n=99), as assessed by immunohistochemistry. Increased and diffuse expression in mesenchymal stromal cells (MSC) and osteoblasts correlated with high myelofibrosis (MF) grade in MPN ( $p_{NRP2} < 0.05$ ,  $p_{NCAM1} < 0.05$ ) and NRP2 and NCAM1 correlate directly ( $p < 0.005$ ). ScRNAseq re-analysis demonstrated NRP2 expression in endothelial cells and partial co-expression of NRP2 and NCAM1 in normal bone BM MSC and osteoblasts. Potential ligands included transforming growth factor  $\beta$ 1 (TGF $\beta$ 1) from osteoblasts and megakaryocytes. Murine ThPO and JAK2<sup>V617F</sup> myelofibrosis models

showed co-expression of *Nrp2* and *Ncam1* in osteolineage cells, while fibrosis-promoting MSC only express *Nrp2*. *In vitro* experiments with MC3T3-E1 pre-osteoblasts and analysis of *Nrp2*<sup>-/-</sup> mouse femurs indicated that *Nrp2* is functionally involved in osteogenesis.

### Conclusion

Further studies are needed to assess the result of NRP2 inhibition in myeloid neoplasms *in vivo*. In summary, NRP2 represents a novel druggable target in patients with myelofibrosis.

AG03.04

## ***Altered IFN-gamma signaling remodels the bone marrow tumor microenvironment in MPN and is associated with disease progression***

M. Bauer<sup>1</sup>, A. Wilfer<sup>1</sup>, H. K. Al-Ali<sup>2</sup>, B. Seliger<sup>3</sup>, C. Wickenhauser<sup>1</sup>

<sup>1</sup>Universitätsmedizin Halle (Saale), Institut für Pathologie, Halle (Saale), Germany, <sup>2</sup>Universitätsmedizin Halle (Saale), Krukenberg Krebszentrum, Halle (Saale), Germany, <sup>3</sup>Medizinische Hochschule Brandenburg, Institut für Transnationale Immunologie, Brandenburg an der Havel, Germany

### Background

Constitutive activation of the Janus kinases and signal transducer and activator of transcription (JAK/STAT) signaling pathway is crucial in disease initiation and progression of myeloproliferative neoplasm (MPN). However, its' interaction with altered interferon (IFN)-gamma signaling has not been analyzed in detail yet.

### Methods

Therefore, publicly RNA expression data of MPN samples, human *JAK2* V617F mutated HEL and SET-D2 cell lines and 152 bone marrow biopsies (BMB) of MPN patients with known treatment and survival were analyzed for components of the IFN-gamma signaling pathway and compared with 50 non-neoplastic BMBs.

### Results

Publicly datasets showed an activation of IFN-g signaling in MPN diseases when compared with HC. Moreover, this activation was independent of IFN-g expression in HEL and SET-D2 cells *in vitro*. MPN BMBs showed a heterogeneous expression of components of IFN-g signaling that was associated with the local immune cell infiltration in the TME, as well as the expression of human leukocyte antigens class I molecules (HLA) and immune checkpoint expression (ICP). IFN-g signaling correlated with higher numbers of CD8<sup>+</sup> T cells and a closer proximity of T cell subpopulations, that all demonstrated to be favorable prognostic factors in these patients. However, in the course of disease a more pronounced myelofibrosis correlated with impaired IFN-g signaling and aberrant immune cell infiltration, while Stat3 signaling was unaffected.

### Conclusion

In conclusion, we found an increasing alteration of both, IFN-gamma signaling and the local BM TME within the course of the disease that was associated with the degree of myelofibrosis and patients' survival.

AG03.05

## ***Histomorphological Spectrum of Nodal Marginal Zone Lymphoma***

F. Spada<sup>1</sup>, A. Fürstberger<sup>1</sup>, A. Rosenwald<sup>2</sup>, W. Klapper<sup>3</sup>, G. Ott<sup>4</sup>, N. T. Gaisa<sup>1</sup>, P. Möller<sup>1</sup>, T. F. E. Barth<sup>1</sup>

<sup>1</sup>Universitätsklinikum Ulm, Pathologie, Ulm, Germany, <sup>2</sup>Julius-Maximilians-Universität Würzburg, Pathologie, Würzburg, Germany, <sup>3</sup>University Hospital Schleswig-Holstein, Department of Pathology, Hematopathology Section and Lymph Node Registry, Kiel, Germany, <sup>4</sup>Robert-Bosch-Krankenhaus, and Dr. Margarete Fischer-Bosch Institute of Clinical Pharmacology, Department of Clinical Pathology, Stuttgart, Germany

### Background

Primary nodal marginal B cell lymphoma (nMZoL) is rare and its patterns of lymph node involvement are as variable as its cytomorphology. In the case of large cell cytology, the distinction between nMZoL and nodal diffuse large B cell lymphoma (nDLBCL) is an unsolved problem in daily routine. To this end, we contributed 89 nMZoL and 47 nDLBCLs cases. Our aim was to establish routinely useable parameters to help recognizing large cell nMZoL and excluding nDLBCL.

## Methods

For the growth pattern, we adopted the definitions of Salama et al. (2009). Lymph follicles were characterized morphologically and by means of CD21 immunostaining highlighting the follicular dendritic cells (FDC). IgD expression status was scored with an immunohistochemical stain. The KI-67 proliferation rate was determined by estimating the percentage of KI-67-positive neoplastic cells. For the morphometric analysis a high-resolution representative picture was acquired from the hematoxylin eosin staining of each lymphoma sample. For each picture the diameter of 30 cells and their nuclear diameter was measured. With centroblasts as a reference for the largest normal B cell we defined the labels “small”, “large” and “abnormally large” for both measurements. The same procedure was followed for the nDLBCL cohort.

## Results

nMZoLs grew mostly interfollicular, nDLBCL cases mostly had a diffuse growth pattern. In nMZoL colonized follicles were prevalent; in nDLBCL there was a very strong prevalence of complete effacement of the follicle and its FDC network. The compression of the FDC network was exclusive to nMZoL. The 51% IgD positivity rate in nMZoL as opposed to the 17% in nDLBCL may also serve as an ancillary indicator. nMZoL covered the whole range of proliferation, while nDLBCL cases showed the highest proliferation rate (KI-67>40%) in all cases except one. Morphometric analysis showed that cases with abnormally large cells and nuclei are most likely to be a nDLBCL and a lymphoma can be identified as nMZoL if the cell and nuclear size are smaller than 10.5  $\mu\text{m}$  and 7.7  $\mu\text{m}$  respectively.

## Conclusion

We generated an operational tool with techniques already available in routine pathology practice to help recognize large cell nMZoL and exclude nDLBCL and composed a decision tree (CyclinD1, CD10, morphometrics) followed by an evaluation of ordinal or continuous scale parameters (growth pattern, follicular colonization, FDC network, IgD, KI-67) and a final majority vote if these parameters fall under the non-decisive value ranges.

AG03.06

## ***Improving the diagnosis, therapy and understanding of severe blood diseases with AI***

C. Marr

Helmholtz Zentrum München - German Research Center for Environmental Health, Institute of AI for Health, Neuherberg, Germany

### Background

The use of AI for the diagnosis of diseases has led to the new research field of computational pathology. With the availability of increasingly comprehensive data sets and powerful computer capacities, the application possibilities are also becoming ever broader.

### Methods

The use of modern deep neural networks and pre-trained foundation models allows accurate classification of individual cells, tissues and patients. In addition, the composition of human tissue can be analyzed in high resolution using single-cell transcription atlases. Finally, mathematical models allow the incorporation of prior biomedical knowledge and the processing of smaller data sets.

### Results

We show how supervised learning can be used to classify diseases in blood smears for which there was previously no clear morphological indication. The use of vision/text models allows a description of pathological patterns close to that of experts. Finally, we show how mathematical models can be used to describe the kinetics of blood stem cells.

### Conclusion

Despite the impressive successes of computational pathology, there are still many hurdles to the application of AI in real medicine. These include, in particular, dealing with the natural diversity of diseases and patients and the technical integration of prior knowledge into machine learning models.

## ***FDC network in human lymph nodes: structure and function based on 3D confocal microscopy***

H. Schäfer<sup>1</sup>, E. C. Hemming<sup>2</sup>, M.-L. Hansmann<sup>3</sup>, P. Wurzel<sup>3</sup>, S. Scharf<sup>1</sup>

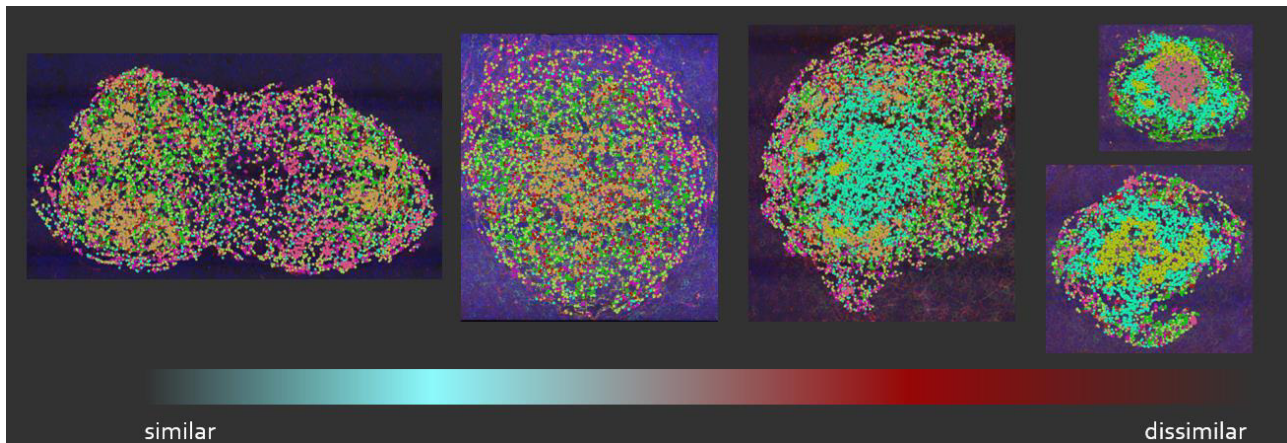
<sup>1</sup>Dr. Senckenbergisches Institut für Pathologie, Universitätsklinikum Frankfurt, Frankfurt am Main, Germany, <sup>2</sup>Universitätsklinikum Frankfurt, Frankfurt am Main, Germany, <sup>3</sup>Institut für Allgemeine Pharmakologie und Toxikologie, Frankfurt am Main, Germany

### **Background**

The human immune response, a complex and decentralized system, protects us effectively against many pathogens. Follicular dendritic cells (FDCs) take part in the defense in the germinal center (GC) reaction. Our working hypothesis is that the structure of the FDC network and their cell morphology contain detailed information about the condition of the GC and functional capabilities, e.g., when malignant cells alter the microenvironment.

### **Methods**

Thick sections of human lymph node stained for the three FDC marker CD21, CD23 and CD35 were digitized with a confocal microscope. We applied a computer vision pipeline to transfer the raw voxel data to graphs. By testing multiple graph properties and descriptors for the FDC structure, we selected a set of features to describe different regions in the GC.



FDC networks of multiple germinal centers ordered by similarity. Colored nodes visualize the different network structures. To connect FDC structure and biological function additional double immune stains were investigated. A correlation analysis of CD3 and FDC revealed that T cells prefer and avoid certain FDC structures. Contact areas of T cells and FDCs were computed and compared for reactive and neoplastic cases.

### **Results**

The graph analysis visualizes also structural differences in the FDC network. Similarity or dissimilarity of GCs can be measured by the outcome of the FDC clustering. The positions of T cells in the FDC network, based on CD3 staining, were highly correlated with FDC structure. Two of the FDC structures were positively correlated with T cells, while two clusters were negatively correlated. The contact areas of T and FDC cells were significantly higher in AITL cases compared to FL and Lymphadenitis cases.

### **Conclusion**

A computer vision pipeline was established to enable the analysis of FDC networks based on graphs. We could determine structural different areas within the GC and by including additional immune markers the correlation between FDC structure and biological function becomes visible. T cells preferably are located at certain network structures, which may indicate that FDC network structure and biological function are closely related. We started to expand the approach for macrophages and will investigate additional cell markers in future.

AG03.08

### ***The three-dimensional landscape of reactive and neoplastic human lymph nodes***

V. J. Diederich<sup>1</sup>, S. Scharf<sup>1,2</sup>, H. Schäfer<sup>1</sup>, M.-L. Hansmann<sup>1,3</sup>, P. Wurzel<sup>1</sup>

<sup>1</sup>Goethe-Universität Frankfurt, Allgemeine Pharmakologie und Toxikologie, Frankfurt am Main, Germany, <sup>2</sup>Goethe-Universität Frankfurt, Molekular Bioinformatik, Frankfurt am Main, Germany, <sup>3</sup>Frankfurt Institute for Advanced Studies, Frankfurt am Main, Germany

#### **Background**

An adaptive immune response is always accompanied by a shift in cellular composition in the lymph node. Lymph nodes are compartmentalized and subdivided into functional subunits. The type of shift in cellular composition is determined by the function of the compartment. After an immune reaction, the balance within the compartments is restored. However, the occurrence of a tumor leads to an irreversible shift in the cellular composition. This work aimed to quantitatively describe reactive shifts of cellular balances and to contrast these with neoplastic conditions.

#### **Methods**

This work was based on 3D fluorescence images of thick sections of human lymph nodes. These are stained for alpha-actin to visualize fibroblastic reticulum cells (FRC) and another stain to visualize dendritic cells, macrophages, T- and B-cells. The data set includes tissue samples with diagnosed lymphadenitis (8 cases), nodular sclerosis classical Hodgkin lymphoma (5 cases), mixed cellularity classical Hodgkin lymphoma (5 cases), follicular lymphoma (7 cases), and diffuse large B-cell lymphoma (2 cases).

#### **Results**

Based on the structure of the FRC, we defined the compartments of the lymph node. Within these compartments, we determined the respective cell volume. Furthermore, three-dimensional visualization allowed us to identify fully enclosed extracellular vesicles. Based on this we were able to define the three-dimensional landscape of the lymphoid compartments.

In the course of tumorigenesis, the compartmentalization of the lymph node is progressively abolished. This is accompanied by structural changes in the FRC network. Despite this ongoing destruction, distinct regions within the tumor tissue are still visible. These can be mostly subdivided into FRC-free, follicle-like compartments and FRC-rich, T-zone-like compartments.

A comparison of reactive and neoplastic analogues reveals a progressive cellular homogenization of the tissue. In addition, higher masses of CD68<sup>+</sup> macrophages and CD8<sup>+</sup> T cells were found under neoplastic conditions. Finally, an increased occurrence of vesicles was found in all neoplasms.

#### **Conclusion**

This three-dimensional landscape of reactive lymph nodes and the elucidated specific changes in various neoplasias may contribute to a holistic understanding of neoplastic alterations in the future.

AG03.02

### ***CD70/CD27 Signaling Promotes the Expansion of Clonal Plasma Cells in Multiple Myeloma and Is a Promising Therapeutic Target in Advanced Disease***

S. Forster<sup>1</sup>, C. Bachmann<sup>2</sup>, M. Boy<sup>2,3</sup>, R. Radpour<sup>2,3</sup>, C. Schuerch<sup>4</sup>, F. Bruehl<sup>5</sup>, F. Fend<sup>4</sup>, C. Riether<sup>2,3</sup>, A. Ochsenbein<sup>3</sup>

<sup>1</sup>Institute of Pathology, Technical University of Munich, Munich, Germany, <sup>2</sup>University of Bern, Department for Biomedical Research, Bern, Switzerland, <sup>3</sup>University Hospital of Bern, Bern, Switzerland, <sup>4</sup>Department of Pathology and Neuropathology, University Hospital Tübingen, Tübingen, Germany, <sup>5</sup>From Robert J. Tomsich Pathology and Laboratory Medicine Institute, Cleveland Clinic, Cleveland, United States of America

#### **Background**

Multiple Myeloma (MM) is a hematological cancer characterized by the expansion of malignant plasma cells within the bone marrow (BM). In the last decade, substantial advances in the treatment of MM patients have been made resulting in improved progression-free and overall survival rates. However, to date, MM still remains incurable. Physiologically, the CD70/CD27 interaction is involved in the regulation of immune cell expansion. Aside, CD70 and CD27 co-expression has been described on leukemic stem cells (LSC) in acute myeloid leukemia patients where the autonomous signaling activation drives LSC self-renewal and expansion. In contrast, only little is known about its impact on myelomagenesis



and MM progression.

## Methods

CD70 and CD27 gene expression levels and its correlations with overall survival (OS), MM progression and high-risk molecular alterations were evaluated using different databases (CoMMpass IA15, GSE6477). CD70 and CD27 protein expression patterns were analyzed in a newly established MM tissue microarray (TMA) and a collection of matched BM samples from initial and advanced disease stages (in collaboration with the Institutes of Pathology in Bern, Basel and Tübingen). For functional studies, CD70 knock-out MM cell lines and patient-derived xenografts (PDX) were generated or CD70 signaling was blocked using different monoclonal antibody constructs.

## Results

High CD70 gene expression levels correlate with increased *MKI67* gene expression and elevated lactate dehydrogenase serum levels indicating a more rapid proliferation of CD70-expressing myeloma cells. In addition, high CD70 expression in MM patients correlated with shorter OS. Longitudinal analyses of CD70 gene expression in the precursor stages monoclonal gammopathy of undetermined significance and smoldering myeloma as well as MM and relapsed MM stages showed highest CD70 gene expression levels in relapsed MM patients. Functionally, we found that CD70/CD27 signaling promotes plasma cell survival inducing the expansion of MM cell lines and primary malignant plasma cells. CD70 blockade or CD70 knock-out resulted in a significant inhibition or complete abrogation of growth of CD70-expressing MM cell lines and patient-derived xenografts.

## Conclusion

Our results indicate that CD70-expressing MM cells propagate the disease. Targeting CD70 is a promising new therapy especially in advanced disease stages.

# AG Hämatopathologie 2

AG03.09

## ***The Tumor Genome of the future - from a bioinformatics perspective***

T. Rausch

European Molecular Biology Laboratory (EMBL), GeneCore, Heidelberg, Germany

Recent technological advances in long-read sequencing have led to human telomere-to-telomere assemblies and the release of the first 47 high-quality human genome assemblies by the Human Pangenome Reference Consortium (HPRC) have enabled the construction of graph-based reference genomes. This talk will discuss potential future approaches for cancer genome analysis that, instead of short-reads and linear reference genomes like GRCh38, use long-reads and graph-based pangenome references to guide disease variant prioritization. The genetic and epigenetic information available through long reads will be an important pillar of future multimodal tumor genomes to ultimately enable precision medicine in cancer.

AG03.10

## ***Targeted panel sequencing for refining B cell lymphoma diagnosis: A real-life, reference center experience***

J. Böck<sup>1</sup>, K. Maurus<sup>1</sup>, K. Kurz<sup>2</sup>, G. Ott<sup>2</sup>, I. Anagnostopoulos<sup>1</sup>, S. Brändlein<sup>1</sup>, A. Rosenwald<sup>1</sup>, A. Zamo<sup>1</sup>, E. Gerhard-Hartmann<sup>1</sup>

<sup>1</sup>Institute of Pathology, University of Würzburg, Würzburg, Germany, <sup>2</sup>Robert-Bosch-Krankenhaus, Department of Clinical Pathology, Stuttgart, Germany

## Background

Diagnosis of one of the many types of B-cell lymphoma (BCL) currently requires an integrated approach comprising morphological expertise, immunophenotyping and the incorporation of clinical data, but may also include flow cytometry, cytogenetics and clonality analysis. In recent years, several studies have defined the mutational landscape of BCLs, which may also serve as a complementary diagnostic tool.

We have developed a custom NGS panel for the routine diagnostics of BCL based on available literature and our own

diagnostic questions. The panel was designed to i) provide high informative value relative to cost, ii) include mutations with diagnostic or prognostic value, iii) ensure rapid turnaround time, and iv) allow the analysis of individual samples. We have applied this panel to challenging cases in our routine work in order to obtain further diagnostic support.

## Methods

The panel contained 40 genes selected based on specific criteria, such as entity-specific mutation frequencies, minimization of co-mutated genes, inclusion of recurrent hotspots, and functional domains. Library preparation was performed using the Ion AmpliSeq Library Kit Plus chemistry and sequencing was performed on the Ion GeneStudio S5 Plus System. Data were analyzed using the Torrent Suite and the Ion Reporter Software (Thermo Fisher). A total of 151 cases were analyzed, comprising 135 BCL and 16 cases, in which a differential diagnosis between a reactive condition and a BCL was considered.

## Results

Evaluable results were obtained in all sequenced cases, although fixation artefacts were present in 3 cases. Diagnostically informative molecular genetic profiles were identified in 72% of cases. Focusing on challenging cases with the differential diagnosis of Burkitt's lymphoma (BL) and diffuse large B-cell lymphoma (DLBCL), we detected at least one mutation in all cases. In 1 out of 14 cases, the diagnosis was changed based on the mutation profile, and in all other cases, panel sequencing provided significant decision support.

## Conclusion

We have successfully applied a custom NGS panel to 151 cases of BCL and samples with this differential diagnosis. Although morphology and immunohistochemistry remain the backbone of diagnosis, panel sequencing provided substantial diagnostic assistance supporting the correct diagnosis in many cases. It was particularly useful in resolving the differential diagnosis between BL and DLBCL in challenging cases.

AG03.11

## ***In-depth molecular profiling of predominantly diffuse follicular lymphoma***

K. S. Kurz<sup>1</sup>, S. Kalmbach<sup>1,2</sup>, A. Zamo<sup>3</sup>, E. Leich<sup>3</sup>, A. Rosenwald<sup>3</sup>, G. Ott<sup>1</sup>, H. Horn<sup>1,2</sup>

<sup>1</sup>Abteilung für Klinische Pathologie, Robert Bosch Krankenhaus, Stuttgart, Germany, <sup>2</sup>Dr. Margarete Fischer-Bosch-Institut für Klinische Pharmakologie, Stuttgart, Germany, <sup>3</sup>Pathologisches Institut, Würzburg, Germany

## Background

Lymphomas with an entirely or predominantly diffuse growth pattern (DFL) are rare. WHO-HAEM5 regards DFL as related to classical FL because of their overlapping cytological features, however showing varying immunophenotypic and genetic characteristics. A systematic evaluation of a larger DFL cohort, especially taking into account also *BCL2* translocation-negative localized (IFL) and systemic FL (sFL) with follicular growth pattern, are missing.

## Methods

To gain detailed insights into the underlying genetic profile, 75 DFL were systematically analyzed by immunohistochemistry (CD5, CD10, CD23, *BCL2*, Ki67), fluorescence in situ hybridization (FISH) (*BCL2* and *BCL6* break-apart), somatic copy number analysis (SCNA) and NGS-based targeted re-sequencing, and compared to follicular *BCL2* translocation-negative IFL and sFL with SCNA and whole exome sequencing (WES) data (Kalmbach et al. 2023<sup>1</sup>).

## Results

SCNA data were available from 68 DFL, 73 *BCL2* translocation-negative follicular IFL and 6 sFL. In general, similar SCNA profiles of DFL, *BCL2* translocation-negative IFL and sFL were observed without significant changes in the frequency of deletions. However, in DFL a significantly higher proportion of samples harboured gains of chromosome 9q. Deletions in chromosome 1p36 were evident in 14 cases (14/68, 21%).

The mutational landscape of DFL was comparable to that of *BCL2* translocation-negative follicular IFL and sFL with mutations in *CREBBP*, *STAT6*, *BCL2*, *TNFRSF14*, *IGLL5*, *KMT2D* and *EZH2* being among the most frequent mutated genes. Mutations in the *BCL2* gene were more frequently detected in *BCL2* translocation-positive DFL, while *STAT6* mutations were predominantly found in *BCL2* translocation-negative DFL. In addition, mutations in the *PDXDC1* gene were observed in 25% of DFL that hitherto have not been described in follicular IFL and sFL.

## Conclusion

Considering the deletion status of chromosome 1p, mutations of *STAT6*, *EZH2* and *PDXDC1* were enriched in samples without deletion, while *TNFRSF14*, *IGLL5* and *BCL2* mutations accumulated in DFL with 1p deletions.

AG03.12

## **Targeted genomic sequencing of Epstein-Barr virus-positive inflammatory follicular dendritic cell sarcomas in comparison to classic follicular dendritic cell sarcomas**

S. Schelbert<sup>1</sup>, K. Maurus<sup>1</sup>, G. Ott<sup>2</sup>, K. Kurz<sup>2</sup>, G. Kristiansen<sup>3</sup>, S. Roth<sup>1</sup>, S. Gramlich<sup>1</sup>, I. Anagnostopoulos<sup>1</sup>, A. Rosenwald<sup>1</sup>, E. Gerhard-Hartmann<sup>1</sup>

<sup>1</sup>Institute of Pathology, University Würzburg, Würzburg, Germany, <sup>2</sup>Robert-Bosch-Krankenhaus, Department of Clinical Pathology, Stuttgart, Germany, <sup>3</sup>Institute of Pathology of the University Hospital Bonn, Bonn, Germany

## Background

Follicular dendritic cell sarcoma (FDCS) is a rare neoplasm of low to intermediate malignancy arising from follicular dendritic cells in extranodal and nodal sites. The even rarer Epstein-Barr virus (EBV)-positive inflammatory FDC sarcomas (IFDCS) also show FDC differentiation but are almost exclusively located in the spleen or liver. Due to their rarity, little is known about the molecular basis of these neoplasms (for overview see [1]).

We analysed 25 samples from 23 patients using next-generation sequencing to better understand the genetic makeup of these uncommon tumours.

## Methods

We investigated 13 samples from 11 patients diagnosed with FDCS and 12 samples from patients diagnosed with EBV-positive IFDCS. DNA and RNA were extracted from formalin-fixed paraffin-embedded tissue (FFPE). Libraries were generated using the TruSight Oncology 500 DNA/RNA High-Throughput Assay (Illumina) and sequenced on the NovaSeq 6000 (Illumina).

Bioinformatic analyses of small variants, copy number variations, fusions, tumor mutational burden and microsatellite status were performed using the Dragen Bio-IT platform (Illumina) and a custom pipeline.

## Results

Mutational profiling of FDCS revealed oncogenic alterations in several signaling pathways including TP53 and NFκB signaling as well as cell cycle regulation and epigenetic modification. The most recurrent alterations were identified within the NFκB signaling pathway, but only in FDCS (4 out of 12 patients). TP53 mutations were found in 2 patients with FDCS and in one patient with EBV-positive IFDCS. All analysed samples were fusion negative. The tumour mutation burden tended to be higher in FDCS (mean: 5.6 mutations per Mb, median: 2.5 mutations per Mb) than in EBV-associated IFDCS (mean: 2.66 mutations per Mb, median: 0.4 mutations per Mb). The same trend was observed with copy number variations (CNV).

## Conclusion

In the here investigated cohorts of FDCS and EBV-positive IFDCS, the genetic landscape is heterogeneous. However, unifying alterations within prominent oncogenic pathways were identified in FDCS, whereas fewer alterations were observed in the latter. By comprehensive analysis of this well-characterized case series, we aim to further elucidate the biological basis of these very rare neoplasms.

Literaturangaben:

[1] Facchetti F, Simbeni M, Lorenzi L, (2021), Follicular dendritic cell sarcoma, *Pathologica*, 316-329

# AG Herz-, Gefäß-, Nieren- und Transplantationspathologie

AG04.01

## **Cardiac transplantation: the role of pathology**

J. Wohlschläger

Cardiac transplantation is an established treatment for terminal chronic heart failure resistant to medical treatment. Although histomorphological diagnosis and grading of various forms of rejection is a main task, the role of pathology in the setting encompasses various other fields. An overview is given about entities of the explanted heart that can recur in the allograft, pathological conditions of the donor heart, histomorphological grading of both acute cellular (ACR) and antibody mediated rejection (AMR), transplant vasculopathy and myocardial changes after mechanical ventricular support by left ventricular assist devices (LVAD).

## AG04.03

### ***A podocentric view on glomerular disease***

C. Schell

Institut für Klinische Pathologie, Freiburg, Germany

Glomerular disease is a major decisive and contributing factor to the increasing incidence of chronic kidney disease (CKD). Glomeruli present a multicellular filtration unit consisting of mesangial, endothelial and parietal cells, as well as podocytes. With the advent of human genetics and further omics-based technologies it is becoming increasingly clear that podocytes are at the center of glomerular disease. While our knowledge regarding this cell type has been evolving in the last decades, there are still unanswered questions: What is the potential of podocytes to regenerate? How is the complex morphology of this massively polarized cell type maintained and regulated? How do podocytes contribute to metabolic glomerular diseases? Within this talk, I will give an overview about milestones in podocyte research and how these shaped our understanding of glomerular disease.

## AG04.04

### ***High CD163<sup>+</sup> macrophage densities in pre-implantation renal biopsies - precisely quantified and localized by convoluted neural networks (CNNs) - are predictive for delayed graft function (DGF)***

T. Zachrau<sup>1</sup>, D. Christensen<sup>1,2</sup>, F. Größler<sup>1</sup>, J. Hänisch<sup>2</sup>, D. Plesch<sup>2</sup>, R. Qasem<sup>1,3</sup>, J. Schmitz<sup>1</sup>, J. H. Bräsen<sup>1</sup>

<sup>1</sup>Hannover Medical School, Nephropathology Unit, Institute of Pathology, Hannover, Germany, <sup>2</sup>MetaSystems Hard- & Software GmbH, Altlußheim, Germany, <sup>3</sup>Klinikum Wahrendorff, Sehnde, Germany

#### **Background**

Deep learning allows reliable segmentation of tissue compartments and quantitative histomorphometric analysis, or “pathomics”. This enables the search for new predictive biomarkers as indicators for disease outcome. In this study, we developed semantic segmentation for kidney structures including all histological compartments. As show case, we compared the densities of macrophages in pre-implantation biopsies of patients showing initial graft function (IGF) versus delayed graft function (DGF).

#### **Methods**

Tissue was digitized with Metafer slide scanner (MetaSystems Hard & Software GmbH). Manual data labelling was done in the QuPath Software. The training resulted in several Convolutional Neural Networks (CNNs), covering the classes cortex, medulla, arteries, glomeruli, tubules, interstitium, peritubular capillaries (PTC) and separately trained macrophages. The performance of each CNN was evaluated in terms of global pixel accuracy on a test dataset. To quantify the histomorphometric difference between the patients with IGF versus DGF, 43 biopsies were stained with DAB against macrophage specific epitopes (CD68, CD206, CD163) and counterstained with hemalum, resulting in 129 digitized whole slide images (WSI). Finally, all CNNs were applied in MetaSystems VSViewer Software on each WSI for morphometric analysis of structures and macrophage densities (percent area per compartment).

#### **Results**

CNN performance was measured as global test accuracy across all classes: For cortex, medulla and extrarenal tissue combined 97.0%, for big arteries 98.7%, for small arteries 99.2%, for glomeruli 99.2%, for interstitium, tubulus and PTC combined 94.1% and for macrophages 98.7%. Significant higher interstitial and tubular CD163<sup>+</sup> macrophage densities were observed in the DGF compared to IGF group (p<0.05). In whole renal cortex a similar tendency was detected (p =

0.061).

### Conclusion

Precise quantification and localization of macrophages to specific anatomical compartments by using different CNNs was successfully demonstrated. We highlighted the predictive value of higher CD163<sup>+</sup> macrophage infiltration for DGF in pre-implantation biopsies, especially in interstitium and tubules.

AG04.05

### ***The role of MIF-2 (D-DT) in kidney fibrosis***

L. Herkens<sup>1</sup>, P. Droste<sup>1,2</sup>, K. Karyniotakis<sup>1</sup>, P. Boor<sup>1,2,3</sup>, S. Djudjaj<sup>1</sup>

<sup>1</sup>RWTH Aachen University, Institute of Pathology, Aachen, Germany, <sup>2</sup>RWTH Aachen University, Division of Nephrology and Clinical Immunology, Aachen, Germany, <sup>3</sup>RWTH Aachen University, Electron Microscopy Facility, Aachen, Germany

### Background

The progression of most kidney diseases leads to kidney fibrosis. Despite scientific progress, mechanisms of kidney disease progression and fibrosis are not completely understood. D-dopachrome tautomerase (D-DT), also known as macrophage migration inhibitory factor 2 (MIF-2), is a cytokine that is a structural and functional homolog of MIF. MIF acts as an endogenous nephroprotective factor in fibrosis, by abrogating cell cycle arrest of tubular cell cycle arrest of tubular cells and thereby limiting kidney fibrosis. On the other hand, very little is known about the role of D-DT in kidney (fibrosis).

### Methods

We analyzed the expression of D-DT in kidney fibrosis in different animal models, i.e., unilateral ureteral obstruction (UUO), ischemia-reperfusion (IR), 2,8-dihydroxyadenine nephropathy, and patient biopsies using immunohistochemistry, immunofluorescence, rt-PCR, RNA *in situ* hybridization, Western blot and re-analyzed publicly available datasets and arrays. We used D-DT knockout (KO) and wildtype (WT) littermate mice treatment with recombinant D-DT in models of kidney fibrosis to analyze the functional role of D-DT. Completed was the study by *in vitro* studies using human embryonic kidney (HEK) 293T cells.

### Results

In both healthy murine and human tissues, D-DT was mainly expressed in proximal tubules. The mRNA and protein expression of D-DT was significantly reduced after fibrosis induction in the UUO and IR. Also in human fibrotic tissue, we have detected significantly decreased mRNA and protein expression of D-DT. This was further confirmed by the re-analysis of D-DT expression in murine and human public array data. *In vitro*, HEK293T cells showed significantly decreased D-DT expression after treatment with transforming growth factor- $\beta$ 1 (TGF- $\beta$ 1). *In vivo*, D-DT KO mice developed significantly more severe fibrosis in the UUO compared to WT while treatment with recombinant D-DT significantly improved fibrosis.

### Conclusion

We have shown that D-DT is downregulated in kidney fibrosis similarly in mice and humans and this downregulation is consistent across various diseases. *In vitro* experiments suggested a protective role of D-DT in kidney fibrosis. With this research, the mechanism of D-DT can be investigated.

## AG Uropathologie 1

AG05.01

### ***Revision of Patient-derived Kidney Organoids for Disease Modelling***

J. Rohe<sup>1</sup>, A. P. K. Ashraf<sup>2</sup>, M. Kehl<sup>1</sup>, K. Fuchs<sup>1</sup>, Y. Li<sup>1</sup>, X. Thielmann<sup>1</sup>, M. Berg<sup>1</sup>, A. Bunes<sup>3</sup>, J. Ellinger<sup>4</sup>, G. Kristiansen<sup>5</sup>, D. Wachten<sup>2</sup>, M. Toma<sup>1</sup>

<sup>1</sup>Institute of Pathology, University Hospital Bonn, Experimental Pathology, Bonn, Germany, <sup>2</sup>Institute of Innate Immunity, Medical Faculty, University of Bonn, Bonn, Germany, <sup>3</sup>Core Unit for Bioinformatics Data Analysis, Medical Faculty, University of Bonn, Bonn, Germany, <sup>4</sup>Clinic and Polyclinic for Urology and Pediatric Urology, University Hospital Bonn, Bonn, Germany, <sup>5</sup>Institute of Pathology,

## Background

Autosomal dominant polycystic kidney disease (ADPKD) is one of the most common causes of end-stage renal disease, yet it remains poorly understood. Increase of cyclic adenosine monophosphate (cAMP) within the primary cilium is caused by the loss of Polycystin 1/2 function and has been a highly relevant target for *in vitro* ADPKD research. As cyst formation is a spatio-temporal remodeling process in a 3D environment, common 2D cell culture models do not meet the necessary requirements. Recently, adult stem cell-derived kidney organoids have been described as suitable candidates for the recapitulation of the highly complex disease. However, current studies lack a common method to identify induced cysts and often solely depend on unspecific pharmacological cAMP increase. Thus, we aimed to create a reproducible model that provides a clear and specific read-out for ADPKD research.

## Methods

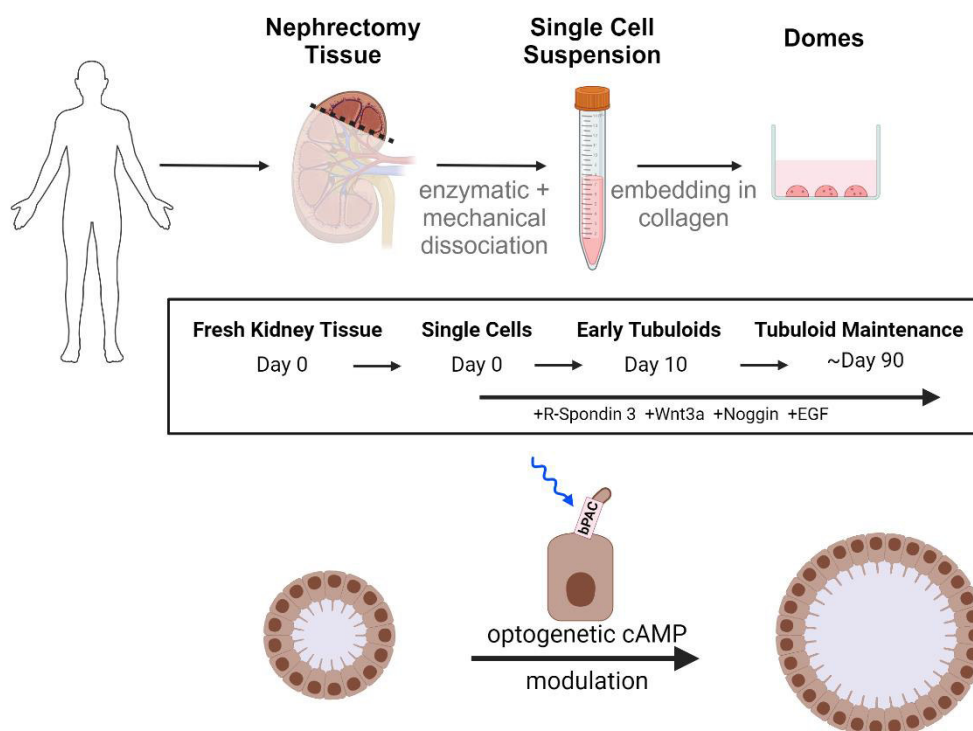
We established ASC-derived kidney organoids from five patients and analyzed them through histological and immunofluorescent imaging for their morphological stability and utility as disease models. Furthermore, we investigated the role of the extracellular matrix (ECM) scaffold on organoid morphology. Using the adenylyl cyclase (AC) activator Forskolin, we characterized the response of organoids to general cAMP elevation. Then we confirmed the specificity of these findings by introducing a ciliary-localized, light-activated AC to organoids through viral transduction.

## Results

Organoid cultures were morphologically stable over eight passages and mimicked collecting duct marker expression. Removal of the ECM scaffold resulted in „apical-out“ organoids, which developed cysts upon Forskolin treatment. Organoids grown in ECM domes already had a cyst-like morphology before treatment but increased significantly in size after pharmacological and spatially-restricted cAMP elevation through Forskolin and optogenetic tools, respectively.

## Conclusion

We characterized a stable *in vitro* model to study ADPKD in human tissue on a cellular and structural level. Moreover, we demonstrated the role of ciliary cAMP elevation in cyst growth and provided a platform for further studies.



## ***Assessing the risk to develop a growing teratoma syndrome based on molecular and epigenetic subtyping as well as novel secreted biomarkers***

F. Bremmer\*<sup>1</sup>, P. Pongratanakul\*<sup>2,3</sup>, S. Pauls<sup>4</sup>, G. Poschmann<sup>4</sup>, C. Kresbach<sup>5</sup>, F. Parmaksiz<sup>6</sup>, M. A. Skowron<sup>6</sup>, A. Stephan<sup>6</sup>, P. Paffenholz<sup>7</sup>, K. Stühler<sup>4</sup>, U. Schüller<sup>5</sup>, P. Ströbel<sup>1</sup>, A. Heidenreich<sup>7</sup>, Y. Che<sup>3</sup>, P. Albers<sup>3</sup>, D. Nettersheim<sup>2</sup>

<sup>1</sup>University Medical Center, Institute of Pathology, Göttingen, Germany, <sup>2</sup>Medical Faculty and University Hospital Düsseldorf, Heinrich Heine University Düsseldorf, Department of Urology, Urological Research Laboratory, Translational UroOncology, Düsseldorf, Germany, <sup>3</sup>Medical Faculty and University Hospital Düsseldorf, Heinrich Heine University Düsseldorf, Department of Urology, Düsseldorf, Germany, <sup>4</sup>Medical Faculty and University Hospital Düsseldorf, Heinrich Heine University Düsseldorf, Molecular Proteomics Laboratory (MPL), Biological and Medical Research Center (BMFZ), Düsseldorf, Germany, <sup>5</sup>University Hospital Hamburg-Eppendorf, Institute of Neuropathology, Hamburg, Germany, <sup>6</sup>Medical Faculty and University Hospital Düsseldorf, Heinrich Heine University Düsseldorf, Department of Urology, Urological Research Laboratory, Translational UroOncology, Düsseldorf, Germany, <sup>7</sup>University Hospital Cologne, University of Cologne, Department of Urology, Cologne, Germany

\*Geteilte Erstautorenschaft

### **Background**

The “Growing teratoma syndrome” (GTS), firstly described by Logothetis et al. in 1982, is defined as a growing teratoma during chemotherapy, while tumor markers are decreasing or normalized. The pathogenesis remains elusive, development to somatic-type malignancy (STM) is unclear and specific treatment options of GTS are limited. By molecular and epigenetic characterization, we aimed at deciphering the origin of GTS and identifying biomarkers to detect patients with aggressive GTS who urgently need surgical treatment before developing a STM.

### **Methods**

We identified 50 patients with a GTS for clinical characterization. 12 patients with n = 73 GTS samples were analyzed on epigenetic, transcriptional and proteome/secretome level. We included 2 longitudinal cases with 1 patient developing a STM, and both developing a yolk-sac tumor (YST) late during disease progression. Teratomas (TER) showing no features of GTS served as controls.

### **Results**

GTS were subtyped into a slow (<0.5 cm/month), medium (0.5-1.5 cm/month) and rapid (>1.5 cm/month) group.

Analyzing the proteome, we found differentially regulated proteins in GTS compared to low proliferative TER. Proteins enriched in all GTS subtypes were involved in DNA replication and repair, and the cell cycle, while proteins interacting with the immune system were depleted.

In longitudinal GTS samples, increasing AFP levels and the subsequent detection of a YST indicated a persisting occult non-seminoma germ cell tumor (GCT) component in GTS. A qRT-PCR analysis, showing low but detectable expression of pluripotency (e.g. OCT3/4, SOX2) and YST marker genes (e.g. FOXA2, GPC3), supports this hypothesis. Based on proteome data, GTS<sup>rapid</sup> seems to metastasize more quickly and more distal from the primary tumor due to a strong interaction with the surrounding microenvironment and a higher migratory capacity than GTS<sup>slow</sup>. In contrast, GTS<sup>slow</sup> seems to be in an ongoing differentiation process into cells of all 3 germ layers. From all datasets, we deduced an atlas of putative epigenetic and secreted biomarkers for GTS and its subgroups.

### **Conclusion**

We have identified novel epigenetic and molecular biomarkers indicative for GTS, enabling the detection of patients harboring a GTS at early time points to adjust the therapeutic concept in time. The newly defined GTS presents an aggressive subtype of highly proliferative GCT including non-seminoma GCT. Patients representing these features of GTS need urgent and complete resection of residual disease after chemotherapy.

AG05.03

## ***Ultra-high resolution imaging of prostate cancer using synchrotron-based virtual histology***

G. Müller<sup>1</sup>, M. Eckermann<sup>2</sup>, S. Leybold<sup>1</sup>, M. Saar<sup>3</sup>, M. Ackermann<sup>1</sup>, D. D. Jonigk<sup>1</sup>

<sup>1</sup>UK Aachen, Pathologie, Aachen, Germany, <sup>2</sup>ESRF, Grenoble, France, <sup>3</sup>UK Aachen, Urologie, Aachen, Germany

### **Background**

Prostate cancer is the most common cancer in male with a prevalence of 66,000 in Germany. The histopathological determination of the Gleason score has some limitations as the poor agreement between biopsy and prostatectomy due to the intratumoral morphological heterogeneity. The aim of the study is the first three-dimensional characterization of acinar prostate carcinoma using high-resolution synchrotron radiation based nanotomography and with the focus on the visualization and the morphometry of the growth pattern of the various Gleason scores and the three-dimensional segmentation of tumor-stroma interaction.

### **Methods**

We included 12 patients in this study with a clinically and pathological confirmed diagnosis of acinar prostate carcinoma. FFPE biopsy samples with Gleason scores of 3+3 (n=3), 3+4 (n=3), 4+3 (n=2), 4+4 (n=2) and 4+5 (n=2) confirmed by two independent pathologists were analyzed at the beamline ID16A at the European Synchrotron Radiation Facility in Grenoble France. The punched biopsies scanned and reconstructed at a resolution and image quality, which allows for the segmentation of individual cells. Using the zoom capability of the cone beam geometry, regions-of-interest are reconstructed with a minimum voxel size of 30 nm.

### **Results**

Overall, in all 12 cases, a disproportionately high correlation could be verified between the areas recorded in the synchrotron and annotated in ultra-high-resolution images and the histomorphological workup of the prostate carcinomas. The Gleason score 3+3 pattern could be confirmed at any time. In regard to the Gleason score 3+4, ultra-high-resolution nanotomography is diagnostically superior to two-dimensional histomorphology, and there is a clear underrepresentation of the Gleason 4 pattern. Furthermore, significantly better resolution of the basal membrane and the peri-/ transtumoral stroma to differentiate Gleason 4 atrophic from Gleason 5 pattern single-cell variant.

### **Conclusion**

Using high-resolution synchrotron radiation, the specific representation of the individual Gleason patterns in a three-dimensional framework with more precise Gleason classification is possible. Therefore, therapeutically relevant statements regarding tumor volume determination in individual cases are more valid for the entire prostate and require a possible changed therapeutic approach. In the future, reliable statements about tumor spread, differentiation and heterogeneity will be possible using AI-supported evaluation methods by segmenting the data sets.

AG05.04

## ***Long term treatment with darolutamide increases neddylation of the androgen receptor***

M. V. Cronauer, T. Mayr, A. Kremer, G. Kristiansen

Institut für Pathologie/UKB, Bonn, Germany

### **Background**

Prostate cancer (PCa) shows a remarkable dependence on the androgen/androgen receptor(AR)-signaling axis at almost all stages of the disease. Unfortunately, current endocrine therapies are only palliative and tumor progression almost inevitably occurs within a few years with the formation of therapy-resistant PCa cells. Mechanisms that allow PCa to evade endocrine therapies include adrenal and intratumoral androgen synthesis, AR-overexpression, AR-mutations and AR-splice variants. In the present study we show that AR-neddylation, a posttranslational modification allowing the covalent conjugation of the ubiquitin-like peptide NEDD8 to proteins, is a further mechanism involved in the failure of endocrine therapies.



## Methods

Androgen sensitive LNCaP cells were treated with increasing concentrations of darolutamide/ODM-201 for >18 months. The high affinity AR-antagonist darolutamid is the latest second generation antiandrogen with a broad efficacy against important AR-mutations like W742L, T878A, F876L. The resulting cells termed L-DaroLT as well as darolutamide untreated LNCaP (L-LT) and PC-3 cells, served as experimental models. Expression of AR, PSA and NEDD8 activating enzyme E1 subunit 1 (NAE1) were determined by RNAseq and Western Blot. Effects of NAE1 and NEDD8-overexpression on AR-signalling were monitored by reporter gene assays.

## Results

RNAseq revealed that L-DaroLT cells showed a 60% increase in NAE1-expression as compared to untreated control cells (L-LT). The increase of NAE1 in L-DaroLT was accompanied by an increase in AR and a decrease in PSA mRNA/protein levels. As shown by reporter gene studies in PC-3 cells, both NAE1- and NEDD8-are able to diminish AR-transactivation. Although functionally inhibited, the AR is paradoxically stabilized by high levels of NAE1 or NEDD8. This suggests a previously unknown resistance mechanism. Our working hypothesis that the AR is a „bona fide“ substrate for neddylation is furthermore supported by *in silico* data confirming two putative NEDD8 binding sites in the human AR.

## Conclusion

The present data suggest that aberrant neddylation of the AR in PCa is a further mechanism involved in the failure of endocrine therapies.

AG05.05

## ***Molecular subtypes of urothelial muscle-invasive bladder cancer – assessing immune cell infiltration and survival***

F. Koll<sup>1</sup>, C. Döring<sup>2</sup>, L. Herwig<sup>2</sup>, B. Hoeh<sup>1</sup>, M. Wenzel<sup>1</sup>, C. Cano Garcia<sup>1</sup>, S. Banek<sup>1</sup>, L. Kluth<sup>1</sup>, J. Köllermann<sup>2</sup>, F. Chun<sup>1</sup>, P. Wild<sup>2</sup>, H. Reis<sup>2</sup>

<sup>1</sup>Universitätsklinikum Frankfurt, Goethe-Universität, Klinik für Urologie, Frankfurt am Main, Germany, <sup>2</sup>Universitätsklinikum Frankfurt, Goethe-Universität, Dr. Senckenbergisches Institut für Pathologie, Frankfurt am Main, Germany

## Background

Molecular subtypes of muscle-invasive bladder cancer (MIBC) show different immune cell infiltration and survival rates. However, their predictive value to guide treatment decisions is controversial and data to use subtypes as guidance for adjuvant chemotherapy is sparse. We characterized the tumor-micro environment of different molecular subtypes and assessed survival rates with and without adjuvant chemotherapy.

## Methods

The gene expression was retrieved using Massive Analysis of 3' cDNA Ends (MACE) and the HTG transcriptome panel from formalin-fixed, paraffin-embedded (FFPE) samples. We assigned consensus molecular subtypes of 143 MIBC patients undergoing radical cystectomy. The immune cell infiltration and PD-L1 expression were determined using multiplex immunofluorescence (PD-L1, PanCK, aSMA, Vimentin, CD45, Ki67) and a machine learning algorithm was trained to identify cell populations. The overall survival (OS) for patients with and without adjuvant chemotherapy was computed using Kaplan-Meier and Cox regression survival analyses.

## Results

48.9% (n=70) samples had a basal/squamous (Ba/Sq) molecular subtype. Ba/Sq tumors had higher concentrations of PD-L1+ immune and tumor cells than other molecular subtypes. 2.8% (n=4) of samples had a neuroendocrine-like (NE-like) subtype, showing significantly higher concentrations of proliferating tumor cells. Patients with luminal tumors (luminal papillary (LumP): 9.1% (n=13), luminal non-specified (LumNS): 6.3% (n=9), luminal unstable (LumU): 4.9% (n=7)) had better OS rates than Ba/Sq (HR 0.5, 95%CI 0.2-0.9, p=0.01) and NE-like (HR 0.3, 95% confidence interval [CI] 0.1-0.9, p=0.04) tumors. While the OS rates of luminal tumors with and without adjuvant chemotherapy did not differ significantly, Ba/Sq tumors had the highest increase of OS with adjuvant chemotherapy ( $p(\log\text{-rank}) < 0.001$ ).

## Conclusion

Molecular subtypes could help to stratify patients with MIBC. The Ba/Sq subtype shows poorer overall survival, but

patients might derive a significant benefit from platinum-based chemotherapy. Additionally, higher PD-L1 expression in Ba/Sq tumors can create an opportunity for these patients to be treated with immune checkpoint therapy.

AG05.06

### ***ELOC-mutated renal cell carcinoma - a new player in the differential diagnosis of renal neoplasms***

A. Fichtner<sup>1</sup>, K. Reuter-Jessen<sup>1</sup>, A. Strauß<sup>2</sup>, P. Ströbel<sup>1</sup>, F. Bremmer<sup>1</sup>

<sup>1</sup>Universitätsmedizin Göttingen, Institut für Pathologie, Göttingen, Germany, <sup>2</sup>Universitätsmedizin Göttingen, Klinik für Urologie, Göttingen, Germany

#### **Background**

According to the current WHO classification, renal cell carcinomas (RCC) encompass a heterogenous group of molecularly defined RCCs. These tumours might already show a distinct morphology and immunohistochemical staining pattern.

#### **Methods**

Formalin-fixed and paraffin-embedded tissue samples from renal tumor resection specimens of a 25- and a 44-year old male Patient were analyzed morphologically on H.E. stainings and immunohistochemical stainings for CD10, CD117, CK7 and vimentin. Molecular analysis using the TruSight Oncology 500 (TSO500) assay were performed additionally.

#### **Results**

Both tumours contained cells with clear cytoplasm, central to slightly eccentric nuclei, a papillary growth pattern and a prominent fibromyxomatous stromal component. Immunohistochemically, they stained positive for CD10, CK7 and vimentin. TSO500 analysis revealed a mutation of the *ELOC* gene.

#### **Conclusion**

In both cases, distinct morphological characteristics and immunohistochemical staining patterns lead to further molecular analysis that confirmed the diagnosis of a rare *ELOC*-mutated RCC. Less than 20 cases have been reported so far with good prognosis in the majority of cases. Especially for the 25-year old patient further investigations of a germ line mutation are important because of a reported case of an *ELOC* mutation in von-Hippel-Lindau disease.

AG05.07

### ***Immunohistochemical ERG positivity in primary prostate cancer is associated with decreased PSMA expression, and lower visibility in corresponding [68Ga]Ga-PSMA-11 PET scans***

N. J. Rupp<sup>1,2</sup>, S. N. Freiburger<sup>1</sup>, D. A. Ferraro<sup>3,4</sup>, R. Laudicella<sup>3,5</sup>, J. Heimer<sup>6</sup>, U. J. Muehlematter<sup>3</sup>, C. Poyet<sup>7</sup>, H. Moch<sup>1,2</sup>, D. Eberli<sup>2,7</sup>, J. H. Rüschhoff<sup>1</sup>, I. A. Burger<sup>3,8</sup>

<sup>1</sup>Department of Pathology and Molecular Pathology, University Hospital Zurich, Zurich, Switzerland, <sup>2</sup>Faculty of Medicine, University of Zurich, Zurich, Switzerland, <sup>3</sup>Department of Nuclear Medicine, University Hospital Zurich, Zurich, Switzerland, <sup>4</sup>Department of Radiology and Oncology, Faculdade de Medicina FMUSP, Universidade de Sao Paulo, Sao Paulo, Brazil, <sup>5</sup>Department of Biomedical and Dental Sciences and Morpho-Functional Imaging, Nuclear Medicine Unit, University of Messina, Messina, Italy, <sup>6</sup>Seminar for Statistics, Federal Institute of Technology (ETH) Zurich, Zurich, Switzerland, <sup>7</sup>Department of Urology, University Hospital Zurich, Zurich, Switzerland, <sup>8</sup>Department of Nuclear Medicine, Cantonal Hospital Baden, Baden, Switzerland

#### **Background**

*TMPRSS2:ERG* gene fusion negatively regulates PSMA expression in prostate adenocarcinoma (PCa) cell lines.

Therefore, immunohistochemical (IHC) ERG expression, a surrogate for an underlying *ERG* gene rearrangement, and PSMA expression patterns in radical prostatectomy (RPE) specimens of primary PCa, including corresponding PSMA-PET scans were investigated.

#### **Methods**

Two cohorts of RPE samples (total n=148): In cohort #1 (n=62 patients) with available RPE and preoperative [68Ga]Ga-PSMA-11 PET, WHO/ISUP grade groups, IHC-ERG (positive vs. negative) and IHC-PSMA expression (% PSMA-

negative tumor area, PSMA%neg) were correlated with the corresponding SUVmax. In the second cohort #2 (n=86 patients) including RPE only, same histopathological parameters were evaluated.

## Results

Cohort #1: PCa with IHC-ERG expression (35.5%) showed significantly lower IHC-PSMA expression and lower SUVmax values on the corresponding PET scans. Eight of 9 PCa with negative PSMA-PET scans had IHC-ERG positivity and confirmed *TMPRSS2::ERG* rearrangement. In IHC-PSMA positive PCa, IHC-ERG positivity was significantly associated with lower SUVmax values. In cohort #2, findings of higher IHC-PSMA%neg and IHC-ERG expression were confirmed with only 0-10% PSMA%neg tumor areas in IHC-ERG-negative PCa.

## Conclusion

IHC-ERG expression is significantly associated with more heterogeneous and lower IHC-PSMA tissue expression in two independent RPE cohorts. There is a strong association of ERG positivity in RPE tissue with lower [68Ga]Ga-PSMA-11 uptake on corresponding PET scans. Results may serve as a base for future biomarker development to enable tumor-tailored, individualized imaging approaches.

AG05.08

## ***Tumor infiltrating B cells are an independent prognostic factor in penile cancer***

P. Stenzel<sup>1,2</sup>, A. Thomas<sup>3</sup>, M. Schindeldecker<sup>1</sup>, S. Porubsky<sup>1</sup>, S. Macher-Goeppinger<sup>1</sup>, I. Tsaur<sup>4</sup>, A. Haferkamp<sup>3</sup>, W. Roth<sup>1</sup>, K. Tagscherer<sup>1</sup>

<sup>1</sup>Universitätsmedizin Mainz, Institut für Pathologie, Mainz, Germany, <sup>2</sup>Uniklinikum Frankfurt, Dr. Senckenbergisches Institut für Pathologie, Frankfurt am Main, Germany, <sup>3</sup>Universitätsmedizin Mainz, Klinik für Urologie, Mainz, Germany, <sup>4</sup>Universitätsklinikum Tübingen, Klinik für Urologie, Tübingen, Germany

## Background

Penile cancer (PeCa) is an orphan disease. Surgery represents the most common treatment for localized disease. Once metastasized, prognosis of PeCa patients is dismal without significant improvement in the last decade. Since medical need of scientific activities in the field is apparent in order to improve outcomes, the aim of the current project was to characterize the tumor microenvironment in PeCa regarding prognosis.

## Methods

A study cohort consisting of 93 men with PeCa, surgically treated at the Department of Urology at the University Medical Center of the Johannes Gutenberg University Mainz, was utilized for the analysis of tumor infiltrating immune cells and PD-L1. A tissue microarray (TMA) was constructed and immunohistochemically stained against CD8 for cytotoxic T cells (CTLs), CD20 for B cells, CD56 for natural killer cells (NK cells), CD138 for plasma cells and FoxP3 for regulatory T cells (Tregs). The TMA slides were analyzed via digital image analysis after manual annotation of tumor parenchyma and tumor associated stroma. PD-L1 staining was quantified manually on tumor cells (tumor proportion score), tumor cells and immune cells (combined proportion score (CPS)) and on immune cells (immune cell score). Immune cells densities and PD-L1 scores were correlated to clinical outcomes and histopathological tumor characteristics.

## Results

CTLs and Tregs could be detected in >90% of PeCa, B cells in 88%, plasma cells in 85% and NK cells 23%. Higher immune cells densities were detected in the tumor associated stroma for all immune cells subtypes except NK cells. About 50% of PeCa were PD-L1 positive (CPS). In the univariate survival analysis, a high infiltration of CTL, B cells and plasma cells and a high PD-L1 CPS were associated with a favorable overall survival (OS) ( $p < 0.05$ ). In the multivariate analysis with respect to tumor grade and stage and lymph node metastasis, B cells remained a significant factor for favorable OS ( $p = 0.04$ ).

## Conclusion

In this study, tumor infiltrating B cells were an independent prognostic factor for longer OS of patients with PeCa. Different B cells subtypes exert pro- and anti-tumorigenic functions from antibody production over antigen presentation to immunosuppressive effects. Contemporarily, B cells are discussed as a new predictive factor for response to modern immunotherapies. The results of this study strengthen this concept. Further research should focus on the distribution of B

cell subtypes in PeCa.

AG05.09

### ***CoreQuest: Determining Tumor content in prostate biopsies***

M. Bernhardt, O. Hommerding, T. Kreft, G. Kristiansen  
Universitätsklinikum Bonn, Institut für Pathologie, Bonn, Germany

#### **Background**

Prostate cancer is one of the most common cancers in men worldwide [1]. Active Surveillance is an active therapeutic strategy for men with so-called insignificant prostate cancer. Inclusion criteria for Active Surveillance vary between protocols and most commonly include PSA level, tumor volume, and histologic tumor content [2]. According to German national guidelines, tumor content should be reported in mm or as a percentage [3]. However, there is no further definition of how these parameters should be determined. The aim of this study was to understand how pathologists determine tumor content and if the determined tumor content is reproducible between different observers.

#### **Methods**

A questionnaire was distributed to members of the German Society of Pathology asking them to select their preferred method of tumor content determination from a variety of options. In addition, whole slide images of ten tumor cases with varying tumor content were provided. Participants were asked to report tumor content and grade as well as any additional features present.

#### **Results**

Of 67 participants who completed the questionnaire, 32 provided diagnoses for the ten cases. The majority of participants reported tumor content in percent (50.0%) or both percent and length in mm (27.4%), while only a minority reported tumor content in mm only (22.6%). The method of tumor content determination showed less variation, and the relative standard deviation was lower for tumor content measured in mm than in percent.

#### **Conclusion**

The majority of participating pathologists determine tumor content as the percentage of tumor present in the core, however, this method is prone to greater variability between individuals.

Literaturangaben:

[1] Hunya Sung, Jacques Ferlay, Rebecca Siegel, Mathieu Laversanne, Isabelle Soerjomataram, Ahmedin Jemal, Freddie Bray, (2021), Global Cancer Statistics 2020: GLOBOCAN Estimates of Incidence and Mortality Worldwide for 36 Cancers in 185 Countries, CA: a cancer journal for clinicians, 3

[2] Peter-Paul Willemse, Niall Davis, Nikolaos Grivas, Fabio Zattoni, Michael Lardas, Erik Briers, Marcus Cumberbatch, Maria de Santis, Paolo Dell'Oglio, James Donaldson, Nicola Fossati, Giorgio Gandaglia, Silke Gillissen, Jeremy Grummet, Ann Henry, Matthew Liew, (2022), Systematic Review of Active Surveillance for Clinically Localised Prostate Cancer to Develop Recommendations Regarding Inclusion of Intermediate-risk Disease, Biopsy Characteristics at Inclusion and Monitoring, and Surveillance Repeat Biopsy Strategy, European Urology, 4

[3] Arbeitsgemeinschaft der Medizinischen Fachgesellschaften (AWMF), (2021), S3-Leitlinie Prostatakarzinom, Ärztliche Zentralstelle Qualitätssicherung, Deutsche Gesellschaft für Urologie, 2024-02-15, [https://register.awmf.org/assets/guidelines/043-022OLI\\_S3\\_Prostatakarzinom\\_2021-10.pdf](https://register.awmf.org/assets/guidelines/043-022OLI_S3_Prostatakarzinom_2021-10.pdf)

## **AG Uropathologie 2**

AG05.10

### ***The Divine Comedy of Prostate Cancer***

D. Berney  
Barts Health NHS Trust, Department Cellular Pathology, London, United Kingdom

The diagnosis of prostate cancer and its treatment remain a major change for 21st century medicine. We will take a bird's eye view of the last 30 years of diagnosis, screening diagnostic pathology and treatment in prostate cancer, show what we are doing badly and what we are doing well, and how to rationalise pathology diagnostics for good treatment and improve grading and staging by pathologists worldwide in the future.

## ***Proteogenomic Integration Underlines the Stability and Relevance of Proteomic Subtypes in Urothelial Bladder Cancer***

F. F. Dreßler<sup>1</sup>, F. Diedrichs<sup>1</sup>, D. Sabtan<sup>2</sup>, S. Hinrichs<sup>2</sup>, P. Mackedan<sup>2</sup>, M. Schlotfeldt<sup>2</sup>, M. Henning<sup>3</sup>, A. Merseburger<sup>3</sup>, A. Miernik<sup>4</sup>, S. Perner<sup>2</sup>, R. Zubarev<sup>5</sup>, P. Wolf<sup>4</sup>, D. Horst<sup>1</sup>, Á. Végvári<sup>5</sup>

<sup>1</sup>Charité - Universitätsmedizin Berlin, Institut für Pathologie, Berlin, Germany, <sup>2</sup>Universitätsklinikum Schleswig-Holstein, Campus Lübeck, Institut für Pathologie, Lübeck, Germany, <sup>3</sup>Universitätsklinikum Schleswig-Holstein, Campus Lübeck, Klinik für Urologie, Lübeck, Germany, <sup>4</sup>Universitätsklinikum Freiburg, Klinik für Urologie, Freiburg, Germany, <sup>5</sup>Karolinska Institutet, Division of Physiological Chemistry I, Department of Medical Biochemistry and Biophysics, Stockholm, Sweden

### **Background**

Urothelial cancer (UC) is a challenging disease with a wide tumor-biological spectrum. Most molecular classification attempts are transcriptome-based and relate only indirectly to the therapeutically relevant and more stable protein level. Simultaneously, the advent of new targeted therapies has increased the need for quantitative data about the actual tumor specificity of potential target proteins. We have previously turned to the proteome to address these questions and reported the five proteomic PAULA subtypes. We now sought to integrate transcriptomic and genomic data with our subtypes.

### **Methods**

We used machine-learning as well as conventional data integration to align protein abundances and transcriptomic data of the TCGA cohort. We identified a relevant feature subset and used support vector classification with recursive cross-validation to confirm it. Out of 408 samples we could reclassify 287 (70.3 %) samples with a class probability >0.5, which we selected for further comparative analyses.

### **Results**

Proteomic low-risk PAULA I samples correlated with the luminal-papillary mRNA subtype but contained almost all *FGFR3* mutations, in contrast to the more scattered distribution in the transcriptomic subtypes. High-risk PAULA III samples were associated with the basal-squamous subtype, whereas the intermediate-risk PAULA IIa/b/c subtypes were not conclusively mapped. PAULA IIa contained more copy number variations (e.g., amplifications in *PPARG*, *FGFR1*, and *NECTIN4*), while neither *CDKN2A* (p16) gene alterations nor protein abundance were increased. *NECTIN4* protein abundances were also higher in PAULA IIa samples. The correlations with overall survival were comparable between both biological levels, but the proteomic subtypes showed slightly better stratification.

### **Conclusion**

Our proteomic subtypes are in general agreement with established transcriptomic subtypes but tend to map known genomic traits and hallmarks more accurately with improved survival stratification. Higher abundances of the ADC target *NECTIN4* in a specific proteomic subtype were confirmed by a corresponding increase of gene amplifications.

## ***Transcription factor GRHL1 is a key regulator of early differentiation processes during squamous bladder cancer development***

J. Wirtz<sup>1</sup>, R. Wang<sup>2</sup>, L. Seillier<sup>1</sup>, L. Gan<sup>3</sup>, F. Friedland<sup>4</sup>, E. Noetzel-Reiss<sup>4</sup>, E. M. Buhl<sup>1,5</sup>, F. Lammert<sup>1</sup>, J. Maurer<sup>6</sup>, M. J. Hoffmann<sup>7</sup>, D. D. Jonigk<sup>1,8</sup>, K.-V. Lehmann<sup>2,9</sup>, M. Rose<sup>1,10</sup>, N. T. Gaisa<sup>1,10</sup>

<sup>1</sup>RWTH Aachen University Hospital, Institute of Pathology, Aachen, Germany, <sup>2</sup>RWTH Aachen University Hospital, Joint Research Center for Computational Biomedicine, Aachen, Germany, <sup>3</sup>RWTH Aachen University Hospital, IZKF Aachen, Aachen, Germany, <sup>4</sup>Research Centre Jülich, Institute of biological information processing, Jülich, Germany, <sup>5</sup>RWTH Aachen University Hospital, Electron Microscopy Facility, Institute of Pathology, Aachen, Germany, <sup>6</sup>RWTH Aachen University Hospital, Department of Gynecology, Aachen, Germany, <sup>7</sup>Medical Faculty, Heinrich-Heine University Düsseldorf, Department of Urology, Düsseldorf, Germany, <sup>8</sup>German Center for Lung Research, DZL, BREATH, Hanover, Germany, <sup>9</sup>University Hospital Cologne, Cancer Research Center Cologne Essen, Cologne, Germany, <sup>10</sup>Medical Faculty of Ulm University, Institute of Pathology, Ulm, Germany

### **Background**

The GRHL transcription factor (TF) family is associated with development and maintenance of the epithelial phenotype. As tumor suppressor genes, they are known to inhibit epithelial-to-mesenchymal transition (EMT), migration and invasion

of tumor cells. In this study we investigate the specific role of *GRHL1* in differentiation processes during squamous bladder cancer development.

## Methods

Transcriptomic profiling of multi-regional samples of bladder cancer cystectomies, comprising normal urothelium (NU), squamous metaplasia (Sq-Met), squamous carcinoma in situ (Sq-Cis), and squamous cell carcinoma (SCC, overall n=43) was accomplished and compared with genome-wide expression patterns of a squamous differentiation *in vitro* model. *GRHL1* expression was confirmed in validation cohorts by qRT-PCR (n=183) and immunohistochemistry (n=236). Close-to-normal HBLAK and malignant squamous-like SCaBER cell lines were used to establish IPTG- inducible sh*GRHL1* knockdown (KD) pools and pCMV6-*GRHL1* overexpression single cell clones. Corresponding scrambled KD pools and mock clones served as controls. Squamous cell differentiation was triggered by applying calcium *in vitro*. Morphological changes were characterized by scanning electron microscopy. Differentially regulated candidate genes were characterized by qRT-PCR and western blot to clarify mechanistic and regulatory associated networks of *GRHL1*. Cell-cell contacts were evaluated using immunofluorescence (IF) confocal microscopy.

## Results

We identified a set of TFs, including *GRHL1*, being significantly upregulated in patient samples during early phase transition from NU to Sq-Met and upon squamous differentiation of HBLAK cells *in vitro*. Notably, *GRHL1* was downregulated during ongoing tumor progression. *In vitro* knockdown of *GRHL1* in HBLAK cells affected expression of desmosomal (e.g. *DSG1*) and keratinization markers (e.g. *CNFN*), thus impairing cell growth and squamous differentiation upon calcium application. In malignant SCaBER cells, overexpression of *GRHL1* resulted in significant suppression of colony formation (p=0.002).

## Conclusion

We revealed a network of TFs, involving *GRHL1* as key drivers for initial steps of squamous differentiation, while acting tumor suppressive in SCC of the urinary bladder.

AG05.13

## **Acetylation of Lysine 619 abolishes AR-V7 signalling**

M. V. Cronauer, T. Mayr, G. Kristiansen  
Institut für Pathologie/UKB, Bonn, Germany

### Background

The androgen receptor (AR) is a central element in the etiology and progression of prostate cancer (PCa). In consequence the AR is the prime target for the treatment of locally advanced and/or metastatic disease. However, endocrine therapies are only palliative and PCa almost invariably recurs as castration resistant prostate cancer (CRPC), able to grow and survive under castrate levels of circulating androgens. In CRPC aberrant reactivation of AR-signalling is often associated with the expression of AR-V7, a constitutively active AR splice variant. Although AR-V7 has been associated with failure of endocrine or taxane-based therapies in a subgroup of patients, the mere detection of AR-V7 transcripts/proteins does not provide sufficient information on AR-V7 activity and thus limits its predictive/prognostic value.

Accumulating evidence indicates that posttranscriptional modifications are regulating AR-activity during disease progression. There is experimental evidence that acetylation of the lysine residue K619 by the acetyl-transferase ARD1 dramatically increases the transcriptional activity of the AR, making ARD1 an interesting target for modulating AR-signalling. As AR and AR-V7 share the same acetylation site, we analyzed the effects of K619 acetylation on AR-V7 signalling.

### Methods

AR-V7-mutants K619R (non-acetylatable) and K619Q (acetylation mimetic) were generated by *in vitro* mutagenesis. Signalling of AR-V7 species (wild type, K619R, K619Q) was studied by reporter gene assay. Protein expression was analyzed by Western Blot, nuclear localization by fluorescence microscopy. 3D-structures of AR-V7 C-termini were simulated using ColabFold v1.5.2 (AlphaFold2 using MMseq2).

## Results

Mimicking K619 acetylation dramatically inhibited AR-V7 transactivation in the reporter gene assay. The inability of K619Q to activate the reporter gene was not due to diminished protein levels or reduced nuclear translocation. Moreover, K619R and K619Q did not affect the structural integrity of the AR-V7-C-terminus.

## Conclusion

In contrast to full length AR, signals triggered by AR-V7 are not enhanced but inhibited by K619 acetylation. Our data suggest that inhibition of K619 acetylation by small molecule inhibitors of ARD1 to diminish AR-signalling would be counteracted by reactivated AR-V7.

AG05.14

## ***Whole-organ mapping bladder cancers reveal heterogeneous expression patterns of TROP2 and NECTIN-4, varying according to distinct subtypes of urothelial bladder cancer.***

L.-M. Hobisch<sup>1,2,3</sup>, F. Lange<sup>1,2,3</sup>, D. Sikic<sup>2,3,4</sup>, H. Taubert<sup>2,3,4</sup>, S. Wach<sup>2,3,4</sup>, B. Wullich<sup>2,3,4</sup>, R. Stöhr<sup>1,2,3</sup>, A. Hartmann<sup>1,2,3</sup>, M. Eckstein<sup>1,2,3</sup>, V. Bahlinger<sup>1,2,3,5</sup>

<sup>1</sup>Institute of Pathology, University Hospital Erlangen, Friedrich-Alexander-Universität Erlangen-Nürnberg (FAU), Erlangen, Germany, <sup>2</sup>Bayerisches Zentrum für Krebsforschung (BZKF), Erlangen, Germany, <sup>3</sup>Comprehensive Cancer Center EMN, University Hospital Erlangen, Erlangen, Germany, <sup>4</sup>Department of Urology and Paediatric Urology, University Hospital Erlangen, Friedrich-Alexander-Universität Erlangen-Nürnberg (FAU), Erlangen, Germany, <sup>5</sup>Institute of Pathology and Neuropathology, University Hospital and Comprehensive Cancer Center Tübingen, Tübingen, Germany

## Background

Novel therapies like Antibody Drug Conjugates Sacituzumab Govitecan and Enfortumab Vedotin are revolutionizing treatment for urothelial cancer (UC) by targeting TROP2 and NECTIN-4, respectively. However, their efficacy hinges on consistent expression of these targets across the entire bladder tumor. This study investigates distinct histologies within whole-organ bladder specimens and explores the varying levels of TROP2 and NECTIN-4 expression among different subtypes.

## Methods

We evaluated 23 positions from two a priori selected Whole-Organ Mapping Bladder Cancers (WOMBC) (n=46), including one case with lymph node metastasis, across various histologies (tumor-associated urothelium, Carcinoma in situ, papillary and sarcomatoid tumor parts of muscle-invasive bladder cancer) with loss of expression of TROP2 and NECTIN-4 in the most invasive tumor part. Immunohistochemical assessment included four luminal and three basal markers to determine protein-based subtypes, along with evaluating TROP2 and NECTIN-4 expression. All stainings were automatically evaluated using QuPath (<https://qupath.github.io/>). Additionally, DNA and RNA from these bladder areas were isolated and analyzed for Fibroblast Growth Factor Receptor 3 (FGFR3) alterations.

## Results

In both WOMBC specimens, TROP2 and NECTIN-4 exhibited notably high expression levels across tumor-associated normal tissue, metaplasia, and Carcinoma in situ, with mean H-Scores of 295 and 155, respectively. In WOMBC 1, molecular subtypes showed no significant difference between papillary and sarcomatoid tumor parts (P=0.22). However, loss of TROP2 and NECTIN-4 expression was observed exclusively in the sarcomatoid areas of the bladder tumor and in the associated lymph node metastasis. In WOMBC 2, Carcinoma in situ presented as a luminal subtype with expression of TROP2 and NECTIN-4, whereas the invasive tumor demonstrated a double-negative neuroendocrine subtype, characterized by loss of TROP2 and NECTIN-4 expression.

## Conclusion

Our findings underscore the significance of comprehensively sampling all tumor components to evaluate biomarkers effectively, revealing the diminished expression of TROP2 and NECTIN-4 in the most invasive tumor regions and lymph node metastasis. Future analyses will incorporate FGFR3 and PD-L1 status to provide a comprehensive overview of biomarker combinations in UC.

# AG Kopf-Hals-Pathologie

AG06.01

## ***Tumor budding and lymphovascular invasion help to identify high-risk p16-positive oropharyngeal squamous cell carcinomas***

F. Stögbauer<sup>1</sup>, J. Budczies<sup>2</sup>, M. Boxberg<sup>1</sup>

<sup>1</sup>Institut für Pathologie, Technische Universität München, München, Germany, <sup>2</sup>Institut für Pathologie, Universitätsklinikum Heidelberg, Heidelberg, Germany

### **Background**

Human papillomavirus (HPV)-positive oropharyngeal squamous cell carcinomas (OPSCC) are generally associated with superior outcomes compared to their HPV-negative counterparts. However, there is a subset of high-risk HPV-positive OPSCC which cannot be reliably identified.

In a previous publication we could show that tumor budding (TB) might be of prognostic relevance for HPV-associated head and neck cancers. However, in that publication only a small subgroup of HPV-positive tumors was included and all HPV-positive tumors were subsumed irrespective of their location.

Thus, we aimed to validate the prognostic significance of TB in p16-positive OPSCC – the surrogate parameter for an underlying HPV-association.

### **Methods**

We evaluated a multicentric cohort (n=299) of p16-positive OPSCC including primary tumors without a history of neoadjuvant treatment. We analyzed various morphological parameters among them TB, tumor infiltrating lymphocytes (TILs), tumor-stroma-ratio (TSR) and lymphovascular invasion (LVI). For TB the cutoff identified in our previous publication was applied whereas for TILs and TSR the optimal cutoffs were calculated. Clinicopathological associations were assessed and survival analyses were conducted.

### **Results**

TB was weakly correlated with the number of TILs and the TSR. Interestingly, we could not detect an association between TB and the number of lymph node metastases or an extracapsular extension of lymph node metastases. Both in univariate and multivariate survival analysis TB was identified as independent prognostic parameter for overall survival (TB high hazard ratio: 3.08, 95%-confidence interval: 1.71-5.54) and progression-free survival. We obtained similar results for the presence of LVI for overall (hazard ratio: 2.04, 95%-confidence interval: 1.09-3.82) and progression-free survival.

Combining TB and LVI in a prognostic classification system yielded the lowest risk for cases with low TB and no LVI whereas cases with high TB and presence of LVI yielded the worst outcomes.

### **Conclusion**

We could identify TB as an independent prognostic factor along with the established risk factor of LVI in p16-positive OPSCC. Therefore, the evaluation of TB especially in conjunction with the evaluation of LVI might contribute to the establishment of more individualized treatment of patients. Ideally, analyzing TB/LVI might help in the identification of p16-positive OPSCC which might be suitable for treatment de-escalation studies.

AG06.02

## ***CD103+ tissue-resident T-cells accumulate in head and neck squamous cell carcinomas of patients responding to anti-PD1 therapy.***

C. Sanders<sup>1</sup>, D. Kittel<sup>1</sup>, A. Heine<sup>2</sup>, P. Brossart<sup>2</sup>, S. Strieth<sup>3</sup>, G. Kristiansen<sup>1</sup>, M. Toma<sup>1</sup>

<sup>1</sup>Institut für Pathologie, Uniklinik Bonn, Bonn, Germany, <sup>2</sup>Onkologie Uniklinik Bonn, Bonn, Germany, <sup>3</sup>Department of Otorhinolaryngology, University Hospital Bonn (UKB), Bonn, Germany

### **Background**

Anti-PD1 therapy plays an important role in advanced-stage head and neck squamous cell carcinoma (HNSCC), but not all patients respond to immune checkpoint therapy. The aim of the study was to investigate specific subtypes of immune cells in correlation with the response to anti-PD1 therapy.



## Methods

Infiltration density of CD103+, CD69+ or PDL1+ lymphocytes in samples from HNSCC patients (primary tumor n=26, paired local recurrence n=5, paired lung metastasis n=5) who received immune checkpoint therapy (pembrolizumab or nivolumab) was examined by immunohistochemistry. Confirmatory studies of the infiltration density of CD8+, CD69+, CD103+ and PDL1 positive cells were performed in a larger HNSCC cohort (n=125) and correlated with clinic-pathological data.

## Results

Accumulation of CD103+ and/ or CD 69+ cells in the primary tumor was associated with a better response to anti-PD1 therapy (CD103 p-value=0.009, CD69 p-value=0.034). The initial PDL1 score did not show a significant association with response to anti-PD1 therapy in this small cohort (n=11; p=0.140).

In the larger HNSCC cohort, poorer differentiation was associated with higher infiltration density of CD8+, CD69+ and CD103+ lymphocytes (CD8 p-value=0.025, CD69 p-value=0.024, CD103 p-value=0.043). Nodal-positive HNSCC showed a significantly higher infiltration density of CD103+ lymphocytes (p=0.026). In addition, significantly more CD103+ cells were found in non-smokers (p=0.027).

## Conclusion

CD103+ tissue-resident T-cells are more frequently detectable in primary tumors of HNSCC patients who show a better response to anti-PD1 therapy.

AG06.03

## ***Expanding the spectrum of low-grade sinonasal adenocarcinoma with biphasic seromucinous differentiation and activating HRAS/AKT1 mutations***

V. S. Hadnagy<sup>1,2</sup>, M. Körner<sup>3</sup>, M. Rössle<sup>4</sup>, P. Dubach<sup>5</sup>, G. Pabst<sup>6</sup>, E. J. Rushing<sup>4,7</sup>, D. Holzmann<sup>8</sup>, M. Hüllner<sup>9</sup>, S. N. Freiberger<sup>1,2</sup>, N. Rupp<sup>1,2</sup>

<sup>1</sup>Departement of Pathology and Molecular Pathology, University Hospital Zurich, Zurich, Switzerland, <sup>2</sup>University of Zurich, Zurich, Switzerland, <sup>3</sup>Pathologie Laenggasse, Ittigen, Switzerland, <sup>4</sup>Institute of Pathology, Lucerne Cantonal Hospital, Lucerne, Switzerland, <sup>5</sup>ENT Department, Buergerspital Solothurn, Solothurn, Switzerland, <sup>6</sup>Division of Otorhinolaryngology - Head and Neck Surgery, Lucerne Cantonal Hospital, Lucerne, Switzerland, <sup>7</sup>Medica Laboratory Zurich, Zurich, Switzerland, <sup>8</sup>Department of Otorhinolaryngology, Head and Neck Surgery, University Hospital Zurich, Zurich, Switzerland, <sup>9</sup>Department of Nuclear Medicine, University Hospital Zurich, Zurich, Switzerland

## Background

Low-grade sinonasal adenocarcinoma (LGSNAC) is a rare heterogeneous and poorly characterized group of tumors, distinct from intestinal-type and salivary-type neoplasms. Therefore, further characterization is needed for better biological understanding and classification.

## Methods

Clinical, histological and molecular characterization of three cases of biphasic, low-grade adenocarcinomas of the sinonasal tract was performed.

## Results

Patients were male, 48 to 78 years, who presented with polypoid masses in the nasal cavity. Microscopically, virtually all tumors were dominated by tubulo-glandular biphasic patterns, microcystic, focal (micro)papillary, oncocytic and basaloid features. Immunohistochemical staining confirmed biphasic differentiation with an outer layer of myoepithelial cells. Molecular profiling revealed HRAS (p.G13R, p.Q61R) mutations, and concomitant AKT1 (p.E17K, p.Q79R) mutations in two cases. Follow-up periods ranged from 5 – 30 months, with one case relapsing locally after 8 and > 20 years.

## Conclusion

This study further corroborates a distinct biphasic neoplasm within the group of LGSNAC. Although morphological and molecular features overlap with salivary gland epithelial-myoepithelial carcinoma, several arguments favor a distinct tumor entity originating from local seromucinous glands, i.e., a sinonasal biphasic seromucinous adenocarcinoma.

# AG Knochen-, Gelenk- und Weichgewebspathologie

AG07.02

## ***Prognostic factors in the diagnosis of Sarcomas from the perspective of a Reference Center (CSUR)***

E. Mayordomo Aranda<sup>1</sup>, F. Giner Segura<sup>1</sup>, E. Such Taboada<sup>2</sup>, M. Angulo Sánchez<sup>3</sup>, C. De la Calva Ceinos<sup>3</sup>

<sup>1</sup>Hospital La Fe, Pathology, VALENCIA, Spain, <sup>2</sup>Hospital La Fe, Cytogenetics, Valencia, Spain, <sup>3</sup>Hospital La Fe, Orthopedic Surgery, Valencia, Spain

The prognostic factors in the diagnosis of sarcomas are well-known: the specific type of sarcoma, the degree of malignancy, the extent of tumor at diagnosis, treatment response, resection margin status, and individual patient characteristics such as age and overall health. Molecular analyses help solidify the diagnosis and, in certain subtypes, can provide additional prognostic information and offer therapeutic options while being responsible for resistances.

We want to share the measures we have taken as a reference center to improve the prognosis of our sarcoma patients. These measures are divided into pre-analytical and analytical phases.

Factors affecting the prognosis in the pre-analytical phase include diagnostic planning through measures adopted at the tumor board, such as establishing the meeting as a non-presential outpatients clinics, with a monthly in-person meeting serving as a single-act consultation where the patient is present and participates in decision-making. We have defined and automated the patient pathway for sarcoma, enabling us to detect bottlenecks in care and improve the management of our committee.

We have included Pathology Technicians (TEAP) in the reception and preparation of samples received fresh in the Pathology Department. Nationally, we have organized a networking project led by Vall de Ebrón Hospital, IMPERAS, to standardize and improve the diagnosis and therefore the survival of our patients with sarcomas.

We have introduced the BIONANO platform, whose main objective is to map the genome of sarcomas to identify and analyze mutations, structural variants, and copy number alterations (CNV) within the sarcoma cell genome. These findings may be useful in diagnosis, prognosis, and the development of patient-adapted targeted therapies. Additionally, it will contribute to understanding the molecular mechanisms of sarcoma progression.

AG07.03

## ***microRNA profiling in combination with whole exome sequencing reveals insights into long-term recurrence patterns in chordoma***

S. R. Ullmann<sup>1</sup>, J. Schreier<sup>1</sup>, S. Franke<sup>1</sup>, K. Körber-Ferl<sup>2</sup>, D. Schanze<sup>3</sup>, C. Lohmann<sup>4</sup>, M. Röpke<sup>4</sup>, D. Ullmann<sup>5</sup>, M. Georgiades<sup>6</sup>, J. Ullmann<sup>7</sup>, D. Jechorek<sup>1</sup>, A. Roessner<sup>1</sup>, F. Karras<sup>1</sup>

<sup>1</sup>Institut für Pathologie, Universitätsmedizin Magdeburg, Magdeburg, Germany, <sup>2</sup>Institut für Humangenetik, Martin-Luther-Universität Halle-Wittenberg, Deep Sequencing Core Facility, Halle, Germany, <sup>3</sup>Institut für Humangenetik, Universitätsmedizin Magdeburg, Magdeburg, Germany, <sup>4</sup>Orthopädische Universitätsklinik, Magdeburg, Germany, <sup>5</sup>Berufsgenossenschaftliches Universitätsklinikum Bergmannsheil Bochum, Chirurgische Klinik, Abteilung für Unfallchirurgie, Bochum, Germany, <sup>6</sup>Universitätsklinik für Radiologie und Nuklearmedizin, Magdeburg, Germany, <sup>7</sup>Institut für Pathologie, Universitätsmedizin Rostock, Rostock, Germany

### **Background**

While few studies on miRNA profiling in primary chordomas have been published, there is no data on the miRNA landscape of long-term recurrences. Therefore we performed a miRNA analysis and whole exome sequencing (WES) investigating four patients with multiple long-term recurrences over seven to 16 years and eight patients with non-recurrent tumors (NRTs) in order to compare both groups as well as the recurrent cases (RCs) to each other. Our aim was to find typical molecular patterns distinguishing the recurrences from the NRTs.

### **Methods**

After histopathological classification, immunohistochemical and morphometric analysis, DNA and miRNA were extracted from formalin-fixed-paraffin-embedded tissue samples and analysed by WES and Nanostring.

## Results

microRNA regulation patterns showed RCs as a distinct group differing from NRTs, clustering apart in unsupervised clustering. The differential expression showed highly significant differences between both groups (Fig. 1a). Intriguingly tumors that would later develop recurrences differed significantly from NRTs (Fig. 1b).

This suggests a pivotal molecular difference between singular and long-term recurring chordomas.

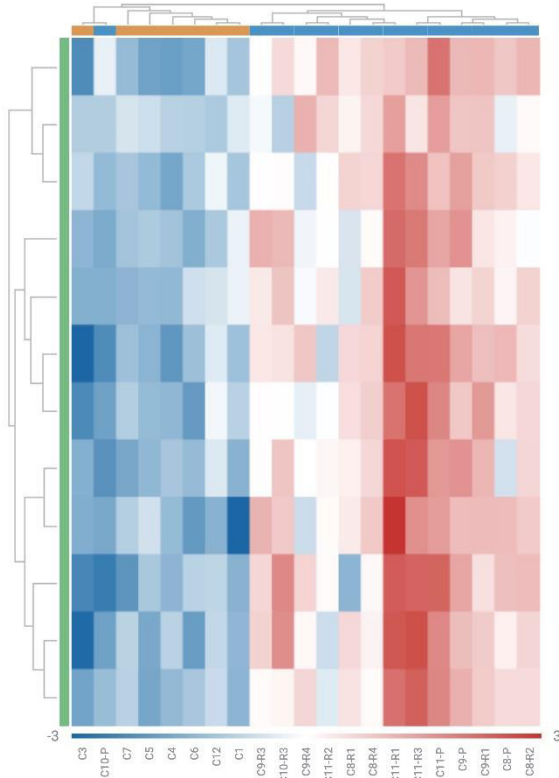


Fig. 1a  
Differential miRNA Expression of all tumor samples.  
(Cx = Case number, P = Primary tumor, Rx = Recurrent tumors)

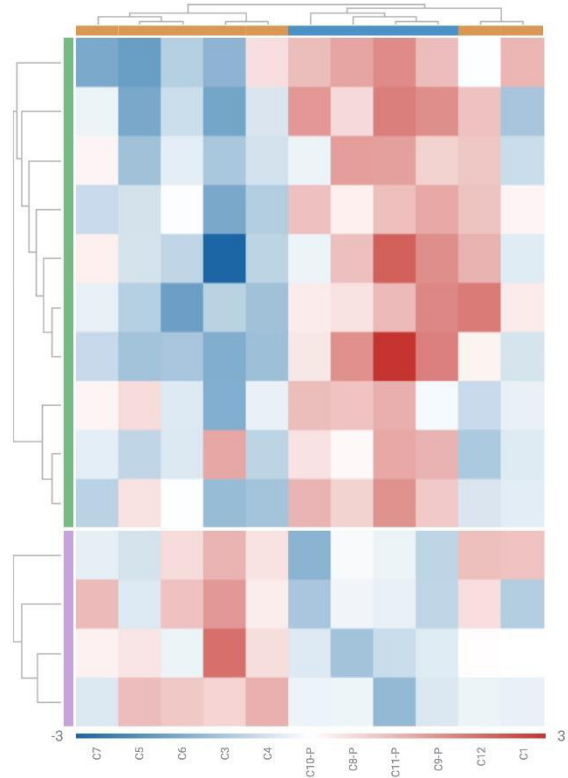


Fig. 1b  
Differential miRNA Expression of all primary and NRT samples.  
(Cx = Case number, P = Primary tumor)

Although no differences could be observed histologically, the differential miRNA expression shows highly significant differences between both groups, with 32 miRNAs upregulated in the RCs being downregulated in the NRTs. Primary tumors, that would later develop recurrences had a distinctive pattern.

Our WES analysis confirmed known and revealed possible new driver genes. Recurring tumors had a higher number of pathogenic mutations as well as increased proliferation rates and pleomorphic changes. Recurrences displayed a change in mutational distribution, showing considerably more disturbances in embryonic signaling and our proposed drivers. Intriguingly our study found a progress in number of alterations throughout the recurrences, most of all affecting chromatin regulation and the new drivers.

## Conclusion

Less disruption of these pathways in NRTs than in RCs implies their pivotal role not only in chordoma formation but also in recurrence evolution.

The miRNA alterations were correlated with the genomic differences. Validated affected genes of miRNAs deregulated primarily in the recurrences are involved in those pathways as well.

As current targeted therapy options are scarce, the progress in number of pathogenic mutations throughout the recurrences as well as the drastic change in miRNA expression could present new research approaches for recurring chordomas and lead to new therapeutic options inhibiting or delaying recurrence formation.

AG07.04

## ***Proteomic and N-Glycan in-situ Characterization of Small Blue Round Cell Tumors***

C. Bollwein, K. Schwamborn, J. P. L. Gonçalves

Institute of Pathology, School of Medicine, Technical University of Munich, Munich, Germany

### **Background**

Small blue round cell tumors (SBRCTs) represent an umbrella term comprising several completely different tumor types, among them ewing sarcoma, rhabdomyosarcoma, neuroendocrine carcinoma, acute lymphoblastic leukemia, nephroblastoma, and neuroblastoma. Correct diagnosis is essential, as treatment concepts and prognosis for each tumor entity differ significantly.

Matrix-assisted laser desorption/ionization (MALDI) mass spectrometry imaging (MSI) is a label-free analytical technique to analyze and visualize the spatial distribution of different classes of molecules, like peptides, glycans, lipids, and metabolites.

In this study, we have measured the protein/peptide and *N*-glycan content from archival samples of SBRCTs utilizing MALDI MSI to create classification algorithms to reliably distinguish the different entities and to identify discriminatory features between the tumor types.

### **Methods**

Samples from small blue round-cell tumors (SBRCT, *n* = 26) were assembled in a tissue microarray: ewing sarcoma (EWS, *n* = 5), rhabdomyosarcoma (RMS, *n* = 5), neuroendocrine carcinoma (NEC, *n* = 5), acute lymphoblastic leukemia (ALL, *n* = 5), nephroblastoma (NEPB, *n* = 3), and neuroblastoma (NEUB *n* = 3). The specimens were subjected to on-tissue enzymatic digestions, utilizing *N*-glycosidase F and trypsin, respectively, followed by matrix application and measurement on a mass spectrometer (rapifleX, Bruker). After matrix removal and histopathological annotation (QuPath, version 0.4.3) data analysis was performed using SCiLS Lab (Bruker, version 2024a) and the open-source programming language python (version 3.9).

### **Results**

MSI data was employed for the training and validation of different classification algorithms (gradient boosting (GB), support vector machine (SVM), *k*-nearest neighbor (KNN), and linear discriminant analysis (LDA)) using 10-fold cross-validation on pixel level. Multiclass classification was implemented as a one vs. rest (one entity vs. all other entities) and one vs. one (one entity vs. every other entity) approach.

For the one vs. rest strategy, overall accuracy was 90.5 % with a mean accuracy of 88.7 % for peptide analysis and 92.4 % for glycan analysis. For the one vs. one approach, overall accuracy was 92.4 % with a mean accuracy of 88.8 % for peptide analysis and 96.1 % for glycan analysis.

### **Conclusion**

In this study, we show that peptide and *N*-glycan mass spectrometry imaging is an auspicious methodology to assist in the classification of different small blue round cell tumors.

AG07.05

## ***Do BAF complexes regulate the differentiation status in synovial sarcoma?***

A. Kuntze<sup>1</sup>, R. Berthold<sup>2</sup>, L. Heinst<sup>2</sup>, M. Trautmann<sup>2</sup>, E. Wardelmann<sup>2</sup>, W. Hartmann<sup>2</sup>, I. Isfort<sup>2</sup>

<sup>1</sup>Gerhard-Domagk-Institute of Pathology, University Hospital Muenster, Münster, Germany, <sup>2</sup>Gerhard-Domagk-Institute of Pathology, University Hospital Muenster, Münster, Germany

### **Background**

Synovial sarcoma (SySa) is a rare malignancy occurring at any age but mostly affects adolescents and young adults. Given its high rate of local recurrence and metastasis, SySa belongs to the group of aggressive mesenchymal tumors. As therapeutic options are limited and advanced disease is associated with a poor prognosis, deciphering the underlying pathomechanism is urgently needed to identify molecular vulnerabilities.

Histologically, SySa exhibit unique features as they can display a pure monophasic spindle cell morphology, a biphasic spindle and epitheloid aspect or a poorly differentiated histological phenotype. Consequently, their expression profile comprises a wide spectrum of mesenchymal, epithelial and pluripotency markers. Despite their morphological variability,

SySa tumorigenesis is driven by a unique chromosomal translocation t(X;18) resulting in a chimeric SS18::SSX fusion protein which drives SySa tumorigenesis.

So far, it is known that the SS18::SSX fusion protein is integrated into BAF chromatin remodeling complexes. These are evolutionary highly conserved key regulators of gene transcription occurring in three functionally distinct subtypes GBAF, CBAF and PBAF, each playing particular roles in embryogenesis and cellular development. Integration of SS18::SSX into GBAF and CBAF complexes changes their relative abundance causing altered BAF complex functionality and dysregulated gene transcription. However, little is known about the subtypes' respective impact on SySa oncogenesis and their exceptional differentiation status.

## Methods

In this research project, we investigate functional dependencies between the different BAF complexes based on protein and RNA expression levels in SySa cell lines. With respect to the essential role of BAF complexes in cellular development, we aim to characterize their pathophysiological impact on SySa differentiation status and their interaction with pluripotency markers. Furthermore, we intend to uncover correlations between the expression of BAF subtypes, pluripotency and differentiation markers via immunohistochemistry and single-cell RNA sequencing in a cohort of human SySa cases.

## Results

Our preliminary results so far indicate distinct roles of the different BAF complexes in SySa differentiation.

## Conclusion

We expect the currently ongoing study to shed light on the pathomechanism of SySa and the respective role of different BAF complexes in oncogenesis.

AG07.06

## ***CDK inhibitors reduce TBXT gene expression in chordoma cell lines***

S. Bette<sup>1</sup>, L. Haase<sup>1</sup>, J. Nell<sup>1</sup>, T. Grieser<sup>2</sup>, R. Marienfeld<sup>1</sup>, N. T. Gaisa<sup>1</sup>, P. Möller<sup>1</sup>, T. F. E. Barth<sup>1</sup>, K. Mellert<sup>1</sup>

<sup>1</sup>Institut für Pathologie, Universitätsklinikum Ulm, Ulm, Germany, <sup>2</sup>Institut für Radiologie Universitätsklinikum Augsburg, Augsburg, Germany

## Background

Chordomas are rare malignant bone tumours of notochordal origin that show a locally infiltrative growth pattern. Radical en-bloc resection, followed by radiotherapy is presently the best long-term disease control. Chemotherapy and targeted therapy options such as tyrosine kinase inhibitors achieve only limited success rates. Chordomas are characterised by the overexpression of the *TBXT* gene and sequentially relevant nuclear amounts of the gene product brachyury. This was shown to be essential for the growth of chordoma cells, making it a promising target for chordoma therapy. Cyclin dependent kinase (CDK) inhibitors have been shown to disrupt the autoregulatory landscape of brachyury and to downregulate cellular brachyury levels. Therefore, we used CDK inhibitors THZ1 and dinaciclib to impede *TBXT* transcription in nine chordoma cell lines of diverse origins. One of these cell lines is the newly established chordoma cell line U-CH22 derived from the pleural effusion of a high-grade disseminated chordoma. With this broad spectrum of chordoma cell lines we tested the effect of CDK inhibitors on the amount of *TBXT* mRNA, brachyury protein and cell viability.

## Methods

Chordoma cell lines (U-CH1, U-CH2, U-CH17PII, U-CH17M, U-CH22, U-CHCF365, UM-Chor1, MUG-Chor1, MUG-CC1) were treated with either THZ1 or dinaciclib in concentrations between 0.1 µM and 10 µM for 24 hours. qPCR was performed to analyse the effect of different inhibitors on the transcription of *TBXT* mRNA. Brachyury protein levels were analysed *via* Western blot. Immunohisto/cytochemistry was used on FFPE-slides with a variety of antibodies.

## Results

U-CH22 was validated as a true poorly differentiated chordoma cell line (vimentin<sup>+</sup>, EMA<sup>+</sup>, pan-cytokeratin<sup>+</sup>, brachyury<sup>+</sup>, and INI-1<sup>-</sup>). THZ1 and dinaciclib significantly reduced *TBXT* mRNA and brachyury protein in nine chordoma cell lines including U-CH22. Both inhibitors decreased *TBXT* mRNA levels to about 10 % and brachyury protein levels to about 45

%. IC50 values ranged from 11 nM to 979 nM for THZ1 and 8 nM to 87 nM for dinaciclib, respectively. Interestingly, the clival chordoma cell lines MUC-CC1 and U-CHCF365 showed the highest susceptibility to THZ1 inhibition.

## Conclusion

We describe the effect of two different CDK inhibitors on a large cohort of chordoma cell lines as well as the newly established cell line U-CH22. CDK inhibitors are a promising class of drugs for the treatment of chordomas, as they can significantly reduce the amount of detectable brachyury in chordoma cells.

AG07.07

## ***TFCP2 - a potential regulator of TBXT expression in chordoma***

J. Neumahr<sup>1</sup>, C. Seeling<sup>2</sup>, P. Oeckl<sup>3</sup>, N. T. Gaisa<sup>1</sup>, P. Möller<sup>1</sup>, T. F. Barth<sup>1</sup>, K. Mellert<sup>1</sup>

<sup>1</sup>Institut für Pathologie, Universitätsklinikum Ulm, Ulm, Germany, <sup>2</sup>Klinik für Innere Medizin III, Universitätsklinikum Ulm, Ulm, Germany,

<sup>3</sup>Klinik für Neurologie und Deutsches Zentrum für Neurodegenerative Erkrankungen (DZNE e.V.) Ulm, Universitätsklinikum Ulm, Ulm, Germany

## Background

Chordoma is a rare primary bone cancer of notochordal origin, occurring almost exclusively along the spine. Chordomas are characterized by strong *TBXT* expression, resulting in nuclear accumulation of its gene product and transcription factor brachyury. Brachyury is essential in chordoma, as its knockdown alters morphology, and inhibits tumor growth through senescence and apoptosis, making *TBXT* a promising therapeutic target. However, the upstream regulatory mechanisms of *TBXT* expression in chordoma remain unclear.

In non-neoplastic tissue, *TBXT* is almost exclusively expressed in the notochord, plays a role in mesoderm differentiation, and its expression is partly regulated by the WNT/ $\beta$ -catenin pathway. In chordoma cell lines, knockdown of  $\beta$ -catenin resulted in decreased *TBXT*, suggesting its involvement in a regulatory complex acting upstream of *TBXT* in chordomas. Therefore, this study aims to identify  $\beta$ -catenin-dependent regulators of *TBXT* in chordoma.

## Methods

$\beta$ -catenin accumulation in cytosol and nuclear fractions was assessed by Western blot.  $\beta$ -catenin immunoprecipitations were performed on total protein lysates from three chordoma cell lines followed by mass spectrometry analysis to identify its binding partners. Proximity ligation assays (PLAs) on cytospins were used to validate these interactions in chordoma cell lines. Additionally, siRNA-mediated knockdown of *TFCP2* and WNT signaling inhibition using SSTC3 were performed to assess the impact on *TBXT* expression and cell viability.

## Results

Western blot analysis of fractioned protein lysates confirmed the presence of nuclear  $\beta$ -catenin in chordoma, indicating an involvement as transcriptional upstream regulator of *TBXT*. Mass spectrometric analysis of co-immunoprecipitated  $\beta$ -catenin identified 37 proteins, primarily associated with cell-cell interaction and the WNT/ $\beta$ -catenin pathway, consistently present in all three tested chordoma cell lines. Among these proteins, the transcription factor *TFCP2*, known to interact with  $\beta$ -catenin in pancreatic cancer, was identified. PLAs confirmed a significant accumulation of  $\beta$ -Catenin-*TFCP2* complexes in chordoma compared to control cells. Preliminary data from *TFCP2* knockdown and WNT inhibition using the CK1 $\alpha$  activator SSTC3 suggest *TBXT* repression and reduced cell viability in chordoma cell lines.

## Conclusion

*TFCP2* was identified as a novel  $\beta$ -Catenin associated transcription factor potentially affecting the expression of the key regulator *TBXT* and, hence, cell viability in chordoma cell lines.

# AG Dermatopathologie

AG08.01

## **Genitaler Lichen sclerosus - eine weiße Gefahr?**

S. Braun

Universitätsklinikum Münster, Münster, Germany

Der genitale Lichen sclerosus (LS) ist eine häufige chronisch-entzündliche Dermatose, dessen Diagnose sowohl klinisch als auch histologisch eine Herausforderung sein kann. Eine frühe und sichere Diagnosestellung ist jedoch wichtig, da unbehandelte, chronisch-entzündliche Verläufe ein Risiko für die Entstehung von Plattenepithelkarzinomen darstellen. Pathologen kommt somit eine besondere Verantwortung zu, sowohl den LS also auch bereits Vorstufen der Plattenepithelkarzinome sicher zu identifizieren. In diesem Vortrage beleuchten wir deshalb das breite histologische Spektrum des genitalen LS und beschäftigen uns mit der Diagnostik der differenzierten und verrukösen intraepithelialen Neoplasie. Ein besonderes Anliegen ist dabei, die häufig verwirrende Terminologie (hypertropher LS, VAAD, DEVIL und co.) zu ordnen und am Ende sowohl dem Diagnostiker als auch Kliniker einen praktischen Arbeitsalgorithmus an die Hand zu geben.

AG08.03

## **Giant Dermatofibroma with associated basal cell carcinoma: A case report of a rare collision**

J. Schwenke<sup>1</sup>, H.-P. Heinlein<sup>2</sup>, T. Mentzel<sup>3</sup>, N. Gaisa<sup>1</sup>, M. Mühlberger<sup>1</sup>

<sup>1</sup>Institut für Pathologie, Universitätsklinikum Ulm, Ulm, Germany, <sup>2</sup>Radiologische Praxis Dillingen, Dillingen, Germany, <sup>3</sup>MVZ Dermatopathologie, Friedrichshafen, Germany

### **Background**

Dermatofibroma and basal cell carcinoma are common lesions of the skin. Giant dermatofibroma is a rare variant of benign dermatofibroma with only few reported cases. Typical features are a size > 5 cm, pedunculated lesion, benign biological behavior and identical histopathology to conventional dermatofibroma. In many cases, the overlying epidermis of a dermatofibroma demonstrates hyperplasia or proliferation of basaloid cells (so called hair follicle induction), very similar to basal cell carcinoma. Only single case reports document the rare association of dermatofibroma with basal cell carcinoma or other malignant lesions.

### **Methods**

We report a case of a 57-year old man presenting with a persisting tumor at the left gluteus region. 2021 we received a 27 mm biopsy of the lesion and diagnosed dermatofibroma. Two years later in 2023 we saw a 12,5 x 9,2 x 3,6 cm resection specimen from the same location with an accompanying smaller separate fragment (4,5 x 2,6 x 1,1 cm). The tissue was examined using routine hematoxylin-eosin staining and immunohistochemistry.

### **Results**

On gross dissection the resection specimen was predominantly covered by skin like in a pedunculated lesion. The section surface showed a 12 cm subcutaneous homogeneous beige tumor in both fragments with focal cyst-like structures filled with blood clots. Histologically a solid, well defined spindle cell tumor with storiform pattern, low mitotic rate and without tumor necrosis was seen. The main tumor was immunoreactive for Vimentin, CD64, HMGA2 and CD68 (partial) as well as negative for CKAE1/3, p40, EP4, Caldesmon, SMA, CD34 and S100. A low proliferative index was observed with KI-67. Focally interspersed basaloid cell populations without contact to the surface epithelium showed expression of CKAE1/3, p40 and EP4 (partial), while being negative for Vimentin, S100, Caldesmon, CD34, CD68 and SMA.

### **Conclusion**

The final diagnosis was a rare collision of a giant dermatofibroma with aneurysmatic features associated with a basal cell carcinoma. Unsparing sampling should be performed to rule out malignancy in giant dermatofibroma. The occurrence of other malignant tumors in giant dermatofibroma is a rare incidental finding, for which histological staging can be difficult. Complete excision of both the malignant tumor and the giant dermatofibroma should be guaranteed to prevent a tumor relapse.

# AG Geschichte und Ethik der Pathologie

AG09.01

## ***Translational Biomedical Research at the Institute of Veterinary Pathology (LMU Munich)***

A. Parzefall

Institut für Tierpathologie am Zentrum für Klinische Tiermedizin Ludwig-Maximilians-Universität München, München, Germany

Following a brief introduction of the >100 years of history of the Institute of Veterinary Pathology, the lecture will provide an overview of current translational collaborative research projects at the Institute. The generation and characterization of translational

large animal models, in particular genetically modified pig models, represents a current interdisciplinary research focus at the Faculty of Veterinary Medicine, which has appropriately specialized facilities for generation and husbandry of pig models for therapeutic trials (Chair of Molecular Animal Breeding and Biotechnology & Center for Innovative Medical Models (CiMM)). Over the past decade, pigs have increasingly become popular as translational large animal models due to their “physiological similarity” to humans, and are now established in biomedical research worldwide. Targeted genetic modifications now make it feasible to create tailored pig models for a large number of different human diseases. At the LMU-Faculty of Veterinary Medicine, various pig models have been developed so far, including models for metabolic diseases such as Diabetes mellitus and the metabolic syndrome, for cardiovascular and endocrine diseases, as well as for various monogenic hereditary diseases (e.g., muscular dystrophies, Laron syndrome, Usher syndrome), and for xenotransplantation. These models have been pathomorphologically characterized at the Institute of Veterinary Pathology. The lecture will provide insight views to selected pig models and their pathological alterations, biobank strategies developed for the efficient use of the models, downstream multi-omics analysis approaches, as well as future perspectives of translational research on porcine models at the LMU.

AG09.02

## ***Die Siegfried Oberndorfer Präparate-Lehrsammlung - Von der Magazinsammlung zum Museum***

A. Riepertinger

Klinikums München-Schwabing, Institut für Pathologie, München, Germany

In 1910, the new built Institute of Pathology of the Hospital Munich-Schwabing was opened.

The first director of the Institute, Professor Siegfried Oberndorfer placed special glass vitrine storing boards in the demonstration room for the collection of specimens used only for teaching of medical students.

Being Jewish, Professor Oberndorfer lost his position as Prosector of the Institute of Pathology Schwabing the 1. of April 1933.

He was replaced by Professor Ludwig Singer being the director of the institute until 1961. During that period, he added specimen from autopsies to that collection relocated to the attic of the institute.

Between 1945 and 1954 the building of the Institute of Pathology came under the command of the US military administration. It is very likely that many of the collectives were dumped meanwhile. Being able to return to the institute in 1954, due to shortage of room and storage capacity, specimens were moved within the institute to and fro and under the new director, Professor Erich Langer finally stored in the basement. As the collection was not the main focus in that time, only few new objects were added and the collection was no longer used for teaching.

In 1980, Professor Karlheinz Wurster became the new director of the institute and the collection was gaining again importance. Specimen were restored, better sorted, tagged and came to a presentable form in the basement. In 1984, as plastination was introduced as an additional technique, new vitrines with differently conserved objects were presented. Professor Andreas Nerlich led the institute from 2005 to 2023, supporting the preparators to enlarge and improve the collection. On 70 sqm and additional 15 sqm for the “historical cabinet” holding objects of the 19<sup>th</sup> century, the collection contains 1150 objects demonstrating a broad spectrum of diseases, including about 700 specimen as permanent loans from other institutes or institutions.

As the institute will be closed in the next years, A. Riepertinger, the leading preparator since several years struggle to convince the city of Munich to settle and preserve the collection as the “Pathologisches Museum München - Siegfried Oberndorfer”.



AG09.03

## ***Survey on working and training conditions and professional satisfaction of residents in surgical pathology***

V. Warm<sup>1</sup>, P. Jurmeister<sup>2</sup>, J. Maas<sup>3</sup>, B. Märkl<sup>4</sup>, G. Blumenstock<sup>5</sup>, M. Sulyok<sup>1</sup>, G. Baretton<sup>6</sup>, F. Fend<sup>1</sup>

<sup>1</sup>Universitätsklinikum Tübingen, Institut für Pathologie, Tübingen, Germany, <sup>2</sup>Ludwig-Maximilians-Universität, Pathologisches Institut, München, Germany, <sup>3</sup>Deutsche Gesellschaft für Pathologie e.V., Berlin, Germany, <sup>4</sup>Universität Augsburg, Pathologie, Medizinische Fakultät Augsburg, Augsburg, Germany, <sup>5</sup>Universitätsklinikum Tübingen, Klinische Epidemiologie und angewandte Biometrie, Tübingen, Germany, <sup>6</sup>Institut für Pathologie des Universitätsklinikums Carl Gustav Carus Dresden, Institut für Pathologie, Dresden, Germany

### **Background**

One of the greatest challenges of the German health care system is the lack of young talents and well-trained professionals. In the field of pathology young academics are also urgently needed. Therefore, it is of utmost importance to understand why young resident physicians choose to specialize in pathology, what they are looking for in a university hospital, what they plan for their professional development and what contributes to their professional satisfaction.

### **Methods**

In order to investigate this issue an online survey was conducted. The questionnaire included three open-ended and five closed-ended questions with free-text answers, 14 single-choice questions, one multiple-choice question and 47 Likert scales. The questionnaire was designed with SurveyMonkey and distributed via the German Society of Pathology and the working group Young Pathology. Descriptive and statistical analyses by chi-square-test were performed with SPSS 28.0.0.0.

### **Results**

120 participants took part in the survey (54.2% male, 40.0% female, 5.8% n/a) with an average training period of 3.7 years and of whom 85% work fulltime. 70% of the participants are employed in institutions with 5-10 residents. Particularly decisive for the choice of career is interest in the subject, but also the compatibility of career and family. In addition to sign out, the activities most frequently performed are grossing and taking part in lecturing. 67% of participants are satisfied or very satisfied with their current professional situation, although 70% of participants often or very often/always work overtime, most of which is spent on diagnostics. Around half of the participants aspire to an academic or university career and a habilitation. Participants aiming for a habilitation are statistically significantly more likely to be dissatisfied and work more overtime. 84% of participants would recommend their peers a career in pathology. The participants particularly value a good working atmosphere. They would like to see a reduction in the workload and better working hours as well as better time management and structured organization in order to do justice to diagnostics, teaching and research.

### **Conclusion**

Despite the high workload, many of the residents are passionate about pathology. This representative survey highlights the main factors important for recruiting residents into academic pathology and delineates areas where improvement is needed, such as staffing and structured work schedules.

AG09.04

## ***Lost Journals – forgotten journals and series of books in pathology***

T. Braunschweig<sup>1</sup>, K. Schierle<sup>2</sup>

<sup>1</sup>Pathologisches Institut, LMU München, München, Germany, <sup>2</sup>Institut für Pathologie, SLK Kliniken Heilbronn, Heilbronn, Germany

### **Background**

First scientific journals as periodic printed booklets or books containing different chapters or articles, mostly written by diverse authors, were published in the second half of the 17<sup>th</sup> century, beginning in France. In the 18<sup>th</sup> century, more focused journals were founded, first general scientific and on medicine, followed by purely medical journals. Subspecific journals about specialties in medicine as surgery, ophthalmology, obstetrics or also pathology developed within the 19<sup>th</sup> century. Especially in the second half of this century, journals and series of books of and about pathology were published. Only a few lasted long and a single one continues until today since 1848: "Virchows Archive".

## Methods

By internet research in different platforms, as the “Karlsruher virtueller Katalog”, “PubMed”, “Internet Archive” and the institute library in Munich, journals and series of books were sorted and registered. On the base of this Register and accessibility via internet, publications were listed not being available online.

## Results

Several online unavailable journals and book series could be identified being published over years as „Ziegler (und Nauwerck), Beiträge zur pathologischen Anatomie“, „Handbuch der allgemeinen Pathologie und der pathologischen Anatomie“, Handbuch der speziellen Pathologie und Histologie“ as well as „Centralblatt für allgemeine Pathologie und pathologische Anatomie“ and several more.

## Conclusion

The aim of this study is an extensively complete register of these “lost journals”, in order to 1) to remember these publications and authors, 2) making it easier for researchers and 3) creating one location in Germany where these journals and book series are available for researchers. A digitalization would be a big step forward, but as these journals and books are numerous, it is beyond our means.

# AG Thoraxpathologie 1

AG10.01

## ***Extensive Autoptic Morphomolecular Characterization of a Metastatic Small Cell Lung Cancer with Promising Response to SSTR-directed Peptide Receptor Radionuclide Therapy***

J. S. Enke<sup>1</sup>, N. G. Reitsam<sup>2</sup>, S. Dintner<sup>2</sup>, E. Sipos<sup>2</sup>, F. Liesche-Starnecker<sup>2</sup>, M. Trepel<sup>3</sup>, R. Claus<sup>2,3</sup>, C. Lapa<sup>1</sup>, R. A. Bundschuh<sup>1</sup>, B. Märkl<sup>2</sup>

<sup>1</sup>Fakultät für Medizin, Universität Augsburg, Nuklearmedizin, Augsburg, Germany, <sup>2</sup>Fakultät für Medizin, Universität Augsburg, Pathologie und Molekulare Diagnostik, Augsburg, Germany, <sup>3</sup>Fakultät für Medizin, Universität Augsburg, Hämatologie und Onkologie, Augsburg, Germany

## Background

As most patients with small cell lung cancer (SCLC) present with metastatic disease, prognosis is still devastating, despite the recent addition of immune checkpoint inhibitors to first-line chemotherapy. For the subset of SCLCs with somatostatin receptor (SSTR) overexpression, peptide receptor radionuclide therapy (PRRT) might be an effective targeted treatment option. However, conclusive results and insights into the tumor biology under SSTR-guided radionuclide therapy are currently missing.

## Methods

Tumor tissue of various tumor sites was obtained over the disease course (initial biopsy, recurrence, autopsy) and extensive histopathologic, immunohistochemical (SSTR2/5, PD-L1, Ki67) and molecular analyses (Illumina TSO 500 NGS panel) were performed.

## Results

Here, we present the case of a male patient with extensively pre-treated stage IV SCLC showing an exceptional treatment response to third-line SSTR-directed PRRT. The primary tumor lesion as well as local recurrence revealed a SCLC with typical histomorphology and characteristic immunophenotype. Interestingly, almost all tumor cells showed intense membranous SSTR2 expression (3+), lacking any SSTR5 expression. SSTR-directed PRRT induced radiologic partial remission; a progression-free survival of 6 months and an overall survival of 8 months was reached. At autopsy, cerebral progression was found to be the most likely cause of death. Interestingly, liver and bone metastases showed a downregulation of the previously highly overexpressed SSTR2 receptor. Genetically, all lesions were characterized by a *TP53* mutation. Up-regulation of PDL1 expression was not observed over the course of therapy.

## Conclusion

This interesting case highlights the great potential of SSTR-guided radionuclide therapy in SSTR overexpressing SCLCs.

Moreover, receptor downregulation of the tumor cells can be considered as potential evasion mechanism. Interestingly, tumor genetics remained comparably stable during the course of treatment, and no up-regulation of PD-L1 expression could be observed.

## AG10.02

### ***Is the association of small cell lung carcinoma with ectopic Cushing's syndrome as frequent as suggested in the literature?***

A. Ura<sup>1</sup>, E. Moser<sup>1</sup>, M. Evert<sup>2</sup>, K. Evert<sup>2</sup>, B. Märkl<sup>3</sup>, E. Sipors<sup>3</sup>, M. Kremer<sup>4</sup>, K. Steiger<sup>1</sup>, C. Moguler<sup>1</sup>, H. Hoffmann<sup>5</sup>, A. Werder von<sup>6</sup>, D. Kaemmerer<sup>7</sup>, G. Klöppel<sup>1</sup>, A. Kasajima<sup>1</sup>

<sup>1</sup>TUM School of Medicine and Health, Department of Pathology, Munich, Germany, <sup>2</sup>University of Regensburg, Institute of Pathology, Regensburg, Germany, <sup>3</sup>Medical Faculty Augsburg, Pathology, Augsburg, Germany, <sup>4</sup>Städtisches Klinikum München, Institute of Pathology, Munich, Germany, <sup>5</sup>TUM School of Medicine and Health, Department of Thoracic Surgery, Munich, Germany, <sup>6</sup>TUM School of Medicine and Health, Internal Medicine II, Munich, Germany, <sup>7</sup>Zentralklinik Bad Berka, Department of General and Visceral Surgery, Bad Berka, Germany

#### **Background**

In the lung and the thymus, ectopic Cushing syndrome (ECS) has been reported either in association with neuroendocrine tumors (NETs) or neuroendocrine carcinomas (NECs). In contrast, in digestive organs, hormone related syndromes, including ECS, are found to be only associated with NETs. Since we wondered whether this biological difference between thoracic and digestive NECs may be due to inappropriate interpretation of the tumor or a true biological phenomenon, we reviewed the published NECs with ECS and in addition searched for ACTH expression in thoracic NECs without ECS. Our aim is to clarify the association of ECS with thoracic small cell (SCLC) and large cell NECs (LCNEC).

#### **Methods**

Histological, immunohistochemical and clinical features of previously reported thoracic NENs patients with ECS were systematically reviewed. In addition, 102 thoracic NENs were assembled from multiple institutions and their histology and immunohistochemical ACTH expression were studied. Presence of clinically evident ECS was carefully reviewed.

#### **Results**

In a systematic literature review, 579 patients were identified between 1964 and 2024, who presented with ECS due to thoracic NENs (421 from lung, 158 from thymus) including 405 (70%) NETs and 174 (30%) NECs. Among NEC patients, the reported entity was SCLC in 163 (94%) and LCNEC in 11 (6%) patients. After careful reassessment of the reported clinical and pathological findings, 14 SCLCs and 8 LCNECs were re-classified as NET, either based on morphology (N=17), clinical manifestation (N=3) or unclear terminology (N=2). No sufficient information was provided for reassessment in 157 reports. In our cohort of 42 resected SCLCs and 10 LCNECs, 5 (11%) SCLCs, but no LCNEC, showed single cell ACTH expression. None of the patients had Cushing syndrome. In contrast, 10 NETs (20%) showed single cell ACTH expression (<10% of tumor cells) and 9 (18%) focal to diffuse positivity. 5 (10%) of the NET patients had ECS.

#### **Conclusion**

Many (17/22) of the reported thoracic NECs with ECS with appropriate information corresponded to NETs. Only in 3 cases, the diagnosis of SCLC could not be excluded with certainty. In the remaining cases, the provided data were insufficient to confirm the diagnosis of NEC. Since NECs contain single ACTH cells, the development ACTH cell neoplasm is possible, however, probably in much lower frequency than the reported cases suggest.

## AG10.03

### ***Predictive biomarkers for checkpoint inhibitor therapy in NSCLC: KRAS/TP53 co-mutations and brain metastasis-specific PD-L1 expression – two real-world cohort analyses***

P. Bischoff<sup>1</sup>, D. Wasilewski<sup>2</sup>, P. Vajkoczy<sup>2</sup>, M. Reck<sup>3</sup>, N. Frost<sup>4</sup>, D. Horst<sup>1</sup>

<sup>1</sup>Charité - Universitätsmedizin Berlin, Institut für Pathologie, Berlin, Germany, <sup>2</sup>Charité - Universitätsmedizin Berlin, Klinik für Neurochirurgie mit Arbeitsbereich Pädiatrische Neurochirurgie, Berlin, Germany, <sup>3</sup>LungenClinic Großhansdorf, Abteilung für Onkologie,

## Background

Advanced NSCLC patients without targetable genomic alterations are eligible for immune checkpoint inhibitor (ICI) treatment, either as monotherapy or in combination with chemotherapy, depending on PD-L1 expression status. However, additional biomarkers are required for precise prediction of ICI therapy response in clinical routine. Moreover, the significance of PD-L1 expression in primary versus metastatic sites, in particular in brain metastases, remains elusive.

## Methods

We analyzed two separate cohorts. The first cohort comprised 696 non-squamous NSCLC patients with high PD-L1 expression (TPS $\geq$ 50%) who received first-line palliative treatment with the ICI pembrolizumab. Treatment efficacy and outcomes were correlated with *KRAS* and *TP53* mutational status and the number of tumor-infiltrating lymphocytes. We conducted complementary gene expression analysis using The Cancer Genome Atlas (TCGA) lung adenocarcinoma cohort.

The second cohort included 64 NSCLC patients treated with ICIs after brain metastasis resection. PD-L1 expression in matched brain metastasis and extracranial tumor tissue was assessed by immunohistochemistry. Optimal PD-L1 cut points for intracranial and extracranial progression-free survival, and overall survival were defined and evaluated in multivariable analyses.

## Results

In the first cohort, *KRAS* mutations were present in 53% of patients, with G12C and non-G12C mutations occurring in 25% and 28%, respectively. *TP53* mutations were found in 51% of patients. Among *KRAS*-mutant patients, *TP53* co-mutations were associated with better outcomes. Patients harboring G12C/*TP53* co-mutations exhibited the longest progression-free survival and overall survival, correlating with increased tumor-infiltrating lymphocytes and upregulation of interferon gamma target genes.

In the second cohort, PD-L1 expression was significantly lower in brain metastases than in matched extracranial tumor tissue. Notably, high PD-L1 expression in brain metastases (TPS $>$ 40%) was independently associated with prolonged intracranial and extracranial progression-free survival, and overall survival.

## Conclusion

Our findings suggest that the combined assessment of *KRAS* and *TP53* mutations in PD-L1-high non-squamous NSCLC may help to identify patients who will likely benefit from ICI therapy. Furthermore, PD-L1 expression in brain metastasis tissue shows promise as a predictive biomarker for ICI response, particularly useful in cases where extracranial tissue is not available for PD-L1 assessment.

AG10.04

## ***One-Carbon-Metabolismus in Karzinomen der Lunge***

S. Yao<sup>1</sup>, Y. Li<sup>1</sup>, O. Elakad<sup>1</sup>, A. von Hammerstein-Equord<sup>2</sup>, S. Küffer<sup>1</sup>, P. Ströbel<sup>1</sup>, H. Bohnenberger<sup>1</sup>

<sup>1</sup>Universitätsmedizin Göttingen, Institut für Pathologie, Göttingen, Germany, <sup>2</sup>Universitätsmedizin Göttingen, Klinik für Herz-, Thorax- und Gefäßchirurgie, Göttingen, Germany

## Background

Lung cancer, particularly driven by *KRAS* mutations, leads in global cancer mortality. Despite progress in targeted therapies for specific mutations like *KRAS* G12C, many patients lack effective treatments. One-carbon metabolism (1CM) enzymes like MTHFD2, known to influence cancer progression, have not been fully explored in lung cancer. This gap underscores the need for our investigation into 1CM's role and therapeutic potential in lung cancer, especially in the context of *KRAS* mutations.

## Methods

We evaluated the significance of five 1CM enzymes in lung cancer subtypes (AC, SQCLC, SCLC) using immunohistochemistry in 323 patient samples and cell proliferation assays in 15 cell lines. This study also assessed the correlation between MTHFD2 expression and *KRAS* mutations in AC, aiming to identify potential therapeutic targets.

## Results

Our study found a significant link between high levels of MTHFD2 and PGDH3 and poor survival in pulmonary adenocarcinoma (AC) patients, highlighting their prognostic significance. MTHFD2, in particular, was strongly associated with increased resistance to Pemetrexed, pointing to a specific mechanism of chemoresistance in AC. Cell proliferation assays across lung cancer subtypes revealed a crucial role for 1CM enzymes in AC cell line growth, with a less pronounced effect in squamous cell lung cancer (SQCLC) and small cell lung cancer (SCLC) lines. This suggests a unique therapeutic target opportunity in AC. Moreover, MTHFD2 expression was markedly upregulated in AC with KRAS mutations, suggesting KRAS-driven cancers rely more on 1CM pathways. This upregulation, coupled with MTHFD2's impact on proliferation and chemoresistance, underlines its central role in AC biology and therapeutic potential. The vulnerability of KRAS-mutant AC cell lines to MTHFD2 inhibition opens new therapeutic avenues for NSCLC patients with these mutations.

## Conclusion

MTHFD2's expression significantly affects AC prognosis and chemoresistance, highlighting its minimal presence in healthy tissue as an advantageous therapeutic target. Targeting MTHFD2 could counteract resistance and improve outcomes in AC, suggesting a promising direction for future therapy development.

AG10.05

## ***The growth-inhibitory role of bile acids in non-small cell lung cancer cells in the presence of PD-L1 and the clinical implication***

Y. Chen<sup>1</sup>, L. Ludewig<sup>1</sup>, J. M. Boehlke<sup>1</sup>, M. Nenkov<sup>1</sup>, Y. Ma<sup>1</sup>, J. Hoff<sup>2</sup>, A. Press<sup>2</sup>, M. Gräler<sup>2</sup>, N. G. Gaßler<sup>1</sup>

<sup>1</sup>University Hospital Jena, Section Pathology of the Institute of Forensic Medicine, Jena, Germany, <sup>2</sup>University Hospital Jena, Department of Anaesthesiology and Intensive Care Medicine, Jena, Germany

## Background

Bile acids (BAs) produced in the liver function as detergents to facilitate the digestion and absorption of lipids. BAs bind their receptors, activating the signaling pathways to regulate metabolic diseases, immune responses, and carcinogenesis. The role of BAs in tumors of the digestive system is well studied, however, the involvement of BAs in lung cancer, especially in the context of PD-L1 overexpression, is not yet clear.

## Methods

In our study, lung cancer cells stably transfected with PD-L1, primary lung tumor tissues as well as plasma samples, and mouse tissues derived from BA-fed mice were used for real-time RT-PCR, western blotting, immunohistochemistry, cell-based functional assay, metabolic analysis (Seahorse assay), and mass spectrophotometry analysis.

## Results

We found that plasma samples from the patients with lung adenocarcinoma (ADC) displayed a significantly higher amount of total BAs compared to that from the patients with lung squamous cell carcinoma (SCC). Treatment of PD-L1 overexpressing ADC cell line H1299 with lithocholic acid (LCA) or ursodeoxycholic acid (UDCA) led to decreased cell proliferation, migration, and invasion, accompanied with reduced mitochondrial ATP production rates. In primary lung tumors, higher expression of the farnesoid X receptor (FXR), one of the BA receptors, was significantly associated with lung SCC and probably involved in tumor immunity. In lung tissues derived from BA-fed mice, an altered expression of proliferation-associated genes was observed.

## Conclusion

Taken together, our data suggest that bile acids LCA and UDCA suppress NSCLC cell growth, migration, and invasion, and cause metabolic reprogramming, even in the presence of the oncogene PD-L1, FXR might be a potential diagnostic marker for lung SCC, and the amount of plasma BAs may be associated with primary lung ADC.

AG10.06

## ***Upregulation of Serpin B13 in squamous cell carcinomas of the lung predicts favorable prognosis***

C. Kümpers<sup>1</sup>, D. Nitschkowski<sup>2,3</sup>, K. Stein<sup>2,3</sup>, T. Jagomast<sup>4</sup>, C. Heidel<sup>5</sup>, J. Kirfel<sup>5</sup>, S. Perner<sup>6</sup>, M. Reck<sup>3,7</sup>, C. Kugler<sup>3,8</sup>, O. Ammerpohl<sup>3,9</sup>, T. Goldmann<sup>2,3</sup>

<sup>1</sup>Institute of Pathology University Hospital Schleswig Holstein, Campus Luebeck, Lübeck, Germany, <sup>2</sup>Histology Research Center Borstel, Leibniz Lung Center, Borstel, Germany, Borstel, Germany, <sup>3</sup>Airway Research Center North (ARCN), German Center for Lung Research (DZL), Germany, Borstel, Germany, <sup>4</sup>Medical Clinic III, University Hospital Schleswig-Holstein, Campus Luebeck, Lübeck, Germany, <sup>5</sup>Institute of Pathology University Hospital Schleswig-Holstein Campus Luebeck, Lübeck, Germany, <sup>6</sup>MVZ Center for Outpatient Oncology, Tuebingen, Germany, Tübingen, Germany, <sup>7</sup>Oncology LungenClinic Grosshansdorf, Großhansdorf, Germany, Großhansdorf, Germany, <sup>8</sup>Surgery, LungenClinic Grosshansdorf, Großhansdorf, Germany, Großhansdorf, Germany, <sup>9</sup>Institute of Human Genetics, University Medical Center Ulm, Germany, Ulm, Germany

### **Background**

Therapy of NSCLC has made immense progress in recent years. However, in the context of personalized therapy, there are much more options for pulmonary adenocarcinomas than for squamous cell carcinomas (SCC). For the latter, valid prognostic markers in addition to common markers such as TNM and grading are also lacking. Serpin B13 belongs to the superfamily of serpins and acts as a serine proteinase inhibitor. Serpin B13 is a cytoplasmic protein that plays a role in the proliferation and differentiation, e.g. of keratinocytes. Here, we describe serpin B13 expression at the protein level and its epigenetic modifications and examine the impact on overall survival using lung squamous cell carcinoma tissues.

### **Methods**

We analyzed epigenetic modifications of the serpin B13 gene in NSCLC and its expression on RNA-level by transcriptome analysis. The expression of serpin B13 on the protein level was assessed by immunohistochemistry using an independent cohort of 125 SCC patients and its expression was correlated with overall survival and immune infiltration.

### **Results**

We revealed a significant difference in methylation of serpin B13 loci in NSCLC and showed that mRNA- and protein expression of serpin B13 is upregulated in pulmonary SCC. High protein expression of serpin B13 was significantly associated with a better overall survival. Moreover, carcinomas with low immune infiltration showed significantly less protein expression of serpin B13 than carcinomas with high immune infiltration. *In-vitro* analyses are currently pending.

### **Conclusion**

Our results suggest serpin B13 to be a novel prognostic biomarker for pulmonary SCC. Its implementation in future routine diagnostic workup could be reasonable.

## **AG Thoraxpathologie 2**

AG10.07

### ***Pathologic diagnosis of lung cancer: my approach to selected topics***

S. Mukhopadhyay

Cleveland Clinic, Pathology, Cleveland, Ohio, United States of America

The aim of this presentation is to outline my approach to the pathologic diagnosis of lung cancer in lung biopsies and resections. The goal is not to cover the entire field of neoplastic lung pathology but rather to focus on selected issues where recent advances have led to developments in the field, or in which difficult-to-resolve difficulties or controversies exist, requiring some degree of judgment by individual pathologists. I will outline my approach to the diagnosis of adenocarcinoma in small biopsies, to the staging of multiple lung adenocarcinomas in resection specimens, to the diagnosis of neuroendocrine neoplasms in the lung (in small biopsies and resections), and how I use (or do not use) immunohistochemistry in lung cancer, including diagnosis, subtyping, and determination of site of origin. I will briefly also address the topic of frozen sections in thoracic pathology with a focus on adenocarcinoma and its mimics.

AG10.08

### ***Computational pathology platform for lung cancer: development and validation of diagnostic and prognostic algorithms***

Y. Wang<sup>1</sup>, C. Kludt<sup>1</sup>, W. Ahmad<sup>1</sup>, A. Pryalukhin<sup>2</sup>, F. Mairinger<sup>3</sup>, A. Bychkov<sup>4</sup>, J. Fukuoka<sup>4</sup>, D. Jonigk<sup>5</sup>, M. Kühnel<sup>5</sup>, A. Schultheis<sup>1</sup>, W. Hulla<sup>2</sup>, N. Gaisa<sup>6</sup>, S. Klein<sup>7</sup>, A. Quaas<sup>1</sup>, R. Büttner<sup>1</sup>, Y. Tolkach<sup>1</sup>

<sup>1</sup>University Hospital Cologne, Institute of Pathology, Cologne, Germany, <sup>2</sup>Landeskrankenhaus Wiener Neustadt, Wiener Neustadt, Austria, <sup>3</sup>University Hospital Essen, Essen, Germany, <sup>4</sup>Kameda Medical Hospital, Kamogawa, Japan, <sup>5</sup>University Hospital Aachen, Aachen, Germany, <sup>6</sup>University Hospital Ulm, Institute of Pathology, Ulm, Germany, <sup>7</sup>University Hospital Cologne, Cologne, Germany

#### **Background**

Non-small cell lung cancer (NSCLC) is one of the most common malignant tumors. ranks as a leading cause of cancer-related deaths globally. Despite the digital revolution in pathology, a significant gap exists in the availability of potent, clinical-grade tools specifically for NSCLC. The study aimed to develop a clinically useful computational pathology platform for NSCLC that can be a foundation for multiple downstream applications and provide immediate value for patient care optimization and individualization.

#### **Methods**

We trained the primary multi-class tissue segmentation algorithm on a substantial, high-quality, manually annotated dataset of whole slide images (WSI) with lung adenocarcinoma (LUAD) and lung squamous cell carcinomas (LUSC). Two downstream applications are investigated. NSCLC subtyping algorithm is trained and validated using a large, multi-institutional (n=6), multi-scanner (n=5), international cohort of NSCLC cases (slides/patients 4097/1527). Five expert pathologists were included in the validation. Four new, AI-derived, fully explainable, quantitative, prognostic parameters are developed and validated for different clinical endpoints.

#### **Results**

The computational platform we developed enables the high-precision, quantitative analysis of H&E-stained slides. The downstream subtyping algorithm allows for high-accuracy classification into LUSC and LUAD (including mucinous) subtypes. The newly developed prognostic parameters facilitate robust and independent risk stratification of patients with LUAD and LUSC.

#### **Conclusion**

We developed a comprehensive computational pathology platform specifically for NSCLC. It could be immediately leveraged to optimize diagnostics and patient care. We also introduced four novel, independent prognostic parameters with significant potential for patient stratification.

AG10.09

### ***Pleural manifestation of a spindle cell tumor with prominent vascular pattern: A rare manifestation of Dermatofibrosarcoma protuberans, a diagnostic pitfall***

M. Forberger<sup>1</sup>, P. Geßner<sup>2</sup>, M. Stiller<sup>1</sup>, D. Geister<sup>3</sup>, H. Bisanz<sup>3</sup>, H. Bläker<sup>1</sup>, M. von Laffert<sup>1</sup>

<sup>1</sup>University Hospital Leipzig, Institute of Pathology, Leipzig, Germany, <sup>2</sup>University of Leipzig, Institute of Clinical Immunology, Faculty of Medicine, Leipzig, Germany, <sup>3</sup>St. Georg Hospital, Institute of Pathology, Leipzig, Germany

#### **Background**

Dermatofibrosarcoma protuberans (DFSP) is a malignant neoplasm that typically arises in the skin or subcutaneous tissues of the trunk or proximal extremities. [1] Histologically the tumor shows spindle cells with storiform pattern and diffuse infiltration of the surrounding stroma. Tumors are positive for CD34 and molecular pathology often reveals a COL1A1/PDGFB fusion. Whereas the tumor is local destructive, metastases are rare. As risk factors for metastasis, tumor size [2] and transformation into a Dermatofibrosarcoma, fibrosarcomatous variant (FS-DFSP) have been described.

Solitary Fibrous Tumors (SFT) typically manifest as slow-growing soft tissue tumors, frequently originating in connective tissues, notably the pleura. Histologically, SFTs exhibit a patternless pattern of spindle-shaped cells, highlighted by staghorn vessels.

## Methods

We present the case of a 59-year-old male with a clinically identified pulmonary mass measuring 2.6 x 2.3 cm in the left upper lobe, initially suspected to be a primary lung tumor. PET-CT revealed mildly increased metabolic activity in the biopsied lung lesion. Another pulmonary nodule and a thigh lesion also exhibited metabolic activity.

Histopathological analyses, including H&E and immunohistochemical stainings (CD34, bcl2, STAT6, Ki67, p53, AE1/3, EMA, S-100, CD31, TLE1, Desmin, and SMA) were conducted.

## Results

Histologically, the left upper lobe biopsy revealed a cellular spindle-shaped tumor with prominent vascular features and a hemangiopericytoma-like growth pattern. Immunohistochemically, the cells were positive for CD34, occasionally weakly positive for bcl-2, and negative for STAT6 and the remaining markers. p53 was wild-type, Ki67 exhibited intermittent positivity at approximately 30%. The immunohistochemical profile confirmed the diagnosis of DFSP. Solitary fibrous tumor was ruled out due to STAT6 negativity. Other differentials were excluded.

The histology was matching with a previously diagnosed and resected DFSP of the right inguinal region.

## Conclusion

In the context of a pleural spindle cell lesion one might initially think of a SFT. In this case, immunohistochemical staining for STAT6 aids in differentiation from SFT. The immunohistochemical staining confirmed the diagnosis that the pulmonary lesions were a rare case of metastases of a previously diagnosed and resected classical Dermatofibrosarcoma protuberans without progression to a fibrosarcomatous variant.

Literaturangaben:

[1] Mentzel T, (2015), Fibrohistiocytic tumors of the skin: a heterogeneous group of superficially located mesenchymal neoplasms, Pathologe, 79-88

[2] Hayakawa K, Matsumoto S, Ae K, et al., (2016), Risk factors for distant metastasis of dermatofibrosarcoma protuberans, J Orthop Traumatol., 261-266

# AG Molekularpathologie 1

AG11.02

## ***MCPIP1 is a novel regulator of necroptotic cell death in colorectal cancer***

J. Rossmannith<sup>1</sup>, A. Hoffmann<sup>2</sup>, W. Roth<sup>1</sup>, M. Oliver Metzger<sup>1</sup>

<sup>1</sup>Universitätsmedizin Mainz, Institut für Pathologie, Mainz, Germany, <sup>2</sup>UCLA, Signaling Systems Laboratory, Department of Microbiology, Immunology and Molecular Genetics and Institute for Quantitative and Computational Biosciences, Los Angeles, United States of America

### Background

Apoptosis resistance is a hallmark of colorectal cancer (CRC) and important reason why chemotherapy fails. Necroptosis is an alternative form of regulated cell death that may help to overcome apoptosis resistance and trigger an anti-tumor immune response. Our previous work has shown that the targeted induction of necroptosis in CRC is feasible. Dissecting the regulatory network of necroptosis is of clinical significance.

### Methods

We quantified necroptotic cell death including live-cell microscopy and automated image analysis in wildtype and CRISPR-Cas9-knockout cells. To address the molecular mechanisms, we performed gene expression analysis and protein biochemistry.

### Results

We identified the endoribonuclease MCPIP1 as a novel positive regulator of necroptotic cell death in CRC. CRISPR-mediated gene knockout significantly protected CRC cells from necroptotic cell death. Preliminary mechanistic studies suggest that MCPIP1 may prime cells for necroptosis by lowering the basal expression of NFκB/RelA-responsive pro-survival regulators. MCPIP1 expression correlated with necroptosis sensitivity in a cohort of patient-derived CRC cell lines.



## Conclusion

MCPIP1 is a novel necroptosis regulator and potential marker of necroptotic capacity in CRC. Patients with MCPIP1-positive CRC may benefit from necroptotic therapies.

AG11.03

## ***Amyloid typing by mass spectrometry***

A. Soltermann<sup>1</sup>, M. Stumpe<sup>2</sup>, P. Dzubak<sup>3</sup>, A. Tzankov<sup>4</sup>, R. Biral<sup>1</sup>, D. Kressler<sup>2</sup>

<sup>1</sup>Pathologie Länggasse, Ittigen, Switzerland, <sup>2</sup>Metabolomics and Proteomics Platform, Department of Biology, University of Fribourg, Fribourg, Switzerland, <sup>3</sup>Institute of Molecular and Translational Medicine, Faculty of Medicine and Dentistry, Palacky University, Olomouc, Czech Republic, <sup>4</sup>Institute of Medical Genetics and Pathology, University Hospital Basel, Basel, Switzerland

## Background

The most frequent variants of amyloidosis are AL (kappa/lambda light chains), AA (serum amyloid A protein), AF (familial, hereditary with mutated amyloid transthyretin, ATTR-mut) and AS (senile, cardiac with wild type amyloid transthyretin, ATTR-wt). Novel drug therapeutics are available for ATTR-mut, and some also for ATTR-wt patients, making amyloid typing key. Immunohistochemistry (IHC) panels have shown some limited specificity and sensitivity. Next to IHC, mass spectrometry is an alternative technology for protein determination. It allows for identifying thousands of proteins in a single run of high-performance liquid chromatography (HPLC).

## Methods

We have implemented a filter- and a bead-based protein extraction protocol for formalin-fixed paraffine-embedded tissue (FFPE), starting with 20 micrometer thick cut sections. Nanoflow HPLC followed by tandem mass spectrometry (MS/MS) using an Orbitrap Exploris 480 was performed at the Department of Biology, University of Fribourg. Samples are independently analyzed at the Institute of Molecular and Translational Medicine, Palacky University, Olomouc.

## Results

With the bead protocol we achieved a robust ion current flow across the HPLC gradient. The filter-based protocol showed a 10-fold lower ion current and clogging of HPLC due to insufficient removal of sodiumdodecylsulfat (SDS). Typically, more than 4000 different proteins were identified per sample. In cases of localized amyloidosis of the seminal vesicle, we identified the specific amyloidogenic protein semenogelin-1 (ASem-1) as well as the generic amyloidosis markers apolipoprotein E (ApoE) and serum amyloid P component (SAP). In a case of AL-lambda, lambda light chains were detected in FFPE omental fat tissue with a ratio lambda to kappa > 10. Mass spectrometric protein quantification indices such as intensity based absolute quantification (iBAQ), LQF intensity and MS/MS counts gave consistent results.

## Conclusion

Amyloid typing by shotgun mass spectrometry is able to detect specific amyloid types in a single assay. It supports the diagnosis and treatment of amyloidosis patients in routine clinical practice, as the causing protein is specifically identified.

## AG Molekularpathologie 2

AG11.04

## ***Implementation of plasma-based ESR1 mutation testing for breast cancer patients in Germany - a harmonization study***

C. Jonas<sup>1</sup>, J. Fassunke<sup>1</sup>, A. Escherich<sup>2</sup>, W. Dietmaier<sup>3</sup>, S. Dintner<sup>4</sup>, S. Herold<sup>5</sup>, L. C. Heukamp<sup>6,7</sup>, K. Neumann<sup>8</sup>, S. Merkelbach-Bruse<sup>1</sup>, R. Büttner<sup>1</sup>

<sup>1</sup>University of Cologne, Faculty of Medicine and University Hospital Cologne, Institute of Pathology, Köln, Germany, <sup>2</sup>A. Menarini GmbH, Zürich, Switzerland, <sup>3</sup>University Hospital Regensburg, Institute of Pathology, Regensburg, Germany, <sup>4</sup>General Pathology and Molecular Diagnostics, Faculty of Medicine, University of Augsburg, Augsburg, Germany, <sup>5</sup>University Hospital Carl Gustav Carus Dresden, Institute of Pathology, Dresden, Germany, <sup>6</sup>Lungenkrebsmedizin Oldenburg, Oldenburg, Germany, <sup>7</sup>Institute for Hematopathology Hamburg, Hamburg, Germany, <sup>8</sup>City Hospital Dessau, Institute of Pathology, Dessau, Germany

## Background

Systemic first-line therapy of advanced hormone receptor positive and HER2 negative breast cancer is often carried out with aromatase inhibitors and CDK4/6 inhibitors. During therapy, often a resistance to aromatase inhibitors, which is caused by a mutation in the estrogen receptor 1 gene (*ESR1*), is developed. Patients with activating mutations in the *ESR1* gene benefit from a change of therapy to ORSERDU®. The approval determines that the *ESR1* analysis must be carried out using plasma as a liquid biopsy.

## Methods

Fourteen *ESR1* mutated artificial plasma samples (8x single mutation, 1x wild type, 5x double mutations) with an allele frequency of 1% were analyzed by parallel sequencing and/or dPCR in different institutes of pathology (Augsburg, Dessau, Dresden, Oldenburg, Regensburg, Cologne). Assays and platforms from Qiagen, ThermoFisher, BioRad and Gencurix were used for the dPCR analysis. Custom and commercial assays from Qiagen, Agilent, Roche, ThermoFisher and Twist Biosciences as well as sequencing platforms from Illumina and ThermoFisher were used for parallel sequencing.

## Results

dPCR: 2 participants correctly analyzed the mutation status of all 14 samples, 2 participants were unable to correctly analyze 2 samples. 1 participant was unable to analyze 4 samples correctly. 1 participant performed dPCR with two different assays. Due to a technical error, he was only able to analyze 2 samples correctly in the first analysis and was able to analyze 13 samples correctly when performing the analysis again with an assay from another provider.

Parallel sequencing: 3 out of 6 participants correctly analyzed the mutations of all 14 plasma samples, 3 participants correctly analyzed all 14 samples after changing the filter criteria. 1 participant could not detect a double mutation due to quality control parameters.

## Conclusion

Parallel sequencing proved to be a suitable method for detecting *ESR1* variants. As the samples to be tested may have a very low allele frequency, it is advisable to check the filter criteria of the evaluation pipeline beforehand. The use of suitable reference standards for the establishment of plasma-based *ESR1* testing seems mandatory. With the exception of one assay, the dPCR assays used here only allow to identify the mutated codon of the *ESR1* gene; a differentiation at base pair level is hardly possible.

AG11.05

## Conclusions from the QuIP MSI ring trial 2023 for practical application in MSI diagnostics

W. Dietmaier<sup>1</sup>, M. Trummer<sup>1</sup>, D. Hirsch<sup>1</sup>, K. Utpatel<sup>1</sup>, K. Jöhrens<sup>2,3</sup>, K. Ilm<sup>3</sup>

<sup>1</sup>Institute of Pathology, University of Regensburg, Regensburg, Germany, <sup>2</sup>Institut für Pathologie, Klinikum Chemnitz, Chemnitz, Germany, <sup>3</sup>QuIP, Berlin, Germany

## Background

Microsatellite instability (MSI) is an important biomarker both in diagnostics and in therapy planning for various tumor entities. Both suitable and quality-assured methods are essential for the detection of MSI in routine molecular pathology applications, which were tested in the 2023 MSI round robin test offered by QuIP.

## Methods

A total of 10 pre-tested and validated samples from colorectal carcinoma (n=5), endometrial carcinoma (n=4) and gastric carcinoma (n=1) were processed to investigate the microsatellite status (MSS/MSI-H) of 47 participants. PCR-based systems with subsequent fragment length analysis, ddPCR and PCR with melting point analysis as well as a next generation sequencing method were used. In-house methods were used, including the Bethesda panel (consisting of mono- and dinucleotide markers) and Pentaplex mononucleotide panel, as well as various commercially available mononucleotide assays from Promega (OncoMate™ MSI Dx Analysis System, MSI Analysis System Version 1. 2 and LMR MSI Analysis System), Thermo Fisher Scientific (TrueMark MSI Assay), Bio-Rad (ddPCR Microsatellite Instability (MSI) Kit), Biocartis (Idylla™ MSI Assay) and AmoyDx (AmoyDx® HANDLE Classic NGS Panel) were used.

## Results

3 out of 10 cases (3 colorectal carcinomas) were correctly assessed by all 47 (100%) participants. 2 cases (endometrial carcinomas) could not be assessed by 1/47 (2%) participants and 1 case (endometrial carcinoma) by 2/47 (4%) participants ("technically not evaluable"). 4 cases (1 gastric carcinoma, 2 colorectal carcinomas, 1 endometrial carcinoma) were each correctly assessed by at least 44/47 participants (94%). In one MSI-H endometrial carcinoma case, MSI was detected by only 26/47 (55%) participants. Each of these used a PCR procedure with subsequent fragment length analysis. The MSI-H in another endometrial carcinoma was correctly detected by 33/47 (70%) participants.

## Conclusion

While the detection of MSI in colorectal carcinoma proved to be relatively unproblematic in the round robin test, there were clear difficulties in detecting MSI in endometrial carcinoma. This shows that the choice of a suitable examination method (in this case PCR with fragment length analysis using suitable markers) is essential. In addition, precise microdissection, examination of normal and tumor tissue in pairs where possible and visual representation of the microsatellite peaks, in which even small microsatellite shifts are clearly visible, are important for MSI detection and interpretation.

AG11.06

## ***Dissecting the Methylomes of Non-Small Cell Lung Cancer with high and low PD-L1 expression***

G. Hutarew, B. Alinger-Scharinger, K. Sotlar, T. Kraus  
Uniklinikum Salzburg, Universitätsinstitut für Pathologie, Salzburg, Austria

### Background

Non-small cell lung cancer (NSCLC) is one of the most frequent cancers. In the last years, there was an increase in molecularly targeted therapies. A novel approach in lung cancer therapy is programmed cell death ligand 1 (PD-L1). PD-L1 has been identified as an important candidate in precision medicine. PD-L1 is a key player in modulating interactions between the immune system and the tumor triggering the immune response in human cancers. Thereby, PD-L1 overexpression is a druggable target in lung cancer. The aim of this study is to identify differentially methylated genes and pathways of PD-L1 high and low expressing NSCLCs.

### Methods

In this study, we performed epigenome-wide methylation analysis on 20 NSCLCs with high and low PD-L1 expression. Thereby, 10 tumors showed high PD-L1 expression with tumor proportion score (TPS) of more than 50% and 10 tumors showed low PD-L1 expression with TPS of less than 1%. Applying the Illumina Infinium EPIC bead chip array we interrogated more than 850,000 methylation sensitive CpGs sites in parallel. Computational analyses were performed to identify differentially methylated genes. Gene ontology analysis was processes to reveal altered pathways.

### Results

We found that NSCLCs with high and low PD-L1 expression show distinct epigenomic alterations of the DNA methylation landscape. Analysis revealed 252,729 tiling regions, 34,988 gene regions, 44,852 promoter regions, and 26,540 in CpG islands. Differential methylation analysis revealed S100A7L2 (S100 Calcium Binding Protein A7 Like 2) gene as top hit being hypermethylated in PD-L1 high NSCLCs (delta beta of 0.17,  $p = 0.002$ ) and LINC00528 (Long Intergenic Non-Protein Coding RNA 528) being hypermethylated in PD-L1 low NSCLCs (delta beta of 0.19,  $p = 0.001$ ).

### Conclusion

In summary, in this pilot study, we found significantly differentially methylated gene regions in NSCLCs with high and low PD-L1 expression enabling to identify novel biomarkers in lung cancer.

## ***Multimodel, AI-based, data-integrated cell-omics derived cell niches advance UICC staging system in non-small cell lung cancer patients.***

S. Schallenberg<sup>1</sup>, G. Dernbach<sup>1,2</sup>, S. Ruane<sup>2</sup>, C. Böhm<sup>2</sup>, L. Ruff<sup>2</sup>, K. Standvoss<sup>2</sup>, S. Ghosh<sup>2</sup>, M. Frentsch<sup>3,4</sup>, M. P. Dragomir<sup>1</sup>, R. Fritz<sup>1</sup>, I. Koch<sup>5</sup>, C. Friedrich<sup>6</sup>, I.-K. Na<sup>3,7</sup>, S. Merkelbach-Bruse<sup>8</sup>, A. Quaas<sup>8</sup>, N. Frost<sup>9</sup>, K. Boschung<sup>10</sup>, W. Randerath<sup>10</sup>, G. Schlachtenberger<sup>11</sup>, M. Heldwein<sup>11</sup>, U. Keilholz<sup>12</sup>, K. Hekmat<sup>11</sup>, J.-C. Rückert<sup>13</sup>, R. Büttner<sup>8</sup>, A. Vasaturo<sup>14</sup>, D. Horst<sup>1</sup>, M. Alber<sup>2</sup>, F. Klauschen<sup>1,15</sup>

<sup>1</sup>Charité - Universitätsmedizin Berlin, Pathologie, Berlin, Germany, <sup>2</sup>Aignostics GmbH, Berlin, Germany, <sup>3</sup>Charité - Universitätsmedizin Berlin, Department of Hematology, Oncology, and Tumor Immunology, Berlin, Germany, <sup>4</sup>Charité - Universitätsmedizin Berlin, IH Center for Regenerative Therapies (BCRT), Berlin Institute of Health at Charite, Berlin, Germany, <sup>5</sup>Berliner Medizinhistorisches Museum der Charité, Pathologie, Berlin, Germany, <sup>6</sup>Max-Delbrück-Center for Molecular Medicine in the Helmholtz Association, Proteomics Platform, Berlin, Germany, <sup>7</sup>Charité - Universitätsmedizin Berlin, BIH Center for Regenerative Therapies (BCRT), Berlin Institute of Health at Charite, Berlin, Germany, <sup>8</sup>Uniklinik Köln, Pathologie, Köln, Germany, <sup>9</sup>Charité - Universitätsmedizin Berlin, Department of Infectious Diseases and Respiratory Medicine, Berlin, Germany, <sup>10</sup>Bethanien Hospital, Clinic of Pneumology and Allergology, Center for Sleep Medicine and Respiratory Care, Solingen, Germany, <sup>11</sup>Uniklinik Köln, Department of Cardiothoracic Surgery, Köln, Germany, <sup>12</sup>Charité - Universitätsmedizin Berlin, Charite Comprehensive Cancer Center, Berlin, Germany, <sup>13</sup>Charité - Universitätsmedizin Berlin, Department of General, Visceral, Vascular and Thoracic Surgery, Berlin, Germany, <sup>14</sup>Ultivue, Cambridge, United States of America, <sup>15</sup>Institute of Pathology, Ludwig-Maximilians-University, Munich, Germany

### **Background**

Lung cancer is the leading cause of cancer death worldwide. Non-small cell lung cancer (NSCLC) represents about 80% of all lung cancer cases. The tumor microenvironment (TME) influences the clinical outcome, whereby the location and composition of immune cells relate to their function and activity. Therefore, we developed a multiplex immunofluorescence (miF)-based, AI-driven approach for spatially resolved TME characterization at the cellular level and used this to successfully predict the patient survival.

### **Methods**

We collected FFPE tissue and clinicopathological data from 1182 patients with resected NSCLC from Berlin and Cologne. After tissue microarray (TMA) construction, sections were stained with a 12-plex immunofluorescence (IF) panel and with hematoxylin and eosin (H&E), respectively, and all stains were scanned and co-registered with single cell accuracy. An H&E-based tissue segmentation model was trained to detect the different tissue regions: carcinoma, stroma, necrosis and healthy tissue. Next, a nucleus-based cell detection model, and 12 binary cell classification models were developed to classify each detected cell by their H&E and miF staining. At last, we trained a model on the Berlin cohort using the spatially resolved cell readouts of cell densities in regions, marker expression, cell neighborhood niches, to predict patient survival which we validate on a separate cohort from Cologne.

### **Results**

Our model identified complex spatially resolved cell signatures to predict patient survival. The model significantly improves over the UICC8 baseline for lung adenocarcinoma (63.3 to 66.5 C-Score) and lung squamous cell carcinoma (63.0 to 69.2 C-Score) on the hold-out cohort.

### **Conclusion**

Our approach illustrates the utility of cell-based spatial analyses and highlights how AI can improve our understanding of TME features that underlie clinical outcome. The combination of our large real-world clinical cohort, multiplex panel, and automated AI approach enabled the detection of a specific cell neighborhood signature to predict patient survival, outperforming the commonly used UICC8 staging system.

## ***Implementation and Optimization of a Single Cell DNA Sequencing Assay for Reconstructing the Clonal Evolution of Tumors from FFPE Samples***

E. Lueftl<sup>1</sup>, M. Cattaneo<sup>2</sup>, I. Lukic<sup>2</sup>, G. Fuerte<sup>2</sup>, A. Immel<sup>3,4</sup>, M. Evert<sup>1</sup>, R. Durruthy-Durruthy<sup>2</sup>, D. Hirsch<sup>1</sup>

<sup>1</sup>Institute of Pathology, University of Regensburg, Regensburg, Germany, <sup>2</sup>Mission Bio, Inc., San Francisco, CA, United States of America, <sup>3</sup>Comprehensive Cancer Center Ostbayern, University Hospital Regensburg, Regensburg, Germany, <sup>4</sup>Institute of Pathology, University of Regensburg, Regensburg, Germany

## Background

Intratumor heterogeneity affects various aspects of tumor behavior including the development of resistance to therapy. It is characterized by the emergence of multiple subclones within a tumor that show unique molecular, phenotypic, and genetic variations. Understanding the clonal dynamics throughout the course of disease is essential for a more effective and personalized therapy. Single cell sequencing techniques are powerful tools to unravel the complex landscape and trace the developmental trajectories that influence treatment responses. However, studying tumors at a single cell level presents challenges, such as low input and amplification bias, allele dropout events, and compromised DNA quality from formalin-fixed paraffin-embedded (FFPE) samples. Hence, we aimed to implement and optimize a single cell DNA sequencing (scDNA-seq) assay suitable for the analysis of FFPE tissue to reconstruct the clonal tumor evolution contributing to tumor progression and therapy resistance.

## Methods

We performed cell disintegration of FFPE colorectal cancer (CRC) specimens from the archive of the Institute of Pathology, University of Regensburg. For cell capturing, we used the microfluidics system from Mission Bio (Tapestri) which included droplet-based cell encapsulation, DNA isolation, barcoding, and targeted multiplex PCR as well as library preparation. For initial testing purposes, we used the pre-designed Myeloid panel which targets 312 genes with amplicon lengths from 125 to 375 bp. We sequenced the libraries on the NovaSeq 6000 (SP Flow Cell, 2 x 150 bp) and analyzed the data using Tapestri Insights and Mosaic.

## Results

Based on this assay, we have thus far successfully analyzed two CRC samples with known mutations in *KRAS* (G12D) and *BRAF* (V600E), respectively, which we were able to detect. As one would expect, those mutations occurred as clonal events. In addition, scDNA-seq revealed subclonal mutations, which point to a linear clonal evolution in the *BRAF*-mutated case, while the *KRAS*-mutated case favors a branched phylogeny. We further identified copy number profiles typical for CRC, e.g., gains of chromosome 7 and 20.

## Conclusion

Our preliminary findings support that scDNA-seq is feasible from FFPE tissue and can provide more detailed insights into tumor evolutionary processes. We consider exploring the genomic landscape at the single cell level a crucial step towards a better understanding of tumor evolution, and it might help tailor individualized cancer treatment strategies in the future.

AG11.09

## ***P-PROFILER: Homologous recombination deficiency in pancreatic ductal adenocarcinoma***

C. Kling<sup>1,2</sup>, S. Lange<sup>3</sup>, M.-L. Koppermann<sup>1</sup>, E.-M. Mayr<sup>1</sup>, M. Walker<sup>1</sup>, A. Terron Kwiatkowski<sup>1</sup>, Y. Wagner<sup>1</sup>, A. Muckenhuber<sup>1</sup>, K. Schwaborn<sup>1</sup>, M. Martis-Thiele<sup>1</sup>, S. Chakraborty<sup>1,2</sup>, Q. Heiß<sup>1,2</sup>, M. Quante<sup>4</sup>, W. Weichert<sup>1</sup>, N. Pfarr<sup>1</sup>

<sup>1</sup>Technische Universität München, Institut für Pathologie, Molekularpathologie, München, Germany, <sup>2</sup>German Cancer Research Center (dkfz), German Cancer Consortium (DKTK), Heidelberg, Germany, <sup>3</sup>Klinikum rechts der Isar, Klinik und Poliklinik für Innere Medizin II, München, Germany, <sup>4</sup>Universitätsklinikum Freiburg, Klinik für Innere Medizin II, Freiburg, Germany

\*Contributed equally

## Background

Homologous recombination deficiency (HRD) is a recognized biomarker for predicting the efficacy of poly(ADP-ribose) polymerase (PARP) inhibitor therapy and platinum-based chemotherapy in cancer treatment, especially in ovarian cancer. Emerging evidence indicates HRD also as a crucial biomarker for other cancers, including pancreatic ductal adenocarcinoma (PDAC). However, the HRD criteria currently in clinical use are tailored to ovarian cancer and may not directly apply to other cancer types. In ovarian cancer, either a pathogenic *BRCA1/2* variant and/or a genomic instability score (GIS) of 42 or higher classifies a cancer as HRD-positive. This GIS threshold was selected to identify 95% of ovarian tumors with *BRCA*-deficiency, yet its accuracy remains unknown for cancers where pathogenic *BRCA* variants are rare. The ongoing P-PROFILER study aims to refine the GIS threshold for PDAC by assessing the GIS and pathogenic variants in genes involved in homologous recombination repair (HRR).

## Methods

In the P-PROFILER study, the GIS of 250 samples from patients with metastatic PDAC is determined using the Illumina TruSight™ Oncology 500 HRD sequencing panel. In addition, the panel allows the detection of single nucleotide variants in 523 cancer-associated genes including 29 HRR-genes, along with RNA fusions, copy number variations and other metabiomarkers such as tumor mutational burden or microsatellite instability.

## Results

183 samples were sequenced, with 127 samples fully analyzed currently. The mean GIS observed was  $16.9 \pm 13.1$  (SD). 15% of the samples contained at least one pathogenic or likely pathogenic HRR-gene variant. Applying the current HRD-criteria, only 7% of these samples qualified as HRD-positive, with two thirds harboring pathogenic or likely pathogenic *BRCA1/2* variants. In 67% of these cases, *BRCA*-deficiency resulted in a GIS greater than 42.

## Conclusion

These preliminary results from the P-PROFILER study underscore the rarity of pathogenic *BRCA* variants in PDAC, along with a generally lower GIS. The GIS threshold of 42 identified only 67% of PDAC samples with pathogenic *BRCA*-variants as opposed to 95% in ovarian cancer. Consistent with these findings, only a small number of tumors met the criteria for a positive HRD status under current guidelines. Moreover, the identification of pathogenic variants in other HRR-genes point towards the existence of *BRCA*-independent mechanisms in pancreatic HRD, and argues for refined HRD-criteria for this entity.

# AG Molekularpathologie 3

AG11.10

## **Resistance testing of *Helicobacter pylori*: Analysis of gyrase B is essential to detect the whole spectrum of resistance mutations against Levofloxacin**

M. Ihle, S. Wagener-Rydzek, J. Fassunke, S. Newton, U. Siebolts, R. Büttner, S. Merkelbach-Bruse  
Uniklinik Köln, Institut für Pathologie, Köln, Germany

### Background

Infection with *Helicobacter pylori* is the main cause for duodenal ulcers, gastritis, mucosa associated lymphoid tissue lymphoma and gastric adenocarcinoma. First line treatment is a triple-therapy with a proton pump inhibitor and two antibiotics (clarithromycin and amoxicillin or metronidazole). Unfortunately, resistance against these agents is increasing. Levofloxacin, a fluoroquinolone, is an alternative antibiotic in second line treatments. However, resistance mutations are also observed. Therefore, a precise mutational analysis is essential to gain the best therapeutic option. Most commercially available assays only cover the detection of *H. pylori* and the resistance against clarithromycin to evaluate first line treatment resistance but resistance testing against second line treatment, e.g. levofloxacin, is lacking. In this study we aimed at evaluating the incidence of *H. pylori* and resistance mutations against clarithromycin and levofloxacin.

### Methods

A cohort of 111 formalin-fixed paraffin embedded tissue samples were analyzed for *H. pylori* in routine diagnostics between June 2023 and December 2023. Of these, 72 samples were further analyzed for resistance. *H. pylori* and resistance against clarithromycin were detected using the RIDA®GENE *Helicobacter pylori* assay. As no commercially available assay for the detection of levofloxacin resistance was available, Sanger sequencing was set up for the mutational analysis of *gyrase A* and *gyrase B* to evaluate the resistance against levofloxacin.

### Results

*H. pylori* was detectable in 70.6% of the analyzed cases. Only 2 of 111 cases were not suitable for analysis. Resistance against clarithromycin was detected in 33.8%, resistance against levofloxacin was detected in 48.3% of 72 samples which were further analyzed. *Gyrase A* was evaluable in 63 cases of whom 31.7% showed a mutation. Mutation hotspots were codon 87 and 91. *Gyrase B* was evaluable in 56 cases of whom 26.8% showed a mutation. Mutation hotspots in *gyrase B* were codon 481 and 484. Overall, a resistance mutation could be detected in 60% of the samples whereas 23.6% of the samples harbored two or more resistance mutations.

## Conclusion

This study shows that the RIDA@GENE *Helicobacter pylori* assay is a fast, robust and sensitive method to detect *H. pylori* and its resistance against clarithromycin. Furthermore, many samples harbored more than one resistance mutation. The analysis of *gyrase A* and *B* is essential to detect the whole spectrum of resistance mutations against levofloxacin.

AG11.11

## **Automation of molecular pathology NGS dataflow, processing and reporting**

S. J. Lambrecht<sup>1,2</sup>, E. Adam<sup>1,2,3</sup>, S. Wolter<sup>1,2,3</sup>, I. Weber<sup>1,2</sup>, A. Hummel<sup>1,2</sup>, U. Matysiak<sup>1,2,3</sup>, M. Werner<sup>1,2,3,4</sup>, S. Lassmann<sup>1,2,3</sup>

<sup>1</sup>Institute for Surgical Pathology, Medical Center, University of Freiburg, Germany, Freiburg, Germany, <sup>2</sup>Comprehensive Cancer Center Freiburg, Medical Center, Freiburg, Germany, Freiburg, Germany, <sup>3</sup>Zentrum für Personalisierte Medizin, partner site Freiburg, Germany, Freiburg, Germany, <sup>4</sup>German Cancer Consortium (DKTK), partner site Freiburg, Germany, Freiburg, Germany

## Background

Molecular pathology diagnostics is based on multiple steps of wet-lab and dry-lab processes. Whilst wet-lab sample processing is increasingly more automated due to integrated technology solutions, the variety of techniques used still requires time consuming efforts to prepare laboratory data for analyses and to integrate results from various output formats into diagnostic reports. Here, we present a custom solutions to optimize time management and team co-work schedules in NGS-based diagnostics.

## Methods

Data workflows of current NGS-based analyses using the custom nNGM Panel (Qiagen), custom RNA-Fusion Panel (Qiagen), TSO500 Panels (DNA/RNA, DNAonly, DNAonly+HRD; Illumina) and Whole Exome Sequencing (WES) were automated starting from output files of the NGS-sequencers (MiSeq, NextSeq; Illumina). Data analyses included custom pipelines on the CLC Genomics Server/Workbench (Qiagen) and the Dragen Server (Illumina) as well as a subsequent annotation pipeline for TSO500 data. Data flow was connected between sequencers, computing and storage servers by pipeline scripts programmed by PowerShell, Bash Shell.

## Results

For small NGS-Panels (nNGM, RNA-Fusion), the established pipelines allow automated transport of sequencing data to the CLC Genomics Server and starting of the bioinformatic analyses. This allows overnight data processing (range 1-5 hrs, depending on sample numbers), quality control and starting of results file evaluation with diagnostic report writing starting early the next day. The data storage structure and data workflow enables working jointly on the generated results files from up to 40-60 samples per run and finalizing diagnostic reports the same day. Similarly, for large NGS panels (TSO500) automated data processing, including annotation for 8 samples per run can be achieved in 3 – 4 hrs. As such, also here data evaluation and diagnostic reporting can start immediately. In addition, with the need to adhere to a multitude of QC-parameters for large panel or WES analyses, an additional bioinformatical script/pipeline here provides the diagnostic report layout with 10 -15 structured QC-parameters included.

## Conclusion

Automation of data flow from sequencers to server processing and final diagnostic reporting 1) reduces the risk of manual errors, 2) reduces turnaround time and 3) provides resources for other associated molecular pathology tasks.

AG11.12

## **Long term effect of choline-deficient high fat diet and correlation of carbohydrate response element binding protein (ChREBP) to NAFLD-mediated hepatocarcinogenesis**

M. Yasser, J. Prey, H. Leiner, F. Dombrowski, S. Ribback

Universitätsmedizin Greifswald, Institut für Pathologie, Greifswald, Germany

## Background

Carbohydrate response element binding protein (ChREBP) is a glucose responsive, glycolytic & lipogenic transcription factor [1, 2], mainly expressed in the liver & emerged as a pioneer factor for de-novo lipogenesis regulation in NAFLD

(non-alcoholic fatty liver disease) development [3]. Choline is an essential nutrient & reports suggest that feeding choline-deficient high fat diet (CD-HFD) to mice causes liver injury that resembles morphological features of human NAFLD [4]. Previously, our group have also suggested an associative role of ChREBP in development of hepatocellular carcinoma [5,6].

However, molecular pathogenesis of ChREBP related hepatocarcinogenesis during prolonged CD-HFD feeding in mice-model remains unexplored.

Inspired by the fact that mitochondrial morphology also changes in NAFLD [7], we want to explore the role of PI3K/AKT/mTOR- RAS/RAF/MAPK pathways & mitochondrial associative pathological features in our CD-HFD induced hepatocarcinogenesis model.

## Methods

Male-C57BL/6J (WT), Liver ChREBP-KO (L-KO) & total body ChREBP-KO (TB-KO) mice were maintained on either a CD-HFD (46% fat, n=219) or control-diet (10% fat, n=232) for 3,6 & 12 months to induce metabolic syndrome. Body weight & glucose levels were measured monthly. After perfusion, frozen liver tissues were examined by Western-blotting & Real-time PCR. While osmium (OSO<sub>4</sub>) & formalin-fixed liver sections were examined by Transmission electron microscopy (TEM) & histologically.

## Results

We have investigated, role of PI3K/AKT/mTOR & RAS/RAF/MAPK pathways & its correlation with ChREBP hepatic deficiency in long-term (12 months) fed CDHFD or control diet in TB-KO, L-KO & WT-mice. Our data suggest a notable downregulation in key PI3K/AKT/mTOR & RAS/RAF/MAPK pathway candidates in KO-mice compared to the WT group. At ultrastructural level, KO-group mice revealed elongated mitochondria of variable shape with whorl-type cristae arrangements. Such 'Megamitochondria' appearance is more prominent in L-KO mice, by their considerably larger size, pale matrix & marginal cristae structure. Mitochondrial shape, size & inter-cristae distances also showed prominent differences.

## Conclusion

Our study provides new exploratory insight into role of PI3K/AKT & RAS/RAF pathway in mice fed with long term CD-HFD diet & important indications about mitochondrial aberrations as an early structural hallmark of NASH. Also understanding into the connecting role of ChREBP with PI3K/AKT - RAS/RAF inhibition, which could reduce mitochondrial oxidative stress.

AG11.13

## ***MSI: colorectal cancer and beyond-The complexity of specific biomarkers within genome wide NGS***

J. Siemanowski-Hrach, P. Poon, S. Merkelbach-Bruse, U. Siebolts  
University Hospital of Cologne, Institute of Pathology, Cologne, Germany

## Background

In order to find new therapeutic targets, genome wide next generation sequencing (NGS) approaches for the analysis of multiple biomarkers are used. Microsatellite instability (MSI) is one of them. As validated cut-offs are not available for a wide range of entities we aimed to establish suitable thresholds for prostate (PCa) and cholangiocellular carcinoma (CCC) in comparison to colorectal cancer (CRC).

## Methods

For mismatch repair (MMR) immunohistochemistry (IHC) tumor sections were stained for MLH1 (Clone: M1, Ventana), MSH2 (G219-1129), MSH6 (EPR3947) and PMS2 (Clone: 44, Ventana) on a Ventana Benchmark stainer. For MSI analysis, the TruSight Oncology 500 Kit was used (Illumina). Sequencing was performed using the Nextseq or Novaseq (Illumina). MSI analysis of 130 noncoding homopolymer regions was done with the TSO500 Local App (Illumina), analysis of additional di-, tri- and tetranucleotide repeats was done with MSIsensor-pro<sup>1</sup>.



## Results

55 CRC, 53 CCC and 60 PCa samples were analysed. Using published thresholds (20-30% of unstable MSI loci)<sup>2, 3</sup>, all CRC, one CCC and no PCa were identified as MSI-High (MSI-H). Another CCC case and two PCa cases harbouring mutations in MLH1, MSH2 or MSH6 were identified as MSI-H after MMR IHC testing. In these samples, percentage of unstable loci ranged from 3.23% (CCC) to 7.26-13.76% (PCa). Using a borderline cut-off of 7% at least the two PCa were also identified as MSI-H<sup>4</sup>.

## Conclusion

Since MSI profiles can differ between cancer entities, thresholds for instability must be determined for each of them individually<sup>5</sup>. Especially when using mononucleotide markers small shifts might be missed. Here we showed that already published cut-offs works for CRC but cannot be easily transferred to PCa and CCC. MSI estimation using NGS is therefore suitable as a quick screening tool. Since thresholds for MSI-H might differ between entities, additional IHC testing is recommended at least in samples where VUS or pathogenic mutations are found in one of the mismatch repair genes.

AG11.14

## ***Up-date of molecular pathology diagnostics for the Molecular Tumorboard in Freiburg***

U. Matysiak<sup>1,2,3</sup>, E. Adam<sup>1,2,3</sup>, S. Wolter<sup>1,2,3</sup>, S. Riemer-Cysar<sup>1,2,3</sup>, E.-P. Dopfer<sup>1,2,3</sup>, S. Timme-Bronsert<sup>1,2,3</sup>, M. Werner<sup>1,2,3,4</sup>, S. Lassmann<sup>1,2,3</sup>

<sup>1</sup>Institute for Surgical Pathology, Medical Center, University of Freiburg, Germany, Freiburg, Germany, <sup>2</sup>Comprehensive Cancer Center Freiburg, Medical Center, Freiburg, Germany, Freiburg, Germany, <sup>3</sup>Zentrum für Personalisierte Medizin, partner site Freiburg, Germany, Freiburg, Germany, <sup>4</sup>German Cancer Consortium (DKTK), partner site Freiburg, Germany, Freiburg, Germany

## Background

Molecular pathology diagnostic is the key for the biweekly molecular tumorboard (MTB) Freiburg since starting 2015. Whilst both numbers and complexity of molecular diagnostic analyses increased, also SOP-driven workflows and MTB-associated duties were professionalized further. Here, we provide an up-date about molecular pathology diagnostic activities in 2023.

## Methods

The molecular pathology diagnostic team participated at 26 MTBs for 1007 case presentations (range 19 to 54 per MTB) and performed diagnostic analyses for 416 MTB cases. About 1-2 week post initial MTB case presentation, clinical diagnostic requests (entity-specific SOPs) were submitted. Diagnostic analyses were by immunohistochemistry (IHC), in-situ hybridization (ISH), NGS-based analyses and other molecular assays (e.g. HPV infection) according to routine accredited procedures. Final signed diagnostic reports were provided latest 3 working days prior to the MTB, where diagnostic reports were presented. Clinical-therapeutic treatment recommendations were discussed interdisciplinary.

## Results

Diagnostic analyses for MTB cases in 2023 were 6 HPV-analyses, 30 ISHs, 821 IHCs and 374 NGS-based analyses. For the latter, mainly the TSO500 Panel (Illumina) was used (n=293) with sub-types of DNA+RNA (n=215), DNAonly (n=45), DNAonly+HRD (n=27), DNA+RNA+HRD (n=4) and RNAonly (n=2), whilst the rest were specific RNA-Fusion panels and/or also smaller NGS-based Panel (e.g. "nNGM-Panel"). Whole Exome Sequencing with diagnostic reporting was performed in 4 cases. The median turn-around time from clinical request to diagnostic reporting was 40 days, including external cases. Next to tissue specimen and/or technical limitations, diagnostic challenges were seen for complex comparative and/or follow-up NGS-based analyses and/or complex cases (e.g. CUPs), where detailed re-evaluation of histopathology, tumor cell content, re-evaluation of all NGS-data sets was necessary. Here, integration of technical, molecular(biological), pathological, in part medical data and plausibility checks are necessary for final diagnostic reporting.

## Conclusion

Molecular pathology diagnostic is a core part of the molecular tumorboard within a dynamically evolving technological and biomarker-driven field of personalized medicine, therefore requiring continuing optimization of workflows and

education of molecular pathology teams.

AG11.15

### ***Histomorphological and molecular analysis of pancreatic neuroendocrine tumours***

A. Kerner<sup>1</sup>, F. Kellers<sup>1</sup>, V. Stoll<sup>1</sup>, C. Röcken<sup>1</sup>, N. Pfarr<sup>2</sup>, B. Konukiewicz<sup>1</sup>

<sup>1</sup>Department of Pathology, University Medical Center Schleswig-Holstein, Campus Kiel, Kiel, Germany, <sup>2</sup>Institute of Pathology, School of Medicine and Health, Technische Universität München, Munich, Germany

#### **Background**

According to the current WHO classification, pancreatic neuroendocrine neoplasms (PanNEN) are divided into well-differentiated PanNEN (pancreatic neuroendocrine tumours, PanNET), which are furthermore subdivided into G1-G3 tumours based on their proliferation index, and poorly differentiated PanNEN (pancreatic neuroendocrine carcinomas, PanNEC) [1]. The genetic landscape of PanNET has already been well studied. However, the correlation of molecular alterations to morphological findings (growth patterns, hormonal expression) is still not clear. The aim of this study was to evaluate the genetic background according to classical morphological parameters.

#### **Methods**

We established a cohort of 24 PanNET and re-evaluated them for growth pattern and grading. We then performed immunohistochemical analysis of neuroendocrine markers (synaptophysin, chromogranin A) and peptide hormones (serotonin, gastrin, insulin, glucagon, somatostatin, pancreatic polypeptide). DNA was extracted from FFPE tissue of 14 cases after microdissection using QIAamp DNA Mini Kit (Illumina). Library preparation was facilitated using TruSeq DNA PCR-free construction kit (Illumina). Whole-exome sequencing was performed on a NovaSeq system (Illumina). For data analysis (tumour only) we used the cBioPortal [2][3] and MIRACUM Pipeline and for methylation analysis of 9 cases we used the Infinium MethylationEPIC Kit (Illumina).

#### **Results**

Five cases were classified as G1, 16 as G2 and 3 as G3 tumours. Among the 19 cases showing peptide hormone expression, pancreatic polypeptide (15 cases) and glucagon (11 cases) were most frequently expressed. Eight cases showed positivity for insulin, 4 for somatostatin, 3 for gastrin and 1 for serotonin. Alterations affecting chromatin remodelling genes and DNA repair genes occurred mostly within the 14 cases.

#### **Conclusion**

PanNET are heterogeneous regarding hormone expression as well as molecular genetic alterations. Further investigations and a larger case series are needed to identify correlations between histology, molecular pathology and hormonal expression.

Literaturangaben:

[1] WHO Classification of Tumours Editorial Board, (2019), Digestive System Tumours, 5th Edition

[2] Cerami E, Gao J, Dogrusoz U, Gross BE, Sumer SO, Aksoy BA, et al., (2012), The cBio cancer genomics portal: an open platform for exploring multidimensional cancer genomics data, *Cancer Discovery*, 401-4, 2(5)

[3] Gao J, Aksoy BA, Dogrusoz U, Dresdner G, Gross B, Sumer SO, et al., (2013), Integrative analysis of complex cancer genomics and clinical profiles using the cBioPortal, *Science Signaling*, p11, 6(269)

## **AG Kinder- und Fetalpathologie 1**

AG12.01

### ***Differentialdiagnosen der Molenschwangerschaft***

R. Hiller, L.-C. Horn

University Hospital Leipzig, Leipzig, Germany

Die orthologe Proliferation und Differenzierung des Trophoblastepithels sind entscheidend für die regelrechte Bildung und Reifung der Plazenta und die adäquate Ausbildung des fetoplazentaren Kreislaufs. Schwerwiegende Störungen können zur Ausbildung einer gestationsbedingten Trophoblasterkrankung, zum Abort oder fetalen intrauterinen Wachstumsretardierungen führen. Eine wesentliche Voraussetzung für eine adäquate Therapie bzw. weiterführende

klinische Diagnostik ist eine exakte Histopathologie. Der Vortrag soll die wesentlichen histomorphologischen Kriterien und immunhistochemischen Charakteristika trophoblastärer Läsionen und ihre Abgrenzung zu retentionsbedingten Veränderungen darstellen, um die Diagnostik und Differenzierung in der täglichen Routine zu erleichtern.

AG12.02

### ***Post-mortem trio genome sequencing in families with children or adolescents with an unexplained cause of death - initial results and outlook***

C. Hendrich<sup>1</sup>, S. von Hardenberg<sup>1</sup>, M. Richter<sup>2</sup>, F. Dohle<sup>3</sup>, L. Doil<sup>4</sup>, T. Engelmann<sup>4</sup>, B. Erdlenbruch<sup>5</sup>, H. Freitag<sup>6</sup>, L. Hagemeyer<sup>4</sup>, M. Reger<sup>7</sup>, J. W. Richter<sup>8</sup>, K. Schoner<sup>9</sup>, T. Ripperger<sup>1</sup>, E. Gradhand<sup>10</sup>, A. K. Bergmann<sup>1</sup>

<sup>1</sup>Medizinische Hochschule Hannover MHH, Institut für Humangenetik, Hannover, Germany, <sup>2</sup>Kinder- und Jugendkrankenhaus Auf der Bult, Hannover, Germany, <sup>3</sup>St. Vincenz Krankenhaus, Frauen - & Kinderklinik, Paderborn, Germany, <sup>4</sup>Medizinische Hochschule Hannover MHH, Institut für Rechtsmedizin, Hannover, Germany, <sup>5</sup>Johannes Wesling Klinikum Minden Universitätsklinikum der Ruhr Universität Bochum, Universitätsklinik für Kinder- und Jugendmedizin, Minden, Germany, <sup>6</sup>Medizinische Hochschule Hannover MHH, Institut für Pathologie, Hannover, Germany, <sup>7</sup>Varisano Klinikum Frankfurt Höchst, Klinik für Kinder- & Jugendmedizin, Frankfurt am Main, Germany, <sup>8</sup>Städtisches Klinikum Braunschweig, Kinder – und Jugendmedizin, Braunschweig, Germany, <sup>9</sup>Universitätsklinikum Marburg, Institut für Pathologie, Marburg, Germany, <sup>10</sup>Universitätsklinikum Frankfurt, Institut für Pathologie, Frankfurt am Main, Germany

#### **Background**

Derzeit werden unklare Todesursachen bei Kindern und Jugendlichen nur in begrenztem Umfang aufgeklärt und nach dem Versterben und dem Ausschluss eines nicht natürlichen Todes i. d. R. keine weitergehende Diagnostik durchgeführt, da Möglichkeiten der Kostenübernahme und entsprechende Versorgungsstrukturen fehlen. Allerdings kann bei unklaren Todesursachen die postmortale genetische Analyse wertvolle Ergebnisse für die Angehörigen liefern und Verdachtsdiagnosen aus einer klinischen oder forensischen Obduktion bestätigen.

Zwischen November 2023 und Februar 2024 haben wir prospektiv 15 Familien mit einem an einer unbekanntem Grunderkrankung gestorben Kind oder Jugendlichen beraten und ggf. eine Trio-Genom-Sequenzierung veranlasst.

#### **Methods**

Postmortale Trio-Genomsequenzierung und HPO-basierte Auswertung anhand von Krankenakten, Obduktionsbefunden und ggf. Photoaufnahmen.

#### **Results**

Vorstellung der Ergebnisse geklärter und ungeklärter Fälle sowie Darstellung der Arbeitsabläufe im Rahmen unterschiedlicher Konstellationen.

#### **Conclusion**

Ziel des Projekts ist neben der diagnostischen und wissenschaftlichen Aufarbeitung die Etablierung interdisziplinärer Versorgungsstrukturen für betroffene Familien zu schaffen. Weiterhin erfolgt eine Erhebung des diagnostischen Bedarfs postmortaler genetischer Diagnostik und die Identifikation von Versorgungslücken. Beteiligte Fachrichtungen wie PathologInnen, RechtsmedizinerInnen, GeburtshelferInnen, PädiaterInnen, die Polizei, Mitarbeitende des Rettungswesens und Staatsanwaltschaft sollen für die Thematik sensibilisiert und Interdisziplinarität gestärkt werden. Die Schaffung einheitlicher logistischer und diagnostischer Boas sollen Grundlagen schaffen, Versorgungsstrukturen und Möglichkeiten der Kostenübernahme für postmortale genetische Untersuchungen zu etablieren.

**Förderung:** Dr. August und Erika Appenrodt-Stiftung Hannover, Deutschland

AG12.03

### ***Placenta pathology in COVID-19-pregnancies – an update***

N. Schaumann<sup>1</sup>, J.-T. Sühren<sup>2</sup>

<sup>1</sup>Medizinische Hochschule Hannover, Institut für Pathologie, OE 5110, Hannover, Germany, <sup>2</sup>Medizinische Hochschule Hannover, Institut für Pathologie, Hannover, Germany

#### **Background**

During the COVID-19 pandemic, increased rates of premature birth and intrauterine fetal deaths were reported. We

updated our previously presented systematic review with the aim to clarify whether there is a typical COVID-19-associated pattern of placenta lesions.

### Methods

Systematic literature search was performed, according to PRISMA guidelines. Publications of  $\geq 10$  cases of COVID-19-positive pregnancies with histological placenta examinations according to Amsterdam criteria were taken into account (38 reports on 3677 placentas).

### Results

Placenta examinations showed similar frequencies of histopathological patterns in COVID-19-placentas as are known for non-COVID-19-pregnancies (maternal vascular malperfusion in 32%, fetal vascular malperfusion in 19%, acute inflammation in 20% and chronic inflammation in 22% of cases). The so called "COVID-19 placentitis" pattern (histiocytic intervillitis, trophoblast necrosis and massive intervillous fibrin deposition), occurs in up to 2% of cases.

### Conclusion

This updated systematic review does not show an increased rate of any specific placenta pathology in cases of COVID-19 pregnancies. Materno-placental transmission of SARS-CoV-19 is rare. The main prognostic factor are not placenta pathologies but maternal pneumonia-associated respiratory distress with secondary fetal brain hypoxia.

## AG Kinder- und Fetalpathologie 2

AG12.04

### ***The role of fluorescence confocal microscopy in evaluation of vitality in pediatric tumor specimens and tumor cell isolation.***

S. Gretser<sup>1</sup>, M. N. Kinzler<sup>2</sup>, T. Theilen<sup>3</sup>, M. Vogler<sup>4</sup>, E. Gradhand<sup>1</sup>

<sup>1</sup>Dr. Senckenbergisches Institut für Pathologie, Universitätsklinikum Frankfurt am Main, Frankfurt am Main, Germany, <sup>2</sup>Abteilung Innere Medizin I, Universitätsklinikum Frankfurt am Main, Frankfurt am Main, Germany, <sup>3</sup>Abteilung pädiatrische Chirurgie und Urologie, Universitätsklinikum Frankfurt am Main, Frankfurt am Main, Germany, <sup>4</sup>Institut für experimentelle Krebsforschung in der Pädiatrie, Goethe Universität Frankfurt am Main, Frankfurt am Main, Germany

### Background

Fluorescence confocal microscopy (FCM) is an optical technique that uses laser light sources of different wavelengths to generate real-time images of fresh, unfixed tissue samples. FCM has been most extensively studied in dermatopathology, but it has also been investigated in other human surgical tissues, such as breast, genitourinary, and gastrointestinal. However, the role of FCM in pediatric tumor specimens has not yet been explored. The objective of this study was to prospectively investigate pediatric tumor specimens and evaluate their adequacy for fresh tumor sampling. Additionally, we aimed to determine whether tumor cell isolation for stable cell culture is still feasible after FCM imaging.

### Methods

This study included pediatric tumor specimens submitted by our Department of Pediatric Surgery and Urology for diagnosis between January and December 2023. The specimens were imaged using FCM and subsequently embedded in paraffin. In cases of heterogeneous tumors, multiple areas were imaged. Tumor vitality and adequacy for tissue sampling were estimated first on FCM images and later on the corresponding H&E. Tumor vitality was determined by estimating the percentage of viable tumor cells. The adequacy of tissue sampling was evaluated based on vitality, cellularity, and the presence of vital non-tumor tissue. If viable tumor was identified, an additional section was imaged using FCM and later submitted for tumor cell isolation. An adjacent tumor section was also isolated without FCM processing for comparison purposes.

### Results

When comparing the estimated tumor cell vitality using FCM and H&E, we found correlated estimates with an average discrepancy of 15% (95% CI = 11.05-19.95). We observed substantial agreement regarding whether the tissue was adequate for fresh tissue collection ( $\kappa = 0.762$ ). Passagable cell cultures could be obtained from all tissue samples submitted for cell isolation without FCM. After FCM, seven out of eight samples yielded passagable cell cultures.

## Conclusion

FCM enables real-time histologic identification of viable tumor areas in pediatric tumor samples without the need to use frozen sections and the associated cryo-artifacts. Our study suggests that the use of FCM in tumor sampling can increase the yield of suitable fresh tumor samples by identifying viable tumor areas and ensuring that sufficient tissue remains for diagnosis. We are also the first to show that the isolation and growth of tumor cells in culture is not compromised by the FCM technique.

AG12.05

## ***Congenital gastrointestinal malformations: Pathological perspectives and diagnostics***

T. Manuylova<sup>1</sup>, F. Fend<sup>2</sup>

<sup>1</sup>Universität Tübingen, Institut für Pathologie und Neuropathologie, Tübingen, Germany, <sup>2</sup>Universitätsklinikum, Institut für Pathologie und Neuropathologie, Tübingen, Germany

### Background

Gastrointestinal malformations are a significant concern in paediatric medicine. In Germany, around one in 15 newborns are diagnosed with significant malformations such as spina bifida or cleft lip and palate, with approximately a fifth of these cases being serious and life-threatening.

### Methods

Most congenital malformations of the gastrointestinal tract present as intestinal obstructions, causing feeding difficulties, abdominal distension, vomiting, and the inability to pass gas and stool within the first 1 to 2 days after birth. Although some gastrointestinal malformations, such as malrotation, have a favourable prognosis, others, such as congenital diaphragmatic hernia, have an unfavourable prognosis with a mortality rate of 10 to 30% or higher, depending on the study. The abdominal wall can be affected by several congenital defects, such as omphalocele and gastroschisis, which allow the protrusion of viscera through the defect.

### Results

The pathogenesis of these malformations is based on an extremely complex embryogenesis of the gastrointestinal tract. In close cooperation with the Perinatal Centre of the Women's Hospital at the University Hospital of Tübingen, we at the Institute of Pathology investigate the entire spectrum of gastrointestinal malformations in fetuses and newborns. Over the past 5 years we have identified a large number of different congenital gastrointestinal malformations such as various atresia, stenoses, fistulas, abdominal wall defects and secondary changes in the intestinal wall such as focal intestinal perforation or necrotising enterocolitis.

### Conclusion

Pathological examination plays an important role in identifying both congenital defects and secondary changes in the tissues of the gastrointestinal tract. These findings are essential for the selection of optimal strategies. In addition, pathological examinations make an important contribution to research by providing insights into the pathophysiology of these malformations and contributing to the development of innovative diagnostic approaches.

AG12.06

## ***Single-Shot Cardioplegia: Del Nido or HTK solution?***

A. M. Müller<sup>1</sup>, A. Macion<sup>2</sup>, C. Preusse<sup>3</sup>

<sup>1</sup>Praxis für Pathologie - Zentrum f. Kinderpathologie, an der UK Köln, Köln, Germany, <sup>2</sup>Praxis für Kinderpathologie an der Uniklinik Köln, Köln, Germany, <sup>3</sup>Universitätsklinik Bonn, Klinik für Herzchirurgie, Bonn, Germany

### Background

Intraoperative or early postoperative myocardial failure after cardiac surgery in the first month of life can be due to inadequate intraoperative myocardial protection. Due to the structural and physiological peculiarities of the newborn heart, challenges for intraoperative myocardial protection are more diverse than with adult hearts. As for example the ischemic newborn heart produces significantly more lactate than the ischemic adult heart. Accordingly, it must be cardioplegically reperfused more frequently. Yet, it is known that each turn of cardioplegic reperfusions harms the

newborn heart. For this reason, methods allowing single-shot application even with extended cardiac arrest, are preferred. Currently this is provided by 2 solutions: HTK or Del Nido solution. By electron microscopy their efficiencies for structural protection of the cardioplegically arrested myocardium was analyzed.

### **Methods**

6 neonate piglet hearts (3 per group, 4 days old), protected with HTK resp. Del Nido solution, were analyzed: after intubation of the animals and subsequent thoracotomy, cardioplegic in-situ perfusion was performed. After heart extirpation, simulating cardioplegic arrest, all hearts were incubated at 25°C for 180 minutes. At defined times (0,60,120,180 min) 50 samples/timepoint were taken from the left ventricle for electronmicroscopic examination of mitochondria (cristae, matrix, membranes) and myofibrils (edema,architecture).

### **Results**

Damages to cell structures increased significantly in both groups as ischemia was progressing, but overall protection with HTK was more effective for almost all analyzed parameters except for edema of myocytes. Here According to this parameter, the hearts protected by Del Nido group displayed better results.

### **Conclusion**

According to the ultrastructural investigations HTK provides a better protection of the newborn heart, especially the mitochondria than the Del Nido solution. The differences between the two methods which are used as single-shot technique, became even more pronounced when ischemia time was extended (> 90 min). Our experimental series, which took place under standardized conditions, is the first study that has been carried out worldwide on this question.

AG12.07

## ***Fetal autopsy in comparison to prenatal diagnostics***

J.-T. Suhren<sup>1,2</sup>, K. Hussein<sup>3</sup>, H.-H. Kreipe<sup>2</sup>, N. Schaumann<sup>2</sup>

<sup>1</sup>Medizinische Hochschule Hannover, Institut für Pathologie, Hannover, Germany, <sup>2</sup>Institut für Pathologie, Medizinische Hochschule Hannover, Hannover, Germany, <sup>3</sup>MVZ Pathologie Hildesheim Hannover-Zentrum GmbH, Hildesheim, Germany

### **Background**

Intrauterine fetal death (IUFD) and abruption due to fetal malformations are two primary factors leading to death during the prenatal period. In these cases, post-mortem examination remains the gold standard diagnostic procedure for verifying prenatal ultrasound diagnostics and human genetics. Furthermore, pathological evaluation of the placenta can reveal findings undetectable by sonography. However, most studies comparing prenatal ultrasound and post-mortem evaluations do not include placenta pathology. Therefore, we aimed to correlate prenatal diagnoses, autopsy findings and placenta pathologies to assess the frequency of prenatally missed relevant diagnoses.

### **Methods**

We conducted a retrospective review of fetal autopsies (arbitrary time interval 2006 to 2021, Institute of Pathology of Hannover Medical School). Prenatal findings and autopsy results were classified into three groups: i) prenatal ultrasound findings matching those of the fetal autopsy, ii) autopsy uncovering additional findings, and iii) post-mortem findings altering the diagnosis. Examination of placental pathology was integrated to ascertain the cause of death.

### **Results**

251 autopsy cases were included: 199 spontaneous IUFDs and 52 induced abortions. Complete agreement between autopsy findings and prenatal ultrasound results was found in 91% of IUFD and 87% of induced abortion cases. Additional findings were identified in 7% of IUFD and 12% of induced abortion cases. Significant additional findings were found in five cases (IUFDs n=4/2% and induced abortions n=1/2%). In 89% of IUFDs, placental pathologies contributed to fetal death.

### **Conclusion**

The frequency of complete agreement between prenatal ultrasound and fetal autopsy is high. Nonetheless, in rare instances, autopsy findings lead to revision of the prenatal diagnosis. This may enable more precise counselling regarding the risks of recurrence and the evaluation of genetic testing.

AG12.08

## ***Viral Myocarditis in Childhood***

M. Overkamp, L. Pelzl, F. Fend, K. Klingel, T. Manuylova  
Institut für Pathologie Tübingen, Tübingen, Germany

### **Background**

Myocarditis can exhibit variable clinical manifestations, ranging from asymptomatic or subclinical disease to the development of fulminant myocarditis with potentially life-threatening conditions including arrhythmias, heart failure, cardiogenic shock and sudden death. Viral infections are the most frequent cause of myocarditis in childhood.

### **Methods**

Clinical suspicion for myocarditis should initiate a timely and thorough diagnostic workup. The definitive diagnosis of myocarditis can be established via diagnostic findings in endomyocardial biopsies. The 2023 Consensus Statement on Myocarditis in Childhood by the German Society for Pediatric Cardiology reflects on the importance of a structured diagnostic workup including the histopathological evaluation of endomyocardial biopsies. An endomyocardial biopsy is indicated if hemodynamic instability is present or if an impaired cardiac function persists for more than two weeks [1]. In addition to histology, immunohistochemistry and molecular pathology can help elucidate the underlying etiology of myocarditis and guide clinical and therapeutic decision-making. Further studies on endomyocardial biopsies, i. e., next generation sequencing (NGS), can be applied to identify genes associated with cardiomyopathy.

### **Results**

The Cardiopathology and Infection Pathology unit at the Department of Pathology in Tübingen receives approximately 3500 endomyocardial biopsies annually. From 2004 to 2022, the diagnosis of myocarditis was made more than 1000 times in patients 16 years of age or younger. 270 cases of lymphocytic myocarditis were analyzed via polymerase chain reaction (PCR) and viral genome was detected in 152 cases. Parvovirus B19 was detected most frequently, followed by human herpesvirus 6 or a combination of both.

### **Conclusion**

Diagnosing or excluding viral myocarditis informs the clinical decision between administering antiviral or immunosuppressive therapy and can greatly impact the clinical outcome. We aim to present current diagnostic guidelines and contextualize them with the retrospective analysis of endomyocardial biopsies evaluated at the Cardiopathology unit at the Institute of Pathology in Tübingen from 2004 to 2022.

Literaturangaben:

[1] Paul T, Klingel K, Tschöpe C, Bertram H, Seidel F. . (2023), Leitlinie Myokarditis der Deutschen Gesellschaft für Pädiatrische Kardiologie., *Klin Padiatr.*, e1-e15, 235(3), doi: 10.1055/a-2039-2604.

## **AG Informatik, digitale Pathologie und Biobanking 2**

AG13.08

### ***Key Steps when Implementing New Diagnostic Technologies in Routine Practice***

J. Lennerz

BostonGene, Waltham, United States of America

The diagnostic technology landscape is rapidly evolving. Novel modalities include AI integration, molecular diagnostics, and data services that require adaptation of our practice. Successfully innovation relies on domain expertise coupled with a strategic approach. However, the essential components for navigating this process often remain unclear, highlighting a critical gap in understanding. First and foremost, a great team is crucial because fostering innovation depends on collaboration and expertise. This involves re-purposing of existing positions and alignment of innovation initiatives with funding sources. Understanding the integration framework comprises both conceptual and procedural aspects including financial sustainability and the different levels of approaching it. Furthermore, interoperability and recognizing the value of safety and effectiveness analyses is essential in ensuring the successful adoption of new diagnostic technologies. The distinction of utilization (what we do now), utilization management (what we should do), and utilization management strategies (how we get there) is paramount in navigating equitable access to testing. Finally, diagnostic quality

management requires new frameworks to maintain and improve accuracy at the operational level. Pathologists are uniquely positioned to embrace innovation and drive improvements in patient care. Expanding our toolkit is an option to remain relevant in the multifaceted landscape of value-based healthcare.

AG13.09

### ***Lessons learned from 10+ years using Digital Pathology***

P. van Diest

University Medical Center Utrecht, Department of Pathology, Utrecht, The Netherlands

At the Department of Pathology of the University Medical Center Utrecht in The Netherlands, we started in 2008 to create a complete digital archive by prospectively scanning all our slides as a prior cases archive, for digital multidisciplinary meetings, teaching and research, and incidental remote digital diagnostics. In 2015, we implemented a fully digital diagnostic pathology workflow. It consisted of the Sectra PACS and the LMS laboratory information system from Finalist, the latter replaced by Delphic AP from Sysmex in 2022. In this presentation, the experiences and lessons learned from the first and second phases of going and staying digital will be shared. In addition, an outlook for the upcoming 5 years will be given.

AG13.10

### ***Automatic Detection of Esophageal Cancer in Whole Slide Image***

H. Q. Nguyen<sup>1</sup>, A. Kazem<sup>1,2</sup>, J. Horstmann<sup>3</sup>, M. Quante<sup>4</sup>, J. Slotta-Huspenina<sup>1</sup>, P. J. Schöffler<sup>1</sup>

<sup>1</sup>Institute of General and Surgical Pathology, Technical University of Munich, München, Germany, <sup>2</sup>Mashhad University of Medical Sciences, Department of Medical Informatics, School of Medicine, Mashhad, Iran, Islamic Republic of, <sup>3</sup>Klinikum Rechts der Isar der TUM, Klinik und Poliklinik für Innere Medizin II, München, Germany, <sup>4</sup>University Medical Center Freiburg, Department of Medicine II, Freiburg, Germany

#### **Background**

Esophageal adenocarcinoma (EAC) is one of the most rapidly increasing cancers in the world, and a known precursor is Barrett's Esophagus. In this project, we explore the ability of Artificial Intelligence (AI) to detect EAC in Whole Slide Images (WSIs) of Barrett biopsies.

#### **Methods**

##### **Dataset**

BarrettNet [barrettNet] is a clinical cohort collected in Germany at 25 different institutions to follow and record the progression of Barrett patients from 2013 to 2023. We utilize 1294 labeled WSIs of 500 distinct cases from this cohort to develop our classifier.

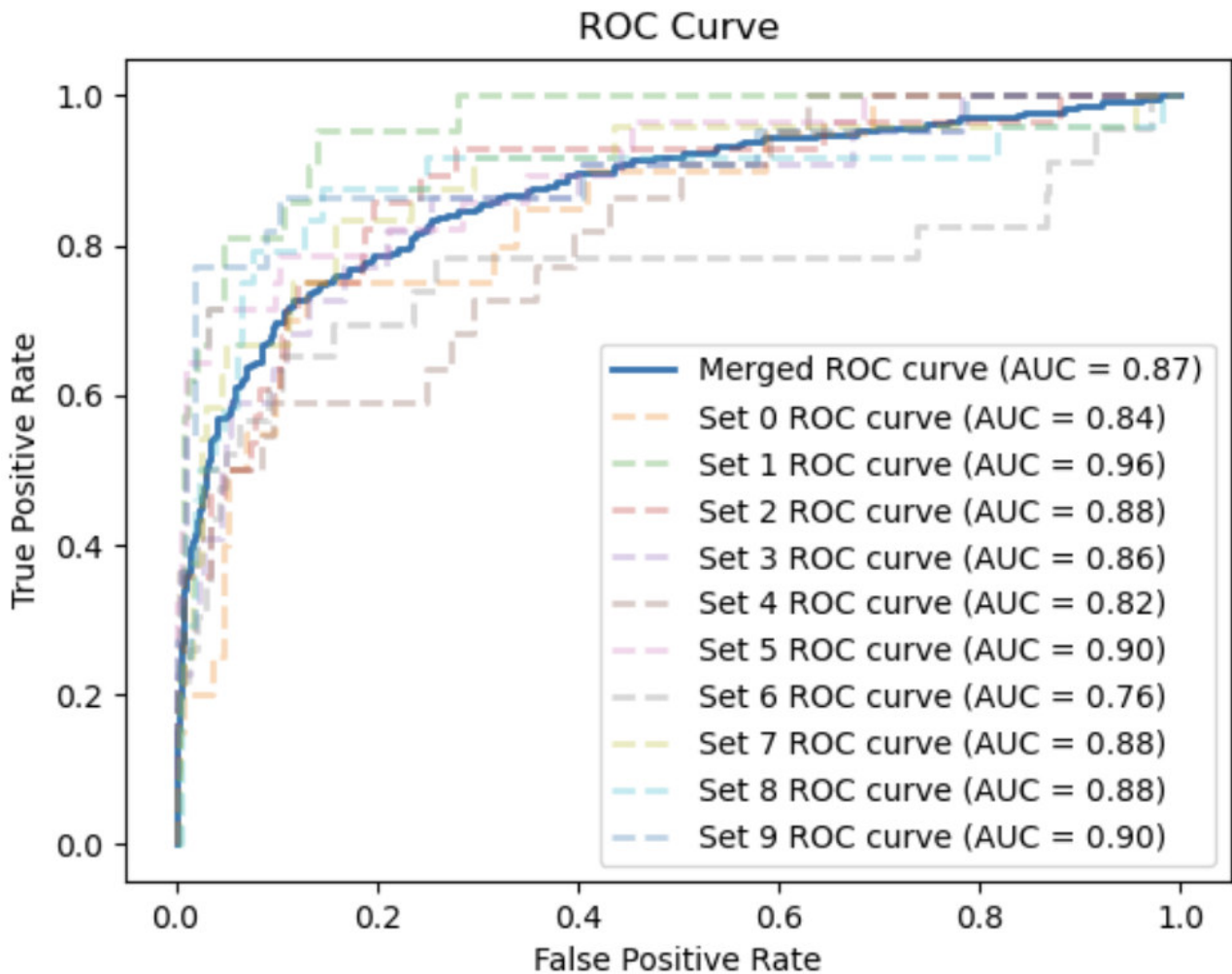
##### **Method**

Our model is based on Multiple Instance Learning (MIL), where only slide-level annotation is required; thus, the annotation time is effectively minimized. Our approach is inspired by "Clustering-constrained Attention Multiple Instance Learning" (CLAM) [clam] and therefore adopts an attention-based mechanism that facilitates slide-level aggregation from patch-level representations. During pre-processing, we incorporate Otsu thresholding for tissue segmentation, and tissue patches of 256×256 pixels are generated. A pre-trained ResNet50 is then used for feature extraction, followed by an inference step, where patch-level binary clustering happens and predictions are made. To prevent overfitting, a dropout of P=0.25 is applied during training. For validation, we employed 10-fold Monte Carlo cross-validation, with 80% of slides for training, and 10% each for validation and testing.

##### **Results**

Our model achieves an average Area Under the Curve (AUC) of 0.87 with an accuracy of 0.91, which outperforms other MIL-based methods. The performance of our model is shown in the following figure.





Model's performance, as evaluated by Area Under the Curve (AUC) of the Receiver Operating Characteristic (ROC) curves

### Conclusion

Based on these outcomes, it is evident that our model exhibits significant proficiency in the case of esophageal cancer, and we affirm that the detection of this cancer using deep learning models on Barrett WSIs is totally feasible.

Literaturangaben:

[barrettNet] Wiethaler M, Slotta-Huspenina J, Brandtner A, (2019), BarrettNET-a prospective registry for risk estimation of patients with Barrett's esophagus to progress to adenocarcinoma, Dis Esophagus  
 [clam] Lu, Ming Y and Williamson, Drew FK and Chen, Tiffany Y and Chen, Richard J and Barbieri, Matteo and Mahmood, Faisal, (2021), Data-efficient and weakly supervised computational pathology on whole-slide images, Nature Publishing Group, Nature Biomedical Engineering, 555-570

AG13.11

### ***Morphometry of tissue architecture distortion and inflammatory environments in IBD-associated crypt branching***

D. Fimbach<sup>1,2</sup>, C. Lang-Schwarz<sup>3</sup>, A. Hartmann<sup>1,2</sup>, C. Matek<sup>2,4</sup>

<sup>1</sup>Universitätsklinikum Erlangen Pathologisches Institut, Erlangen, Germany, <sup>2</sup>Bayerisches Zentrum für Krebsforschung, Erlangen, Germany, <sup>3</sup>Institute of Pathology, Klinikum Bayreuth GmbH, Bayreuth, Germany, <sup>4</sup>Pathologisches Institut Universitätsklinikum Erlangen, Erlangen, Germany

### Background

Crypt branching has been described as a histological reaction pattern of the colon mucosa in inflammatory bowel diseases (IBDs) [1]. Specifically, crypt branching can occur both in a symmetric and asymmetric fashion, representing

two distinct reaction patterns of the colon mucosa. Quantification and automated detection of these architectural distortions is required in order to analyse histology samples in an automated way for both reaction patterns and allow for a better understanding of its significance in tissue reaction with respect to chronic inflammation in IBD.

## Methods

Our data consists of whole slide images of patients with ulcerative colitis (n=100), Crohn's disease (n=100), infective colitis (n=50), and colitis ulcerosa with low-grade intraepithelial neoplasia *alio loco* (n=50). We segmented crypts using an epithelial segmentation model [2].

We furthermore classify the segmented crypts based on various machine learning approaches, including deep learning. Shape features of colon crypts form the basis of our classification, allowing for a robust distinction between symmetric and asymmetric crypt fission. Furthermore, we characterise the concomitant inflammatory infiltrate on a single-cell basis using a single-cell classifier [3].

## Results

At crypt classification, our top performing classic ensemble models achieve a mean balanced accuracy of about 0.80, while our best-performing deep-learning model achieves a mean balanced accuracy of 0.78. Combination with our single-cell classifier allows us to study in detail the inflammatory infiltrate associated with different crypt fission modes.

## Conclusion

Our models are able to detect and classify crypt branching based on shape-based information alone, corroborating a previous, qualitative morphological observation. Combined with the interpretability of classic ensemble models and hand-crafted features, this allows tracking the decision process for an individual crypt and discerning important characteristics for distinguishing the symmetric and asymmetric crypt fission modes. Combining the classifier with a single-cell classification model allows characterising the inflammatory microenvironment of crypt branching in detail.

Literaturangaben:

[1] Rubio CA, Schmidt PT, Lang-Schwarz C, Vieth M, (2022), Branching crypts in inflammatory bowel disease revisited., J Gastroenterol Hepatol, 440–445, 37

[2] Pettersen HS, Belevich I, Røyset ES, et al., (2022), Code-Free Development and Deployment of Deep Segmentation Models for Digital Pathology., Front Med, 816281, 8

[3] Graham S, QC Vu, Jahanifar M, et al., (2023), One model is all you need: Multi-task learning enables simultaneous histology image segmentation and classification., Med Image Anal, 102685, 83

AG13.12

## ***Learning by doing: Iterative development of software and a seminar format to teach computational pathology in interdisciplinary teams***

N. S. Schaadt<sup>1</sup>, J. Neemann<sup>2</sup>, G. Forestier<sup>3</sup>, D. Allerkamp<sup>2</sup>, F. Sprengel<sup>2</sup>, C. Wemmert<sup>4</sup>, T. M. Deserno<sup>5</sup>, F. Feuerhake<sup>1,6</sup>

<sup>1</sup>Institut für Pathologie / Medizinische Hochschule Hannover, Hannover, Germany, <sup>2</sup>Hochschule Hannover, Department of Computer Science, Hannover, Germany, <sup>3</sup>University of Haute-Alsace, Institut de Recherche en Informatique, Mathématiques, Automatique et Signal, Mulhouse, France, <sup>4</sup>University of Strasbourg, Le laboratoire des sciences de l'ingénieur, de l'informatique et de l'imagerie ICube, Strasbourg, France, <sup>5</sup>Peter L Reichertz Institute for Medical Informatics of TU Braunschweig and Hannover Medical School, Medical Informatics, Braunschweig, Germany, <sup>6</sup>Institut für Neuropathologie / Universitätsklinikum Freiburg, Freiburg i. Br., Germany

## Background

Curricular teaching in medicine and computer science does not sufficiently cover computational pathology. Our aim was to enable interactive learning on digital whole slide images (WSIs) addressing (1) active skill development by integration of formative feedback [1] and (2) application of Artificial Intelligence (AI)-based analysis workflows on segmentation and classification tasks relevant for quantitative biomarker evaluation.

## Methods

We developed a browser-based software ("PathoLearn") for interactive microscopy teaching [2] and extended it by a module enabling students to design an own AI-algorithm [3]. Students learn to independently identify informative areas in WSIs and solve relevant tasks, including outlining areas or anatomical structures and labeling single structures (e.g., cells) and jointly solve tasks in a real-time team collaboration by designing and testing individual AI-based analysis

workflows. They describe a sequence of pre-existing tasks (giving examples), specifying only the parameters and the inputs and outputs. We iteratively integrated the software into a new interdisciplinary seminar concept that brings together students of computer science and medicine.

## Results

Previous evaluation showed that voluntary participating students of supplementary sessions liked the teaching concept and perceived a significant learning progress particularly by drawing outlines [4], helping to better understand and interpret histological structures in the medical context. Performance increased in final exam-like tasks from 66.0% after the regular curricular course to 79.6% after solving additional exercises using PathoLearn. In a debriefing, participants could comprehensively describe opportunities and potential limitations of AI-based approaches in computational pathology.

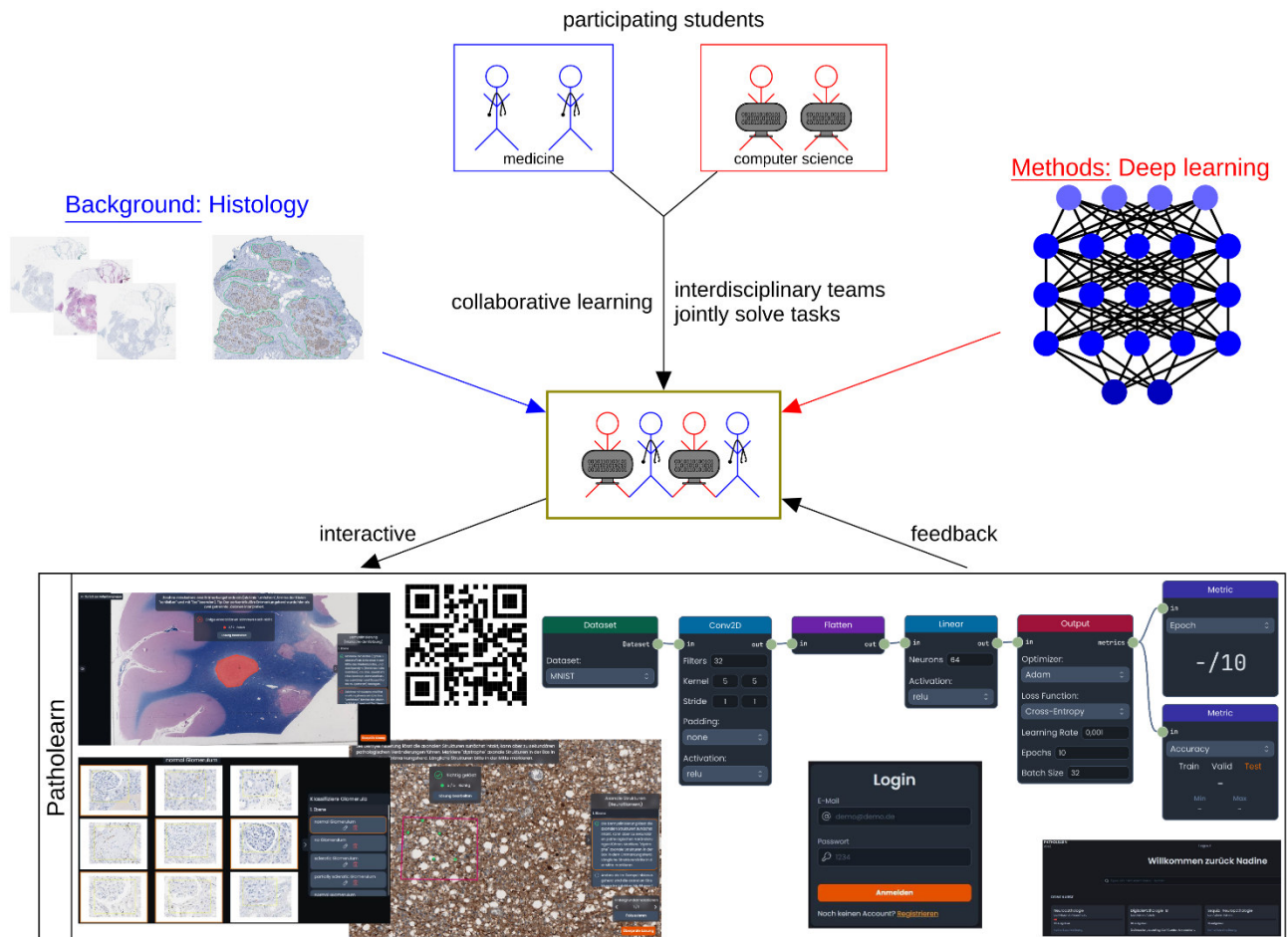


Figure 1. New seminar concept: Collaborative learning in interdisciplinary teams of medicine and computer science students. Using an interactive software (PathoLearn) that automatically generates personalized feedback and provides a synchronized platform to jointly create deep learning architectures.

## Conclusion

The software and the seminar format improved skills and knowledge necessary for efficient interdisciplinary collaboration between students of computer science and medicine, considered to be essential in an era of emerging digitization of medicine.

Literaturangaben:

- [1] Hattie, J., (2008), Visible learning: A synthesis of over 800 meta-analyses relating to achievement, <https://doi.org/10.4324/9780203887332>
- [2] Neemann, J., (2021), Entwicklung einer Lernsoftware für das Fach Pathologie, Hochschule Hannover, <https://doi.org/10.25968/opus-1972>
- [3] Neemann, J., (2023), Extending PathoLearn with an End-To-End Artificial Intelligence Platform, Hochschule Hannover, <https://doi.org/10.25968/opus-3064>

[4] Schaadt, N.S., Grote A., Forestier, G., Wemmert, C., Feuerhake F. , (2018), Role of task complexity and training in crowdsourced image annotation, *Comp Path Ophthalmic Med Image Ana*, 44–51, Best paper award MICCAI 2018, <https://germain-forestier.info/publis/compay2018.pdf>

AG13.13

### ***Identification of relevant tumor tissue structures and corresponding metastasis over deep learning of annotated $\mu$ CT data***

V. Stehl<sup>1</sup>, J. Chen<sup>2</sup>, M. Thalwaththe Gedara<sup>3</sup>, M. Al Kallaa<sup>1</sup>, C. Lölkes<sup>3</sup>, M. Wiczorek<sup>2</sup>, V. Heusinger-Heß<sup>3</sup>, M. Olbinado<sup>4,5</sup>, V. Novak<sup>4</sup>, M. Seidl<sup>1</sup>

<sup>1</sup>Institut für Pathologie, Universitätsklinikum Düsseldorf, Düsseldorf, Germany, <sup>2</sup>ImFusion GmbH, München, Germany, <sup>3</sup>Fraunhofer Institut für Kurzzeitdynamik, Ernst-Mach-Institut, Efringen-Kirchen, Germany, <sup>4</sup>ANAXAM, Villigen, Switzerland, <sup>5</sup>Paul-Scherrer-Institut, Villigen, Switzerland

#### **Background**

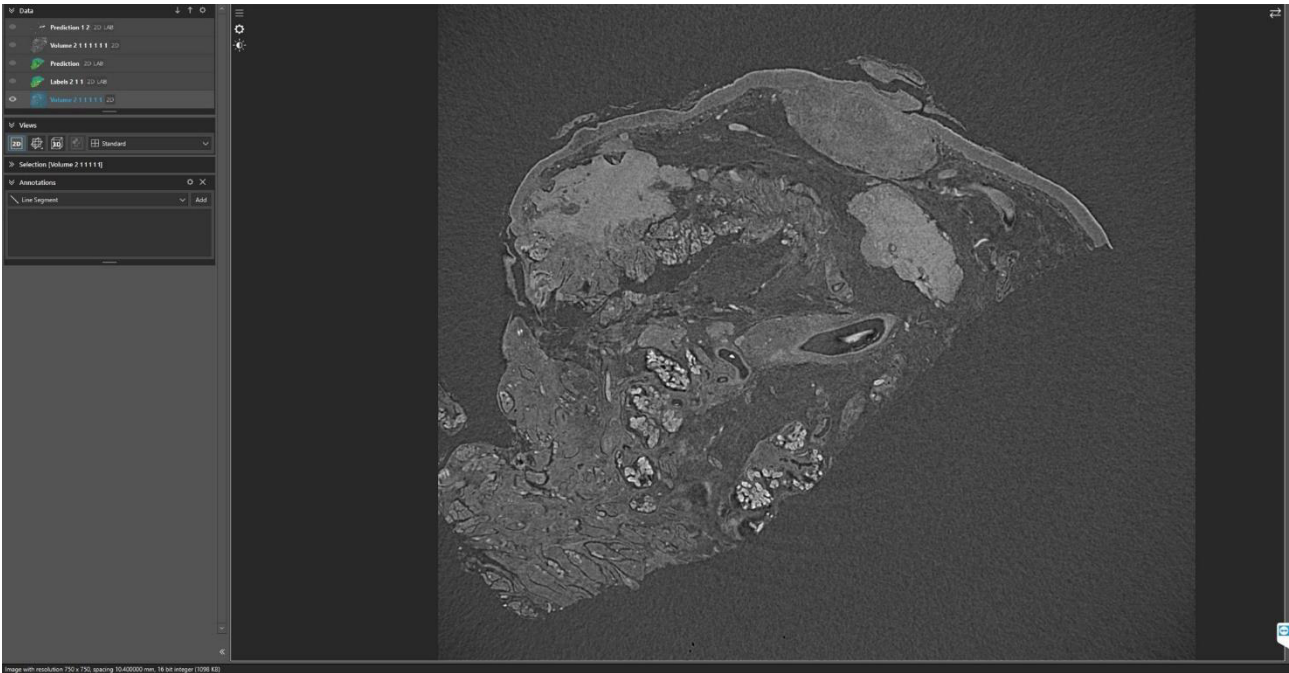
Roughly 1600 pathologists in Germany analyze around 40 million tissue samples per year. To really benefit from digitization, histological techniques should improve the quality and reduce the personal workload. Previously, we successfully demonstrated the non-destructive identification of relevant tissue structures in FFPE blocks, which is a necessary condition to supervised FFPE block sectioning. To further facilitate the method, we **aim** to visualize structures of at least 10  $\mu$ m within a 3D  $\mu$ CT data set with a beforehand trained deep learning model and guide the technical assistant through the sectioning process of the FFPE block.

#### **Methods**

3D morphological data was captured from FFPE tissue samples with  $\mu$ CT and synchrotron derived x-ray. The model was trained on several markers first on tonsil tissue and then transferred to head-neck tumors with corresponding lymph node metastasis. The annotation was done manually in the software provided by our collaborators, which performed the model development and training.

#### **Results**

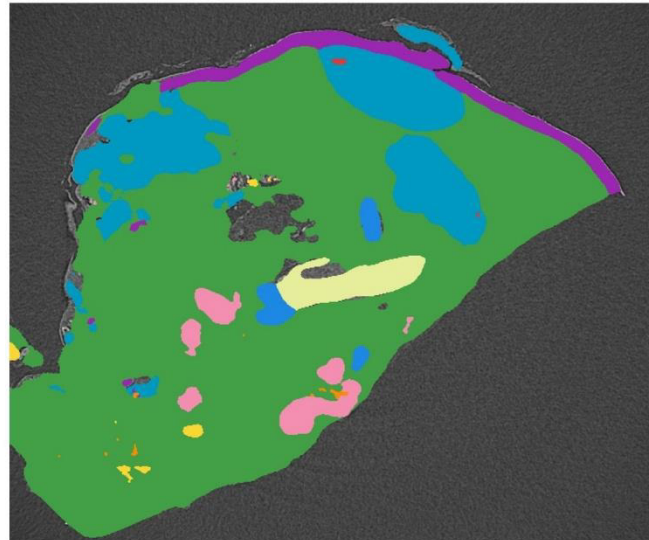
We could train a model with high accuracy on single markers annotated beforehand manually in tonsil tissue and a subset of tumor samples. Further tumor samples are in progress. The following structures are visualized: nuclei, tumor infiltration, vessels, glands, muscle fibers, germinal centers, and larger structures.



Manual



Model



Initial black and white image from the  $\mu$ CT data set: with the help of the annotations, the relevant structures are displayed in color). The comparison of manually annotated structures with those annotated by the model display a high accuracy. Connective tissue (green), salivary glands (pink) and vessels (light yellow, dark blue).

### Conclusion

With high resolution  $\mu$ CT images and software-based analysis, relevant structures can be identified in a three-dimensional context and not only on an approximately 2D plane. For the future we will investigate the use of virtual immunohistochemical markers in the 3D dataset, to reach feasible digital pathology without further workload. The experiments are part of the collaboration project HORUS (BMBF 13GW0571D). Collaborating institutions: ImFusion GmbH, Munich; DORNER Health IT Solutions, Muellheim; Fraunhofer EMI, Efringen-Kirchen; Institute for Surgical Pathology, Medical Center-University of Freiburg; Institute of Pathology, Heinrich Heine University and University Hospital of Duesseldorf.

# AG Informatik, digitale Pathologie und Biobanking 1

AG13.02

## ***Why we need clinical trials to validate AI-assays: a proposal***

R. Salgado

ZAS Hospitals, Laboratorium voor Pathologische Anatomie PA2, Antwerp, Belgium

At present, in breast cancer, clinico-pathological risk stratification is mostly performed using a limited set of features such as tumour size and lymph node status. Very large adjuvant trials have illustrated the key problem with the current scheme - it does not stratify patients with sufficient granularity to permit optimal selection and this selection hence does not always reflect a clear understanding of the biological diversity of cancer at diagnosis. One of the most rapidly expanding areas of research at present is that focused on combining histopathology, genomics, and artificial intelligence. Several results in this area have identified genomic/transcriptomic features which in hindsight are associated with histological features, that may be identified using AI-assays. This area of research has the potential to significantly impact the management of breast cancer but is challenged by the lack of a robust framework for the validation and dissemination of research tools, including AI-assays. Key to a potential solution is the establishment of a digital pathology platform linked with well-annotated patient information including long term outcomes collected using randomized clinical trials from large collaborative trial groups.

AG13.03

## ***Empowering minimally invasive postmortems with modular standard operating procedures to qualify for scientific demands***

F. A. Kammerstetter<sup>1</sup>, C. Schustetter<sup>1</sup>, F. Fusco<sup>1</sup>, A. Kasajima<sup>1</sup>, C. Delbridge<sup>1</sup>, P.-H. Kuhn<sup>1</sup>, K. Steiger<sup>1</sup>, L. Schul<sup>2</sup>, K. Hollerith<sup>2</sup>, T. Lahmer<sup>3</sup>, U. Heemann<sup>2</sup>, K. F. Stock<sup>2</sup>, J. Slotta-Huspenina<sup>1,2,4</sup>, G. Weirich<sup>1</sup>

<sup>1</sup>Institute of Pathology, School of Medicine, Technical University Munich, Ismaninger Straße 22, 81675 Munich, Germany, <sup>2</sup>Department of Nephrology, School of Medicine, Technical University Munich, Ismaninger Straße 22, 81675 Munich, Germany, <sup>3</sup>Department of Internal Medicine II, Klinikum Rechts der Isar, School of Medicine, Technical University of Munich, Ismaninger Straße 22, 81675 Munich, Germany, <sup>4</sup>Pathologie Starnberg MVZ GmbH, Starnberg, Germany

### **Background**

Compared to clinical autopsies (CA), ultrasound-guided minimally invasive tissue sampling (US-MITS) is a slender method to obtain tissue samples from deceased patients. US-MITS is accessible to clinicians, resulting in short post-mortem intervals beneficial to high-end tissue analyses. In-clinic US-MITS profits from a scalable workflow, and a modular orchestration of standard operating procedures (SOPs) to maintain a high-quality output. This survey established and evaluated SOPs relevant to US-MITS performance at different sites.

### **Methods**

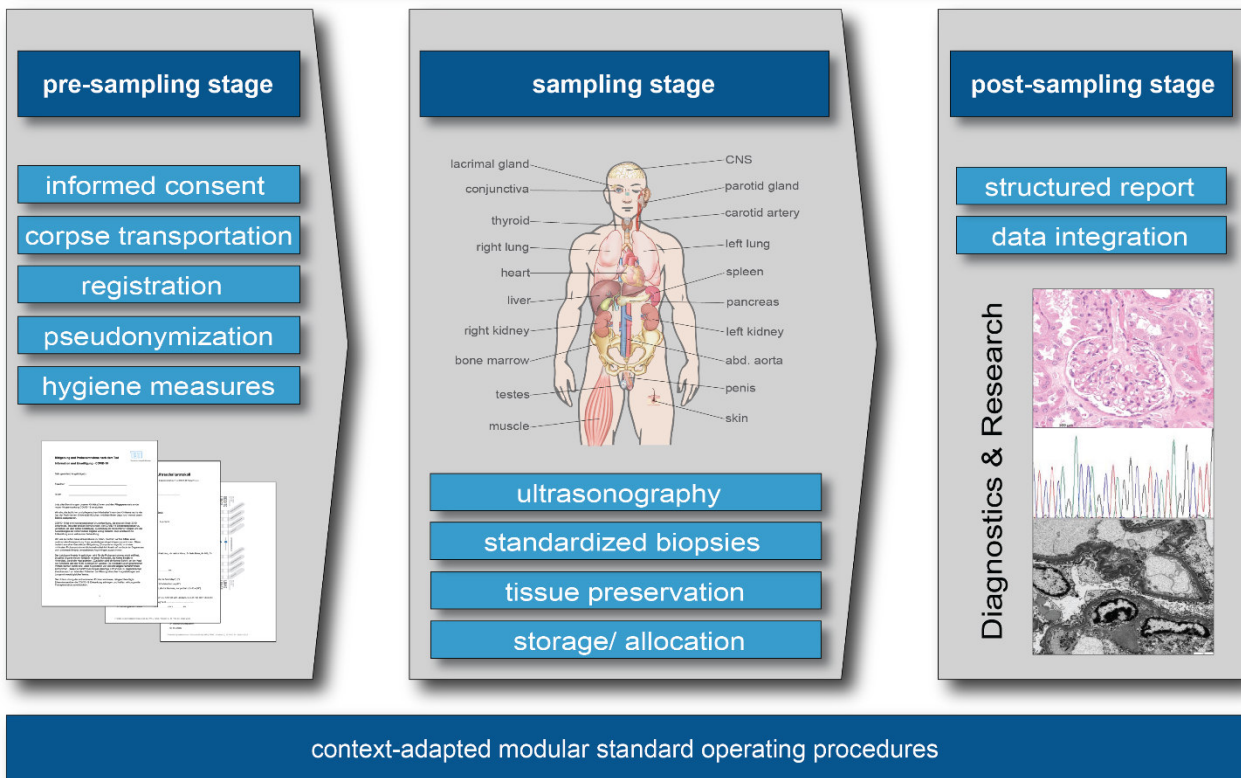
COVID-19 set the frame for SOP implementation and evaluation to establish the US-MITS method. Between 6/20 and 9/22, SOPs were evaluated at two different sites: the TUM pathology and at the bedside in an intensive care unit of the TUM University hospital. An interdisciplinary rotating team (8 members) carried out US-MITS. The procedure's workflow started with a patient's expiry and ended with the diagnostic report. SOPs concerned three workflow stages: pre-sampling, sampling, and post-sampling.

### **Results**

Pre-sampling SOPs comprised next-of-kin information, prearrangement activities (e.g. pseudonymization), and the setting up of US-MITS locations, including hygiene issues. Sampling SOPs involved standardized US examinations, organ-specific biopsy, biopsy preservation, post-sampling SOPs the biopsy processing, digitalization, tissue quality assessments (postmortem interval, biopsy length, organ specificity, and vitality) and a structured diagnostic report. Altogether, we assessed 3024 multi-organ biopsies from 36 deceased COVID-19 patients. Team members considered the SOPs easy to understand and practical. The elaboration of SOPs concerning tissue quality was especially helpful in establishing a reproducible and scalable technique for modular site-specific workflows.



# Workflow US-guided minimally invasive tissue sampling



## Conclusion

Defining SOPs for US-MITS helped to settle this clinical method as a dependable flexible, and scalable postmortem biopsy tool. SOP-based US-MITS bears the potential of an ideal supplement or alternative to CA when specific diagnostic and scientific issues are at stake beyond mere causes of death.

AG13.04

## ***Low-resource finetuning of foundation models beats state-of-the-art in histopathology***

B. Roth<sup>1</sup>, V. Koch<sup>1,2</sup>, S. J. Wagner<sup>1,2</sup>, J. A. Schnabel<sup>1,2,3</sup>, C. Marr<sup>2</sup>, T. Peng<sup>2</sup>

<sup>1</sup>Technische Universität München, School of Computation and Information Technology, München, Germany, <sup>2</sup>Helmholtz Zentrum München, German Research Center for Environmental Health, München, Germany, <sup>3</sup>King's College, School of Biomedical Engineering and Imaging Sciences, London, United Kingdom

## Background

To handle the large scale of whole slide images in computational pathology, most approaches first tessellate the images into smaller patches, extract features from these patches, and finally aggregate the feature vectors with weakly-supervised learning. The performance of this workflow strongly depends on the quality of the extracted features. Recently, foundation models in computer vision have showcased strong generalizability.

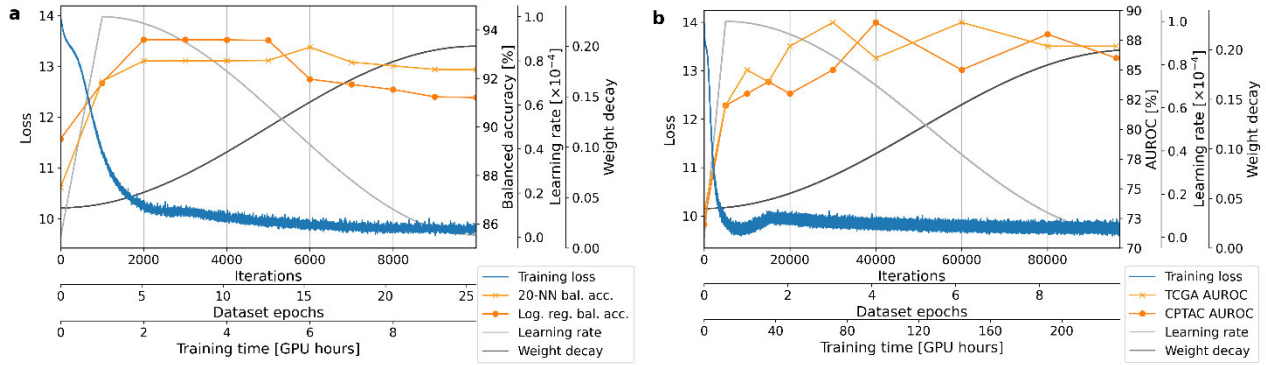
## Methods

In this study, we benchmark the most popular vision foundation models as feature extractors for histopathology data: DINOv2 [REF3], BEiT [REF4], SAM [REF5], and ImageBind [REF6] versus existing histopathology-specific extractors CTransPath [REF1] and RetCCL [REF2]. We evaluate the models as feature extractors in two settings. On slide-level we use the cohorts COAD and READ from TCGA [REF7] and CPTAC's [REF8] CRC cohort. For evaluation we train a slide-level classifier using transformer-based aggregation [REF10]. In patch-level classification, we utilize the NCT-CRC-100K [REF9] dataset. We train our model on the entire dataset and validate it on CRC-VAL-HE-7K. We use logistic regression

and KNN for evaluation.

Most importantly, we finetune the model DINOv2 on TCGA and the NCT dataset using the adapted DINOv2 code and evaluate the result.

## Results



Performance over time of finetuning a ViT-s with DINOv2: a) on NCT-CRC and evaluating on the external NCT-CRC testset on patch-level classification and b) on TCGA and testing on TCGA and CPTAC (external testset) on WSI-level classification.

Model	Histo	AUROC	
		TCGA	CPTAC
ResNet50		0.67±0.10	0.65±0.05
ResNet50 truncated		0.68±0.02	0.68±0.02
SAM (ViT-B)		0.56±0.07	0.62±0.03
SAM (ViT-H)		0.55±0.05	0.64±0.02
BEiT (ViT-B)		0.52±0.07	0.51±0.02
ImageBind (ViT-h)		0.64±0.06	0.71±0.02
DINOv2 (ViT-S)		0.73±0.07	0.72±0.06
DINOv2 (ViT-g)		0.66±0.12	0.60±0.03
RetCCL (ResNet50)	✓	0.84±0.08	0.77±0.05
CTransPath (Swin-T)	✓	<u>0.85±0.05</u>	<u>0.82±0.04</u>
DINOv2 (ViT-S)	✓	<b>0.89±0.05</b>	<b>0.85±0.02</b>
DINOv2 (ViT-g)	✓	0.84±0.05	0.79±0.03

Finetuned DINOv2 outperforms dedicated feature extractors CTransPath and RetCCL on AUROC scores on WSI classification (MSI detection) in CRC tissue from TCGA and CPTAC (external). Also, DINOv2 ViT-S notably outperforms



the ViT-g variant.

Model	Histo	20-NN		linear probe	
		ACC	F1	ACC	F1
ResNet50		0.78	0.81	0.86	0.88
ResNet50 truncated		0.87	0.91	0.88	0.89
SAM (ViT-B)		0.75	0.76	0.83	0.81
SAM (ViT-H)		0.69	0.71	0.79	0.84
BEiT (ViT-B)		0.63	0.66	0.59	0.65
ImageBind (ViT-h)		0.87	0.89	0.90	0.91
DINOv2 (ViT-S)		0.88	0.90	0.90	0.92
DINOv2 (ViT-g)		0.91	0.93	0.92	0.94
RetCCL (ResNet50)	✓	0.91	0.93	0.92	0.94
CTransPath (Swin-T)	✓	<b>0.95</b>	<b>0.96</b>	<b>0.94</b>	<u>0.95</u>
DINOv2 (ViT-S)	✓	<u>0.94</u>	<u>0.95</u>	<u>0.93</u>	0.94
DINOv2 (ViT-g)	✓	0.93	<u>0.95</u>	<b>0.94</b>	<b>0.96</b>

Finetuned DINOv2 matches the performance of the best-scoring feature extractor, CTransPath, on balanced accuracy (ACC) and weighted F1-scores (F1) for CRC tissue classification on NCT-patches.

### Conclusion

Our experiments demonstrate that by finetuning a foundation model on a single GPU for only two hours or three days depending on the dataset, we can match or outperform state-of-the-art feature extractors for computational pathology. These findings imply that even with little resources one can finetune a feature extractor tailored towards a specific downstream task and dataset.

### Literaturangaben:

- [REF1] Xiyue Wang and Sen Yang and Jun Zhang and Minghui Wang and Jing Zhang and Wei Yang and Junzhou Huang and Xiao Han, (2022), Transformer-based unsupervised contrastive learning for histopathological image classification, Medical Image Analysis, <https://www.sciencedirect.com/science/article/pii/S1361841522002043>, 2024-02-27
- [REF2] Xiyue Wang and Yuexi Du and Sen Yang and Jun Zhang and Minghui Wang and Jing Zhang and Wei Yang and Junzhou Huang and Xiao Han, (2023), RetCCL: Clustering-guided contrastive learning for whole-slide image retrieval, Medical Image Analysis, <https://www.sciencedirect.com/science/article/pii/S1361841522002730>
- [REF3] Maxime Oquab and Timothée Darcet and Théo Moutakanni and Huy Vo and Marc Szafraniec and Vasil Khalidov and Pierre Fernandez and Daniel Haziza and Francisco Massa and Alaaeldin El-Nouby and Mahmoud Assran and Nicolas Ballas and Wojciech Galuba and Russell Howes and Po-Yao Huang and Shang-Wen Li and Ishan Misra and Michael Rabbat and Vasu Sharma and Gabriel Synnaeve and Hu Xu and Hervé Jegou and Julien Mairal and Patrick Labatut and Armand Joulin and Piotr Bojanowski, (2023), DINOv2: Learning Robust Visual Features without Supervision, <https://arxiv.org/abs/2304.07193>
- [REF4] Hangbo Bao and Li Dong and Songhao Piao and Furu Wei, (2022), {BEiT: BERT Pre-Training of Image Transformers, <https://arxiv.org/abs/2106.08254>
- [REF5] Alexander Kirillov and Eric Mintun and Nikhila Ravi and Hanzi Mao and Chloe Rolland and Laura Gustafson and Tete Xiao and Spencer Whitehead and Alexander C. Berg and Wan-Yen Lo and Piotr Dollár and Ross Girshick, (2023), Segment Anything, <https://arxiv.org/abs/2304.02643>

[REF6] Rohit Girdhar and Alaaeldin El-Nouby and Zhuang Liu and Mannat Singh and Kalyan Vasudev Alwala and Armand Joulin and Ishan Misra, (2023), ImageBind: One Embedding Space To Bind Them All, <https://arxiv.org/abs/2305.05665>

[REF7] Cancer Genome Atlas Network and others, (2012), Comprehensive molecular characterization of human colon and rectal cancer, Nature Publishing Group, Nature

[REF8] Edwards, Nathan J. and Oberti, Mauricio and Thangudu, Ratna R. and Cai, Shuang and McGarvey, Peter B. and Jacob, Shine and Madhavan, Subha and Ketchum, Karen A., (2015), The CPTAC Data Portal: A Resource for Cancer Proteomics Research, Journal of Proteome Research, 2707-2713, 14, <https://doi.org/10.1021/pr501254j>

[REF9] Kather, Jakob Nikolas and Halama, Niels and Marx, Alexander, (2018), 100,000 histological images of human colorectal cancer and healthy tissue, Zenodo, <https://doi.org/10.5281/zenodo.1214456>

[REF10] Sophia J. Wagner and Daniel Reisenbüchler and Nicholas P. West and Jan Moritz Niehues and Jiefu Zhu and Sebastian Foersch and Gregory Patrick Veldhuizen and Philip Quirke and Heike I. Grabsch and Piet A. {van den Brandt} and Gordon G.A. Hutchins and Susan D. Richman and Tanwei Yuan and Rupert Langer and Josien C.A. Jenniskens and Kelly Offermans and Wolfram Mueller and Richard Gray and Stephen B. Gruber and Joel K. Greenson and Gad Rennert and Joseph D. Bonner and Daniel Schmolze and Jitendra Jo, (2023), Transformer-based biomarker prediction from colorectal cancer histology: A large-scale multicentric study, Cancer Cell, 1650-1661.e4, 41, <https://www.sciencedirect.com/science/article/pii/S1535610823002787>

AG13.05

## ***Tissue Concepts: Supervised Foundation Models for Resource-Efficient, Robust Deep Learning in Pathology***

T. Nicke<sup>1</sup>, J. R. Schäfer<sup>2</sup>, L. O. Schwen<sup>3</sup>, H. Höfener<sup>3</sup>, F. Thielke<sup>3</sup>, A. Turzynski<sup>4</sup>, T. Bisson<sup>5</sup>, N. Flinner<sup>6</sup>, N. Zerbe<sup>5</sup>, F. Feuerhake<sup>7</sup>, D. Merhof<sup>8</sup>, H. Hahn<sup>3</sup>, J. Lotz<sup>1</sup>

<sup>1</sup>Fraunhofer MEVIS, Lübeck, Germany, <sup>2</sup>Fraunhofer MEVIS, Aachen, Germany, <sup>3</sup>Fraunhofer MEVIS, Bremen, Germany,

<sup>4</sup>Gemeinschaftspraxis für Pathologie Lübeck, Lübeck, Germany, <sup>5</sup>Charité - Universitätsmedizin Berlin, Institut für Pathologie, Berlin, Germany, <sup>6</sup>Dr. Senckenbergisches Institut für Pathologie, Universitätsklinikum Frankfurt, Frankfurt, Germany, <sup>7</sup>Institut für Pathologie, Medizinische Hochschule Hannover, Hannover, Germany, <sup>8</sup>Universität Regensburg, Lehrstuhl für Bildverarbeitung, Regensburg, Germany

### **Background**

Deep Learning is the cornerstone of the automation of image analysis in pathology but requires large problem-specific training datasets. Recently, training of foundation models (FM) using self-supervision has demonstrated great potential to provide robust solutions in data-scarce situations [1],[2],[3],[4]. However, training FM requires even larger, diverse datasets. Additionally, the CO<sub>2</sub> emitted during training has raised concerns among researchers [5].

### **Methods**

We propose “Tissue Concepts”, a data-efficient supervised pre-training for foundation models in pathology. The foundational backbone was simultaneously pre-trained on 16 labeled tasks in a multitask learning scheme for 160 hours on a single GPU (Nvidia RTX A5000). The resulting FM was frozen after pre-training and [SO1] was evaluated by training a task-specific, random-forest-based regressor on unseen external data and measuring sample efficiency (i.e., the effect of small training datasets on classifier performance). We further evaluated the model's ability to segment unseen images based on an interactive training using LightGBM [6].

### **Results**

When applied to an unseen breast cancer cellularity estimation task (BreastPathQ), a combination of Tissue Concepts with a task-specific head outperforms the state of the art with a mean squared error (MSE) of 0.024 on the test set. In comparison, a model pre-trained on ImageNet only achieves an MSE of 0.041. The Tissue-Concepts-based head can be trained to this performance using only 6% of the available training data.

Furthermore, a segmentation can be interactively trained using the features extracted by Tissue Concepts. In the presented demo, 3–6 patches of sparsely annotated training data are sufficient (<https://s.fhg.de/tissue-concepts-few-shot>).

Supervised training of Tissue Concepts emitted approx. 19 kg CO<sub>2</sub>, whereas self-supervised FM training to similar performance usually requires more data and emits more than one ton of CO<sub>2</sub>.

### **Conclusion**

Supervised FMs are a basis for developing robust and reliable deep neural networks that generalize well to external data and new tasks. With adequate pre-training, state-of-the-art performance can be obtained using a small number of

training samples. In the BMBF-funded project PROSurvival, FMs will serve as performant feature extractors for federated learning in prostate cancer survival.

#### Literaturangaben:

- [1] Wang, X et al., (2022), Transformer-based unsupervised contrastive learning for histopathological image classification., Medical Image Analysis, <https://doi.org/10.1016/j.media.2022.102559>
- [2] Vorontsov, E. et al., (2023), Virchow: A Million-Slide Digital Pathology Foundation Model, arXiv preprint, <https://doi.org/10.48550/ARXIV.2309.07778>
- [3] Filiot, A. et al., (2023), Scaling Self-Supervised Learning for Histopathology with Masked Image Modeling, Medrxiv preprint, <https://doi.org/10.1101/2023.07.21.23292757>
- [4] Schäfer, JR. et al., (2023), Overcoming Data Scarcity in Biomedical Imaging with a Foundational Multi-Task Model, arXiv preprint, <https://doi.org/10.48550/ARXIV.2311.09847>
- [5] Vafaei Sadr, A. et al., (2024), Operational greenhouse-gas emissions of deep learning in digital pathology: a modelling study, The Lancet Digital Health, [https://doi.org/10.1016/S2589-7500\(23\)00219-4](https://doi.org/10.1016/S2589-7500(23)00219-4)
- [6] Ke, G. et al., (2022), LightGBM: A Highly Efficient Gradient Boosting Decision Tree, Advances in Neural Information Processing Systems 30 (NIPS 2017), [https://papers.nips.cc/paper\\_files/paper/2017/hash/6449f44a102fde848669bdd9eb6b76fa-Abstract.html](https://papers.nips.cc/paper_files/paper/2017/hash/6449f44a102fde848669bdd9eb6b76fa-Abstract.html)

## AG13.06

### ***Surface microscopic techniques for distortion-free digital pathology***

M. Al Kallaa<sup>1</sup>, V. Stehl<sup>1</sup>, M. Seidl<sup>1</sup>, J. Chen<sup>2</sup>, M. Wieczorek<sup>2</sup>, M. Thalwaththe Gedara<sup>3</sup>, V. Heusinger-Heß<sup>3</sup>, S. Moser<sup>3</sup>

<sup>1</sup>Institute of Pathology, University Hospital of Duesseldorf, Duesseldorf, Germany, <sup>2</sup>ImFusion GmbH, Munich, Germany, <sup>3</sup>Fraunhofer EMI, Efringen-Kirchen, Germany

#### **Background**

Histopathological techniques serve as the benchmark for cancer diagnosis, yet they are constrained by the analysis of small, nearly two-dimensional tissue samples, presenting a limitation in tissue examination. To address this limitation, there's a need for a routine-applicable, three-dimensional histological method. We therefore aim to tackle a pre-analytical problem: virtual imaging with comparable detail resolution to conventional histology requires the identification of similar microanatomical structures between virtual and histological sections. Although histological sections on slides provide high resolution, they are not distortion-free. In contrast, the cutting surface of tissue blocks is undistorted. Therefore, **the goals** of the work include scrutinizing the method of paraffin block surface microscopy, developed by project HORUS for histological examination.

#### **Methods**

The technique was refined using tonsil samples, which exhibit stratified squamous epithelium and lymphoid tissue germinal centers, serving as test structures for identification purposes. Annotation was conducted using QuPath software to assess the developed surface microscopic technique relative to digitized HE sections, which served as the benchmark.

#### **Results**

We examined the HORUS technique in comparison with digitized HE sections and were able to identify structures such as capillaries, salivary glands (10-25 µm), muscle fibers, stratified squamous epithelium (25-100 µm), and germinal centers (500+ µm).

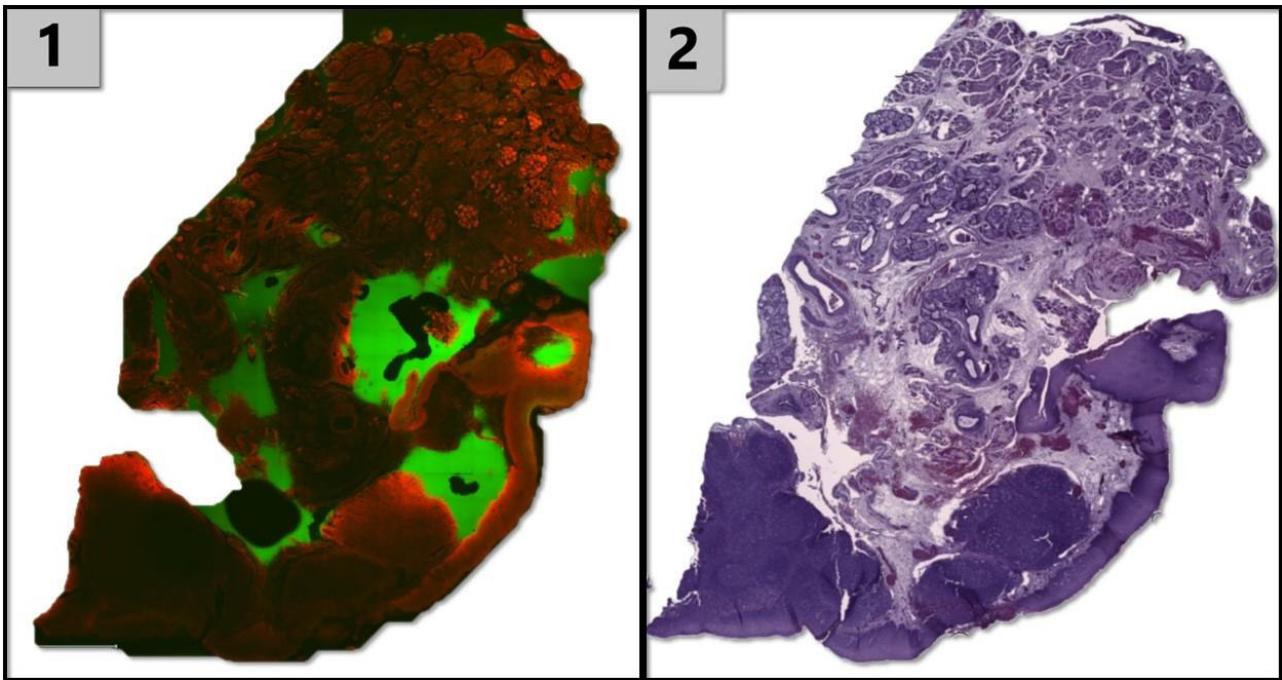


Figure 1: Fluorescence scan of of FFPE tonsil tissue (Our newly developed surface microscopic technique). Figure 2: the corresponding HE scan.

### Conclusion

The method of paraffin block surface microscopy, developed by project HORUS offers a comprehensive approach to tissue analysis with comparable detail resolution to conventional histology. The method will undergo further refinement and application to paired samples of head and neck tumors and their lymph node metastasis.

AG13.07

### ***Visualizing histopathological images through Activation Atlases: a tool for enhancing model explainability and discovering novel features with AI***

C. Glasner<sup>1</sup>, S. Schulz<sup>1</sup>, F. Wolf<sup>2</sup>, M. Gustav<sup>2</sup>, J. N. Kather<sup>2</sup>, M. Jesinghaus<sup>3</sup>, F. Kellers<sup>4</sup>, A. Fernandez<sup>1</sup>, D. Truhn<sup>5</sup>, S. Strobl<sup>1</sup>, D.-C. Wagner<sup>1</sup>, W. Roth<sup>1</sup>, [S. Foersch<sup>1</sup>](#)

<sup>1</sup>University Medical Center Mainz, Institute of Pathology, Mainz, Germany, <sup>2</sup>Medical Faculty Carl Gustav Carus, Technical University Dresden, Else Kroener Fresenius Center for Digital Health, Dresden, Germany, <sup>3</sup>University Hospital Giessen-Marburg, Institute of Pathology, Marburg, Germany, <sup>4</sup>University Hospital of Schleswig Holstein, Campus Kiel, Department of Pathology, Kiel, Germany, <sup>5</sup>University Hospital Aachen, Department of Diagnostic and Interventional Radiology, Aachen, Germany

### Background

Deep learning models have shown remarkable accuracy in classifying histopathological images, aiding in the diagnosis and understanding of diseases. However, their complexity often results in a lack of transparency, obscuring the learned features and decision-making processes. This opacity hinders both the establishment of trust among medical professionals and patients, and the discovery of novel insights into disease characteristics that the models may contain.

### Methods

We propose the use of Activation Atlases<sup>1</sup>, a technique for visualizing the features a trained model extracts from an image dataset. This method involves clustering, averaging and inverting the activations of numerous input images to produce a grid that represents how the network perceives the data up to any selected layer. Our study applies Activation Atlases to different computer vision models fine-tuned on a subset of the NCT-CRC-HE-100K dataset to explore the dataset through the models' "eyes".

### Results

Preliminary findings suggest that Activation Atlases offer a comprehensive visualization of the features learned by the neural networks, revealing visual characteristics relevant to histopathological diagnosis. These insights have the potential

to augment human pathologists' understanding and identification of disease markers.

## Conclusion

Activation Atlases serve as a valuable tool for demystifying the decision-making processes of deep learning models in histopathology, potentially fortifying trust in AI-assisted diagnostics and uncovering novel diagnostic features. Future work will focus on extending this technique to a wider range of architectures and datasets, further bridging the gap between AI and clinical practice.

<sup>1</sup>Carter, et al., "Activation Atlas", Distill, 2019.

# AG Gastroenteropathologie 1

AG14.01

## ***Immunohistochemical In-situ Protein Expression Analysis for Anti-Claudin-18.2 Therapies - Which is the Correct Antibody?***

O. Basturk, D. Frosina, P. Ruh, E. Hernandez, A. Jungbluth

Memorial Sloan Kettering Cancer Center, Pathology, New York, United States of America

### Background

Several novel antibody-drug conjugate (ADC) based therapies targeting isoform 2 of Claudin-18 (CLDN18.2) have recently become available and are tested for the treatment of gastric cancer. For eligibility testing, most current trials require presence of target antigen above certain threshold levels as analyzed by IHC. Interestingly, IHC testing for most anti-CLDN18.2 therapies employ primary reagents reactive to both isoforms, CLDN18.1 and 18.2. In the present study we test two mAbs to CLDN18.2 and to CLDN18.1/18.2 respectively and compare the expression of both antigens in a series of gastric carcinomas.

### Methods

The following mAbs were employed: mAb EPR19202 (Abcam, ab222512) to CLDN-18.2 and mAb EPR19203 (ab222513) detecting CLDN-18.1/18.2. Specificity testing and assay development was done in panels of normal tissues including lung and stomach.

Next, a series of 32 gastric carcinomas was analyzed with both mAbs. Staining was graded based on immunopositive tumor cell as follows: negative, focal (<5%), + (5-<25%), ++ (25-<50%), +++ (50-<75%), ++++ (75-100%). Intensity was graded as weak (w); moderate (m), strong (s).

### Results

Previous data show that in normal tissues, CLDN-18.2 is restricted to gastric mucosa while CLDN-18.1 is solely present in lung. EPR19202 immunostaining was restricted to normal gastric mucosa, while EPR19203 was immunoreactive in lung and gastric mucosa, confirming specificity of both primary reagents.

Full sections of 32 gastric carcinoma resections were analyzed. Immunopositivity for CLDN18.1&2 versus CLDN18.2 was as follows: Negative: 18.8%/31.2%; focal:6.3%/21.9%; +:5.6%/21.9%; ++:12.5%/6.2%; +++:21.8%/9.4%; ++++:25%/9.4%. All 15 CLDN18.1&2 +++/++++ positive cases showed moderate or strong staining, while for CLDN18.2, only 3/6 +++/++++ cases were moderate or strongly positive and only 1 case showed strong staining in >75% of the tumor.

### Conclusion

Current anti-CLDN18.2 ADC therapies require IHC expression typing for eligibility employing various, usually rather high threshold levels of immunopositive tumor cells as well as intensity levels. Interestingly, current eligibility typing for clinical trials is based on a mAb detecting CLDN18.1&2. Here we show a big discrepancy between the expression of CLDN18.1&2 versus CLDN18.2 in gastric carcinoma. Our data suggest that current eligibility typing employing an anti-CLDN18.1&2 mAb vastly overstates the number of eligible patients. The use of a mAb specific for the target antigen CLDN18.2 should be considered.

## AG14.02

### ***Investigating Unconfirmed HER2 Status***

L. Haffner<sup>\*1,2</sup>, K. Kolbe<sup>\*1,3</sup>, E. Raimundez<sup>4</sup>, A. Walch<sup>5</sup>, J. Hasebauer<sup>4</sup>, F. Lordick<sup>1,3</sup>

<sup>1</sup>University of Leipzig Medical Center, Department of Oncology, Gastroenterology, Hepatology, Pulmonology, Leipzig, Germany,

<sup>2</sup>Comprehensive Cancer Center Central Germany, Leipzig, Germany, <sup>3</sup>UCCL, Leipzig, Germany, <sup>4</sup>University of Bonn, Faculty of Mathematics and Natural Sciences, Bonn, Germany, <sup>5</sup>Helmholtz Zentrum München, Research Unit Analytical Pathology, Neuherberg, Germany

\*Contributed equally

#### **Background**

Trastuzumab is an approved targeted therapy in HER2 positive advanced gastric cancer (GC). Unfortunately not all patients respond and the majority of initial responders eventually experience progression. The VARIANZ study aimed to find biomarkers to predict response to trastuzumab treatment in advanced gastric cancer. Locally assessed HER2 status was reassessed by central pathology using immunohistochemistry (IHC) and in situ hybridization, resulting in a HER2 test deviation rate of 22.3%. The aim of this study was to identify reasons that may have caused the deviating HER2 test results.

#### **Methods**

Data about the local HER2 test procedure including IHC antibodies used and participation in round robin tests from 105 local pathologies were collected. HER2 status was verified centrally according to algorithm of the ToGA study using immunohistochemistry and chromogenic-in-situ hybridization. Patients were followed up to 48 months.

#### **Results**

Central confirmation of the local HER2 IHC scores were seen for the majority of locally HER2- IHC 0/1 (172/178; 96.6%), but less frequently for locally HER2+ IHC3+ (57/124; 46.0%) cases. Deviation rate was not associated with IHC antibody platform used in the local pathology institute neither with participation in quality-assuring tests. Regarding tumor characteristics, deviating test results were more frequently found in GC vs. EGJC (69.1% vs. 39.7%;  $p = 0.001$ ) and in Laurén diffuse vs. intestinal subtype (23.5% vs. 5.9%,  $p = 0.004$ ). Patients who received trastuzumab for confirmed HER2+ mGC (central HER2+/local HER2+) lived significantly longer as compared with patients who received trastuzumab for local HER2+ but central HER2- mGC (20.5 months,  $n = 60$  v 10.9 months,  $n = 65$ ; hazard ratio, 0.42; 95% CI, 8.2 to 14.4;  $P < .001$ ).

#### **Conclusion**

Our results suggest that HER2 positivity and therefore benefit of HER2 targeted therapy with trastuzumab is associated with GEJ tumor location and intestinal Laurén classification. The heterogeneity of GEJC/GC results in deviating HER2 results and decreased trastuzumab benefit.

## AG14.03

### ***Low microsatellite instability – a distinct instability type in gastric cancer?***

M. Kohruss<sup>1</sup>, S. Chakraborty<sup>1</sup>, A. Hapfelmeier<sup>2</sup>, M. Jesinghaus<sup>1,3</sup>, J. Slotta-Huspenina<sup>1</sup>, A. Novotny<sup>4</sup>, L. Sasic<sup>5</sup>, M. M. Gaida<sup>6,7,8</sup>, K. Ott<sup>9</sup>, W. Weichert<sup>1,10</sup>, N. Pfarr<sup>1</sup>, G. Keller<sup>1</sup>

<sup>1</sup>Technical University of Munich, Institute of Pathology, TUM School of Medicine and Health, München, Germany, <sup>2</sup>Technical University of Munich, Institute of AI and Informatics in Medicine, München, Germany, <sup>3</sup>University of Marburg, Institute of Pathology, Marburg, Germany, <sup>4</sup>Technical University of Munich, Department of Surgery, TUM School of Medicine and Health, München, Germany,

<sup>5</sup>University of Heidelberg, Department of Surgery, Heidelberg, Germany, <sup>6</sup>University of Heidelberg, Institute of Pathology, Heidelberg, Germany, <sup>7</sup>University Medical Center Mainz, Institute of Pathology, Mainz, Germany, <sup>8</sup>University Mainz, TRON-Translational Oncology at the University Medical Center Mainz, Mainz, Germany, <sup>9</sup>Klinikum Rosenheim, Department of Surgery, Rosenheim, Germany,

<sup>10</sup>German Cancer Consortium, Partner Site Munich, Institute of Pathology, München, Germany

#### **Background**

We recently showed that low microsatellite instability (MSI-L) was associated with decreased survival in primarily resected gastric cancer (GC), but was associated with a good response to platinum/5-fluorouracil (5-FU) neoadjuvant chemotherapy (CTx) (1). The purpose of this study was to characterize the instability pattern of the MSI-L tumors and to investigate an association of MSI-L with mutations in genes of DNA repair pathways, the homologous recombination

(HR) deficiency score and with total tumor mutation burden (TMB) using whole exome sequencing (WES) (2).

## Methods

MSI had been determined by PCR using DNA from formalin-fixed paraffin-embedded tissues in recent studies (1). Two mononucleotide- (BAT25, BAT26) and three dinucleotide repeat markers (D2S123, D5S346, D17S250) were analyzed. Tumors were classified as MSI-High (H) if at least 2 markers showed instability and as MSI-L if only one marker was unstable. MSI patterns were compared between 67 MSI-H and 35 MSI-L tumors. WES was performed in 34 microsatellite stable (MSS) and 20 MSI-L tumors after or without neoadjuvant CTx (2).

## Results

MSI-H tumors showed instability at mono- and dinucleotide repeat markers, with BAT25 being unstable in 96% of tumors. Of the 35 MSI-L tumors, 33 tumors showed instability at only one dinucleotide repeat marker, with 31 of them demonstrating an insertion of typically two base pairs. In the HR pathway, 10 of the 34 (29%) MSS and 10 of the 20 (50%) MSI-L tumors showed variants ( $p=0.154$ ). In the DNA damage tolerance pathway, 6 of the 34 (18%) MSS and 7 of the 20 (35%) MSI-L tumors had variants ( $p=0.194$ ). The HR deficiency score was similar in both tumor groups. TMB was significantly higher in MSI-L compared to MSS tumors after CTx ( $p=0.046$ ). In the MSS and MSI-L tumors without CTx no difference was observed ( $p=1.00$ ).

## Conclusion

MSI-L due to instability at dinucleotide repeat markers was associated with increased TMB after neoadjuvant CTx treatment. This suggests that it is a specific type of MSI indicating sensitivity to platinum/5-FU-CTx. This is consistent with our previous results showing a good response of MSI-L tumors when analyzing biopsies prior to CTx (1). If confirmed in further studies, this could help refine chemotherapeutic options including immune-based strategies for GC patients with MSI-L tumors.

Ref.:

1. Kohlruss, Grosser et al., J Path of Clin Res 5: 227-239, 2019
2. Kohlruss et al. J Cancer Res Clin Oncol 149:17727-17737, 2023

AG14.04

## ***The clinical importance of the locoregional host anti-tumour immune reaction in patients with oesophagogastric cancer***

H. I. Grabsch

Maastricht University Medical Center+, GROW Research Institute for Oncology and Reproduction, Pathology, Maastricht, The Netherlands

Oesophagogastric cancer remains a significant health concern worldwide with a very poor prognosis and limited therapy options. The host anti-tumour response largely depends on the activation of T cells and B cells in tumour draining lymph nodes (LN) initiated by tumour antigen presenting dendritic cells. Any immune response activation in LN leads to an increase in LN size and microarchitectural changes such as paracortical hyperplasia, follicular hyperplasia or sinus histiocytosis. For decades, pathologists are looking at LNs of cancer resection specimens in order to identify and count LN with tumour metastasis. Yet, the microarchitectural features visible in tumour negative LN, most likely indicative of the host's ability to mount an anti-tumour response and their potential predictive/prognostic value has not been studied in detail in patients with OeG cancers. This lecture will first provide a brief overview of how the host anti-tumour reaction in patients with cancer works and then discuss the potential clinical importance of our own recent quantitative results from LN microarchitecture studies in OeG resection specimens from patients treated either by neoadjuvant chemotherapy or surgery alone. In the second part of the lecture, results from relating the LN microarchitectural features to the primary tumour microenvironment (tumour stroma content, tumour infiltrating lymphocytes) in OeG will be presented. The potential implications of our findings for clinical practice and future research directions will be discussed.

# AG Gastroenteropathologie 2

AG14.05

## ***Sacituzumab govitecan represents a novel therapeutic approach in cholangiocarcinoma***

R. Hosni<sup>1</sup>, N. Klümper<sup>2</sup>, V. Branchi<sup>3</sup>, N. Pelosi<sup>1</sup>, S. Ng<sup>4</sup>, D. J. Ralser<sup>5</sup>, S.-E. Abedellatif<sup>1</sup>, H. Matthaei<sup>3</sup>, J. Kalf<sup>3</sup>, J. Boovadira Poonacha<sup>6</sup>, V. Lukacs-Kornek<sup>6</sup>, G. Kristiansen<sup>1</sup>, M. A. Gonzalez-Carmona<sup>7</sup>, M. Hölzel<sup>4</sup>, M. Toma<sup>1</sup>

<sup>1</sup>Universitätsklinikum Bonn, Pathologie, Bonn, Germany, <sup>2</sup>Universitätsklinikum Bonn, Urologie, Bonn, Germany, <sup>3</sup>Universitätsklinikum Bonn, Surgery, Bonn, Germany, <sup>4</sup>Universitätsklinikum Bonn, Experimental Oncology, Bonn, Germany, <sup>5</sup>Universitätsklinikum Bonn, Gynecology, Bonn, Germany, <sup>6</sup>Universitätsklinikum Bonn, Molecular Medicine and Experimental Immunology, Bonn, Germany, <sup>7</sup>Universitätsklinikum Bonn, Internal Medicine, Bonn, Germany

### **Background**

Cholangiocarcinoma is an aggressive cancer type with very limited therapeutic options. Patient-derived organoids (PDOs), *in vitro* 3D cultures generated from a tumor biopsy or resection specimen, represent a valuable preclinical model for drug testing. Several antibody-drug conjugates (ADCs) were recently approved for the treatment of breast and urothelial cancers. This study aimed to elucidate the expression profile of the antibody targets of recently-approved ADCs in cholangiocarcinoma and to employ PDOs as an *in vitro* model for drug testing.

### **Methods**

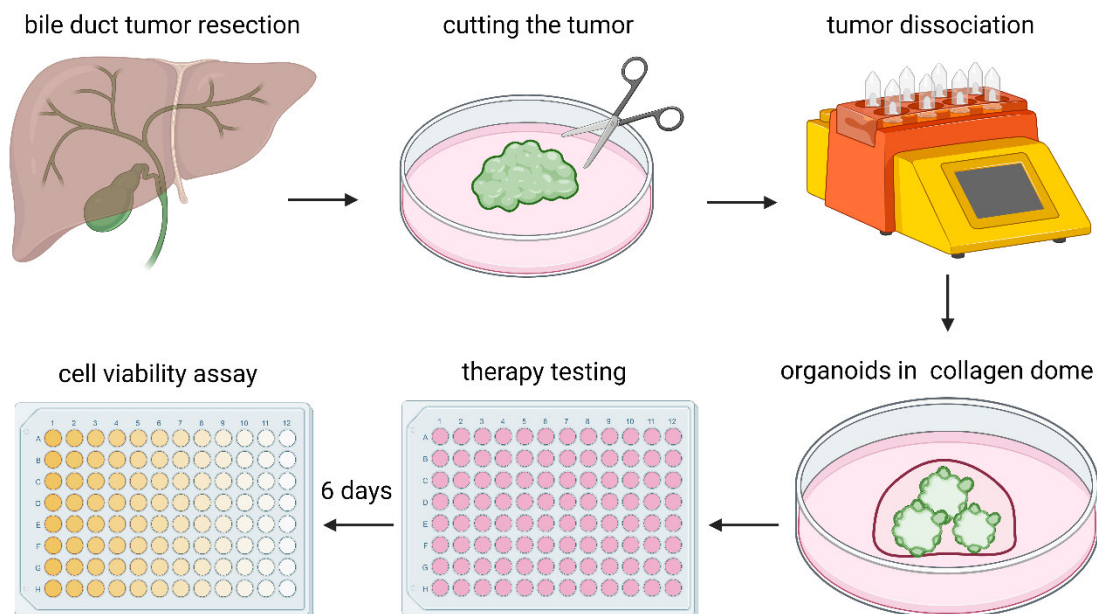
We investigated the expression profile of the antibody targets of recently-approved ADCs; namely, Trop 2, Nectin 4, folate receptor, Her 2, and Her 3 in a cholangiocarcinoma cohort (n=65) via immunohistochemistry (IHC). Thereafter, we analyzed the expression level with respect to clinicopathological parameters and patient survival. Furthermore, we established PDO cultures from four cholangiocarcinoma patients and tested their response *in vitro* to sacituzumab govitecan, an ADC targeting Trop2, using the CellTiter-Glo® luminescent cell viability assay.

### **Results**

Of all 5 targets, Trop 2 was the most frequently expressed (92 % of cases positive); 71% of cases expressed Trop 2 at moderate to high levels (H-score  $\geq 100$ ). Nectin 4 was the second most frequently expressed (58 % of cases positive), followed by folate receptor (48 %), Her 3 (47 %), and Her 2 (30 %). Associations between expression and clinicopathological data were only observed for Her 3, in which a 3+ staining intensity was significantly correlated with lower-staged tumors (pT1/2). All four cholangiocarcinoma PDO cultures expressed Trop 2 concordantly with their parental tumor tissue. PDO drug sensitivity testing revealed growth inhibition in response to sacituzumab govitecan.



## Conclusion



This study reveals that Trop 2 is widely expressed in cholangiocarcinoma. Moreover, it provides preclinical evidence for the potential for use of sacituzumab govitecan as a new therapeutic strategy in treating cholangiocarcinoma patients, especially those harboring Trop2 positive tumors.

AG14.06

## ***The Clinical and Biological Dichotomy of Early-Onset Pancreatic Cancer: A Matched Case Study***

M. D. Arslan<sup>1</sup>, M. Guenther<sup>1,2</sup>, S. A. Surendran<sup>1</sup>, A. Jung<sup>1</sup>, J. Kumbrink<sup>1</sup>, S. Ormanns<sup>1,2</sup>

<sup>1</sup>Institute of Pathology, Ludwig-Maximilians-University, Munich, Germany, <sup>2</sup>Innpath Institute of Pathology, Tirol Kliniken, Innsbruck, Austria

### **Background**

Pancreatic cancer (PDAC) is an aggressive malignancy with a dismal prognosis. PDAC typically occurs at higher patient ages. Early-onset pancreatic cancer (EOPC) is defined as a diagnosis before the age of 50. EOPC is a rare, but heterogeneous form of the disease. In this study, we compared the biology of EOPC patients with matched average-onset pancreatic cancer (AOPC) patients at the genomic and transcriptional level and in the composition of their tumor microenvironment (TME).

### **Methods**

This retrospective study included 50 PDAC patients resected between 2000 and 2016. To 25 EOPC patients, 25 AOPC patients were propensity-score-matched by UICC stage, differentiation grade, R-status, sex, localization and applied chemotherapy. Clinicopathological data and FFPE samples were retrieved from the institutes archive and the hospitals database. Nucleic acids from FFPE samples were extracted using the truXTrac Kit. NGS analysis was performed on 50 cases using the OncoPrint Comprehensive Assay v3, and RNA expression was assessed for 48 cases using the NanoString nCounter Tumor Signaling 360 panel. TME composition was assessed by multiplex immunohistochemistry (mIHC) on a Phenolmager HT platform and by metagenomic 16S rRNA sequencing.

## Results

Mean patient age for EOPC was 43.4 years and 74.1 years for AOPC. There were no significant differences between the groups in sex distribution, tumor size, histology, stage, perioperative chemotherapy and tumor localization. EOPC patients had significantly longer overall survival (OS) than AOPC patients (28.6 vs. 22.4 months,  $p=0.034$ ) and a trend towards longer disease-free survival (DFS, 11.9 vs. 9.5 months,  $p=0.08$ ). We detected no significant differences in pathogenic gene variants but a lower frequency of KRAS and TP53 alterations in the EOPC group. RNA-based gene expression analysis indicated several differentially expressed genes. While microbiome profiles showed no significant differences, a decreased prevalence of the *Fusicatenibacter* genus was noted in the EOPC group ( $p=0.046$ ). Interestingly, mIHC revealed significant differences in the TME composition, indicating a stronger immune response in EOPC patients.

## Conclusion

The preliminary findings of our matched case study suggest that EOPC and AOPC possess distinct biologic characteristics, especially in their TME composition, which may have substantial implications for treatment strategies. Further studies are needed to validate these findings.

AG14.07

## ***Subtyping of PanNETs by transcription factors, hormones, histology and patient outcome***

E. Moser<sup>1</sup>, A. Ura<sup>1</sup>, L. Vogel<sup>2</sup>, K. Steiger<sup>1</sup>, C. Mogler<sup>1</sup>, M. Kremer<sup>3</sup>, M. Evert<sup>4</sup>, B. Märkl<sup>5</sup>, I. Marinoni<sup>6</sup>, A. Perren<sup>6</sup>, K. Scheidhauer<sup>2</sup>, M. Martignoni<sup>7</sup>, H. Friess<sup>7</sup>, A. von Werder<sup>8</sup>, G. Klöppel<sup>1</sup>, A. Kasajima<sup>1</sup>

<sup>1</sup>Institute of Pathology, TUM School of Medicine and Health, Munich, Germany, <sup>2</sup>Department of Nuclear Medicine, TUM School of Medicine and Health, Munich, Germany, <sup>3</sup>Institute of Pathology, München Klinik, Munich, Germany, <sup>4</sup>Institute of Pathology, University Hospital Regensburg, Regensburg, Germany, <sup>5</sup>Pathology, Medical Faculty Augsburg, University Augsburg, Augsburg, Germany, <sup>6</sup>Institute of Tissue Medicine and Pathology (IGMP), University of Bern, Bern, Switzerland, <sup>7</sup>Department of Surgery, TUM School of Medicine and Health, Munich, Germany, <sup>8</sup>Department of Internal Medicine II, TUM School of Medicine and Health, Munich, Germany

## Background

Pancreatic NETs (PanNETs) show pronounced heterogeneity in hormone and transcription factor expression. Transcription factors such as ARX and PDX1 seem to be related to alpha cell and beta cell type features, respectively, and partly associate with patient outcome. However, detailed studies correlating pancreatic hormone expression, histology, proliferation, and clinical data are lacking.

## Methods

185 surgically resected PanNETs (nonfunctioning 164, functioning 21, including 18 insulinomas) between 1996 and 2023, were subdivided by cluster analysis based on the expression signatures of the transcription factors ARX, PDX1, ISL1 and CDX2. Five groups (Group A1, A2, B, C, D) were identified and correlated to the expression of insulin, glucagon, PP, somatostatin, serotonin, gastrin, calcitonin, ACTH and DAXX/ATRX as well as ALT activation status (alternative lengthening of telomeres detected by FISH), histological pattern (trabecular vs. solid vs. paraganglioma-like), Ki67 index and progression free survival.

## Results

Group A1 (ARX+/ISL1+/PDX1-/CDX2-) was the dominant subtype (47%), followed by Group B (17%, ARX-/ISL1+/PDX1+/CDX2-), Group A2 (15%, ARX+/ISL1+/PDX1+/CDX2-), Group C (15%, ARX-/ISL1-/PDX1-/CDX2-) and Group D (6%, ARX-/ISL1-/PDX1+/CDX2+). Group A1 and A2 showed a strong association with trabecular growth pattern and glucagon and PP expression ( $p<0.001$ ), with Group A2 in addition associated with gastrin expression. Group B was linked with insulin production ( $p<0.001$ ) and included 15 of the 18 insulinomas. Group C was associated with solid or PG-like morphology and the expression of serotonin, calcitonin, and somatostatin. Group D showed solid morphology and the expression of ACTH, somatostatin or serotonin but was negative for glucagon or PP. Patient outcome was worse in Group D than Group A2 and Group B ( $p<0.01$ ). ALT positivity was associated with poorer outcome in Group A1/A2 but not in other types.

## Conclusion

PanNETs can be divided based on different transcription factor signatures into five groups which associate strongly with histology, hormone production, functionality, and patient outcome. The worst patient outcome was related to the group expressing PDX1 and CDX2 concomitantly.

AG14.08

## ***PITX2 as a Sensitive and Specific Marker of Midgut Neuroendocrine Tumors: Results from a Cohort of 1157 Primary Neuroendocrine Neoplasms***

A. Grass<sup>1</sup>, A. Kasajima<sup>2</sup>, S. Förtsch<sup>3</sup>, M. Kriegsmann<sup>4</sup>, A. Brobeil<sup>4</sup>, M. Schmitt<sup>5</sup>, D. Wagner<sup>3</sup>, J. Poppinga<sup>6</sup>, D. Wiese<sup>6</sup>, E. Maurer<sup>6</sup>, A. Kirschbaum<sup>6</sup>, H. Winter<sup>7</sup>, T. Muley<sup>7</sup>, A. Rinke<sup>8</sup>, T. Gress<sup>8</sup>, M. Kremer<sup>9</sup>, M. Evert<sup>10</sup>, B. Märkl<sup>11</sup>, A. Quaas<sup>12</sup>, M. Eckstein<sup>13</sup>, M. Tschurtschenthaler<sup>14</sup>, G. Klöppel<sup>2</sup>, C. Denkert<sup>1</sup>, D. Bartsch<sup>6</sup>, M. Jesinghaus<sup>1</sup>

<sup>1</sup>Institut für Pathologie, Philipps-Universität Marburg, Marburg, Germany, <sup>2</sup>Technische Universität München, Institut für Pathologie, München, Germany, <sup>3</sup>Universitätsmedizin Mainz, Institut für Pathologie, Mainz, Germany, <sup>4</sup>Universitätsklinikum Heidelberg, Institut für Pathologie, Heidelberg, Germany, <sup>5</sup>Institut für Pathologie, Philipps-Universität Marburg, Institut für Pathologie, Marburg, Germany, <sup>6</sup>Universitätsklinikum Gießen und Marburg, Klinik für Viszeralchirurgie, Marburg, Germany, <sup>7</sup>Universitätsklinikum Heidelberg, Thoraxklinik, Heidelberg, Germany, <sup>8</sup>Universitätsklinikum Gießen und Marburg, Klinik für Gastroenterologie, Marburg, Germany, <sup>9</sup>Städtisches Klinikum München, Institut für Pathologie, München, Germany, <sup>10</sup>Universitätsklinikum Regensburg, Institut für Pathologie, Regensburg, Germany, <sup>11</sup>Universitätsmedizin Augsburg, Institut für Pathologie, Augsburg, Germany, <sup>12</sup>Universitätsmedizin Köln, Institut für Pathologie, Köln, Germany, <sup>13</sup>Universitätsklinikum Erlangen, Institut für Pathologie, Erlangen, Germany, <sup>14</sup>Technische Universität München, Institut für translationale Krebsforschung und experimentelle Krebstherapie, München, Germany

## Background

As Neuroendocrine Tumors (NET) often present as metastatic lesions, immunohistochemical assignment to a site of origin is one of the most important tasks in their pathological assessment. Since a fraction of NETs eludes the typical expression profiles of their primary localization, additional sensitive and specific markers are required to improve diagnostic certainty.

## Methods

We investigated the expression of the transcription factor Pituitary Homeobox 2 (PITX2) in a large-scale cohort of 909 NET and 248 Neuroendocrine Carcinomas (NEC) according to the Immunoreactive Score (IRS) and correlated PITX2 expression groups with general tumor groups and localization of the primary.

## Results

PITX2 expression (all expression groups) was highly sensitive (98.1%) for midgut-derived NET, but not perfectly specific, as non-midgut NET (especially pulmonary/duodenal) were quite frequently weak or moderately positive. The specificity rose to 99.5% for a midgut origin of NET if only a strong PITX2 expression was considered, which was found in only 0.5% (one pancreatic/one pulmonary) of non-midgut NET. In metastases of midgut-derived NET, PITX2 was expressed in all cases (87.5% strong, 12.5% moderate), while CDX2 was negative or only weakly expressed in 31.3% of the metastases. In NEC, a fraction of cases (14%) showed a weak or moderate PITX2 expression, which was not associated with a specific tumor localization.

## Conclusion

Our study independently validates PITX2 as a very sensitive and specific immunohistochemical marker of midgut-derived NET in a very large collective of Neuroendocrine Neoplasms. Therefore, our data argue towards implementation into diagnostic panels applied for NET as a first line midgut marker.

## ***Deciphering histological growth patterns in colorectal carcinoma liver metastasis: insights from single-cell RNA sequencing and spatial transcriptomics***

M. Mühlbauer<sup>1</sup>, M. Vogl<sup>1</sup>, A. Immel<sup>1,2</sup>, T. Pukrop<sup>3</sup>, M. Evert<sup>1</sup>, D. Hirsch<sup>1</sup>

<sup>1</sup>Institute of Pathology, University of Regensburg, Regensburg, Germany, <sup>2</sup>Comprehensive Cancer Center Ostbayern, Regensburg, Germany, <sup>3</sup>Department of Internal Medicine III, Hematology and Oncology, University Hospital Regensburg, Regensburg, Germany

### **Background**

Liver metastasis remains a primary cause of mortality in colorectal carcinoma (CRC) patients. It has been shown that different histological growth patterns (HGPs) are associated with distinct outcomes. Thus far, five different HGPs have been described: desmoplastic, replacement, pushing, sinusoidal, and portal. This study focuses on the most common, i.e., desmoplastic and replacement, patterns, with desmoplastic HGP being defined by a strong peri-metastatic capsule and associated with a more favorable prognosis [1]. As much remains unknown about the specific determinants of these patterns, our primary goal is to uncover the factors that contribute to their development, leading to a better understanding of how the distinct patterns impact prognosis.

### **Methods**

Formalin-fixed and paraffin-embedded liver samples from six CRC patients (three samples per HGP) were subjected to single-cell RNA sequencing (scRNAseq) and spatial transcriptomics (ST). A representative area of the metastasis-parenchyma interface was selected. ScRNAseq was performed using the droplet-based 10x Genomics Chromium platform. Robust scRNAseq data preprocessing involved ambient RNA and doublet removal. Multi-sample data integration and dimensionality reduction enabled cell type identification and labeling. ST was conducted with the 10x Visium solution.

### **Results**

Analysis of single-cell expression of 30,378 cell profiles showed distinctive cell types, including CRC cells, hepatocytes, stromal cells, endothelial cells, and diverse immune cell populations. Stromal and immune cells showed multiple differentially expressed genes in pseudobulk analysis across the two HGPs, such as upregulation of S100A4 in replacement-type T-cells and upregulation of TPM4 in replacement-type plasma cells. Gene set enrichment analysis revealed upregulation of genes associated with oxidative phosphorylation across multiple cell types in the replacement HGP. Spatial decomposition of the ST dataset unveiled the presence of S100A4-positive T-cells concentrated at the replacement HGP invasion front.

### **Conclusion**

Our preliminary findings indicate a pivotal role of the metastatic tumor microenvironment in the development of HGPs. However, the identified pathways and genes require validation through follow-up experiments. Our data contributes deeper insights into the complex interplay between metastatic tumors and their microenvironment, adding to existing data and paving the way for future advancements in CRC treatment strategies.

### Literaturangaben:

[1] Latacz E, Höppener D, Bohlok A, Leduc S, Tabariès S, Fernández Moro C, Lugassy C, Nyström H, Bozóky B, Floris G, Geyer N, Brodt P, Llado L, van Milieghem L, Schepper M de, Majeed AW, Lazaris A, Dirix P, Zhang Q, Petrillo SK, Vankerckhove S, Joye I, Meyer Y, Gregorieff A, Roig NR, Vidal-Vanaclocha F, Denis L, Oliveira RC, Metrakos P, Grünhagen DJ, Nagtegaal ID, Mollevi DG, Jarnagin WR, D'Angelica MI, Reynolds AR, Doukas M, Desmedt C, Dirix L, Donckier V, Siegel PM, Barnhill R, Gerling M, Verhoef C, (2022), Histopathological growth patterns of liver metastasis: updated consensus guidelines for pattern scoring, perspectives and recent mechanistic insights, British journal of cancer, 127(6): 988–1013, <https://doi.org/10.1038/s41416-022-01859-7>

## AG Gastroenteropathologie 3

AG14.11

### ***Why liver metastases of colon cancer don't all look the same: gene expression analysis of colorectal carcinoma liver metastases with different patterns of infiltration.***

F. Keil<sup>1</sup>, M. Mühlbauer<sup>1</sup>, D. Hirsch<sup>1</sup>, M. Evert<sup>1</sup>, T. Pukrop<sup>2</sup>, H.-J. Schlitt<sup>3</sup>, S. M. Brunner<sup>3</sup>, R. Spang<sup>4</sup>, A. Lösch<sup>4</sup>, Y. L. Hu<sup>4</sup>, K. Evert<sup>1</sup>

<sup>1</sup>Institute of Pathology, University of Regensburg, Regensburg, Germany, <sup>2</sup>University Hospital Regensburg, Department of Internal Medicine III, Hematology and Oncology, Regensburg, Germany, <sup>3</sup>University Hospital Regensburg, Department of Surgery, Clinic and Policlinic for Surgery, Regensburg, Germany, <sup>4</sup>University of Regensburg, Department of Statistical Bioinformatics, Regensburg, Germany

#### **Background**

The infiltrative pattern of colorectal adenocarcinoma liver metastases (histological growth pattern, HGP) has been shown to provide prognostic information, but little is known about the transcriptomic background behind different HGPs. The aim of this study was to identify differentially expressed genes between the two most common HGPs.

#### **Methods**

We retrospectively evaluated the HGPs of 491 liver metastases from colorectal adenocarcinoma of 239 patients who underwent metastasectomy at the University Hospital Regensburg between 2003 and 2016. Resection specimens from synchronous liver metastases were available from 87 patients and 39 patients had metachronous liver metastases that were evaluable for HGP. A representative sample of 104 metastases from 49 patients was subjected to RNA expression analysis using the nanoString nCounter PanCancer Progression Panel.

#### **Results**

The two most common HGPs were the replacement type (rHGP, 59%) and the desmoplastic type (dHGP, 37%). Although the predominant HGP was mostly constant across synchronous or metachronous metastases, it varied in a substantial proportion and cannot be regarded as a persistent feature within one patient's disease course. Comparative gene expression analysis revealed significant differences between predominant rHGP and predominant dHGP metastases in genes related to the extracellular matrix structure, epithelial-to-mesenchymal transition and cell adhesion, among others. When comparing pure rHGP and pure dHGP only, statistical significance increased and additional genes showed differential expression.

#### **Conclusion**

HGPs differ not only histologically but also at the transcriptomic level. These differences in gene expression are most accentuated in metastases with only one infiltration pattern. The differentially expressed genes discovered in this study with the IVDR conform nanoString nCounter assay can be used for diagnostic and therapeutic purposes, when histological evaluation of the HGP cannot be performed. This can potentially allow drawing prognostic information from liver biopsies or blood samples before metastasectomy to guide therapeutic decision making.

AG14.12

### ***Stroma AReactive Invasion Front Areas (SARIFA) and the plasmin/plasminogen system in gastric and colorectal cancer***

B. Grosser<sup>1</sup>, N. G. Reitsam<sup>1</sup>, E. Sipos<sup>1</sup>, F. Sommer<sup>2</sup>, J. Hardt<sup>3</sup>, B. Märkl<sup>1</sup>

<sup>1</sup>Institut für Pathologie und Molekulare Diagnostik, Augsburg, Germany, <sup>2</sup>Klinik für Allgemein-, Viszeral- und Transplantationschirurgie, Augsburg, Germany, <sup>3</sup>Institut für Labormedizin und Mikrobiologie, Augsburg, Germany

#### **Background**

Recently, we were able to validate Stroma AReactive Invasion Front Areas (SARIFA) as a new histomorphologic prognostic marker in gastric and colon cancer in local and external cohorts, including two clinical phase II-III trials (Grosser et al. 2024 [1]; Reitsam et al. 2024 [2]). SARIFA is defined as the direct contact between tumor cells and fat cells. As underlying mechanisms, our analyses indicated an interaction of tumor cells with tumor-promoting adipocytes. Since typical mutations can be largely ruled out as a cause for the occurrence of SARIFAs, matrix degradation and

immune response could instead play a significant mechanistic role.

The hypothesis of the project was therefore that the plasmin/plasminogen system, which is involved in matrix degradation in neoplastic processes, in particular its important components uPA and PAI1, plays an important role in the mechanisms underlying the SARIFA phenomenon.

## Methods

SARIFA status was assessed in the TCGA STAD cohort (n = 191) and on H&E-stained tissue sections from a local series of primary resection specimens of colon carcinomas and adenocarcinomas of the stomach and gastroesophageal junction. A spatially resolved transcriptome analysis of GC samples (n = 12) was conducted in tumor cells and the stroma and data were analyzed in regard to SARIFA-status and genes involved in the plasmin/plasminogen system. Expression on protein level was validated with previously measured, commercially available uPA and PAI1 ELISAs in CRC patients (n = 97).

## Results

Indeed, we found upregulation of the plasminogen system in SARIFA-positive gastric cancers. In TCGA-STAD, *SERPINE1* (PAI1), as well as *SERPINE2*, were significantly upregulated on mRNA level (each LFC 0.73; p < 0.001). In the spatial transcriptomic data set PLAU (uPA) (LFC 1.30; p = 0.02), PLAUR (uPAR) (LFC 1.95; p = 0.001) and *SERPINE2* (LFC 1.52; p = 0.04) were significantly upregulated in SARIFA positive GC samples.

In our local CRC cohort for which uPA and PAI1 ELISA data were available, SARIFA status proves its prognostic relevance (p < 0.027; SARIFA-positive n=35, SARIFA-negative n=61). Here the upregulation of uPA in SARIFA-positive CRCs could be validated on the protein level (p=0.0027).

## Conclusion

Our results suggest that the formation of SARIFA and the consecutive adipocyte /tumor-microenvironment interaction may rely on alterations in the plasmin/plasminogen system. Thus, plasmin/plasminogen system targeting agents may have the potential to benefit SARIFA-positive GC and CRC patients.

AG14.13

## ***Linking H&E-Based Histopathological Indicators of Tumor-Adipocyte Interaction SARIFA and TAF to Gene-Expression Based Consensus Molecular (CMS), Pathway-Derived (PDS) and Immune Subtyping in Colorectal Cancer***

N. G. Reitsam<sup>1</sup>, B. Grosser<sup>1</sup>, P. Grochowski<sup>1</sup>, V. Grozdanov<sup>2</sup>, D. F. Steiner<sup>3</sup>, V. L'Imperio<sup>4</sup>, H. S. Muti<sup>5,6</sup>, J. N. Kather<sup>6,7,8</sup>, B. Märkl<sup>1</sup>

<sup>1</sup>Universitätsklinikum Augsburg, Institut für Pathologie und Molekulare Diagnostik, Augsburg, Germany, <sup>2</sup>Universitätsklinikum Ulm, Klinik für Neurologie, Ulm, Germany, <sup>3</sup>Google LLC, Google Health, Palo Alto, California, United States of America, <sup>4</sup>University of Milano-Bicocca, IRCCS (Scientific Institute for Research, Hospitalization and Healthcare) Fondazione San Gerardo dei Tintori, Department of Medicine and Surgery, Pathology, Monza, Italy, <sup>5</sup>Universitätsklinikum, Klinik für Viszeral-, Thorax-, und Gefäßchirurgie, Dresden, Germany, <sup>6</sup>Technische Universität Dresden, Else Kröner Fresenius Zentrum für Digitale Gesundheit, Dresden, Germany, <sup>7</sup>Universitätskrankenhaus Heidelberg, Nationales Zentrum für Tumorerkrankungen (NCT), Heidelberg, Germany, <sup>8</sup>University of Leeds, Pathology & Data Analytics, Leeds Institute of Medical Research at St James's, Leeds, United Kingdom

## Background

Tumor-Adipose-Feature (TAF) as well as SARIFA (Stroma AReactive Invasion Front Areas) are both novel H&E-based histopathological biomarkers linking tumor-associated adipocytes to poor outcomes and an aggressive tumor biology in colorectal cancer (CRC). Besides SARIFA and TAF several other histopathologic biomarkers such as conventional grading, tumor budding or histologic subtypes exist. Recently, different gene-expression RNA-based approaches have been established to better stratify CRCs as biologically heterogeneous disease.

## Methods

Based on histopathological assessment of SARIFA-status (positive vs negative) and TAF (presence or absence) in TCGA cohorts COAD and READ, we aimed to link gene-expression based established CRC consensus molecular subtypes (CMS), pan-cancer immune subtypes (IS), as well as just recently published pathway-derived subtypes (PDS) to SARIFA/TAF as novel H&E biomarkers. Subtyping was performed on normalized gene-expression counts (number of CRC cases: n=196) by deploying R packages *CMScaller*, *PDSclassifier*, and *ImmuneSubtypeClassifier*.

## Results

We observed a statistically significant enrichment of CMS1 (immune) and CMS4 (mesenchymal) as well as PDS2 (stromal & inflammatory phenotype) in SARIFA-positive CRCs as well as CRCs with the presence of TAF (each  $p \leq 0.05$ ). These results are in line with our findings that SARIFA-positive CRCs show a lower proportion of tumor (hence higher stroma content) on a histological level at the luminal tumour component. Especially, CMS4 as well as PDS2 are both linked to a poor prognosis, just as SARIFA-positivity and the presence of TAF. Interestingly, pan-cancer IS did not differ significantly based on SARIFA-status and TAF, with most CRC cases in general being of 'wound healing' or 'interferon-gamma dominant' subtype, indicating that site-specific transcriptomic CRC classifiers (CMS & PDS) may better correlate with prognostically and biologically relevant histologic features.

## Conclusion

Even though gene-expression based subtyping is a powerful tool in stratifying CRC patients, it has not been implemented into clinical routine so far as challenging assays are needed. Here, we show that SARIFA and TAF as solely H&E based histologic indicators of tumor-adipocyte-interaction show a strong association with CMS and PDS subtyping. Exploiting the underlying biological properties (lipid metabolism, stromal changes, inflammatory dysregulation) could enable targeted therapies, for which SARIFA/TAF would provide simple H&E biomarkers.

AG14.14

## ***Single cell quantitative analysis of H&E tumor slides for survival prediction in colorectal cancer***

V. Mitchell Barroso, R. Büttner, A. Quaas, Y. Tolkach  
University Hospital Cologne, Institute of Pathology, Cologne, Germany

### Background

The management of colorectal carcinoma (CRC) relies on pathological interpretation. Computational pathology approaches allow for extraction of deep features from tumor images and development of potent AI-based prognostic parameters that complement traditional variables such as tumor stage/grade. The aim of this project was 1) to develop an AI-based computational platform allowing tumor tissue analysis from H&E-stained whole slide images (WSI) at any resolution including cellular, and 2) to systematically study the prognostic role of different cell populations in resectable colorectal cancer.

### Methods

Two well characterized cohorts of digitized H&E-stained tissue sections were included: 614 CRC patients from The Cancer Genome Atlas and 248 CRC patients from the University Hospital Cologne. All WSIs underwent analysis by a quality control tool. The WSIs were then analyzed by a previously developed, AI-based tissue segmentation algorithm allowing precise segmentation of 11 tissue classes. The second AI algorithm was trained that detects and classifies cells from H&E-stained slides into 6 classes (tumor cells, lymphocytes, plasma cells, neutrophilic and eosinophilic granulocytes, and stromal cells). All WSIs were analyzed by this algorithm, whereby cell detections were attributed to different tissue compartments (tumor and tumoral stroma). Systematic analysis of the immune infiltrate was performed regarding prognostic role for available end points (overall, progression-free, cancer-specific survival).

### Results

Analysis of immune cells and stromal cells in epithelial and stromal tumor compartments provides a powerful source for prognostic insights, with some variations for microsatellite-stable and -instable tumors. In general, high proportions of stromal cells and low proportions of lymphocytes, granulocytes, and plasma cells are associated with negative prognostic effects, with independent prognostic value in multivariable models. We define and validate optimal cut-offs and constellations of cellular parameters in an integrative prognostic model.

### Conclusion

Our results confirm that quantitative, AI-based analysis of cellular compositions allow for prognostic stratification of patients with resectable CRC, independent of microsatellite instability status. These new prognostic parameters are fully quantitative, analyzable directly from H&E-stained images, and might be considered for inclusion into extended aggressivity grading histological systems for CRC.

AG14.15

### ***Investigation of intratumoral heterogeneity as influencing factor in the development of therapy resistance in rectal carcinoma***

M. Vogl<sup>1</sup>, M. Mühlbauer<sup>1</sup>, A. Immel<sup>2</sup>, M. Evert<sup>1</sup>, D. Hirsch<sup>1</sup>

<sup>1</sup>Institut für Pathologie, Universität Regensburg, Regensburg, Germany, <sup>2</sup>Comprehensive Cancer Center Ostbayern, Universitätsklinikum Regensburg, Regensburg, Germany

#### **Background**

Colorectal tumors constitute the third most common cancer worldwide with rectal cancer accounting for one third of cases and with increasing incidence in younger adults. Therapeutic approaches comprise neoadjuvant radiochemotherapy, resection, and adjuvant chemotherapy depending on tumor stage, localization, and individual risk. Factors for resistance development include genomic alterations, gut microbiota composition and both the extracellular and cellular tumor microenvironment (TME). In the latter, pro-inflammatory fibroblasts and immune cell populations seem to play a pivotal role.

Rectal cancer specimen before and after neoadjuvant therapy and surgery were examined using single cell RNA sequencing (scRNAseq) to broaden the insight into subpopulations of tumor, immune and stromal cells and the TME as putative variables in the development of therapy resistance.

#### **Methods**

Intratumoral heterogeneity in rectal carcinoma was studied on formalin-fixed paraffin-embedded (FFPE) archival tissue including therapy-naive biopsies and surgical resection specimen after radiochemotherapy. FFPE tissue slices were disintegrated into single cell suspensions. Single cells were hybridized with probe pairs targeting mRNA and encapsulated as gel beads in emulsion using a microfluidic chip system from 10x Genomics. Inside the gel beads, the RNA probe pair was ligated, and cell specific barcodes were added. After two PCR and clean-up steps, the final cDNA library was sequenced on a NovaSeq 6000 platform. Single cell RNA sequencing data was analyzed using the CellRanger software (10x Genomics) and software package Seurat besides others in R.

#### **Results**

Neoadjuvant therapy induces fibrotic remodeling with a shift from predominantly epithelial to elevated proportions of stromal cells and B cell infiltrates. Preliminary data suggest that inflammatory TNF and IL1B from myeloid and stromal cells may characterize the therapy-naive TME with yet unclear impact on therapy resistance. In surgical specimen, early results indicate that LYVE1 upregulation in myeloid populations may be associated with an adverse therapeutic response. Hence, myeloid and stromal traits will be of major interest for subsequent comprehensive analysis.

#### **Conclusion**

ScRNAseq from FFPE delivered good quality results for rectum cancer specimen. Therapy-related cellular alterations in rectum carcinoma and putative targets will be investigated in more detail. To this end, scRNAseq data will be complemented with spatial transcriptomics analysis.

AG14.16

### ***Fast track development and multi-institutional clinical validation of the AI algorithm for detection of lymph node metastasis in colorectal cancer***

A. Giammanco<sup>1</sup>, A. Bychkov<sup>2</sup>, J. Fukuoka<sup>2</sup>, W. Hulla<sup>3</sup>, S. Klein<sup>4</sup>, F. Mairinger<sup>5</sup>, A. Pryalukhin<sup>3</sup>, A. Seper<sup>6</sup>, A. Quaas<sup>1</sup>, A. Tsvetkov<sup>1</sup>, R. Büttner<sup>1</sup>, Y. Tolkach<sup>1</sup>

<sup>1</sup>University Hospital Cologne, Institute of Pathology, Cologne, Germany, <sup>2</sup>Kameda Medical Hospital, Kamogawa, Japan,

<sup>3</sup>Landesklinikum Wiener Neustadt, Wiener Neustadt, Austria, <sup>4</sup>University Hospital Cologne, Cologne, Germany, <sup>5</sup>University Hospital Essen, Essen, Germany, <sup>6</sup>Danube Private University, Krems an der Donau, Austria

#### **Background**

Lymph node metastasis (LNM) detection can be automated using AI-based diagnostic tools. Only limited studies addressed this task for colorectal cancer. The aim of the study was the development of a clinical-grade digital pathology tool for LNM detection in colorectal cancer (CRC) using the original fast-track framework.



## Methods

Training cohort included 432 slides from one department. A segmentation algorithm detecting 8 relevant tissue classes was trained. Test cohorts consisted of materials from five pathology departments digitized by four different scanning systems.

## Results

High-quality, large training dataset was generated within 7 days and minimal amount of annotation work using fast-track principles. The AI tool showed very high accuracy for LNM detection in all cohorts, with sensitivity, negative predictive value, and specificity ranges of 0.980-1.000, 0.997-1.000, and 0.913-0.990, correspondingly. Only 5 of 14460 analyzed test slides with tumor over all cohorts were classified as false negative (3/5 representing clusters of tumor cells in lymphatic vessels).

## Conclusion

A clinical-grade tool was trained in a short time using fast-track development principles and validated using the largest international, multi-institutional, multi-scanner cohort of cases to date, showing very high precision for LNM detection in CRC. We release a part of the test datasets to facilitate academic research.

# Poster Computational Pathology 1

P.ComPath.01.01

## ***AI-based Anomaly Detection for Clinical-Grade Histopathological Diagnostics***

J. Dippel<sup>1,2</sup>, N. Preni<sup>3,4</sup>, J. Hense<sup>1,2</sup>, P. Liznerski<sup>5</sup>, T. Winterhoff<sup>6</sup>, S. Schallenberg<sup>3</sup>, M. Kloft<sup>5</sup>, O. Buchstab<sup>7</sup>, D. Horst<sup>3,8</sup>, M. Alber<sup>3,6</sup>, L. Ruff<sup>6</sup>, K.-R. Müller<sup>1,2,9,10</sup>, F. Klauschen<sup>2,3,7,8</sup>

<sup>1</sup>Technische Universität Berlin, Machine Learning Group, Department of Electrical Engineering and Computer Science, Berlin, Germany, <sup>2</sup>BIFOLD – Berlin Institute for the Foundations of Learning and Data, Berlin, Germany, <sup>3</sup>Charité Universitätsmedizin Berlin, Institute of Pathology, Berlin, Germany, <sup>4</sup>Charité Universitätsmedizin Berlin, Berlin Institute of Health, Berlin, Germany, <sup>5</sup>Rheinland-Pfälzische Technische Universität, Kaiserslautern, Germany, <sup>6</sup>Aignostics GmbH, Berlin, Germany, <sup>7</sup>Ludwig-Maximilians-Universität, Institute of Pathology, Munich, Germany, <sup>8</sup>German Cancer Research Center (DKFZ) & German Cancer Consortium (DKTK), Munich Partner Site, Germany, <sup>9</sup>Korea University, Department of Artificial Intelligence, Seoul, Republic of Korea (South Korea), <sup>10</sup>Max-Planck Institute for Informatics, Saarbrücken, Germany

\*Contributed equally

## Background

A major unsolved challenge for the broad implementation of AI in histopathological diagnostics lies in the highly heterogeneous frequencies of diseases. As most current AI models in histopathology follow the paradigm of supervised learning, they perform well only on common diseases with ample amounts of available training data. Less frequent diseases (which show, collectively, a sizeable number), however, need to be taken into account whenever a diagnosis is rendered and may cause severe misclassifications in models trained by supervised learning [1] [2]. An effective technique for detecting infrequent (i.e. anomalous) diseases from long-tail disease distributions is needed.

## Methods

We collected a large real-world dataset of GI biopsies, which are prototypical of the problem, from two large university hospitals. We adapted different state-of-the-art deep anomaly detection (AD) methods to our setting, namely AD based on self supervised learning and Outlier Exposure. Further, we generated explanatory heatmaps to guide pathologists' view to anomalous tissue areas.

## Results

Our best-performing approach, which only requires training data from common findings and is based on Outlier Exposure, reached over 95% (stomach) and 91% (colon) AUROC in detecting anomalous findings with a wide range of different morphological patterns. It provides interpretable heatmaps locating the anomalous tissue and generalizes across hospitals and scanners.

## Conclusion

This study establishes the first effective clinical application of AI-based AD in histopathology that can facilitate case prioritization and reduce the amount of missed diagnoses. Further, when combined with supervised classification of common findings, AI-AD could eliminate the risk of overlooking less frequent and potentially severe diseases, thereby driving automation in routine diagnostics.

Literaturangaben:

[1] Jeroen Van der Laak, Geert Litjens, Francesco Ciompi, (2021), Deep learning in histopathology: the path to the clinic., Nature Medicine, 775-784, 27(5)

[2] Harriet Evans, David Snead, (2024), Why do errors arise in artificial intelligence diagnostic tools in histopathology and how can we minimize them?, Histopathology, 279-287, 84(2)

P.ComPath.01.02

## **Mediating diverging expectations for AI-based applications in pathology: Providing best practice AI recommendations for pathologies**

J. Helmer<sup>1,2</sup>

<sup>1</sup>FH Münster, Science-to-Business Marketing Research Centre, Münster, Germany, <sup>2</sup>University of Adelaide, Adelaide Business School, Adelaide, Australia

## Background

The emergence of Artificial Intelligence (AI) dominates discussions in pathology[1][2]. While some actors envision a promising future, others voice deep concerns by highlighting factors like technological maturity[3], regulatory developments[4], and ethical and practical challenges[5]. To strategically guide the future of AI in pathology and avert potential disappointments, a deeper understanding of pathologists' diverging technological expectations plays a vital role[6]. This study aims to better understand AI expectations in pathology by questioning: How do AI expectations influence its application in pathology and the future ahead?

## Methods

This study employs the Eisenhardt approach[7] to conduct a qualitative comparative market study in German (1) pathologies and (2) clinics. A document analysis of 105 scientific articles, practical reports, and governmental publications reveals 24 factors influencing AI expectations (see fig. 1). These guide the subsequent 30 in-depth interviews aiming to identify within-case and cross-case patterns[8].

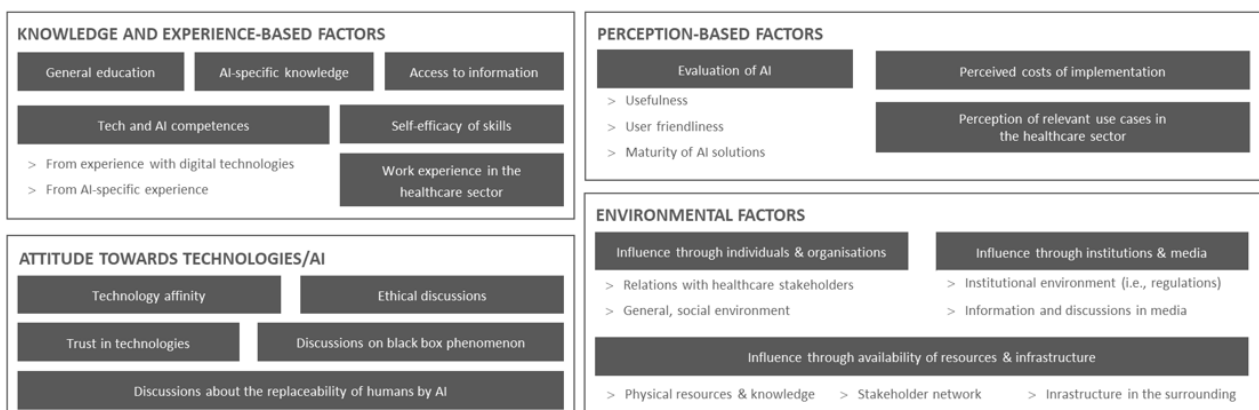


Figure 1: Identified factors influencing AI-expectations in pathologies and clinics

Identified factors influencing AI-expectations in pathologies and clinics

## Results

The results offer nuanced insights into diverse – heightened and lowered – expectations of pathologies and clinics shaped by multiple factors. While the study provides insights into shared factors such as AI knowledge, regulations, and data security, the investigated heterogeneous cases enable a differentiated view on varying influential factors which cause the split into positive and negative expectations. These are, e.g., anticipated business cases and costs, digital

maturity, resource accessibility, or trust. Thus, observed actions of cases range from ignorance to passive and active waiting to acting and shaping.

## Conclusion

The resulting framework serves as the first cornerstone in pathologies' strategic AI implementation process. Examining and comparing diverging views in pathologies and clinics, the framework enables actors to reflect on their status quo and identify hindrances to a strategic AI implementation. Moreover, it offers essential market insights and mediates discussions on the future of AI applications in pathology.

## Literaturangaben:

- [1] Davenport, T., & Kalakota, R., (2019), The potential for artificial intelligence in healthcare, *Future Healthcare Journal*, 94-98, 6(2), <https://doi.org/10.7861%2Ffuturehosp.6-2-94>
- [2] Alhatem, A., Wong, T., & Clark Lambert, W., (2024), Revolutionizing diagnostic pathology: The emergence and impact of artificial intelligence-what doesn't kill you makes you stronger?, *Clinics in dermatology*, <https://doi.org/10.1016/j.clindermatol.2023.12.020>
- [3] Klauschen, F., Dippel, J., Keyl, P., Jurmeister, P., Bockmayr, M., Mock, A., Buchstab, O., Alber, M., Ruff, L., Montavon, G., & Müller, K.-R., (2024), Toward Explainable Artificial Intelligence for Precision Pathology, *Annual Review of Pathology*, 541–570, 19, <https://doi.org/10.1146/annurev-pathmechdis-051222-113147>
- [4] Gerke, S., Babic, B., Evgeniou, T., & Cohen, I. G., (2020), The need for a system view to regulate artificial intelligence/machine learning-based software as medical device, *NPJ Digital Medicine*, 1-4, 3(53), <https://doi.org/10.1038/s41746-020-0262-2>
- [5] Ahmad, Z., Rahim, S., Zubair, M., & Abdul-Ghafar, J., (2021), Artificial intelligence (AI) in medicine, current applications and future role with special emphasis on its potential and promise in pathology: Present and future impact, obstacles including costs and acceptance among pathologists, practical and phil, *Diagnostic Pathology*, 1-16, 16(24), <https://doi.org/10.1186/s13000-021-01085-4>
- [6] Borup, M., Brown, N., Konrad, K., & van Lente, H., (2006), The sociology of expectations in science and technology, *Technology Analysis & Strategic Management*, 285–298, 18(3-4), <https://doi.org/10.1080/09537320600777002>
- [7] Eisenhardt, K. M., (1989), Building Theories from Case Study Research, *Academy of Management Review*, 532-550, 14(4), <https://doi.org/10.2307/258557>
- [8] Miles, M., & Huberman, A. M., (1984), *Qualitative data analysis*, Sage Publications, Beverly Hills, CA

## P.ComPath.01.03

### **Scanner Contest: Comparison of Whole Slide Scanners in Digital Pathology**

F. Fliedner<sup>1</sup>, A. Laib<sup>2</sup>, J. Bein<sup>2</sup>, P. J. Wild<sup>2</sup>, N. Flinner<sup>2</sup>

<sup>1</sup>Universitätsklinikum, Goethe-Universität Frankfurt, Dr. Senckenbergisches Institut für Pathologie, Frankfurt am Main, Germany,

<sup>2</sup>Universitätsklinikum Frankfurt am Main, Dr. Senckenbergisches Institut für Pathologie, Frankfurt am Main, Germany

#### Background

A reliable scanner is essential for digital pathology. Important parameters include scanning speed, digital footprint of the resulting images and image quality. Here we evaluate six different scanners using a unique curated set of slides.

#### Methods

Our dataset consists of 270 slides of prostate tissue from 43 cases. One PIN4 stain is available for each case, as well as several H&E-stained slides. All slides were digitized using scanners from six different companies. To collect information about the actual image quality, HistoQC was applied to a subset (one representative H&E slide per patient and scanner).

#### Results

Although the scanners performed well overall when scanning the slides, there were still some errors. In some cases, up to five slides were not scanned at all, or the resulting file was corrupted. In other cases, the slide was scanned correctly, but the barcode was not read properly, resulting in incomplete metadata. The average file size ranged from ~1 GB to ~4.5 GB per slide, with the largest file being ~8 GB. The file sizes between the different scanners show moderate to strong positive correlation (0.48 to 0.82), indicating the influence of the amount of tissue. The time required to scan the entire dataset ranges from 11.0 to 26.4 hours, with no correlation found between the scan times per slide. This indicates that different slides had to be rescanned with different scanners. The performance of HistoQC showed a high variance depending on the scanner, with analysis of the images often resulting in no tissue being detected.

#### Conclusion

Which scanner is most suitable depends on the requirements of the respective application. For example, when

examining frozen sections, the scanning time is more important than the file size - however, if all diagnostic sections of an institute are to be digitized, the file size becomes an important cost factor.

P.ComPath.01.04

## ***AI Model Transferability: Using NoisyEnsembles to Overcome Domain Differences Without Prior Knowledge***

R. Mayer<sup>1</sup>, S. Gretser<sup>1</sup>, A. Stoll<sup>1</sup>, M. N. Kinzler<sup>1,2</sup>, A. Vogel<sup>3</sup>, P. J. Wild<sup>1,4,5,6</sup>, N. Flinner<sup>1,4,6,7</sup>

<sup>1</sup>Goethe-Universität Frankfurt, Universitätsklinikum, Dr. Senckenbergisches Institut für Pathologie, Frankfurt am Main, Germany, <sup>2</sup>Goethe-Universität Frankfurt, Universitätsklinikum, Medizinische Klinik 1, Frankfurt am Main, Germany, <sup>3</sup>Medizinische Hochschule Hannover, Klinik für Gastroenterologie, Hepatologie, Infektiologie und Endokrinologie, Hannover, Germany, <sup>4</sup>Frankfurt Institute for Advanced Studies (FIAS), Frankfurt am Main, Germany, <sup>5</sup>Goethe-Universität Frankfurt, Universitätsklinikum Frankfurt MVZ GmbH, Wildlab, Frankfurt am Main, Germany, <sup>6</sup>University Cancer Center (UCT) Frankfurt-Marburg, Frankfurt am Main, Germany, <sup>7</sup>Frankfurt Cancer Institute (FCI), Frankfurt am Main, Germany

### **Background**

Artificial Intelligence holds the potential to make significant advancements in pathology. However, its actual implementation and certification for practical use are currently limited, often due to challenges related model transferability to a target domain. To mitigate the many factors influencing this transferability, targeted methods are often required. In this context we tested methods aimed at decreasing staining and scanner related differences within datasets through stain normalization and augmentation, as well as taking a look at the generally applicable transferability enhancing method NoisyEnsemble which does not require any prior knowledge of the target domain.

### **Methods**

Various Convolutional Neural Networks (CNN) were trained on a multitude of datasets of different tissue and institutional origin. Key was the designation of one institute as external test, keeping the training independent from the Whole Slide Images (WSI) of the designated institute. On this basis the effect of classic stain normalization was observed and compared to Hue- and Saturation-Value augmentation (HSV). Further, the effectiveness of the NoisyEnsemble method was tested for cancer detection in urothel and ovarian carcinoma, as well as differentiation of the histological small- and large-duct in intrahepatic cholangiocarcinoma (iCCA). Finally, the CNN architectures were compared to Vision Transformers (ViT) in individual, ensemble and NoisyEnsemble scenarios.

### **Results**

The normalization methods of Vahadane and HSV perform increase transfer to the external set for cancer detection in urothelial carcinoma by around 12% with a slight lead to HSV. The NoisyEnsemble method increases CNN accuracy in all observed scenarios as compared to individual models (1) and a regular ensemble (2): Carcinoma detection in ovarian tissue: (1) +6%, (2) +6%; Differentiation of histological small- and large-duct in iCCA: (1) +18%, (2) +17%; Carcinoma detection in urothelial tissue: (1) +5%, (2) +2%. ViTs show great performance in single model and ensemble scenarios, using them for NoisyEnsembles is not advised.

### **Conclusion**

It is crucial to be aware of the transferability challenge: achieving good performance during development does not necessarily translate to good performance in real-world applications. The inclusion of existing methods to enhance transferability such as stain normalization and NoisyEnsemble and their ongoing refinement, is of importance.

P.ComPath.01.05

## ***RudolfV: A Foundation Model by Pathologists for Pathologists***

J. Dippel<sup>1,2,3</sup>, B. Feulner<sup>\*1</sup>, T. Winterhoff<sup>\*1</sup>, S. Schallenberg<sup>4</sup>, G. Dernbach<sup>1,3,4</sup>, A. Kunft<sup>1</sup>, S. Tietz<sup>1</sup>, P. Jurmeister<sup>5,6</sup>, D. Horst<sup>4,5</sup>, L. Ruff<sup>1</sup>, K.-R. Müller<sup>2,3,7,8</sup>, F. Klauschen<sup>3,4,5,6</sup>, M. Alber<sup>1,4</sup>

<sup>1</sup>Aignostics, Berlin, Germany, <sup>2</sup>Machine Learning Group, TU Berlin, Berlin, Germany, <sup>3</sup>BIFOLD – Berlin Institute for the Foundations of Learning and Data, Berlin, Germany, <sup>4</sup>Institute of Pathology, Charité – Universitätsmedizin Berlin, Berlin, Germany, <sup>5</sup>German Cancer Research Center (DKFZ) & German Cancer Consortium (DKTK), Berlin & Munich Partner Sites, Germany, <sup>6</sup>Institute of Pathology, Ludwig-Maximilians-Universität München, München, Germany, <sup>7</sup>Korea University, Department of Artificial Intelligence, Seoul, Republic of Korea (South Korea), <sup>8</sup>Max-Planck Institute for Informatics, Saarbrücken, Germany

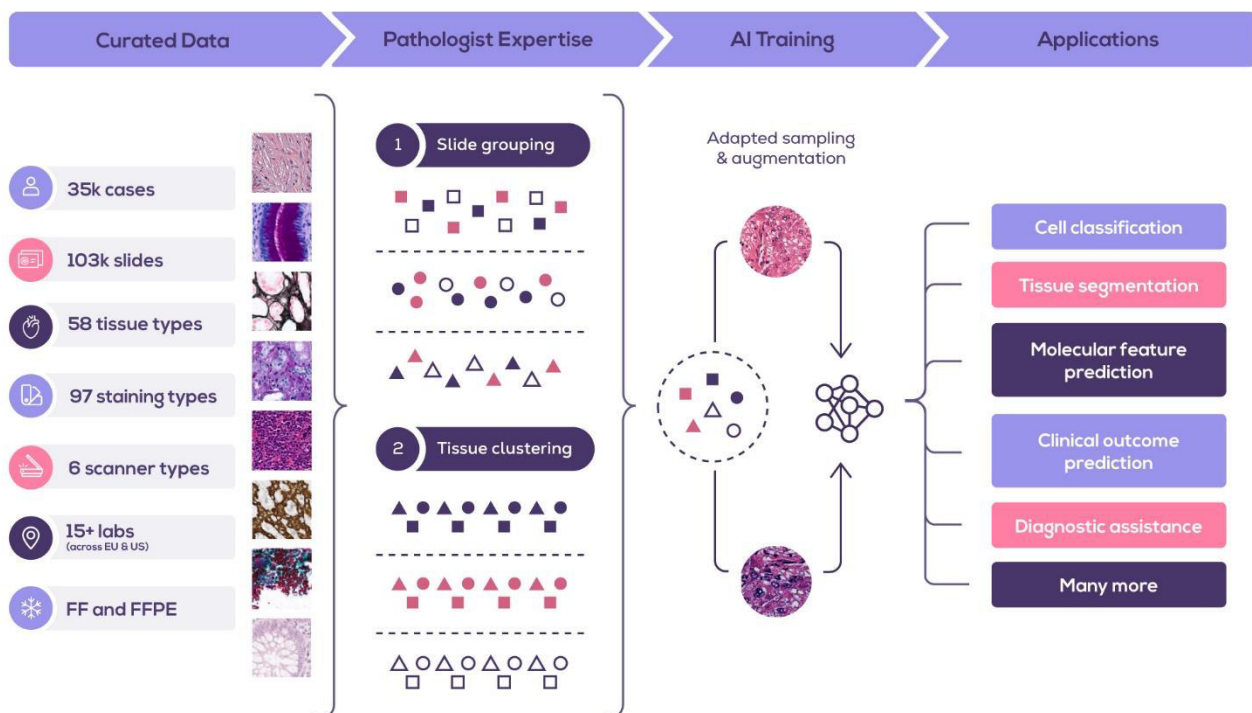
\*Contributed equally

## Background

Histopathology plays a central role in clinical medicine and biomedical research. While artificial intelligence shows promising results on many pathological tasks, generalization and dealing with rare diseases, where training data is scarce, remains a challenge. Distilling knowledge from unlabeled data into a foundation model before learning from, potentially limited, labeled data provides a viable path to address these challenges. In this work, we extend the state of the art of foundation models for digital pathology whole slide images by semi-automated data curation and incorporating pathologist domain knowledge.

## Methods

We combine computational and pathologist domain knowledge (1) to curate a diverse dataset of 103k slides corresponding to 750 million image patches covering data from different fixation, staining, and scanning protocols as well as data from different indications and labs across the EU and US, (2) for grouping semantically similar slides and tissue patches, and (3) to augment the input images during training. We train a ViT-L model with the DINOv2 framework.



We curated a dataset of 103k slides with diverse properties. With Pathologist input, we grouped the slides into 26 groups, and the patches into semantically meaningful clusters. The resulting foundation model can be used for various applications in digital pathology.

## Results

We evaluate the resulting model on a set of public and internal benchmarks and show that although our foundation model is trained with an order of magnitude less slides, it performs on par or better than competing models. We expect that scaling our approach to more data and larger models will further increase its performance and capacity to deal with increasingly complex real world tasks in diagnostics and biomedical research.

## Conclusion

This work shows that careful integration of pathological domain knowledge can lead to substantial performance gains with using an order of magnitude less slides and a model with less parameters than competing models. We assume that scaling the amount and diversity of data and the number of model parameters will further increase the performance of our approach.

We would like to note that while the present work is a machine learning focused study, we expect the results to be of

great usefulness in future diagnostic real world settings and biomedical research. Future research will therefore explore exposing RudolfV to assisting clinical routine diagnostics in histopathology and more complex tasks including multimodal modeling.

P.ComPath.01.06

### ***Development and clinical validation of a digital pathology algorithm for stroma-tumor ratio quantification in lung adenocarcinoma***

W. K. M. Ahmad<sup>1</sup>, S. Michels<sup>2</sup>, A. Rasokat<sup>2</sup>, A. Quaas<sup>1</sup>, R. Büttner<sup>1</sup>, Y. Tolkach<sup>1</sup>

<sup>1</sup>Institute of Pathology, University Hospital Cologne, Köln, Germany, <sup>2</sup>Clinic I of Internal Medicine, Centrum for Integrated Oncology, Köln, Germany

#### **Background**

Lung cancer is currently the leading cause of cancer-related deaths worldwide, highlighting the urgent need for improvements in tumor diagnosis, prediction of outcomes, and treatment. Computational pathology allows deep analysis of tumors and extraction of clinically relevant information. The aim of this study was to develop an algorithm for quantification of stroma/tumor-ratio (STR) in lung adenocarcinoma patients that provides clinically meaningful prognostic stratification of patients with a resectable tumor.

#### **Methods**

As a backbone for STR quantification, a powerful lung cancer segmentation algorithm was used. It segments digitized Hematoxylin and eosin (H&E) stained whole-slide images of lung cancer. Another algorithm working with segmentation masks was employed for quantifying the STR values in the tumor slides. One retrospective resectable lung adenocarcinoma cohort (patients n=451) was used for exploration alongside two other independent validation cohorts (in total patients n=420). The best STR cutoff was identified in an exploration cohort and subsequently validated in the 2 validation cohorts. The prognostic impact of the proposed cutoff on overall survival (OS), cancer-specific survival (CSS) and progression-free survival (PFS) endpoints was evaluated in univariate and multivariate setting together with other typical prognostic parameters.

#### **Results**

Based on the identified STR cut-off, patients were stratified into low- and high-risk groups. In the exploration cohort, the chosen cut-off led to the identification of a high-risk patient group with hazard ratio (HR) 2.12 (95%CI 1.47-3.06; p<0.001) for OS, HR 2.35 (95%CI 1.43-3.82; p<0.001) for CSS, and HR of 1.50 (95%CI 1.02-2.2;p=0.038) for PFS. In the merged validation cohorts, it led to a hazard ratio (HR) of 1.62 (95%CI 1.26-2.09;p<0.001) for OS, HR 1.66 (95%CI 1.2-2.3;p=0.002) for CSS and HR 2.15 (95%CI 1.19-3.87;p=0.012) for PFS.

#### **Conclusion**

The developed algorithm confirms that STR is a prognostic parameter in patients with resectable lung adenocarcinoma, with independent prognostic value in context of typical prognostic variables. This parameter can be used to identify high-risk patients post-resection and to inform clinical decisions regarding the necessity of postoperative adjuvant therapy.

P.ComPath.01.07

### ***Stable Diffusion for generation of synthetic histopathological image data of clear cell renal cell carcinoma (ccRCC)***

S. Schulz<sup>1</sup>, S. Engelhardt<sup>2</sup>, J. N. Kather<sup>3</sup>, C. Glasner<sup>1</sup>, O. Saldanha<sup>3</sup>, F. Laqua<sup>4</sup>, A. Fernandez<sup>1</sup>, W. Roth<sup>1</sup>, P. Stenzel<sup>1</sup>, S. Strobl<sup>1</sup>, D.-C. Wagner<sup>1</sup>, D. Truhn<sup>5</sup>, B. Baessler<sup>4</sup>, S. Foersch<sup>1</sup>

<sup>1</sup>University Medical Center Mainz, Institute of Pathology, Mainz, Germany, <sup>2</sup>Heidelberg University Hospital, Internal Medicine III, Heidelberg, Germany, <sup>3</sup>Medical Faculty Carl Gustav Carus, Technical University Dresden, Else Kroener Fresenius Center for Digital Health, Dresden, Germany, <sup>4</sup>University Hospital Würzburg, Department of Diagnostic and Interventional Radiology, Würzburg, Germany, <sup>5</sup>University Hospital Aachen, Department of Diagnostic and Interventional Radiology, Aachen, Germany

#### **Background**

Histopathological analysis is a cornerstone in the diagnosis and research of clear-cell renal cell carcinoma (ccRCC). The availability of high-quality, diverse histopathological image data is crucial for advancing diagnostic algorithms and

understanding disease mechanisms. However, the acquisition of such datasets faces ethical, privacy, and logistic challenges. This project explores the potential of Stable Diffusion for generating synthetic histopathological images of ccRCC, aiming to augment existing datasets and potentially facilitate research without the aforementioned constraints.

## Methods

Methods: The project employs a generative deep learning model based on the Stable Diffusion architecture and was trained on a dataset of annotated histopathological images of ccRCC. Generated images are evaluated through a combination of quantitative metrics and qualitative assessment by expert pathologists. Furthermore, the impact of synthetic images on the performance of diagnostic algorithms is assessed by integrating them into training datasets and comparing model accuracy with and without their inclusion.

## Results

Preliminary results indicate that the stable diffusion model can generate synthetic images closely resembling real histopathological samples of ccRCC. Quantitative metrics will likely show a high degree of similarity between synthetic and real images, while qualitative evaluations will confirm their diagnostic relevance. Incorporating synthetic images into diagnostic model training datasets might result in improved accuracy and robustness, highlighting their potential to support medical AI research.

## Conclusion

This project demonstrates the viability of AI as a tool for generating high-quality synthetic histopathological images of ccRCC. Future work will focus on further refining the generation process, expanding the range of represented ccRCC variants, and exploring the implications of synthetic data usage in medical research.

P.ComPath.01.08

## ***Contribution of specific cell types to the development of Barrett's esophagus and carcinoma via germline genetic risk***

A. Hillmer<sup>1</sup>, M. Wenzel<sup>1</sup>, A.-S. Giel<sup>2</sup>, P. Plum<sup>3</sup>, S. Hoppe<sup>4</sup>, M. Franitza<sup>4</sup>, C. Jonas<sup>4</sup>, P. Dasmeh<sup>2</sup>, R. Thieme<sup>3</sup>, Y. Zhao<sup>4</sup>, D. Heider<sup>5</sup>, C. Palles<sup>6</sup>, R. Fitzgerald<sup>7</sup>, R. Buettner<sup>4</sup>, A. Quaas<sup>4</sup>, I. Gockel<sup>3</sup>, C. Maj<sup>2</sup>, S.-H. Chon<sup>4</sup>, J. Schumacher<sup>2</sup>

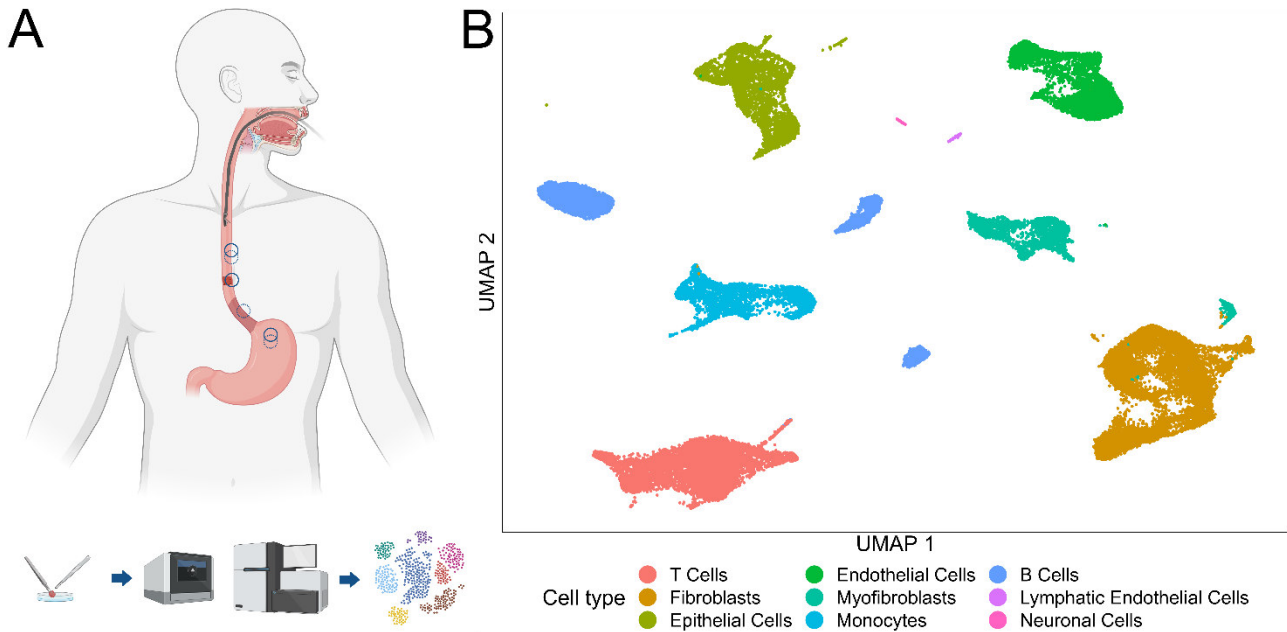
<sup>1</sup>Universität zu Köln, Institut für Pathologie, Köln, Germany, <sup>2</sup>University Hospital of Marburg, Marburg, Germany, <sup>3</sup>University Hospital of Leipzig, Leipzig, Germany, <sup>4</sup>Universität zu Köln, Köln, Germany, <sup>5</sup>Heinrich-Heine University Düsseldorf, Düsseldorf, Germany, <sup>6</sup>University of Birmingham, Birmingham, United Kingdom, <sup>7</sup>University of Cambridge, Cambridge, United Kingdom

## Background

We sought to elucidate how individual cell types in Barrett's esophagus (BE) and esophageal adenocarcinoma (EAC) contribute to disease development via germline genetic risk.

## Methods

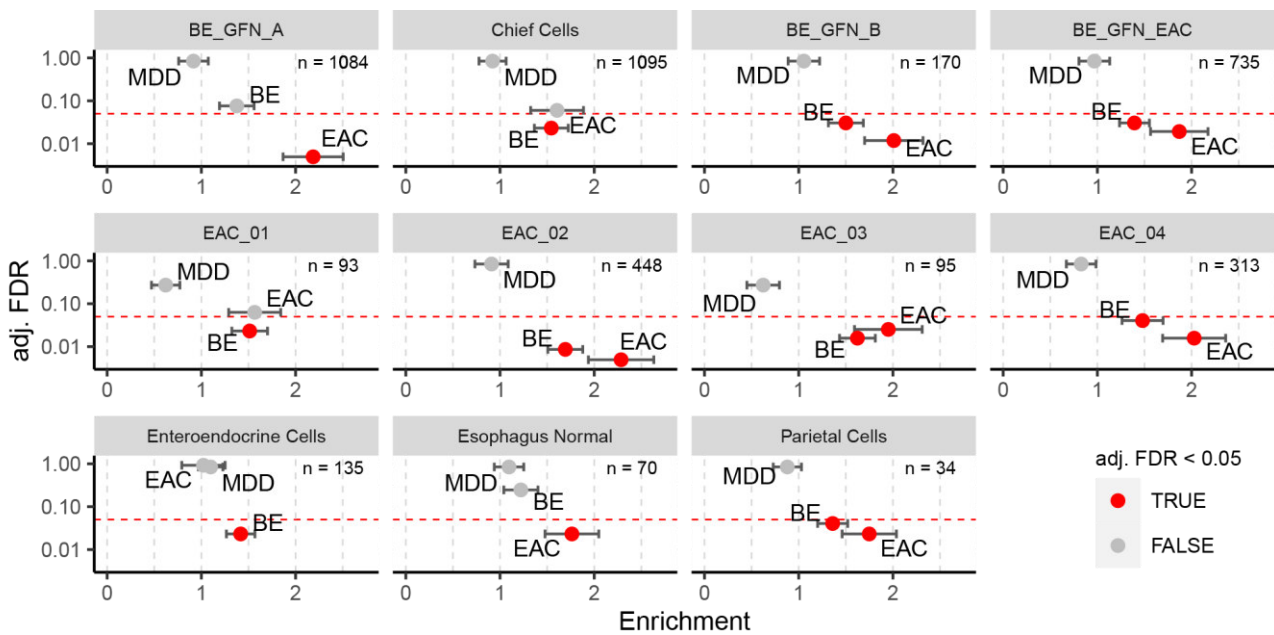
We performed single cell RNA-sequencing (scRNA-seq) of BE, EAC and paired normal esophagus and gastric fundus tissue samples (Fig. 1). After analyzing individual cell types, we integrated the scRNA-seq data and data of a genome-wide association study (GWAS) on BE/EAC to determine cell type-specific genetic risk.



Single cell RNA-sequencing from biopsies from the esophagus and gastric fundus. A Samples are taken from healthy esophageal and stomach tissue of every patient and either BE or EAC depending on patient's disease. B UMAP representation of single cell RNA-seq data with coloring according to initial cell type family annotation.

### Results

The integration of single cell transcriptome and germline genetic data revealed that EAC development is driven to a greater extent by local cellular processes than the development of BE (Fig. 2). In particular, one cell type of gastric fundus and BE origin (named BE-GFN-A) appears to be of particular relevance for EAC development (Fig. 2). BE-GFN-A cells are characterized by the expression of *TFF1*, *TFF2*, *MUC5AC*, and *MSMB*, while the expression of *REG1A* and *REG3A* is low. This cell type shows the highest cell proliferative index of non-cancer cells and large somatic copy number alterations (SCNAs) are missing. In addition, we found specific subtypes of fibroblasts, endothelial cells, B cells, and memory T cells that contribute to EAC development through germline genetic risk.



Partitioned heritability analysis of GWAS risk variants for BE and EAC applied on cell type-specific expression profiles. Enrichment describes the level of enrichment of GWAS risk variants within cell type-specific gene sets of epithelial cells. Significant enrichments are indicated by red data points. Dashed line: FDR of 0.05.



## Conclusion

EAC development is based on germline risk through multiple cell types. Among them, the premalignant gastric fundus-derived cell type BE-GFN-A is of utmost importance for the progression towards EAC and represents a potential biomarker and target for research and therapy.

P.ComPath.01.09

## ***Utilizing AI to employ microvasculature as new diagnostic marker for routine pathological diagnostics in interstitial lung disease***

N. Engler<sup>1,2</sup>, M. Legnar<sup>1</sup>, C. Schwab<sup>1</sup>, T. Pfeffer<sup>1,3</sup>, M. Allgäuer<sup>1</sup>, J. Hesser<sup>4,5,6,7</sup>, P. Schirmacher<sup>1</sup>, C.-A. Weis<sup>1,5</sup>

<sup>1</sup>Institute of Pathology, University Hospital Heidelberg, 69120 Heidelberg, Germany, <sup>2</sup>Translational Lung Research Center Heidelberg (TLRC), Member of the German Center for Lung Research (DZL), 69120 Heidelberg, Germany, <sup>3</sup>Tissue Bank of the German Center for Infection Research (DZIF), Institute of Pathology, Heidelberg University Hospital, 69120 Heidelberg, Germany, <sup>4</sup>Institute for Intelligent Systems in Medicine (MIISM), Medical Faculty Mannheim of the University of Heidelberg, 68167 Mannheim, Germany, <sup>5</sup>Interdisciplinary Center for Scientific Computing (IWR), Heidelberg University, 69120 Heidelberg, Germany, <sup>6</sup>Interdisciplinary Center for Computer Engineering (ZITI), Heidelberg University, 69120 Heidelberg, Germany, <sup>7</sup>CZS Heidelberg Center for Model-Based AI, Heidelberg University, 69120 Heidelberg, Germany

## Background

Interstitial lung disease (ILD) encompasses various diagnostically challenging subtypes of lung diseases. Among these, idiopathic pulmonary fibrosis (IPF) is the most common, with a poor median survival of 3-5 years, emphasizing the need for rapid and accurate diagnosis. Histologically, ILDs are classified based on fibrosis, inflammation, and distribution patterns, requiring significant diagnostic expertise. It is noteworthy that the diagnosis is not solely reliant on histology but is typically made in a multi-disciplinary setting. Due to the complexity of these diseases, there is an urgent need for additional diagnostic criteria to enhance reproducibility and reliability. Morphologically and in terms of imaging, diverse histopathological patterns of microvasculature have been associated with different ILD subtypes. This study aims to establish microvascular alterations in ILD subtypes as new markers for routine pathological diagnostics using Artificial Intelligence (AI).

## Methods

Slides (HE, MG, EvG) of patients with pathologically diagnosed ILD are scanned, and the resulting whole slide images (WSI) are stored. Samples of COVID-19 autopsy cases will be used as controls (altered lung tissue: positive control; non-altered lung tissue: negative control). Cases are annotated on the case level using text-based clustering of the diagnostic reports, similar to a previous study in nephropathology [1]. To identify diagnostically relevant subregions of the WSI, multiple-instance machine learning (MIL) is performed.

## Results

In the proposed ongoing project, we aim to identify microvascular 2D patterns in various ILD subtypes based on different histochemical staining using a combination of computer linguistics and vision techniques.

## Conclusion

In this proposed project, promising microvascular patterns are identified as novel morphological 2D biomarkers in interstitial lung diseases.

Literaturangaben:

[1] Legnar M, Daumke P, Hesser J, Porubsky S, Popovic Z, Bindzus JN, Siemoneit J-HH, Weis C-A., (2022), Natural Language Processing in Diagnostic Texts from Nephropathology., *Diagnostics*, 12(7):1726, <https://doi.org/10.3390/diagnostics12071726>

P.ComPath.01.10

## ***Diff-ST: Staining Translation between HE and IHC by Diffusion Models***

J. Liu, Ž. Stanonik, P. Schüffler

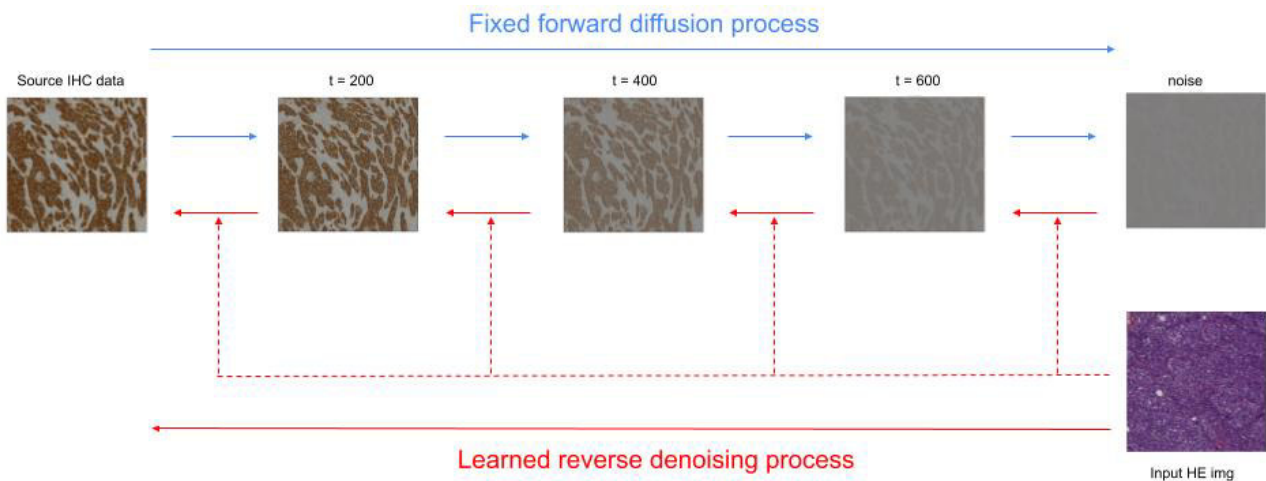
Institute of Pathology, Technical University of Munich, München, Germany

## Background

Histopathological examinations use often hematoxylin and eosin (HE) staining to visualize tissue structure and immunohistochemistry (IHC) to detect specific protein expression. Various IHC staining reagents can highlight markers linked to different tumors, like HER2 in breast and gastric cancers [BCI]. However, IHC is costly and time-consuming. Moreover, restaining HE slides or using adjacent slides for IHC may reduce diagnostic accuracy due to missing data.

## Methods

To address these challenges, we propose Diff-ST, a Denoising Diffusion Probabilistic Models (DDPM) [ddpm] based method to generate IHC images given HE images, thus the synthetic IHC images could provide high-resolved, detailed and structural reserved information for clinical decisions. In contrast to Generative Adversarial Network (GAN) based approaches, the diffusion models could introduce stochasticity into staining translation, yielding more diverse generated samples. However, a notable drawback of DDPM lies in the color deviation induced by domain bias. To address this inherent issue, we enhance the loss function design by incorporating an additional similarity-based loss function alongside the common mean squared error (MSE) loss.



The Diff-ST pipeline involves two key components: the diffusion process (green) and the denoising process (red). In the diffusion phase, incremental noise levels are added to the IHC images. Conversely, in the denoising phase, a U-Net, conditioned on the HE image, is trained to reduce noise in the images at each timestep.

## Results

Empirical study shows that incorporating this structural constraint accelerates the model training and improve the overall efficiency. Consequently, the proposed Diff-ST method achieves comparable performance to state-of-the-art (SOTA) GAN-based approaches in quantitative evaluation metrics, such as Structural Similarity (SSIM) and Peak Signal-to-Noise Ratio (PSNR).

Model	PSNR	SSIM
<b>Pix2pix GAN (reproduced)</b>	18.29	0.36
<b>CutMix (reproduced)</b>	15.83	0.34
<b>BCI-Stainer (reproduced)</b>	21.93	0.577
<b>Vanilla Diff-ST (ours)</b>	17.13	0.511
<b>Diff-ST (ours)</b>	20.71	0.557

Quantitative evaluations for HER2-stained image generation: Pixel2pixel, CutMix, and BCI-Stainer are GAN-based methods, whereas vanilla Diff-ST is diffusion model-based. We propose Diff-ST by introducing a structural similarity constraint

## Conclusion

Overall, Diff-ST presents promising prospects for advancing clinical virtual staining and further facilitating histological diagnosis.

Literaturangaben:

[BCI] Liu, Shengjie and Zhu, Chuang and Xu, Feng and Jia, Xinyu and Shi, Zhongyue and Jin, Mulan, (2022), BCI: Breast Cancer

Immunohistochemical Image Generation Through Pyramid Pix2pix, IEEE, Proceedings of the IEEE/CVF Conference on Computer Vision and Pattern Recognition (CVPR) Workshops, New Orleans, 1815-1824, <https://bci.grand-challenge.org/>, 2022-06-01 [ddpm] Ho, Jonathan, Ajay Jain, and Pieter Abbeel, (2020), Denoising diffusion probabilistic models, Advances in neural information processing systems, 6840-6851

## Poster Computational Pathology 2

P.ComPath.02.01

### ***AI-based detection of oral squamous cell carcinoma with Raman histology***

A. Weber<sup>1,2</sup>, K. Enderle-Ammour<sup>1</sup>, K. Kurowski<sup>1,3,4</sup>, M. C. Metzger<sup>5</sup>, P. Poxleitner<sup>5,6,7</sup>, M. Werner<sup>1,3</sup>, R. Rothweiler<sup>5</sup>, J. Beck<sup>6,8</sup>, J. Straehle<sup>6,8</sup>, R. Schmelzeisen<sup>5,6</sup>, D. Steybe<sup>5,6,7</sup>, P. Bronsert<sup>1,3,4</sup>

<sup>1</sup>Institute for Surgical Pathology, Medical Center, University of Freiburg, Freiburg, Germany, <sup>2</sup>Faculty of Biology, University of Freiburg, Freiburg, Germany, <sup>3</sup>Tumorbank Comprehensive Cancer Center Freiburg, Medical Center, University of Freiburg, Freiburg, Germany, <sup>4</sup>Core Facility for Histopathology and Digital Pathology, Medical Center, University of Freiburg, Freiburg, Germany, <sup>5</sup>Department of Oral and Maxillofacial Surgery, Medical Center, University of Freiburg, Freiburg, Germany, <sup>6</sup>Center for Advanced Surgical Tissue Analysis (CAST), University of Freiburg, Freiburg, Germany, <sup>7</sup>Department of Oral and Maxillofacial Surgery and Facial Plastic Surgery, University Hospital, LMU Munich, Munich, Germany, <sup>8</sup>Department of Neurosurgery, Medical Center, University of Freiburg, Freiburg, Germany

#### **Background**

Accurate evaluation of surgical margins is vital in oral squamous cell carcinoma (OSCC) treatment. Conventional methods, reliant on hematoxylin and eosin (H&E)-stained frozen sections, face limitations. Stimulated Raman Histology (SRH) emerges as a promising alternative, utilizing Stimulated Raman Scattering (SRS) microscopy to produce H&E-like images without preprocessing. Deep learning (DL) has transformed medical image analysis, offering potential to enhance SRH's diagnostic capabilities.

#### **Methods**

This prospective study involved 80 tissue specimens from 8 OSCC patients. SRH images were acquired with the NIO Laser Imaging System and annotated for six tissue types (tumor, stroma, adipose tissue, muscle, squamous epithelium, and glandular tissue) using QuPath software. A dataset of 21,703 labeled tiles was generated, and a VGG19-based convolutional neural network (CNN) was trained and tested on SRS and SRH images.

#### **Results**

The CNN achieved an overall balanced accuracy of 0.90 (0.87 for SRH) across tissue types. Precision and recall varied, with adipose tissue showing the highest performance and glandular tissue the lowest. Confusion between squamous epithelium and tumor was evident in both SRS and SRH images.

#### **Conclusion**

DL-based identification of OSCC and sub-classification of non-neoplastic tissues on SRS and SRH images demonstrate promising outcomes. Integrating SRH and DL holds potential for advancing intraoperative tissue assessment in OSCC treatment.

P.ComPath.02.02

### ***Quantitative Continuous Scoring of IHC assays using computational pathology allows superior patient selection for biomarker-informed cancer treatments***

S. Haneder<sup>1</sup>, M. Gustavson<sup>1</sup>, A. Kapil<sup>1</sup>, A. Shumilov<sup>1</sup>, M. Schick<sup>1</sup>, J. C. Barrett<sup>2</sup>, H. Sade<sup>1</sup>

<sup>1</sup>AstraZeneca Computational Pathology GmbH, München, Germany, <sup>2</sup>AstraZeneca, Early Oncology Translational Medicine, Gaithersburg, United States of America

#### **Background**

Targeted cancer therapies often rely on protein expression biomarkers assessed visually by pathologists through immunohistochemically stained tissue. This approach is subjective, semi-quantitative and does not assess expression heterogeneity. To address these challenges, we have developed a computational pathology approach called Quantitative Continuous Scoring (QCS). QCS deploys the power of Deep Learning (DL) to provide objective and continuous expression data of biomarkers in digitized IHC whole slide images (WSI), particularly of proteins expressed at low levels.

## Methods

To this end we utilize two DL-based algorithms, which we developed fully supervised by using pathologist input as the reference standard. These algorithms identify invasive tumor areas and segment each tumor cell across the WSI into cell nuclei, cytoplasm and/or membrane. Based on an accurate subcellular segmentation, we can compute biomarker expression, on a continuous scale, as mean Optical Density (OD) in each subcellular compartment based on the Hue-Saturation-Density (HSD) model. Therefore, this approach enables precise detection of the low biomarker expression range. Importantly, it also allows the computation of the spatial distribution of tumor cells across the WSI.

## Results

We have successfully used QCS to drive the selection of antibody clones for IHC assays and to delineate the mode of action and PK/PD mechanisms. Beyond this, QCS outperformed traditional pathologist scoring in identifying patient populations having maximum treatment benefit through retrospective analysis of multiple clinical trials. Of note, the combination of assessing continuous target expression and capturing the spatial distribution of tumor cells has provided surrogate markers to predict potential bystander activity of antibody drug conjugates (ADCs).

## Conclusion

In summary, we describe and discuss here a computational pathology-based approach for precise biomarker quantification and superior patient selection with broad applicability and potential to transform pathology, thus addressing one of the key challenges of precision oncology.

P.ComPath.02.03

## ***From CLL to Richter syndrome: at the interface of Boolean network modeling and experimental readouts***

J. Maier<sup>1,2</sup>, J. D. Schwab<sup>2</sup>, S. D. Werle<sup>2</sup>, R. Marienfeld<sup>1</sup>, N. T. Gaisa<sup>1</sup>, P. Möller<sup>1</sup>, N. Ikonomi<sup>2</sup>, H. A. Kestler<sup>2</sup>

<sup>1</sup>Institut für Pathologie, Universitätsklinikum Ulm, Ulm, Germany, <sup>2</sup>Institut für Medizinische Systembiologie, Ulm, Germany

## Background

Chronic lymphocytic leukemia (CLL) is an indolent B-cell neoplasm which, in 5-10% of cases, undergoes malignant transformation into an aggressive B-cell lymphoma, termed Richter syndrome (RS). Considering the rather limited availability of *in vitro* and *in vivo* models for RS, we set up an *in silico* dynamic modeling strategy, namely Boolean networks, to study RS pathogenesis.

## Methods

Boolean network models allow the dynamic analysis of large molecular crosstalk[1][2], retrieving stable long-term behaviors, representing biological phenotypes. In Boolean networks each gene/node can either be active (ON) or inactive (OFF). Regulatory dependencies are summarized qualitatively by logical connectives (AND, OR, and NOT). Simulations were conducted using the R-package BoolNet[3]. To validate the model, we conducted dynamic simulations of CLL and RS-associated lesions and matched the resulting stable states to known behaviors of the tumors. Furthermore, we set up a strategy to compare model predictions to published single cell-RNA sequencing (sc-RNA seq) results. Specifically, we binarized the expression values from 3 different patients who were diagnosed with RS. Activities of genes were then classified as active or inactive within the selected cell populations using a 30% threshold of expression, according to the Hans-Score.

## Results

We established a large network model of 49 genes and 147 interactions, representing molecular crosstalks between frequently altered pathways in CLL and RS. Simulation of the unperturbed CLL model as well as RS-like phenotypes could correctly predict the experimentally observed phenotypical traits from 10 different conditions in terms of proliferation, cell survival, and gene specific activities. To also validate the model quantitatively, we applied the sc-RNA seq evaluation pipeline described above and matched the results with the predicted phenotypes. Here, 10 of the 14 mainly transcriptionally regulated nodes of the model were correctly predicted. After additionally adding a NOTCH1 deletion to the validation process which is present in 2 of the 3 patients, all 14 gene activities could be explained from our model simulations.

## Conclusion

The presented CLL model can reliably recapitulate the main gene activity patterns shown during tumor evolution. Thus, it can be further applied to predict disease drivers and druggable targets.

Literaturangaben:

- [1] Kauffman SA, (1969), Metabolic stability and epigenesis in randomly constructed genetic nets., J Theor Biol., Mar 1969;22(3):437-67
- [2] Schwab JD, Kühlwein SD, Ikonomi N, Kühl M, Kestler HA, Concepts in Boolean network modeling: What do they all mean?, Comput Struct Biotechnol J., 2020;18:571-582.
- [3] Müssel C, Hopfensitz M, Kestler HA., BoolNet--an R package for generation, reconstruction and analysis of Boolean networks., Bioinformatics, May 15 2010;26(10):1378-80.

P.ComPath.02.04

## ***AI-based stroma-tumor ratio quantification algorithm: comprehensive evaluation of prognostic role in primary colorectal cancer***

R. Carvalho<sup>1,2</sup>, T. Zander<sup>3</sup>, V. Mitchell Barroso<sup>2</sup>, A. Bekisoglu<sup>2</sup>, N. Zerbe<sup>1</sup>, S. Klein<sup>4</sup>, R. Büttner<sup>4</sup>, A. Quaas<sup>4</sup>, Y. Tolkach<sup>4</sup>

<sup>1</sup>Charité - Universitätsmedizin Berlin, Institute of Pathology, Berlin, Germany, <sup>2</sup>University of Cologne, Medical Faculty, Cologne, Germany, <sup>3</sup>University Hospital Cologne, Clinic of Internal Medicine, Oncology, Cologne, Germany, <sup>4</sup>University Hospital Cologne, Institute of Pathology, Cologne, Germany

### Background

Stroma-tumor ratio (STR) quantification in primary colorectal cancer is an important prognostic parameter. Earlier studies involved relevant region selection and STR quantification by human analysts, prone to interobserver variability. The aim of the current study was to develop a fully automatized, fully quantitative algorithm for STR analysis based on precise segmentation of H&E-stained histological tissue sections.

### Methods

STR quantification algorithm was developed based on a segmentation backbone, allowing accurate pixel-wise mapping of all relevant tissue classes (n=12), including tumor cells, tumoral stroma, necrosis, and mucin. Two well characterized cohorts of patients with stage I-IV primary operable colorectal cancer and available digital H&E histological slides were included (n=548 and n=231, correspondingly). Three sizes of analytical "window" for STR analysis were tested (1.0, 1.5, and 2.0 mm). The maximal STR value per case was used for prognostic analysis involving different clinical endpoints.

### Results

Regional heterogeneity of STR was high in most tumors, with the algorithm effectively finding the most relevant region for analysis. Maximal case-level STR values depend on the size of the analytical "window", which also significantly influences the prognostic performance of the STR and must be a matter of standardization. The prognostic value of the STR was limited to patients with microsatellite stable (MSS) tumors in both cohorts. In Cox survival analysis, an analytical "window" size of 1 mm allowed best performance, with an independent prognostic role retained in the context of other pathological variables for overall survival endpoint.

### Conclusion

A powerful, fully automatized, fully quantitative, objective tool for STR assessment in primary colorectal cancer was developed. STR might be of limited value in patients with microsatellite instable tumors, with most prognostic benefits of analysis in patients with MSS tumors. Boa\_Image\_Frameization of STR quantification is important given that analytical parameters can substantially influence the prognostic performance.

P.ComPath.02.05

## ***Computer-aided claudin-18.2 assessment in gastric cancer***

S. Köfler<sup>1</sup>, K. Mühlberger<sup>1</sup>, V. Girking<sup>1</sup>, D. H. W. Liu<sup>1</sup>, B. Dislich<sup>2</sup>, B. Gloor<sup>3</sup>, R. Langer<sup>1</sup>

<sup>1</sup>Johannes Kepler University Linz, Kepler University Hospital GmbH, Department of Pathology and Molecular Pathology, Linz, Austria, <sup>2</sup>Universität Bern, Institut für Gewebemedizin und Pathologie, Bern, Switzerland, <sup>3</sup>Universität Bern, Inselspital, Universitätsklinik für Viszerale Chirurgie und Medizin, Bern, Switzerland

## Background

Gastric cancer (GC) is the fourth most common cause of cancer-related death worldwide. With a majority of cases having already metastasized upon diagnosis the five-year survival rate for those patients is below 7 percent. Claudin-18.2 is advancing from trials to routine diagnostics to identify cancer patients eligible for immunotherapy with Zolbetuximab with the expectation to increase disease-free survival for patients with advanced cancer stages. Its specificity in stomach entities positions it as the next diagnostic biomarker. Current research focuses on (i) developing scoring guidelines, and (ii) acquiring data to understand molecular mechanisms driving claudin-18.2 in various cancer types.

## Methods

Leveraging HALO and HALO AI image analysis software from Indica Labs, New Mexico, USA, we developed a Deep Learning algorithm based on a DenseNet to identify tumor tissue on HE-stained Tissue microarray (TMA) slides of primary resected GC from 109 patients. Subsequent analysis steps include cell segmentation followed by DAB stain intensity estimation in cells previously identified as tumorous. This computational approach enables us to provide quantitative values for positively stained tissue.

## Results

On a cohort subset of a TMA constructed from the tumor front and center (306 / 268 cores) our classifier demonstrated an overall F1 score of 0.82/0.77 (neg./pos. class) (0.77/0.75, 0.86/0.78), providing strong evidence of its effectiveness in the studied context. In support of the need to objectify claudin-18.2 scoring, we report that inter-rater reliability between two expert pathologists but in an untrained setting was only moderate ( $\kappa$  0.605 / 0.456). Utilizing a previously reported claudin-18.2 positivity cutoff ( $\geq$  75% of tumor cells membranes stained moderately (2+) or strongly (3+)) we identified 15% positive cases from the tumor center TMA, among them an equal number of intestinal and diffuse type GC.

## Conclusion

Using a computational workflow we can objectively quantify IHC staining intensity and reproducibly report the proportion of positive tumor cells resulting in reduced inter and intra-observer variability. Our lower-than-expected positivity rate as well as the lower F1 score for positive cases suggests a tendency for pathologists to overestimate positive cases. Aiming to facilitate pathologists in interpreting claudin-18.2 assays we will further develop our computer-aided diagnostics tool on 300 additional cases.

P.ComPath.02.06

## ***Automated Locoregional Antigen Determination as a Prerequisite for CAR T-Cell Therapy Target Selection***

M. Dinser<sup>1,2,3</sup>, D. Hieber<sup>1,2,3</sup>, R. Pryss<sup>2</sup>, C.-M. Monoranu<sup>4</sup>, F. Liesche-Starnecker<sup>3</sup>, J. Schobel<sup>1</sup>, V. Nickl<sup>5</sup>

<sup>1</sup>Neu-Ulm University of Applied Sciences, DigiHealth Institute, Neu-Ulm, Germany, <sup>2</sup>University Hospital of Würzburg, Institute of Medical Data Science, Würzburg, Germany, <sup>3</sup>Medical Faculty University of Augsburg, Pathology, Augsburg, Germany, <sup>4</sup>Institute of Pathology, University of Würzburg, Department of Neuropathology, Würzburg, Germany, <sup>5</sup>Department of Neurosurgery University Hospital of Würzburg, Section Experimental Neurosurgery, Würzburg, Germany

## Background

Clinical studies show that the genetic modification of T-cells to express chimeric antigen receptors (CARs) provide promising results in tumor therapy [1]. CAR T-cells are retargeted to recognize tumor associated antigens (TAAs). However, the selection of suitable TAAs for CAR T-cell therapy poses a challenge. Striking a balance is crucial, aiming for minimal overlap of target antigens to mitigate the risk of off-tumor toxicity, while simultaneously ensuring comprehensive coverage across the entire tumor to avoid antigen escape and recurrence. This work presents an automated Artificial Intelligence pipeline that determines TAAs with maximum coverage and minimal overlap based on immunohistochemical (IHC) stained pathological slides.

## Methods

The pipeline utilizes one Hematoxylin and Eosin (HE) stained slide and six IHC slides, stained for different TAAs. Initial alignment of all slides was performed using the VALIS framework [2], accounting for varying tissue distribution. Subsequently, a Machine Learning (ML) model identified the tumor area in the HE-slide, and the resulting tumor mask

was applied to all IHC-slides. Tumor regions from all IHC-slides were then extracted, segmented into smaller tiles, and subjected to a color deconvolution algorithm [3]. A quantification algorithm analyzed the antigen coverage [4]. Finally, combining antigen expressions from all IHC-slides, antigen pairs or triplets with minimal overlap and maximum coverage were determined.

## Results

The proposed pipeline is currently evaluated in a medical study determining optimal TAAs for a dual or triple CAR T-cell therapy strategy in Glioblastoma (GBM) patients. The study evaluates six TAAs. A GBM-specific ML model is used for tumor segmentation [5]. First results align with medical analyses from an accompanying study.

## Conclusion

This work presents an automated and feasible pipeline for selecting TAAs with a maximum coverage and minimal overlap for optimizing CAR T-cell therapy strategies. The initial results are promising and consistent with accompanying medical analyses. An upcoming large-scale evaluation of GBM slides will confirm its suitability for clinical use. The pipeline uses a minimum of ML, limited to tumor detection, ensuring easy-to-understand results.

Literaturangaben:

- [1] Cappell, K. M., & Kochenderfer, J. N. , (2023), Long-term outcomes following CAR T cell therapy: what we know so far, *Nature Reviews Clinical Oncology* , 359–371, 20(6), <https://doi.org/10.1038/s41571-023-00754-1>
- [2] Gatenbee, C. D., Baker, A. M., Prabhakaran, S., Swinyard, O., Slebos, R. J. C., Mandal, G., Mulholland, E., Andor, N., Marusyk, A., Leedham, S., Conejo-Garcia, J. R., Chung, C. H., Robertson-Tessi, M., Graham, T. A., & Anderson, A. R. A, (2023), Virtual alignment of pathology image series for multi-gigapixel whole slide images, *Nature Communications*, 14(1), <https://doi.org/10.1038/s41467-023-40218-9>
- [3] Ruifrok, A. C., & Johnston, D. A. , (2001), Quantification of histochemical staining by color deconvolution, *Analytical and quantitative cytology and histology*, 291–299, 23(4)
- [4] Varghese, F., Bukhari, A. B., Malhotra, R., & De, A. , (2014), IHC Profiler: an open source plugin for the quantitative evaluation and automated scoring of immunohistochemistry images of human tissue samples, *PloS one*, 9(5), <https://doi.org/10.1371/journal.pone.0096801>
- [5] Hieber, D., Prokop, G., Karthan, M., Märkl, B., Schobel, J., & Liesche-Starnecker, F. , (2023), Neural Network Assisted Pathology for Labeling Tumors in Whole-Slide-Images of Glioblastoma, In 106. Jahrestagung Deutsche Gesellschaft für Pathologie e.V..

P.ComPath.02.07

## ***Continuous AI-supported surveillance of IHC assay performance for sustainable staining quality***

R. Huss<sup>1</sup>, J. Raffler<sup>2,3</sup>, C. Herbst<sup>1</sup>, J. Warkotsch<sup>1</sup>, C. Wengenmayr<sup>2</sup>, T. Schaller<sup>1</sup>, B. Märkl<sup>1</sup>

<sup>1</sup>Institut für Pathologie und Molekulare Diagnostik, Augsburg, Germany, <sup>2</sup>Institut für Digitale Medizin, Augsburg, Germany,

<sup>3</sup>Comprehensive Cancer Cancer Augsburg, Augsburg, Germany

## Background

In diagnostic histopathology, tissue sections with a few µm thickness are examined microscopically, whereby the thickness and quality of the tissue can vary. In the context of a specific investigation, e.g. for biomarkers by immunohistochemistry (IHC), various antibodies and detection systems are used.

In recent years, efforts have been made to unify the technologies and standardize the processes in the laboratory in order to ensure consistent quality and avoid misinterpretation, even by experienced pathologists. Here we present a workflow supported by artificial intelligence (AI) that continuously captures quality parameters and even makes early deviation trends obvious.

## Methods

In addition to the paraffin sections, antigen-specific cell lines are applied to the slide as standardized reference samples and stained in the staining machine (in this case Roche Benchmark Ultra). The stained slides are then scanned with high resolution (Philips UFS). With the help of in-house developed software, image and relevant metadata are extracted and aggregated from the LIS. These data are uploaded to the Qualitopix® web suite (Visiopharm A/S) where they are analyzed in near real time.

## Results

Since the start of the project in May 2022, a total of 545 quality tests have been carried out almost continuously. Since June 2023, a systematic evaluation of the test results for HER2/Neu, Ki-67 and PD-L1 has also been carried out with the help of a standardized reference sample (total n = 178).

Due to the cloud-based software Qualitopix®, deviations could be detected at an early stage and usually eliminated at a very reasonable time (e.g. through early batch replacements or changing the position in the staining device).

There were also noticeable quality fluctuations due to a combination of two otherwise non-critical reagents or batches, the analysis of which would otherwise have been much more time-consuming and cumbersome.

## Conclusion

Thanks to an AI-supported quality control workflow using Qualitopix® from Visiopharm, relevant quality fluctuations can even be recognized as a trend in histopathological routine operation at an early stage.

The standardized evaluation of a large number of relevant parameters thus enables early root cause research and problem solving.

P.ComPath.02.08

## ***What you can learn from Pokémon for nephropathology: About the creation of diagnostic decision trees based on different types of knowledge graphs.***

M. Legnar<sup>1</sup>, J.-H. H. Siemoneit<sup>2</sup>, Z. Popovic<sup>3</sup>, S. Porubsky<sup>4</sup>, C.-A. Weis<sup>1,5</sup>

<sup>1</sup>Pathologisches Institut Heidelberg, Universitätsklinikum Heidelberg, Universität Heidelberg, Abteilung Allgemeine Pathologie, Heidelberg, Germany, <sup>2</sup>Pathologisches Institut Mannheim, Universitätsmedizin Mannheim, Universität Heidelberg, Mannheim, Germany, <sup>3</sup>Pathologisches Institut Mannheim, Universitätsmedizin Mannheim, Universität Heidelberg, Mannheim, Germany, <sup>4</sup>Institut für Pathologie, Universitätsmedizin Mainz, Johannes-Gutenberg-Universität, Mainz, Germany, <sup>5</sup>Interdisziplinäres Zentrum für wissenschaftliches Rechnen, Universität Heidelberg, Heidelberg, Germany

## Background

In pathology, diagnoses typically represent clearly defined concepts with established criteria. However, this critical information is scattered across diverse sources, including textbooks, publications, and diagnostic texts, rather than being systematically documented through algorithms. Knowledge graphs seem to be a fitting tool to collect this information or store it in a way that is understandable to humans and computers. Alas, the creation of comprehensive knowledge graphs is not a trivial task.

The next step would be leveraging machine learning to construct decision trees based on this dispersed knowledge.

But how do you prove that the methods used deliver good results and that the lack of classification quality, for example, is not due to the graph quality or topology?

This study employs toy datasets from the Pokémon franchise as examples of near-perfect graphs and a real dataset from nephropathology to illustrate the generation of interpretable decision trees from knowledge graphs.

## Methods

The initial step involves knowledge graph generation by means of computer linguistics. Subsequently, two distinct methodologies are evaluated on different kinds of knowledge graphs: Firstly, a concept-frequency-based approach, and secondly, the application of different modified variations of the Mindwalc algorithm.

## Results

Employing Pokémon datasets as a meticulously curated toy dataset, we can demonstrate through artificial gradual graph degradation by removing edges that the complexity of the resultant decision trees correlates with the increasing deterioration of the graph. Additionally, the predictive performance diminishes correspondingly.

Moreover, for both methodologies, we can illustrate that distinct graph topologies—flat topology versus hierarchical topology like in medicine with ontologies like SNOMEDCT or KBC—can serve as foundations for decision tree generation.

## Conclusion

The use of a quasi-perfect knowledge graph generated by fans over countless hours has the advantage that a method can be first established and then second applied on a real data set of interest - in this case, from nephropathology -



regardless of the subsequent graph quality.

P.ComPath.02.09

## **Gene expression prediction for patient stratification in muscle invasive bladder cancer**

I. Froeberg Mathisen<sup>1</sup>, A. Stoll<sup>1</sup>, J. Triesch<sup>2</sup>, P. J. Wild<sup>1</sup>, N. Flinner<sup>1</sup>

<sup>1</sup>Dr. Senckenberg Institute of Pathology, University Hospital Frankfurt, Frankfurt am Main, Germany, <sup>2</sup>Frankfurt Institute for Advanced Studies (FIAS), Frankfurt am Main, Germany

### **Background**

Muscle-invasive bladder cancer (MIBC) is associated with poor survival. Traditionally, MIBC is treated with a combination of neoadjuvant chemotherapy (NAC) and radical cystectomy. In recent years, immunotherapy and targeted therapies have been approved and patient stratification has become increasingly important. A set of six consensus subtypes has been described by Khamoun et al. (2020). They are assigned on the basis of the expression of 857 selected genes and are thought to have different responses to NAC. In this study, we aim to predict the expression of genes relevant for the stratification of MIBC patients based on hematoxylin and eosin (H&E) stain whole slide images.

### **Methods**

A ResNet18 model pre-trained on ImageNet was used to extract features from H&E stained tissue from the TCGA BLCA cohort. Multilayer perceptrons of different architectures were trained to predict expression of the 857 relevant genes and evaluated using 5-fold cross-validation with non overlapping patient groups.

### **Results**

The best performing model could predict the expression of 276 out of 857 genes with significant positive Pearson correlations ( $\alpha = 0.05$ ), with maximum correlations of about 0.50. These included KRT5 and KRT20, which may predict response to neoadjuvant chemotherapy, and TUBA1A, which has been identified as a potential target for several drugs in high-risk patients. Several other model architectures were able to predict the expression of over 200 genes, including NECTIN4 (Pearson = 0.27), which is targeted by Enfortumab vedotin (EV) and approved for patients with metastatic disease. We also attempted to predict NECTIN4 gene expression alone and found that this achieved a significant Pearson correlation of 0.29 (up from 0.25 with the same architecture).

### **Conclusion**

The results suggest that the expression of several potentially treatment-relevant genes can be predicted simultaneously from H&E-stained whole slide images, but prediction of a single gene of interest may be superior.

Literaturangaben:

[1] Carissa E. Chu, (2021), Heterogeneity in NECTIN4 Expression Across Molecular Subtypes of Urothelial Cancer Mediates Sensitivity to Enfortumab Vedotin, *Clinical Cancer Research*, <https://doi.org/10.1158/1078-0432.CCR-20-4175>

[2] Ping-Bao Zhang, (2019), Systematic analysis of gene expression profiles reveals prognostic stratification and underlying mechanisms for muscle-invasive bladder cancer, *Cancer Cell International*

[3] Benoît Schmauch, (2020), A deep learning model to predict RNA-Seq expression of tumours from whole slide images, *Nature Communications*, <https://www.nature.com/articles/s41467-020-17678-4>

[4] Henrik Jütte, (2021), KRT20, KRT5, ESR1 and ERBB2 Expression Can Predict Pathologic Outcome in Patients Undergoing Neoadjuvant Chemotherapy and Radical Cystectomy for Muscle-Invasive Bladder Cancer, *Journal of Personalized Medicine*, <https://www.mdpi.com/2075-4426/11/6/473>

[5] Aurélie Kamoun, (2020), A Consensus Molecular Classification of Muscle-invasive Bladder Cancer, *European Urology*, <https://www.sciencedirect.com/science/article/pii/S0302283819306955>

P.ComPath.02.10

## **AI-based identification of lung carcinoma with Stimulated Raman Histology**

K.-M. Schröder<sup>\*1</sup>, A. Weber<sup>\*1,2</sup>, K. Kurowski<sup>1,3,4</sup>, M. Werner<sup>1,3</sup>, B. Passlick<sup>5</sup>, S. Schmid<sup>5</sup>, B. Ohm<sup>5</sup>, U.-T. Le<sup>5</sup>, P. Bronsert<sup>1,3,4</sup>

<sup>1</sup>Institut für Klinische Pathologie, Freiburg, Germany, <sup>2</sup>Fakultät für Biologie, Freiburg, Germany, <sup>3</sup>Tumorbank Comprehensive Cancer Center Freiburg, Freiburg, Germany, <sup>4</sup>Core Facility Histopathologie und Digitale Pathologie, Freiburg, Germany, <sup>5</sup>Klinik für

## Background

Frozen section represents the gold standard guiding the surgical resection. Stimulated Raman Histology employs stimulated Raman scattering (SRS) of photons at specific wavelengths interacting with biomolecules to visualize cellular structures in tissue samples. This process generates images akin to H&E-stained tissues and bypasses tissue sectioning and staining. Our study focused on evaluating the effectiveness of AI-based lung cancer identification in Stimulated Raman Histology of lung cancer patients.

## Methods

SRH images were acquired with the NIO Laser Imaging System. 459 SRS images were categorized and annotated in the tissue types Tumor, Stroma, Necrosis, Fat, Normal, and Other using QPath (Version 0.4.3). A dataset of 21,703 labeled tiles was generated, and a VGG19-based convolutional neural network (CNN) was trained and tested on SRS and SRH images. Training a VGG19-based convolutional neural network was done using 64 SRS and corresponding SRH images, with a validation set of 16 images.

## Results

Annotation of 6 tissue types was performed on SRH images in 459 tissue samples from 136 cases. The model achieved a balanced accuracy of 0.93 (for SRH), precision (non-tumor) 0.94 (Recall: 0.93, F1: 0.93) and precision (tumor) 0.92 (Recall: 0.93, F1: 0.93).

For SRS we performed a balanced accuracy of 0.88; precision 0.93 (non-tumor) (Recall: 0.84, F1: 0.88) and precision 0.83 (tumor) (Recall: 0.93, F1: 0.88).

## Conclusion

Our data underscore the potential of deep learning in the intraoperative identification of tissue types using SRS and SRH images, offering significant advancements in lung cancer diagnostics.

P.ComPath.02.11

## A biomathematical approach to separate nodal marginal zone B-cell lymphoma from nodal diffuse large B-cell lymphoma on the basis of H&E-morphology.

P. Thiam<sup>1</sup>, F. Spada<sup>2</sup>, T. Barth<sup>2</sup>, P. Möller<sup>2</sup>, H. Kestler<sup>1</sup>

<sup>1</sup>Ulm University, Institute of Medical Systems Biology, Ulm, Germany, <sup>2</sup>Ulm University Medical Center, Institute of Pathology, Ulm, Germany

## Background

Between the large cell variant of nodal Marginal Zone B-cell Lymphoma (nMZoL) and the Diffuse Large B-Cell Lymphoma (nDLBCL) is a considerable grey zone with respect to histo- and cytomorphology. Since nMZoL and nDLBCL might differ in their clinical behaviour and prognosis, which by this grey zone is not clear at all, it is highly desirable to use novel methods to solve this differential diagnostic problem. Based on a set of 86 nMZoL and 47 nDLBCL, we set out to perform a novel image analysis on these Lymphoma cases.

## Methods

The analysis consists of applying a deep learning [LeCun2015] approach to perform the differentiation between both forms of Lymphoma based on a set of whole slide images. First a segmentation of each whole slide image into small size patches is performed. These patches are subsequently used to optimize an inference model by using a transfer learning approach. Once optimized, the model is used to perform inference on a set of patches extracted from an unseen image. The prediction corresponding to the whole slide image is finally computed by aggregating the resulting patch specific scores.

## Results

The approach is assessed by performing a total of 100 evaluation experiments. During each experiment, a stratified random split is performed to generate the training, validation and testing sets following the ratios 0.5/0.2/0.3 of the entire

set of samples. The results of the performed experiments (see Fig. 1) show the ability of the model to distinguish between both forms of Lymphoma with the following averaged performance scores: sensitivity: 75.07%; specificity: 72.36%; geometric mean: 73.24%; accuracy: 73.33%; Area Under Curve: 73.72%.

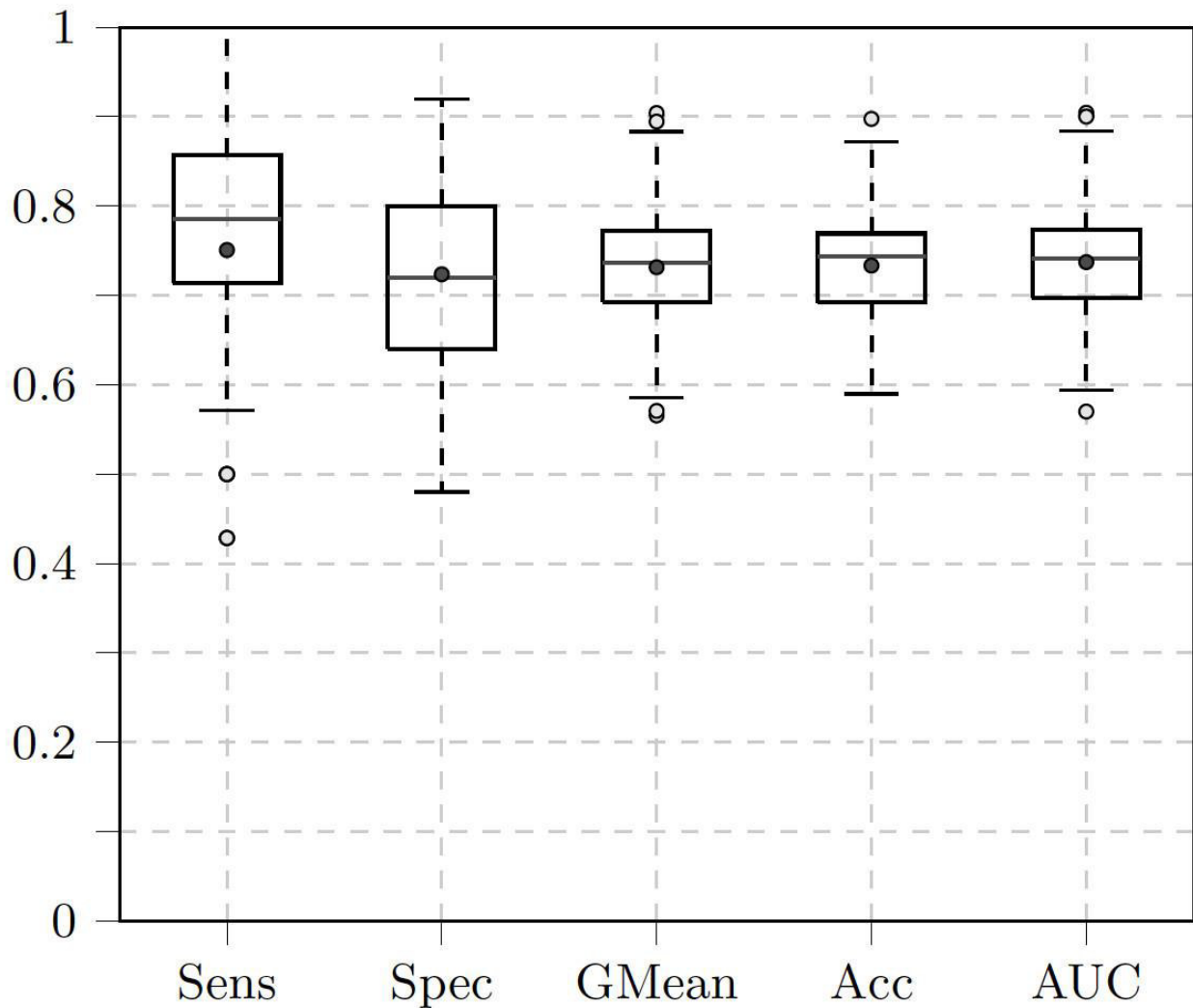
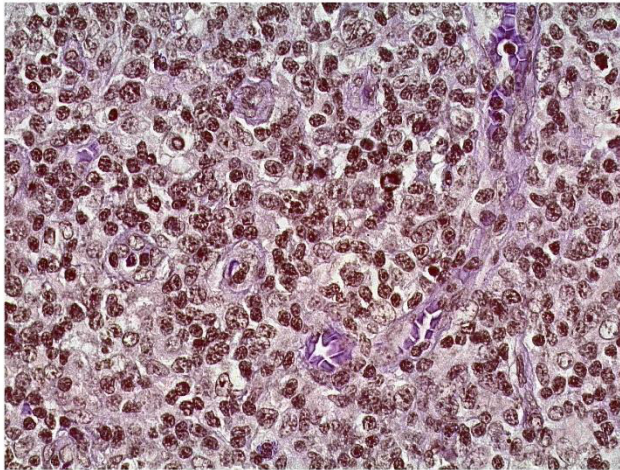


Figure 1: Performance Evaluation (Sensitivity (Sens), Specificity (Spec), Geometric Mean (GMean), Accuracy (Acc), Area Under Curve (AUC)).

### Conclusion

A visualization of the areas upon which the decisions taken by the trained model are based can be generated, therefore providing some insights into the particularities of both forms of Lymphoma and thereby improving the interpretability of the generated output (see Fig. 2). These results are quite promising, since such a task is quite challenging and is bounded with a huge amount of workload for the pathologist.

Groundtruth: nMZoL



Prediction: nMZoL

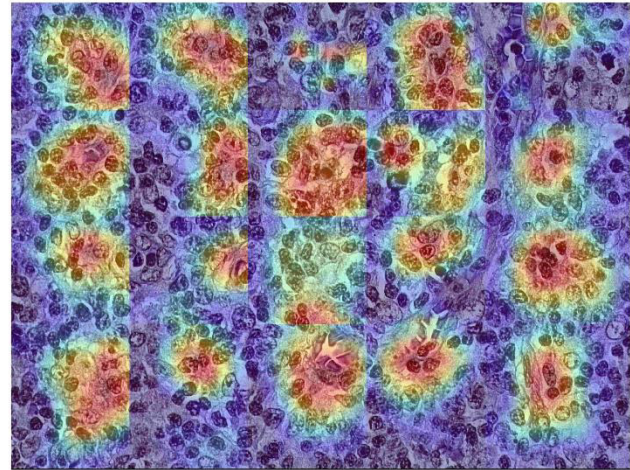


Figure 2: Prediction Visualization (Gradient-weighted Class Activation Mapping): the whole slide image is depicted on the left; the same image with the areas specific to the model's prediction for each of the extracted patches is depicted on the right.

Literaturangaben:

[LeCun2015] Yann LeCun, Yoshua Bengio, Geoffrey Hinton, (2015), Deep Learning, Nature 521, 436-444, <https://doi.org/10.1038/nature14539>, 2024-02-25

## Poster Personalisierte (Krebs-)Medizin 1

P.PersMed.01.01

### ***Tumor budding of pancreatic ductal adenocarcinoma in a chorioallantoic membrane model - potential pitfall in the evaluation.***

F. Schick Tanz<sup>1</sup>, R. Ranjan<sup>2</sup>, M. Reichert<sup>2,3</sup>, K. Steiger<sup>1</sup>

<sup>1</sup>Institute of Pathology, Technical University of Munich, Munich, Germany, <sup>2</sup>Klinikum rechts der Isar, Technical University of Munich, Clinic and Polyclinic for Internal Medicine II, Munich, Germany, <sup>3</sup>German Cancer Consortium, Partner Site Munich, Munich, Germany

#### **Background**

The chorioallantoic membrane (CAM) is a highly vascularized extraembryonic membrane within a fertilized chicken egg. It is used as a model to investigate tumor morphogenesis, angiogenesis, invasion, and metastatic dissemination in several cancer entities, including pancreatic ductal adenocarcinoma (PDAC). [1][2] Tumor budding is a well-established prognostic marker in PDAC that can be used as a simple morphological-based method to stratify patients into prognostic categories. [3] Therefore, PDAC models should also offer the possibility to look into budding behavior.

#### **Methods**

PDAC patient derived organoids (PDOs) were transplanted onto CAM, and engrafted tumors were harvested to prepare paraffin-embedded blocks. The histomorphological evaluation was performed on the HE-stained PDO-CAM xenografts. In addition, immunohistochemical (IHC) staining of CK7 and in situ hybridization of human DNA-specific *ALU* repeats were performed on the PDO-CAM xenografts.

#### **Results**

Small cell clusters qualifying for potential buds were observed at the invasion front on the HE-stained PDO-CAM xenografts. Within these cell clusters two groups with distinct morphological features could be differentiated. One group had prominent nucleoli, pale cytoplasm, and very weak expression for CK7, while the other showed accentuated nuclear hyperchromasia and a more eosinophil cytoplasm with strong positivity for CK7. This raised suspicion that the CAM itself also produces bud-like structures. To clearly discriminate the potential buds from the CAM from tumor buds (TB), an in-situ-hybridization for *ALU* repeats was used, taking advantage of the interspecies differences. Here, the apparent nuclear reaction was observed only in the group that showed accentuated nuclear hyperchromasia and a more eosinophil

cytoplasm with strong positivity for CK7, characterizing them as actual TB of the PDO-CAM xenografts.

## Conclusion

Tumor budding of PDAC PDOs can be evaluated in CAM models, but it is necessary to differentiate between bud-like complexes that derive from the CAM and actual TB. For this purpose, IHC can be very useful, but in incredibly challenging cases, *ALU* ISH offers a conclusive alternative.

Literaturangaben:

[1] Ranjan RA, Muenzner JK, Kunze P, et al., (2023), The Chorioallantoic Membrane Xenograft Assay as a Reliable Model for Investigating the Biology of Breast Cancer., *Cancers* (Basel), <https://doi.org/10.3390/cancers15061704>, 2024-02-16

[2] Pion E, Karnosky J, Boscheck S, et al., (2022), 3D In Vivo Models for Translational Research on Pancreatic Cancer: The Chorioallantoic Membrane (CAM) Model., *Cancers* (Basel), <https://doi.org/10.3390/cancers14153733>, 2024-02-16

[3] Karamitopoulou E, Wartenberg M, Zlobec I, et al., (2018), Tumour budding in pancreatic cancer revisited: validation of the ITBCC scoring system., *Histopathology*, <https://doi.org/10.1111/his.13508>, 2024-02-16

P.PersMed.01.02

## ***A noisy NFκB-A20-RIPK3 circuit controls necroptosis kinetics in fibrosarcoma***

M. Oliver Metzig<sup>1,2,3</sup>, Y. Tang<sup>1,2</sup>, S. Mitchell<sup>1,2</sup>, B. Taylor<sup>1,2</sup>, R. Foreman<sup>2,4</sup>, R. Wollman<sup>2,4</sup>, A. Hoffmann<sup>1,2</sup>

<sup>1</sup>Signaling Systems Laboratory, Department of Microbiology, Immunology and Molecular Genetics, University of California, Los Angeles, United States of America, <sup>2</sup>Institute for Quantitative and Computational Biosciences, University of California, Los Angeles, United States of America, <sup>3</sup>Institute of Pathology, University Medical Center Mainz, Mainz, Germany, <sup>4</sup>Department of Chemistry and Biochemistry, University of California, Los Angeles, United States of America

### Background

Balancing life-death decisions is crucial to maintain tissue homeostasis and prevent disease. Tumor necrosis factor (TNF) is a potent activator of nuclear factor κB (NFκB), which provides pro-survival and pro-inflammatory signals. In certain scenarios, however, TNF triggers necroptotic cell death, an important back-up mechanism in apoptosis resistant tumors, which may install an adaptive anti-tumor response. Whether TNF-induced NFκB affects the decision of cancer cells to undergo necroptosis was previously unclear.

### Methods

Live-cell microscopy, automated image analysis, CRISPR/Cas9-mediated gene editing, gene expression analysis, protein biochemistry, mathematical modeling

### Results

Live-cell microscopy in combination with genetic perturbation revealed that RelA/NFκB encodes a transient mechanism to protect a fraction of fibrosarcoma cells from rapid necroptosis. TNF-induced expression of TNFAIP3/A20 forms an incoherent feedforward loop to interfere with RIPK3 activation in the necrosome. A computational model quantitatively accounted for TNF-induced necroptosis kinetics. Preliminary data point towards additional regulators, particularly in the context of constitutive NFκB.

### Conclusion

Our systems biology approach provides understanding of how NFκB regulates dynamic necroptosis decisions in fibrosarcoma. NFκB-A20 controlled necroptosis kinetics may affect therapeutic outcomes and shape the anti-tumor immune response.

P.PersMed.01.03

## ***αvβ6-Integrin expression in gynaecological and urogenital cancer entities: Eligibility as a theranostic target***

N. M. Schmid<sup>1</sup>, S. Ballke<sup>1</sup>, J. Notni<sup>2</sup>, H. Lisiecki<sup>1</sup>, E. Schmoeckel<sup>1</sup>, M. Remke<sup>1</sup>, M. Boxberg<sup>1</sup>, K. Schwamborn<sup>1</sup>, J. Pereira Lopes Goncalves<sup>1</sup>, T. Groll<sup>1</sup>, K. Steiger<sup>1</sup>

<sup>1</sup>Institut für Pathologie, Technische Universität München, München, Germany, <sup>2</sup>Pharmazeutische Radiochemie, TUM School of Natural Sciences, München, Germany

## Background

The transmembrane adhesion receptor  $\alpha\beta6$ -integrin is exclusively expressed by epithelial cells, including several carcinoma cells, where it drives invasion and metastasis. Since its expression density is also negatively correlated with overall survival, it represents a promising theranostic target. The  $\alpha\beta6$ -integrin selective positron emission tomography (PET) radiopharmaceutical  $^{68}\text{Ga}$ -Trivehexin has already been successfully used for clinical imaging of various human carcinomas [1]. We investigated the membranous expression of  $\alpha\beta6$ -integrin based on immunohistochemistry (IHC) in gynaecological and urogenital cancer entities to determine whether it is suitable for diagnostic imaging, as a therapeutic target or as a prognostic marker.

## Methods

We evaluated tissue microarrays (TMAs) consisting of 79 to 152 bladder-, cervical-, renal-, endometrial-, and prostate cancer cases. Tissue samples were annotated and punched using a TMA Grand Master (3D Histech). TMAs were immunohistochemically examined by using anti-human  $\beta6$ -Integrin antibody [clone 442.5C4] (#407317, dilution 1:100, Merck Millipore, Burlington, Massachusetts, USA). Slides were digitalized and assessed microscopically by using Aperio ImageScope (Leica Biosystems). The expression intensity was evaluated by scoring from 0 (absent) to 3 (high) and the expression frequency was assessed as percentage (%) for each tumor core. A modified version of the  $\beta6$ -integrin scoring scheme proposed by Sipos et al. [2] was used to calculate the final score for each case, considering intensity, frequency and the number of cores.

## Results

The vast majority of cervical (96.2%), bladder (93%), and endometrial cancer cases (92%) showed membranous  $\alpha\beta6$ -integrin expression. In comparison, 63% of renal and 67.8% of prostate cancer cases showed variable, low to strong (score 1 to 3) membranous  $\alpha\beta6$ -integrin expression. The investigated gynaecological cancer entities and bladder cancer presented a significant membranous positivity for  $\alpha\beta6$ -integrin and showed a higher expression than the urogenital cancers.

## Conclusion

$\alpha\beta6$ -Integrin is highly expressed in cervical-, bladder- and endometrial cancer. Hence, it appears to be a promising target for radiotheranostics (i.e., nuclear imaging and targeted radionuclide therapy) in these entities. We also demonstrated a lower membranous  $\alpha\beta6$ -integrin expression for renal and prostate cancer on the protein level.

Literaturangaben:

[1] Quigley, N.G., et al., (2022), PET/CT imaging of head-and-neck and pancreatic cancer in humans by targeting the "Cancer Integrin"  $\alpha\beta6$  with Ga-68-Trivehexin, Eur J Nucl Med Mol Imaging, p. 1136-1147, 49(4)

[2] Sipos, B., et al., (2004), Immunohistochemical screening for beta6-integrin subunit expression in adenocarcinomas using a novel monoclonal antibody reveals strong up-regulation in pancreatic ductal adenocarcinomas in vivo and in vitro, Histopathology, p. 226-36, 45(3)

P.PersMed.01.04

## ***Establishment of an organotypic tissue slice culture for intrahepatic cholangiocarcinoma***

L. Meyer<sup>1,2,3</sup>, N. Meier<sup>1</sup>, B. Vollmer-Kary<sup>1</sup>, K. Kurowski<sup>1</sup>, P. Holzner<sup>4</sup>, M. Werner<sup>1,5</sup>, O. Schilling<sup>1,5</sup>, M. Föll<sup>1,5,6</sup>

<sup>1</sup>Uniklinikum Freiburg, Institut für klinische Pathologie, Freiburg, Germany, <sup>2</sup>Uniklinikum Freiburg, Institut für klinische Pathologie, AG Schilling, Freiburg, Germany, <sup>3</sup>Fakultät für Biologie, Albert-Ludwigs Universität, Freiburg, Germany, <sup>4</sup>Department of General and Visceral Surgery, Universitätsklinikum, Freiburg, Germany, <sup>5</sup>German Cancer Consortium (DKTK) German Cancer Research Center (DKFZ), Heidelberg, Germany, <sup>6</sup>Khoury College of Computer Sciences, Northeastern University, Boston, United States of America

## Background

Intrahepatic cholangiocarcinoma (iCCA) is a rare cancer derived from the bile ducts within the liver. The cancer has a low survival rate and limited therapeutical options. Better patient derived models to study the tumor biology, tumor heterogeneity and therapy efficacy are needed. So far there are three types of patient derived models to study iCCA tumors: patient derived cell lines fail to recapitulate the 3D structure of a tumor, patient derived organoids can do this however they still fail to show the tumor-stroma-interactions as well as the tumor microenvironment. Patient derived xenografts can show the tumor-stroma interactions however they are very expensive and have a low engraftment rate. In

this study, we therefore present the organotypic tissue slice culture (OTSC) which is a cheap, quick, and easy method to cultivate patient derived tumorslices for multiple days while preserving the original tumor architecture and microenvironment.

## Methods

Fresh iCCA tumor was received after surgical resection and cut into slices of 300 µm thickness using a vibratome. The slices were cultivated on cell culture inserts in three different media to identify the best culturing conditions. The tissue slices were harvested between day 1 and 12 in culture and formalin-fixed and paraffin-embedded (FFPE). These FFPE blocks were used for histological and morphological analysis via H&E staining and immunohistochemistry.

## Results

In total, 120 tissue slices from three iCCA patients could be cultivated. Due to the large tumor size, 30 to 40 slices could be generated from each iCCA tumor. The slices could be cultivated for up to one week, during which histological and morphological analysis revealed a decrease in the amount of both tumor and stroma cells during. In future experiments, additional agents such as growth factors and vitamins will be added to the commercially available culture media to optimize the cell culture conditions. Furthermore, the model will be studied by using a mass spectrometry imaging-based approach, for either peptide or metabolite imaging.

## Conclusion

We present the very first description of an organotypic tissue slice culture for iCCA, which holds great potential as an in vitro model to study functional aspects and patient-specific treatment responses in iCCA.

P.PersMed.01.05

## ***Biological Makeup of Pancreatic Ductal Adenocarcinoma Predicts Prognosis and Indicates Treatment Response***

J. Rao<sup>1</sup>, M. Sinn<sup>2,3</sup>, U. Pelzer<sup>2</sup>, H. Riess<sup>2</sup>, H. Oettle<sup>2</sup>, I. E. Demir<sup>4</sup>, H. Friess<sup>4</sup>, C. Jäger<sup>4</sup>, K. Steiger<sup>1</sup>, A. Muckenhuber<sup>1</sup>

<sup>1</sup>Institute of Pathology, Technical University of Munich, München, Germany, <sup>2</sup>Charité – University Medicine Berlin, Department of Haematology, Oncology and Tumour Immunology, Berlin, Germany, <sup>3</sup>University Medical Center of Hamburg-Eppendorf, Department of Internal Medicine II, Hamburg, Germany, <sup>4</sup>Klinikum rechts der Isar, School of Medicine, Technical University of Munich, Department of Surgery, München, Germany

## Background

Despite extensive research over decades of years, pancreatic ductal adenocarcinoma (PDAC) continues to be a highly lethal disease with limited success from conventional therapies. Subclassification of PDAC into distinct biological subtypes has been suggested by various groups to enhance patient's outcome and minimize unnecessary side effects. Recently, a new classification method based on IHC, involving KRT81 and HNF1A, was able to replicate certain existing molecular subtyping methods, offering valuable prognostic, and somewhat predictive insights.

## Methods

The KRT81/HNF1A subtyping method was refined to classify PDAC into 3 distinct biological subtypes. The prognostic value of the IHC-based method was examined in two separate groups, consisting of 269 and 286 primary resected patients, respectively. The predictive effect for response to the chemotherapy erlotinib + gemcitabine was also evaluated in the second cohort.

## Results

In univariate and multivariate analysis, the new HNF1A-positive subtype showed the best survival in both PDAC cohorts, while the KRT81-positive subtype was associated with the worst survival, and the double-negative subtype fell in between ( $P < 0.001$  and  $P < 0.001$ , respectively). In the second cohort, we also noticed that the IHC-based subtype could potentially predict the effectiveness of erlotinib-based treatment.

## Conclusion

The revised classification system using immunochemistry markers KRT81 and HNF1A shows prognostic significance for PDAC patients and might help to tailor treatment strategies for better response to specific drugs.

## ***Modeling Immunotherapies in Live 3D Human cancer tissue Bioreactors***

Y. Zhang<sup>1</sup>, P. Bucher<sup>2</sup>, J. Leibold<sup>2</sup>, J. Feucht<sup>2</sup>, C. M. Schürch<sup>1</sup>

<sup>1</sup>Department of Pathology and Neuropathology, University Hospital and Comprehensive Cancer Center, Tuebingen, Germany, <sup>2</sup>Cluster of Excellence iFIT (EXC 2180) "Image-Guided and Functionally Instructed Tumor Therapies", Eberhard Karls University Tübingen, Tuebingen, Germany

### **Background**

Despite the remarkable efficacy of cancer immunotherapies in advanced malignancies, a significant portion of patients remains unresponsive. With the escalating clinical use of immunotherapies, concerns arise over potential adverse effects and healthcare costs. Predicting individual responses to immunotherapy remains challenging, underscoring the need for better models and predictive biomarkers. The tumor microenvironment (TME) governs tumor-immune cell interactions and influences antitumoral immunity. Understanding how immunotherapies shape the TME can unveil novel targets and biomarkers. However, current experimental platforms inadequately mimic the intact human TME. Advanced models capable of assessing immunotherapy-induced changes in TME composition and architecture are imperative for enhancing treatment outcomes and advancing our understanding of immunotherapies.

### **Methods**

Fresh human lymph node tissue samples were acquired from the Department of Surgery, divided for experimentation and diagnosis. Tissue pieces (~3mm diameter) were then cultured for 3 days in U-cup bioreactors. CAR-T cell and antibody-based therapies were administered during culture. Following culture, tissue pieces were harvested for flow cytometry and histological analysis.

### **Results**

Optimization of the culture system led to a significant enhancement in tissue viability compared to both the previous setup and traditional plate culture methods. Comparative analyses via flow cytometry and fluorescence imaging revealed notable differences between PI3K signaling pathway-enhanced CAR-T therapy and conventional CAR-T therapy. Enhanced CAR-T cells demonstrated superior tissue infiltration, although their cytotoxicity did not significantly differ from conventional CAR-T cells. Treatment with the PD-1 inhibitor pembrolizumab significantly decreased lymphoma cell viability but had no significant effect on benign lymph node tissues. Additionally, preliminary validation demonstrated the efficacy of a novel humanized antibody targeting the melanoma-associated self-antigen tyrosinase-related protein 2 (TRP2) in melanoma immunotherapy.

### **Conclusion**

Our optimized bioreactor culture system effectively sustains lymphoid tissue activity, providing a valuable platform for assessing the efficacy of diverse immunotherapies and personalized treatment approaches.

## ***Trop-2 expression in solid tumors - a molecular tumorboard experience***

E.-P. Dopfer<sup>1,2,3</sup>, S. Riemer-Cysar<sup>1,2,3</sup>, L. Bergmann<sup>1,2,3</sup>, U. Matysiak<sup>1,2,3</sup>, S. Lassmann<sup>1,2,3</sup>, S. Timme-Bronsert<sup>1,2,3</sup>, M. Werner<sup>1,2,3,4</sup>

<sup>1</sup>Institute for Surgical Pathology, Medical Center, University of Freiburg, Germany, Freiburg, Germany, <sup>2</sup>Comprehensive Cancer Center Freiburg, Medical Center, Freiburg, Germany, Freiburg, Germany, <sup>3</sup>Zentrum für Personalisierte Medizin, partner site Freiburg, Germany, Freiburg, Germany, <sup>4</sup>German Cancer Consortium (DKTK), partner site Freiburg, Germany, Freiburg, Germany

### **Background**

Trophoblast surface antigen 2 (Trop-2) is a type I transmembrane glycoprotein, which is highly expressed in multiple tumors and which associates with malignant progression. As such, Trop-2 has evolved as a novel therapeutic target for antibody-drug conjugate (ADC; Sacituzumab-Govitecan). Here, we provide an overview of Trop-2 expression and its relevance in solid tumors of the molecular tumorboard Freiburg.

### **Methods**

The cohort included 50 cases of the CCC-Freiburg Molecular Tumorboard (MTB) from 10/2023 to 01/24, diagnosed with solid tumors (e.g. colorectal, lung, ovarian, prostate carcinomas) and completion of approved guideline therapy. Next to



other protein stains and NGS panel-based molecular pathology, Trop-2 staining was included for decision on therapy recommendations. Trop-2 IHC-staining was on Formalin-Fixed and Paraffin-Embedded tissue specimens using the Trop-2 antibody clone EPR20043 (Abcam). Trop-2 expression was evaluated in tumor cells using the H-Score by two pathologists independently.

### Results

Trop-2 staining was successful in all 50 cases. No (H-Score = 0), low (H-Score 1-99), moderate (H-Score 100-199) and high (H-Score 200-300) Trop-2 expression was negative in 8/50 (16%) seen in 10/50 (20%), 9/50 (18%) and 23/50 (46%) of cases, respectively. Whilst melanomas/skin tumors were Trop-2 negative, colorectal carcinomas mainly exhibited a low Trop-2 expression and hormone-dependent carcinomas (e.g. prostate, ovarian, breast carcinomas) frequently a high Trop-2 expression. Other tumors (e.g. cholangio carcinoma) showed variable Trop-2 expression. Treatment recommendations including Trop-2 ADC were provided in 26/44 (59%) cases and Trop-2 ADC was prioritized as 1<sup>st</sup> treatment recommendation in 8/26 (31%) of cases. Trop-2 ADC was recommended for a single case with low Trop-2 expression (H-Score 60) due to lack of other therapeutic options.

### Conclusion

In the “real word” of the CCCF Molecular Tumorboard “Trop-2” was established, applied and identified as important immunohistochemical biomarker in solid tumors to enable treatment recommendations for the novel Trop-2 ADC (Sacituzumab-Govitecan).

P.PersMed.01.08

## ***The Novel HSF1 Inhibitor NXP800 Possesses Antineoplastic Activity in Human Hepatocellular Carcinoma***

S. Steinmann, A. Kleinle, M. Evert, D. F. Calvisi

Institut für Pathologie der Universität Regensburg, Experimentelle Tumorpathologie, Regensburg, Germany

### Background

Hepatocellular carcinoma (HCC) is the most frequent primary liver tumor, characterized by a dismal prognosis and limited therapeutic options. Previous data from our and other groups showed that heat shock factor 1 (HSF1), a critical transactivator of stress responses, plays a critical role in hepatocarcinogenesis. Nevertheless, the importance of HSF1 as an actionable target in this disease remains elusive. Therefore, in the present study, we tested the therapeutic relevance of NXP800 (CCT361814), a newly developed HSF1 inhibitor currently in clinical trials for ovary tumors, in experimental models of HCC.

### Methods

In vitro, we treated several HCC cell lines (HLE, HLF, PLC/PRF/5, and SNU449) with increasing concentrations of NXP800. MTT assay was applied to determine the effect on cell viability and this agent's half inhibitory concentration (IC50). Relevant oncogenic signaling pathways, such as PI3K/AKT, MAPK/ERK, and Hippo cascades, were examined utilizing Western Blotting and Real-time PCR. Additionally, the effects of NXP800 on tumor growth were monitored in vivo using the chick embryo chorioallantoic membrane (CAM) xenograft model. Moreover, the impact of NXP800 administration on mitochondrial performance was explored utilizing Seahorse (Agilent) real-time cell metabolic assays (Mito Stress Test, Glycolytic Rate Assay) and transmission electron microscopy (TEM).

### Results

In sum, NXP800 displayed relevant anti-growth activity in HCC cell lines in vitro and reduced tumorigenicity in vivo at nanomolar concentrations. Besides, TEM imaging revealed extensive tumor cell mitochondrial damage and lysosomal degradation under NXP800 treatment.

### Conclusion

Thus, the present data suggest that targeting HSF1 with NXP800 might be a potent therapeutic modality for treating human HCC.

## Poster Personalisierte (Krebs-)Medizin 2

P.PersMed.02.01

### ***Proteomic characterisation of pancreatic ductal adenocarcinoma (PDAC) by MALDI-TOF with regard to protein expression profiles, biological subtypes and clinical outcomes***

C. Koch\*<sup>1</sup>, J. Pereira Lopes Goncalves\*<sup>1</sup>, C. Bollwein<sup>1</sup>, I. E. Demir<sup>2</sup>, C. Jäger<sup>2</sup>, M. Schlitter<sup>3</sup>, J. Rao<sup>1</sup>, K. Steiger<sup>1</sup>, K. Schwamborn<sup>1</sup>, A. Muckenhuber<sup>1</sup>

<sup>1</sup>Institut für Pathologie, Technische Universität München, München, Germany, <sup>2</sup>Technische Universität München, Klinik und Poliklinik für Chirurgie, München, Germany, <sup>3</sup>BioNTech, Mainz, Germany

\*Contributed equally

#### **Background**

Pancreatic ductal adenocarcinoma (PDAC) is the 7th most common cause of cancer-related death worldwide, with a 5-year survival rate of less than 10%. In recent years, research has shown that different biological subtypes of pancreatic cancer are of prognostic and possibly predictive importance. Based on these subtypes, protein expression in PDACs was investigated using mass spectrometry imaging for exploration and immunohistochemistry (IHC) for validation to identify novel prognostic and predictive biomarkers by correlating protein expression profiles with subtypes and clinical outcomes.

#### **Methods**

The cohort consists of 12 tissue microarrays (TMA) with tumor samples from approximately 250 patients. Sections were subjected to *in situ* tryptic digestion, followed by matrix application and acquisition of mass spectrometry data. After HE staining and digitization for histological annotation, tumor cells, tumor stroma and nerve-infiltrating tumor cell clusters were annotated separately. Data analysis was performed using SCiLS and the R programming language.

#### **Results**

After an initial, unfiltered data analysis, no *m/z* values were identified that could be correlated with survival groups. However, *m/z* 944.5 was found to be indicative of immune infiltration regardless of IHC subgroup membership. At a small sample size, *m/z* 944.5 appears to have higher relevance for long-term survival in a subgroup of KRT81-expressing PDACs, paradoxically the group associated with the worst prognosis overall.

#### **Conclusion**

Despite the lack of *m/z* values directly related to survival outcome, the identification of *m/z* 944.5 as a marker of strong immune infiltration is interesting. Bibliographic research suggests that *m/z* 944.5 may be a fragment of H2A.Z, a histone variant involved in several DNA-related processes, which is currently being validated by IHC. In the literature, H2A.Z has been identified as a prognostic biomarker correlating with TP53 mutations and immune infiltration in HCC. In PDAC, overexpression of H2A.Z isoforms has been associated with chemoresistance and tumor growth and identified as a protein of higher relevance for gradient boost classifiers in distinguishing between PDACs and cholangiocarcinomas. As our study progresses, we find the identification of *m/z* 944.5 as a marker for immune infiltration, especially in specific subgroups, intriguing. Ongoing investigations aim to gain further insights into the interplay between proteomic markers and clinical outcomes.

P.PersMed.02.02

### ***Cytokine profiling in cerebrospinal fluid after intraoperative radiation of primary and secondary brain tumors***

Z. Mielewczyk<sup>1</sup>, P. Krauss<sup>2</sup>, K.-H. Kahl<sup>3</sup>, T. Mögele<sup>1</sup>, B. Märkl<sup>1</sup>, E. Shiban<sup>2</sup>, F. Liesche-Starnecker<sup>1</sup>

<sup>1</sup>University of Augsburg, Pathology, Augsburg, Germany, <sup>2</sup>University of Augsburg, Department of Neurosurgery, Augsburg, Germany,

<sup>3</sup>University of Augsburg, Department of Radiooncology, Augsburg, Germany

#### **Background**

Intraoperative radiation therapy (IORT) is an ascending treatment approach which provides targeted radiation, reduced

local recurrence and induction of an anti-tumor effect by activating an immune response. Aim of our study is to characterize the immunological signature represented by the cytokine profile in the cerebrospinal fluid (CSF) after IORT of primary and secondary brain tumors.

### Methods

We analyzed the cytokine patterns in 63 CSF samples obtained from 18 patients with tumor resection and IORT. Samples were taken from test group at four time points: 1. intraoperatively, before tumor resection and IORT, 2. intraoperatively, after tumor resection, before IORT, 3. intraoperatively, after tumor resection and IORT, 4. ~24 hours postoperatively from drainage and from control group at three time points: 1. intraoperatively, before tumor resection, 2. intraoperatively, after tumor resection and 3. ~24 hours postoperatively from drainage. Samples were tested using a multiplex immunoassay (CodePlex Secretome - Human Innate Immune Panel provided by IsoPlexis) according to the manufacturer's instructions. Levels of EGF, GM-CSF, Granzyme B, IFN- $\gamma$ , IL-1 $\beta$ , IL-4, IL-6, IL-7, IL-8, IL-10, IL-15, IP-10, MCP-1, MIP-1 $\alpha$ , MIP-1 $\beta$ , PDGF-BB, sCD137, TNF- $\alpha$  and VEGF were measured and quantified using IsoSpeak software.

### Results

An increase of signal intensity was observed for 16 of the 19 analyzed cytokines (84%) in the test group, of which 7 (37%) displayed significant differences between baseline and postoperative time points: IL-1 $\beta$ , IL-6, IL-8, IP-10, MCP-1, MIP-1 $\beta$  and VEGF. Within these cytokines, a noticeable increase is evident for IL-1 $\beta$ , IL-8, IP-10, and MIP-1 $\beta$  when comparing the control and test groups.

### Conclusion

Our study allows first conclusions about changes in the cytokine profile of cerebrospinal fluid after IORT of primary and secondary brain tumors. The results indicate that IL-1 $\beta$ , IL-8, IP-10 and MIP-1 $\beta$  are involved in the inflammatory response induced by exposure to ionizing radiation of the tumor bed during surgery.

P.PersMed.02.03

## ***Inter-Observer Agreement Assessment in Estimating Tumor-Infiltrating Lymphocytes and Tumor-Stroma Ratio***

A. Kazemi<sup>1,2</sup>, M. Gharib<sup>3</sup>, N. Mohammadian Roshan<sup>3</sup>, S. Taraz Jamshidi<sup>3</sup>, F. Stögbauer<sup>2</sup>, S. Eslami<sup>1,4,5</sup>, P. J. Schöffler<sup>2,6,7</sup>

<sup>1</sup>Department of Medical Informatics, School of Medicine, Mashhad University of Medical Sciences, Mashhad, Iran, Islamic Republic of,

<sup>2</sup>Institute of General and Surgical Pathology, Technical University of Munich, Munich, Germany, <sup>3</sup>Department of Pathology, Faculty of Medicine, Mashhad University of Medical Sciences, Mashhad, Iran, Islamic Republic of, <sup>4</sup>Pharmaceutical Sciences Research Center, Institute of Pharmaceutical Technology, Mashhad University of Medical Sciences, Mashhad, Iran, Islamic Republic of, <sup>5</sup>Department of Medical Informatics, University of Amsterdam, Amsterdam, The Netherlands, <sup>6</sup>TUM School of Computation, Information and Technology, Technical University of Munich, Garching bei Munich, Germany, <sup>7</sup>Munich Data Science Institute, Technical University of Munich, Garching bei Munich, Germany

### Background

To implement the new marker in clinical practice, reliability assessment, validation, and standardization of utilization must be applied. This study evaluated the reliability of tumor-infiltrating lymphocytes (TILs) and tumor-stroma ratio (TSR) assessment through conventional microscopy by comparing observers' estimations. First publication date is 11.06.2023 (1).

### Methods

Three pathologists using 86 CRC HE slides assessed Intratumoral and invasive margins stromal TILs, and TSR. TSR and TILs were categorized using one and four different proposed cutoff systems, respectively, and agreement was assessed using the intraclass coefficient (ICC) and Cohen's kappa statistics. Pairwise evaluation of agreement was performed using the Fleiss kappa statistic and the concordance rate and it was visualized by Bland-Altman plots. To investigate the association between biomarkers and patient data, Pearson's correlation analysis was applied.

### Results

For the evaluation of intratumoral stromal TILs, ICC of 0.505 (95% CI: 0.35-0.64) was obtained, kappa values were in the range of 0.21 to 0.38, and concordance rates in the range of 0.61 to 0.72. For the evaluation of tumor-front TILs, ICC was 0.52 (95% CI: 0.32-0.67), the overall kappa value ranged from 0.24 to 0.30, and the concordance rate ranged from

0.66 to 0.72. For estimating the TSR, the ICC was 0.48 (95% CI: 0.35-0.60), the kappa value was 0.49 and the concordance rate was 0.76. We observed a significant correlation between tumor grade and the median of TSR (0.29 (95% CI: 0.032-0.51),  $p$ -value = 0.03).

## Conclusion

The agreement between pathologists in estimating these markers corresponds to poor-to-moderate agreement; implementing immune scores in daily practice requires more concentration in inter-observer agreements.

Literaturangaben:

[1] Kazemi, A. Gharib, M. Mohamadian Roshan, N. Taraz Jamshidi, S. Stögbauer, F. Eslami, S. Schüffler, Pj, (2023), Assessment of the Tumor-Stroma Ratio and Tumor-Infiltrating Lymphocytes in Colorectal Cancer: Inter-Observer Agreement Evaluation, *Diagnostic*, 2075-4418 (Print)

P.PersMed.02.04

## ***Beyond the norm - unforeseen outcomes in brain autopsies***

P. Grochowski, T. Schaller, I. Kleinlein, B. Märkl, F. Liesche-Starnecker

Universitätsklinikum Augsburg, Institut für Pathologie und Molekulare Diagnostik, Augsburg, Germany

### Background

The role of autopsies decreases in pathologists' routine in recent years. However, postmortal examination often deliver unexpected findings, adding relevant information to clinically known disease patterns. On example of brain autopsies, we present our experiences on patients diagnosed postmortal with relevant and unexpected diseases.

### Methods

The reports from all non-fetal autopsies conducted in our Institute between April 2022 and October 2023 were retrospectively evaluated for relevant neuropathological findings (reported according to a standardised form by pathology/neuropathology specialist) and compared to available clinical data, focusing on previously undiagnosed pathologies. Age-related and terminal changes, were not taken into account. If a brain autopsy was not performed, a case was not included in our register.

### Results

Brain examinations were performed in 180 of 219 autopsies. In overall 80 cases (44,4%) we detected the total of 96 relevant cerebral pathologies, of which 59 (61,5%) were not previously diagnosed. For 16 deceased (8,9%), cerebral involvement was main cause of death, however in 5 cases (2,8%) it was diagnosed only postmortal (two patients with spread of bacterial infection in CNS, one patient with IVLBCL, one with limbic encephalitis and one with brain oedema due to hypoxia). In another 7 cases (3,9%) incidental benign primary CNS tumours could be found (including 4 meningiomas, 1 pituitary adenoma, 1 pineocytoma, 1 craniopharyngioma). Accidental secondary tumours were diagnosed in nine cases (5%). Moreover, postmortal diagnosis of previously not detected strokes were made in 27 cases (15%) with majority ischemic (20 cases, 11%) and the rest haemorrhagic (7 cases, 3,9%). Finally the primary neurodegenerative diseases were diagnosed in 3 cases (1,7%), explaining the clinical course of symptomatic patients without prior diagnosis (1 case of Parkinson's disease, 2 cases of Alzheimer's disease). Although premortal clinically diagnosed, worth mentioning are also 2 fatal cases of Borna encephalitis.

### Conclusion

Whilst nowadays autopsies do not play such an important role in pathologists' routine, as they used to in the past, they can still deliver many unexpected and occasionally unusual findings, especially in examination of CNS. These results are possible only in cooperation with clinicians, but eventually they benefit from pathologists' findings, that contribute to better understanding of clinical patterns and finally help to improve the standard of care.

## ***Spinning disk confocal multiplex immunofluorescence for simultaneous assessment of tissue organization and subcellular protein quantification***

N. Pikki<sup>1</sup>, D. Papić<sup>1</sup>, J. Kluge<sup>1</sup>, S. Ugliano<sup>2</sup>, K. Bozek<sup>2</sup>, D. Horst<sup>1</sup>, S. Florian<sup>1</sup>

<sup>1</sup>Charité - Universitätsmedizin Berlin, Institut für Pathologie, Berlin, Germany, <sup>2</sup>Universität Köln, Center for Molecular Medicine Cologne CMMC, Köln, Germany

### **Background**

Multiplex immunofluorescence (IF) is used to quantify dozens of proteins on one tissue section, preserving their spatial context. Thus, multiple cell populations can be detected on the same slide and their interactions and relationships to each other can be assessed. However, while useful to understand tissue organization, so far, resolution and speed of this technology are too low to measure protein abundance and distribution at the subcellular level in larger patient cohorts. Thus, information about cellular morphology, which is of eminent importance to identify cell types and assess cell dignity in pathology, is completely ignored in multiplex IF studies.

### **Methods**

Here, we show that spinning disk confocal microscopy using water immersion makes high-resolution imaging of large patient collectives with a very high level of detail in x, y and z-planes possible. The higher resolution compared to established multiplex IF technologies allows accurate distinction of even small overlapping cells, e.g. lymphocytes in lymphoid follicles, and leads to a dramatic, up to 3x improvement of nuclear identification accuracy both by software and the human eye.

### **Results**

Moreover, we will show new morphological properties of normal cells like smooth muscle cells or epithelial cells in salivary glands that we discovered through this technology and have so far not been described. Finally, we will present first results from a high-throughput project based on this technology designed to reveal new therapeutic biomarkers in triple negative breast cancer (TNBC) by imaging tissues from 100 patients obtained at diagnosis (biopsy) and surgery (after neoadjuvant chemotherapy). In addition to established analysis strategies like determination of cellular neighborhoods, our image analysis strategy in this study will include measurements of subcellular protein localization and cell and organelle shape, which will serve to improve cell type identification and translate classic cellular attributes from histopathology into digitally quantifiable cell properties.

### **Conclusion**

We believe that the advantages of spinning disk confocal multiplex IF will facilitate the development of new biomarkers and generate new insights into tissue and tumor biology. Being based on commercially available microscopes, we are optimistic that this technology will find wide adoption in the cancer research community.

## ***Peptide-Level Batch Normalization Reduces Variance in Multiplexed Clinical Proteomics***

F. F. Dreßler

Charité - Universitätsmedizin Berlin, Institut für Pathologie, Berlin, Germany

### **Background**

Proteomic analyses are becoming increasingly available and are essential to answer many questions of clinical and preclinical research including the quantitation of targets for the novel ADC class of therapeutics. Technical variance and the quantitative multi-level read-out at the spectrum match, peptide and protein level pose challenges to optimal data quality. Proteomics of clinical cohorts rely increasingly on multiplexed assays to reduce measurement time and costs and to improve analysis depth and comparability across samples. We have previously examined and developed protein-level normalization strategies. Now, we investigated the effects of batch normalization in multiplexed assays at the peptide and protein level.

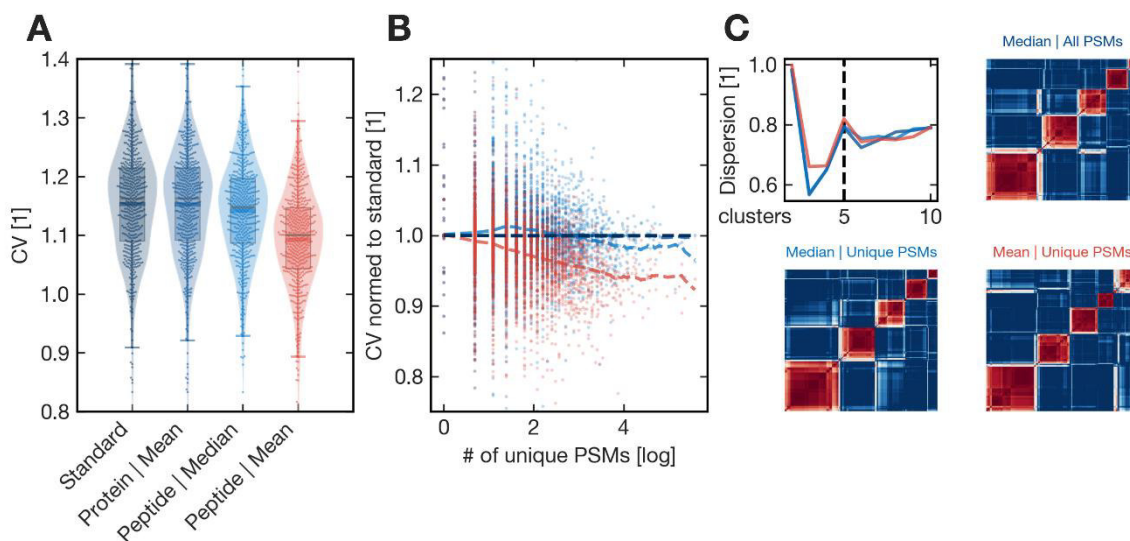
### **Methods**

We used a TMTpro-16-plex dataset with 29 sets/batches and a common pooled standard (always 134N). 69631 unique

peptides were mapped to 9542 distinct proteins. We normalized either the peptide abundances directly with their corresponding standard abundances (peptide-level normalization) or the sum of all protein-grouped peptides (protein-level). We combined peptide-level normalization with both mean and median of the resulting ratios. To evaluate the effect on the dataset, we calculated the protein-wise coefficients of variation (CV) and performed separate, unsupervised cluster analysis with consensus non-negative matrix factorization (NMF).

## Results

Peptide-level normalization with ratio averaging reduced the CVs considerably and showed a negative logarithmic relationship with the number of peptides, in line with theoretical expectations. Median peptide-level ratios showed a similar but reduced trend. These effects propagated to the NMF cluster level, where cross-run dispersion was improved with mean ratios.



The effects of batch normalization at different data levels. A: Coefficients of variation (CV); B: CVs stratified by the number of unique peptide spectrum matches (PSM); C: Consensus matrices of NMF with the different datasets.

## Conclusion

Clinical proteomics can be optimized at various levels, many of which are unique to this type of omics data. Batch effects of multiplexed proteomic assays should be normalized on the peptide level, prior to protein grouping with mean ratios.

P.PersMed.02.07

## ***Proteomic and immunopeptidomic landscape of non-small cell lung cancer***

A. Seredynska<sup>1,2</sup>, R. Fiestas Cueto<sup>1</sup>, L. Goncharenko<sup>1</sup>, A. E. Cabrita Figueiredo<sup>1</sup>, K. Kurowski<sup>1</sup>, P. Westermann<sup>3</sup>, P. Bronsert<sup>1</sup>, M. Werner<sup>1</sup>, C. Messner<sup>1</sup>, K. Baerenfaller<sup>3</sup>, O. Schilling<sup>1,2</sup>

<sup>1</sup>Institute for Surgical Pathology, Faculty of Medicine, Medical Center, University of Freiburg, Freiburg, Germany, <sup>2</sup>German Cancer Consortium (DKTK) and German Cancer Research Center (DKFZ), Heidelberg, Germany, <sup>3</sup>Swiss Institute of Allergy and Asthma Research (SIAF), University of Zurich, Davos, Switzerland

## Background

Non-small cell lung carcinoma (NSCLC) is the most common type of lung cancer, with adenocarcinoma (LUAD) and squamous cell carcinoma (LUSC) being the most prevailing histological subtypes with distinct biological signatures. Correct classification and accurate molecular profiling are essential for effective therapeutic guidance. Therefore, a correct distinction between LUAD and LUSC and deeper understanding of the molecular alterations on the protein level are required in order to detect biologically relevant biomarkers.

In this study, we aim to perform an in-depth mass spectrometry (MS)-based proteomic study of a large patient cohort representing the two aforementioned subtypes of NSCLC. The MS-based profiling of the LUAD and LUSC and their primary types revealed the proteomic alterations that might determine their clinical behaviour. High-coverage proteome

analysis gives the possibility to unravel the mechanisms of immune evasion in NSCLC. Moreover, the immunopeptidomics study should reveal the tumor-associated antigens, which are pivotal for the development of epitope-specific cancer immunotherapies.

### **Methods**

Patient-derived samples were processed with optimized, semi-automated single-pot, solid phase enhanced sample preparation (SP3-beads) workflow utilizing a pipetting BRAVO robot. Thereby, extracted proteins were digested and the resulting peptides were analyzed via liquid-chromatography tandem-mass spectrometry (LC-MS/MS). To study the immunopeptidome, a workflow for enrichment of HLA-I and HLA-II-bound antigens was established and optimized on a BRAVO robot for fresh frozen tissue.

### **Results**

The MS-analysis of the patient cohort (consisting of LUAD (n = 83), LUSC (n = 70) and tumor-adjacent (n = 138)) resulted in high proteome coverage of a total of 6951 proteins. Initial statistical analysis shows significant upregulation of CSTA, ITGA6 in LUSC, suggesting roles in tumor progression. Conversely, LUAD reveals elevated levels of SNTB1, DPP4 and MSLN. Further analysis suggests a possible distinction based on patient's gender. The immunopeptidomic pilot study allowed for identification of 1710 HLA-I and 6183 HLA-II peptides.

### **Conclusion**

Deep proteomic and immunopeptidomic coverage enables us to gain deeper insight into fundamental molecular biology of LUAD and LUSC. Ongoing proteomic analysis should unravel their key differences and give a promising outlook for the future development of therapies.

## **Poster Vergleichende Pathologie**

P.VergPath.01

### ***In-depth histological evaluation and comparison of mouse models for cholangiocarcinoma studies***

M. Tulesin<sup>1</sup>, S. Roessler<sup>2</sup>, A. Beckers<sup>3</sup>, D. Častven<sup>4</sup>, J. Marquardt<sup>4</sup>, K. Steiger<sup>1</sup>, T. H. Wirtz<sup>3</sup>, M.-L. Berres<sup>3</sup>, T. Groll<sup>1</sup>, C. Mogler<sup>1</sup>

<sup>1</sup>Institute of Pathology, Technical University of Munich, Munich, Germany, <sup>2</sup>Institute of Pathology, Heidelberg University Hospital, Heidelberg, Germany, <sup>3</sup>University Hospital RWTH Aachen, Department of Internal Medicine III, Aachen, Germany, <sup>4</sup>University Medical Center Schleswig-Holstein, Campus Luebeck, Department of Internal Medicine I, Luebeck, Germany

### **Background**

Cholangiocarcinoma (CCA) is an aggressive cancer arising in the bile ducts, known for its challenging late-stage detection and limited treatment options. It represents approximately 10-15% of liver cancers. Recent research has revealed new insights into CCA, highlighting its complex nature and exploring more effective treatment options, primarily focusing on mice studies. Therefore, the aim of this study is to characterize the existing mouse models used in the CCA research, compare their characteristics, and evaluate their ability to mimic human CCA, along with their respective advantages and challenges.

### **Methods**

In this study, we used tissue-based techniques, including classical H&E staining and immunohistochemistry, targeting 13 markers. We comprehensively evaluated their histomorphological profile, along with the tumor microenvironment (TME), across seven mouse models that are used in the CCA studies.

### **Results**

In our results, we have observed diverse CCA subtypes in the mouse models, with various tumor growth patterns, morphological variations, and TME changes. Additionally, we found preneoplastic liver lesions and other neoplastic lesions, such as hepatocellular carcinoma and non-neoplastic alterations of the liver parenchyma (e.g., steatosis).

### **Conclusion**

In conclusion, all of the examined mouse models proved to be suitable for the CCA research. However, we strongly

recommend that the objectives and targets of the CCA research be defined in advance, with a selection of the appropriate mouse model to ensure optimal model suitability for future studies.

P.VergPath.02

## ***miRNA profiling in intestinal tumors of dogs – a comparison of FFPE tissue and liquid biopsy***

A. Kehl<sup>1,2</sup>, H. Aupperle-Lellbach<sup>1,2</sup>, B. Schusser<sup>3</sup>, K.-P. Janssen<sup>4</sup>, K. Steiger<sup>2</sup>

<sup>1</sup>Laboklin GmbH&Co.KG, Bad Kissingen, Germany, <sup>2</sup>Technical University of Munich (TUM), Comparative Experimental Pathology, School of Medicine, München, Germany, <sup>3</sup>Technical University of Munich (TUM), Reproductive Biotechnology, School of Life Sciences Weihenstephan, Freising, Germany, <sup>4</sup>Technical University of Munich (TUM), Dept. of Surgery, School of Medicine, Klinikum rechts der Isar, München, Germany

### **Background**

Canine intestinal tumors include lymphoma, carcinomas, and spindle cell tumors. For diagnosis and prognosis, tissue sampling with histological examination is needed. Non-invasive diagnostics based on biomarkers in serum (liquid biopsy) would be great diagnostic progress to differentiate neoplastic from inflammatory lesions commonly induced by foreign bodies.

miRNAs are small, non-coding RNAs important for cell development, differentiation, and apoptosis by translational suppression or enhancement. They are supposed to play a role in oncogenesis by tumor-suppressive or oncogenic effects. miRNAs are potential biomarkers in different diseases since they are released into the bloodstream. The study aimed to investigate the usefulness of selected miRNAs as biomarkers in the differential diagnosis of neoplastic and inflammatory intestinal masses in dogs.

### **Methods**

miRNA profiles (miR-18b, 20b, 192, 194, 126, 214) in FFPE material derived from 27 carcinomas, 27 lymphomas, 18 inflammatory masses, and 17 healthy intestinal tissue samples were evaluated by digital droplet PCR. Additionally, the amount of these miRNAs was measured in the serum of 13 healthy dogs and dogs with carcinomas (n=8) or lymphomas (n=6). All samples were submitted for routine diagnostics at Laboklin GmbH&Co.KG.

### **Results**

Since miRNA profiles differed between large and small intestinal healthy tissues, groups were compared within small or large intestines, respectively. In the small intestine, down-regulation of miR-126 and 194 was observed in carcinoma samples. miR-20b, 126 and 194 in lymphoplasmacytic enteritis samples and miR-20b, 126, 214, 192 and 194 in T-cell lymphoma were down-regulated compared to healthy tissue. In the large intestine, miR-192 in enteritis samples, miR-18b and 192 in carcinoma and miR-126, 214, 192 and 194 in B-cell lymphoma samples were down-regulated. In contrast to tissue sample, in serum, miR-194 was up-regulated in carcinoma samples, and miR-214 was up-regulated in carcinoma and lymphoma, whereby the other miRNAs (miR-18b, 20b, 126 and 192) showed no differences.

### **Conclusion**

Some of our findings corresponded to results from human studies (i.e. miR-194 being down-regulated in colorectal adenomas), emphasising the need for further comparative studies to investigate the relevance of miRNAs in the development of intestinal neoplasms. Further investigation of a greater number of samples, and especially corresponding serum samples, is needed to determine the potential of selected miRNAs as biomarkers.

P.VergPath.03

## ***Spatial transcriptomics reveal multiple clusters in murine pancreatic preneoplastic lesions***

T. Metzler<sup>1,2</sup>, J. Wirth<sup>1,2</sup>, E.-M. Mayr<sup>2</sup>, S. Chakraborty<sup>2</sup>, N. Pfarr<sup>2</sup>, J. Höbart<sup>3</sup>, J. Ruland<sup>3</sup>, K. Steiger<sup>1,2</sup>

<sup>1</sup>Technical University of Munich, Comparative Experimental Pathology (CEP), Munich, Germany, <sup>2</sup>Technical University of Munich, Institute of General and Surgical Pathology, Munich, Germany, <sup>3</sup>Technical University of Munich, Institute of Clinical Chemistry and Pathobiochemistry, Munich, Germany



## Background

Mouse models with a targeted conditional mutation in the *KRAS* gene are commonly used in the research of pancreatic ductal adenocarcinoma (PDAC). Besides invasive carcinomas these models also develop preneoplastic precursor lesions. Mouse pancreatic intraepithelial neoplasia (mPanIN) originate from pre-existing ducts and resemble human PanIN-lesions. The role of mucinous tubular complexes (MTCs), which are morphologically similar to mPanIN, but develop from acinar cells that undergo acinar-ductal metaplasia (ADM), is not yet fully investigated. The aim of this study was to gain further insight into differential gene expression of morphologically similar lesions on a spatial resolution.

## Methods

The pancreata of five p48<sup>Cre/+</sup>;LSL-Kras<sup>G12D</sup> mice between three and six months of age were histologically analysed on HE slides and their transcriptoms subsequently analysed on a spatial resolution using the “Visium Spatial Gene Expression” technology (10x Genomics, Pleasanton, CA, USA). The data was further analysed with Python using the scanpy framework.

## Results

Preliminary results show multiple transcriptional clusters in areas of normal pancreatic acini, preneoplastic lesions and stroma that match well the morphologic annotations of the respective areas. Comparison of differentially expressed genes between different clusters and annotated regions already led to promising candidates for further evaluation and possible use as immunohistologic (IHC) surrogate markers.

## Conclusion

Our preliminary results suggest transcriptional heterogeneity in regions of pancreatic preneoplastic lesions that need to be further investigated and might lead to a better understanding of the development of pancreatic cancer in mouse models and human patients.

P.VergPath.04

## ***β6-integrin expression in genetically engineered mouse models: mouse versus human***

S. Ballke<sup>1</sup>, L. Löprich<sup>2</sup>, T. Kaltenbacher<sup>2</sup>, R. Rad<sup>2</sup>, T. Groll<sup>1</sup>, W. Weichert<sup>1</sup>, J. Notni<sup>3</sup>, K. Steiger<sup>1</sup>

<sup>1</sup>Technische Universität München, School of Medicine and Health, Institut für Pathologie, Comparative Experimental Pathology, München, Germany, <sup>2</sup>Technische Universität München, School of Medicine and Health, Institut für Molekulare Onkologie und Funktionelle Genomik, München, Germany, <sup>3</sup>Targeted Radiopharmaceuticals In Molecular Theranostics (TRIMT) GmbH, Radeberg, Germany

## Background

αvβ6-integrin belongs to a class of 24 transmembrane cell adhesion receptors. It is solely expressed by epithelial cells and upregulated in a variety of carcinomas. It promotes cancer invasion and is linked to poor prognosis, making it a promising target for theranostics. An elevated β6-integrin expression was found in several carcinomas of different entities. Pancreatic ductal adenocarcinomas (PDACs) showed a high expression of β6-integrin in primary tumors (88%) [1]. Several genetically engineered mouse models (GEMMs) are used for cancer research in PDAC and other cancer entities. Therefore, it is of exceptional scientific interest, if GEMMs used for cancer research are appropriate models for β6-integrin screening to allow subsequent translation into human applications.

## Methods

13 PDACs und 5 adenocarcinomas of the lung from two different GEMMs (A: p48-Cre<sup>ki/+</sup>; LSL-Kras<sup>ki/+</sup> and B: Hnf1b<sup>ki/+</sup>; p53<sup>loxki/ki</sup>; LSL-Kras<sup>ki/+</sup>) were evaluated. Samples were fixed in 10% neutral-buffered formalin and routinely processed for histology. Tissue was examined by using anti-ITGB6 antibody (ab229552, dilution 1:500, abcam). Slides were digitalized and evaluated by using Aperio ImageScope (Leica Biosystems). A modified score [2] including intensity and frequency of membranous β6-integrin expression was applied. Results were compared to our findings from a human cohort (103 cases of Non-small cell lung cancer (NSCLCs), thereof 83 adenocarcinomas) and to the published results from PDACs [1].

## Results

All five adenocarcinomas of the lung from mouse model B did not show any positivity for  $\beta 6$ -integrin expression. In contrast, 80.6% of human NSCLCs displayed a strong (54.4%) or moderate (26.2%) positive staining. In murine PDACs no (84.6%) or low (15.4%)  $\beta 6$ -integrin expression was noticed.

## Conclusion

The present results show that the promising data for membranous  $\beta 6$ -integrin expression from human cohorts of PDAC and NSCLC is not reflected in corresponding and commonly used GEMMs. This indicates that complex GEMMs used in cancer research may not be necessarily suitable regarding their experimental  $\beta 6$ -integrin expression and therefore should be screened thoroughly before translating results into human applications.

Literaturangaben:

[1] Steiger, K., et al., (2021), There is a world beyond  $\alpha 5\beta 1$ -integrin: Multimeric ligands for imaging of the integrin subtypes  $\alpha 5\beta 1$ ,  $\alpha 5\beta 2$ ,  $\alpha 5\beta 3$ , and  $\alpha 5\beta 4$  by positron emission tomography., *EJNMMI Res*, p.106, 11(1)

[2] Sipos, B., et al., (2004), Immunohistochemical screening for  $\beta 6$ -integrin subunit expression in adenocarcinomas using a novel monoclonal antibody reveals strong up-regulation in pancreatic ductal adenocarcinomas in vivo and in vitro., *Histopathology*, p. 226-236, 45(3)

P.VergPath.05

## ***Subtyping of murine pancreatic ductal adenocarcinoma (mPDAC)***

L. Arps<sup>1,2</sup>, S. Müller<sup>3,4</sup>, M. Zukowska<sup>3,4</sup>, D. Saur<sup>3,4,5</sup>, R. Rad<sup>3,4,5</sup>, M. Reichert<sup>4,5</sup>, I. Heid<sup>6</sup>, H. Trabelssi<sup>6</sup>, N. Wirges<sup>1</sup>, R. Klopffleisch<sup>2</sup>, K. Steiger<sup>1,5</sup>

<sup>1</sup>Institut für Allgemeine Pathologie und Pathologische Anatomie der TU München, München, Germany, <sup>2</sup>Institut für Tierpathologie der Freien Universität Berlin, Berlin, Germany, <sup>3</sup>TranslaTUM - Zentralinstitut für translationale Krebsforschung der TU München, München, Germany, <sup>4</sup>Innere Medizin II, MRI TU München, München, Germany, <sup>5</sup>Deutsches Konsortium für Translationale Krebsforschung (DKTK), Deutsches Krebsforschungszentrum (DKFZ), Heidelberg, Germany, <sup>6</sup>Interventionelle Radiologie, MRI TU München, München, Germany

## Background

Murine pancreatic ductal adenocarcinoma (mPDAC) replicates the multi-stage progression of human PDAC (hPDAC), the most common pancreatic malignant tumour. Therefore, detecting mPDAC subgroups comparable to human findings is of great interest. At the transcriptome level, one mesenchymal (C1) and three epithelial (C2a, C2b and C2c) mPDAC subtypes were identified.<sup>1</sup> The project aims to detect immunohistochemical surrogate markers to differentiate the epithelial subtypes on histological slides.

## Methods

Based on RNA sequencing data from 38 mPDAC cell lines generated from different genetically engineered mouse models of PDAC<sup>1</sup>, 33 markers were selected, and 28 were established on mouse tissue and analysed immunohistochemically in 29 mPDAC cell pellets. The percentage of positive tumour cells and staining intensity were investigated semi-quantitatively. The markers were further tested on 32 mPDAC orthotopic transplant tumours.

## Results

In the cell pellets, 2 of 28 markers, Nectin (NDN) and Placenta associated 8 (PLAC8), showed differential staining of the subtypes, analogous to the RNA sequencing data. PLAC8 showed lower expression in C2a compared to C2b ( $p = 0,001$ ) or C2c ( $p < 0.001$ ). NDN is more strongly expressed in C2a in contrast to C2b ( $p < 0.001$ ) or C2c ( $p = 0,005$ ). Transplant tumours of subtypes C2b and C2c showed strong staining with NDN in more than 2 % of the tumour cells. In C2a, no cells were stained at this high intensity, and less than 2 % of the cells showed weak to moderate staining. At least 20 % of the tumour cells of C2b and C2c stained moderate to strong with PLAC8, whereas less than 20 % of the cells were stained with the same intensity in C2a.

## Conclusion

Our preliminary results indicate that NDN and PLAC8 may be potential surrogate markers for differentiating the mouse model's mPDAC subtypes C2a and C2b or C2c. Further investigations in endogenous mPDAC tumours have yet to validate their suitability, but they might enable further translational characterisation of mPDAC compared to hPDAC.

1. Mueller S, Engleitner T, Maresch R, et al. Evolutionary routes and KRAS dosage define pancreatic cancer phenotypes. *Nature*. 2018 Feb 1;554(7690):62-68. doi: 10.1038/nature25459. Epub 2018 Jan 24. PMID: 29364867; PMCID: PMC6097607.

P.VergPath.06

## ***Pathology Skills Lab: Tumor models in pathology teaching***

M. Bernhardt, C. Sanders, O. Hommerding, T. Kreft, D. Nagy, X. Zhou, G. Kristiansen  
Universitätsklinikum Bonn, Institut für Pathologie, Bonn, Germany

### **Background**

Demographic change and an aging workforce leading to a shortage in pathologists requires innovative approaches to attract medical students to the field [1][2]. Medical education must aim at teaching skills and competences and address different learning styles to ensure that all students are successful [3][4].

### **Methods**

“Practical Pathology” is a pilot project that aims to enhance students' understanding of pathology. It provides hands-on experience in macroscopic gross analysis by using tumor models built from scratch.

### **Results**

A survey evaluating the program, completed by 63 participating students, yielded positive feedback regarding the course methodology. Students emphasized its relevance in understanding the pathology workflow and its superiority over traditional teaching methods. The majority acknowledged the significance of hands-on training in medical education, with those having prior work experience expressing particularly favorable views on the course's impact on knowledge acquisition.

### **Conclusion**

The course enhanced students' understanding of pathological processes and potential sources of clinical-pathological misinterpretation. An increase in motivation for a potential career in the field of pathology was observed in a minority of students, although this exceeded the percentage of pathologists in the total medical workforce.

Literaturangaben:

[1] Bundesärztekammer, (2022), Ärzttestatistik 2022, <https://www.bundesaerztekammer.de/baek/ueber-uns/aerzttestatistik/2022>, 2023-10-31

[2] Kasch, R; Engelhardt, M; Förch, M; Merk, H; Walcher, F; Fröhlich, S, (2016), Ärztemangel: Was tun, bevor Generation Y ausbleibt? Ergebnisse einer bundesweiten Befragung, *Zentralblatt für Chirurgie*, 2

[3] Leite, W; Svinicki, M; Yuying, S, (2010), Attempted Validation of the Scores of the VARK: Learning Styles Inventory With Multitrait–Multimethod Confirmatory Factor Analysis Models, *Educational and Psychological Measurement*, 2

[4] (2021), Nationaler Kompetenzbasierter Lernzielkatalog Medizin (NKLM) 2.0, Medizinischer Fakultätentag der Bundesrepublik Deutschland, 7, <https://nkml.de/zend/menu>, 2024-02-24

## **Poster Gynäko- und Mammopathologie**

P01.01

### ***An Extremely Rare Differential Diagnosis – Metaplastic Papillary Tumour of the Fallopian Tube***

A. Vlaški, V. Neukunft, F. Klauschen, D. Mayr  
Pathologisches Institut LMU, Pathologie, München, Germany

### **Background**

Metaplastic papillary tumour of the fallopian tube (MPT) is a very unusual lesion, which has been described 13 times in the literature so far. The previous research has proven the metaplastic nature of the MPT, distinguishing it from a true neoplasm.

## Methods

In this case report we would like to present MPT, which we have recently diagnosed at our Institute, with its morphological features and immunohistochemical profile.

## Results

A 67-year-old woman underwent gynecological surgery because of a cystic ovarian lesion suspected to be endometriosis.

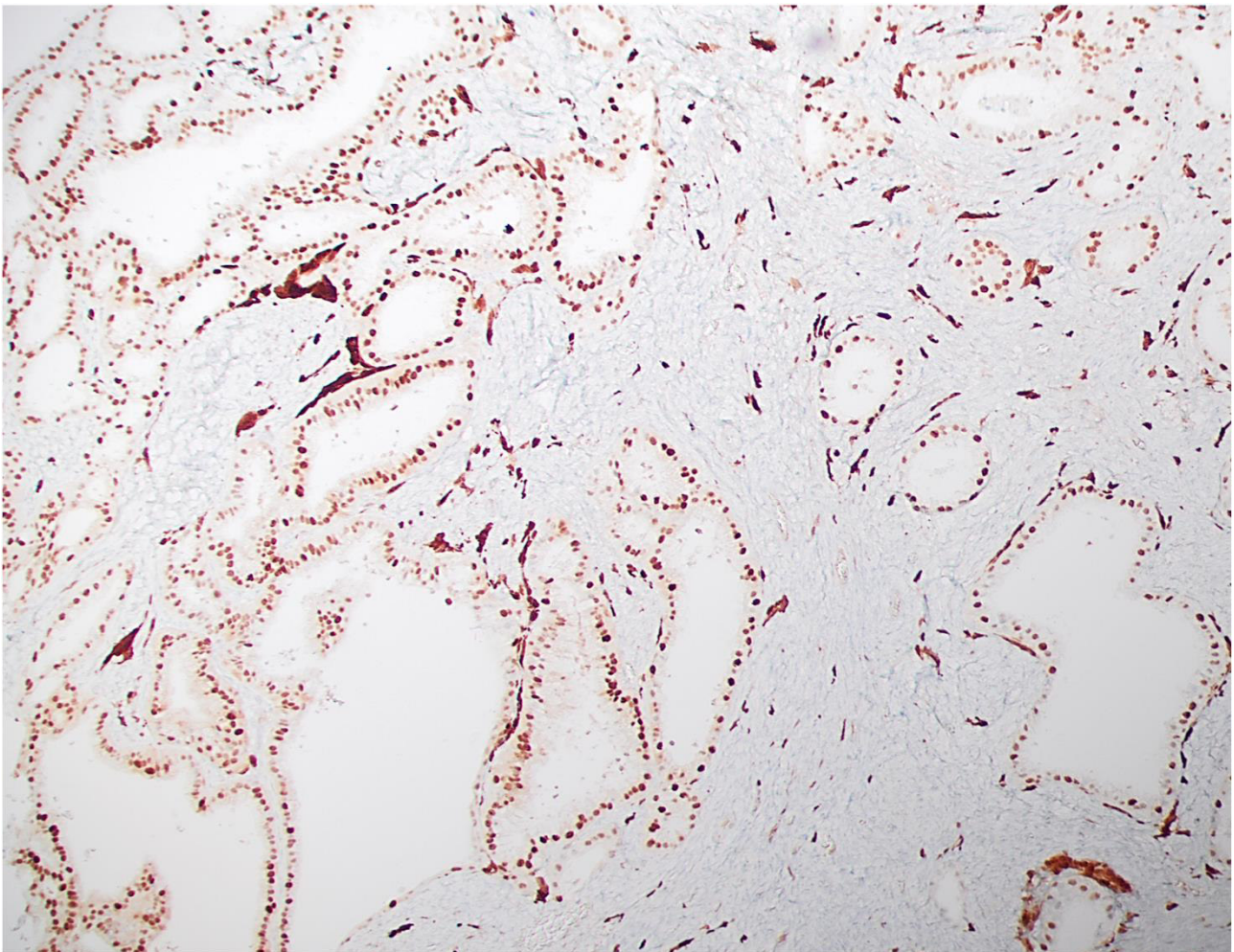
An indistinct 1.5 cm measuring lesion in the paratubal soft tissue was an additional finding. Histopathological examination revealed ovarian serous cysts and a paratubular tubulocystic lesion, consisting of narrow stroma, covered by a single-layer epithelium. The epithelial lining consisted of predominantly cylindrical, partly cuboid cells, which appeared to be occasionally mucinous and oncocytic. The cell nuclei showed modest differences in their size, with focally slight atypia and prominent nucleoli. The back-to-back appearance of these structures was observed.

Immunohistochemical examination demonstrated PAX8, BerEP4, estrogen and progesterone receptors positivity and focally positivity for CDX-2. Nuclear expression of Cyclin D1 was observed (Figure 1). The proliferation index was 2-3%. A wild-type p53 pattern was revealed.

Based on the morphology, microscopical features and immunohistological findings, we classified this papillary, hormone receptor and PAX8 positive, low proliferative paratubular lesion with nuclear expression of Cyclin D1 as a benign, metaplastic papillary lesion of the fallopian tube.

## Conclusion

The importance of the metaplastic papillary tumour of the fallopian tube, as an extremely rare lesion, is reflected in its differentiation from other entities, especially borderline tumours and serous tubal intraepithelial carcinoma. MPT should be presented to clinicians as a condition with an indolent clinical course.



Cyclin D1: nuclear positivity, Magnification: 100x

Literaturangaben:

- [1] Jang MI, Sung JY, Kim JY, et al. , (2017), Metaplastic Papillary Tumor of the Fallopian Tube, *Anticancer Res.* , 3693-701, 37(7), 2023-12-20
- [2] Salazar MF, Moscoso IE, Vázquez LT, et al. , (2015), Fallopian Metaplastic Papillary Tumour: An Atypical Transdifferentiation of the Tubal Epithelium? , *J Pathol Transl Med*, 148-55, 49(2), 2024-01-05
- [3] Solomon AC, Chen PJ, LiVolsi VA., (2003), Pathologic quiz case: an incidental finding in the fallopian tube. Fallopian tube, left, tubal ligation: metaplastic papillary tumor of fallopian tube, *Arch Pathol Lab Med*, e363-4, 127(8), 2023-12-05
- [4] Sunitsch S, Reisinger J, Abete L, et al. , (2020), Metaplastic papillary tumour of the fallopian tube, a rare entity, analysed by next-generation sequencing, *Histopathology*, 923-7, 76(6), 2024-01-14
- [5] WHO Classification of Tumours, (2020), Female Genital Tumours, IARC Press, Lyon, Tumours of the fallopian tube., 2024-01-20

P01.02

## ***Expression of circular LSD1 RNAs and LSD1 protein in endometrial cancer***

M. M. Anokhina<sup>1</sup>, R. Sander<sup>1</sup>, V. M. Wildhagen<sup>1</sup>, C. Neppi<sup>1</sup>, W. Göring<sup>1</sup>, M. Schlensog<sup>1</sup>, E. Ruchhaeberle<sup>2</sup>, W. Meier<sup>2</sup>, T. Fehm<sup>2</sup>, T. T. Rau<sup>1</sup>

<sup>1</sup>Institut für Pathologie, Universitätsklinikum Düsseldorf, Düsseldorf, Germany, <sup>2</sup>Klinik für Gynäkologie und Geburtshilfe, Universitätsklinikum Düsseldorf, Düsseldorf, Germany

### **Background**

LSD1 is often overexpressed in many cancers types and is associated with poor prognosis and high risk of metastasis regulating both, gene repression and activation. Our recent findings in lung cancer cells demonstrate that LSD1 also regulates its own transcription. We identified new circular LSD1-RNAs, derived from the LSD1 gene locus<sup>1</sup>, whose back-splicing was found to compete with the canonical alternative splicing (AS) regulating expression of LSD1 isoforms that differ in the alternative exon2a and are thought to have distinct functions. The role of LSD1 in endometrial carcinoma (EC) is poorly investigated. The question how LSD1 RNA/protein isoforms are expressed in tumor/normal endometrial tissues as well as whether/how circular *LSD1*-RNAs can regulate expression and AS of LSD1 in different molecular subtypes of EC (POLEmut, MMRdef, NSMP, P53abn) was investigated.

### **Methods**

Using RT-qPCR specific to *LSD1* mRNA and circ*LSD1*-RNAs isoforms the expression level of LSD1 RNA species in cancer versus normal tissues in the advanced stage endometrial carcinoma cohort of N= 55 cases was quantified and compared with LSD1 immunostaining. Molecular subtyping of the cohort has been initiated with a half of the cases ready for analysis. Additionally, functional cell culture experiments representing the four molecular subtypes were initiated.

### **Results**

Circ*LSD1*-RNAs were found to be expressed in normal endometrial tissue and downregulated in the tumor. The expression level of LSD1 mRNA in tumor/normal tissue was found not always consistent with LSD1 immunostaining suggesting accumulation of LSD1 protein in tumor cells although the *LSD1* transcription was decreased. Exon2a+ *LSD1* mRNA expression correlated with exon2a containing circ*LSD1* RNAs. In cell culture experiments, the viability of TP53 and POLE mutated cell lines was reduced upon overexpression of circ*LSD1*-RNAs, whereas knockdown of circ*LSD1*-RNAs resulted in significantly increased viability.

### **Conclusion**

LSD1 emerges as a functional relevant biomarker in endometrial carcinoma. Its regulation via circRNAs across entities underpins their pivotal role. Furthermore, cell lines with the different mutational backgrounds responded differently to treatment with LSD1 inhibitors indicating a possible clinical applicability in the future. Thus, the detailed mechanism of how circ*LSD1*-RNAs affect AS and transcription of LSD1 will be deepened by our working group.

Literaturangaben:

- [1] Galang, J.N.; Shen, Y.; Koitzsch, U; Yu, X.; Eischeidt-Scholz, H.; Bachurski, D.; Rau, T.T.; Neppi, C.; Herling, M.; Bulimaga, B.; Vasyutina, E.; Schweiger, M. R.; Büttner, R.; Odenthal, M.; Anokhina, M.M, (2023), Vesicular release and uptake of circular LSD1-RNAs from non-cancer and cancer lung cells, *Int. J. Mol. Sci.*, <https://doi.org/10.3390/ijms241813981>.

P01.03

### ***Prostate specific membrane Antigen (PSMA) expression in Endometrial carcinoma and its metastases***

K. Kurowski<sup>1</sup>, V. Guyon<sup>2</sup>, I. Juhasz-Böss<sup>2</sup>, C. Unger<sup>2</sup>, M. Werner<sup>1,3,4</sup>, P. Bronsert<sup>1,3,4</sup>

<sup>1</sup>Universitätsklinikum Freiburg, Institut für Klinische Pathologie, Freiburg, Germany, <sup>2</sup>Universitätsklinikum Freiburg, Klinik für Frauenheilkunde und Geburtshilfe, Freiburg, Germany, <sup>3</sup>Universitätsklinikum Freiburg, Core Facility für Histopathologie und digitale Pathologie Freiburg, Freiburg, Germany, <sup>4</sup>Universitätsklinikum Freiburg, Tumorbank Comprehensive Cancer Center Freiburg, Freiburg, Germany

#### **Background**

Endometrial cancer is the fifth most common cancer among women in Germany. In the metastatic stage, the five-year survival rate in Germany is approximately 20%. This study focuses on Prostate-Specific Membrane Antigen (PSMA), a marker known for its diagnostic and predictive value in prostate cancer, and its expression in endometrial carcinoma. The aim of the presented study was to investigate PSMA expression in tumor cells and neovasculature of primary and metastatic endometrial cancer. The results are correlated with clinical and pathological parameters.

#### **Methods**

Tissue samples from 123 patients, who underwent primary surgical treatment for endometrial carcinoma, were examined. A Tissue Microarray (TMA) was created, consisting of up to three samples from the central tumor tissue and two samples from the tumor periphery, as well as up to three samples from metastases. Immunohistochemical staining of the TMA was performed using CD31 (clone JC70A from Dako, Carpinteria, USA) as an endothelial cell marker to determine overall vascular density, along with staining using a PSMA antibody (clone 3E6 from Dako). Subsequently, a digital-assisted analysis of the stained TMA sections was conducted using the image analysis program QuPath® (University of Edinburgh, Scotland).

#### **Results**

Tumor cells were PSMA positive in 73.2% of primary tumor samples. In 68.3% of cases, over 59.6% (25th percentile) of tumor vessels were PSMA positive. The log-rank analysis and the univariate Cox regression showed statistically significant correlations between PSMA expression in tumor neovasculature and both overall and progression-free survival.

#### **Conclusion**

The findings suggest that PSMA could function as a notable prognostic and predictive factor in patients with endometrial carcinoma receiving PSMA-targeted therapies, potentially significantly augmenting their prognosis.

P01.04

### ***Predictive biomarkers in uterine cervical cancer - Immunohistochemical analyzation of Her2, Tissue factor, Folate receptor alpha, Trop2, CDH6, Nectin4 and cMet in cervical cancer***

H. Lisiecki, T. Groll, N. Schmid, K. Steiger, K. Schwamborn, C. Mogler, E. Schmoedel  
Institut für Pathologie der Technischen Universität, München, Germany

#### **Background**

Uterine cervical cancer is the fourth most common cancer in woman globally (after breast, colorectal and lung cancer). In recent decades, prevention programs and HPV-vaccination have made great progress and led to a decrease of incidence rates. Nevertheless, the prognosis for patients with advanced disease is still poor. According to data from the USA the 5-year relative survival rate for cervical cancer is about 90%. However, in case of distant metastasis the 5-year relative survival rate decreases to 20% (data <https://www.cancer.gov>).

With regard to the potential use of antibody drug conjugates (ADCs) we analyzed immunohistochemical targets including Her2, Tissue factor, Folate receptor alpha, Trop2, CDH6, Nectin4, and cMet in a cohort of cervical cancer.

#### **Methods**

The study group encompasses 81 cases of uterine cervical cancer, including 57 squamous cell carcinomas, 20

adenocarcinomas and 4 adenosquamous carcinomas. The targets were analyzed by immunohistochemistry on a tissue micro-array (TMA). To test whether the results on small samples are representative for larger tumor samples, additionally, 20% of the samples were analyzed utilizing whole tissue sections. Furthermore, we analyzed matched samples from metastases (12 lymph node metastases and 7 distant metastases) and compared the results to the primary tumor.

## Results

Her2 score 3+ was found in 2.6 % of cases, 2+ in 2.6 % and 1+ in 9.0 %. Trop2 showed strong expression (immunoreactive score (IRS) 9-12) in 41.0 % and intermediate expression (IRS 4-8) in 52.6 %. Tissue factor showed strong expression in 13.9 % and intermediate expression in 55.7 %. Folatreceptor alpha was intermediately expressed in 2.6 % and weakly expressed (IRS 2-3) in 1.3 % and was completely negative in 96.2 % of cases. Further investigations and statistical analyses for CDH6, Nectin4, and cMet as well as comparison to whole tissue sections and metastases are currently being processed.

## Conclusion

This study aims to investigate potential targeted therapy approaches in uterine cervical carcinomas. So far, we could show that Her2, Tissue factor and Trop2 could represent potential therapeutic targets, whereas Folatreceptor alpha appears to be less significant. In the current literature there is also evidence for Her2 and Tissue factor as promising new treatment options. Analyses regarding the remaining targets are currently in process.

P01.05

## ***Trop-2 expression in carcinoma of the uterine cervix - a possible target for the treatment approach with antibody drug conjugates (ADC)***

M. Forberger<sup>1</sup>, B. Wolf<sup>2</sup>, A. Freude<sup>3</sup>, G. G. R. Hiller<sup>3</sup>, S. Droste<sup>2</sup>, A. K. Höhn<sup>3</sup>, L.-C. Horn<sup>3</sup>

<sup>1</sup>University Hospital Leipzig, Institute of Pathology, Leipzig, Germany, <sup>2</sup>University Hospital Leipzig, Division of Gynecologic Oncology, Department of Obstetrics and Gynecology, Leipzig, Germany, <sup>3</sup>Institute of Pathology, University Hospital Leipzig, Leipzig, Germany

## Background

The Trophoblast Cell Surface Antigen 2 (TROP-2) is associated with invasiveness and tumor progression in several malignancies [1]. Strong TROP-2-expression is associated with poor prognosis in cervical carcinoma [2]. Recently, TROP-2 was identified as a target protein for treatment of solid tumors using antibody-drug conjugates (ADC; [3]). The data for the expression of Trop2 in cervical carcinoma is limited [4].

## Methods

Trop2 expression was evaluated using an H-score as previously described [2] [5]. The staining intensity (SI) was scored as negative (0), weak (1), moderate (2) or strong (3). The percentage of positively stained tumor cells was calculated as 0 (complete negative staining of tumor cells), 1 (1-10% positive stained tumor cells), 2 (11-50%) and 3 (51-100%). Overall staining results were calculated by SI x percentage staining. The overall staining scores of Trop2 correlated with the histological subtype of cervical carcinoma and p16-expression as a surrogate marker for HPV-association. The evaluation of immunohistochemistry for Trop2 was blinded to the p16-status.

## Results

100 cases of cervical carcinoma were included in the study. 79 represented squamous (SCC) and 21 adenocarcinomatous (AC) histology. Overall 5% were negative for p16-immunostaining (4 AC, 1 SCC). All cases represented at least moderate diffuse expression of Trop2. There were no differences between histologic subtype ( $p > 0.05$ ), nor p16-expression status ( $p > 0.05$ ).

## Conclusion

It has been shown that the antibody drug conjugate (ADC) topoisomerase-1-inhibitor irinotecan, coupled via a linker to a humanised IgG1k-antibody hRS7 binding to TROP-2 (i.e. sacituzumab) represents an effective treatment approach to several carcinoma types [3]. All examined cases showed at least moderate staining for TROP-2 within the tumor cells. So, TROP-2 may represent a potential target for ADC in cervical cancer. There are no differences of TROP-2 expression within the different histological subtypes (SCC vs. AC) and p16-expression (positive vs. negative).



Literaturangaben:

- [1] Cubas R, Zhang S, Li M, Chen C, Yao Q, (2010), Trop2 expression contributes to tumor pathogenesis by activating the ERK MAPK pathway, *Mol Cancer.*, 253
- [2] Liu T, Liu Y, Bao X, Tian J, Liu Y, Yang X, (2013), Overexpression of TROP2 predicts poor prognosis of patients with cervical cancer and promotes the proliferation and invasion of cervical cancer cells by regulating ERK signaling pathway. , *PLoS One*, 75864
- [3] Bardia A, Messersmith WA, Kio EA, Berlin JD, Vahdat L, Masters GA, Moroosse R, Santin AD, Kalinsky K, Picozzi V, O'Shaughnessy J, Gray JE, Komiya T, Lang JM, Chang JC, Starodub A, Goldenberg DM, Sharkey RM, Maliakal P, Hong Q, Wegener WA, Goswami T, Ocean AJ, (2021), Sacituzumab govitecan, a Trop-2-directed antibody-drug conjugate, for patients with epithelial cancer: final safety and efficacy results from the phase I/II IMMU-132-01 basket trial., *Ann Oncol.*, 746-756
- [4] Dum D, Taherpour N, Menz A, Höflmayer D, Völkel C, Hinsch A, Gorbokon N, Lennartz M, Hube-Magg C, Fraune C, Bernreuther C, Lebok P, Clauditz TS, Jacobsen F, Sauter G, Uhlig R, Wilczak W, Steurer S, Minner S, Marx AH, Simon R, Burandt E, Krech T, Luebke AM, (2022), Trophoblast Cell Surface Antigen 2 Expression in Human Tumors: A Tissue Microarray Study on 18,563 Tumors., *Pathobiology*, 245-258
- [5] Bignotti E, Zanotti L, Calza S, Falchetti M, Lonardi S, Ravaggi A, Romani C, Todeschini P, Bandiera E, Tassi RA, Facchetti F, Sartori E, Pecorelli S, Roque DM, Santin AD, (2012), Trop-2 protein overexpression is an independent marker for predicting disease recurrence in endometrioid endometrial carcinoma., 22

P01.06

### ***Prognostic impact of peritumoral stromal response in surgically treated carcinoma of the uterine cervix***

L.-C. Horn<sup>1</sup>, B. Wolf<sup>2</sup>, G. G. R. Hiller<sup>1</sup>, S. Droste<sup>2</sup>, L. Weydandt<sup>2</sup>, A. K. Höhn<sup>1</sup>

<sup>1</sup>Institute of Pathology, University Hospital Leipzig, Leipzig, Germany, <sup>2</sup>University Hospital Leipzig, Division of Gynecologic Oncology, Department of Obstetrics and Gynecology, Leipzig, Germany

#### **Background**

Desmoplastic stromal response (DSR) is on hallmark of infiltrative tumor growth in morphology and mainly driven by the switch of stromal fibroblast into cancer associated (myo-) fibroblasts (CAF; [1]). For tongue squamous cell carcinomas it has been reported that high DSR was associated with a significant higher rate of lymph node spread and reduced 5-year recurrence free survival. In vulvar cancer DSR is associated with higher rate of inguinal lymph node involvement and poor prognosis [2]. The knowledge about the prognostic impact of DSR in cervical carcinoma (CX) is limited [3] [4].

#### **Methods**

438 patients with primarily surgical treated CX (tumor stage >pT1b1) by radical hysterectomy using the TMMR approach were routinely examined for the presence and the grade of DSR. DSR correlated to clinicopathologic data and prognostic outcome.

#### **Results**

DSR was present in 80.6% of cases and was associated with a significantly higher frequency of lymphovascular space (76.5 vs. 56.5%,  $p < 0.001$ ) and venous involvement (14.4 vs. 2.4%,  $p < 0.001$ ). Pelvic lymph node metastasis was more common in patients with DSR (23.0 vs. 11.8%,  $p < 0.05$ ). Most strikingly, DSR was significantly more frequent in tumors with parametrial involvement (i.e. pT2b; 47.3 vs. 17.6 %,  $p < 0.0001$ ). These prognostically negative parameters in patients with desmoplastic disease translated into inferior overall (80.2% vs. 94.5% hazard ratio [HR] 3.8 [95%-CI 1.4 – 10.4],  $p = 0.002$ ) and recurrence-free survival (75.3% vs. 87.3%, HR 2.3 [95%-CI 1.2 – 4.6],  $p = 0.008$ ).

#### **Conclusion**

In the present study, DSR was associated with a more aggressive phenotype of cervical cancer and inferior survival. Previous studies have shown that DSR is associated with high tumor cell dissociation in CX [5] and CD34<sup>low</sup> and SMA<sup>high</sup> represent the immunohistochemical stromal signature in CX. Targeting desmoplasia may be a promising treatment approach in the future [6].

Literaturangaben:

- [1] Jordan SM, Watanabe T, Osann K, Monk BJ, Lin F, Rutgers JK, (2012), Jordan SM, Watanabe T, Osann K, Monk BJ, Lin F, Rutgers JK. Desmoplastic stromal response as defined by positive  $\alpha$ -smooth muscle actin staining is predictive of invasion in adenocarcinoma of the uterine cervix., *Int J Gynecol Pathol.*, 369-76



- [2] Holthoff ER, Byrum SD, Mackintosh SG, Kelly T, Tackett AJ, Quick CM, Post SR, (2017), Vulvar squamous cell carcinoma aggressiveness is associated with differential expression of collagen and STAT1. , Clin Proteomics., 40
- [3] Horn L-C, Richter CE, Hentschel B, et al., (2005), Juxtatumoral desmoplastic stromal reaction is associated with high tumor cell dissociation in squamous cell carcinomas of the uterine cervix. , Ann Diagn Pathol.
- [4] Wolf B, Weydandt L, Dornhöfer N, Hiller GGR, Höhn AK, Nel I, Jain RK, Horn LC, Aktas B., (2023), Desmoplasia in cervical cancer is associated with a more aggressive tumor phenotype., Sci Rep.
- [5] Horn LC, Schreiter C, Canzler A, Leonhardt K, Eienkel J, Hentschel B, (2013), CD34(low) and SMA(high) represent stromal signature in uterine cervical cancer and are markers for peritumoral stromal remodeling., Ann Diagn Pathol.
- [6] Beavis PA, Slaney CY, Kershaw MH, Gyorki D, Neeson PJ, Darcy PK, (2016), Reprogramming the tumor microenvironment to enhance adoptive cellular therapy., Semin Immunol. , 64-72

P01.07

### ***Anti-HPV16/18-E6 (Clones: C1P5, BF7), Anti-HPV18-E7 (Clone: 8E2) and Anti-HPV (Clone: K1H8) Antibodies are Not Suited to Replace the Anti-p16 Antibody in Routine HPV Diagnostics***

E. Siehr<sup>1</sup>, U. Vogel<sup>2</sup>

<sup>1</sup>Institut für Pathologie, Allgemeine und Molekulare Pathologie und Pathologische Anatomie, Tübingen, Germany, <sup>2</sup>Institute of Pathology, Tübingen, Germany

#### **Background**

In routine diagnostics HPV-related cervical intraepithelial neoplasia (CIN) and cervical cancer (CC) are detected by immunohistochemistry using the surrogate protein marker p16. However, p16 is not exclusively increased by HPV E7 oncoprotein (Stiasny et al. Anticancer Research 2016). Therefore, it would be of advantage to directly detect HPV-proteins.

#### **Methods**

7 paraffin tissue microarrays (PTMAs) were constructed out of routine paraffin blocks of mostly HPV-related CIN and CC with a total of 109 cores (5 mm in diameter) and 120 cores (3 mm in diameter). The HPV subtypes were routinely determined by PCR. Furthermore, three paraffin cell blocks (PCBs) were prepared using HeLa-, MCF7 and SKBR3 cell lines embedded in agarose. The slides of the PTMAs and the PCBs were immunohistochemically stained with anti-HPV16/18-E6 (Clones: C1P5, BF7; 1:100), anti-HPV18-E7 (Clone: 8E2; 1:100) anti-HPV (Clone: K1H8, ready to use) (abcam) and anti-p16 (CINtec, Roche) antibodies using a Roche/Ventana platform (BenchMark Ultra, pretreatment: CC1, incubation time: 30 min, incubation temperature: 37°C, OptiView DAB IHC Detection Kit).

#### **Results**

By PCR well-known low and high risk HPV subtypes could be detected. The anti-HPV16/18-E6 (Clone: C1P5) antibody displayed very much unspecific staining of dysplastic cells, carcinoma cells, endothelium and fibrocytic cells. The anti HPV18-E6 (Clone: BF7) antibody showed no signal, even in the HeLa cell-line. By using the anti-HPV-E7 (Clone: 8E2) antibody the HeLa cells were correctly positive. The anti-HPV (Clone: K1H8) antibody which should recognize the 11 most important HPV low risk and high risk subtypes stained sometimes only few superficial cells in CIN. p16 correlated well with high grade CIN and CC.

#### **Conclusion**

In routine diagnostics p16 immunohistochemistry cannot be replaced by one of the four tested anti-HPV antibodies although p16 is only a surrogate marker for HPV infection. Promising anti HPV-E7 antibodies were described by Shi et al. (Molecular Medicine report, 2018) which are obviously not yet commercially available.

P01.08

### ***Incidental Diagnosis of Lymphangioliomyomatosis (LAM) in Gynecological Surgery - A Case Series***

J. Müller<sup>1</sup>, B. Gilks<sup>2</sup>, J. McAlpine<sup>3</sup>, G. G. R. Hiller<sup>4</sup>, A. K. Höhn<sup>4</sup>, L.-C. Horn<sup>4</sup>

<sup>1</sup>University Hospital Leipzig, Institute of Pathology, Leipzig, Germany, <sup>2</sup>Vancouver General Hospital and the University of British Columbia, Department of Anatomical Pathology, Vancouver, Canada, <sup>3</sup>University of British Columbia, Division of Gynecologic Oncology, Department of Obstetrics and Gynecology, Vancouver, Canada, <sup>4</sup>University Hospital Leipzig, Institute of Pathology, Division of

## Background

Lymphangiomyomatosis (LAM) is a rare, slow progressing, low-grade neoplasm that primarily affects premenopausal women. The disease is of systemic nature and well known for its pulmonary involvement with cystic destruction, but extra-pulmonary disease may occur and present as renal angiomyolipoma or lymphangiomyomatous lesions in different organs. LAM-associated lesions may present mutations in the tuberous sclerosis complex genes and may develop sporadically or in the context of tuberous sclerosis as hereditary disease. Incident LAM may represent the sentinel finding of the disease.

## Methods

A data base research was performed for LAM in gynecological surgical specimens. H&E-stained slides were re-examined for exact localization of the LAM within the specimen. Immunohistochemical stains were re-evaluated for expression patterns. Clinical data were retrieved for the presence of tuberous sclerosis.

## Results

The age ranged from 32 to 78 years (mean = 54 yrs, median = 55 yrs), with 8/13 were  $\leq$  55 years. One woman had a history of LAM with lung involvement and another woman had clinical diagnosis of tuberous sclerosis. Overall, no history of renal angiomyolipoma or PEComa noted. 9/13 women underwent surgery for gynecological malignancy, 2/13 for endometriosis and complex atypical endometrium hyperplasia and 2/13 for pelvic discomfort and pelvic lymphadenopathy. On histological examination 10/13 women incidentally presented LAM involvement in 1 to 9 lymph nodes (median = 1,5) with a lesion size of 0,5 to 12 mm (median = 2,3 mm), mainly located subcapsular or in the nodal parenchyma, one half with extranodal spread in the fatty tissue. 3/13 women showed extranodal involvement of the retroperitoneum, myometrium, and the hilum of the ovary. The neoplasm stained in most cases positive for HMB45 (patchy 9/13, focal 1/13), for desmin (4/7) and smooth muscle actin (3/3), with negativity for broad spectrum cytokeratins (6/6) and S100 (3/3). LAM was associated with tuberous sclerosis in 2/13 patients.

## Conclusion

LAM is a rare systemic disease, which mainly involves the lungs. Nevertheless, abdominal nodal or extranodal manifestations may occur and therefore should be considered as a differential diagnosis in the spectrum of abdominal spindle cell neoplasm. It is important to report the incidental finding of even small foci of LAMs as a clue for women with yet unrecognized tuberous sclerosis complex.

P01.09

## ***A node in the male breast. Case report of an unusual tumor manifestation.***

T. Hansen<sup>1</sup>, Z. E. Kovacs<sup>2</sup>, J. Kriegsmann<sup>1,3</sup>, S. Jud<sup>2</sup>

<sup>1</sup>MVZH ZMD Trier GmbH, Trier, Germany, <sup>2</sup>Klinikum Mutterhaus der Borromäerinnen, Gynäkologie und Geburtshilfe, Trier, Germany,

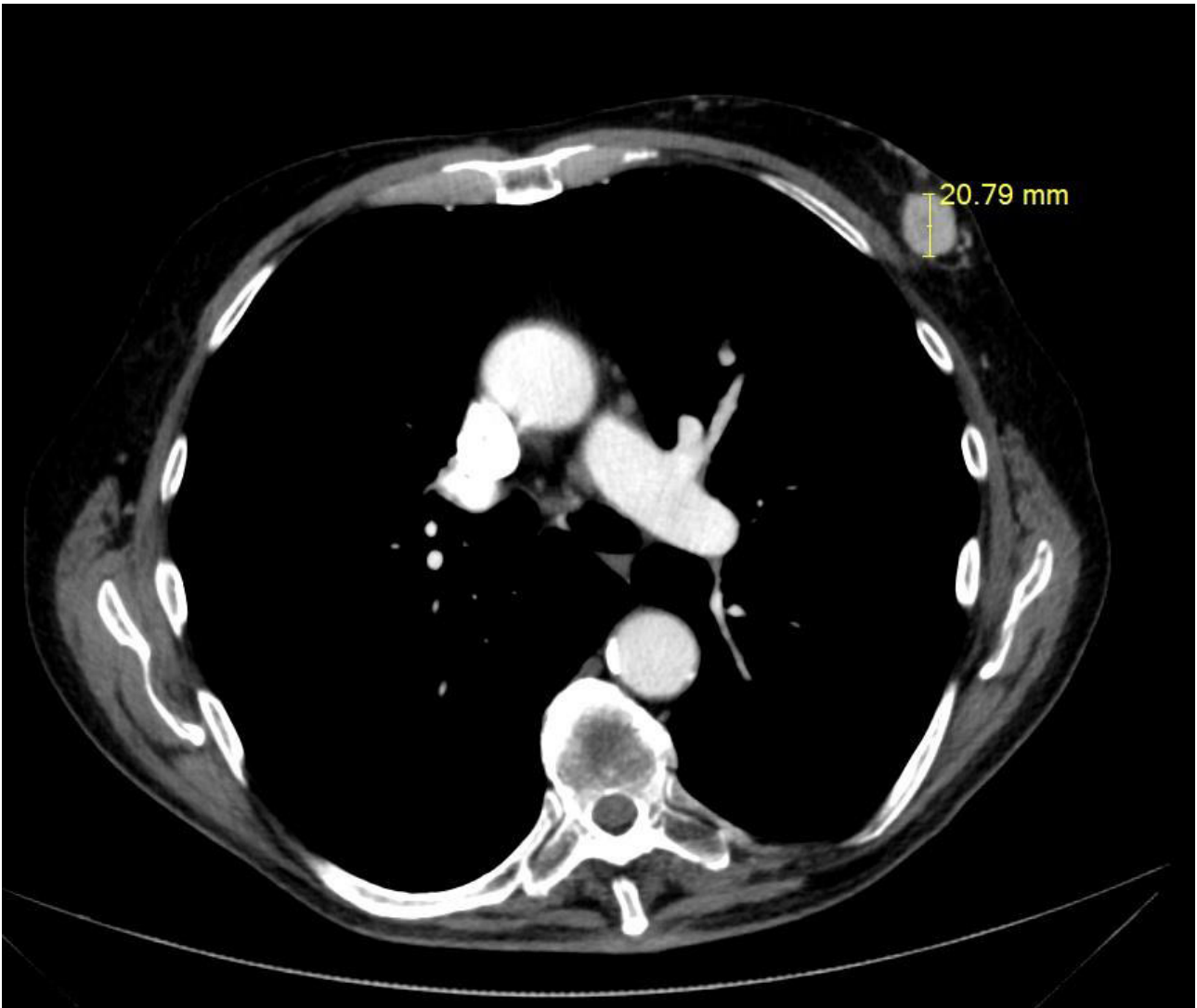
<sup>3</sup>Danube Private University, Department of Medicine, Krems, Austria

## Background

Renal cell carcinoma (RCC) has been described to reveal unusual sites of metastasis. Furthermore, it may retain the tendency to metastasize late in its course[1][2]. We present a case exhibiting both of these mentioned features.

## Methods

We report on a 82-year old male patient presenting with a painless nodule of his left breast and with weight loss of 10 kg during the last months. Further physical examination revealed no abnormal findings. Radiological analysis demonstrated a nodule of the left mammary region measuring up to 20 mm.

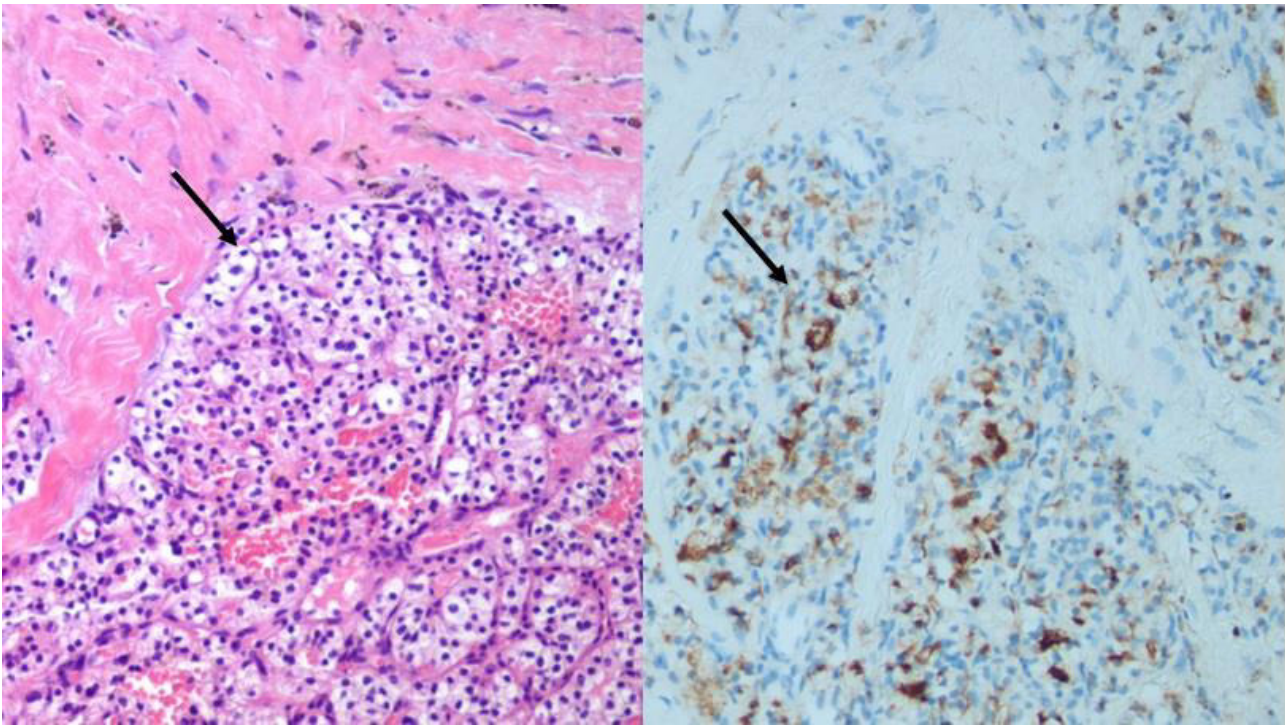


CT scan with the tumor in the left breast

Axillary lymph nodes were inconspicuous. Ultrasonography-guided core needle biopsy was performed. The tissue specimens were processed for further histological examination according to standard protocols.

### Results

Microscopically, we found fibrous tissue with an epithelial tumor, arranged in nests and sheets of clear cells containing glycogen in the PAS reaction. There was slight atypia. By means of immunohistochemistry, the tumor cells were positive for pan-cytokeratin, vimentin, CD10, and renal cell carcinoma marker (RCC marker), while stainings for GATA binding protein-3 and estrogen receptor (ER) were absent.



On the left side, tumor cells (arrows) in H&E staining. on the right side, immunohistochemistry for RCC marker  
 We interpreted the results as breast metastasis of a clear cell carcinoma favouring primary RCC. On questioning, the patient revealed a history of clear cell RCC in the left kidney 15 years ago.

### Conclusion

Breast metastasis of extra-mammary tumors is rare, and it is even more exceptional in male patients[2], as reported herein. This case report highlights the fact that RCC can exhibit an aberrant tendency to metastasize to unusual sites and to metastasize after prolonged periods of primary resection[1][2][3]. On the one hand, long-term surveillance of RCC is mandatory. On the other hand, in patients with a prior history of other tumors, metastatic involvement of the breast has to be suspected.

Literaturangaben:

[1] Malhotra KP, et al, (2021), Metastases from renal cell carcinoma – report of three unpredictable cases and literature review, Indian J Cancer , 273, 58, 2024-02-09

[2] Elouarith I, et al, (2022), Breast metastasis 18 years after nephrectomy for renal cell carcinoma: a case report., J Surg Case Rep, doi: 10.1093/jscr/rjac116, 2024-02-20

[3] Spasic M, et al, (2023), Secondary breast malignancy from renal cell carcinoma: challenges in diagnosis and treatment – case report, Diagnostics, doi: 10.3390/diagnostics13050991, 2024-02-09

## Poster Hämatopathologie

P03.01

### ***The Pathogenesis of Pathological Splenic Rupture in Diffuse Large B-Cell Lymphoma – Enzymatic Degeneration of the Splenic Capsule?***

U. Vogel

Institute of Pathology, Tübingen, Germany

#### Background

Splenic rupture in diffuse large B-cell lymphoma (DLBCL) is a rare event. Concerning the pathogenesis of splenic rupture Hynes et al. described in 1964 three possible mechanisms which seem to be widely accepted till today: (1) Mechanical stress on the capsule by distention of the spleen secondary to cellular (e.g. leukemic) infiltration; (2) Splenic infarct with capsular hemorrhage and subsequent rupture; and (3) Defects in blood coagulation.

## Methods

A 68-year-old male was admitted to hospital with a four week history of night sweats and weight loss (4-5 kg). By punch biopsy of a left cervical lymph node a diffuse large B cell Lymphoma (DLBCL) NOS was histologically diagnosed and a high dose prednisolone therapy was administered. Three days after admission the patient experienced a deep vein thrombosis of the left leg which was treated by full dose anticoagulation therapy. The next day tumor lysis syndrome was detected and intensive intravenous fluid therapy was started. 7 days after admission the patient developed a circulatory failure due to hemorrhagic shock.

## Results

Autopsy revealed extensive infiltration of the DLBCL in the heart, liver, kidneys, thyroid gland, stomach, small intestine, mesovarium, mesosalpinx, ovaries, parapancreatic and retroperitoneal fatty tissue and the spleen (weight: 1455 g). The splenic capsule was ruptured and 2900 ml of blood was found in the abdominal cavity confirming the clinical diagnosis of hemorrhagic shock as cause of death. Histological, histochemical and immunohistochemical examinations of the spleen at the rupture site displayed a thinned out splenic capsule, dense vital, apoptotic and necrotic subcapsular infiltrates of the DLBCL and an infiltrate of neutrophil granulocytes.

## Conclusion

It seems obvious that a rapid enlargement of the spleen by proliferating tumor cells may lead to a mechanical stress of the splenic capsule which may finally rupture as proposed by Hynes et al. Histological examination of the rupture site of the splenic capsule in this case may hint to an additional enzymatic degradation of the splenic capsule due to the release of proteolytic enzymes by spontaneous or corticosteroid-related (Schmidt S et al. Cell Death Differ. 2004) tumor cell necrosis in combination with neutrophils attracted by tumor cell necrosis. Acknowledging this enzymatic mechanism the administration of high dose corticosteroid therapy may be questioned in favour of a slowly increasing dose in cases with huge spleens.

P03.02

## ***Deep Learning (DL) based artificial intelligence (AI) algorithm for diagnostic and prognostic usage in myeloproliferative neoplasm (MPN)***

L. Glamann<sup>1</sup>, M. Bauer<sup>1</sup>, I. Tolkach<sup>2</sup>, C. Wickenhauser<sup>1</sup>

<sup>1</sup>Universitätsmedizin Halle (Saale), Institut für Pathologie, Halle (Saale), Germany, <sup>2</sup>University Hospital Cologne, Institute of Pathology, Cologne, Germany

## Background

Digitization of tissue sections enables the use of artificial intelligence (AI)-based deep learning (DL) image analysis in pathology. DL algorithms can be trained to safely recognize all relevant histomorphological structures in tissue-slides, including the detection of cancer cells. So far, this has mainly been used in solid tumors and only little is known about its relevance in hematological diseases. Therefore, the aim of this multicenter study is to analyze the relevance of AI-based algorithms in MPN diagnostics.

## Methods

In total 1200 bone marrow biopsies of patients with histologically proved BCR-ABL negative MPN, with known clinical data were included. So far, 110 H&E stained and digitized MPN samples have been precisely manually annotated by experienced human analysts for different tissue/cell classes: bone, fat, megakaryocytes, hematopoietic cells, bleeding areas, and artefact by employing the open source software QuPath. 100 slides from UK Halle were split into a training cohort (80%) and a validation cohort (20%). The other 10 slides from UK Cologne were used for the testing of the algorithm.

## Results

In order to train the algorithm in detecting megakaryocytes and to distinguish them from other cells in the bone marrow, e.g. granulocytic and erythropoietic cells, manually annotated pictures served as the ground truth for the semantic segmentation neural network. Our algorithm underwent rigorous training using machine learning techniques to learn features to distinguish of megakaryocytes from other cells in the bone marrow. So far, the algorithm showed a good performance with an accuracy of over 90% that still has to be improved. As a clinical use case we show high accuracy of

the algorithm for quantification of bone marrow cellularity when compared to two expert pathologists.

## Conclusion

So far, the algorithm, trained to detect different tissue classes and megakaryocytes in MPN bone marrow tissue samples, has shown promising results in accurately processing bone marrow specimens and quantifying bone marrow cellularity. Moving forward, our goal is to further train the algorithm to differentiate between healthy and neoplastic megakaryocytes, thereby enhancing its diagnostic capabilities.

P03.03

## ***The challenge of spatially mapping the mononuclear phagocytic system in B-cell lymphoma.***

E. Yalcin<sup>1,2</sup>, I. Iaccarino<sup>1,2</sup>, W. Klapper<sup>1,2</sup>

<sup>1</sup>Institute of Pathology, University Hospital Schleswig-Holstein, Campus Kiel, Hematopathology Section and Lymph Node Registry, Kiel, Germany, <sup>2</sup>Clinical Research Unit "CATCH ALL" (KFO 5010/1) funded by the Deutsche Forschungsgemeinschaft, Bonn, Germany

## Background

Cells of the mononuclear phagocytic system (MPS), including macrophages, dendritic cells and monocytes, play a central role in the tumor microenvironment of B-cell malignancies.[1] However, consistent detection and accurate quantification of these cells in tissue is a challenge. Widely used digital image analysis fail due to the cellular features of the MPS such as variable and complex cell bodies, long cytoplasmic protrusions crossing serial histology sections, varying number of nuclei and uneven expression of proteins within one cell. Our aim is to establish a digital image analysis work-flow for the characterization of the MPS in FFPE-tissue using multiplex immunofluorescence (mIF).

## Methods

A 5-marker mIF panel (CD68, CD14, CD11c, HLA-DR and CD163) and QuPath Bioimage analysis software[2] was used to quantify and subtype cells of the MPS in reactive lymphoid tissue B cell lymphoblastic lymphoma (B-LBL; n = 32) and Burkitt lymphoma (BL; n = 40). Macrophage content was compared between several distinct approaches using machine learning-based algorithms. Validation was performed by manual counting by an experienced pathologist and correlation with RNA-sequencing data.

## Results

Nuclei-based machine-learning algorithms greatly overestimate the macrophage content by e.g. by wrongly classifying cells adjacent to macrophages as macrophages too. In contrast, the Pixel-classifier that ignores nuclear detection to annotate cells consistently detects the polymorphic macrophage population independent of the variability in tissue immunoreactivity. By this classifier normalized CD68+ macrophage counts shows a strong correlation with CD68 mRNA expression validating the method. Initial data of the MPS in B-LBL and BL will be presented.

## Conclusion

Quantification the MPS in lymphoma specimen by digital image analysis requires a dedicated approach that differs from detection of other cell types such as lymphocytes.

Literaturangaben:

[1] Fowler NH, Cheah CY, Gascoyne RD, Gribben J, Neelapu SS, Ghia P, Bollard C, Ansell S, Curran M, Wilson WH, O'Brien S, Grant C, Little R, Zenz T, Nastoupil LJ, Dunleavy K., (2016), Role of the tumor microenvironment in mature B-cell lymphoid malignancies , *Haematologica*, 10.3324/haematol.2015.139493

[2] Bankhead P, Loughrey MB, Fernández JA, Dombrowski Y, McArt DG, Dunne PD, McQuaid S, Gray RT, Murray LJ, Coleman HG, James JA, Salto-Tellez M, Hamilton PW. , (2017), QuPath: Open source software for digital pathology image analysis , *Sci Rep*, 10.1038/s41598-017-17204-5

P03.04

### ***Reduction of intra-cellular ROS levels by NOX inhibitors or BHA attenuates cell survival and JAK/STAT signaling in classical Hodgkin's lymphoma.***

J. Wildfeuer, R. Dheenadayalan, S. Hartung, M. Zahn, N. T. Gaisa, P. Möller, R. B. Marienfeld  
Universitätsklinikum Ulm, Pathologie, Ulm, Germany

#### **Background**

Classical Hodgkin's lymphoma (cHL) is one of the most frequent forms of B cell lymphoma with an incidence of about 3 cases per 100,000 persons per year. The typical feature of classical Hodgkin's lymphoma is the presence of multinucleated Hodgkin's Reed Sternberg cells (HRS cells) and a reactive, inflammatory tumor micro-environment. This inflammatory environment promotes the survival of the HRS cells and a constitutive signalling, including JAK/STAT and NF- $\kappa$ B signalling. Reactive oxygen species (ROS) have been shown to alter the activity of several signaling pathways, including JAK/STAT and NF- $\kappa$ B in different cancers. In cHL, the role of ROS for survival and proliferation still remains largely unclear. In the present study we analyzed the effect of antioxidants or NOX inhibitors on growth and survival of cHL cell lines and on JAK/STAT and NF- $\kappa$ B activity. Our results shed more light onto the importance of ROS for the regulation of crucial survival pathways in cHL.

In this study we aimed to decipher the role of ROS for the growth and survival of cHL as constitutively elevated ROS levels might contribute to the pathogenesis of this B cell lymphoma.

#### **Methods**

The antioxidant BHA as well as the NOX inhibitors (iNOX) Apocynin and DPI were used to determine the effect of ROS in the cHL cell lines. To investigate the effect of iNOX and BHA on cell survival, an MTS assay, western blot, and growth curve were performed. JAK/STAT and NF- $\kappa$ B activity was determined by electromobility shift assays (EMSA), western blot analyses, and by kinase assays. The influence of the protein tyrosine phosphatase PTP1B was investigated by knock down with siRNA.

#### **Results**

We observed a concentration-dependent decrease of cell numbers as well as increasing numbers of dead cells with both iNOX and BHA, with all cHL cell lines. Cleaved caspase 3 revealed an increased apoptosis. STAT6 activation appeared to be diminished by iNOX or BHA, while the effect of the ROS modulating compounds on NF- $\kappa$ B is inconsistent. Knock down of PTP1B showed a partial rescue of cHL survival and STAT6 activity.

#### **Conclusion**

High levels of cytokines and growth factors in the reactive micro-environment of cHL might cause a constant activation of NOX and subsequently increased levels of ROS, which in turn oxidate vulnerable cysteine residues, like in PTP1B, causing a diminished PTP1B activity in cHL as part of the JAK/STAT activation program in cHL.

## **Poster Herz-, Gefäß-, Nieren- und Transplantationspathologie**

P04.01

### ***Representative clinical case with Nutcracker syndrome (NCS) favoring transposition of superior mesenteric artery (SMA) onto the infrarenal aorta***

R. Friebe<sup>1</sup>, S. Arndt<sup>1</sup>, F. Meyer<sup>2</sup>, C. March<sup>3</sup>, U. Barth<sup>1</sup>, Z. Halloul<sup>1</sup>

<sup>1</sup>Dept. of General, Abdominal, Vascular and Transplant Surgery, Otto-von-Guericke University with University Hospital, Division of Vascular Surgery, Magdeburg, Germany, <sup>2</sup>Klinik für Allgemein-, Viszeral-, Gefäß- und Transplantationschirurgie, Otto-von-Guericke-Universität mit Universitätsklinikum, Magdeburg, Germany, <sup>3</sup>Klinik für Radiologie und Nuklearmedizin, Otto-von-Guericke-Universität mit Universitätsklinikum, Magdeburg, Germany

#### **Background**

Pain in the left flank and groin region comprises a broad spectrum of differential diagnosis.

Aim: To illustrate the rare diagnosis as well as a possible and suitable treatment option of "Nutcracker syndrome" (NCS)

## Methods

Scientific case report based on i) clinical experiences obtained in the clinical and perioperative management of this single patient and ii) selective references from the medical scientific literature

## Results

(Case presentation): *Medical history and clinical finding:* A 32-years old male patient was admitted to the Dept. of Radiology for embolization of the left spermatic vein due to a testicular varicocele and pain in the groin region.

*Diagnostic measures:* Digital subtraction angiography (DSA) scans revealed a reversed flow in the left spermatic vein and pronounced collateral circulation of the left renal vein (LRV). A computed tomography(CT)-Angiography scan showed an angle between the longitudinal axis of superior mesenteric artery(SMA) and that of aorta of lower than 17°. Therefore, the finding was interpreted as the diagnosis "NCS".

*Therapy:* The decision was made for a surgical treatment and the patient was electively admitted to the hospital. The surgical therapy comprised transposition of the SMA to the infrarenal section of the aorta.

*Postoperative course:* The patient was transferred to the ICU for one day of observation. On the following day, the patient was transferred back to the normal vascularsurgical ward with stable cardiopulmonary/-circulatory conditions. An immediate post-operative CT-Angio control showed no bleeding complication and regular visceral perfusion. Clinical status improved substantially, there were no further pain attacks.

## Conclusion

NCS is considered a rare diagnosis, with almost unknown prevalence. This diagnosis needs to be taken into account in case of left-side flank and groin pain especially in combination with proteinuria. A possible therapy of the NCS is the placement of a stent in the LRV. Due to the lack of data on the long-term-outcome in case of stent-implantation in the LRV, this approach remains for unoperable or high surgical risk subjects. Transposition of the SMA can be a good alternative therapeutic approach, with a more long-term prospect and prognosis, as shown in the presented case.

P04.02

## ***Aneurysm of the internal jugular vein – case report on a rare entity***

J. Deeb<sup>1</sup>, F. Meyer<sup>2</sup>, M. Petersen<sup>3</sup>, M. Pech<sup>4</sup>, U. Barth<sup>1</sup>, Z. Halloul<sup>5</sup>

<sup>1</sup>Dept. of General, Abdominal, Vascular and Transplant Surgery; Otto-von-Guericke University with University Hospital, Division of Vascular Surgery, Magdeburg, Germany, <sup>2</sup>Klinik für Allgemein-, Viszeral-, Gefäß- und Transplantationschirurgie, Otto-von-Guericke-Universität mit Universitätsklinikum, Magdeburg, Germany, <sup>3</sup>Dept. of General, Abdominal, Vascular and Transplant Surgery; Otto-von-Guericke University with University Hospital, Magdeburg, Germany, <sup>4</sup>Dept. of Radiology and Nuclear Medicine; Otto-von-Guericke University with University Hospital, Magdeburg, Germany, <sup>5</sup>Dept. of General, Abdominal, Vascular and Transplant Surgery, Otto-von-Guericke University with University Hospital, Division of Vascular Surgery, Magdeburg, Germany

## Background

*Aim:* By means of a case description, a patient with the rare entity of an aneurysm of the right internal jugular vein is to be characterized.

## Methods

Scientific case report

## Results

(*case characteristics*): In a 62-years old female patient, primary hyperparathyroidism was diagnosed. Selective jugular vein catheterization (after previous scintigraphy of parathyroid gland and F-18-Cholin-PET/CT) revealed lateralization of hormone secretion of the parathyroid gland on the right side. In addition, an aneurysm of the right jugular vein and "pseudoxanthoma elasticum" were found - therefore, simultaneous surgical intervention was derived: The aneurysm was resected (tangential ablation of a 10-cm segment of the anterior venous wall with a spindle-shaped wall specimen) and longitudinal gathering suture as well as adenoma resection of the parathyroid gland (because of osteoporosis and nephrolithiasis). Postoperatively, local wound seroma developed, which was treated with local cooling (regressive swelling). Histopathological investigation revealed disturbed tissue texture and luminal parts of parietal thrombus (no hint for infection or malignant tumor growth) as well as intima-layer thickening fibrotization. Follow-up investigations over 12 months did not show any pathological finding using Duplex-ultrasonography and clinical examination (no hint for a



residual swelling).

## Conclusion

Venous aneurysms are extremely rare compared with the arterial system. Etiologically, weakness of the vascular wall can be considered the most frequent cause. Further causes are traumas, inflammation, degenerative processes, mechanical stress and venous hypertension (the latter most likely determining the site). To diagnose a venous aneurysm and for postoperative follow-up control investigation, Duplex ultrasonography is a suitable diagnostic measure. Surgical treatment of venous aneurysms is determined by its site and symptomatology – eventually, surgical intervention can be combined with an operative procedure treating accompanying findings if justifiable (typical histological findings: intima-layer thickening and fibrotization). Aneurysm of the internal jugular vein is a rare entity - indication for surgical intervention is derived depending on **i**) aneurysm site (at the head and neck only in case of symptoms, cosmetic problems or associated to other diseases as in the presented case) as well as **ii**) complaints and symptoms (swelling, redness).

P04.03

## ***TGF $\beta$ induced mechanosignaling controls the transcriptome and microenvironmental composition of proximal tubules in chronic kidney disease***

A. Merz<sup>1</sup>, A. Paolini<sup>2</sup>, S. Chakraborty<sup>3</sup>, G. Andrieux<sup>3</sup>, G. Walz<sup>2</sup>, M. Werner<sup>1</sup>, M. Rogg<sup>1</sup>, C. Schell<sup>1</sup>

<sup>1</sup>Institut für Klinische Pathologie, Universitätsklinikum Freiburg, Freiburg, Germany, <sup>2</sup>Klinik für Innere Medizin IV, Universitätsklinikum Freiburg, Freiburg, Germany, <sup>3</sup>Institut für Medizinische Bioinformatik und Systemmedizin, Universitätsklinikum Freiburg, Freiburg, Germany

## Background

Interstitial fibrosis and progressive atrophy of proximal tubules (PT) are hallmarks of chronic kidney disease (CKD). The latter is characterized by thickening and multilamellation of the tubular basement membrane, whereas fibrosis is promoted by accumulation of extracellular matrix (ECM) translating into increased matrix rigidity. The role of mechanotransduction via integrin adhesion complexes (IAC) as well as the corresponding signaling programs activated in this context remain elusive. Here, we aimed to elucidate the functional role of the ILK-Pinch-Parvin (IPP) complex as an essential part of the IAC in PT damage response and CKD.

## Methods

Morphometric assessment of a CKD patient biopsy cohort as well as ischaemia-reperfusion injury (IRI) mouse models was performed. Transcriptome studies of human proximal tubular epithelial cells (hRPTECs) under pro-fibrotic and rigid matrix conditions were analyzed. A CKD mimicking *in vitro* model was established and functionally characterized. Reanalysis of scRNA sequencing from a human CKD cohort was employed for cross-correlation. IPP-complex knockout models were generated by CRISPR/Cas9.

## Results

In IRI mice, we observed a strong recruitment of IPP proteins to the tubular basement membrane of PTs showing features of tubular atrophy. These findings were translated to a CKD patient cohort further assessing markers of mechanosignaling and tubular damage. For detailed analysis of the underlying mechanisms, we employed rigidity sensing assays in a hRPTEC model. Remarkably, transcriptome analysis revealed that only under pro-fibrotic conditions, hRPTECs sensed changes in stiffness that translated into regulation of adhesome-related gene signatures. Cross-correlation with available scRNA seq data from CKD-patients highlighted differential expression of secreted signaling proteins including the matricellular molecule CCN1. Functional studies demonstrated the pivotal role of the IPP-complex as a central signaling node for mechanosignaling.

## Conclusion

In CKD, IPP and other IAC proteins are recruited to the thickened tubular basement membrane of atrophic tubules, indicating a critical role in disease progression. Our results demonstrate that inflammation processes induce a phenotypic switch of PTs, resulting in altered IAC expression signatures. Our data indicate that IAC proteins are crucially involved in sensing of the microenvironmental composition of PTs and thereby reciprocally fine-tune auto-/paracrine signaling properties of epithelial cells.

P04.04

## ***Sustainable Benchmarking of deep learning models for computational pathology***

Y.-C. Lan<sup>1</sup>, M. Strauch<sup>1</sup>, N. Schmitz<sup>1</sup>, P. Pilva<sup>1</sup>, T. Nguyen<sup>2</sup>, J. Kers<sup>3</sup>, P. Boor<sup>1</sup>, R. D. Bülow<sup>1</sup>

<sup>1</sup>Uniklinik RWTH Aachen, Institut für Pathologie, Aachen, Germany, <sup>2</sup>University Medical Center Utrecht, Department of Pathology, Utrecht, The Netherlands, <sup>3</sup>University of Amsterdam, Department of Pathology, Amsterdam, The Netherlands

### **Background**

Deep learning (DL) holds great promise to improve medical diagnostics, with research mainly focusing on developing DL with the best performance. However, DL implementation can have substantial environmental consequences, and metrics allowing us to consider carbon footprint are missing. We aimed to explore and develop an approach for benchmarking DL models for digital pathology that integratively evaluates diagnostic performance and environmental impact measured by CO<sub>2</sub>- or equivalent (CO<sub>2</sub>eq) emissions.

### **Methods**

We collected multicentre datasets for two classification tasks, one with high complexity (kidney transplant pathology classification – three centres, in total 2020 patients) and one with low complexity (subtyping of chromophobe, clear cell and papillary renal cell carcinomas (RCCs), TCGA and one center, in total 1229 patients). A vision transformer, transMIL, CLAM and Inceptionnet were evaluated for their diagnostic performance and environmental impact.

### **Results**

Comprehensive benchmarking revealed differences and similarities of model performance with regard to diagnostic accuracy and environmental sustainability in the two tasks. Our newly developed metric termed ‘Environmentally Sustainable Performance’ (ESPer) score, which integrates performance and environmental impact measured by CO<sub>2</sub>eq of DL models when used in diagnostic practice can be used to integratively investigate environmental sustainability and diagnostic accuracy.

### **Conclusion**

While some of the architectures had comparable performances, ESPer enabled prioritizing those with less carbon footprint. Data reduction approaches, which need to be considered during training, could further improve ESPer. Evaluating environmental sustainability alongside performance when benchmarking deep learning models for specific tasks is inevitable, especially in production settings with a low share of renewable energy in the local energy mix.

P04.05

## ***Two Cases of Lymphofollicular Myocarditis – a Specific Entity?***

U. Vogel<sup>1</sup>, K. Klingel<sup>2</sup>

<sup>1</sup>Institute of Pathology, Tübingen, Germany, <sup>2</sup>Institut für Pathologie, Allgemeine und Molekulare Pathologie und Pathologische Anatomie, Tübingen, Germany

### **Background**

The search in PubMed for the terms “lymphofollicular myocarditis”, “lymphofollicular cardiomyopathy” or “lymphofollicular dilated cardiomyopathy” yields only one publication (Klingel et al. Eur Heart J 2010). Moreover, a lymphofollicular variant of myocarditis is not explicitly mentioned in the 2023 ESC guidelines for the management of cardiomyopathies and in the recently published review on dilated cardiomyopathy (Heymans et al. Lancet 2023). Therefore, the question may be raised whether a lymphofollicular myocarditis represents a specific entity.

### **Methods**

Case 1: In 2009 a 30-year-old male received a left ventricular assist device (LVAD) for terminal heart failure due to dilated cardiomyopathy of unknown reason. Histologically the resected heart tissue displayed a multifocal infiltrate of T- and B-lymphocytes. By PCR examinations an infectious etiology was excluded. In 2023 the patient underwent heart transplantation due to deteriorated heart function (left ventricular ejection fraction (LVEF): 15%; left ventricular enddiastolic diameter (LVEDD): 79 mm).

Case 2: In 2013 a 29-year-old male developed non-infectious autoimmune myocarditis which was treated by azathioprine and corticosteroids for 6 months. In 2014 an endomyocardial biopsy revealed a discrete lymphocytic inflammation which

was interpreted as healing myocarditis. In 2023, the patient underwent heart transplantation due to dilated cardiomyopathy (LVEF: 30%; LVEDD: 62 mm). The explanted heart revealed focal infiltrates of T- and B-lymphocytes.

### Results

In both cases we found in the explanted hearts typical changes for dilated cardiomyopathy but also a lymphofollicular arrangement of T- and B-lymphocytes with germinal centers with follicular dendritic cells.

### Conclusion

Lymphofollicular myocarditis seems to be a rare, but distinct entity of myocarditis probably due to (auto)immune mechanisms. In endomyocardial biopsies the focal arrangement of both T- and B-lymphocytes may hint to a lymphofollicular myocarditis. The histological aspect of the inflammatory infiltrate resembles the well-known autoimmune lymphocytic thyroiditis Hashimoto.

P04.06

## ***Arrhythmogenic Cardiomyopathy and/or Oxymetazoline Abuse as a Putative Cause for Myocardial Fibrofatty Replacement and Sudden Cardiac Death***

U. Vogel<sup>1</sup>, T. Matthäus<sup>2</sup>, S. Waldmüller<sup>2</sup>, T. Haack<sup>2</sup>

<sup>1</sup>Institute of Pathology, Tübingen, Germany, <sup>2</sup>Institute of Medical Genetics and Applied Genomics, Tübingen, Germany

### Background

Arrhythmogenic cardiomyopathy (ACM) is a primary heart muscle disease characterized by progressive transmural fibrofatty replacement of cardiomyocytes accounting for electrical instability and subsequent risk of life threatening ventricular arrhythmias. Oxymetazoline is a direct sympathomimetic which binds to and activates  $\alpha_1$  and  $\alpha_2$  adrenergic receptors. It is administered e.g. as oxymetazoline hydrochloride in nasal sprays to treat nasal congestion in acute rhinitis. Side effects of the treatment may be e.g. nausea, fever, convulsions, hypertension and cardiac arrhythmia. In case of overdose cardiac arrest can occur.

### Methods

A 38-year-old Caucasian female experienced a cardiac arrest at home. Due to immediate cardiopulmonary resuscitation a return of spontaneous circulation was achieved. However, at hospital an irreversible, generalized hypoxic damage of the brain was diagnosed. Treated with palliative therapy she died 7 days later. After autopsy a third-party anamnesis revealed that she used oxymetazoline nasal spray for more than 22 years with at least 2 bottles per month and about up to 12 sprays per day. When she started the abuse, she developed a psychosis and reduced her personal relationships. A psychotherapy for two years was stopped due to ineffectiveness. Besides her profession she was engaged in sports. Family history concerning ACM was not obvious.

### Results

By autopsy generalized hypoxic encephalopathy could be confirmed. The histological examination of both ventricles revealed patchy myocardial necrosis, granulation tissue, diffuse fibrosis and fat tissue. Genetic testing revealed a single very rare missense variant in the desmoplakin gene (*DSP* (ENST00000379802.8):c.1088A>C; p.Gln363Pro, heterozygous) which is of uncertain significance concerning the myocardial findings.

### Conclusion

In contrast to the brain the damage of the heart muscle could not be explained at first. An ongoing viral myocarditis and thrombosis in small coronary arteries were excluded. The severe oxymetazoline abuse in combination with physical exercise may have led to hypoxia in the cardiac muscle due to vasoconstriction. The psychosis and the cardiac arrest may also be attributed to oxymetazoline. ACM caused by the detected *DSP* variant cannot be excluded as differential diagnosis. A combination of both etiologies may be possible.

P04.07

## ***Role of ANXA4 as a modifier in VHL-dependent ccRCC***

M. Wess, T. Feilen, M. Werner, O. Schilling, M. Rogg, C. Schell

Institut für Klinische Pathologie, Universitätsklinikum Freiburg, Freiburg, Germany

### **Background**

The central genetic hallmark feature of clear cell renal cell carcinoma (ccRCC) is the early loss of function of VHL. Previous studies have indicated VHL-dependent alterations of the extracellular matrix (ECM). However, to date comprehensive description and understanding of VHL-dependent ECM signatures are missing.

### **Methods**

Proteomics were used to reveal VHL-dependent protein expression in ccRCC cell lines (A498, 786-O) and CRISPR/Cas9-modified human proximal tubular epithelial cells (hRPTECs) as well as syndromic and sporadic ccRCC patient cohorts. For candidate proteins analysis of proteomic and histological datasets was performed. Further functional analysis was conducted employing CRISPR/Cas9-mediated knockout (KO) approaches.

### **Results**

Proteomic analysis revealed differential regulation of ECM-related proteins with ANXA4 being significantly upregulated. Interestingly, functional genetic titration of ANXA4 employing KD, overexpression or complete ablation did not translate into major changes of cellular proliferation or migration in renal cancer or tubular cells. Detailed localization studies demonstrated that ANXA4 is detectable in distinct cellular compartments, namely the cell membrane and nucleus/nuclear lamina. Exterior factors (stress/density) initiated shuttling of ANXA4 between these different compartments. Remarkably, similar distribution patterns were detectable in situ in tumour tissue of ccRCC patients. Further transcriptomic analysis of ANXA4 KO cells demonstrated a major impact on ECM- and cell-adhesion-associated gene sets, reflected by impaired invasive migratory capacity in conditions of reduced ANXA4-expression.

### **Conclusion**

Loss of VHL distinctly alters the ECM composition in ccRCC. We have identified the ECM-associated protein ANXA4 as a prominently upregulated protein. RNA-sequencing studies and subcellular localization patterns indicate a potential co-regulatory role of ANXA4 affecting matrisome-related transcriptomic signatures. These observations highlight the intricate regulation of ECM-associated signaling pathways in the context of VHL-dependent renal cell carcinoma.

P04.08

## ***A new mouse model of glomerular thrombotic microangiopathy***

P. Droste<sup>1,2</sup>, S. Djudjaj<sup>1</sup>, B. M. Klinkhammer<sup>1</sup>, M. Buhl<sup>1</sup>, R. Wanke<sup>3</sup>, E. Kemter<sup>4</sup>, P. Boor<sup>1,2</sup>

<sup>1</sup>LaBooratory of Nephropathology, Institute of Pathology, Medical Faculty, RWTH Aachen University, Aachen, Germany, <sup>2</sup>Division of Nephrology and Clinical Immunology, Medical Faculty, RWTH Aachen University, Aachen, Germany, <sup>3</sup>Institute of Veterinary Pathology, Center for Clinical Veterinary Medicine, Ludwig-Maximilians-Universität München, München, Germany, <sup>4</sup>Institute of Molecular Animal Breeding and Biotechnology, Gene Center and Department of Veterinary Sciences, Ludwig-Maximilians-Universität München, München, Germany

### **Background**

Thrombotic microangiopathies are rare and severe diseases with a multifaceted manifestation pattern. The kidneys are often affected, which can lead to acute and chronic renal failure. The pathophysiology of these heterogeneous diseases is incompletely understood and therapeutic options are limited. Established animal models of these diseases are lacking. Here we characterize a murine model of chronic glomerular endothelial cell injury generated by random mutagenesis.

### **Methods**

Eight-week-old wild-type mice were compared with homozygous mutated mice. Perfused kidneys and hearts, fixed in methyl-Carnoy's solution, were used for light microscopy, immunohistochemistry, and immunofluorescence staining. Transmission electron microscopy was performed on renal cortex and heart. Serum was taken for creatinine, blood urea nitrogen, and other basic values. Blood pressure was measured with a cuff tail system.

## Results

The mouse model presents with a spontaneous phenotype, a decreased lifespan, a decreased body weight, and impaired kidney function. The glomeruli showed hypertrophy, thrombi, a double contour of the glomerular basement membrane with cell interposition, and endothelial cell swelling. Interstitial fibrosis and infiltration with inflammatory cells were found in the cortex of the kidneys. Mesenchymal markers were expressed in a unique circular pattern around the capillaries in the glomerulus. The glomerular endothelial cells lost specific markers that are typical for them and partially expressed mesenchymal markers indicating an endothelia-to-mesenchymal transition. We detect an increased heart weight, with hypertrophic cardiomyocytes and elevated blood pressure.

## Conclusion

The present mouse model shows a chronic damage of the glomerular endothelium resembling a thrombotic microangiopathy with evidence of a glomerular endothelia-to-mesenchymal transition. In addition, the model shows abnormalities that are compatible with the systemic consequences of chronic kidney disease. A further in-depth and mechanistic investigation of the model should follow to make it usable for further experiments.

P04.09

## ***Effectiveness of Combined Lipoprotein Apheresis and PCSK9 Inhibitor Therapy: A Comprehensive Analysis in the Context of Cardiovascular Risk Reduction***

S. Kuss<sup>1</sup>, U. Julius<sup>2</sup>

<sup>1</sup>Pathologisches Institut der LMU München, München, Germany, <sup>2</sup>Universitätsklinikum Carl Gustav Carus, Medizinische Klinik und Poliklinik III, Dresden, Germany

## Background

Lipoprotein apheresis (LA) is an effective therapy for reducing the incidence of cardiovascular events (CVE) in patients at high risk of atherogenesis due to severe hyperlipoproteinemia. Proprotein-Convertase-Subtilisin/Kexin-Type-9 Inhibitors (PCSK9i) have established as supplementary therapy to further lower LDL levels effectively. This study aims to evaluate the effectiveness of combining LA with PCSK9i in reducing cardiovascular risk.

## Methods

We conducted a comprehensive analysis of patients treated with LA up to 31 December 2018 in five LA centers in Saxony, Germany, which also offered PCSK9i. A total of 200 patients were included in the study. Patients were divided into groups that received either PCSK9i add-on therapy or LA only. The analysis included gender, age, cardiovascular risk factors, lipid profiles, achievement of LDL-C targets recommended by the ESC/EAS guideline and incidence of cardiovascular events.

## Results

Both LA and PCSK9i therapy significantly reduced lipid levels. However, the majority of patients in both groups did not achieve recommended LDL-C targets initially. LA led to a considerable reduction in cardiovascular events across all groups. Patients with additional PCSK9i therapy showed potential benefit, particularly in those with high LDL-C and combined LDL-C and Lp(a) elevation. Notably, the PCSK9i therapy in patients with isolated Lp(a) elevation showed limited additional benefit compared to LA alone.

## Conclusion

Combining LA with PCSK9i offers promise in managing dyslipoproteinemia and reducing cardiovascular risk. While both therapies individually provide lipid-lowering benefits, the combined approach shows potential for enhanced risk reduction, especially in patients with high LDL-C levels. Tailoring therapy based on lipid profiles and cardiovascular risk factors could optimize outcomes in these patients. These results underline the importance of adapting treatment strategies in the treatment of dyslipoproteinaemia to the respective risk profile.

# Poster Uropathologie

P05.01

## ***Real world data on the prevalence of BRCA1/2 and HRR gene mutations in patients with prostate cancer.***

O. Hommerding, M. Hommerding, A.-L. Wulf, V. Tischler, G. Kristiansen  
Institut für Pathologie, Universitätsklinikum Bonn, Bonn, Germany

### **Background**

In May 2020, olaparib received FDA approval for metastatic castration-resistant prostate cancer (mCRPC) with deleterious or suspected deleterious somatic or germline HRR gene mutations. Subsequently, the European Medicines Agency (EMA) endorsed olaparib for patients harboring deleterious or suspected deleterious somatic or germline mutations in BRCA1/2. The prevalence of HRR gene mutations ranges from 19% to 33%, depending on whether primary or metastatic tumor tissue is considered. According to the literature, BRCA2 alterations emerge as the most prevalent, ranging from 6% to 12%.

### **Methods**

This study aims to contribute data on the prevalence of BRCA1/2 and HRR gene mutations in a real world cohort. Therefore, a retrospective analysis of all prostate cancer cases analyzed for BRCA1/2 and HRR gene mutations within the last five years in our institute was performed. 200 cases were identified and all were analyzed using targeted NGS BRCAness multigene panel, which includes 8 HRR genes (ATM, BRCA1, BRCA2, CDK12, CHEK2, FANCA, HDAC2, PALB2).

### **Results**

Interestingly, only a third of the samples sequenced comprised castration-resistant prostate cancer tissue, whereas two thirds were primary tissue samples from the initial diagnosis (e.g. core needle biopsies, RPE specimen), that are expected to be hormone sensitive cancers. In addition, our study demonstrates a comparable prevalence of HRR mutations in our cohort compared to the literature. However, targetable BRCA2 mutations were less frequently identified. Therefore, 20.4% exhibited potentially targetable mutations according to FDA criteria, while only 4.3% met EMA eligibility for olaparib treatment.

### **Conclusion**

The study provides valuable real-world insights into the implementation of BRCA1/2 and HRR gene mutation testing in the clinical practice.

P05.02

## ***Androgen receptor non-genomic signaling as potential androgen sensitizer in castration resistant prostate cancer cells***

T. Mayr<sup>1</sup>, A. Kremer<sup>1</sup>, L. Arèvalo<sup>2</sup>, P. Basitta<sup>1</sup>, F. Hölscher<sup>1</sup>, M. V. Cronauer<sup>1</sup>, G. Kristiansen<sup>1</sup>

<sup>1</sup>Institut für Pathologie, Universitätsklinikum Bonn, Bonn, Germany, <sup>2</sup>Instituto Nacional de Investigación y Tecnología Agraria y Alimentaria, Madrid, Spain

### **Background**

Prolonged androgen deprivation therapy (ADT) often results in tumor recurrence in androgen receptor (AR) expressing prostate cancer (PCa) after 2 – 3 years on average, independent of applied treatment regimen and antiandrogen (AA). To elucidate molecular mechanisms that result in AA-resistance, hormone-sensitive and castration-resistant PCa cells were long-term cultivated in the presence of first and second generation AAs. Resistance formation in resulting PCa sublines was validated by de-inhibition of cell proliferation in the presence of respective AAs. A candidate gene approach combined changes in AR / AR target gene expression with AA-dependent alterations in cancer signaling components in these PCa sublines.

### **Methods**

LNCaP and 22Rv1 cells subjected to long-term (PCa<sup>L<sup>T</sup></sup>) treatment with AAs of increasing affinity (bicalutamide <

apalutamide < darolutamide) to AR and were checked for resistance formation to AAs in androgen-depleted media by MTS assay. 3'RNAseq data were analyzed in a candidate gene approach for changes in cancer-related signaling pathways to find novel mechanisms for PCa resistance formation. Protein expression was confirmed for potential resistance-inducing signaling components and compared with changes in AR target gene expression. pEGFP-AR, pΔt-AR constructs and/or activated pEF-SRC<sub>Y560F</sub> were transfected in HEK293 cells and checked for AR activity using pARE<sub>2</sub>-TATA-luc and pRL-tk constructs.

## Results

We identified upregulation of the glucocorticoid receptor in LNCaP<sup>LT-Apa</sup>, as well as *de novo* expression of ligand-independent AR-V7 splice variant in LNCaP<sup>LT-Bica</sup>. Further cancer signaling components were identified by 3'RNAseq analysis. Consistent with reduced AR activity, 22Rv1<sup>LT</sup> sublines upregulate epidermal growth factor receptor (EGFR) at the RNA and protein levels upon AA treatment, particularly in the 22Rv1<sup>LT-Daro</sup> subline. The non-receptor tyrosine kinase c-SRC mediates EGFR activity as part of non-genomic AR signaling. We identified a specific tyrosine phosphorylation within the AR as critical for sensitizing AR signaling in the presence of low dihydro-testosterone (DHT) levels.

## Conclusion

Upregulation of EGFR/c-SRC signaling may contribute to resistance formation by sensitizing PCa cells to subphysiological androgen concentrations found in patients undergoing ADT.

P05.03

## ***Expression profiles of co-inhibitory receptors in non-urothelial neoplasms of the urinary bladder***

S. Ledderose<sup>1</sup>, L. Eismann<sup>2</sup>, J. Casuscelli<sup>2</sup>, F. Klauschen<sup>1</sup>, C. Ledderose<sup>3</sup>, G. B. Schulz<sup>2</sup>, A. Sendelhofert<sup>1</sup>, S. Rodler<sup>2</sup>

<sup>1</sup>Pathologisches Institut der LMU, München, Germany, <sup>2</sup>Urologische Klinik und Poliklinik der LMU, München, Germany, <sup>3</sup>University of California San Diego, Department of Surgery, San Diego, United States of America

## Background

Pure squamous carcinoma (SCC) and adenocarcinoma (AC) of the urinary bladder are rare malignant diseases and are often diagnosed at an advanced stage. Immune checkpoint inhibitors (ICIs) targeting CTLA-4 and PD-L1/PD-1 have improved prognosis, but have shown low overall response rates and are sometimes associated with severe side effects. New ICIs that target the co-inhibitory receptors (CIR) TIM-3, LAG-3 and TIGIT could represent a further therapeutic option for patients with SCC or AC. Nevertheless, there is only limited data on the expression profiles of these new ICI-targets on tumor-infiltrating lymphocytes (TILs) in SCC and AC.

## Methods

We included patients from a prospectively maintained database of patients undergoing radical cystectomy for SCC and AC. Tissue microarrays were created from representative FFPE tumor-samples and stained for TIM-3, LAG-3 and TIGIT immunohistochemically. The grade of immunoreactive TILs was determined semi-quantitatively. Kaplan-Meier-method and Cox regression models were used to evaluate differences in overall survival (OS) and progression free survival (PFS) between patients with high and low immunoreactive TILs.

## Results

59 patients with SCC and 24 patients with AC were included into this study. TILs showed a high expression of TIM-3 in 24/59 (40.7%) of SCC and in 8/24 (33.3%) of AC (p=0.632). High LAG-3-scores were present in 27/59 (45.8%) of SCC and in 0/24 (0.0%) of AC (p<0.001). High TIGIT expression in TILs was observed in 27/59 patients (45.8%) of all SCC and in 12/24 (50.0%) of AC samples (p=0.810). All three co-inhibitory receptors were highly expressed in 15 (25.4%) patients with SCC. Conversely in AC, no sample showed triple-positivity. In SCC, high TIM-3 expression was associated with poor PFS (p=0.048). High LAG-3 or high TIGIT expression tended to be associated with an impaired PFS, but statistical significance was not reached. In AC, no correlation between co-inhibitory receptor-expression and PFS was observed. In both SCC and AC no statistically significant difference in OS was found based on CIR expression.

## Conclusion

TIM-3, LAG-3 and TIGIT are important regulators of the antitumoral immune response and show variable expression

profiles in SCC and AC. High infiltration with TIM-3 – positive TILs is significantly associated with shorter PFS in patients with SCC. Our results provide new insights into the expression profiles of those molecules in SCC and AC and provide a rationale for innovative CIR-based ICI therapies.

P05.04

## ***Heterogeneity of PSMA-Expression in Primary Prostate Cancer***

M. Remke<sup>1</sup>, H. Wang<sup>2</sup>, S. Chakraborty<sup>1</sup>, K. Schwamborn<sup>1</sup>, N. Pfarr<sup>1</sup>, M. Eiber<sup>2</sup>, K. Steiger<sup>1</sup>

<sup>1</sup>Institute of Pathology, Technical University of Munich, Munich, Germany, <sup>2</sup>Klinikum Rechts der Isar, Technical University Munich, Department of Nuclear Medicine, Munich, Germany

### **Background**

Prostate-specific membrane antigen (PSMA) is a widely used target in the treatment and imaging of prostate cancer. PSMA-PET offers excellent specificity in detecting primary prostate cancer and lymph node metastases. Regarding sensitivity, however, different data can be found in the literature, and PSMA-negativity of primary prostate cancers has also been reported. Therefore, we studied the heterogeneity of PSMA expression in primary prostate cancer within and between individual patients and molecular pathologically analyzed areas with different PSMA expression.

### **Methods**

We established a workflow for the coregistration of PSMA ligand uptake, histology, and PSMA immunohistochemistry (IHC). For this purpose, we used prostatectomies of patients who had undergone radio-guided surgery at the Klinikum rechts der Isar, TUM. These patients received 99mTc-PSMA-I&S intravenously to allow intraoperative detection of lymph node metastases. We performed autoradiography (ARG) of 5 mm prostate slices and matched and compared these images to H&E-stained slides (Gleason score, GS) and PSMA-IHC in a grid-based manner (size of grids: 3x3 mm). Based on IHC, we dissected PSMA-positive and PSMA-negative areas of 8 patients and performed RNA-sequencing using a modified CapSeq protocol optimized for formalin-fixed paraffin-embedded tissues.

### **Results**

17 prostatectomies with a total of 4660 grids were included. Marked intra- and inter-patient heterogeneity of PSMA expression was detected: PSMA negative foci in PSMA-ARG were observed in all samples and 8 patients (47%) showed negative areas in PSMA-immunohistochemistry. Higher PSMA-ligand uptake was observed in  $GS \geq 8$  than in  $GS < 8$  ( $p < 0.001$ ). However, the presence of PSMA-negative areas did not correlate with the GS. Preliminary data from 8 patients points towards a different RNA-expression profile between PSMA-positive and PSMA-negative areas.

### **Conclusion**

PSMA expression (IHC) and PSMA-ligand uptake (ARG) show marked heterogeneity within and between individual patients. Differences in the sensitivity of IHC and ARG are caused primarily by the lower spatial resolution of ARG. Prostate carcinoma with  $GS \geq 8$  showed significantly higher ligand uptake compared with  $GS < 8$  and non-neoplastic prostate tissue, which underlines the role of PSMA imaging as a non-invasive biomarker in prostate cancer. Preliminary results indicate that PSMA-positive and PSMA-negative foci are phenotypically distinct clones with a characteristic RNA signature.

Literaturangaben:

[1] Hui Wang#, Marianne Remke#, Thomas Horn, Kristina Schwamborn, Yiyao Chen, Katja Steiger, Wilko Weichert, Hans-Jürgen Wester, Margret Schottelius, Wolfgang A Weber, Matthias Eiber, (2023), Heterogeneity of prostate-specific membrane antigen (PSMA) and PSMA-ligand uptake detection combining autoradiography and postoperative pathology in primary prostate cancer, *EJNMMI Res.*, Nov 16;13(1):99, <https://ejnmmires.springeropen.com/articles/10.1186/s13550-023-01044-8>, 2024-02-19



P05.05

## **Selective embedding of prostatectomy specimen - is “more” really “better”**

M. Bernhardt<sup>1</sup>, L. Weinhold<sup>2</sup>, O. Hommerding<sup>1</sup>, T. Kreft<sup>1</sup>, M. Schmid<sup>2</sup>, G. Kristiansen<sup>1</sup>

<sup>1</sup>Universitätsklinikum Bonn, Institut für Pathologie, Bonn, Germany, <sup>2</sup>Universitätsklinikum Bonn, Institut für Medizinische Biometrie, Informatik und Epidemiologie, Bonn, Germany

### **Background**

Prostate cancer is one of the most common types of cancer in men [1]. Histopathologic examination of radical prostatectomy specimens is important for determining tumor characteristics that affect prognosis [2]. The extent of tumor embedding required is a subject of ongoing debate [3][4]. This prospective study aimed to develop a time-efficient approach for processing radical prostatectomy specimens with selective embedding while maintaining diagnostic accuracy.

### **Methods**

A total of 226 prostatectomy specimens were analyzed to compare a highly standardized selective embedding protocol with complete embedding as the gold standard. Diagnostic parameters including pT stage, margin status (R), International Society of Urological Pathology (ISUP) grade groups, as well as the presence of intraductal carcinoma of the prostate (IDC-P) and cribriform tumor growth were evaluated for concordance.

### **Results**

Selective embedding demonstrated consistent and accurate diagnostic outcomes, with concordance rates ranging from 90% to 98% across various parameters including pT-stage, margin status (R), ISUP grade groups, IDC-P, and cribriform tumor growth.

### **Conclusion**

Selective embedding demonstrated consistent and accurate diagnostic outcomes, with concordance rates ranging from 90% to 98% across various parameters including pT-stage, margin status (R), ISUP grade groups, IDC-P, and cribriform tumor growth.

**Conclusion:** This study establishes a standardized protocol for selective embedding of radical prostatectomy specimens, with only minimal information loss while reducing material cost by an average of 46.6 %.

### Literaturangaben:

[1] Bergengren, Oskar; Pekala, Kelly; Matsoukas, Konstantina; Fainberg, Jonathan; Mungovan, Sean; Bratt, Ola; Bray, Freddie; Brawley, Otis; Luckenbaugh, Amy; Mucci, Lorelei; Morgan, Todd; Carlsson, Sigrid, (2023), 2022 Update on Prostate Cancer Epidemiology and Risk Factors-A Systematic Review, European Urology, 2

[2] (2022), Urinary and Male Genital Tumors, International Agency for Research on Cancer, World Health Organization classification of tumors, Lyon, 5, International Agency for Research on Cancer

[3] Collette, Eelco; den Bakker, Michael; Klaver, Sjoerd; Vis, André; Kliffen, Mike, (2019), Partial versus complete prostatectomy specimen sampling: prospective non-inferiority study for pT3a tumours and surgical margin involvement, BMJ Open, 4

[4] Montironi, Rodolfo; Lopez Beltran, Antonio; Mazzucchelli, Roberta; Cheng, Liang; Scarpelli, Marina, (2012), Handling of radical prostatectomy specimens: total embedding with large-format histology, International Journal of Breast Cancer

P05.06

## **The coding Toll-like Receptor 4 polymorphism rs4986790 does not influence the risk for penile cancer development in Caucasians**

R. Stöhr<sup>1</sup>, O. Wendler<sup>2</sup>, J. Giedl<sup>1</sup>, N. Gaisa<sup>3</sup>, G. Richter<sup>4</sup>, V. Campean<sup>5</sup>, M. Burger<sup>6</sup>, B. Wullich<sup>7</sup>, S. Bertz<sup>1</sup>, L. Tögel<sup>1</sup>, A. Hartmann<sup>1</sup>

<sup>1</sup>Universitätsklinikum Erlangen, Institut für Pathologie, Erlangen, Germany, <sup>2</sup>Universitätsklinikum Erlangen, Hals-Nasen-Ohren-Klinik – Kopf- und Halschirurgie, Erlangen, Germany, <sup>3</sup>Universitätsklinikum Ulm, Institut für Pathologie, Ulm, Germany, <sup>4</sup>Institut für Pathologie, Hameln, Germany, <sup>5</sup>Institut für Pathologie, Ansbach, Germany, <sup>6</sup>Universitätsklinikum Regensburg, Lehrstuhl für Urologie am Caritas-Krankenhaus St. Josef, Regensburg, Germany, <sup>7</sup>Universitätsklinikum Erlangen, Urologische und Kinderurologische Klinik, Erlangen, Germany

### **Background**

Persistent high risk HPV infection has become an established cause of human carcinogenesis including penile

squamous cell carcinoma (SCC). As not all infected males develop penile SCC variability in host genetic factors might play a role in carcinogenesis. One such factor is pathogen recognition receptors of the innate immunosystem like Toll-like receptors (TLRs). TLRs act as initiators of inflammatory response to infections and tissue injury. Increasing evidence suggests that TLRs also have either antitumor or protumor effects on carcinogenesis. TLR4 was reported to regulate inflammatory responses. In addition, TLR4 was demonstrated to promote EMT and cancer cell migration. The polymorphism rs4986790 in TLR4 results in a substitution of amino acid 299 from aspartic acid to glycine and is known to modify susceptibility to various human pathogens. In addition, many studies suggested a potential relationship between rs40986790 alleles and tumors, e.g. a higher risk for gastric, colorectal, ovarian and cervical cancer. To date no data for a possible influence of TLR4 SNP rs4986790 on penile SCC risk are available. Therefore, the aim of the presented preliminary study was the evaluation of a possible influence of rs4986790 on penile cancer risk.

## Methods

DNA was isolated from archival non-cancerous and tumorous tissue of 87 penile SCC cases. Distribution of rs4986790 (c.896A>G; p.D299G) gene was determined by Sanger sequencing. HPV detection in the SCC tissue was done by usage of GP5+/6+ primers followed by subtype-specific PCR. For comparison genotype distribution data of 920 Caucasian male controls taken from the literature were used.

## Results

Distribution of rs4986790 followed the Hardy-Weinberg equilibrium in both cases and controls. HPV DNA was detected in 39% of the penile SCC cases. Overall, there was no significant difference in the distribution of rs4986790 neither between cases and controls ( $p=0,907$ ) nor between HPV positive and negative cases ( $p=0,705$ ). The frequency of the presence of the risk allele did also not differ significantly between cases and controls ( $p=0,729$ ). There was also no association between rs4986790 genotypes and age of disease onset ( $p=0,670$ ).

## Conclusion

Our preliminary data argue against an influence of the TLR4 rs4986790 SNP on risk for development of penile SCC in Caucasians. Even in combination with HPV status the SNP appears not to be associated with an increased disease risk in HPV positive cases as it was reported for HPV-associated lesions in other organs.

P05.07

## ***Investigating novel treatment options: Inhibition of cullin 1, 4 and 5 reduces viability of testicular germ cell tumour cell lines***

A. Liesen<sup>1</sup>, A. Hansen<sup>1</sup>, K. Funke<sup>1</sup>, R. Islam<sup>1</sup>, G. Kristiansen<sup>2</sup>, H. Schorle<sup>1</sup>

<sup>1</sup>Institute of Pathology, University Hospital Bonn, Germany, Developmental Pathology, Bonn, Germany, <sup>2</sup>Institute of Pathology, University Hospital Bonn, Germany, Pathology, Bonn, Germany

## Background

Testicular germ cell tumours (TGCT) are the most common tumour in young men. The treatment regimen consists of surgery and a combination of radiotherapy and platinum-based chemotherapy (CDDP). However, in 10-30% of patients diagnosed with metastatic non-seminoma, survival rates are low due to CDDP resistance, so new treatment approaches are needed [1]. Using a CRISPR-activation screen in TGCT cell lines, neddylation was shown to contribute to cisplatin resistance [2].

Neddylation triggers the activation of Cullin Ring Ligases (CRL), which ubiquitinylate substrates and thus regulate 20% of the proteasomal protein breakdown process within the cell [3], [4]. The substrates of the E3 ligases are divided into cullins and non-cullins.

## Methods

Here, we tested the effect of various cullin inhibitors using an XTT viability assay on non-seminoma embryonal carcinoma cell lines and a choriocarcinoma cell line as well as a seminoma cell line.

Next, we will perform staining of an in-house generated TGCT-tissue microarray (169 patient samples, 5 controls) using Cullin-antibodies in order to elucidate the protein level and distribution in tumour vs. healthy tissue.

## Results

Treatment with 33-11 (cullin 4 inhibition) or Gossypol (cullin 5 & 1 inhibition) showed a strong decrease in the viability of all tested TGCT cell lines. Inhibition of other cullins using suramin, Nac-Opt and DI591 was less effective.

## Conclusion

The data suggest that inhibition of Cullin 4 using 33-1 and Cullin 1 and 5 using gossypol seems to be the most promising approach. Further, it suggests, that the effect detected using MLN4924, which inhibits neddylation in general might be in the case of the cullins primarily caused by inhibition of cullin 1,4 and 5. Thus, selective inhibition of cullins might open up new avenues for treating (platinum-resistant) GCTs.

Literaturangaben:

- [1] Daniel Nettersheim, Sina Jostes, Simon Schneider, and Hubert Schorle, (2016), Elucidating human male germ cell development by studying germ cell cancer, *Reproduction*, <https://rep.bioscientifica.com/view/journals/rep/152/4/R101.xml>
- [2] Kai Funke, Ulf Einsfelder, Aylin Hansen, Lena Arévalo, Simon Schneider, Daniel Nettersheim, Valentin Stein, Hubert Schorle, (2023), Genome-scale CRISPR screen reveals neddylation to contribute to cisplatin resistance of testicular germ cell tumours, *British Journal of Cancer*, <https://pubmed.ncbi.nlm.nih.gov/37024667/>
- [3] Wu K, Huynh KQ, Lu I, Moustakim M, Miao H, Yu C, Haeusgen MJ, Hopkins BD, Huang L, Zheng N, Sanchez R, DeVita RJ, Pan ZQ., (2021), Inhibitors of cullin-RING E3 ubiquitin ligase 4 with antitumor potential., *Proceedings of the National Academy of Sciences of the United States of America*, <https://pubmed.ncbi.nlm.nih.gov/33602808/>
- [4] Yu Q, Hu Z, Shen Y, Jiang Y, Pan P, Hou T, Pan ZQ, Huang J, Sun Y., (2020), Gossypol inhibits cullin neddylation by targeting SAG-CUL5 and RBX1-CUL1 complexes. *Neoplasia*, <https://pubmed.ncbi.nlm.nih.gov/32145688/>

P05.08

## ***Immunohistochemical validation of potential prognostic biomarkers for prostate cancer***

T. Kreft<sup>1</sup>, G. Kristiansen<sup>2</sup>

<sup>1</sup>Institut für Pathologie Uniklinikum Bonn, Pathologie, Bonn, Germany, <sup>2</sup>Institut für Pathologie, Universitätsklinikum Bonn, Bonn, Germany

### Background

Prostate cancer is one of the most common types of cancer in men[37202314][33538338]. In a previous analysis of the prostate cancer TCGA dataset, we identified approximately 20.000 differentially expressed genes of which 50 were prognostic of biochemical relapse following radical prostatectomy[31170942].

### Methods

In this pursuit, seven prognostic transcripts were meticulously scrutinized (AKAP8, ATP6V1D, DLK1, EMRE, GBAS, RalB, WDR79) through immunohistochemistry, employing a cohort comprising 300 clinically annotated prostate cancer cases. Employing the sophisticated open-source software QuPath, this evaluation unfolded semi-automatically, adhering to the methodology proposed by Bankhead et al.[29203879].

### Results

This investigation failed to establish a significant correlation between the expression levels of the scrutinized markers and various clinicopathological parameters, including Gleason score, pT-stage, pN-stage, and serum PSA levels. However, a noteworthy revelation surfaced in survival analysis, where the overexpression of RalB emerged significantly associated with enhanced overall survival in the Kaplan-Meier analysis. Yet, this association failed to attain statistical significance in the multivariable analysis.

### Conclusion

In conclusion, this exploration underscores the imperative realization that prognostic transcripts unearthed through the data mining of public databases may not seamlessly translate into prognostic biomarkers at the protein level. The subsequent imperative lies in subjecting such findings to rigorous validation through immunohistochemistry. Notably, RalB emerges as a potential prognostic biomarker for prostate cancer progression, prompting the urgency for comprehensive and further investigative studies.

Literaturangaben:

[29203879] Bankhead, P. et al., (2017), QuPath: Open source software for digital pathology image analysis , <https://doi.org/10.1038/s41598-017-17204-5>

[31170942] Kremer A, Kremer T, Kristiansen G, Tolkach Y, (2019), Where is the limit of prostate cancer biomarker research? Systematic investigation of potential prognostic and diagnostic biomarkers., <https://doi.org/10.1186/s12894-019-0479-z>

[33538338] Sung H, Ferlay J, Siegel RL, Laversanne M, Soerjomataram I, Jemal A, Bray F, (2020), GLOBOCAN Estimates of Incidence and Mortality Worldwide for 36 Cancers in 185 Countries

[37202314] Bergengren O, Pekala KR, Matsoukas K, Fainberg J, Mungovan SF, Bratt O, Bray F, Brawley O, Luckenbaugh AN, Mucci L, Morgan TM, Carlsson SV, (2022), Update on Prostate Cancer Epidemiology and Risk Factors-A Systematic Review, European Urology, <https://doi.org/10.1016/j.eururo.2023.04.021>

P05.09

## ***Proteomic signatures in sporadic progressive and localized clear cell renal cell carcinoma***

T. Feilen<sup>1</sup>, A. L. Kössinger<sup>1</sup>, M. Rogg<sup>1</sup>, M. Grabbert<sup>2</sup>, M. Werner<sup>1</sup>, C. Schell<sup>1</sup>, O. Schilling<sup>1,3</sup>

<sup>1</sup>Institute for Surgical Pathology, Faculty of Medicine, Medical Center, University of Freiburg, Freiburg im Breisgau, Germany,

<sup>2</sup>Department of Urology, Faculty of Medicine, Medical Center, University of Freiburg, Freiburg im Breisgau, Germany, <sup>3</sup>German Cancer Consortium (DKTK) and German Cancer Research Center (DKFZ), Heidelberg, Germany

### **Background**

Renal cell carcinoma (RCC) is among the 10 most common cancers worldwide. A major subtype, clear cell RCC (ccRCC) accounts for 75% of all RCC cases and hence is the most common malignancy of the kidney. ccRCC is a highly heterogeneous tumor characterized by diverse clinical outcomes, including progressive disease with the development of distant metastases. Understanding the molecular mechanisms underlying disease progression is crucial for improving prognostic stratification and developing targeted therapies.

### **Methods**

In this study, we performed a comprehensive proteomic analysis of formalin-fixed paraffin-embedded (FFPE) patient samples (n = 41) to investigate the molecular alterations associated with progressive and localized ccRCC. Patient samples comprising tumor tissue and normal adjacent tissue (NAT) were collected for each individual. To ensure robust comparisons, patients with localized ccRCC were matched to those with metastasized disease based on sex, age and tumor grading. A chi-square test confirmed comparable grading and sex between the localized and metastasized patient samples.

### **Results**

In our study, we employed mass spectrometry-based proteomics to analyse ccRCC patient samples with a depth of > 7000 proteins. To enhance confidence, we showed integrability of our data into a proteomic dataset from CPTAC. Differential abundance analysis revealed subtle differences between metastasized and localized tumors in proteins involved in TCA cycle and ribosome biosynthesis. Additionally, the k-means clustering of tumor samples uncovered four distinct clusters exhibiting upregulated proteins associated with extracellular matrix organisation, mitochondrial respiration, immune response and small molecule metabolism.

### **Conclusion**

Our study highlights the proteomic signatures and complexity inherent in ccRCC. We elucidate subtle proteome alterations linked to disease progression, while also revealing four distinct tumor clusters showcasing more pronounced proteomic differences.

## ***The non-clear cell renal cell carcinoma subtype composition of a European cohort- Results from reference pathology of the SUNNIFORECAST study.***

L. Vorfelder<sup>1</sup>, C. Stöhr<sup>1</sup>, C. Matek<sup>1</sup>, M. Ahrens<sup>2</sup>, J. Haanen<sup>3</sup>, B. Escudier<sup>4</sup>, M. Gross-Goupil<sup>5</sup>, E. Boleti<sup>6</sup>, G. Gravis<sup>7</sup>, A. Flechon<sup>8</sup>, M.-O. Grimm<sup>9</sup>, J. Bedke<sup>10</sup>, P. Barthélémy<sup>11</sup>, D. Castellano<sup>12</sup>, B. Mellado<sup>13</sup>, P. Ivanyi<sup>14</sup>, I. Polifka<sup>1,15</sup>, F. Lange<sup>1</sup>, A. Agaimy<sup>1</sup>, L. Bergmann<sup>16</sup>, A. Hartmann<sup>1</sup>

<sup>1</sup>Friedrich-Alexander-Universität-Erlangen-Nürnberg, Institut für Pathologie, Erlangen, Germany, <sup>2</sup>Goethe University, Meizinische Klinik II, Frankfurt am Main, Germany, <sup>3</sup>Netherlands Cancer Institute, Division of Medical Oncology, Amsterdam, The Netherlands, <sup>4</sup>Institut Gustave Roussy, Service des Opérations de Recherche Clinique, Villejuif Cedex, France, <sup>5</sup>Hopital Saint André, Hopital Saint André, Bordeaux, France, <sup>6</sup>Royal Free London NHS Foundation Trust, Department of Oncology, London, United Kingdom, <sup>7</sup>Institut Paoli-Calmettes, Département d'Oncologie Médicale, Marseille, France, <sup>8</sup>Centre Léon Bérard, Département de Cancérologie Médicale, Lyon Cedex 08, France, <sup>9</sup>Universitätsklinikum Jena, Urologische Klinik und Poliklinik, Jena, Germany, <sup>10</sup>Universitätsklinikum Tübingen, Klinik für Urologie, Tübingen, Germany, <sup>11</sup>Hôpitaux Universitaires de Strasbourg - Hôpital de Hautepierre, Service d'Oncologie et d'Hématologie, Strasbourg Cedex, France, <sup>12</sup>Hospital Universitario 12 de Octubre, Medical Oncology Service, Madrid, Spain, <sup>13</sup>Hospital Clinic de Barcelona, Medical Oncology Service, Barcelona, Spain, <sup>14</sup>Medical School Hannover (MHH), Hematology, Hemostasis, Oncology, and Stem Cell Transplantation, Hannover, Germany, <sup>15</sup>Human Pathology Practice Dr. Weiß MVZ GmbH, Erlangen, Germany, <sup>16</sup>Universitätsklinikum Frankfurt / Goethe Universität, Hämatologie/Onkologie, Frankfurt am Main, Germany

### **Background**

The 2022 WHO classification defined several molecular subtypes, resulting in more than 20 entities of renal cell carcinomas (RCC) in total. As several of these subtypes are linked to poor prognosis, clinical studies investigating patients with well characterized tumours are urgently needed. Exact classification of non-clear cell RCC (nccRCC) including histopathological and molecular diagnostics is a prerequisite. The SUNNIFORECAST study (NCT03075423) is a phase 2 randomised open/label investigator initiated trial of nivolumab with ipilimumab vs. standard of care in patients with previously untreated and advanced nccRCC. For study inclusion, a reference pathology to confirm diagnosis of nccRCC was mandatory.

### **Methods**

350 cases were submitted by the primary pathologists for reference pathology as paraffin blocks or unstained slides. Diagnostic procedures followed the recommendations of the WHO 2022 classification and included H&E staining, immunohistochemistry and molecular testing.

### **Results**

In 334 of 350 cases, reference pathology confirmed the diagnoses of nccRCC. During reevaluation, only few cases were diagnosed as ccRCC, liposarcoma or epithelioid angiomyolipoma. Histopathological diagnoses included papillary RCC (n = 138 - 41%), chromophobe RCC (n = 58 - 17%), RCC, NOS, mostly with pure sarcomatoid pattern (n = 30 - 71%), TFE3 or TFEB altered RCC (n = 25 and n = 1, respectively - 8%), FH-deficient RCC (n = 33 - 10%), SDHB-deficient RCC (n = 4 - 1%), SMARCB1-deficient renal medullary carcinoma (n = 9 - 3%), collecting duct carcinoma (n = 14 - 4%) and tubulocystic RCC (n = 1). Interestingly, no tumours from the category of other oncocytic tumours and no clear cell papillary renal cell tumours were detected. Compared to primary pathology, diagnosis changed in 116/350 cases. There was incorrect primary diagnosis in 28/33 cases of FH-deficient RCC, 3/4 cases of SDHB deficient RCC and 17/26 cases of translocation RCC. All chromophobe RCC showed sarcomatoid dedifferentiation or coagulative tumour necrosis. Micropapillary and microcystic architecture were specifically and very frequently detected in G1/G2 papillary RCC tumours.

### **Conclusion**

In conclusion, the diagnosis of molecularly defined RCC is still problematic in daily practice. Therefore, reference pathology is a prerequisite for clinical studies investigating ncc RCC.

# Poster Thoraxpathologie

P10.01

## **Long-term cryopreservation and revitalization of human PCLS**

S. Schubert<sup>1</sup>, L.-J. Schröder<sup>1</sup>, D.-H. Park<sup>1</sup>, E. K. Plucinski<sup>1</sup>, C. Werlein<sup>1</sup>, M. Kühnel<sup>2</sup>, D. D. Jonigk<sup>1,2</sup>, J.-C. Kamp<sup>1,3</sup>, L. Neubert<sup>1</sup>

<sup>1</sup>Institut für Pathologie, Medizinische Hochschule Hannover, AG Lungenforschung, Hannover, Germany, <sup>2</sup>Institut für Pathologie, Universität Aachen, Aachen, Germany, <sup>3</sup>Klinik für Pneumologie, Medizinische Hochschule Hannover, Hannover, Germany

### **Background**

Human precision-cut lung slices (hPCLS) are a relevant *ex vivo* organ slice culture model for studying the basic mechanisms and novel treatment approaches of lung diseases such as asthma, idiopathic pulmonary fibrosis (IPF) and other interstitial lung diseases (ILD). The hPCLS preserve the natural 3-dimensional tissue architecture of the lung parenchyma, airways, interstitial connective tissue, vasculature, and immunocompetent cells, therefore allowing for a more accurate representation of the lung compared to traditional 2-dimensional models. The preparation and cultivation of hPCLS for large-scale clinical studies or personalized therapy response prediction relies on the collection of fresh human lung tissue. The cryopreservation of hPCLS would mean a valuable advancement of this model as the availability of fresh human lung tissues is always limited. To date, no reliable cryopreservation protocol for hPCLS is available.

### **Methods**

Our aim is to establish a robust cryopreservation protocol by optimizing cryomedia and freezing conditions. Ultimately, the protocol should allow for the preservation of tissue integrity and viability, enabling the creation of a flexible on-demand biobank of hPCLS for future use.

### **Results**

Investigation of n=12 donors (female to male ratio 7:5, aged 40-78 years) with reported ILDs and lung carcinomas used for generation of hPCLS showed that DMEMF12 with 10% DMSO and additional 10% FCS, but not more, has a positive effect on the viability and tissue integrity of hPCLS after cryopreservation for up to 28 days and rapid thawing. Methodologically, we used for the first time a combination of WST1/WST8 and LDH assays to demonstrate elevated viability up to 90% and comparison to hPCLS parallel culture. Our study highlights a ciliary motility recovery rate of 97% at d1 post cryopreservation in comparison to respective controls. Utilizing histomorphological grading, we found out that the bronchial epithelium is almost unaffected by freezing of hPCLS, while a moderate preservation of the alveolar epithelium and low preservation of the endothelium is observed.

### **Conclusion**

Our preliminary data holds out the prospect of more flexible application options and improved therapy response predictions by the utilization of cryopreserved hPCLS with increased viability for a range of lung diseases.

P10.02

## **Machine-learning based BAL cytology of lung transplant patients**

M. Gerckens<sup>1</sup>, C. Mümmler<sup>1</sup>, J. Strodel<sup>1</sup>, G. Burgstaller<sup>2</sup>, J. Behr<sup>1</sup>, N. Kneidinger<sup>1</sup>

<sup>1</sup>Department of Medicine V, LMU University Hospital, LMU Munich, Comprehensive Pneumology Center (CPC), Member of the German Center of Lung Research (DZL), München, Germany, <sup>2</sup>Institute of Lung Health and Immunity (LHI), Comprehensive Pneumology Center (CPC), Helmholtz Munich, Member of the German Center of Lung Research (DZL), München, Germany

### **Background**

Long-term survival after lung transplantation (LTX) is limited by the poorly understood chronic lung allograft dysfunction (CLAD). Differential cytology of bronchoalveolar lavage (BAL) plays an important role for the surveillance of LTX recipients, as BAL neutrophilia and eosinophilia are important risk factors for CLAD development. Usually, BAL differential cytology is manually assessed, which is time-consuming and examiner dependent. We used a machine-learning based BAL cytology computer vision (BAL-ML) model for the evaluation of differential cytology of BAL cytopins.

## Methods

More than 500 BAL cytopsins of LTX patients were imaged using a Zeiss AxioScan slide scanner. Manual cell segmentation and differential cell labeling for the ground truth generation for training was performed by two respiratory physicians independently. Labeled training data contained representative as well as granulocyte- and lymphocyte-enriched image-subsets. Differential cell counts from clinical reports were obtained separately.

## Results

Preliminary Mask-RCNN based models achieved a performance comparable to human interrater reliability in single cell macrophage, lymphocyte and granulocyte evaluation. Macrophage, lymphocyte, neutrophil, and lymphocyte cell counts generated by the BAL-ML model and clinical reports correlated significantly ( $R^2=0.86$ ,  $p<0.001$ ;  $R^2=0.62$ ,  $p<0.001$ ;  $R^2=0.81$ ,  $p<0.001$ ;  $R^2=0.34$ ,  $p<0.001$ ; respectively). Cell count derived neutrophilia between BAL-ML model and clinical reports reached a interrater reliability for neutrophilia (>15%) with a Cohens Kappa of 0.75, for lymphocytosis (>15 %) of 0.46 and for eosinophilia (>1%) of 0.51, respectively.

## Conclusion

BAL differential cytology by BAL-ML models is feasible and reliable. Further validation of the models is ongoing. In the future, these validated models could assist BAL cytology in clinical routine for rapid and accurate BAL reports.

P10.03

## ***Correlation of pulmonary ultrasound features with histopathology in conventional and minimally invasive postmortems***

G. Weirich<sup>1</sup>, J. Slotta-Huspenina<sup>1,2,3</sup>, K. Stock<sup>3</sup>

<sup>1</sup>Technical University Munich, School of Medicine, Institute of Pathology, München, Germany, <sup>2</sup>Pathologie Starnberg MVZ GmbH, Starnberg, Germany, <sup>3</sup>Technical University Munich, School of Medicine, Department of Nephrology, München, Germany

## Background

Computed tomography (CT) and ultrasound (US) are commonly used in forensic medicine, but not in clinical postmortems. The gold standard remains conventional autopsy (CA), but its popularity among clinicians and the public has decreased. As a substitute for CA, imaging-based postmortems and minimally invasive procedures gained attention. We employed an interdisciplinary approach to conduct lung US in COVID-19 victims, and then used US-MITS and CA to compare US findings with histomorphology.

## Methods

Following informed consent from the next-of-kin, we employed a standardized pulmonary ultrasound protocol established for COVID-19 patients [1] using a Siemens-Accuson S 3000 ultrasound system in 23 individuals who died from COVID-19, then proceeded with US-MITS (n=23) and CA (n=10). Two cases involved using US/CT fusion. The CA included removing the lungs, applying a standardized inking protocol, and performing transverse sectioning. Microscopical analyses were conducted on sections taken from pathologic US sites and MITS puncture sites. Altogether, 20 lung wings were investigated to compare the results of CA with those of US-MITS.

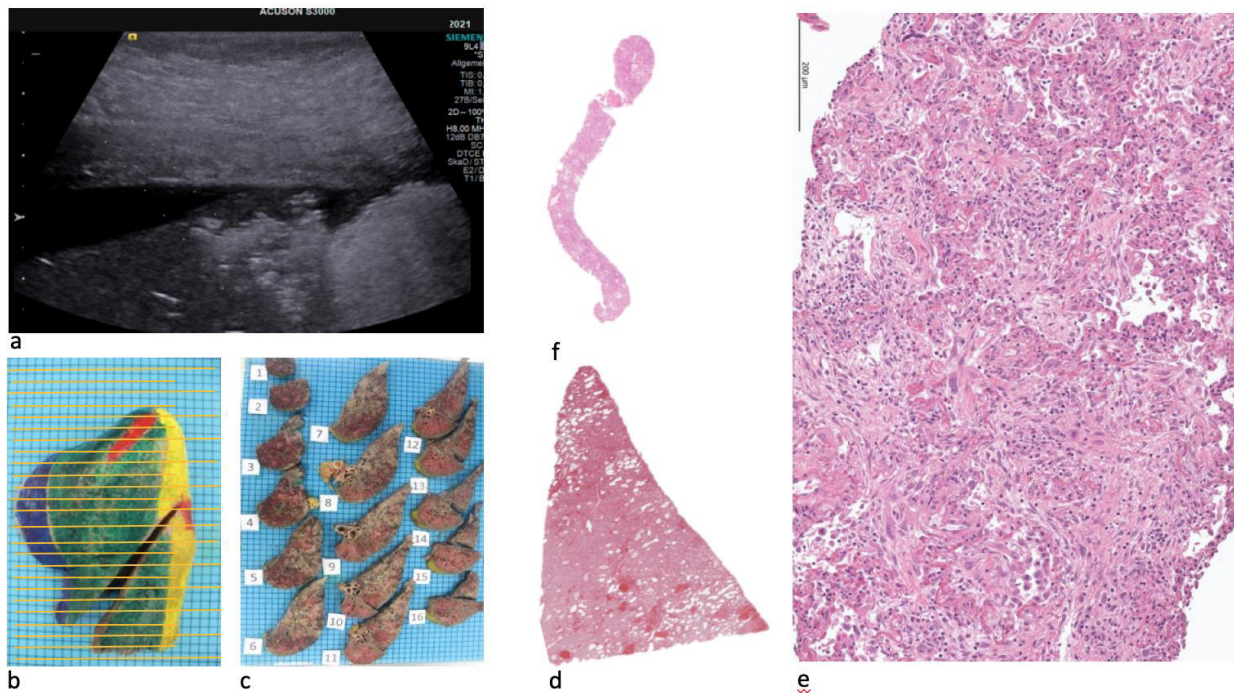


Fig. 1: a - Pulmonary US, subpleural consolidation, b - standardized inking, c - sectioning, d & e - fibrosis, (H&E), f - similar finding in MITS sample

## Results

Lung US detected 200 peripheral lung lesions in 23 deceased (mean 8,7): consolidation (161/200), air trapping (64/200), fragmented pleura (58/200), and B-lines (22/200). Air trapping was highly associated with consolidation ( $p < 0,001$ ). Microscopic analysis of lung samples holding US changes revealed severe fibrosis in cases of consolidation (fig.1), various stages of diffuse alveolar damage in samples with fragmented pleura and distended air spaces and lung remodeling in samples with air trapping. The comparison of CA samples with those from US-MITS did not reveal substantial discrepancies.

## Conclusion

To detect peripheral lung lesions in COVID-19 pneumonia, lung US can be a valuable tool. In our study, we found that similar lesions can also be detected postmortally. In addition, US-MITS provided pathologic lung samples that are diagnostically as powerful as CA-derived specimens, making postmortal US-MITS a viable alternative to CA.

## Literaturangaben:

[1] Kiefl, D., Eisenmann, S., Michels, G., Schmid, M., Ludwig, C., Pin, M., Gloeckner, E., Petersen, P.F., Damjanovic, D., Schellhaas, S., Janssens, U., Fandler, M., Blaschke, S., Geuting, M., Mueller, T., Menze, J., Heinzmann, A., Helm, M., Lambracht, A., D., Bernhard, M., Spethmann, S., Stock, K.F., Clevert, D.A., Breitkreutz, R., (2020), German recommendations on lung and thoracic ultrasonography in patients with COVID-19., *Med Klin Intensivmed Notfmed*, 654-667, 115(8)

P10.04

## ***mRNA expression analysis of explanted decellularized allogenic cardiovascular heart valves***

A. Seidel<sup>\*1</sup>, L. Neubert<sup>\*1,2</sup>, C. Werlein<sup>1,2</sup>, P. Braubach<sup>1,2</sup>, H. Freitag<sup>1,2</sup>, C. Riehle<sup>3</sup>, D. Jonigk<sup>2,4</sup>, J.-C. Kamp<sup>1,2</sup>, S. Sarikouch<sup>5</sup>

<sup>1</sup>Institute of Pathology, Medical School Hannover, Hannover, Germany, <sup>2</sup>Biomedical Research in Endstage and Obstructive Lung Disease Hannover (BREATH), Deutsches Zentrum für Lungenforschung (DZL), Hannover, Germany, <sup>3</sup>Department of Cardiology and Angiology, Medical School Hannover, Hannover, Germany, <sup>4</sup>Institute of Pathology, Medical Faculty, RWTH University Aachen, Aachen, Germany, <sup>5</sup>Department for Cardiothoracic, Transplant, and Vascular Surgery, Medical School Hannover, Hannover, Germany

\*Contributed equally



## Background

Implanted human heart valves' long-term survival is primarily determined by the immune response against the allogeneic tissue. Decellularized human donor valves have been developed, tested, and clinically used at the Hannover Medical School over the past 20 years. In pulmonary valve replacement, decellularized human donor valves are now the new gold standard. However, a few patients show early degeneration.

The study objective was to gain histomolecular insight into the mechanisms leading to tissue degeneration and immune response.

## Methods

Therefore, Formalin-fixed and paraffin-embedded tissues from fresh explanted decellularized aortic valves (n=14) and pulmonary valves (n=13) were used. RNA was isolated and analyzed using NanoString® technology, focusing on fibrosis and inflammation-related genes. Formalin-fixed and paraffin-embedded tissues from fresh explanted donor aortic valves (n=7) and donor pulmonary valves (n=8) served as controls.

## Results

Our analysis revealed 56 differentially expressed genes in decellularized aortic valves compared to donor aortic valves, of which 21 are upregulated and 35 are downregulated. Furthermore, compared to the donor pulmonary valves, decellularized pulmonary valves showed 115 differentially expressed genes, including 66 upregulated and 49 downregulated genes. In both aortic and pulmonary valve explants, we found increased expression of fibrosis-, inflammation-, and endothelium- related genes and a decreased expression of complement encoding genes consistent with the pathway activity pattern assessed by IPA.

## Conclusion

Once we better understand the molecular mechanisms behind the immunological activation after decellularized human heart valve implantation, the possibility of masking the corresponding antigens before implantation through appropriate silencing methods may arise.

# Poster Molekularpathologie I

P11.01.01

## ***Cloud-based software for visualization and data analysis of Visium-measured tissue cohorts.***

W. Zhang<sup>1</sup>, P. T. Tran<sup>1</sup>, F. Wee<sup>2</sup>, W. Yim<sup>2</sup>, L. Y. Chong<sup>2</sup>, Z. W. Neo<sup>2</sup>, M. C. Lau<sup>2,3</sup>, J. P. S. Yeong<sup>2,4</sup>, [A. Ly](#)<sup>1</sup>, N. Verbeeck<sup>1</sup>, M. Claesen<sup>1</sup>, N. H. Patterson<sup>1</sup>

<sup>1</sup>Aspect Analytics NV, Genk, Belgium, <sup>2</sup>A\*STAR, Institute of Molecular and Cell Biology (IMCB), Singapore, Singapore, <sup>3</sup>A\*STAR, Bioinformatics Institute (BII), Singapore, Singapore, <sup>4</sup>Singapore General Hospital, Department of Anatomical Pathology, Singapore, Singapore

## Background

Spatial profiling technologies enable the investigation of various molecular classes in a tissue-based context, providing valuable insights into spatial patterns within tumors and their microenvironment. The spatial transcriptomic Visium assay (ST) has been widely adopted as it maps quantitative gene expression data to their original location in tissue sections. This has produced demand for software where multiple ST datasets can be viewed and analyzed together. We present a software package allowing simultaneous viewing of a cohort of ST measurements, and includes integration of complementary data (pathologist annotations, bioinformatics results).

## Methods

Fresh frozen samples were collected from EBV-associated cancer tissue that received anti-PD-1/PD-L1 immunotherapy treatment (responder n = 2, non-responder n = 6). ST sample preparation, hematoxylin and eosin (H&E) staining, and measurement were conducted following recommended protocols (version 1, 10X Genomics).

The H&E-stained sections were digitized using an Axioscan 7 (Zeiss), and full-resolution images co-registered to the genomic data using a non-rigid registration algorithm (Aspect Analytics). Pathology annotation was performed in QuPath. Batch correction was conducted using ComBat, PRECAST and Scanorama. A pre-trained deep neural network model

was applied to the H&E images for morphological and color feature extraction.

## Results

The software has a panel view allowing visualization of all 8 samples in the study cohort. The ST capture spots and gene expression data can be viewed on top of the corresponding H&E images; users can zoom and pan across the samples, either collectively or for single images. H&E images are not downsampled during data ingestion and can be viewed at full, sub-cellular resolution.

Complementary information, e.g. pathology annotations, batch corrected data in lower dimensions (e.g., UMAP or PCA), morphological features or other data analysis results, can be either overlaid into the spatial visualization or viewed simultaneously with the images with actions in one visualization coordinating others. This cloud-based software allows communication of results between collaborators without the limitation of a specific workstation or operating system.

## Conclusion

We present a cloud-based software solution, enabling simultaneous visualization of multiple ST datasets, and integration of high-resolution microscopy, pathologist annotations, and spatial data analysis results.

P11.01.03

## ***TU-SIMPL - our solution for a digitalized molecular pathology lab***

M. Martis-Thiele\*<sup>1</sup>, A. Abdouli\*<sup>2</sup>, Y. Wagner<sup>1</sup>, S. Chakraborty<sup>1</sup>, M.-L. Koppermann<sup>1</sup>, A. Terron Kwiatkowski<sup>1</sup>, M. Walker<sup>1</sup>, E. Mayr<sup>1</sup>, N. Pfarr<sup>1</sup>, Q. Heiß\*<sup>1</sup>

<sup>1</sup>Institut für Pathologie, TUM School of Medicine and Health, Technische Universität München, Molekulare Pathologie, München, Germany, <sup>2</sup>Technische Hochschule Deggendorf, Life Science Informatics, Deggendorf, Germany

\*Contributed equally

## Background

The rise of next generation sequencing has significantly shaped the landscape of modern molecular diagnostics, unlocking new insights into targeted treatments and becoming the standard of care in precision medicine. These advancements come at the price of increased amount of laboratory processes, genomic and patient data, and complexity in variant interpretation and reporting. To cope with the general management and organization of this huge laboratory and information flows, many labs need to face this neglected challenge and search for straightforward solutions to replace the insecure and inefficient spreadsheets and e-mails used so far.

## Methods

Although commercial LIMS (Laboratory Information Management Systems) are available, they are often too costly and do not meet all our needs. Searching for the best approach to move on from spreadsheets to a more efficient system in our lab, we opted to use a free and open-source system (SIMPL - System for Informatics in the Molecular Pathology Laboratory), which has been developed at the Genomic and Molecular Pathology Division at the University of Chicago Medicine.

## Results

The SIMPL database is a modular end-to-end information system, which can handle all stages of a typical NGS workload from sample accessioning through bioinformatic analysis and reporting. The database also considers and fulfills data security and patient privacy requirement, recording every action performed.

## Conclusion

Here we present our adaptations of the SIMPL database, TU-SIMPL, in order to digitalize the processes in our lab. The TU-SIMPL derivative takes in account German law restrictions in displaying and storing patient information, as well as lab specific work cycles, and variant interpretation and reporting.

P11.01.04

## ***Rapid simultaneous detection of 16 pathogenic NRAS mutations in advanced colorectal cancer specimens***

I. Michalk<sup>\*1,2</sup>, F. Baenke<sup>3</sup>, D. Aust<sup>1,2</sup>, D. E. Stange<sup>3,4</sup>, J. Weitz<sup>3,4</sup>, N. Dressel<sup>5</sup>, A. Hennig<sup>\*6</sup>

<sup>1</sup>University Hospital Carl Gustav Carus Technische Universität Dresden, Institute of Pathology, Dresden, Germany, <sup>2</sup>Tumour- and Normal Tissue Bank of the University Cancer Center (UCC), University Hospital Carl Gustav Carus, Medical Faculty, Dresden, Germany, <sup>3</sup>Medical Faculty and University Hospital Carl Gustav Carus, Department of Visceral, Thoracic and Vascular Surgery, Dresden, Germany, <sup>4</sup>National Center for Tumor Diseases Dresden (NCT/UCC), a partnership between DKFZ, Faculty of Medicine and University Hospital Carl Gustav Carus, TUD Dresden University of Technology, and Helmholtz-Zentrum Dresden - Rossendorf (HZDR), Dresden, Germany, <sup>5</sup>Biotype GmbH, Productmanagement, Dresden, Germany, <sup>6</sup>Biotype GmbH, Research and Development, Dresden, Germany

\*Contributed equally

### **Background**

NRAS status determination in patients with advanced colorectal cancer (CRC) is recommended by multiple guidelines (ESMO, S3) at the time of diagnosis to support first-line therapy decision-making. Historically, this marker has been mainly assessed by sequencing and qPCR but recently NGS technologies become more widely used. The number of reported pathogenic mutations in the NRAS gene is limited. Using a condensed multiplex PCR assay consisting of the most relevant actionable aberrations of the NRAS gene can be useful for reporting variants.

### **Methods**

A novel assay, allowing the detection of 16 oncogenic NRAS mutations in two PCR reactions, was established on the BIOTYPE MODAPLEX Platform, a technology combining conventional PCR with capillary gel electrophoresis. Assay development was performed using artificial material to cover rare NRAS mutations. FFPE tissue-derived tumor DNA from 30 CRC patients (EK59032007) which underwent surgical resection of the primary tumor at University Hospital Dresden and for which the NRAS status was determined in routine diagnostics using NGS methods were tested in a beta-site study. This sample cohort was analyzed with the new targeted assay to confirm concordance.

### **Results**

Assay verification confirmed the detection of all 16 NRAS mutations with a limit of detection between 1 % to 5 %. Within the beta-site study, all four NRAS cases (G13D, Q61K, Q61L, Q61R) were correctly identified using the new MODAPLEX NRAS Mutation assay. No false positive signals were detected in the 26 NRAS wildtype samples. Confusion matrix analysis showed 100 % sensitivity, specificity, and accuracy.

### **Conclusion**

The new MODAPLEX NRAS mutation assay allows the stratification of advanced CRC patients by determination of the NRAS mutational status with 100 % concordance compared to NGS sequencing. The NRAS assay covers 16 oncogenic driver mutations, which cover 98.4 % of all CRC cases with oncogenic NRAS mutations reported in the AACR GENIE v14.0 cohort. Consequently, this offers an actionable panel with a low input amount of 20 ng DNA in total. The workflow can be carried out within one working day, starting from microdissection (not required) of tumor material until the data evaluation using the provided intuitive MODAPLEX Reporter software. In addition, the NRAS analysis can be combined with POLE mutational and MSI assessment on the same platform concurrently, streamlining pathology workflows.

P11.01.05

## ***The BMP/TGF- $\beta$ Signaling in the Development of Dedifferentiated Chondrosarcoma***

F. S. Karras<sup>1</sup>, J. Schreier<sup>1</sup>, S. R. Ullmann<sup>1</sup>, S. Franke<sup>1</sup>, K. Körber-Ferl<sup>2</sup>, D. Jechorek<sup>1</sup>, A. Roessner<sup>1</sup>

<sup>1</sup>Otto-von-Guericke University Magdeburg, Institute of Pathology, Magdeburg, Germany, <sup>2</sup>Martin-Luther University Halle, Institute of Human Genetics, Halle, Germany

### **Background**

Dedifferentiated chondrosarcoma (DDCS) is a rare and aggressive cartilage tumor originating out of a conventional low-grade chondrosarcoma [1]. The typical histological appearance is characterized by a coexistence of a well-differentiated low-grade tumor component and a dedifferentiated high-grade sarcoma component. Despite the obvious histological

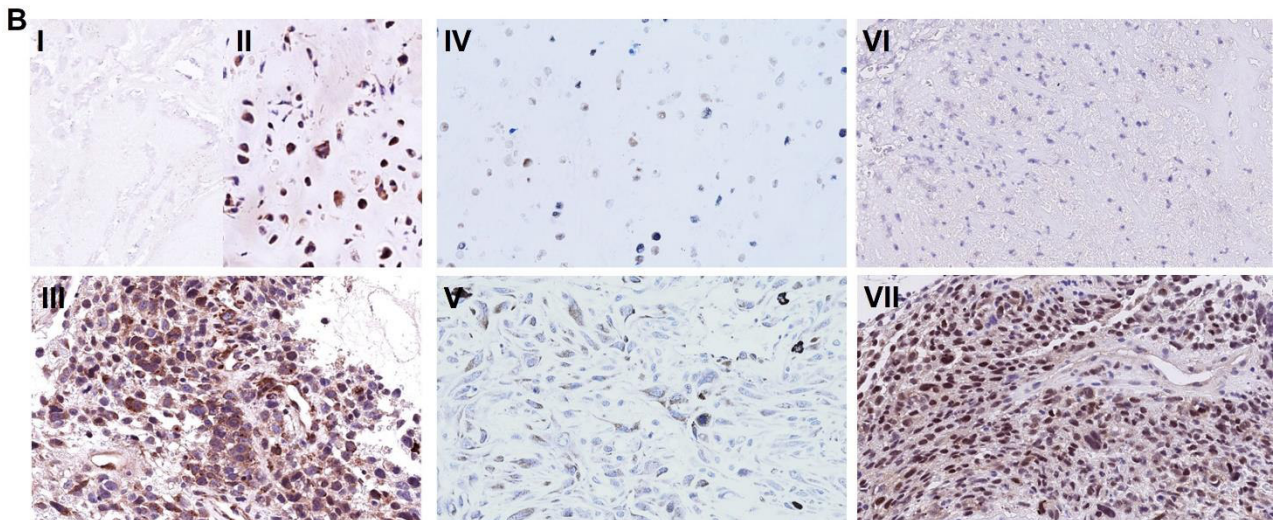
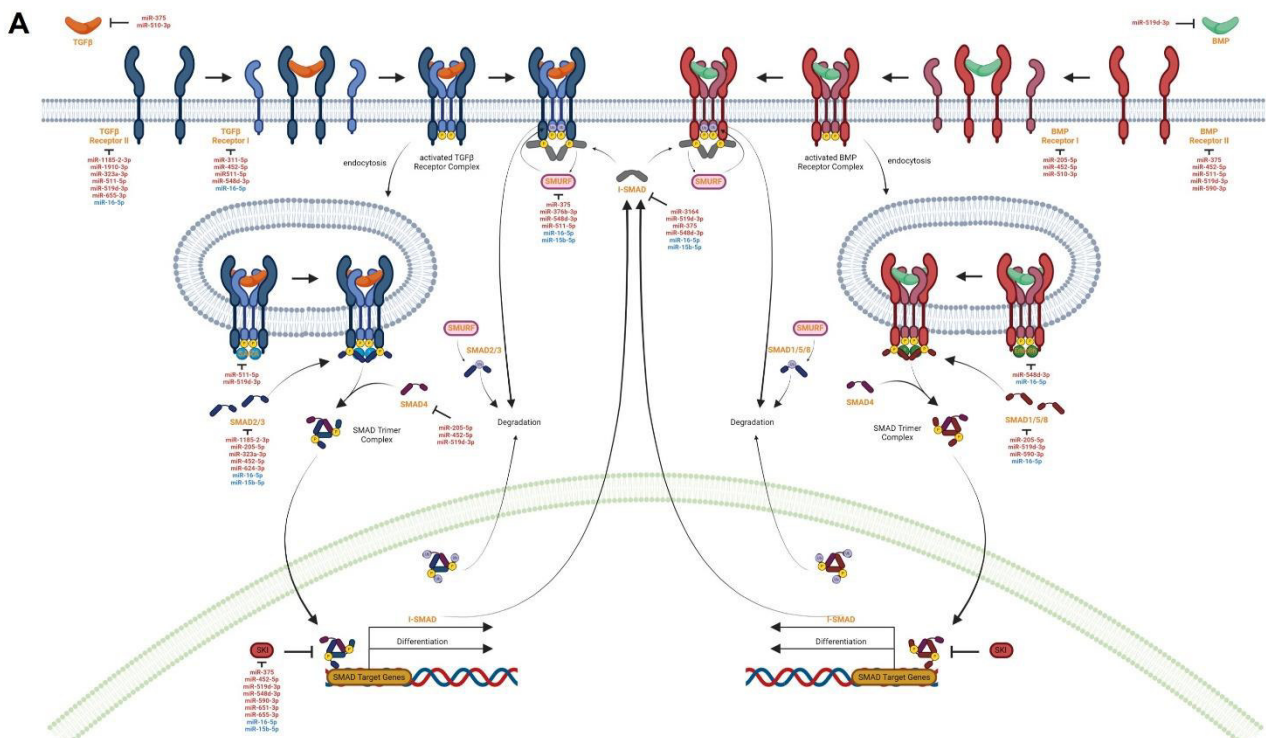
differences, the underlying mechanisms of DDCS development are widely unknown [2]. In a preliminary study, we identified differentially expressed miRNAs in the dedifferentiated components in comparison to the well-differentiated components of paired DDCS samples [3]. Validated targets of these miRNAs are components of BMP/TGF- $\beta$  signaling. Therefore, we performed a genomic and epigenetic analysis of 10 DDCS cases with focus on BMP/TGF- $\beta$  signaling.

## Methods

We extracted DNA and miRNA from FFPE tissue samples of both components of 10 DDCS cases. The DNA was analyzed by WES and data was analyzed using Varvis. MiRNA expression was analyzed using the miRNA Expression Panel for the nCounter MAX analysis system (NanoString Technologies). Immunohistochemical expression of BMPR2, TGFBR2 and SMADs was evaluated in detail in the well-differentiated and dedifferentiated tumor components.

## Results

We could identify several pathogenic and likely pathogenic mutations, as well as significantly deregulated miRNAs, which influence many components of the BMP/TGF- $\beta$  signaling (Fig. 1A). However, staining of BMPR2, TGFBR2 and SMAD4 revealed no uniform appearance (Fig. 1B).



A) BMP/TGF- $\beta$  signaling pathway with mutated genes (orange) and deregulated miRNAs (red - up, blue - down) (Created with BioRender.com). B) Immunohistochemical staining of BMPR2 (I, 100x; II, 400x; III, 400 x), TGFBR2 (IV,

400x; V, 400x), and SMAD4 (VI, 200x; VII, 400x).

## Conclusion

So far, the underlying mechanisms of the development of DDCS is widely unknown. In this study, we combined the analyses of the mutation profile and the differential miRNA expression as well as immunohistochemical staining to analyze the role of the BMP/TGF- $\beta$  signaling in the dedifferentiation of DDCS. Taken together, we were able to identify more likely pathogenic mutations in the dedifferentiated components, as well as many deregulated miRNAs, which are targeting the main components of the BMP/TGF- $\beta$  signaling pathway. However, staining of BMPR2, TGFBR2 and SMAD4 revealed no uniform appearance. Nevertheless, the revealed differences between the both components could be a new hint for the underlying mechanisms.

Literaturangaben:

[1] WHO, (2020), Soft tissue and bone tumours. vol. 3, 5th ed, WHO

[2] Lucas, Calixto-Hope G.; Grenert, James P.; Horvai, Andrew, (2021), Targeted Next-Generation Sequencing Identifies Molecular and Genetic Events in Dedifferentiated Chondrosarcoma, Archives of pathology & laboratory medicine, 1009-17

[3] Karras, Franziska S.; Schreier, Julian; Körber-Ferl, Kerstin; Ullmann, Sarah R.; Franke, Sabine; Roessner, Albert; Jechorek, Dörthe, (2023), Comparative Analysis of miRNA Expression in Dedifferentiated and Well-Differentiated Components of Dedifferentiated Chondrosarcoma, Pathology - Research and Practice

P11.01.06

## ***The role of ChREBP deletion in hepatocellular carcinoma pathogenesis in high-fat diet mouse model***

M. Karim, J. Prey, M. Yasser, F. Willer, H. Leiner, S. Mortoga, F. Dombrowski, S. Ribback  
Universitätsmedizin Greifswald, Institut für Pathologie, Greifswald, Germany

### Background

Background and Aims: The transcription factor carbohydrate response element binding protein (ChREBP) senses intracellular carbohydrates and is involved in regulation of glucose and lipid metabolism in the liver [1]. Previous studies from our lab report that ChREBP activity plays an essential role in the progression and development of hepatocellular carcinoma (HCC) [2,3]. In the present study, we aimed to investigate the contribution of ChREBP to HCC tumorigenesis in the high-fat diet (HFD) induced mouse model.

### Methods

Methods: Male C57BL/6J (WT) and global ChREBP-KO (KO) mice were maintained on either a HFD (46% of calories from fat; n=195) or a control diet (10% of calories from fat; n=75) for 12, 24, and 48 weeks starting at the age of 4 weeks. Body weight and blood glucose levels were recorded once in a month. After perfusion, liver tissue was formalin-fixed, paraffin embedded, sectioned into serial slides, and stained for histological and immunohistochemical analysis.

### Results

Results: Prolonged HFD feeding induced hepatic steatosis along with inflammation in HFD mice, which was significantly different from control group ( $p < 0.05$ ). ChREBP-KO mice displayed significantly more glycogen accumulation in the liver than the WT mice. In addition, HFD-fed mice displayed significantly higher cell proliferation index compared to the control ( $p < 0.05$ ). Furthermore, liver and body weight were significantly increased in ChREBP-KO mice compared to WT mice ( $p < 0.05$ ) in 48-week group. Mice fed with HFD exhibited significantly higher blood glucose levels compared to the control group ( $p < 0.05$ ). We observed a 1.51% incidence of HCC development in WT mice, whereas ChREBP deficiency resulted in a 2.27% incidence of HCC development.

### Conclusion

Conclusion: Excess HFD feeding implicates significant fat accumulation, leading to non-alcoholic fatty liver disease (NAFLD), which further progresses to non-alcoholic steatohepatitis (NASH). Our results suggest that ChREBP seems to be involved in the NASH-associated hepatocarcinogenesis.

Literaturangaben:

- [1] Uyeda, K. and Repa, J.J., (2006), Carbohydrate response element binding protein, ChREBP, a transcription factor coupling hepatic glucose utilization and lipid synthesis, *Cell metabolism*, 107-110., 4(2), doi: 10.1016/j.cmet.2006.06.008
- [2] Ribback, S., Sonke, J., Lohr, A., Frohme, J., Peters, K., Holm, J., Peters, M., Cigliano, A., Calvisi, D.F. and Dombrowski, F., (2017), Hepatocellular glycogenotic foci after combined intraportal pancreatic islet transplantation and knockout of the carbohydrate responsive element binding protein in diabetic mice, *Oncotarget*, 104315, 8(61), doi: 10.18632/oncotarget.22234
- [3] Ribback, S., Che, L., Pilo, M.G., Cigliano, A., Latte, G., Pes, G.M., Porcu, A., Pascale, R.M., Li, L., Qiao, Y. and Dombrowski, F., (2018), Oncogene-dependent addiction to carbohydrate-responsive element binding protein in hepatocellular carcinoma, *Cell Cycle*, 1496-1512, 17(12), doi: 10.1080/15384101.2018.1489182

P11.01.07

## ***Entity specific prediction of single-nucleotide variants in carcinomas of the bladder and urinary tract***

J. Möller<sup>1</sup>, L. Seillier<sup>1</sup>, M. Rose<sup>1,2</sup>, D. D. Jonigk<sup>1,3</sup>, N. Ortiz-Brüchle<sup>1</sup>, N. T. Gaisa<sup>1,2</sup>

<sup>1</sup>Institute of Pathology, University Hospital RWTH Aachen, Aachen, Germany, <sup>2</sup>Institute of Pathology, University Hospital Ulm, Ulm, Germany, <sup>3</sup>German Center for Lung Research, DZL, BREATH, Hanover, Germany

### **Background**

Advanced carcinomas of the bladder and urinary tract show poor prognosis and limited therapy options. Thus, personalized targeted therapies after Next-generation-sequencing (NGS) of tumor tissue are an additional option. NGS provides an increasing wealth of data where variant effect predictors (VEPs) can be a useful tool to simplify the analysis, helping to identify and prioritize mutations of clinical significance. Since VEPs are based on different background models and training data, it seems to be of great importance to evaluate entity specific differences in the prediction performance of pathogenicity prediction algorithms.

### **Methods**

The publicly available databases ClinVar and cBioPortal were used to collect datasets of variations in bladder and urinary tract cancer (BC) (n=441), PanCancer (PC) (n=361) and benign (n=357) variants. The performance of 16 different prediction algorithms (e.g. SIFT, MutationTaster) were evaluated individually and as combinations of two or three algorithms. For a variant to be predicted as Deleterious in a combination of tools thresholds of t=1, t=2 (two algorithms) or t=1, t=2 or t=3 (three algorithms) were defined, analyzing the possibilities of decision making in VEP combinations. A PanCancer data set (n=2811) by Suybeng et al. (J Mol Diagn., 2020) was included for further evaluation of entity specific prediction differences of tools.

### **Results**

The individual and combinatorial performance of VEPs varies dramatically. MutationTaster was the best performing individual tool regarding sensitivity (96.4%) in the oncogenic BC data set, the specificity was 76.75%. Combinations of three tools showed sensitivities up to 100% and specificities up to 97.48%. The best performing combination of VEPs varies between data sets of oncogenic BC and PC variants. Regarding sensitivity the best combination in oncogenic BC variants was MutationTaster/MetaSVM/ListS2 (100%), in our PC data set it was SIFT/MutationTaster/Vest4 (99.72%) and in the PC data set adapted by Suybeng et al. it was BayesDeladdAF/PolyPhen2HDIV/MutationTaster(98.51%).

### **Conclusion**

Combinations of pathogenicity prediction tools increase the value of individual predictions in the analysis of mutational data from cancer patients. However, our benchmarking shows that it is necessary to choose the tool in the context of the study and included entities. For further validation, larger data sets with a broader variety of genes should be investigated.

P11.01.08

## ***Exploring Tumor Evolution in Advanced Colorectal Cancer: Comprehensive Genomic Profiling Using Tissue and Liquid Biopsy in a Research Autopsy Case***

S. Dintner<sup>1</sup>, L. Siebenhüter<sup>1</sup>, R. Ihringer<sup>1</sup>, É. Sipos<sup>1</sup>, S. Eser<sup>2</sup>, A. Probst<sup>3</sup>, T. Kröncke<sup>4</sup>, B. Märkl<sup>1</sup>

<sup>1</sup>Universitätsklinikum Augsburg, Institut für Pathologie und Molekulare Diagnostik, Augsburg, Germany, <sup>2</sup>Donau-Ries Kliniken, Klinik für Innere Medizin, Donauwörth, Germany, <sup>3</sup>Universitätsklinikum Augsburg, Gastroenterologie, Augsburg, Germany, <sup>4</sup>Universitätsklinikum Augsburg, Radiologie, Augsburg, Germany

### **Background**

Tumor heterogeneity in colorectal cancer (CRC) poses significant challenges for personalized medicine, affecting diagnosis, treatment response, and prognosis. Traditional tissue sampling may not fully capture the complexity of advanced tumors, especially inaccessible metastases. Liquid biopsy offers a promising, minimally invasive method to monitor tumor heterogeneity during therapy. Additionally, postmortem autopsy examinations provide a unique opportunity to comprehensively investigate tumor heterogeneity by analyzing multiple metastatic lesions alongside the primary tumor site. This combined approach enhances our understanding of intertumoral heterogeneity and offers valuable insights into tumor progression and therapeutic strategies, serving as indispensable resources for unraveling the complexities of tumor biology.

### **Methods**

To analyze autopsy tissue specimens comprehensively, DNA was extracted and a whole exome library was generated using HyperExomeV2 (Roche), sequenced on a NextSeq2000 system. Simultaneously, circulating cell-free DNA (ccfDNA) from blood plasma was isolated and enriched with the AVENIO ctDNA Surveillance Kit V2 (Roche), then sequenced on a NextSeq550Dx platform. Genetic data from primary tumors, progression samples, and metastatic lesions were integrated for comprehensive analysis.

### **Results**

The study examined a metastatic colorectal carcinoma, conducting a thorough molecular analysis covering DNA alterations including SNVs, INDELS, CNVs, TMB, HRD, MSI, and mutational signatures. Samples were obtained from the primary tumor and metastatic sites over the patient's clinical course from initial diagnosis in 2020 to demise in 2023. Additionally, 16 liquid biopsy specimens were collected longitudinally during therapy, with postmortem autopsy tissues analyzed. Although analysis is ongoing, this unique dataset holds promise for elucidating the complex tumor heterogeneity in colorectal carcinomas.

### **Conclusion**

In conclusion, tumor heterogeneity emerges as a pivotal determinant shaping the prognosis of colorectal cancer (CRC), exerting profound impacts on treatment resistance, disease trajectory, and overall survival outcomes. Comprehensive comprehension and targeted management of tumor heterogeneity stand as imperative steps towards advancing personalized medicine and fostering the innovation of highly efficacious therapeutic interventions tailored to the intricate dynamics of CRC.

P11.01.09

## ***Tumor heterogeneity analysis of malignant melanoma***

K. Peters<sup>1</sup>, A. Manukyan<sup>2</sup>, T. Redmer<sup>3,4</sup>, E. Wyler<sup>2</sup>, J. Radke<sup>5</sup>

<sup>1</sup>Institute of Pathology, University Medicine Greifswald, Greifswald, Germany, <sup>2</sup>Institute for Medical Systems Biology, Max Delbrueck Center in the Helmholtz Association, Berlin, Germany, <sup>3</sup>Institute for Medical Biochemistry, University of Veterinary Medicine Vienna, Vienna, Austria, <sup>4</sup>Institute of Pathology, Unit of Laboratory Animal Pathology, University of Veterinary Medicine Vienna, Vienna, Austria, <sup>5</sup>Institute of Pathology, University Medicine Greifswald, Greifswald, Germany

### **Background**

Despite therapeutic advances, brain metastasis remains the major therapeutic obstacle in melanoma patients and is often associated with resistance to BRAF/MEK inhibitors [1] and a median survival time of around 4 months [2]. Likely, symptomatic macrometastases develop from dormant micrometastases which may have already crossed the blood-brain barrier at an early stage of the disease [3]. The transition from dormant micrometastases to symptomatic macrometastases is not fully understood, offering numerous opportunities to explore the genetic and epigenetic



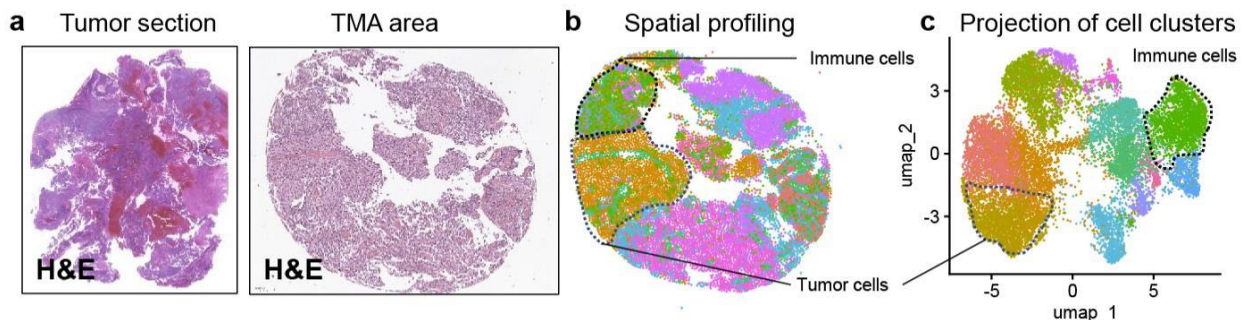
landscape of melanoma progression. The transition from a dormant to a proliferative phase of metastases is influenced significantly by the tumor microenvironment [4].

## Methods

To unravel the tumor-stroma cell crosstalk that significantly impact on the progression of symptomatic macrometastases, tumor recurrence, and therapy resistance we performed single-cell spatial transcriptomic analysis and epigenetic profiling.

## Results

Single-cell spatial transcriptomics generated in both, primary tumors and brain metastases revealed the expression profiles of tumor cells and their microenvironment, ultimately leading to the definition of various cell clusters.



Spatial transcriptomics to identify intra-tumor heterogeneity in melanoma. a) Hematoxylin-eosin staining (H&E) of tumor and tissue microarray (TMA) sections. b) Spatial images of unsupervised clustering results and c) UMAP plot of cell types

## Conclusion

Our analyses provide insights into cellular subsets, tumor heterogeneity and the composition of the tumor microenvironment in malignant melanoma.

Literaturangaben:

- [1] Bai X, Flaherty KT, (2021), Targeted and immunotherapies in BRAF mutant melanoma: where we stand and what to expect, Br J Dermatol, 185(2):253-262
- [2] Alcida Karz et al, (2022), Melanoma central nervous system metastases: An update to approaches, challenges, and opportunities, Pigment Cell Melanoma Res, 35: 554-572
- [3] Xiaoshuang Li et al, (2020), Disseminated Melanoma Cells Transdifferentiate into Endothelial Cells in Intravascular Niches at Metastatic Sites, Cell Rep., 16;31(11):107765
- [4] Dairan Zhou et al, (2023), Harnessing immunotherapy for brain metastases: insights into tumor-brain microenvironment interactions and emerging treatment modalities, J Hematol Oncol, 16(1):121

P11.01.11

## ***Comprehensive genomic instability testing: Empowering analysis beyond conventional boundaries***

E.-M. Mayr, N. Pfarr, C. Kling, S. Chakraborty, M.-L. Koppermann

Institut für allgemeine Pathologie und pathologische Anatomie, TU München, München, Germany

### Background

HRD-testing plays a crucial role in cancer diagnostics as a predictive biomarker for determining the suitability of patients for PARPi therapies and other DNA-damaging agents. However, this analysis is in routine diagnostics mainly limited to specific cancer types, such as ovarian, breast, pancreatic and prostate cancer.

In this study, we addressed the general abundance of this deficiency throughout different cancer entities and explore whether HRD-testing should be considered as standard of care. Additionally, we examined the correlation between HRD high tumors and alterations in specific HRR (homologous recombination repair) genes.



## Methods

To assess this, tumor samples from lung (n=23), colon/colorectal (n=8), urothelial (n=5) and endometrial (n=7) cancer as well as sarcomas (n=10) were selected including those with known pathogenic or likely pathogenic HRR gene mutations, excluding *BRCA1/2* (based on TSO500 sequencing data).

Genomic instability was measured using the Infinium CytoSNP-850K Beadchip (Illumina). Tumor ploidy and copy number profiles were calculated using the ASCAT R package and the GIS (Genomic Instability Score) was determined using the scarHRD R package, which incorporates HRD-LOH, TAI, LST. The cut-off for HRD-high tumors was set at  $\geq 42$ . To increase validity, the study will be further expanded.

## Results

Our findings revealed a significant presence of HRD-high tumors, particularly in lung samples, with half of the samples exhibiting a GIS (Genomic Instability Score)  $\geq 42$  or in close proximity to the cut-off. Additionally, one-third of sarcoma samples were categorized as HRD-high though colorectal cancer samples only showed HRD-negative results. Several HRD-positive samples exhibited mutations in known HRR genes, although not exclusively.

## Conclusion

Our study highlights the widespread prevalence of HRD-positive tumors across different cancer entities. These findings suggest the need to expand HRD- testing to include other cancer types, thereby offering patients putative alternative therapeutic options (e.g. within molecular tumor boards). Furthermore, HRR gene mutations might serve as indicators but not as predictors for the occurrence of HRD-high tumors.

P11.01.12

## ***Tumours with low level of MSI, ERBB2- and/or MET-amplification reveal more patients who can benefit from targeted therapies***

A. Terron-Kwiatkowski, Y. Wagner, M. Walker, F. Seiler, A. Mihalkov, N. Rete, R. Zemankova, Q. Heiß, N. Pfarr  
Institute of Pathology, Technical University of Munich, Munich, Germany

## Background

Microsatellite instability (MSI), ERBB2 (Her2)-amplification and MET-amplification are known biomarkers long used for the detection of colorectal, breast or lung tumours that can benefit from targeted therapies. With the increasing molecular testing, other tumour types have been reported to present these biomarkers and may also profit from the directed therapies.

In our laboratory, the molecular DNA analysis of tumours is routinely performed using the TruSight Oncology NGS Panel (TSO 500 Genes, Illumina). The threshold for amplifications was established to be at least 5 gene copies and 10% of unstable microsatellite sites for MSI, the latter was validated mainly in colorectal tumours. Therefore, we looked at the borderline range of our MSI as well as ERBB2- and MET-amplification thresholds in all tumour types with the aim of identifying more patients who could opt for the corresponding targeted therapies.

## Methods

For this purpose, tumours harboring 4-10% MSI sites and/or two or more copies of ERBB2 or MET genes identified with the TSO500 Panel (Illumina) were analyzed by alternative methods such as fragment analysis/immunohistochemistry for MSI, Her2-neu and/or MET-FISH or qPCR and the results of the different methods compared.

## Results

Among 42 tumours with MSI in the range of 4-10% identified by the NGS panel, 14% were confirmed to be true MSI positive by fragment analysis or immunohistochemistry in different tumour types. Approximately 11 tumours were found to have 2.5-5 MET copies by the NGS Panel and nearly 20% of these were confirmed positive by FISH. Similarly, of over 80 tumours with 2-10 ERBB2 copies by NGS ca. 5% were confirmed to have a Her2 amplification.

## Conclusion

Our preliminary data shows that a proportion of tumours (5-20%) with low level of MSI, MET- or ERBB2-amplification detected by NGS are confirmed positive for these biomarkers by alternative methods, revealing a further number of patients who can benefit from the corresponding targeted therapies. Taken together a cut-off especially for NGS based

pan cancer approaches for borderline cases should be taken into account adapted to different tumor types.

P11.01.13

### **Classification of cancer types using RNA-seq data from cancer panel TSO500**

S. Chakraborty<sup>\*1,2</sup>, M.-L. Koppermann<sup>\*1</sup>, M. Martis-Thiele<sup>1</sup>, Q. Heiß<sup>1,2</sup>, C. Kling<sup>1,2</sup>, E. Mayr<sup>1</sup>, M. Walker<sup>1</sup>, Y. Wagner<sup>1</sup>, A. Terron-Kwiatkowski<sup>1</sup>, W. Weichert<sup>1</sup>, N. Pfarr<sup>1</sup>

<sup>1</sup>TUM, Institute of Pathology, München, Germany, <sup>2</sup>DKFZ, DKTK, Heidelberg, Germany

\*Contributed equally

#### **Background**

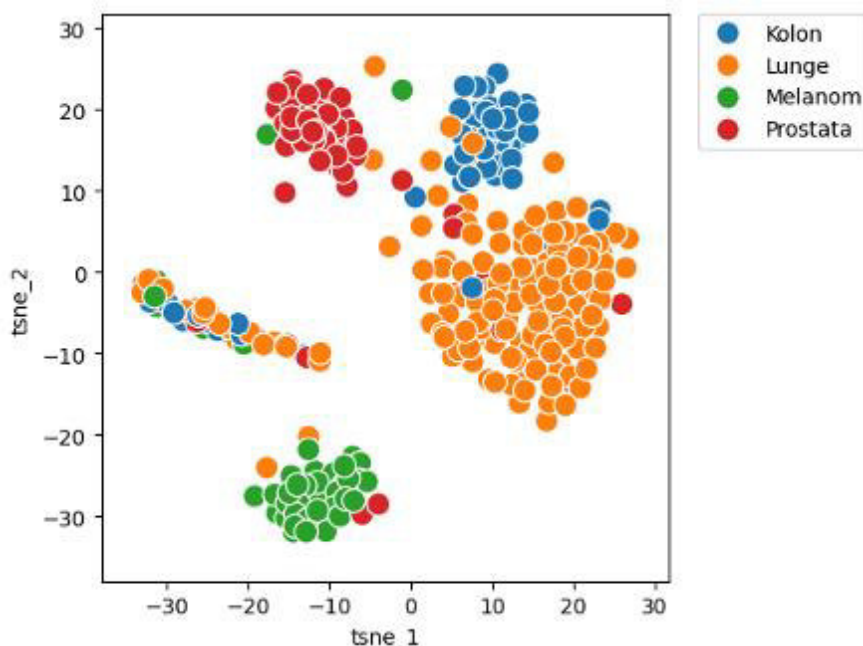
TruSight Oncology 500 (TSO500) is a pan cancer NGS assay which allows inhouse genomic and transcriptomic profiling of cancer tissues from FFPE samples. The gene panel comprises 523 genes and the RNA panel has 53 fusion driver genes.

Our training data consists of around 600 TSO500 assays containing various cancer types including lung, colon, ovarian, breast, pancreas, prostate cancers.

#### **Methods**

This study used the available gene expression data to train five ML based clustering methods, linear support vector machines (linear SVM), polynomial support vector machines (poly SVM), ridge regression, random forests and k-nearest neighbor (kNN).

#### **Results**



t-SNE plot of four major cancer types based on TSO500 RNA-seq data

A t-SNE analysis revealed some very well defined clusters indicating the classification potential of the 53 genes in the panel. Prostate, melanoma, colon and lung cancers seem to cluster separately (figure 1) but it is difficult to differentiate between pancreas, colon and cholangiocarcinoma as well as between ovarian and endometrial cancer. There are also subtypes seen within some of the entities such as breast cancer.

The highest five fold cross validation score for classification of 0.7504 was achieved by Ridge Regression when the class labels of the training dataset contained all the cancer types. However when we grouped cancer types that were close together, we got a cross validation score of 0.8952 with Ridge Regression again performing the best.

An additional cluster was seen which contained samples from all the cancer types which might coincide with known primary tumor samples which metastasized to other parts of the body. However this needs to be validated further with

clinical data and expanded to include subtyping of the tumors.

### **Conclusion**

In this study, we show that the 53 therapy relevant genes from the TSO500 pan cancer assay can be used to effectively classify and predict certain cancer types while some other types are difficult to differentiate from each other. This sort of classification can be used to gain insights into the therapy relevant genes which explain the variance in gene expression amongst different tumor classes. Additionally such a method can also be used to classify samples which have metastasized to different parts of the body, but the origin of the primary tumor is unknown (cancers of unknown primary, CUP).

## **Poster Molekularpathologie II**

P11.02.01

### ***Single-cell multi-omic detection of DNA methylation and histone modifications reconstructs the dynamics of epigenetic maintenance***

C. Geisenberger<sup>\*1</sup>, J. van den Berg<sup>\*2,3</sup>, V. van Batenburg<sup>\*2,3</sup>, B. de Barbanson<sup>2,3</sup>, J. Verity-Legg<sup>2,3</sup>, J. de Ridder<sup>2,3</sup>, A. van Oudenaarden<sup>2,3</sup>

<sup>1</sup>Ludwig-Maximilians-Universität, Institut für Pathologie, München, Germany, <sup>2</sup>Hubrecht Institute-KNAW (Royal Netherlands Academy of Arts and Sciences), Utrecht, The Netherlands, <sup>3</sup>University Medical Center Utrecht, Oncode Institute, Utrecht, The Netherlands

\*Contributed equally

### **Background**

DNA methylation and histone modifications encode epigenetic information. Recently, major progress was made to measure either mark at single-cell resolution. However, a method for simultaneous detection is lacking, preventing study of their interactions.

### **Methods**

To bridge this gap, we developed single-cell Epi2-seq. This technique provides single-molecule and single-cell readout of histone modifications and DNA methylation.

### **Results**

Our results show how the local chromatin context influences DNMT1 dynamics and provides evidence that replication-coupled remethylation proceeds slower in nucleosome-covered regions.

### **Conclusion**

Single-cell multiomic measurements provide unprecedented insight into the mechanics underlying faithful methylation inheritance.

P11.02.02

### ***Is the Prediction of the TP53 Mutation Status By Immunohistochemistry in Breast Carcinoma With a Wild-Type Pattern Really Feasible in the Individual Case?***

U. Vogel<sup>1</sup>, I. Bonzheim<sup>2</sup>

<sup>1</sup>Institute of Pathology, Tübingen, Germany, <sup>2</sup>Institut für Pathologie, Allgemeine und Molekulare Pathologie und Pathologische Anatomie, Tübingen, Germany

### **Background**

The mutational status of TP53 highly affects the prognosis in many malignant tumors. The prediction of the TP53 mutation status by immunohistochemistry gained increasing acceptance in the last decade. P53 immunohistochemistry was described as an accurate surrogate reflecting the underlying TP53 mutation status (Köbel et al. Int J Gynecol Pathol 2019). Four patterns of p53 staining has been described: wild type, complete absence, overexpression and cytoplasmic.

## Methods

In 2022 a 41-year-old female was diagnosed with breast carcinoma and underwent mastectomy in our hospital. One year later a liver metastasis was detected, punched and histologically processed elsewhere.

## Results

The immunohistological p53 pattern in both tumors were described by two different institutes of pathology as wild-type with an admixture of negative, weakly and strongly positive cells. At the request of the clinicians genetic testing was performed revealing a TP53 mutation (exon 7, c.743G>A, p.R248Q).

## Conclusion

In 2006 M. Olivier et al. (Clin Cancer Res) described immunohistochemistry as a poor surrogate for TP53 gene mutation. In 2019 Köbel et al. admitted that about 5% of normal wild-type pattern are mutated. So, the question may be raised whether additional genetic testing should be performed in every case with a p53 wild-type pattern. Moreover, according to Miller et al. (PNAS 2005) only the transcriptional fingerprint describing the downstream p53 functional effects may predict clinical breast cancer behavior.

P11.02.04

## ***The diagnostic value of ACSL1, ACSL4 and ACSL5 and the clinical application of ACSL inhibitor in non-small cell lung cancer***

Y. Ma<sup>1</sup>, M. Nenkov<sup>1</sup>, A. Berndt<sup>1</sup>, M. Abubrig<sup>1</sup>, M. Schmidt<sup>2</sup>, T. Sandhaus<sup>3</sup>, O. Huber<sup>2</sup>, J. H. Clement<sup>4</sup>, S. M. Lang<sup>5</sup>, Y. Chen<sup>1</sup>, N. Gaßler<sup>1</sup>

<sup>1</sup>Section Pathology of the Institute of Forensic Medicine, Jena University Hospital, Jena, Germany, <sup>2</sup>Institute of Biochemistry II, Jena University Hospital, Jena, Germany, <sup>3</sup>Clinic of Cardiothoracic Surgery, Jena University Hospital, Jena, Germany, <sup>4</sup>Department of Hematology and Medical Oncology, Jena University Hospital, Jena, Germany, <sup>5</sup>Department of Internal Medicine V, Jena University Hospital, Jena, Germany

## Background

Long chain Acyl-CoA synthetase (ACSL) family members are involved in long chain fatty acid activation, a crucial step for cells to utilize fatty acids (FAs) in regulation of FA homeostasis. Cancer cells utilize the limited environmental FAs via dysregulation of ACSL isoforms to adapt to altered lipid metabolism. Dysregulated ACSLs are associated with either cancer promotion or inhibition, dependent on cellular context. The role of ACSLs in different cancer types has not yet been fully elucidated, and particularly, its role in lung cancer is obscure.

## Methods

The expression pattern of ACSLs was analyzed via real-time RT-PCR and western blotting. The ACSL enzymatic activity was measured by liquid scintillation counting using [<sup>3</sup>H]-palmitic acid as substrate. The tissue distribution of the ACSL family members and the association between ACSLs and clinicopathological parameters were evaluated by Multiplex immunofluorescence and immunohistochemistry, respectively. The effect of the ACSL inhibitor Triacsin C (TC) and TC combined with Gemcitabine or EGFR-TKIs were explored via the cell viability.

## Results

Compared to normal human bronchial epithelial cells (NHBE), ACSL1, ACSL4, and ACSL6 were highly expressed while ACSL3 and ACSL5 were lost in the majority of lung cancer cell lines. The ACSL activity was associated with the expression levels of ACSLs. In normal lung tissue, all ACSLs were expressed in normal bronchial and alveolar epithelia, especially type II pneumocytes. In primary lung tumors, higher expression of ACSL1, ACSL4 and ACSL5 was significantly correlated with adenocarcinoma (ADC). Besides, ACSL5 was significantly reversely related to the proliferation marker Ki67 in low grade tumors, while ACSL3 was positively associated with Ki67 in high grade tumors. Combination therapy with TC and Gemcitabine enhanced the growth inhibitory effect in EGFR wild type cells, while TC combined with EGFR-TKIs sensitized the EGFR-mutant cells to EGFR-TKI treatment.

## Conclusion

ACSLs have a similar distribution/expression pattern in normal lung tissue. ACSL1 may be a biomarker for lung ADC, and ACSL1, ACSL4 and ACSL5 may be involved in lung cancer differentiation, and TC in combination with chemotherapy or EGFR-TKIs may help to overcome drug resistance.

## ***Fast-track analysis of lung cancer samples - implementation and evaluation of a customized Easy®PGX assay in routine diagnostics***

J. Fassunke\*, S. Wagener-Ryczek\*, R. Pappesch, C. Jonas, V. Welter, C. Heydt, J. Siemanowski-Hrach, C. Heydt, M. Ihle, S. Merkelbach-Bruse, U. Siebolts  
Uniklinik Köln, Institut für Pathologie, Köln, Germany

\*Geteilte Erstautorenschaft

### **Background**

In cancer precision medicine, the detection of somatic gene variants, splicing variants and targetable fusion events plays an important role. The spectrum of molecular targets tested increased with improvement of multiplex DNA and RNA-based sequencing methods. A major disadvantage is the growing turnaround time until delivery of results. An implementation of a fast-track analysis upfront parallel sequencing (NGS)-based analyses offers a solution to face the demand for comprehensive best standard molecular diagnostics allowing fast therapy decisions.

### **Methods**

For the detection of variants and fusions of lung cancer patients, a customized qPCR assay system was applied on an Easy®PGX platform. In brief, 10ng DNA and 15ng RNA extracted separately from formalin-fixed paraffin-embedded (FFPE) tissue samples were taken as input for each reaction well of the customized Easy®PGX fast-track assay (Diatech Pharmacogenetics S.R.L). Data analysis was performed with the Easy®PGX software for DNA and RNA.

### **Results**

Until now, 1600 DNA and 1600 RNA samples were analysed using the above described fast-track system for lung cancer patients. On DNA level, variants in exon 19, 20 and 21 of EGFR, BRAF Codon V600 and KRAS codon 12 variants were analysed, whilst targetable fusions in ALK, RET and ROS1 as well as MET exon 14 skipping were analysed on RNA level. Individual thresholds of ct values for each assay were evaluated and detection limits were identified that deviate from the manufacturer's specifications.

### **Conclusion**

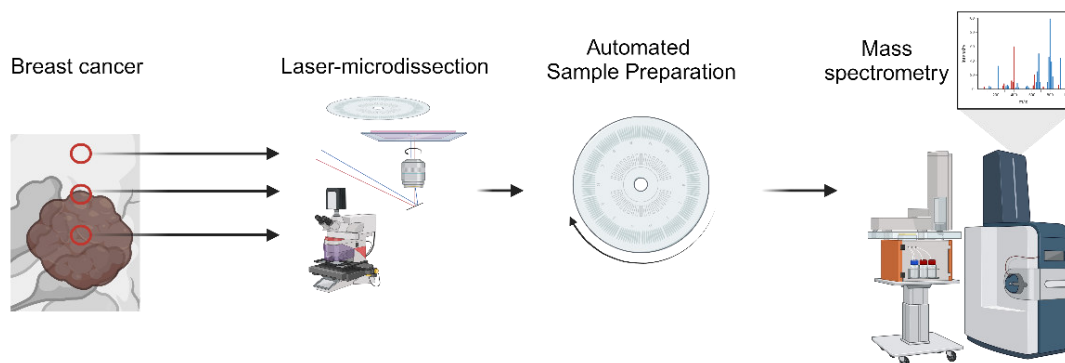
The technical feasibility of rapid analysis of therapeutically relevant molecular targets in lung cancer samples prior to NGS was investigated. The robustness and detection limits of each variant and fusion assay included was evaluated. Rapid delivery of molecular results with high precision and sensitivity of molecular testing is guaranteed by individual thresholds for ct values for each assay and the effective use of downstream validation assays. This method demonstrated robust detection of therapeutically relevant target aberrations leading to faster therapy decision and complements molecular diagnostics via larger NGS-based methods.

## ***Catching Proteomic Intratumoral Heterogeneity in Breast Cancer - A Miniaturized Low Input Proteomic Approach with a Microfluidic System***

M. Maldacker<sup>1</sup>, M. Metzger<sup>2</sup>, J. Heyer<sup>1,3</sup>, A. Seredynska<sup>1,4</sup>, I. D. Steenbuck<sup>1,3,5</sup>, P. Bronsert<sup>1,3,4,6,7</sup>, M. Werner<sup>1,3,4,6,7</sup>, N. Klatt<sup>2</sup>, O. Schilling<sup>1,3,4,6,7</sup>

<sup>1</sup>Institute for Surgical Pathology, Freiburg, Germany, <sup>2</sup>Hahn-Schickard, Freiburg, Germany, <sup>3</sup>Faculty of Medicine, University of Freiburg, Freiburg, Germany, <sup>4</sup>German Cancer Consortium (DKTK), Partner Site Freiburg, Germany, <sup>5</sup>Department of Cardiology and Angiology, University Heart Center Freiburg-Bad Krozingen, University of Freiburg, Freiburg, Germany, <sup>6</sup>Center for Personalized Medicine, Partner Site Freiburg, Germany, <sup>7</sup>Comprehensive Cancer Center Freiburg, Medical Center, Freiburg, Germany

### **Background**



### **A low input proteomic workflow for laser-microdissected central, adjacent and peripheral regions from breast cancer using microfluidics and mass spectrometry.**

Mass spectrometry (MS) is pivotal in tumor characterization from clinical, patient-derived paraffin-embedded and formalin-fixed tissues (FFPE). However, mixing proteomes from distinct cell populations leads to a loss of information on prognosis and therapeutic resistances. Our goal is to implement a robust microfluidic-based workflow for low input proteomics to elucidate proteomic intratumoral heterogeneity in breast cancer across different intrinsic subtypes.

### **Methods**

To counter the loss of proteomic heterogeneity, we implemented a proteomic workflow utilizing a laser-capture microdissection compatible microfluidics based sample preparation. The automated processing was coupled to high throughput liquid chromatography and mass spectrometry (LC-MS). The herein developed workflow is applied for dissection and analysis of central, adjacent and peripheral regions of breast cancer tumors from 40 patients.

### **Results**

We were able to show, that our surfactant-based protocol for miniaturization in a centrifugal disc was able to extract up to

3000 proteins from microdissected paraffin-embedded and formalin-fixed tissue slices. In addition, microfluidic and centrifugal-based miniaturization reduced the variation between samples. Furthermore, our laser-microdissection and microfluidics-based workflow enabled the proteomic analysis of breast cancer tumors for which alternative dissection approaches are not applicable. By dissection of central, adjacent and peripheral, we aim to display the intratumoral diversity on the proteome level. Thereby we currently opt to implement mass spectrometry-based approaches that spatially deconvolute the mechanisms underlying therapeutic resistance and recurrence in breast cancer.

## Conclusion

In our highly collaborative developmental process, we are able to show that proteomics is well on the way to resolve heterogeneity from patient derived FFPE samples with increased depth, easy handling combined in a robust workflow.

P11.02.07

## ***Understanding the Impact of Macrophages on Lung Transplant Outcomes***

E. K. Plucinski\*<sup>1</sup>, J.-C. Kamp\*<sup>1,2</sup>, C. Werlein<sup>1</sup>, J. Gottlieb<sup>2</sup>, H.-H. Kreipe<sup>3</sup>, D. D. Jonigk<sup>4</sup>, L. Neubert<sup>1</sup>, M. P. Kühnel<sup>4</sup>

<sup>1</sup>Medizinische Hochschule Hannover, Institut für Pathologie, AG Lungenforschung, Hannover, Germany, <sup>2</sup>Medizinische Hochschule Hannover, Klinik für Pneumologie, Hannover, Germany, <sup>3</sup>Medizinische Hochschule Hannover, Institut für Pathologie, Hannover, Germany, <sup>4</sup>Uniklinik RWTH Aachen, Institut für Pathologie, Aachen, Germany

\*Geteilte Erstautorenschaft

## Background

Lung transplantation (LTx) is often the last remaining therapeutic option for patients with end-stage lung disease such as idiopathic pulmonary fibrosis (IPF), chronic obstructive pulmonary disease (COPD) or pulmonary hypertension (PH). Despite many advances in transplantation surgery and follow-up, median graft survival after LTx varies widely depending on the underlying disease, ranging from 7.1 to 6.0 years for PH and COPD and 5.2 years for IPF (Bos et al., 2020). Various complications, such as cellular or humoral rejection, continue to challenge clinicians and recipients, highlighting the urgent need for effective interventions to prevent them. Nevertheless, we have been able to identify a group of patients who live for years without complications after LTx, the so-called 'super survivors'. At the histological level, this group is characterised by a high number of alveolar macrophages in the absence of clinical signs of infection or lung remodelling.

## Methods

To investigate the role of the innate immune system with macrophages as major players in graft tolerance, we analysed lung tissue from transbronchial biopsies. We performed a whole transcriptome analysis of alveolar macrophages in super survivors (n=16) and healthy controls (n=12) using the novel Nanostring GeoMx spatial transcriptomics technology. Additionally, we investigated whether these macrophages are of donor or recipient origin using fluorescence in situ hybridization (FISH) of X and Y chromosomes in gender-mismatched transplanted patients.

## Results

We identified a specific gene expression pattern in alveolar macrophages of LTx super survivors that differs from the classical M1-M2 scheme. We found alveolar macrophages with characteristics of anti-arteriosclerotic and anti-inflammatory macrophages in the context of long-term survival after LTx, which are mostly donor-derived.

## Conclusion

These studies show that macrophages may have a protective effect on the allograft. Understanding the dynamics and functions of macrophages in the context of LTx can be critical to improving patient outcomes and developing targeted interventions to reduce complications.

P11.02.08

## ***The next generation of cell death research: enhancing immunotherapy***

J. Krummeich, J. Rossmannith, W. Roth, M. Oliver-Metzig  
Universitätsmedizin Mainz, Institut für Pathologie, Mainz, Germany

### **Background**

Over several decades, substantial research effort has elucidated mechanisms and identified molecular targets to overcome cell death resistance in cancer. In the era of immunotherapy, however, the focus should extend beyond simply maximizing cancer cell death, and also consider the immunological effects of cytotoxic treatments. While certain cell death modalities remain immunologically silent, the targeted induction of immunogenic cell death (ICD) promises to mount an effective anti-tumor immune response and prime for successful immunotherapy.

### **Methods**

Cytotoxicity assays, co-culture experiments, gene expression analysis, protein biochemistry, ELISA

### **Results**

We provide a comprehensive overview of different forms of ICD and their inducers with a focus on RIPK1-dependent apoptosis and necroptosis. We present an arsenal of *in vitro* and *in vivo* tools to investigate the immunological consequences of cell death. Preliminary data show that switching between death modalities in cancer cells is feasible and may affect bystander cells of the microenvironment to render tumors more immunogenic.

### **Conclusion**

Controlling cancer cell death is a deliberate approach to optimize anti-tumor immunity. Switching between apoptosis and necroptosis may prime the tumor microenvironment and enhance immunotherapy.

P11.02.09

## ***Tumor heterogeneity of glioblastoma analyzed via SpatialOMx and HiPLEX-IHC***

B. Wendik<sup>1</sup>, C. Henkel<sup>1</sup>, S. Frost Frederiksen<sup>1</sup>, M. Szensny<sup>1</sup>, J. Bartsch<sup>2</sup>, M. Föll<sup>3</sup>, O. Schilling<sup>3</sup>

<sup>1</sup>Bruker Daltonics GmbH & Co KG, MALDI Imaging, Bremen, Germany, <sup>2</sup>Universitätsklinikum Marburg, Neurochirurgie, Marburg, Germany, <sup>3</sup>Uniklinikum Freiburg, Institute for Surgical Pathology, Freiburg, Germany

### **Background**

Glioblastoma is the most common and a highly malignant primary brain tumor with five-year survival rates below 10 %. Glioblastomas are characterized by high levels of heterogeneity within the tumor cells and the tumor microenvironment, which consists of blood vessels and necrosis intermingled with differentiated and stem-like tumor cells. Tumor heterogeneity influences chemotherapy resistance and local cancer cell dissemination, both connected to the high recurrence rate of > 90%. Disturbed metabolism has been reported in glioblastoma, however the spatial context that allows assessment of intratumor heterogeneity and the tumor microenvironment have hardly been studied.

### **Methods**

Fresh frozen tissue sections from three glioblastoma patients and one astrocytoma patient as were measured by lipid mass spectrometry imaging, as well as antibody based HiPLEX-IHC imaging on a TimsTOF fleX MALDI-2 with 20 µm spatial resolution. TIMS ion mobility was switched on for the lipid imaging. Bulk tumor tissue from the same patient was homogenized and lipids were extracted via MTBE phase separation and measured via LC-MS/MS and TIMS ion mobility (4D-Lipidomics) on the TimsTOF fleX. Results provided by MetaboScape were used for the annotation of MALDI-imaging m/z values in combination with the ccs information.

### **Results**

HiPLEX imaging based on cell type specific antibodies revealed different cellular compositions in the four brain tissue samples. Glia cells were more evenly distributed over the tissue and showed variation between the four samples compared to immune cells. CD4 T-cells were more intense in the tumor tissue areas, while macrophages partially colocalized with collagen 1 in round structures, which we hypothesize to be areas of stem cells. One glioblastoma tumor contained many B-cells, which are rarely studied in this tumor type. Some lipids and metabolites were co-localized with



macrophages, B-cells and astrocytes indicating cell-type specific molecular compositions. Lipid mass spectrometry imaging showed spatial heterogeneity in the tumor microenvironment as well as inside the tumor areas.

## Conclusion

Novel aspect: SpatialOMx in combination with HiPLEX-IHC imaging showed that spatial and cell-type specific lipid analysis overcome the inherent heterogeneity of bulk tumors and allow detailed assessment of intratumor heterogeneity and the tumor microenvironment, which are both relevant to glioblastoma recurrence and therapy success.

P11.02.10

## ***Molecular detection of Severe Acute Respiratory Syndrome Coronavirus 2 (SARS-CoV-2) by mass spectrometry in formalin-fixed paraffin embedded (FFPE) post-mortem tissue specimens.***

T. Hansen<sup>1</sup>, B. Sauerbrei<sup>1</sup>, U. Titze<sup>2</sup>, B. Schulz<sup>2</sup>, I. Hansen<sup>2</sup>, K. Kriegsmann<sup>3</sup>, M. Kriegsmann<sup>4</sup>, J. Kriegsmann<sup>1,5</sup>

<sup>1</sup>MVZH ZMD Trier GmbH, Trier, Germany, <sup>2</sup>Klinikum Lippe GmbH, Institut für Pathologie, Detmold, Germany, <sup>3</sup>Laborarztpraxis Rhein-Main MVZ GbR, Frankfurt am Main, Germany, <sup>4</sup>Zentrum für Histologie, Zytologie und Molekularpathologie, Wiesbaden, Germany, <sup>5</sup>Danube Private University, Department of Medicine, Krems, Austria

## Background

The coronavirus disease 2019 (COVID-19) pandemic has induced a great recovery of autopsy studies. In addition, there has been an immense research effort aimed at establishing molecular diagnostic modalities[1][2][3]. Matrix-assisted laser desorption/ionization time-of-flight (MALDI-TOF) mass spectrometry has been described as an alternative molecular method for the detection of virus particles such as SARS-CoV-2[4]. Here, we used mass spectrometry analyzing SARS-CoV-2 RNA on COVID-19 autopsy FFPE tissue samples.

## Methods

Tissue specimens were routinely processed from autopsies of 10 patients (M = 7; F = 3; mean age: 84 yrs) according to the protocols of the DEFEAT Pandemics study group[2][5]. All patients deceased from COVID-19. Tissue samples of a SARS-CoV-2-negative patient served as control. We performed SARS-CoV2 qualitative detection using the MALDI-TOF Mass ARRAY system [Agena, Germany] and analyzed the mutation D614G (associated with the B.1.1.7 variant), as previously described[4]. The MassARRAY SARS-CoV-2 Panel includes 5 targets within the SARS-CoV-2 genome (N1, N2, N3, ORF1, and ORF1ab). According to the manufacturer's instructions, the detection of at least 2 targets is required for the result "positive". The examination procedure was repeated three times. For evaluation, only triple positive result was listed.

## Results

The results of this study are summarized (TABLE01).

Pat.-No.	Lungs	Heart	Liver	Kidney	Spleen	Muscle	Cerebrum	Cerebellum	D614G
<b>1 + 2</b>	neg	neg	neg	neg	neg	neg	neg	neg	pos
<b>3</b>	neg	neg	neg	neg	neg	neg	neg	neg	neg
<b>4</b>	pos (5/5)	pos (5/5)	pos (2/5)	pos (4/5)	pos (3/5)	ND	neg	neg	pos
<b>5</b>	pos (5/5)	neg	neg	neg	neg	neg	neg	neg	pos
<b>6</b>	pos (5/5)	pos (2/5)	neg	neg	neg	neg	pos (4/5)	pos (5/5)	pos
<b>7</b>	pos (5/5)	neg	neg	neg	neg	neg	neg	neg	pos
<b>8</b>	pos (4/5)	pos (4/5)	pos (4/5)	neg	ND	pos (3/5)	pos (3/5)	pos (3/5)	pos
<b>9</b>	pos (5/5)	pos (4/5)	pos (4/5)	pos (2/5)	pos (5/5)	pos (5/5)	pos (3/5)	neg	pos
<b>10</b>	pos (3/5)	neg	neg	neg	neg	ND	neg	ND	pos

SARS-CoV-2 RNA (encountered as number of positive targets/ 5 targets) in autopsy tissue specimens [Legend: neg = negative; ND = not done; pos = positive]

In 7/10 COVID-19 patients, we thoroughly were able to detect SARS-CoV-2. We mainly found virus RNA in the lungs (n = 7) and the heart (n = 4), while N1 and N2 were the targets being mostly positive. Most interestingly, the D614G mutation could be identified in the majority of the study cohort (9/10 patients).

## Conclusion

In FFPE autopsy tissue specimens, MALDI-TOF mass spectrometry can be used as an alternative molecular technique, e.g. for the detection and subtyping of virus RNA. Due to its large load capacity (96 samples per batch)[4], it might be a useful method in high-throughput molecular testing of tissue samples such as in postmortem cohort analysis in the case of future possible pandemics.

Literaturangaben:

[1] Jongigk D, et al., (2022), Organ manifestations of COVID-19: what have we learned so far (not only) from autopsies?, *Virchows Arch*, 139, 481, 2022-04-04

[2] von Stillfried S, et al., (2022), First report from the German COVID-19 autopsy registry, *Lancet Reg Health Eur*, doi 10.1016/j.lanepe.2022.100330, 2022-02-18

[3] Schweizer L, et al., (2023), Quantitative multiorgan proteomics of fatal COVID-19 uncovers tissue-specific effects beyond inflammation., *EMBO Mol Med*, doi 10.15252/emmm.202317459, 2024-02-16

[4] Wierz M, et al., (2022), Detection of severe acute respiratory syndrome coronavirus 2 (SARS-CoV-2) including variant analysis by mass spectrometry in placental tissue, *Viruses*, doi 10.3390/v14030604, 2024-02-16

[5] Boor P, et al., (2021), Praktische Aspekte von COVID-19 Obduktionen, *Pathologie*, 197, 42, 2021-11-01

P11.02.11

## ***The transcription factor CREB1 is a regulator of IKK2 expression***

L. Savini<sup>1</sup>, Y. Gallenmiller<sup>1</sup>, J. Lindauer<sup>1</sup>, U. Marienfeld<sup>2</sup>, N. T. Gaisa<sup>1</sup>, P. Möller<sup>1</sup>, R. Marienfeld<sup>1</sup>

<sup>1</sup>Institut für Pathologie, Ulm, Germany, <sup>2</sup>Institut für Physiologische Chemie, Ulm, Germany

### Background

Dysregulated canonical NF- $\kappa$ B signalling is crucial for solid tumours and B cell lymphomas. The I $\kappa$ B kinase complex (IKK complex), composed of IKK1, IKK2 and NEMO is the key element of the NF- $\kappa$ B system. However, IKK1 and IKK2 are thought to exert different while overlapping functions and thus the composition of the IKK complex appears to activate different sets of NF- $\kappa$ B dimers leading to a distinct NF- $\kappa$ B target gene profile. Despite the importance of the IKKs, the mechanisms by which the IKK expression are regulated are poorly understood. To get an insight into the control of the IKK expression, we analysed expression of IKK1 and IKK2 in different cell lines, tissues and tumour entities and analysed their proximal promoters. With this work we aimed at a better understanding of the expression of IKK1 and IKK2 as central regulators of the canonical NF- $\kappa$ B signalling pathways in cancer.

### Methods

In-silico analyses were performed to analyse the protein expression of IKK1 and IKK2 in tissues and their role as prognostic tumor markers. Proximal IKK1 and IKK2 promoters were characterised using luciferase constructs. Supershift analyses and chromatin immunoprecipitation experiments were performed to investigate the binding of CREB1 to the IKK2 promoter and western blot to examine the IKK1 and IKK2 expression.

### Results

Heterogeneous IKK1 and IKK2 protein expression was found in tissues, with IKK1 in the kidney and IKK2 in the testis and prostate. High IKK1 expression correlated with renal cancer prognosis, and IKK2 expression with urothelial carcinoma. Collectively indicating a regulated expression of IKK components. Fine mapping revealed a crucial ETS/CREB site for IKK2 promoter activity. CREB1 was found to bind to this site in the IKK2 promoter, implicating it as an IKK2 regulator. Knockdown of CREB1 led to a significant decrease in IKK1 and IKK2 expression, supporting this role.

### Conclusion

IKK1 or IKK2 expression are considered negative prognostic markers in various tumours such as renal carcinoma and urothelial cancer while IKK1 and IKK2 expression was heterogeneous in tissues. Characterization of the IKK2 promoter revealed a critical role of the CREB/ATF family for IKK1 and IKK2 expression, which was supported by decreased IKK1 and IKK2 levels upon knockdown of CREB1 in HEK293T. In summary, this work identified CREB transcription factors as

regulators of the NF- $\kappa$ B/IKK system, which is of great interest in the context of various tumour diseases.

P11.02.12

### ***Longitudinal transcriptomic profiling of dystrophin-deficient satellite cells***

S. Franzmeier<sup>1,2</sup>, S. Chakraborty<sup>2</sup>, N. Pfarr<sup>2</sup>, E. Wolf<sup>3,4</sup>, J. Schlegel<sup>2,5</sup>, K. Matiassek<sup>1</sup>

<sup>1</sup>Institut für Tierpathologie, Ludwig-Maximilians Universität München, München, Germany, <sup>2</sup>Institut für Pathologie, Technische Universität München, München, Germany, <sup>3</sup>Genzentrum, Ludwig-Maximilians Universität München, München, Germany, <sup>4</sup>Center for Innovative Medical Models, Ludwig-Maximilians Universität München, München, Germany, <sup>5</sup>Department für Health und Sport Sciences, Technische Universität München, München, Germany

#### **Background**

The contribution of dystrophin-deficient satellite cells (SC) to Duchenne Muscular Dystrophy (DMD) is still not fully understood. Elucidating pathways in affected SC constitutes an urgent and compelling research question especially as stem-cell based treatment approaches for new therapies are gaining more popularity. Consequently, we aimed to investigate SC's behavior outside their dystrophic niche to reveal any cell intrinsic changes at pre-contractile stages of muscle development.

#### **Methods**

To examine this, we used a well-characterized translational porcine model for DMD and collected muscle biopsies at three different ages (fetal, 3-days-, and 3-months-old). We established a targeted isolation protocol using magnetic beads to isolate SC from affected male DMD and age-matched WT control muscle samples. Subsequently, cells were cultivated *in vitro* and harvested for analysis at two different stages: in a proliferative state and after differentiation into multinucleated myotubes. 3' mRNA sequencing was performed, followed by bioinformatic data analysis.

#### **Results**

Transcriptome profiles from DMD SC in both developmental stages clustered distinctively from WT control in all three age groups. Principal component analysis (PCA) separated profiles of 3-days-old DMD SC from fetal and 3-months-old DMD SC. Among the top differentially regulated genes in the DMD cohort we detected the myogenic transcription factors *MYF5*, *MYOD1* and *MYOG*, as well as important muscle contraction-related genes like *MYLPP* and *MYL1*. Additionally, several genes demonstrated an altered expression pattern when compared across the age groups, such as *ACTA1*, which was upregulated in the 3-days-old DMD SC in relation to the fetal stage and downregulated in the 3-months-old DMD SC in relation to the 3-days stage.

#### **Conclusion**

Our data revealed a dynamic regulation of myogenesis genes over time and provides a detailed view on longitudinal expression signatures during DMD disease progression. These findings could help to identify crucial molecular events for developing targeted interventions at specific stages of disease development.

P11.02.13

### ***2NA FISH: a novel spatial transcriptomics tool for therapy decisions based on mRNA diagnostics in the tissue context***

T. Neuß, A. Malinova, J. Stiller, A. Bausch, C. Port

Technische Universität München, Zelluläre Biophysik, Garching, Germany

#### **Background**

Therapy response prediction is complex. Recent advances have emphasised the importance of the spatial tissue architecture, tumour microenvironment (TME) and single-cell RNA expression patterns in determining molecular subtypes, as well as tumour behavior and therapy response. The emerging trend of measuring mRNA expression in the tissue context - Spatial Transcriptomics - integrates these factors and has been named Nature Method of the Year 2020. However, there is no application of Spatial Transcriptomics in clinical diagnostics yet.

#### **Methods**

Utilising nanotechnology, we have developed an RNA FISH-based approach for measurement of up to 5-20 RNAs on a

single slide in the tissue context. The approach is non-destructive and can be expanded to up to 50 RNAs, as well as combined with multimodal analyses such as H&E staining and immunohistochemistry (IHC). We have developed an AI-based analysis software which visualizes the results and gives quantitative RNA molecule counts per cell, integrated into the location in the sample.

### **Results**

Using conventional epifluorescence microscopes, our 2NA FISH technology reliably detects mRNAs with higher signal-to-noise ratio than commercially available RNA FISH. Detection of up to 7x RNAs was demonstrated in 2D cell culture, and up to 5 RNAs in cryosections. Measurement of 10 RNAs and application on FFPE samples are currently under development.

### **Conclusion**

2NA FISH provides a robust, cost-effective microscopy-based spatial transcriptomics approach for routine clinical diagnostics. Using only standard equipment enables the use of 2NA FISH as a simple “staining” approach in the pathology lab to deliver simple, spatial transcriptomics insights. Given the emerging relevance of the spatial tissue architecture and the influence of the TME on tumour behaviour and therapy response, 2NA FISH presents a high-potential technology for diagnostics development to support therapy decisions for heterogeneous cancers.

## **Poster Kinder- und Fetalpathologie**

P12.01

### ***Comparison of neonatal autopsy findings with prenatal diagnoses***

J.-T. Suhren<sup>1,2</sup>, K. Hussein<sup>3</sup>, H.-H. Kreipe<sup>2</sup>, N. Schaumann<sup>2</sup>

<sup>1</sup>Medizinische Hochschule Hannover, Institut für Pathologie, Hannover, Germany, <sup>2</sup>Institut für Pathologie, Medizinische Hochschule Hannover, Hannover, Germany, <sup>3</sup>MVZ Pathologie Hildesheim Hannover-Zentrum GmbH, Hildesheim, Germany

#### **Background**

In a clinical setting, in Germany neonatal death within the first week of life is rare. Autopsy may confirm the clinical diagnoses but can also show additional findings. Our study aimed to assess the correlation between clinical diagnoses and post-mortem findings in early neonatal deaths.

#### **Methods**

In this retrospective study from the Institute of Pathology of Hannover Medical School we included autopsy cases after death within the first seven days of life (arbitrary time interval 2006 to 2021). Discrepancies between clinical and histopathological findings were classified into three groups: i) full agreement, ii) additional findings, which do not change the main diagnosis, or iii) additional findings, which change the main diagnosis.

#### **Results**

A total of 27 cases were included. Predominance of malformations (81%), particularly in the pulmonary system, characterized the cohort. Additional findings could be discovered in 48% of cases, predominantly in pulmonary, urogenital, and cardiac organs. Major discrepancies, which changed the clinical diagnosis, could be found in 11%.

#### **Conclusion**

In most cases, autopsy confirms the clinical diagnosis. In a few cases, autopsy findings can provide previously unrecognized pathologies which may help to identify the underlying cause of death.

P12.02

### ***Congenital diarrhea, severe metabolic acidosis and retinal dystrophy: Syndromic Microvillus Inclusion Disease caused by homozygous Syntaxin 3 mutation***

A. Müller<sup>1</sup>, A. R. Janecke<sup>2</sup>, J. Keck<sup>3</sup>

<sup>1</sup>Universitätsklinik Köln, Praxis für Pathologie / Zentrum für Kinderpathologie, Köln, Germany, <sup>2</sup>Universitätsklinik Innsbruck, Klinik für Pädiatrie I, Innsbruck, Austria, <sup>3</sup>Sana Klinikum Offenbach, Kindergastroenterologie, Offenbach, Germany

#### **Background**

Microvillous inclusion disease (MVID) is characterized by near complete loss of microvilli and accumulation of microvilli-containing vacuoles in intestinal epithelial cells. We are reporting the case of a newborn with partial loss of microvilli but lack of typical microvillous inclusion bodies on electron microscopy, that was diagnosed with syndromic MVID caused by an extremely rare syntaxin 3 (STX3) mutation via trio-exome-analysis.

#### **Methods**

A female newborn presented with intractable congenital diarrhea, severe metabolic acidosis with bicarbonate loss and hypertonic dehydration on the 6th day of life. Bowel rest showed a partial response with improvement of stool frequency / consistency, normalization of stool-pH, and reducing substances. On upper gastrointestinal endoscopy, macroscopic total villous atrophy from the duodenal bulb to the deep duodenum was present.

#### **Results**

On histopathology there was severe duodenitis with crypt hyperplasia, eosinophilia, and focal enhancement of capillarization of the superficial mucosa. The mucosal epithelium showed irregular PAS, CD10, and EpCAM staining. Electron microscopy revealed a reduced number of microvilli, epithelial patches with microvilli completely missing, and very few microvilli embedded in the cytoplasm. Large microvilli-containing vacuoles - as would be expected in classic MVID - were not seen. Trio-exome-analysis identified a homozygous STX3 mutation in the patient (c.372\_373dup (exon 6), p. (Arg125LeufsTer7)). This frameshifting mutation affects both the intestinal and retinal transcript of the STX3 gene, coding for a soluble N-ethylmaleimide-sensitive factor attachment receptor (SNARE)-protein that catalyzes trafficking and fusion between vacuoles and their target membranes, underlying intestinal microvillous inclusion disease as well as an early onset retinal dystrophy. Both were recognized in this patient.

The same homozygous mutation was described only once before in a patient showing a very similar clinical presentation with atypical MVID and retinal dystrophy.

#### **Conclusion**

STX3 mutations can underlie the rare instance of an oculo-intestinal disorder, presenting as syndromic MVID with atypical findings on GI-histopathology and electron microscopy.

P12.03

### ***Life-threatening hemorrhage of congenital hemangioma in unborn infant at 32 weeks of gestation***

J. Müller<sup>1</sup>, B. Vogt<sup>2</sup>, C. Roth<sup>3</sup>, L.-C. Horn<sup>4</sup>, G. G. R. Hiller<sup>4</sup>

<sup>1</sup>University Hospital Leipzig, Institute of Pathology, Leipzig, Germany, <sup>2</sup>University Hospital Leipzig, Department of Obstetrics and Gynecology, Leipzig, Germany, <sup>3</sup>University Hospital Leipzig, Department of Pediatric Radiology, Leipzig, Germany, <sup>4</sup>University Hospital Leipzig, Institute of Pathology, Division of Gynecologic, Breast and Perinatal Pathology, Leipzig, Germany

#### **Background**

The majority of vascular tumors of infancy have no clinical impact. A rare subtype within that group is congenital hemangiomas (CH). These tumors develop intrauterine and are fully formed at birth with different postnatal clinical behavior as rapidly involuting, non-involuting or partially involuting hemangioma. Large CH may cause hemodynamic complications due to high blood-flow rates.

#### **Methods**

We report the case of an intrauterine fetal demise at 32 weeks of gestation with a large hemorrhagic facial hemangioma.

## Results

**Case report:** Admission of a 28-year-old gravida 1, para 0 for intrauterine fetal transfusion due to suspected progression and relevant bleeding of a monitored fetal facial tumor. Follow-up fetal assessment showed regular findings. On the second post-interventional day no fetal cardiac action could be registered with diagnosis of intrauterine fetal demise at 31 + 5 weeks of gestation.

The autopsy of the male fetus revealed a large facial vascular tumor of 9.5 x 9.5 x 5.0cm localized at the right side of the face with involvement of the ipsilateral eyelid and ear. The surface of the tumor showed erosion and ulceration. On histological examination the tumor presented variably sized capillary lobules surrounded by fibrous tissue with small thin-walled dilated vessels and associated larger extralobular vessels with overall massive blood stasis, partially ruptured vessels and extensive hemorrhage. The endothelium stained positive for CD34 and WT1, with ambiguous staining for GLUT-1 due to intravascular blood congestion. The fetus showed morphologic features of long standing anemia with pale colored skin and inner organs and hypertrophic myocardium.

## Conclusion

Based on the clinical and diagnostic features we classified the tumor as congenital hemangioma. Individual cases of life-threatening massive hemorrhages and an increased mortality rate of CH have been reported in literature. Therefore, particularly large CH require special care and close intrauterine monitoring may be suggested to prevent complications.

# Poster Informatik, digitale Pathologie und Biobanking

P13.01

## ***Retrospective Analysis of Rare, Triple-Negative Breast Carcinomas with Low Malignant Potential Utilizing the Forschungsdatenportal Gesundheit (FDPG)***

F.-L. Klaus, A. Muckenhuber

Institut für Pathologie, Technische Universität München, München, Germany

## Background

Triple-negative breast carcinomas (TNBCs) are invasive breast carcinomas typically exhibiting highly aggressive behavior and poorer overall survival compared to stage-matched non-triple-negative breast carcinomas. Consequently, (neo-)adjuvant chemotherapy is often utilized. However, certain histological subtypes of TNBCs demonstrate low malignant potential and may have a favorable prognosis even without chemotherapy [1][2]. Accurate diagnosis of these subtypes is crucial to avoid overtreatment [3]. Due to their rarity, there are few publications on these entities with limited case numbers (e.g., TNBC with apocrine differentiation). Therefore, multicenter databases such as the Forschungsdatenportal Gesundheit (FDPG) within the framework of the Medical Informative Initiative (MII) are essential for expanding knowledge in this area [4]. Using the FDPG in this project, our aim is to characterize the clinical course of rare subtypes of TNBCs, assess the efficacy of chemotherapy, and investigate clinicopathological variables for their prognostic relevance.

## Methods

Prior to requesting data provision, a feasibility inquiry is made to assess data availability. The basic modules diagnosis, laboratory findings, procedures, and medication from the MII core dataset can be utilized. The available data can be centrally analyzed with patient consent or made available solely for "Distributed Analyses". Based on the assessment of the data availability, a data usage request specifying all required clinicopathological variables can be sent out.

## Results

The following inclusion criteria were defined: Diagnosis: Malignant neoplasms of the breast gland [Mamma] (C50) AND Procedure: Excision and resection of the breast [OPS code: 5-87] between 01-01-2005 and 31-12-2020. The feasibility inquiry yielded 18,810 patients for "Distributed Analyses" and 260 cases for patients consenting to central analysis. A data usage request specifying the required clinicopathological parameters was subsequently submitted. Data provision is pending.

## Conclusion

For the investigation of rare tumor entities such as TNBCs with low malignant potential, the FDPG offers a means to

achieve a sufficiently high case number for retrospective analysis, at least when using "Distributed Analysis". It seems to be possible to meaningfully supplement the existing limited data on individual subtypes through analysis of the requested data.

Literaturangaben:

- [1] Hans-Peter Sinn, Zsuzsanna Varga, (2023), Triple-negatives Mammakarzinom Klassifikation, aktuelle Konzepte und therapierelevante Faktoren
- [2] Cserni G, Quinn CM, Foschini MP, Bianchi S, Callagy G, Chmielik E, Decker T, Fend F, Kovács A, van Diest PJ, Ellis IO, Rakha E, Tot T , (2021), Triple-Negative Breast Cancer Histological Subtypes with a Favourable Prognosis, Cancers (Basel)
- [3] Cima L, Kaya H, Marchiò C, Nishimura R, Wen HY, Fabbri VP, Foschini MP, (2022), Triple-negative breast carcinomas of low malignant potential: review on diagnostic criteria and differential diagnoses, Virchows Arch.
- [4] Prokosch HU, Gebhardt M, Gruendner J, Kleinert P, Buckow K, Rosenau L, Semler SC, (2023), Towards a National Portal for Medical Research Data (FDPG): Vision, Status, and Lessons Learned., Stud Health Technol Inform.

P13.02

## ***Digitalization of Histopathological Routine Diagnostics - Do's and Don'ts***

V. Iwujoku\*<sup>1</sup>, A. Haas<sup>2</sup>, K. Ekici<sup>2</sup>, M. Z. Khan<sup>1</sup>, F. Stögbauer<sup>2</sup>, K. Steiger<sup>2</sup>, C. Mogler\*<sup>2</sup>, P. Schöffler\*<sup>1</sup>

<sup>1</sup>Institut für Pathologie, TUM School of Medicine and Health, Technische Universität München, Computational Pathology, Munich, Germany, <sup>2</sup>Institut für Pathologie, TUM School of Medicine and Health, Technische Universität München, Munich, Germany

\*Contributed equally

### **Background**

Digital pathology is primarily the interpretation of pathology images from digitally scanned slides. There were early beginnings of digitalization decades ago, when pathology images were transmitted in real time microscopy between Logan Airport Medical Station and Massachusetts General Hospital in Boston[1]. Since then, it has evolved into virtual scanned imaging using slide scanners to generate high resolution digital images in real time. As a result, digital pathology became feasible for routine clinical use[2][3][4]

The digitalization of histopathological routine laboratory, is an important and decisive step in the digital transformation of pathology. It enables numerous new options such as mobile working and home office for medical specialists, faster provision of images and access to data set for research papers, conferences and tumour boards. However, the switch to a fully digital workflow also means considerable efforts in technical and personnel areas.

### **Methods**

We started by digitalizing archive slides and in 2022 we initialized the process of routine scans.

Various work shifts in the laboratory were pulled further apart in terms of time. In addition, the scanning process was also carried out in stages of urgency: biopsies first, in order to avoid a waiting loop until slides with larger tissue samples were available to be scanned and to have a workflow that was as continuous as possible.

Work stations were colour coded differentiating scanned and unscanned slides. A further measure to increase the efficiency of the scanning process included retraining the laboratory staff on how to apply the paraffin sections in the water bath to the slides by placing the paraffin sections more closely and linearly.

### **Results**

We digitalize approximately 700 routine slides daily and almost 1000 on peak days.

We are currently in the validation stage.

We have 6 Leica GT450 scanners and 2 20SL Glissando scanners for large slides.

Our pathologists now sign out IHC cases digitally.

We have built an almost perfect digital pathology with just a few technical glitches.

## Conclusion

The implementation of digital pathology is costly and personnel-intensive, at least in the early days. Most costs level out over time due to the resulting invaluable benefits such as flexible and more efficient work, AI-supported analytics as a tool for optimized reporting and action against the growing gap in pathology specialists.

Literaturangaben:

- [1] Navid Farahani ,Liron Pantanowitz , (2015), Overview of Telepathology, Surg Pathol Clin, 223-231, 2, <https://doi.org/10.1016/j.path.2015.02.018>
- [2] Stephan W. Jahn, Markus Plass, Farid Moinfar 11 Page: 3697 DOI: 10.3390/jcm9113697 URL: , (2020), Digital Pathology: Advantages, Limitations and Emerging Perspectives, Journal of Clinical Medicine, 3697, 11, <https://www.mdpi.com/2077-0383/9/11/3697/htm>
- [3] Liron Pantanowitz, Ashish Sharma, AlexisB Carter, Tahsin Kurc, Alan Sussman, Joel Saltz, (2018), Twenty years of digital pathology: An overview of the road travelled, what is on the horizon, and the emergence of vendor-neutral archives, Journal of Pathology Informatics, 40, 1
- [4] Liron Pantanowitz, (2010), Digital images and the future of digital pathology, Journal of Pathology Informatics, 15, 1

P13.03

## **Quantitative tissue analysis with easily customizable AI-based segmentation**

P. Kuritcyn<sup>1</sup>, M. Benz<sup>1</sup>, D. Firmbach<sup>2,3</sup>, C. Matek<sup>2,3</sup>, A. Hartmann<sup>2,3</sup>, C. I. Geppert<sup>2,3</sup>, V. Bruns<sup>1</sup>

<sup>1</sup>Fraunhofer-Institute for Integrated Circuits IIS, Digital Health and Analytics, Erlangen, Germany, <sup>2</sup>University Hospital Erlangen, FAU Erlangen-Nuremberg, Institute of Pathology, Erlangen, Germany, <sup>3</sup>University Hospital Erlangen, FAU Erlangen-Nuremberg, Comprehensive Cancer Center Erlangen-EMN (CCC), Erlangen, Germany

### Background

Accurate delineation of different tissue types like stroma or active tumor supports the analysis of tissue sections in two ways: a) quantitative analysis of tissue areas to determine e.g. tumor-stroma ratio, b) definition of regions of interest (ROIs) for quantitative evaluation of a subsequent cell detection (e.g. cell densities within different ROIs). Given the variety of different entities and diseases an easily adaptable AI-based segmentation with only a few user provided annotated examples is highly desirable.

### Methods

We applied a so-called prototypical few-shot segmentation method as described in [1] but used an EfficientNetB0 instead of MobileNetV2 architecture. The key idea of this approach is to train the deep neural network to derive a representative feature description from the input image and assign class labels to the pixels based on their similarity to so-called class prototypes. These prototypes are representatives of a class and are derived from a few annotated image sections. Thus the model can be adapted to a new task by simply replacing the prototypes.

The few-shot model was trained on a dataset with images from hematoxylin and eosin (HE) stained colon sections with pixel-wise annotation of five classes (tumor, stroma, necrosis, mucus, background). Then the model was adapted to a new task: segmentation of epithelial tissue in HE stained images of breast sections using one public dataset from [2]. The new prototypes were calculated based on five images (512x512 pixels) per class.

### Results

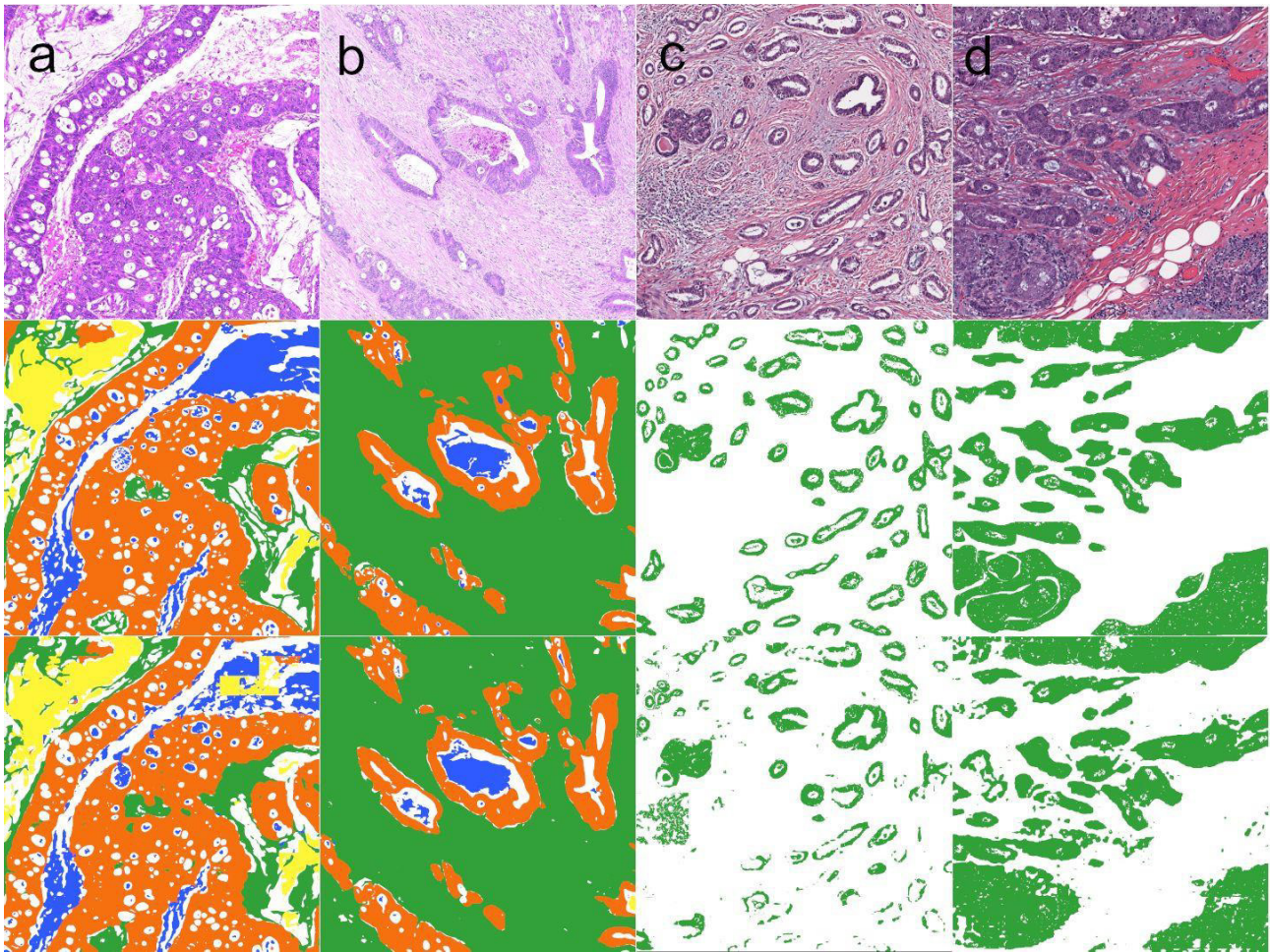
The table presents the results for the tumor microenvironment and epithelial tissue segmentation. For each task the evaluation was repeated with ten different sets of prototypes calculated from a randomly chosen set of images.

task	accuracy	average recall	average precision
tumor microenv. segmentation	0.888	0.800	0.798
epithelium segmentation	0.840	0.805	0.811

The accuracy is the ratio of correctly predicted pixels to all pixels. Recall is the ratio of all pixels of a class that were correctly predicted. Precision is the ratio of all pixels with the predicted class label that actually belong to this class.



Segmentation examples of each task are displayed in the figure below.



Images in column a and b are from the tumor microenvironment and the ones in c and d from the epithelium segmentation task. First row: original images. Second row: ground truth masks (a,b: tumor (orange), stroma (green), necrosis (blue), mucus (yellow), background (white)); c,d: epithelium (green), background (white)). Third row: predicted masks.

### Conclusion

The few-shot model achieved promising results for both tasks. Only five annotated examples per class were sufficient to adapt the model to a new task. This is an ideal technique to realize a customizable AI-based segmentation tool.

### Literaturangaben:

- [1] Firmbach, Daniel; Benz, Michaela; Kuritcyn, Petr; Bruns, Volker; Lang-Schwarz, Corinna; Stuebs, Frederik A.; Merkel, Susanne; Leikauf, Leah-Sophie; Braunschweig, Anna-Lea and Oldenburger, Angelika and Gloßner, Laura; Abele, Niklas; Eck, Christine; Matek, Christian; Hartmann, Arndt; Geppert, Carol I., (2023), Tumor–Stroma Ratio in Colorectal Cancer—Comparison between Human Estimation and Automated Assessment., *Cancer*, 2675, 15, <https://doi.org/10.3390/cancers15102675>
- [2] Janowczyk Andrew and Madabhushi, Anant , (2016), Deep learning for digital pathology image analysis: A comprehensive tutorial with selected use cases., Elsevier, *Journal of Pathology Informatics*, 7:29, <http://www.andrewjanowczyk.com/deep-learning/>, 2024-02-16

P13.04

## ***A Systematic Review of Machine Learning-Based Tumor-Infiltrating Lymphocytes Analysis in Colorectal Cancer: Overview of Techniques, Performance Metrics, and Clinical Outcomes***

A. Kazemi<sup>1,2</sup>, A. Rasouli-Saravani<sup>3</sup>, M. Gharib<sup>4</sup>, T. Albuquerque<sup>5</sup>, S. Eslami<sup>1,6,7</sup>, P. J. Schüffler<sup>2,8,9</sup>

<sup>1</sup>Department of Medical Informatics, School of Medicine, Mashhad University of Medical Sciences, Mashhad, Iran, Islamic Republic of,

<sup>2</sup>Institute of General and Surgical Pathology, Technical University of Munich, Munich, Germany, <sup>3</sup>Department of Immunology, School of Medicine, Shahid Beheshti University of Medical Sciences, Tehran, Iran, Islamic Republic of, <sup>4</sup>Department of Pathology, Faculty of Medicine, Mashhad University of Medical Sciences, Mashhad, Iran, Islamic Republic of, <sup>5</sup>INESC TEC -Rua Dr. Roberto Frias, Porto, Portugal, <sup>6</sup>Pharmaceutical Sciences Research Center, Institute of Pharmaceutical Technology, Mashhad University of Medical Sciences, Mashhad, Iran, Islamic Republic of, <sup>7</sup>Department of Medical Informatics, University of Amsterdam, Amsterdam, The Netherlands, <sup>8</sup>TUM School of Computation, Information and Technology, Technical University of Munich, Garching bei Munich, Germany, <sup>9</sup>Munich Data Science Institute, Technical University of Munich, Garching bei Munich, Germany

## Background

Tumor-infiltrating lymphocytes (TIL) can have a crucial impact on diagnosis or decision-making for treating patients with colorectal cancer (CRC), but the inter-observer agreement for quantifying TIL is not perfect. We aimed to systematically review the machine learning (ML) techniques applied for TIL identification on CRC histopathological images to investigate their performance, patient outcomes, and clinical aspects.

## Methods

Original TIL-related publications from 2000 to 2022 on PubMed and Scopus databases were retrieved. Articles focused on manually identifying or quantifying TIL or using prebuilt tools for whole TIL analysis were excluded. All articles were screened based on inclusion and exclusion criteria in the title, abstract, and full text. In the initial stage, 722 records were identified. Finally, clinical and technical data extraction was done in ten studies (1-10). The association of TIL levels with patient outcomes was investigated.

## Results

Deep neural networks (1-6, 8) and traditional ML models (7, 9, 10) are promising in aiding pathologists. Compared to traditional ML models, deep learning models achieved higher performance for identifying TIL. The main applications of ML techniques are segmentation, classification, detection, quantification, and spatial distribution analysis of TIL. Most studies aimed to identify specific subtypes of TIL, such as CD3 and CD8 cells. Stromal or intraepithelial-TIL were identified in a few studies (1-3, 9). However, most studies identified TIL in the whole tumor region. Only two studies focused on TIL infiltrated from invasive margins (4, 10). There is no standard threshold for categorizing TIL densities; therefore, some studies have tried different cut-off points to determine the association of TIL levels with patients' outcomes. Higher TIL density in different locations in tumor regions is associated with outcomes.

## Conclusion

Despite some differences in methodology, pipelines, and datasets, most studies have shown a significant positive association between the higher level of TIL and favorable outcomes in CRC. A large multi-institutional CRC dataset with a diverse and multi-ethnic population must validate and generalize ML methods.

Literaturangaben:

- [1] Xu, Y.; Yang, S.; Zhu, Y.; Yao, S.; Li, Y.; Ye, H.; Ye, Y.; Li, Z.; Wu, L.; Zhao, K.; Huang, L.; Liu, Z., (2022), Artificial intelligence for quantifying Crohn's-like lymphoid reaction and tumor-infiltrating lymphocytes in colorectal cancer, *Comput Struct Biotechnol J*, 5586-5594, 2001-0370 (Print), 2023-12-01
- [2] Yang, J. Ye, H. Fan, X. Li, Y. Wu, X. Zhao, M. Hu, Q. Ye, Y. Wu, L. Li, Z. Zhang, X. Liang, C. Wang, Y. Xu, Y. Li, Q. Yao, S. You, D. Zhao, K. Liu, Z., (2022), Artificial intelligence for quantifying immune infiltrates interacting with stroma in colorectal cancer, *J Transl Med*, 451, 1
- [3] Xu, Z. Li, Y. Wang, Y. Zhang, S. Huang, Y. Yao, S. Han, C. Pan, X. Shi, Z. Mao, Y. Xu, Y. Huang, X. Lin, H. Chen, X. Liang, C. Li, Z. Zhao, K. Zhang, Q. Liu, Z., (2021), A deep learning quantified stroma-immune score to predict survival of patients with stage II-III colorectal cancer, *Cancer Cell Int*, 585, 1
- [4] Xu, H. Cha, Y. J. Clemenceau, J. R. Choi, J. Lee, S. H. Kang, J. Hwang, T. H., (2022), Spatial analysis of tumor-infiltrating lymphocytes in histological sections using deep learning techniques predicts survival in colorectal carcinoma, *J Pathol Clin Res*, 4
- [5] Pai, R. K. Hartman, D. Schaeffer, D. F. Rosty, C. Shivji, S. Kirsch, R. Pai, R. K., (2021), Development and initial validation of a deep learning algorithm to quantify histological features in colorectal carcinoma including tumour budding/poorly differentiated clusters, *Histopathology*, 391-405, 3
- [6] Pai, R. K. Banerjee, I. Shivji, S. Jain, S. Hartman, D. Buchanan, D. D. Jenkins, M. A. Schaeffer, D. F. Rosty, C. Como, J. Phipps, A. I. Newcomb, P. A. Burnett-Hartman, A. N. Le Marchand, L. Samadder, N. J. Patel, B. Swallow, C. Lindor, N. M. Gallinger, S. J. Grant, R. C. Westerling-Bui, T. Conner, J. Cyr, D. P. Kirsch, R. Pai, R. K., (2022), Quantitative Pathologic Analysis of Digitized Images of Colorectal Carcinoma Improves Prediction of Recurrence-Free Survival, *Gastroenterology*, 1531-1546 e8, 6
- [7] Failmezger, H. Zwing, N. Tresch, A. Korski, K. Schmich, F., (2021), Computational Tumor Infiltration Phenotypes Enable the Spatial and Genomic Analysis of Immune Infiltration in Colorectal Cancer, *Front Oncol*, 552331
- [8] Bian, C. Auid-Orcid Wang, Y. Lu, Z. An, Y. Wang, H. Kong, L. Du, Y. Tian, J., (2021), ImmunoAIzer: A Deep Learning-Based

Computational Framework to Characterize Cell Distribution and Gene Mutation in Tumor Microenvironment, *Cancers (Basel)*, 7  
[9] Stachtea, X. Loughrey, M. B. Salvucci, M. Lindner, A. U. Cho, S. McDonough, E. Sood, A. Graf, J. Santamaria-Pang, A. Corwin, A. Laurent-Puig, P. Dasgupta, S. Shia, J. Owens, J. R. Abate, S. Van Schaeuybroeck, S. Lawler, M. Prehn, J. H. M. Ginty, F. Longley, D. B., (2022), Stratification of chemotherapy-treated stage III colorectal cancer patients using multiplexed imaging and single-cell analysis of T-cell populations, *Mod Pathol*, 564-576, 4  
[10] Yoo, S. Y. Park, H. E. Kim, J. H. Wen, X. Jeong, S. Cho, N. Y. Gwon, H. G. Kim, K. Lee, H. S. Jeong, S. Y. Park, K. J. Han, S. W. Kim, T. Y. Bae, J. M. Kang, G. H., (2020), Whole-Slide Image Analysis Reveals Quantitative Landscape of Tumor-Immune Microenvironment in Colorectal Cancers, *Clin Cancer Res*, 870-881, 4

P13.05

### ***Decoding pan-cancer treatment outcomes using multimodal real-world data and explainable artificial intelligence***

J. Keyl<sup>1</sup>, P. Keyl<sup>2</sup>, G. Montavon<sup>3</sup>, K.-R. Müller<sup>3</sup>, M. Schuler<sup>4</sup>, F. Klauschen<sup>5</sup>, J. Kleesiek<sup>1</sup>

<sup>1</sup>Institute for Artificial Intelligence in Medicine, Essen, Germany, <sup>2</sup>Pathologisches Institut, LMU, München, Germany, <sup>3</sup>Machine Learning Group, Technical University of Berlin, Berlin, Germany, <sup>4</sup>Department of Medical Oncology, Essen, Germany, <sup>5</sup>Pathologisches Institut, LMU, Thalkirchner Straße 36, Germany

#### **Background**

The accurate prognostic assessment of patients for personalized medicine remains a challenge. Although large amounts of routine clinical data are available, they are not systematically used for predicting a patient's individual prognosis and developing tailored therapies. Modern explainable AI methods are able to integrate large amounts of data and provide valuable insight into factors that determine a patient's outcome.

#### **Methods**

We developed an xAI-based approach for exploring patient characteristics in large-scale real-world data. We predicted the prognosis of 15,726 patients across more than 30 cancer types based on 350 patient markers including clinical records, genetic data, and histologic subtypes. xAI was used to disentangle the contribution of each feature to clinical outcomes at the patient and cohort levels.

#### **Results**

xAI identified 114 key markers that accounted for 90% of the neural network's decision process. This provided novel representations of the prognostic landscape, revealing that the prognostic impact of many features depended strongly on the specific patient context. We identified subgroups of patients for which specific markers were associated with high risk and validated our main results in an independent cohort of 3,288 lung cancer patients from a US nationwide electronic health record-derived database.

#### **Conclusion**

This work demonstrates that the combination of real-world data and explainable artificial intelligence can transform research on prognostic factors in oncology.

P13.06

### ***AI-driven analysis for real-time detection of morphologic characteristics in unstained microscopic cell culture images***

K. Hildebrand\*<sup>1</sup>, T. Mögele\*<sup>1</sup>, D. Raith<sup>2,3,4</sup>, M. Eberle<sup>1</sup>, E. Meerdink<sup>2</sup>, J. Bödecker<sup>3,4</sup>, J. Bermeitinger<sup>2</sup>, M. Trepel<sup>5</sup>, R. Claus<sup>1,5,6</sup>

<sup>1</sup>Institut für Pathologie und Molekulare Diagnostik, Medizinische Fakultät, Universität Augsburg, Augsburg, Germany, <sup>2</sup>LABMaiTE, Freiburg, Germany, <sup>3</sup>Neurorobotics Lab, Department of Computer Science, Universität Freiburg, Freiburg, Germany, <sup>4</sup>BrainLinks-BrainTools, Universität Freiburg, Freiburg, Germany, <sup>5</sup>Hämatologie und Onkologie, Medizinische Fakultät, Universität Augsburg, Augsburg, Germany, <sup>6</sup>Personalisierte Tumormedizin und Molekulare Onkologie, Medizinische Fakultät, Universität Augsburg, Augsburg, Germany

\*Contributed equally

#### **Background**

AI-based image recognition has significantly advanced the analysis of tissues and individual cells both in diagnostics and translational studies. To date, recognition is primarily based on the identification of certain cell characteristics (e.g. by

staining). The morphological assessment of unstained cells holds additional potential, as it allows for virtually real-time assessment without the need to manipulate the cells. This facilitates longitudinal observations as required for drug testing and constitutes a prerequisite for autonomous execution of experiments, e.g. for treatment optimization.

## Methods

A semi-automated cell culture system (AICE3, LabMaite) was used to culture myeloid leukemic cell lines (K562, HL60, Kasumi-1). K562 cells were treated with 50  $\mu$ M hemin (six days) and 5 nM phorbol ester (PMA, 48 hours) to induce erythroid and megakaryocytic differentiation, respectively. Cell images were obtained by automated bright field microscopy. The images were used for training on an NVIDIA DGX A100 GPU with Ultralytics YOLOv8. Morphologic features were extracted using RedTell.

## Results

The model was trained to recognize K562 cells from morphologically similar HL-60 and Kasumi-1 based on 436 and 399 images with an average of 15.5 and 23.8 cells, respectively. mAP@.5 >98% indicated that bounding boxes were generated correctly. Precision and recall/sensitivity for K562 detection were >97%. Validation with an external K562 dataset was highly similar. The model-based separation of K562, HL-60, and Kasumi-1 achieved an average sensitivity and specificity of >97 % and a precision of 94.6 %. To test applicability to drug testing, we used a K562-based model for drug-induced differentiation. Based on >3,000 annotations, YOLOv8-s achieved exceptional precision, sensitivity and specificity of >95% in recognizing and distinguishing untreated K562 cells from those stimulated to erythroid (K562/hemin) or megakaryocytic (K562/PMA) differentiation. Mixing experiments demonstrated highly reliable distinction between the three classes. Using RedTell, we identified three of 74 predefined morphological traits that contributed significantly to the distinction of the classes and explained most of the dataset variance.

## Conclusion

We show that AI-assisted detection of unstained cells in suspension culture can be reliably performed in near real-time and enables accurate identification cell lines and monitoring of morphological differences. This forms the basis for future AI-based automated drug testing.

P13.07

## ***Puzzling in pathology: Post-operative tissue reconstruction***

C. Blattgerste<sup>1</sup>, A. Jessen<sup>1</sup>, K. Rohr<sup>2,3</sup>, C. Scherl<sup>4</sup>, C.-A. Weis<sup>1,5</sup>

<sup>1</sup>Institute of Pathology, Heidelberg University Hospital, AG Computational Pathology, Heidelberg, Germany, <sup>2</sup>Universität Heidelberg, BioQuant, IPMB, Biomedical Computer Vision Group, Heidelberg, Germany, <sup>3</sup>German Cancer Research Center, Heidelberg, Germany, <sup>4</sup>Universitätsmedizin Mannheim, Klinik für Hals-Nasen-Ohrenheilkunde, Kopf- und Halschirurgie (HNO), Mannheim, Germany, <sup>5</sup>Interdisciplinary Center for Scientific Computing, Heidelberg, Germany

## Background

The concept of assembling puzzles transcends mere child's play when applied to computational analysis, particularly in the context of reconstructing irregularly shaped fragments like, for instance, tissue fragments in pathology. In addition to their heterogeneous shape, these fragments are often overlaid by artifacts and occasionally missing elements. This ongoing research project focuses on reassembling surgical specimens from head and neck surgeries through histological sections after the standard tissue workup procedure. With a micrometer accurate three-dimensional (3D) reconstruction, the long-term goal is to develop a tool to determine tumor dimensions and locations, thereby facilitating more reliable assessments of safety margins.

## Methods

The methodology employs a three-step approach as suggested for comparable reassembly problems in, e.g., archeology [1]: First, each tissue fragment is extended using a self-supervised Generative Adversarial Network (GAN) [2]. Second, the extended tissue is registered with adjacent fragments [3]. Third, the pairwise matching fragments are pieced together based on a graph-based algorithm identifying the optimal arrangement of puzzle pieces. The resulting transformations lead to the reconstruction of tissue cross-sections into a 3D form.

## Results

By the time of writing, the initial tissue fragment extension is established and several registration approaches including intensity and feature as well as machine learning based approaches are tested.

## Conclusion

The outcome of this not yet fully established process is the generation of a 3D histological dataset of the surgical specimen, augmented with additional resection samples. This dataset permits navigational and measurement capabilities akin to those found in radiological imaging, offering a novel perspective in the post-operative analysis of tissue fragments.

Literaturangaben:

[1] Derech, N., Tal, A., & Shimshoni, I., (2021), Solving Archaeological Puzzles, Pattern Recognition, <https://doi.org/10.1109/ICCV.2019.01062>

[2] Teterwak, P., Sarna, A., Krishnan, D., Maschinot, A., Belanger, D., Liu, C., & Freeman, W.T., (2019), Boundless: Generative Adversarial Networks for Image Extension, IEEE International Conference on Computer Vision, 10520-10529, <https://api.semanticscholar.org/CorpusID:201106503>, 2024-02-26

[3] Junyu Chen, Eric C. Frey, Yufan He, William P. Segars, Ye Li, Yong Du, (2022), TransMorph: Transformer for unsupervised medical image registration, Medical Image Analysis, <https://doi.org/10.1016/j.media.2022.102615>, 2024-02-26

P13.08

## ***A versatile and non-proprietary multiplex immunohistochemistry approach for tissue-based spatial phenotyping***

G. Andreev<sup>1</sup>, M. Grabbert<sup>2</sup>, M. Werner<sup>1</sup>, M. Rogg<sup>1</sup>, C. Schell<sup>1</sup>

<sup>1</sup>Institut für Klinische Pathologie, Freiburg, Germany, <sup>2</sup>Klinik für Urologie, Universitätsklinikum Freiburg, Freiburg, Germany

### Background

The rapidly emerging field of tissue-based spatial analysis is crucial for understanding both physiological and pathological conditions. Advanced techniques like cellular neighborhood characterization within tissue compartments have propelled the study of complex pathologies. However, the widespread adoption of commercial systems is hindered by costs and proprietary limitations. Our study explores a non-proprietary cyclic immunohistochemistry (cyclIHC) method paired with an open-source digital processing workflow for multiplex spatial phenotyping of FFPE-tissue samples.

### Methods

We adapted a cyclIHC approach to enable for multiplex spatial phenotyping. A computational pipeline was established allowing for automated co-registration and further segmentation of whole-slide-images (WSI) as well as tissue-microarrays (TMA). Generation of merged multiplex data was based on transformation of individual IHC stainings towards single channel pseudo-colored images. Core extraction from TMAs and further image processing relied on a workflow utilizing QuPath, Python scripts and ImageJ.

### Results

Our cyclIHC method proved robust across various FFPE tissue types, maintaining quality up to 10-12 antibody cycles. Further cycles led to reduced tissue quality or staining intensities, affecting cell segmentation and quantification. Modular workflows for co-registration were evaluated and established. Comparison with other low-plex technologies confirmed competitive performance, even against single IHC protocols. Moreover, cyclIHC was successfully applied to classify and phenotype immune infiltrates in TMAs of lung and renal carcinoma, demonstrating its potential for increased throughput capacities.

### Conclusion

The demand for spatial analysis of complex tissues is growing. Our cyclIHC workflow offers a cost-effective, non-proprietary solution for low-plex phenotyping. Although accurate co-registration presents challenges in cyclIHC data processing, our easy to set up, open-source workflow effectively overcomes these limitations and is potentially facilitating its accessibility towards the broader research community.

# Poster Gastroenteropathologie I

P14.01.01

## ***Structured evaluation of histopathological findings for future research puposes using the example of chronic inflammatory bowel disease***

J. Shakhtour<sup>1</sup>, M. Middelhoff<sup>2</sup>, D. Schult-Hannemann<sup>2</sup>, C. Mogler<sup>1</sup>, L. Arps<sup>1</sup>, F. Kohlmayer<sup>3</sup>, K. Steiger<sup>1</sup>

<sup>1</sup>Institut für allgemeine Pathologie und pathologische Anatomie der TUM, München, Germany, <sup>2</sup>Klinikum rechts der Isar der TUM, Klinik und Poliklinik für Innere Medizin II, München, Germany, <sup>3</sup>Bitcare GmbH, München, Germany

### **Background**

A definitive diagnosis of chronic inflammatory bowel disease (IBD) and follow-ups of Crohn's disease (CD) and ulcerative colitis (UC) is often only possible through a combination of clinical parameters and histology, because landmark findings such as granulomas are not always found[1]. Therefore, a standardized reporting based on the histological image is essential for the optimal combination of pathological and clinical criteria for definitive diagnosis or follow-up of IBD.

### **Methods**

Cohort:

In cooperation with the department of Gastroenterology at the Hospital rechts der Isar, a cohort of currently 727 patients was compiled as part of the Collaborative Research Project (SFB) 1371 in the "ColoBAC" registry study from 2019-2023. The patients received colonoscopic examinations and stepwise biopsies. All biopsies were formalin fixed and paraffin embedded according to standard protocols.

Data integration system (DIS):

All histological parameters were entered into an internal database and got pseudonymized. The database can be searched for the presence of certain criteria. This enables simple cohort compilation based on histological criteria.

### **Results**

The reports collected at our Pathology institute were systematically evaluated on the basis of relevant parameters, including recommendations of the ECCO guidelines[2]. These consist of the localization of the inflammatory infiltrate in the intestine, severity (low, moderate or high), spread (focal, diffuse or multifocal), and composition of the inflammatory cells. For better comparability, the Nancy index, a recognized index for determining disease activity, was also recorded[3]. In addition, erosions, ulcerations, cryptitis, crypt abscesses, basal plasmocytosis, and granulomas were recorded as particularly noteworthy inflammatory changes. Morphologic changes of the mucosa were considered based on the degree of crypt architectural disorder (low, moderate or high) and the degree of regenerative changes (low, moderate or high).

### **Conclusion**

In this project, a structured evaluation of the histopathological findings of study patients with a (suspected) diagnosis of IBD was carried out using clearly defined histological parameters, which were entered into an internal database system. This enables histological data to be quickly and easily incorporated into future research projects, which can contribute to a better understanding of IBD.

Literaturangaben:

[1] Heresbach D, Alexandre JL, Branger B, et al., (2005), Frequency and significance of granulomas in a cohort of incident cases of Crohn's disease, Gut, 215-222, 54(2)

[2] Magro F, Langner C, Driessen A, et al., (2013), European consensus on the histopathology of inflammatory bowel disease, J Crohns Colitis, 827-851, 7(10)

[3] Marchal-Bressenot A, Salleron J, Boulagnon-Rombi C, et al., (2017), Development and validation of the Nancy histological index for UC, Gut, 43-49, 66(1)



P14.01.02

### ***Prospective multicenter observational study on the impact of intestinal anastomosis onto early postoperative and long-term oncological outcome in resection of colon cancer (CA)***

E. Hajduk<sup>1</sup>, F. Meyer<sup>2</sup>, K. Ridwelski<sup>3</sup>

<sup>1</sup>Institute of Quality Assurance in operative Medicine, Otto-von-Guericke University with University Hospital, Magdeburg, Germany,

<sup>2</sup>Klinik für Allgemein-, Viszeral-, Gefäß- und Transplantationschirurgie, Otto-von-Guericke-Universität mit Universitätsklinikum,

Magdeburg, Germany, <sup>3</sup>Dept. of General and Abdominal Surgery; Municipal Hospital (, Magdeburg, Germany

#### **Background**

Aim: To investigate the influence of intestinal anastomosis on postop. outcome

#### **Methods**

Through a 7-years time period, all consecutive patients w/ the histologically diagnosed primary colon CA were registered.

#### **Results**

- *Basic data*: From 2010–2016, data from a total of 14,466 patients were documented (mean age, 72.8 [range, 22–96] years; sex ratio, m:f=7,696:6,770). From this group, 717 patients (4.96%) were included in a matched-pair analysis. The majority of these patients underwent elective surgery ( $n=12,620$  patients; 87.2%) regardless of whether a bowel anastomosis or an “anus praeter” was created. In emergency surgery, a bowel anastomosis was possible in a large proportion ( $n=1,332$  patients [72.1%]). In contrast, in 514 patients (27.9%) who underwent emergency surgery, a stoma was created. Interestingly, stoma had to be created even less frequently in patients who had undergone planned surgery ( $n=366$  [2.5%]).

- *Early postop. outcome*: Cases of postop. mortality were mainly due to general complications. Especially among the patients treated in an emergency situation w/o intestinal anastomosis, a high proportion died of their pre-existing condition (17.0%). Patients who underwent anus praeter creation or emergency surgery had a worse risk profile (risk factors such as arterial hypertension, diabetes mellitus & secondary cardiac or renal diseases), which led to the decision to operate w/o anastomosis. Furthermore, data show no matter which technique was used, patients that had been operated w/o anastomosis were more likely to develop complications.

- *Long-term oncosurgical outcome*: Early postop. mortality had major impact onto survival. The most important factors influencing long-term survival were age, resection status & tumor stage (according to TNM & UICC). The more advanced the tumor stage was classified, the lower the long-term survival. Kaplan-Meier curves for surgical technique & urgency showed significant differences in survival time in the matched-pair analysis. Patients categorized with the same tumor stage, age & risk factors had a better chance of survival, if they had been operated electively & w/ intestinal anastomosis. Interestingly, the multivariable analysis showed that older patients & such w/ distant metastasis benefit from a discontinuity resection.

#### **Conclusion**

Current studies agree - as indicate in the presented study - that older patients & such w/ reduced general condition by preexisting risk factors benefit from discontinuity resection.

P14.01.03

### ***Prospective multicenter observational study including propensity score analysis on the impact of multivisceral resection of advanced colon and rectal cancer onto outcome characterized by morbidity, mortality and survival***

M. Arndt<sup>1</sup>, H. Lippert<sup>1</sup>, R. S. Croner<sup>2</sup>, F. Meyer<sup>2</sup>, R. Otto<sup>1</sup>, K. Ridwelski<sup>3</sup>

<sup>1</sup>Institute for Quality Assurance in operative Medicine, Otto-von-Guericke University with University Hospital, Magdeburg, Germany,

<sup>2</sup>Klinik für Allgemein-, Viszeral-, Gefäß- und Transplantationschirurgie, Otto-von-Guericke-Universität mit Universitätsklinikum,

Magdeburg, Germany, <sup>3</sup>Dept. of General and Abdominal Surgery; Municipal Hospital (, Magdeburg, Germany

#### **Background**

Aim: To analyze the impact of non-multivisceral resection (nMVR) versus MVR onto outcome such as overall survival incl. to determine the influencing factors.

## Methods

The data of 25.321 patients from 364 hospitals who had undergone surgery for CRC (the UICC stages I–III) during a defined time period were registered in a computer-based data file & evaluated.

## Results

From 2008 to 2015, the MVR rates were 9.9% ( $n=1,551$ ) for colon cancer (colon CA) & 10.6% ( $n=1,027$ ) for rectal cancer (rectal CA). CRC was more common in men (colon/rectal CA: 53.4/62.0%) than in women; all MVR groups had high proportions of women (53.6 vs. 55.2%; pairs of values in previously mentioned order). Resection of another organ frequently occurred (75.6 vs. 63.7%). The MVR group had a high prevalence of intraop. (5.8%; 12.1%) & postop. surgical complications (30.8 vs. 36.4%; each  $p<0.001$ ). Wound infections (colon CA: 7.1%) & anastomotic insufficiencies (rectal CA: 8.3%) frequently occurred after MVR. The morbidity rates of the MVR groups were also determined (43.7 vs. 47.2%). The hospital mortality rates were 4.9% in the colon CA-related MVR group & 3.8% in the rectal CA-related MVR group & were significantly increased compared with those of the nMVR group (both  $p<0.001$ ). Results of the MPA showed that the morbidity rates in both MVR groups (colon CA: 42.9 vs. 34.3 %; rectal CA: 46.3 vs. 37.2%; each  $p<0.001$ ) were significantly increased. The hospital mortality rate tended to increase in the colon CA-related MVR group (4.8 vs. 3.7%;  $p=0.084$ ), while it significantly increased in the rectal CA-related MVR group (3.4 vs. 3.0%;  $p=0.005$ ). Moreover, the 5-yr-overall survival rates were 53.9% (nMVR: 69.5%;  $p<0.001$ ) in the colon CA group & 56.8% (nMVR: 69.4%;  $p<0.001$ ) in the rectal CA group. Comparison of individual T stages (MVR vs. nMVR) showed no significant differences in the survival outcomes ( $p<0.05$ ); however, according to the MPA, a significant difference was observed in the survival outcomes of those with pT4 colon CA (40.6 vs. 50.2%;  $p=0.017$ ). By contrast, the 5-yr-local recurrence rates after MVR were not significantly different (7.0 vs. 5.8%; both  $p>0.05$ ). The risk factors common to both tumor types were advanced age ( $>79$  yr), pT stage, sex & morbidity (each hazard ratio:  $>1$ ;  $p<0.05$ ).

## Conclusion

MVR allows curative resection with adequate long-term survival.

In the overall data, MVR was associated with significant increases in hospital mortality rates, as indicated by the MPA (significant only for rectal CA).

P14.01.04

## ***Intraabdominal inflammation indicated by diverticulitis of the sigmoid colon under immunosuppressive medication after previous lung transplantation***

D. Strischewski<sup>1</sup>, F. Meyer<sup>2</sup>

<sup>1</sup>Klinik für Allgemein-, Viszeral-, Gefäß- und Transplantationschirurgie; Otto-von-Guericke-Universität mit Universitätsklinikum, Magdeburg, Germany, <sup>2</sup>Klinik für Allgemein-, Viszeral-, Gefäß- und Transplantationschirurgie, Otto-von-Guericke-Universität mit Universitätsklinikum, Magdeburg, Germany

## Background

**Ziel:** Aufgrund klin. Managementerfahrg. & selektiver Referenzen d. med.-wiss. Literatur soll die eher seltene Fallkonstellation einer akuten intraabd. Inflammation als ungewönl. Komplikation od. visz.-med. Nebenwirkg. einer immunsuppr. Medikation b. zugr.-lieg. Z.n. Lungentransplantation(LTx) illustriert werden.

## Methods

Wissenschaftl. Fallbericht

## Results

Kasuistik: *Anamnese:* - Jetzig: Eine 54-j. Patientin(Patn.) stellte sich mit seit 5 d bestehenden li-seitigen UB-Beschwerden in der Notaufnahme vor. Miktion, Stuhlgang & Nahrgr.-aufnahme waren unauffällig. Fieber, Erbrechen & Übelkeit wurden verneint.

- Eigen: **1)** Medikation: u.a. Advagraf/Prednisolon/Mycophenolat; **2)** Neben-Dx: Akut auf chron. Nierenversagen, Z.n. SARS-CoV-2-Infektion 2 Jahre[J.] zuvor, Z.n. Ulcera ventriculi, Z.n. Teilthrombosierg. d. V. cava inf. n. Femoraliskatheter (vor 6 J.), Sigmadivertikulose, Folsäuremangel, Anämie, Z.n. Herpes zoster (vor 3 J.), Osteoporose, Ex-Nikotinabusus 30 p/y, COPD Gr. IV



*Klinisch:* Patn. in red. AZ & adipösem EZ; 4-fach orientiert, kreislaufstabil - Abdomen: weich, allerdings gebläht. Min. Resistenz im Bereich des li MB & UB palpabel, hier lokaler DS. Keine AWS, kein Peritonismus.

*Diagnostik:* - Labor (SI) - L: 11 Gpt/l; CrP: 143,39 mg/l; CKD-EPI: 23 ml/min/1,73m<sup>2</sup>

- CT: unkomplizierte Divertikulitis am Sigma & der li Kolonflexur mit leichter umgebender Fettgewebsimbibierung. ohne Anzeichen v. fr. Luft, Abszess, Perforation od. Ileuszeichen

*Diagnose:* 1. Schub einer unkompliz. Sigma-Diverticulitis

*Entsch.-findung:* konservative Therapie

*Therapie:* Init. Nahrungskarenz, Bettruhe, lokale Kühlg., Schmerz- & antibiot. Therapie mittels Tazobac, Infus.-Behandlg.

*Verlauf:* Klin. & laborchem. Befundbesserg., Kostaufbau verträglich, stat. Entlassung bei subj. Wohlbefinden am 7. Tag.

*Procedere:* Klin./laborchem. Verl.-Kontr. beim HA, weitere Einnahme v. Unacid PD 750 mg 1-0-1 ab 5.-10. Ther.-tag, weiterhin Schonkost & ballaststoffreiche Ernährung. sowie Koloskopie im entz.-freien Intervall (frühestens nach 6-8 Wo.), WV in der LTx-Sprechstunde zur Nachsorge

## Conclusion

Beim beschr. Fall handelt es sich entweder um eine der zahlr. im Beipackzettel gelisteten Nebenwirkg. von Mycophenolat mofetil, Prednisolon bzw. Tacrolimus, die als „Kolonentzündg.“ bzw. „Magen-Darm-Entzündg.“ aufgeführt sind, oder eine Entz.-Reaktion b. einer sukzeptiblen (gastro-)intest. Mukosa durch die transpl.-bedingte imm.-suppr. Medikation darstellen (diff.-diagnost. ebenso Diverticulitis-Auftreten i.R. des reg. Vorkommenrisikos zu prüfen).

P14.01.05

## **Detection of oncofetal matrix proteins in collagenous colitis.**

T. Hansen<sup>1</sup>, R. Aurora<sup>2</sup>, M. Dederer<sup>3</sup>, T. Stolz<sup>4</sup>, R. Wulff<sup>5</sup>, T. Zimmer<sup>6</sup>, M. Otto<sup>1</sup>, J. Kriegsmann<sup>1,7</sup>, A. Berndt<sup>8</sup>

<sup>1</sup>MVZHZMD Trier GmbH, Trier, Germany, <sup>2</sup>Internistische Fachpraxis, Bitburg, Germany, <sup>3</sup>Krankenhaus Maria Hilf, Innere Medizin, Daun, Germany, <sup>4</sup>Zentrum für Innere Medizin, Gastroenterologie, Völklingen, Germany, <sup>5</sup>Gemeinschaftspraxis Wulff & Wulff, Birkenfeld, Germany, <sup>6</sup>Zentrum für Magen- und Darmgesundheit, Wittlich-Wengerohr, Germany, <sup>7</sup>Danube Private University, Department of Medicine, Krems, Austria, <sup>8</sup>Institut für Rechtsmedizin, Sektion Pathologie, Jena, Germany

## Background

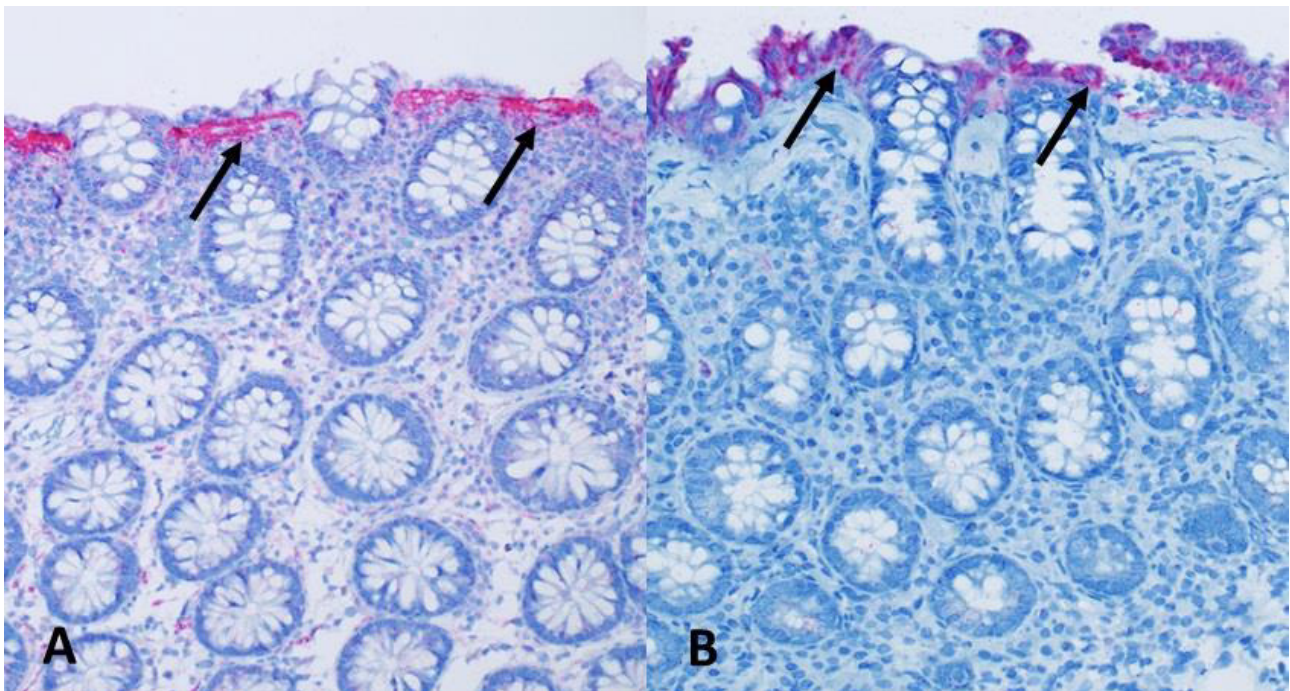
Extracellular matrix (ECM) remodelling is a crucial mechanism of collagenous colitis (CC). Besides several types of collagen, the glycoprotein tenascin has been demonstrated as major factor for both pathogenesis and diagnosis of CC[1][2]. In inflammatory and neoplastic disorders, especially tenascin C contributes to a particular ECM reorganization (known as oncofetal ECM) in a typical large, low spliced oncofetal isoform (oncfTnC). Interaction of oncfTnC with the g2 subunit of the hemidesmosomal adhesion protein laminin 332 (Lng2) and the extra domain A containing cellular fibronectin (EDA-Fn) is important for the formation of a provisional ECM[3]. So far, these specialized matrix molecules have not been investigated in CC.

## Methods

We examined 15 patients with CC (M = 4, F = 11, mean age: 54.3 yrs, range: 23 – 88 yrs). We conducted routine histological and immunohistochemical studies according to standard protocols including immunohistochemistry. All cases were examined for the expression of B domain containing oncfTnC [clone 4C8MS, Thermo], Lng2 [clone CL2980, Thermo], and EDA-Fn [clone IST-9, Santa Cruz]. For negative control, we studied biopsies of 4 patients without any signs of colitis.

## Results

We found strong immunoreaction for oncfTnC and Lng2 in the majority of patients with CC (13/15 and 12/15 respectively). While labelling for oncfTnC was mainly confined to basement membrane, we observed a remarkable cytoplasmic staining of Lng2 in the colonic epithelium (Fig. 1). By contrast, only one CC patient revealed a significant expression of EDA-Fn. In negative controls, we did not detect relevant labeling of these molecules.



A. Expression of oncofetal tenascin C (red) at the basement membrane (arrows); B. Expression of Lng2 (red) in the cytoplasm of colonic epithelium (arrows).

### Conclusion

In CC, tissue remodelling demonstrates features of an oncofetal ECM. Our finding of cytoplasmic Lng2 expression in colonic epithelium is especially remarkable since this staining reaction has been particularly described for colonic carcinoma [4]. Moreover, it needs to be further examined whether the spatially associated oncofetal tenascin C / cytoplasmic Lng2 expression might have pathobiological, diagnostic and prognostic importance for CC.

### Literaturangaben:

- [1] Miehke S, et al., (2021), European guidelines on microscopic colitis: United European Gastroenterology and European Microscopic Colitis Group statements and recommendations, *United European Gastroenterol J*, 13, 9, 2022-10-27
- [2] Anagnostopoulos I, et al., (1999), Tenascin labelling in colorectal biopsies: a useful marker in the diagnosis of collagenous colitis, *Histopathology*, 425, 34, 2024-02-07
- [3] Berndt A, et al., (2022), Invasion-associated reorganization of laminin 332 in oral squamous cell carcinomas: the role of laminin g2 chain in tumor biology, diagnosis, and therapy, *Cancers*, 4903, 14, 2023-01-11
- [4] Pyke C, et al., (1995), Laminin-5 is a marker of invading cancer cells in some human carcinomas and is coexpressed with the receptor for urokinase plasminogen activator in budding cancer cells in colon adenocarcinomas, *Cancer Res*, 4132, 55, 2024-02-07

P14.01.06

## ***Neuroendocrine differentiation in conventional adenocarcinomas and adenoneuroendocrine carcinomas of the colorectum***

F. Kulow<sup>1</sup>, F. Kellers<sup>1</sup>, V. Stoll<sup>1</sup>, M. Jesinghaus<sup>2</sup>, S. Försch<sup>3</sup>, C. Röcken<sup>1</sup>, B. Konukiewitz<sup>1</sup>

<sup>1</sup>University Hospital Schleswig-Holstein, Campus Kiel, Institute of Pathology, Kiel, Germany, <sup>2</sup>Philipps-University Marburg and University Hospital Marburg (UKGM), Department of Pathology, Marburg, Germany, <sup>3</sup>University Medical Center Mainz, Institute of Pathology, Mainz, Germany

### Background

Colorectal cancer is accounting for around 10% of all cancers and is the second most common cause of cancer-related death [1]. The histological classification is based on the current WHO classification of tumours of the digestive system [2]. Histological criteria are used to group the carcinomas into distinct subtypes. The expression of neuroendocrine markers in conventional adenocarcinomas without a neuroendocrine carcinoma morphology was shown not to be biologically relevant [3]. Our aim of the study was to classify the colorectal cancer cohort according to the criteria of the current WHO classification [2] and, in a next step, to evaluate the molecular background and implications of the expression of the neuroendocrine marker synaptophysin.

## Methods

In this study, a cohort of 171 patients with colorectal carcinomas was analysed. The tumors were histomorphologically re-evaluated at the Institute of Pathology, University Hospital Schleswig-Holstein, Campus Kiel and subtyped according to the current WHO classification. Synaptophysin expression was determined in 150 cases by immunohistochemistry and evaluated semiquantitatively on a three-tiered scale 0-3 (0= none, 1= 1-9 %, 2=10-29 %, 3= 30-100 %).

## Results

The distribution of growth patterns of colorectal carcinomas represented the distribution according to the WHO classification: 74 % were carcinomas not otherwise specified (NOS), 9 % mucinous carcinomas, 3 % medullary carcinomas, 4 % adenoma-like carcinomas, 5 % serrated carcinomas, 3 % micropapillary carcinomas, 0.6 % signet-ring cell carcinomas and 2 % undifferentiated carcinomas. Synaptophysin expression was detected in 11 cases, mostly represented by few scattered cells. One NOS and one mucinous carcinoma showed 100 % synaptophysin expression.

## Conclusion

Synaptophysin expression occurs in 7 % of conventional colorectal carcinomas. The carcinomas do not show a neuroendocrine carcinoma morphology and therefore do not fulfill criteria of mixed neuroendocrine-non-neuroendocrine carcinomas. Clinical implications and underlying molecular mechanisms of synaptophysin expression need further investigation.

Literaturangaben:

[1] World Health Organization, (2023), Colorectal cancer, <https://www.who.int/news-room/fact-sheets/detail/colorectal-cancer>, 2023-12-12

[2] WHO Classification of Tumours Editorial Board, (2019), Digestive System Tumours, IARC, Lyon, 5th Edition ed.

[3] Konukiewicz B, Kasajima A, Schmitt M, Schwamborn K, Groll T, Schick Tanz F, et al., (2021), Neuroendocrine Differentiation in Conventional Colorectal Adenocarcinomas: Incidental Finding or Prognostic Biomarker?, *Cancers*, Basel, 13(20)

P14.01.07

## ***The role of the host: Stroma Areactive Invasion Front Areas (SARIFA) - concordance in double carcinoma of the colon and rectum.***

F. J. Farfán López<sup>1</sup>, A. Wiegering<sup>2</sup>, É. Sipos<sup>1</sup>, F. Sommer<sup>3</sup>, G. Schenkirsch<sup>4</sup>, B. Lohner<sup>1</sup>, B. Märkl<sup>1</sup>, A. Rosenwald<sup>5</sup>, F. Kurz<sup>5</sup>

<sup>1</sup>Pathology, Medical Faculty Augsburg, University Augsburg, Augsburg, Germany, <sup>2</sup>Department of General, Visceral, Transplant, Vascular and Pediatric Surgery, Würzburg University Hospital, Würzburg, Germany, <sup>3</sup>General, Visceral and Transplantation Surgery, University Augsburg, Augsburg, Germany, <sup>4</sup>Tumor Data Management, University Hospital Augsburg, Augsburg, Germany, <sup>5</sup>Institute of Pathology, University of Würzburg, Würzburg, Germany

## Background

The evaluation of tumour areas in direct contact with adipocytes has been proposed as a strong prognostic biomarker among others in colorectal cancers. It is simple to assess and can be performed on H&E histology. Genetics, as a mechanistic background for the occurrence of SARIFA, could be ruled by our recently published investigations. Therefore, we hypothesised that patient depended factors, like the individual's immune system might be responsible for the development of this phenomenon. If this is the case, double cancers in the same patient should show the identical SARIFA-status.

## Methods

We are currently assessing the tumour front in patients with either syn- or metachronous double carcinomas of the colon and rectum. In two academic medical centers, we identified retrospectively a total of 112 patients aged 21-85 years with more than one primary adenocarcinoma of the colon or rectum. The SARIFA status has been assessed on all available tumor slides by at least two experienced pathologists.

## Results

All tumours showed a histology of conventional adenocarcinoma or one of its subtypes. Tumour classification ranged from pT1 to pT4.

SARIFA-positivity on the basis of individual tumours was found in 75 out of 228 cancers (33 %) which is in the expected range. Concordant SARIFA-positivity or -negativity occurred in 17 (15%) and 54 (48%) patients, respectively.

Disconcordance, however, was found in 41 (37%) patients. In part, this discordance can be explained by widely differing pT stages of the tumours. Nevertheless, these discrepancies also occur in cases with identical pT stage.

### **Conclusion**

The first results of this ongoing study indicate that our hypothesis that SARIFA is driven by the sum of the patients' individual factors does not hold true. This situation, however, offers now the chance to analyse concordant and disconcordant tumors within the same individual. This appears to be a particular interesting approach to further investigate the tumour biology.

P14.01.08

### ***Morpho-proteomic analyses differentiate between crohn's disease and ulcerative colitis in routine diagnostic colon stage biopsies***

V. Hollfoth<sup>1</sup>, S. Mattern<sup>1</sup>, H. Reichle<sup>1</sup>, S. Fusco<sup>2</sup>, M. Franz-Wachtel<sup>3</sup>, N. Malek<sup>2</sup>, B. Macek<sup>3</sup>, S. Singer<sup>1</sup>

<sup>1</sup>Universitätsklinikum Tübingen, Institut für Pathologie, Tübingen, Germany, <sup>2</sup>Universitätsklinikum Tübingen, Innere Medizin I, Tübingen, Germany, <sup>3</sup>Universität Tübingen, Proteome Center Tübingen, Tübingen, Germany

### **Background**

Inflammatory bowel disease (IBD) presents as a chronic disease, typically with acute episodes of abdominal pain and diarrhea. Differentiation between the subtypes crohn's disease (CD) and ulcerative colitis (UC) is a frequent task in routine diagnostics, which can be challenging in a subset of cases. In this study, we aim to differentiate between colorectal manifestations of CD and UC with a morpho-proteomic approach.

### **Methods**

We analyzed and compared FFPE biopsy samples (stage biopsies) including CD (n=25), UC (n=23) as well as inconspicuous reference samples (n=18) by using a mass spectrometry-based proteomic approach (LC-MS/MS). With this approach we identified up to 5000 proteins.

### **Results**

Comparing the IBD samples to the inconspicuous references, we detected significant increase of calprotectin (consisting of S100A8 and S100A9) in samples with active inflammation. Comparing UC and CD samples (adapted to the severity of inflammation), we identified a discriminating protein signature. Included in this signature, we found STAT1, STAT3 and TAP1 higher abundant in CD, and CTSH in UC consistent with previous transcriptomic analyses. Enrichment analyses using the STRING- and Metascape databases suggest in CD patients high 'interferon signaling' (innate immune response) indicated by a switch from the constitutive proteasome to the immunoproteasome (upregulation of PSMB8, 9 and/or 10 and downregulation of PSMB5, 6 and/or 7). Applying our signature-based proteomic diagnostic approach to IBD cases discussed in the local molecular inflammatory board of the University Hospital Tuebingen, we could either confirm the respective diagnosis or clarify unclear or challenging cases.

### **Conclusion**

Morpho-proteomic analysis of FFPE colonic stage biopsies is a promising tool in IBD diagnostics, especially in CD/UC borderline cases. It will also contribute to a better understanding of the disease-specific underlying alterations as the basis for an improved molecularly guided therapy in personalized IBD medicine.

P14.01.09

### ***Proteomic Insights into Treatment Response in Crohn's Disease Patients***

J. Thiery<sup>1,2,3</sup>, M. Fahrner<sup>1</sup>, A. Fritsch<sup>4</sup>, F. Röttele<sup>4</sup>, P. Bronsert<sup>1</sup>, M. Werner<sup>1</sup>, P. Hasselblatt<sup>4</sup>, O. Schilling<sup>1</sup>

<sup>1</sup>Institute for Surgical Pathology, Medical Center, University of Freiburg, Freiburg, Germany, <sup>2</sup>German Cancer Consortium (DKTK), partner site Freiburg, Freiburg, Germany, <sup>3</sup>Faculty of Biology, University of Freiburg, Freiburg, Germany, <sup>4</sup>Clinic for Internal Medicine II, Gastroenterology, Hepatology, Endocrinology, and Infectious Diseases, Medical Center, University of Freiburg, Freiburg, Germany

### **Background**

Crohn's Disease (CD) represents a complex inflammatory bowel disease. Treatment response rates are approximately 40%. Predictive biomarkers are lacking. This study aims to elucidate the proteomic profile of CD patients undergoing

treatment, with the objective of predicting therapeutic outcomes.

## Methods

We analyzed 48 patient samples, comprising ileum biopsies collected either pre-therapy initiation or during treatment with anti-TNF or Ustekinumab. Treatment response was assessed via clinical and endoscopic criteria. Formalin-fixed, paraffin-embedded (FFPE) biopsies were subjected to robotic sample preparation, followed by liquid chromatography-mass spectrometry (LC-MS) analysis.

## Results

A diverse proteomic landscape, with an average identification of 6,700 proteins per sample was observed. Using clustering analyses, we successfully differentiated between inflammation and clinical remission states. Considering acute inflammation, a substantial upregulation of 2,100 proteins compared to remission states was noted. Among these upregulated proteins known inflammation markers, such as myeloperoxidase, lactotransferrin, fibrinogen, neutrophil elastase, metalloproteinases, and calprotectin, highlighted the inflammatory milieu characteristic of CD pathophysiology. Conversely, proteins involved in cellular respiration and metabolic processes were downregulated.

Notably, treatment interventions demonstrated a significant attenuation of inflammatory pathways in responders, characterized by a decreased intensity of inflammatory proteins. In contrast, non-responders exhibited minimal changes in proteomic composition after treatment, highlighting the heterogeneity in treatment response among CD patients. Gene Ontology enrichment analyses further elucidated the functional significance of treatment responses, revealing an upregulation of metabolic and cellular respiration processes post-successful treatment. These findings suggest a potential restoration of cellular homeostasis and metabolic balance following effective therapy.

## Conclusion

Integrating proteomic data with clinical parameters provides a comprehensive understanding of CD pathophysiology and treatment response. The next steps will focus on leveraging these findings to predict therapy response, thereby advancing personalized medicine approaches in CD management.

P14.01.10

## ***Mesenteries as a novel ex vivo co-culture model to study peritoneal metastasis***

K. Huebner<sup>1</sup>, L. Blind<sup>1</sup>, C. Lang-Schwarz<sup>2</sup>, S. Bootsma<sup>3</sup>, L. Vermeulen<sup>3</sup>, R. Palmisano<sup>4</sup>, A. Agaimy<sup>5</sup>, A. Hartmann<sup>5,6</sup>, R. Schneider-Stock<sup>1,6</sup>

<sup>1</sup>University Hospital, Friedrich-Alexander-University Erlangen-Nürnberg, Experimental Tumorpathology, Institute of Pathology, Erlangen, Germany, <sup>2</sup>Friedrich-Alexander-University Erlangen-Nuremberg, Institute of Pathology, Bayreuth, Germany, <sup>3</sup>Center for Experimental and Molecular Medicine, Amsterdam, The Netherlands, <sup>4</sup>Friedrich Alexander University Erlangen-Nürnberg, OICE, Erlangen, Germany, <sup>5</sup>University Hospital, Friedrich-Alexander-University Erlangen-Nürnberg, Institute of Pathology, Erlangen, Germany, <sup>6</sup>Comprehensive Cancer Center Erlangen-EMN (CCC ER-EMN), Erlangen, Germany

## Background

Peritoneal metastasis is the result of disseminating tumor cells originating predominantly from gynecological and gastrointestinal tumors, such as ovarian or colorectal cancer (CRC). In particular, tumor cell adhesion is mediated by the interaction of cancer cells with the mesothelial cell layer lining the peritoneal cavity. Although studies have shown the feasibility of culturing peritoneal tissues *ex vivo*, knowledge on the attachment and invasion of tumor cells and the genes involved in these processes is rare. Thus, our aim was to establish a novel *ex vivo* mesentery model to study peritoneal metastasis.

## Methods

Mesenteries of C57BL/6J mice (3-4 weeks age) were isolated, washed and placed onto a semi-porous membrane in a 6-well plate. Mesenteries were incubated in an air-liquid-interface (ALI) system for up to 48 h at 37°C and 5% CO<sub>2</sub> in a humidified atmosphere. Viability of mesenteries was determined by terminal deoxynucleotidyl transferase dUTP nick end labeling (TUNEL) and lactate dehydrogenase (LDH) assays. Spheroids from GFP-labelled CRC cell lines were generated in ultra-low attachment plates and transplanted onto freshly isolated mesenteries for up to 48 h. Mesentery integrity as well as tumor cell adhesion and invasion were evaluated by immunohistochemistry (IHC). For this, mesenteries were fixed in 4% PFA, paraffin embedded, sectioned and subjected for staining (HE, calretinin, Ki-67, GFP, pan-CK).

## Results

TUNEL and LDH assays revealed high viability of the mesenteric tissue after 48 h of *ex vivo* cultivation. Tissue integrity was further validated by HE staining and allowed to identify the key components of the mesentery, including mesothelial cell monolayer, adipocytes, fibroblasts, immune cells, and extracellular matrix. The presence of calretinin-positive cells further confirmed intact mesothelial cells. Attached and invading tumor cells were identified specifically by GFP IHC staining. By spinning disc confocal microscopy, we observed genotype-specific differences regarding the invasion pattern and capacity of transplanted tumor cells.

## Conclusion

We have successfully established a novel *ex vivo* mesentery model for tumor cell co-culture approaches. By using ALI culture, we maintained mesentery tissue viability and integrity over the course of the experiment. Our system constitutes an alternative approach to the frequently used *in vivo* peritoneal metastasis mouse models and contributes to the 3R principles as reduction and partial replacement.

P14.01.11

## ***Disseminated spread of a well-differentiated neuroendocrine tumor in the small bowel potentially associated with a HOXB13 G84E mutation***

L. Rentschler<sup>1,2</sup>, S. Dintner<sup>1,2</sup>, T. Wagner<sup>1,2</sup>, A. Mair<sup>2,3</sup>, T. Pfeiffer<sup>2,4</sup>, T. Pusch<sup>2,5</sup>, B. Märkl<sup>1,2</sup>

<sup>1</sup>Pathology, Medical Faculty, Augsburg, Germany, <sup>2</sup>Bavarian Cancer Research Center (BZKF), Augsburg, Germany, <sup>3</sup>General and Visceral Surgery, Medical Faculty, Augsburg, Germany, <sup>4</sup>Hematology and Oncology, Medical Faculty, Augsburg, Germany, <sup>5</sup>Cardiology and Endocrinology, Medical Faculty, Augsburg, Germany

## Background

Neuroendocrine tumors (NET) of the small bowel are known to sometimes occur as multifocal tumors but do not typically occur as part of a tumor predisposition syndrome. There is only a limited number of cases with extensive primary NET reported in the literature and none as extensive as presented here.

We present a rare case of a patient with more than 40 tumor nodules in the small bowel. These are potentially associated with an HOXB13 G84E mutation, which is linked with an elevated risk for prostate cancer and might be associated with other types of cancer in male individuals. [1]

## Methods

Routine work-up of a right hemicolectomy specimen including immunohistochemical staining (Chromogranin A, Synaptophysin, Ki-67, Serotonin, CDX2, SSTR2) and NGS-550 gene-panel analysis.

## Results

**CASE DESCRIPTION:** A male patient in his 60s presented for right hemicolectomy due to an endoscopically non-resectable adenoma of the ascending colon. Multiple smaller masses in the ileum as well as conspicuous mesenteric nodules were noticed intraoperatively and a 50-cm segment of the small bowel was resected.

Pathologic examination revealed more than 40 tumor nodules of a well-differentiated NET in the terminal ileum, measuring 0.5 to 2.5 cm each, as well as multiple lymph node metastases. Immunohistochemistry showed positivity for Chromogranin A, Synaptophysin, CDX2, Serotonin, SSTR2 and a proliferation index of 2%. Next generation sequencing revealed the potentially pathogenic HOXB13 mutation (G84E) in a suggestive allele frequency of 46%. Follow-up staging with DOTA-PETCT suggests an even more extensive disseminated tumor spread throughout the remaining small bowel.

## Conclusion

This is a very rare case of a multifocal neuroendocrine tumor of the small bowel with disseminated spread. The detection of a HOXB13 could be causally related. Further examinations of the next of kin could provide additional information after appropriate human genetic counseling.

Literaturangaben:

[1] Wei, J., Shi, Z., Na, R. et al., (2020), Germline HOXB13 G84E mutation carriers and risk to twenty common types of cancer: results from the UK Biobank, *British Journal of Cancer*, 1356–1359, 123, <https://pubmed.ncbi.nlm.nih.gov/32830201/>

P14.01.12

## ***Mass spectrometry imaging of a large cohort of rare intrahepatic cholangiocarcinoma deploying tissue micro arrays***

B. A. Barta<sup>1</sup>, A. Weber<sup>1</sup>, P. Hönscheid<sup>2</sup>, K. Kurowski<sup>1</sup>, M. Werner<sup>1</sup>, O. Schilling<sup>1</sup>, P. Bronsert<sup>1</sup>, M. C. Föll<sup>1</sup>

<sup>1</sup>Faculty of Medicine, University of Freiburg Medical Center, Institute of Surgical Pathology, Freiburg, Germany, <sup>2</sup>University Hospital Carl Gustav Carus at the Technische Universität, Institute of Pathology, Dresden, Germany

### **Background**

Intrahepatic cholangiocarcinoma (ICC) is a rare and aggressive type of cancer that originates from the bile ducts within the liver. It accounts for approximately 8-10% of all cholangiocarcinoma cases. It poses significant challenges in early detection and treatment due to its asymptomatic nature and aggressive behaviour. Understanding ICC at the spatio-molecular level could help unravel intratumor heterogeneity, which is crucial for developing effective diagnostic methods and therapies.

### **Methods**

Here, we present a spatially resolved mass-spectrometric analysis of a large ICC cohort of 70 patients with patient-matched malignant tumor and tumor-adjacent non-malignant tissue samples deploying tissue micro arrays (TMAs) with 409 cores. Employing a state-of-the-art matrix-assisted laser desorption/ionization coupled to time-of-flight mass spectrometry (MALDI TOF MS) allowed a high precision of the molecular distribution. Tryptic peptide imaging was performed to elucidate the spatial distribution of proteins. Data preprocessing was carried out using an automated workflow within the Galaxy framework. Hematoxylin and eosin (H&E) staining was conducted post measurement to visualize tissue morphology. H&E images were annotated to delineate tumor positive and healthy regions. To extract meaningful insights from the data, supervised machine learning algorithms were used.

### **Results**

The application of supervised partial least squares (PLS) and spatial shrunken centroids (SSC) algorithms succeeded in classifying tumor positive regions remarkably accurately (accuracy: 0.93, 0.84; sensitivity: 0.92, 0.86; specificity: 0.94, 0.83 for PLS and SSC respectively), demonstrating the efficacy of this approach in discerning distinct biomolecular patterns. In the comparison between tumor and tumor-adjacent liver tissue, a prominent peptide originating from collagen 1 emerged as the most discriminative feature. This finding highlights the robust presence of locally distributed extracellular matrix (ECM) components in ICC, indicative of its desmoplastic nature. Ultimately, we aim to provide a detailed characterization of the intratumor heterogeneity in our samples.

### **Conclusion**

This innovative approach may complement current diagnostic tools, and has the potential to guide therapeutic decisions based on the uncovered spatio-molecular characteristics of tumors.

P14.01.13

## ***Strawberry Notch 1 is essential in hepatocellular carcinoma and cholangiocarcinoma***

S. Roessler<sup>1</sup>, S. Fritzsche<sup>1</sup>, M. Le Marois<sup>1</sup>, K. Gür<sup>1</sup>, A. Fraas<sup>1</sup>, R. Sugiyanto<sup>1</sup>, T. Albrecht<sup>1</sup>, V. Da Silva Mourato Henriques<sup>1</sup>, C. Sticht<sup>2</sup>, C. De La Torre<sup>2</sup>, K. Breuhahn<sup>1</sup>, P. Schirmacher<sup>1</sup>, B. Goeppert<sup>1</sup>

<sup>1</sup>Institute of Pathology, Heidelberg, Germany, <sup>2</sup>Medical Research Centre, Mannheim, Germany

### **Background**

Aberrant Notch signaling has been identified as a possible catalyst for the development of hepatocellular carcinoma (HCC) and cholangiocarcinoma (CCA). Through genetic studies in *Drosophila*, it was observed that the knockout of strawberry notch (*sno*) mimics loss of Notch. Here, we elucidated the role of the mammalian Strawberry Notch 1 (SBNO1) in HCC and CCA development.

### **Methods**

HCC and CCA gene expression and proteomics datasets were analyzed for SBNO1 expression. Tissue microarrays were subjected to immunohistochemical staining for SBNO1 protein expression. In cell lines, SBNO1 was downregulated

using siRNA or sgRNA followed by cell viability, colony formation and migration assays and gene expression analysis. BioID was employed to identify interaction partners of SBNO1. Syngeneic mouse models using Hep55.1C cells and hydrodynamic tail vein injection (HDTV) were applied for in vivo study.

## Results

In HCC and CCA, SBNO1 protein but not mRNA was significantly increased. The localization of SBNO1 protein to the nucleus suggested its involvement in gene regulation. SBNO1-inhibition reduced cell viability, colony formation and migration and induced distinct expression patterns in HCC and CCA cell lines. However, BioID revealed that SBNO1 similarly modulates gene regulation in HCC and CCA by binding to general transcription factors TAF4 and TAF3. Deletion of *Sbno1* in Hep55.1C reduced tumor growth in vivo and inhibited liver tumor development in three different models of HCC and CCA using HDTV. Furthermore, *Sbno1*-deletion reduced biliary differentiation and angiogenesis in the tumor margin, underscoring the necessity of *Sbno1* in Notch-driven CCA formation.

## Conclusion

We identified SBNO1 as a new epigenetic driver required for HCC and iCCA tumor cell proliferation in vitro and in vivo.

# Poster Gastroenteropathologie II

P14.02.01

## ***Methylprednisolon-induced liver injury - a case series***

M. Wühr<sup>1</sup>, M. Ringelhan<sup>2</sup>, U. Ehmer<sup>2</sup>, C. Mogler<sup>1</sup>

<sup>1</sup>Institut für Allgemeine Pathologie und Pathologische Anatomie der TU München, München, Germany, <sup>2</sup>Klinikum Rechts der Isar der TU München, Klinik und Poliklinik für Innere Medizin II, München, Germany

## Background

Methylprednisolone-induced liver injury affects patients following high-dose pulse treatments with methylprednisolone. Patients suffering from autoimmune-mediated diseases, such as multiple sclerosis, are a risk group. Here we present a case series of 8 liver biopsies of patients with methylprednisolone-induced liver injury that were diagnosed at our department.

## Methods

We included 8 core needle liver biopsy samples that were examined between 2018 and 2023. 7 patients had a past medical history of either multiple sclerosis or acute disseminated encephalomyelitis, having received high dose pulse treatment with methylprednisolone within the last few weeks. All patients were biopsied following abnormal liver function tests without any apparent clinical cause. Routine liver biopsy stainings were performed after formalin fixation and paraffin embedding. Ancillary testing with immunohistochemistry and molecular pathology was done in select cases.

## Results

The severity of histopathologic liver injury in our cohort ranges from slight to severe. Biopsies from all patients showed a hepatitic injury pattern with single hepatocyte necrosis and mild to moderate inflammation of the portal tracts and acini with a predominance of lymphocytes. Viral infection was ruled out in all patients. A diagnosis of drug-induced liver injury was made in all cases.

## Conclusion

Methylprednisolone-induced liver injury is a rare but potentially underreported disease. The histopathologic liver injury pattern is consistent with drug-induced liver injury. The mechanism is still unclear. Previous studies suggest an immune reconstitution syndrome following prolonged immunosuppression in susceptible patients [1]. It seems likely that the association of liver injury with a strong immunosuppressant as causative drug might lead to misdiagnosis.

Literaturangaben:

[1] Allgeier J, Weber S, Todorova R, Neumann J, Gerbes A., (2022), Acute liver injury following methylprednisolone pulse therapy: 13 cases from a prospectively collected cohort., *Eur J Gastroenterol Hepatol*, doi: 10.1097/MEG.0000000000002334, 2024-02-12



P14.02.02

## ***Sister Mary Joseph nodule (SMJN): clinicopathological analysis in a cohort of ten patients.***

T. Hansen<sup>1</sup>, K. Schürheck<sup>2</sup>, U. Titze<sup>3</sup>, B. Schulz<sup>3</sup>, J. Kriegsmann<sup>1</sup>, W. Hiller<sup>2</sup>

<sup>1</sup>MVZH ZMD Trier GmbH, Trier, Germany, <sup>2</sup>Klinikum Lippe GmbH, Klinik für Allgemein- und Viszeralchirurgie, Detmold, Germany,

<sup>3</sup>Klinikum Lippe GmbH, Institut für Pathologie, Detmold, Germany

### **Background**

According to the literature, umbilical metastases (also called SMJN) still present a challenging diagnosis. Despite a growing number of case studies [1][2], a thorough clinicopathological analysis is restricted to a small number of larger cohorts. In addition, the origin as well as the pathogenesis and the biological behavior of this tumor are still a matter of debate. We therefore examined a cohort of ten patients with a SMJN diagnosis.

### **Methods**

From the archival records (Inst. f. Pathology Detmold) between January 2004 and December 2021, we found ten patients with SMJN (M = 5, F = 5, mean age: 65.2 yrs, range: 43 – 90 yrs). We conducted routine histological and immunohistochemical studies according to standard protocols. All cases were examined for the expression of podoplanin [clone D2-40, Agilent] and CD31 [clone JC70A, Agilent] in order to detect lymphangiosis and/or haemangiosis carcinomatosa respectively. Moreover, we performed next-generation sequencing (NGS) applying the Ion Torrent system [ThermoFisher]. Follow-up information was available in all patients (duration time 1 – 60 months). At the end of follow-up (31 December 2021), six patients have been deceased. Overall survival (OS) was defined as the interval between the date of metastasis until the date of death.

### **Results**

Pancreatic adenocarcinoma was mostly diagnosed (n=4), followed by ovarian carcinoma (n=2). Performing further clinical and radiological examinations, we interpreted seven cases as a result of a local or disseminated peritoneal carcinosis. In 6 cases, we found lymphangiosis carcinomatosa, while there was only one patient with haemangioinvasion. In accordance to the various primary neoplasms, different mutations were revealed by NGS with KRAS Exon 2 mutations in the majority of patients (n=4), comprising all patients with pancreatic adenocarcinoma. Mean OS was 6.5 months.

### **Conclusion**

SMJN is mainly caused by intraabdominal tumors. The biological behavior and survival is dependent on origin of the primary neoplasm. Considering that the umbilical lymphatic vasculature typically is beyond the classical drainage of these intraabdominal tumors and reflecting our results, SMJN is suggested to be primarily caused by either local or disseminated peritoneal carcinosis. Lymphangioinvasion is therefore interpreted as secondary phenomenon.

Literaturangaben:

[1] Chalya PL, et al., (2013), Sister Mary Joseph's nodule at a university teaching hospital in northwestern Tanzania: a retrospective review of 34 cases, *World J Surg Oncol*, doi 10.1186/1477-7819-11-151, 2024-02-03

[2] Hugen N, et al., (2021), Umbilical metastases: real-world data shows abysmal outcome, *Int J Cancer*, 149:1266, 2024-02-04

P14.02.03

## ***Investigating the significance of CEACAM6 in GBC and clinical relevance***

C. Metzger, R. N. Sugiyanto, A. Inal, T. Albrecht, A. Charbel, P. Schirmacher, B. Goeppert, S. Roessler

Institute of Pathology, University Hospital Heidelberg, Heidelberg, Germany

### **Background**

Gallbladder cancer (GBC) is the most common carcinoma of the biliary tract characterized by late diagnosis and poor outcome. The glycoproteins carcinoembryonic cell adhesion molecule 5 (CEACAM5) and CEACAM6 play a role in cell adhesion, differentiation and cell growth. High expression of CEACAM5/6 has been associated with oncogenic characteristics like invasiveness, metastasis and overall poor survival in different cancer types. In GBC, the functions of CEACAM5 and CEACAM6 are still unknown.

## Methods

Overexpression and knockdown were used to study CEACAM6 protein function in GBC cell lines. To demonstrate the different expression patterns of targeted proteins, a TMA consisting of >500 paraffin embedded GBC tissues was used. TMA slides were stained utilizing specific antibodies for CEACAM5 and CEACAM6. The expression pattern was compared to non-neoplastic gallbladder tissue. Upon different expression gradients, an IRS score was created, which included the multiplication of intensity (0-3) of the staining pattern and percentage of positive stained cells with 1 point (pt) for <25%, 2pts for 26-50%, 3pts for 51-75%, and 4pts for >75%.

## Results

CEACAM6 promoted migration and invasion but reduced cell adhesion and colony formation in GBC cell lines. The knockdown of CEACAM5 comparably reduced GBC cell migration suggesting that both proteins function similarly. The immunohistochemical staining revealed that both CEACAM5 and CEACAM6 localized to the cytoplasm and membrane in normal gallbladder and GBC tissue samples. CEACAM5 showed strong, intermediate, absent expression in 54.5%, 18.2% and 27.3% of non-neoplastic gallbladder epithelium. Likewise, GBC exhibited strong expression in 48.9%, intermediate expression in 33.3% and absence in 17.8% of samples. In contrast, CEACAM6 was strongly positive in 35.9%, intermediate positive in 48.4% and undetectable in 15.7% of non-neoplastic gallbladder tissues, whereas 45.8% of GBC had high expression, 33.1% intermediate and 21.2% no expression of CAEACM6. Thus, a subset of patients with GBC showed overexpression of CEACAM6.

## Conclusion

Enhanced expression of CEACAM6 in GBC endorsed the oncogenic function observed in GBC cell lines.

P14.02.04

## ***Pathogenetic, Prognostic, and Therapeutic Role of Fucosylation in Intrahepatic Cholangiocarcinoma***

C. E. Ament

Institute of Pathology, University of Regensburg, Regensburg, Germany

## Background

Aberrant protein glycosylation is a cancer hallmark, associated with tumor development and progression. In the present dissertation, I thoroughly investigated the role of fucosylation (a type of glycosylation) in intrahepatic cholangiocarcinoma (iCCA), a lethal malignancy with increasing incidence worldwide and limited therapeutic options.

## Methods

Global protein fucosylation was determined using lectin histochemistry and Western blotting. The GDP-L-fucose synthetase (FX) and the GDP-fucose transmembrane transporter (SLC35C1), both prominent players of cellular fucosylation, were silenced via small interfering RNA. iCCA cell lines were treated with L-Fucose and 6-Alkynylfucose (6AF), a fucosylation inhibitor. In these cells, the fucosylation effect on the NOTCH and NF- $\kappa$ B pathway, two predominant cascades in cholangiocarcinogenesis and fucosylation targets, as well as the effect on proliferation and migration was investigated. Moreover, iCCA cell lines were treated with 6AF and used in the chick chorioallantoic membrane (CAM) assay.

## Results

I discovered that the levels of global fucosylation and members of the fucosylation pathway are ubiquitously upregulated in human iCCA tissues compared to non-tumorous surrounding livers and normal biliary cells. In addition, total fucosylation levels correlate with poor patients' prognosis. Furthermore, the fucosylation inhibitor 6-alkynylfucose (6AF) triggered a dose-dependent decrease in the proliferation and migration of iCCA cell lines that were annulled by adding fucose to the cell medium. At the molecular level, 6AF administration or small interfering RNA-mediated silencing of GDP-L-fucose synthetase (FX) and the GDP-fucose transmembrane transporter (SLC35C1), both pivotal players of cellular fucosylation, decreased NOTCH activity, NOTCH1/Jagged1 interaction, NOTCH receptors, and related target genes in iCCA cell lines. In the same cells, EGFR, NF- $\kappa$ B p65, and Bcl-xL protein levels diminished, whereas I $\kappa$ B $\alpha$  (a critical cellular NF- $\kappa$ B inhibitor) increased after FX/SLC35C1 knockdown or 6AF administration. In the CAM assay, 6AF

treatment profoundly suppressed the growth of iCCA cells.

### Conclusion

In conclusion, elevated global fucosylation characterizes human iCCA, contributing to cell growth and migration via the upregulation of the NOTCH and EGFR/NF- $\kappa$ B pathways. Thus, aberrant fucosylation is a novel pathogenetic player and a potential therapeutic target for human iCCA.

P14.02.05

### ***Analysis of neoplastic steatogenesis in hepatocellular neoplasia in relation to Wnt/CTNNB1 status***

R. S. Hofmann<sup>1</sup>, H. R. Witzel<sup>1</sup>, D. A. Ridder<sup>2</sup>, M. Schindeldecker<sup>1</sup>, D. S. Duret<sup>1</sup>, A. Weinmann<sup>3</sup>, W. Roth<sup>1</sup>, B. K. Straub<sup>1</sup>

<sup>1</sup>Institute of Pathology, University Medicine, Mainz, Germany, <sup>2</sup>Institute of Pathology, Ludwigshafen, Germany, <sup>3</sup>1st Medical Clinic, University Medicine, Mainz, Germany

### Background

Carcinogenesis is triggered by molecular genetic alterations, resulting in pathological activation of signaling pathways and aberrant gene expression patterns, which determine tumor biology and impact on morphology. Alterations in the Wnt-signaling cascade play a major role in the development of hepatocellular carcinoma (HCC), subtypes of hepatocellular adenoma (HCA), hepatoblastoma and are discussed to be altered in focal nodular hyperplasia (FNH). About 30 % of HCC harbour a mutation in the *CTNNB1* gene, which encodes  $\beta$ -catenin, a crucial factor in the Wnt-signaling pathway. In previous work, we could show that chronic liver diseases due to alcohol, metabolic syndrome or hepatitis C, but also liver tumors are frequently characterized by an accumulation of lipid droplets (LD) and display different patterns of expression of respective LD-associated proteins of the perilipin-family. While perilipin 2 is widely expressed in normal liver and liver tumors, perilipin 1 is restricted to hepatocytes of zone 3 in normal liver, the zone in which the Wnt-signaling cascade is activated, and is also detected in *CTNNB1*-mutated HCA.

### Methods

We therefore started to analyse neoplastic steatogenesis and perilipin-expression with regard to the *Wnt/CTNNB1*-status in two different hepatocellular cell lines, Huh7 and HepG2, as well as in well characterized clinico-pathologic collectives of 50 HCAs and 870 HCCs of 574 patients *in situ*. In addition, tissue slice cultures of vital human liver were analysed, a model system that reflects the different cell types of the tissue.

### Results

Using immunohistochemistry in HCA and HCC, expression of the Wnt-target glutamine synthetase correlated with the expression of perilipin 1 ( $p < 0.001$ ), but not perilipin 2 *in situ*, although only minimal microvesicular steatosis was observed in these cases. Patients with HCCs with high perilipin 1- and low perilipin 2-expression displayed a more favourable outcome. To functionally validate these results in cell culture, the Wnt-pathway was induced by chemical inhibition of glycogen synthase kinase 3 $\beta$  (lithium chloride, CHIR99021, BIO) and showed induction of the known Wnt-downstream target genes *AXIN2*, *MYC* and *LEF1*. In addition, quantitative real-time PCR analysis further showed an increase in *PLIN1* and a decrease in *PLIN5* upon Wnt-induction.

### Conclusion

Our data suggest that Wnt-signaling plays a crucial role in the regulation of perilipin 1 in liver steatogenesis and may even impact on prognosis in HCCs.

P14.02.06

### ***Three-Dimensional and Molecular Characterization of the Human Ductular Reaction in Liver Cirrhosis***

C. Ganter<sup>1</sup>, L. Hagemann<sup>1</sup>, D. Beckmann<sup>2</sup>, D. van de Loo<sup>3</sup>, F. Kiefer<sup>1</sup>, S. Bobe<sup>1,4</sup>

<sup>1</sup>University of Münster, European Institute for Molecular Imaging, Münster, Germany, <sup>2</sup>University of Münster, Institute for Geoinformatics, Münster, Germany, <sup>3</sup>University Hospital Münster, Department of Internal Medicine B, Münster, Germany, <sup>4</sup>Gerhard-Domagk-Institute of Pathology, University Hospital Muenster, Münster, Germany

## Background

Inflammatory processes in the liver are often accompanied by bile ductular proliferation known as ductular reaction (DR). Although considered a general principal of disease, different patterns of DR can be recognized in liver histology but have not been of any specific diagnostic value so far. As cirrhotic end stage liver disease hardly allows to unambiguously trace back the underlying disease, a diagnostic blind spot is faced in cryptogenic cirrhosis. In this project, we investigated the DR's three-dimensional architecture and microenvironment in Alcoholic and Non-Alcoholic Liver Disease (ALD & NALD) to evaluate its diagnostic potential.

## Methods

A cohort of explanted liver specimens obtained from patients undergoing transplantation due to NALD or ALD was examined. Healthy liver tissue of surgical specimens served as controls. Light sheet fluorescence microscopy was performed on FFPE samples for morphological analysis of the 3D bile ductular structure and computational analysis was implemented towards volumetric rendering and quantification. Further, a multi-marker staining on thin sections allowed a molecular characterization investigating the DR microenvironment.

## Results

Light sheet fluorescence microscopy revealed three structural patterns of the biliary tree, which were distinctive for the three subgroups - healthy control, ALD and NALD. The immunostaining indicated a correlation between the extend of DR and the severeness of the disease (MELD score) as well as the stage of fibrosis.

## Conclusion

To our knowledge, this study for the first time used light sheet fluorescence microscopy on immunostained FFPE tissue. With the structural 3D analysis as well as the evaluation of multi-marker stainings our work revealed that cirrhotic ALD and NALD livers in a small cohort of explanted livers show morphological differences in the DR, which were inconspicuous in routine histology, hinting at diagnostic potential for the volumetric analysis of DR.

P14.02.07

## ***An often-unrecognized side effect in dialysis patients and its histological detection using a special stain.***

J. Schläiß, S. Weingardt-Kocher, S. E. Weißinger

Institute of Pathology, Alb Fils Kliniken GmbH, Göppingen, Germany

## Background

Around 80.000 patients currently require dialysis in Germany. Lanthanum carbonate (LC) (Fosrenol®) is a safe and well tolerated drug to treat hyperphosphatemia in dialysis patients. Small amounts of absorbed lanthanum are known to deposit in liver and bones but do not cause organ damage[1]. However, lanthanum deposition in the stomach and duodenum can cause endoscopically detectable white lesions in the mucosa, ranging histologically from just white mucosa with deposited material, generally phagocytosed by macrophages in the lamina propria, up to ulceration and regenerative changes[2]. Since the morphological description of lanthanum pathology is variably described and medication information is not always available, direct detection of lanthanum deposits could confirm the diagnosis of lanthanum gastroenteropathy.

## Methods

We searched our archive for lanthanum gastroenteropathies within the last 3 years. A protocol for visualization of lanthanum deposits in tissue was modified and established. In a buffered, weakly acidic solution, fluoride ions react with alizarin complexone and lanthanum to form a violet complex (alizarin complexone stain)[3]. Histomorphology was evaluated on H&E, PAS and alizarin complexone stains. Clinical data was retrospectively analyzed in relation to any dialysis treatment and medication.

## Results

Archival searches revealed 11 patients. Female to male ratio was 2:9, median age was 76 years and the biopsies were from stomach (n=10) and/or duodenum (n=3). Histology varied from deposits only to granulomatous inflammation and severe intestinal metaplasia. LC medication information was previously provided in none of the patients. With the alizarin

complexone staining method 8/9 biopsies could confirm the diagnosis of lanthanum gastroenteropathy. In 10/11 patients previous histologically diagnosed lanthanum gastroenteropathy could retrospectively be confirmed by clinical data.

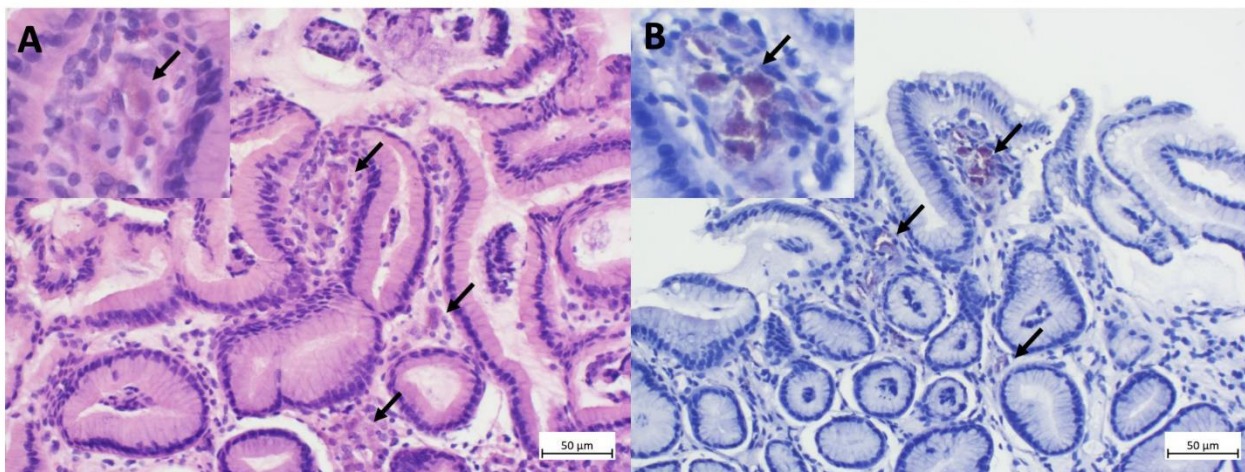


Figure 1. Gastric antrum biopsy with lanthanum deposits (arrows) in macrophages within the lamina propria. (A) H&E stain. Insert shows 40x magnification. (B) Alizarin complexone stain visualizing lanthanum. Insert shows 40x magnification.

### Conclusion

Alizarin complexone stain for the detection of lanthanum in gastroduodenal biopsies of dialysis patients is a reliable method to confirm the diagnosis of lanthanum gastroenteropathy, even if clinical data is missing or histomorphology is discrete.

### Literaturangaben:

- [1] Spasovski, G.B.; Sikole, A.; Gelev, S.; Masin-Spasovska, J.; Freemont, T.; Webster, I.; Gill, M.; Jones, C.; De Broe, M.E.; D'Haese, P.C., (2006), Evolution of Bone and Plasma Concentration of Lanthanum in Dialysis Patients before, during 1 Year of Treatment with Lanthanum Carbonate and after 2 Years of Follow-Up., *Nephrol Dial Transplant*
- [2] Nakamura, T.; Tsuchiya, A.; Kobayashi, M.; Naito, M.; Terai, S., (2019), M2-Polarized Macrophages Relate the Clearance of Gastric Lanthanum Deposition., *Clin Case Rep*
- [3] Miyagawa, M., (2007), Alizarin Complexone Stain for Histochemical Localization of Lanthanum., *Biomedical Research on Trace Elements*

P14.02.08

## ***Expression of fibroblast activation protein (FAP) in neuroendocrine tumours of ileum and lung***

M. Wessels, F. Kellers, V. Stoll, C. Röcken, B. Konukiewitz

Institut für Pathologie, Universitätsklinikum Schleswig-Holstein, Campus Kiel, Kiel, Germany

### Background

Fibroblast activation protein (FAP) can be found in cancer-associated fibroblasts and could be a promising target for diagnostics and therapy of solid tumors. We examined the protein in stromal and tumoural tissue of neuroendocrine tumours (NET) of the lung, as well as in NET of the ileum.

### Methods

The neoplasms were classified according to the current WHO classification. Measurement of FAP expression was performed on a group of NET of the ileum and the lung, of which 19 ileal and 21 lung NET were eligible for immunohistochemical analysis. FAP staining abundance and intensity was examined on tumour sections via semiquantitative analysis in tumour cells as well as in stromal cells. The results were confirmed by digital image analysis with QuPath [1].

### Results

In the semiquantitative analysis, FAP-positive tumour cells were found in 9 out of 21 lung NET cases (43 %), in 8 cases

with staining in singular cells (< 5 %) and in 1 case with focal spreading throughout the section (> 5 %). In the analysis of ileal NET, FAP positivity was detected in none of the tumour cells.

The semiquantitative analysis of the stromal cells of the tumours showed a positive staining in cases of both the lung and ileal NET. The NET of the ileum had positive stromal staining in 12 of 19 cases (63 %), 2 with focal positivity in 1-10 % cells (17 %), 9 with focal positivity in 10-50 % of cells (75 %) and 1 with focal positivity for FAP in over 50 % of stromal cells (8 %). 7 cases did not show FAP positivity (37 %). The NET of the lung showed a stromal staining in all 21 cases (100 %), in 3 cases with a focal (1-10 % of cells, 14 %), in 6 cases with an intermediate (10-50 % of the cells, 29 %) and in 12 cases with a strong positivity (more than 50 % of the cells, 57 %).

## Conclusion

FAP is expressed in NET of ileum and lung. The semiquantitative analysis showed a tendency of higher FAP expression in tumor-associated stromal cells than in tumor cells. FAP expression in NET offers diagnostic and therapeutic options and potential for further investigations.

Literaturangaben:

[1] Bankhead P, Loughrey MB, Fernandez JA et al. (2017) QuPath: Open source software for digital pathology image analysis. Sci Rep 7:16878

P14.02.09

## ***Characterization of neuroendocrine differentiation in conventional pancreatic ductal adenocarcinomas***

A. Kraus, F. Kellers, V. Stoll, C. Röcken, B. Konukiewitz

Department of Pathology, University Medical Center Schleswig-Holstein, Campus Kiel, Kiel, Germany

### Background

Pancreatic ductal adenocarcinomas (PDAC) are classified according to histological criteria [1][2]. The expression of the neuroendocrine marker synaptophysin has already been analyzed in conventional adenocarcinomas of the colorectum and was shown not to be biologically relevant when not associated with a true neuroendocrine carcinoma histology, in contrast to "true" mixed adenoneuroendocrine carcinomas, which harbor a dismal prognosis [3]. In this study, we investigated the expression of neuroendocrine markers in PDAC without histological characteristics of a neuroendocrine carcinoma.

### Methods

We analysed a cohort of n=58 PDAC patients who underwent complete resection at the University Medical Center Schleswig-Holstein, Campus Kiel. All cases were re-evaluated histologically, subtyped and forwarded to immunohistochemical (IHC) staining using antibodies directed against synaptophysin. Immunostaining for synaptophysin was analysed semiquantitatively. Selected cases were additionally immunostained for insulin, glucagon, PP, INSM1, SSTR2 and CGA. IHC double-staining for synaptophysin and Ki-67 was performed in selected cases.

### Results

Our cohort was predominantly composed of conventional adenocarcinomas (48/58), followed by 4 clear cell carcinomas, 3 cribriform carcinomas, 2 adenosquamous carcinoma and 1 colloid carcinoma. Occasionally, in about 10% of the cases, neuroendocrine cells were present in small clusters in close association to neoplastic glands. These cells stained with physiological pancreatic hormones, but did not always represent the exact hormone distribution profile as in normal islet tissue. Double staining showed that synaptophysin-positive cells did not correlate with higher proliferation, making them unlikely to be of neoplastic origin. There was no association in the occurrence of these neuroendocrine cells to a specific PDAC-subtype. No carcinoma expressed synaptophysin in tumor cells.

### Conclusion

Synaptophysin expression, as seen in conventional adenocarcinomas of colorectal origin, seems not to occur in PDAC. Scattered neuroendocrine cell rather represent residual Islets of Langerhans.

Literaturangaben:

- [1] Board WCoTE, (2019), WHO classification of tumours of the digestive system, IARC, Lyon
- [2] Schlitter A., Segler A., Steiger K. et al, (2017), Molecular, morphological and survival analysis of 177 resected pancreatic ductal adenocarcinomas (PDACs): Identification of prognostic subtypes, Scientific reports, 41064, 7
- [3] Konukiewitz B, Kasajima A, Schmitt M, Schwamborn K, Groll T, Schick Tanz F, et al, (2021), Neuroendocrine Differentiation in Conventional Colorectal Adenocarcinomas: Incidental Finding or Prognostic Biomarker?, Cancers, Basel, 5111, 13(20)

P14.02.10

### ***Improved survival of mouse colon precision cut tissue slices (cPCTS) using Air liquid cultivation***

D. Thalheim<sup>1</sup>, P. Kunze<sup>1</sup>, J. Prochazka<sup>2</sup>, A. Hartmann<sup>3,4</sup>, R. Nagy<sup>5</sup>, R. Tietze<sup>6</sup>, R. Schneider-Stock<sup>1,4</sup>

<sup>1</sup>University Hospital, Friedrich-Alexander-University Erlangen-Nürnberg, Experimental Tumorpathology, Institute of Pathology, Erlangen, Germany, <sup>2</sup>Czech Center for Phenogenomics, Institute of Molecular Genetics of the ASCR, Prague, Czech Republic, <sup>3</sup>University Hospital, Friedrich-Alexander-University Erlangen-Nürnberg, Institute of Pathology, Erlangen, Germany, <sup>4</sup>Comprehensive Cancer Center Erlangen-EMN (CCC ER-EMN), Erlangen, Germany, <sup>5</sup>Friedrich-Alexander-University Erlangen-Nürnberg, Institute of Applied Quantum Technologies (AQuT.), Erlangen, Germany, <sup>6</sup>University Hospital, Friedrich-Alexander-University Erlangen-Nürnberg, Department of Otorhinolaryngology, Head & Neck Surgery, Section of Experimental Oncology & Na-nomedicine (SEON), Erlangen, Germany

#### **Background**

Mouse colon precision cut tissue slices (cPCTS) can be used for a variety of different research topics such as physiology, toxicology or even immunology. They have an intact three-dimensional structure with the physiological cell composition and intact metabolic and immunological functions. In addition, a large number of cPCTS can be produced from a single organ, thus fulfilling the 3R principles in terms of reducing the number of animals. Since long-term cultivation is still difficult, we aimed to improve various culture conditions.

#### **Methods**

In contrast to the current standard cultivation of cPCTS floating in medium with 80 % O<sub>2</sub>, we have established an air-liquid (ALI) cultivation procedure of cPCTS. In ALI cultivation, the cPCTS lie on a semi-permeable insert membrane, so medium is only present on the bottom side of the insert, while on the top side the cPCTS have direct contact with ambient air. In the first part of our study we investigated the relevance of growth factors supplemented to the medium, in the second part the oxygen content of the ambient air was changed. Survival of cPCTS was assessed by lactate dehydrogenase (LDH) assay, qPCRs of various cell type-specific and immunological marker genes and immunohistochemical staining on fixed cPCTS.

#### **Results**

The addition of growth factors to the medium did not lead to any improvement in cell integrity. In contrast, a significant improvement in stem cell and proliferation markers was achieved with cultivation at 21 % oxygen instead of the currently usual 80 %, even over a period of 120 h. Intact stem cell compartment over time was confirmed in Lgr5-GFP mice.

#### **Conclusion**

The ALI cultivation simplifies handling when changing medium and allows for long-term microscopy, since the cPCTS lie stable on the insert membrane and do not move out of the microscopy focus. The addition of expensive growth factors seems to be not necessary.

P14.02.11

### ***Invasive Fungal Disease in Chronic Liver Transplant Failure – an Underestimated Burden***

K. Hofmann<sup>1,2</sup>, A. V. Puzalkova<sup>2</sup>, T. Pfeffer<sup>1,2</sup>, I. M. Klein<sup>1,2</sup>, A. Mehrabi<sup>3</sup>, U. Merle<sup>4</sup>, R. Penzel<sup>2</sup>, A. Stenzinger<sup>2</sup>, C. Flechtenmacher<sup>2</sup>, P. Schirmacher<sup>1,2</sup>

<sup>1</sup>Tissue Bank of the German Center for Infection Research (DZIF), Institute of Pathology, Heidelberg University Hospital, Heidelberg, Germany, <sup>2</sup>Institute of Pathology, Heidelberg University Hospital, Heidelberg, Germany, <sup>3</sup>Department of General, Visceral and Transplantation Surgery, Heidelberg University Hospital, Heidelberg, Germany, <sup>4</sup>Department of Gastroenterology, Infectious Diseases and Intoxication, Heidelberg University Hospital, Heidelberg, Germany

## Background

Invasive fungal infection (IFI) is a significant complication in solid organ transplant patients and a diagnostic challenge. To elucidate occurrence and significance of IFI in chronic liver transplant failure, a comprehensive retrospective histo- and molecular pathological analysis was performed at the Institute of Pathology Heidelberg in collaboration with the accredited Tissue Bank of the German Center for Infection Research (DZIF).

## Methods

FFPE tissue samples and pathological findings from all explanted liver transplants due to chronic transplant failure from the liver transplant database of Heidelberg University Hospital (1991-2021,  $\geq 90$ -day graft survival) were reexamined. Additional staining with periodic acid-Schiff and Grocott methenamine silver was used in the light-microscopic investigations to uncover occurrence, severity, and associated conditions of IFI. Molecular fungal species identification was performed chip-based by DNA hybridization.

## Results

Light-microscopic examination revealed fungal infection in 43 (28.5%) of the 151 analyzed cases with 2/3 being newly specified. Female patients presented a slightly higher risk for IFI. Typically the large bile ducts were affected, accompanied by acute inflammation with frequent abscess and concrement formation (78.1%). In 37 cases, molecular identification of the fungal species was achieved. *Candida albicans* was the most common species (70%) with mixed infections in 24% of cases.

## Conclusion

This data show the underestimated prevalence and high diagnostic and clinical relevance of IFI in chronic liver transplant failure and highlights the diagnostic challenges and needs. The contribution of structured registries and qualified biobanking is evident in such retrospective (but also prospective) studies and improves the diagnostic approach and development of adequate therapeutic strategies.

P14.02.12

## ***Multimodal and site-specific differentiation dynamics of type 2 conventional dendritic cells in liver damage and cholestasis***

S. Thomann<sup>1</sup>, A. Agrawal<sup>1</sup>, H. Hemmer<sup>1</sup>, S. Sagar<sup>2</sup>, P. Kießling<sup>3</sup>, E. Scheidereit<sup>3</sup>, T. Poth<sup>4</sup>, M. Tóth<sup>5</sup>, K. Breitkopf-Heinlein<sup>6</sup>, N. Rahbari<sup>7</sup>, C. Kuppe<sup>3</sup>, D. Grün<sup>1</sup>

<sup>1</sup>University of Würzburg, Institute of Systems Immunology, Würzburg, Germany, <sup>2</sup>University Hospital Freiburg, Department of Gastroenterology, Hepatology, Endocrinology and Infectious Diseases, Freiburg, Germany, <sup>3</sup>University Hospital Aachen, Department of Nephrology and Clinical Immunology, Aachen, Germany, <sup>4</sup>University Hospital Heidelberg, Center for Model System and Comparative Pathology, Heidelberg, Germany, <sup>5</sup>University Hospital Heidelberg, Institute of Pathology, Heidelberg, Germany, <sup>6</sup>Medical Faculty Mannheim, Department of Surgery, Mannheim, Germany, <sup>7</sup>University Hospital Ulm, Department of Surgery, Ulm, Germany

## Background

Biliary-niche residing conventional dendritic cells (cDCs) regulate T cell responses and may contribute to disease pathogenesis in auto-immune related liver diseases. In cholangitis, cDCs may act as disease initiators of a dysfunctional and self-perpetuating immunologic response, however the dynamics and spatiotemporal properties of cDCs remain largely unexplored.

## Methods

Time-point specific single cell RNA-sequencing (scRNA-seq) was performed on a mouse model of 3,5-diethoxycarbonyl-1,4-dihydrocollidine (DDC)-induced cholangitis. Cell state-specific transition probabilities and transcription factor regulon activity were predicted using VarID2 and SCENIC. Multimodal scRNA/scATAC-seq was used to measure genomic accessibility. Combined indexing of transcriptomes and epitopes was used to subtype immune cells in liver-draining lymph nodes (LN). Functional validation was performed using an inducible mouse model of cDC2-depletion and Il17a- and Tcrd-knockout mice.

## Results

Disease onset was characterized by an induction of a Sox9<sup>+</sup> cholangiocyte-derived Nfkb2-regulated gene expression



programme including Macrophage colony-stimulating factor 1 (Csf1) and CC-chemokine ligand 2 (Ccl2). Early onset cholestasis was associated with a change of frequency towards cDC2 abundance and the recruitment of immature and epigenetically restricted preDCs, while mature cDC2 egressed into draining LN. In liver, cDC2-specific disease trajectories were linked with positive regulation of a T17 immune response and both conventional and unconventional T cell subsets were found to be Interleukin 17-producers. Cholangitis resolution was associated with an incomplete restoration of the cDC2 cell state and T17 polarization was attenuated by cDC2-depletion *in vivo*.

## Conclusion

DDC-induced cholangitis is associated with a multicellular crosstalk at the biliary niche, which results in the recruitment of epigenetically restricted cDC2, while draining LNs harbour mature cDC2 to induce site-specific T cell responses.

P14.02.13

## ***STAT1 and STAT3 are associated with increased Inflammation in Hepatocellular Carcinoma***

J. Schreck<sup>1,2</sup>, C. Ploeger<sup>1</sup>, T. Albrecht<sup>1,2</sup>, A. Charbel<sup>1,2</sup>, P. Schirmacher<sup>1,2</sup>, B. Goeppert<sup>3</sup>, S. Roessler<sup>1,2</sup>

<sup>1</sup>Pathologisches Institut Universitätsklinikum Heidelberg, Allgemeine Pathologie, Heidelberg, Germany, <sup>2</sup>Liver Cancer Center Heidelberg (LCCCH), Heidelberg, Germany, <sup>3</sup>RKH Klinikum Ludwigsburg, Institut für Pathologie und Neuropathologie, Ludwigsburg, Germany

## Background

Constant activation of IL6-signaling is associated with HCC tumorigenesis. The regulatory function of IL6-signaling is mediated by STAT3, which can be inhibited by SH2D4A by retaining STAT3 dimers in the cytoplasm [1]. In Addition, STAT3 and STAT1 show a divergent functionality in HCC tumorigenesis [2]. Our aim was to find a possible association between STAT1 and STAT3 expression and tumoral immune cells.

## Methods

A Tissue microarray consisting of 127 HCC samples taken from the University hospital Heidelberg was constructed. Sections were stained with antibodies against STAT1, STAT3, CD3, CD4, CD8, CD20, CD68, CD117, FOXP3 and PD-L1. STAT1 and STAT3 were scored using immunoreactivity score. Immune cells were already counted before [2][3]. PD-L1 was scored in tumor cells using TP- and CP-Scores. Paired Spearman correlation coefficients were calculated.

## Results

STAT1 expression in tumor cells and STAT1 positive immune cells showed a strong correlation with infiltrating T-cells. STAT3 expression in tumor cells was moderately correlated with CD4 and FOXP3 positive immune cells. STAT1 expression in tumor and immune cells showed a strong correlation with PD-L1 Scores in tumor cells, with T-Cells and a bit weaker for B-Cells. Absolute T- and B-cell counts as well as macrophages were significantly increased around tumors with high PD-L1 expression (TPS). This effect was also detectable in STAT1 but not in STAT3 positive immune cells. Tumors with a high STAT3 expression showed a significantly increased infiltration by T-cells. When looking at the peritumoral immune cells, those tumors with a high level of STAT3 expressing immune cells had significantly more infiltrating T- and B-cells. Tumor cells with a high nuclear STAT1 and STAT3 expression showed a high cytoplasmic STAT1 and STAT3 expression, respectively. In Addition, tumor cells with a high nuclear STAT3 expression showed a high nuclear STAT1 expression as well.

## Conclusion

We could show a subset of HCC tumor samples with activated STAT1 and STAT3 signaling, associated with increased infiltrating immune cells, mainly consisting of cytotoxic and regulatory T-cells, often associated with a worse prognosis in HCC. High PD-L1 expression in STAT3 positive tumor cells could indicate a subset of tumors with STAT3-associated immunotolerant behaviour, possibly facilitating a new approach for blocking PD1-/PD-L1-axis.

Literaturangaben:

[1] Dirk Schmidt-Arras, (2016), IL-6 pathway in the liver: From physiopathology to therapy, *Journal of hepatology*, Jun;64(6):1403-15, <https://pubmed.ncbi.nlm.nih.gov/26867490/>

[2] Carolin Ploeger, (2016), Chromosome 8p tumor suppressor genes SH2D4A and SORBS3 cooperate to inhibit interleukin-6 signaling in hepatocellular carcinoma, *Hepatology*, Sep;64(3):828-42, <https://pubmed.ncbi.nlm.nih.gov/27311882/>

## Poster Gastroenteropathologie III

P14.03.01

### ***Helicobacter pylori* recurrence: clinico-pathological evaluation of molecular analysis in FFPE specimens of 968 patients**

T. Hansen<sup>1</sup>, M. Diederichs<sup>1</sup>, N. Arens<sup>1</sup>, M. Balsliemke<sup>2</sup>, S. Burg<sup>3</sup>, H. Heinzow<sup>4</sup>, R. Mahlberg<sup>5</sup>, E. Rambusch<sup>5</sup>, J. Kriegsmann<sup>1</sup>

<sup>1</sup>MVZHZMD Trier GmbH, Trier, Germany, <sup>2</sup>Verbundkrankenhaus Wittlich, Innere Medizin II, Wittlich, Germany, <sup>3</sup>Kreis Krankenhaus Saarburg, Innere Medizin, Saarburg, Germany, <sup>4</sup>Krankenhaus der Barmherzigen Brüder, Innere Medizin I, Trier, Germany, <sup>5</sup>Klinikum Mutterhaus der Borromäerinnen, Innere Medizin 1, Trier, Germany

#### **Background**

Resistance of *H. pylori* to antibiotics has reached alarming levels worldwide. It has become clear that in FFPE-based tissue specimens molecular testing of *H. pylori* mutations (in particular, those associated with resistance against clarithromycin and fluoroquinolones) is comparable to phenotypical methods[1]. However, data on clinicopathological analysis yielded by this method has not been described in detail yet.

#### **Methods**

From January 2014 to December 2023, we analyzed FFPE specimens of 968 patients with *H. pylori* gastritis (M: 335; F: 633; mean age: 51 yrs, Range: 5-89 yrs) by performing strip-assay based molecular analysis to detect *H. pylori* and resistance to clarithromycin as well as fluoroquinolones (GenoType Helico DR kit, Hain Lifesciences) as previously reported [2]. For statistical analysis, we conducted binary regression analysis using SPSS programme (IBM SPSS Statistics 27).

#### **Results**

Overall resistances were found in 65% of patients analyzed (629/968), the majority of them with clarithromycin resistance (64%), followed by patients with dual resistance to both clarithromycin and fluoroquinolones (24%), and patients resistant to fluoroquinolones alone (12%). Female sex ( $p = 0.037$ ) and increasing age ( $> 60$  yrs;  $p = 0.038$ ) were significantly associated with clarithromycin resistance, while there were no significant sex and age differences in the fluoroquinolone-resistant patients. For the dual resistance, female sex ( $p = 0.009$ ) and increasing age ( $> 50$  yrs,  $p = 0.01$ ) were significant factors. In 339/968 patients (35%), we did not detect any mutations conferring resistance. This cohort was significantly associated with male sex ( $p = 0.014$ ), and with younger age ( $< 40$  yrs,  $p = 0.019$ ).

#### **Conclusion**

Our results concerning clarithromycin and fluoroquinolone resistance are mainly in line with previously published clinical and epidemiological data, which were mainly based on examination of cultures and native samples[3][4]. Together with the known benefits (lower turnaround time, cost effectiveness etc.) [5], we confirm the view that molecular analysis on FFPE-based tissue specimens is a feasible approach for routine diagnosis as well as scientific issues. Further investigation should elucidate a morpho-molecular association between *H. pylori* mutation and specific histological findings.

#### Literaturangaben:

[1] Malfertheiner P, et al., (2022), Management of helicobacter pylori infection: the Masstricht VI/Florence consensus report, Gut, doi: 10.1136/gutjnl-2022-327745, 2024-01-29

[2] Cambeau E, et al., (2009), Evaluation of a new test, GenoType Helico DR, for molecular detection of antibiotic resistance in Helicobacter pylori, J Clin Microbiol, 3600, 47, 2024-01-28

[3] Bluemel B, et al, (2020), Antimicrobial resistance of helicobacter pylori in Germany, 2015 to 2018, Clin Microbiol Infect , 235, 26, 2024-03-01

[4] Megraud F, et al., (2021), Helicobacter pylori resistance to antibiotics in Europe in 2018 and its relationship to antibiotic consumption in the community, Gut, 1815, 70, 2022-11-15

[5] Pastukh N, et al., (2017), GenoType Helico DR test in comparison with histology and culture for Helicobacter pylori detection and identification of resistance mutations to clarithromycin and fluoroquinolones, Helicobacter, doi: 10.1111/hel.12447, 2024-01-30

## **Combining gene expression analysis of gastric cancer cell lines and tumor specimens of the VARIANZ study to identify biomarkers for anti-HER therapies**

M. Hufnagl<sup>1</sup>, J. Maier<sup>1</sup>, C. Heck<sup>1</sup>, K. Ebert<sup>1</sup>, I. Haffner<sup>2</sup>, G. Zwingenberger<sup>1</sup>, E. Raimundez<sup>3</sup>, R. Geffers<sup>4</sup>, R. Wirtz<sup>5</sup>, A. Walch<sup>6</sup>, J. Hasenauer<sup>3</sup>, F. Lordick<sup>2</sup>, B. Lubber<sup>1</sup>

<sup>1</sup>Institut für Allgemeine Pathologie und Pathologische Anatomie, Technische Universität München, TUM School of Medicine and Health, München, Germany, <sup>2</sup>University Cancer Center Leipzig (UCCL), University Leipzig Medical Center, Leipzig, Germany, <sup>3</sup>Faculty of Mathematics and Natural Sciences, University of Bonn, Bonn, Germany, <sup>4</sup>Helmholtz Zentrum für Infektionsforschung, Braunschweig, Germany, <sup>5</sup>STRATIFYER Molecular Pathology GmbH, Köln, Germany, <sup>6</sup>Helmholtz Zentrum München, Research Unit Analytical Pathology, Neuherberg, Germany

### **Background**

The standard treatment for patients with advanced HER2-positive gastric cancer is a combination of the antibody trastuzumab and platin-fluoropyrimidine chemotherapy. As some patients do not respond to trastuzumab therapy or develop resistance during treatment, the search for alternative treatment options and biomarkers to predict therapy response is the focus of research. Two objectives were pursued: (1) We compared the efficacy of trastuzumab and other HER-targeting drugs such as cetuximab and afatinib. We also hypothesized that treatment-dependent regulation of a gene indicates its importance in response and that it can therefore be used as a biomarker for patient stratification. (2) We investigated whether a combination treatment of trastuzumab and other receptor tyrosine kinase inhibitors against members of the HER family (tucatinib, pyrotinib and poziotinib) is more effective than trastuzumab mono-treatment.

### **Methods**

(1) A selection of gastric cancer cell lines (Hs746T, MKN1, MKN7 and NCI-N87) was treated with EGF, cetuximab, trastuzumab or afatinib for a period of 4 or 24 hours. The effects of treatment on gene expression were measured by RNA sequencing and the resulting biomarker candidates were tested in an available cohort of gastric cancer patients from the VARIANZ trial (NCT02305043) or functionally analyzed *in vitro*. (2) MKN1, MKN7 and NCI-N87 cells were treated with trastuzumab and combinations of trastuzumab with tucatinib, pyrotinib or poziotinib for 48 h. The effects on signal transduction were measured by Western blot analysis using phospho-specific antibodies.

### **Results**

(1) After treatment of the cell lines with afatinib, the highest number of regulated genes was observed, followed by cetuximab and trastuzumab. Although trastuzumab showed only relatively small effects on gene expression, *BMF*, *HAS2* and *SHB* could be identified as candidate biomarkers for response to trastuzumab. Subsequent studies confirmed *HAS2* and *SHB* as potential predictive markers for response to trastuzumab therapy in clinical samples from the VARIANZ trial. (2) The combination treatments were more effective than treatment with trastuzumab alone.

### **Conclusion**

By confirming *HAS2* and *SHB* as biomarkers for trastuzumab therapy, we provide evidence that the regulation of gene expression after treatment can be used for biomarker discovery. Based on our results on combinations of trastuzumab with small molecular inhibitors, further gene expression studies with combination treatments should be carried out.

### Literaturangaben:

[1] Ebert K, Haffner I, Zwingenberger G, Keller S, Raimundez E, Geffers R, Wirtz R, Barbaria E, Hollerith V, Arnold R, Walch A, Hasenauer J, Maier D, Lordick F, Lubber B, (2022), Combining gene expression analysis of gastric cancer cell lines and tumor specimens to identify biomarkers for anti-HER therapies-the role of HAS2, SHB and HBEGF, *BMC Cancer* 22(1):254

[2] Melina Hufnagl, (2023), Master Thesis, Analysis of biomarkers for response prediction of HER inhibitors in gastric cancer, TUM School of Life Sciences, Technische Universität München

[3] Jasmin Maier, (2021), Master Thesis, Investigation of molecular effects of HER inhibitors and the role of IL-8 as a resistance factor in gastric cancer cell lines, TUM School of Life Sciences, Technische Universität München

[4] Corinna Heck, (2020), Master Thesis, Analysis of molecular and phenotypical effects of new HER2 inhibitors in gastric cancer cell lines, TUM School of Life Sciences, Technische Universität München

P14.03.03

## ***Familial Mediterranean Fever (FMF) - an exotic but rising differential diagnosis of "unclear abdominal illness" in Germany due to increasing migration over the last decade, a Late-Onset-Case***

M. R. Kanaan<sup>1</sup>, F. Meyer<sup>2</sup>

<sup>1</sup>Department of Urology and Urologic Oncology, Hannover Medical School, Hannover, Germany, <sup>2</sup>Klinik für Allgemein-, Viszeral-, Gefäß- und Transplantationschirurgie, Otto-von-Guericke-Universität mit Universitätsklinikum, Magdeburg, Germany

### **Background**

Aim: To raise awareness of rare autoinflammatory diseases as a differential diagnosis in patients with recurrent febrile attacks accompanied by unexplained acute abdominal pain

### **Methods**

Scientific case report

### **Results**

Case presentation: - Medical history (hx): 1) *Present*: A 19-years old male patient had presented to the surgical emergency department because of an episode of fever accompanied by acute abdominal pain for 2 d with worsening tendency in the right lower abdomen with associated arthralgia and thoracic pain during breathing. The patient reported similar episodes in the past with complete healing after 2 to 3 days without any specific treatment.

2) No Medication or other known illnesses in the past. No surgical intervention in hx.

3) *Social and family hx*: The patient grew up in Syria and has been in Germany for 3 years.

- Physical examination: The patient was in severely reduced general condition by normal nutritional status. Vital signs were stable. Examination of the abdomen revealed marked rigidity and tenderness in the right lower quadrant. The abdominal wall was rigid and there was peritonism.

- Diagnostic measures indicated a CRP level of 35.0 mg/L and a normal range white blood cell count of 8.6 GpT/L. Abdominal ultrasound did not show any signs of appendicitis or other serious illnesses.

- The patient received a conservative therapeutic approach, which involved infusion therapy, administration of analgesics, and an initial "nil per os" period. Oral nutrition was then gradually resumed. The patient's family history was reexamined after recovery, revealing a similar case in a related family member.

- The clinical course was uneventful, the patient was free of fever and pain after 2 days of conservative therapy.

- Diagnosis with familial mediterranean fever (FMF) was given after assessing the Tel-Hashomer criteria with a resulting positive score. Therapy with colchicine of 1.0 mg per day as being a gold standard in disease management to prevent renal and cardiac amyloidosis and were advised to seek prompt medical attention during episodes of fever and serositis.

### **Conclusion**

The case described a late manifestation of FMF with typical clinical symptoms. This diagnosis should be considered a significant disease in case of positive familial history or case of descent from high-incidence areas. This case emphasizes the importance of taking a precise medical history and highlights FMF as an increasing disease in Germany as an up-coming consequence of migration.

P14.03.04

## ***Characterization of Septins as proteins of the nucleoskeleton in cancer cells***

T. Klessinger<sup>1</sup>, M. Bissinger<sup>1</sup>, M. Luzarowski<sup>2</sup>, P. Schirmacher<sup>1</sup>, K. Breuhahn<sup>1</sup>, S. M. E. Weiler<sup>1</sup>

<sup>1</sup>Institute of Pathology, Heidelberg University Hospital, Heidelberg, Germany, <sup>2</sup>Center for Molecular Biology of Heidelberg University (ZMBH), Core Facility for Mass Spectrometry & Proteomics, Heidelberg, Germany

### **Background**

As demonstrated for actin, nuclear cytoskeletal proteins can control gene expression, DNA repair, and tumorigenesis. Another filament-forming protein family, Septins, is detectable in the cytoplasm and affects various cellular processes such as cytokinesis, cell polarity, and membrane dynamics. Our previous results illustrated that Septins were frequently dysregulated in hepatocarcinogenesis. However, it is unclear whether Septins are present in tumor cell nuclei and how the transition of Septins between cellular compartments occurs at the molecular level. This project aims to detect nuclear

Septins, their nuclear interactome, and subcellular shuttling mechanisms in hepatocellular carcinoma (HCC) cells.

## Methods

Cytoplasmic/nuclear fractionation of different cell lines followed by Western Blot analysis and immunofluorescence microscopy (with TritonX-100 and Digitonin pretreatment) were used to detect nuclear Septins. Different truncated and mutated forms of Septin-10 were expressed to define the nuclear localization sequence (NLS). HCC cells with inducible expression of Septin-6/10 fused to the biotin ligase BirA were used for BioID proximity-dependent labeling after cytoplasmic/nuclear fractionation and subsequent liquid chromatography/mass spectrometry (LC/MS). Potential binding partners were confirmed using co-immunoprecipitation (co-IP) and proximity ligation assay (PLA).

## Results

All investigated Septin family members are localized in the cytoplasm and the nucleus; however, the ratio between nuclear/cytoplasmic enrichment differs between Septin family members. The Septin Unique Element (SUE), part of all Septin family members at the C-terminal end, is essential for the nuclear localization of Septin-10. In detail, deleting a motive of the amino acids "KMVKAR" or replacing one single arginine (R299) with glycine R299G significantly reduces the nuclear import of Septin-10. The nuclear interactome of Septin-6 and Septin-10 illustrated physical interaction with other Septin family members. Importantly, the interaction of both Septins with different nuclear proteins was detected. We confirmed the binding of Septin-6/10 with Importin-7, which is a known nuclear transport receptor.

## Conclusion

Septins are expressed in the cytoplasmic and nuclear components. Their active subcellular transport is mediated by a so far not described NLS and probably binding to Importin-7. Further studies are needed to clarify the pro-tumorigenic function of nuclear Septins in tumor cells.

P14.03.05

## ***Gene expression analysis of gastric cancer cell lines reveals modulation of PD-L1 expression by HER inhibitors***

J. Hacker, K. Anzenhofer, M. Hufnagl, J. Farah, V. Simion, V. Jackermaier, L. Wolff, F. Hartmann, A. Notter, K. Ebert, B. Luber  
Institut für Allgemeine Pathologie und Pathologische Anatomie, Technische Universität München, TUM School of Medicine and Health, München, Germany

## Background

Gene expression analysis revealed that treatment of gastric cancer cell lines with afatinib, a receptor tyrosine kinase inhibitor against members of the HER family, reduces PD-L1 (*CD274*) gene expression in cell lines with *HER2* amplification (NCI-N87 and MKN7) [1, 2]. Based on these data, we investigated whether other HER inhibitors (tucatinib, pyrotinib, poziotinib) have an inhibitory effect on the expression of PD-L1 and what role the epidermal growth factor EGF plays in this context.

## Methods

The gastric cancer cell lines Hs746T, MKN1, MKN7 and NCI-N87 were treated with EGF, cetuximab, trastuzumab or afatinib for a period of 4 or 24 hours. The effects of treatment on gene expression were measured by RNA sequencing [1, 2]. To determine the effects of afatinib, tucatinib, pyrotinib and poziotinib as mono-treatment and in combination with EGF, MKN7 and NCI-N87 cells were treated for 24 h and PD-L1 gene expression was analysed by quantitative PCR analysis (qPCR).

## Results

The gene expression results that treatment of gastric cancer cell lines with afatinib reduces PD-L1 gene expression in cell lines with *HER2* amplification (NCI-N87 and MKN7) were confirmed by qPCR [1]. Furthermore, we found that the HER inhibitors tucatinib, pyrotinib and poziotinib have a similar inhibitory effect on the gene expression of PD-L1 as afatinib. EGF, on the other hand, causes a strong stimulation of PD-L1 gene expression, which can be largely reversed by the simultaneous administration of a HER inhibitor (afatinib, tucatinib, pyrotinib or poziotinib).

## Conclusion

Overall, the integration of HER inhibitors into existing immunotherapies with checkpoint inhibitors offers a promising approach to reduce the immune evasion of cancer and thus improve the overall treatment success of immunotherapies. The underlying signaling mechanisms should be investigated in more detail.

Literaturangaben:

[1] Ebert K, Zwingenberger G, Barbaria E, Keller S, Heck C, Arnold R, Hollerieth V, Mattes J, Geffers R, Raimundez E, Hasenauer J, Lubner B, (2020), Determining the effects of trastuzumab, cetuximab and afatinib by phosphoprotein, gene expression and phenotypic analysis in gastric cancer cell lines., *BMC Cancer* 20(1):1039

[2] Ebert K, Haffner I, Zwingenberger G, Keller S, Raimundez E, Geffers R, Wirtz R, Barbaria E, Hollerieth V, Arnold R, Walch A, Hasenauer J, Maier D, Lordick F, Lubner B, (2022), Combining gene expression analysis of gastric cancer cell lines and tumor specimens to identify biomarkers for anti-HER therapies-the role of HAS2, SHB and HBEGF, *BMC Cancer* 22(1):254

P14.03.06

## ***Successful pancreatic cancer operation annihilated by port infection: A case report***

L. Engelbrecht<sup>1</sup>, F. Scheufele<sup>2</sup>, M. Wühr<sup>1</sup>, S. M. Naisar<sup>2</sup>, M. Idzikowski<sup>1</sup>, J. Shakhtour<sup>1</sup>, I. E. Demir<sup>2</sup>, G. Weirich<sup>1</sup>

<sup>1</sup>Institute for Pathology, TUM School of Medicine and Health, Technical University of Munich, München, Germany, <sup>2</sup>University Hospital "Klinikum rechts der Isar", Technical University of Munich, Department of Surgery, München, Germany

### Background

Ductal adenocarcinoma represents the most common cancer type of the pancreas (PDAC, app. 90%). Rapid tumour growth and symptom scarcity contribute to the late-stage detection of this neoplasm. Since treatment options are limited for advanced disease, the 5-year survival rate is < 8% [1]. However, a novel surgical approach to locally advanced PDAC, the Triangle operation (TO), has shown promising results concerning life expectancy [2]. TO involves radical tumour resection, and dissection of the triangle formed by the celiac trunk, the superior mesenteric artery, and the portal vein, which are often the site of local relapse. After the exclusion of peritoneal and hepatic metastases and vascular tumour infiltration by frozen section (superior mesenteric artery (SMA), celiac trunk (CT)), TO may be applied.

### Methods

A 66-year-old female patient diagnosed with ductal adenocarcinoma of the pancreas in 09/2022 presented to the clinic after three cycles of unsuccessful neoadjuvant chemotherapy with unchanged tumour size and no reduction of peripancreatic spread and celiac axis blood vessel encasement. Following treatment of a chest port infection, TO was performed by total pancreateosplenectomy, left adrenalectomy, hepaticojejunostomy, gastrojejunostomy, and the resection of a proximal segment of the superior mesenteric vein, divestment of the SMA, and the CT. Two days later, there were signs of mesenteric ischemia, upon which the patient was stented for an AMS stenosis (38%). Subsequently, the patient developed signs of sepsis and died three days later. An abdominal autopsy was performed to clarify the cause of death.

### Results

Inspection of the operative site found patent surgical anastomoses and minimal tumour residues at the portal vein. There were gross and microscopic signs of acute ischemia at the gastrojejunal anastomosis, the small intestine, and the right colon. Close to the gastrojejunal anastomosis, there was transmural granulocytic inflammation, accompanied by acute peritonitis. There was no evidence of vascular thrombosis or thromboembolism.

### Conclusion

This case demonstrates that transient hypotension, presumably caused by the port infection in this case, may lead to detrimental gastrointestinal perfusion culminating in lethal sepsis[3].

Literaturangaben:

[1] Orth, M., et al., (2019), Pancreatic ductal adenocarcinoma: biological hallmarks, current status, and future perspectives of combined modality treatment approaches, *Radiat Oncol*, p.141

[2] Hackert, T., et al, (2017), The TRIANGLE operation - radical surgery after neoadjuvant treatment for advanced pancreatic cancer: a single arm observational study, *HPB, Oxford*, p.1001-1007

[3] Lebeaux, D., et al., (2012), Clinical outcome after a totally implantable venous access port-related infection in cancer patients: a

P14.03.07

### ***Mechanisms of local adipose tissue-tumour crosstalk in pancreatic cancer***

S. Marquard, H. R. Witzel, S. Allmang, N. Marnet, W. Roth, M. M. Gaida  
Universitätsmedizin Mainz, Institut für Pathologie, Mainz, Germany

#### **Background**

Adipose tissue is an important but rather unattended component of the tumour microenvironment in various invasive cancers, especially those of the digestive system. In pancreatic cancer (PDAC) infiltration of the peripancreatic adipose tissue occurs in about 90% of the cases and is certainly one reason for local recurrence and incomplete resection. In addition, even small tumours often metastasise, with the peritoneum being the most commonly affected site after the liver. Adipose tissue has been shown to promote tumour progression through its secretome and the release of fatty acids, with several studies demonstrating that adipose tissue derived conditioned medium (ATCM) fosters e.g. invasiveness or chemoresistance of tumour cells. Little is known about the mechanisms underlying these effects in PDAC and how visceral fat depots from different anatomic locations impact on downstream signalling in tumour cells. Our aim is to unravel local interactions at the interface of tumour cells and adipose tissue.

#### **Methods**

As an exploratory experiment, we used a transcriptomic approach based on the cultivation of different PDAC cell lines with ATCM from patient derived peripancreatic and perirenal adipose tissue as a model for local and metastatic disease, respectively.

#### **Results**

Functional profiling of differentially expressed genes revealed significant enrichment of gene sets upregulated in proinflammatory and protumorigenic signalling pathways (e.g. TNF $\alpha$  signalling via NF $\kappa$ B or KRAS activation), as well as gene signatures, which are for example associated with epithelial-mesenchymal transition, when comparing culture with peripancreatic versus perirenal ATCM. Similar gene sets and pathways were significantly enriched comparing cultivation with ATCM independent of its origin versus cells cultured in common cell culture medium. These initial findings suggest that, depending on the location of the adipose tissue, it may not be the secretome itself that is substantially altered, but rather the intensity of its downstream effects.

#### **Conclusion**

Further investigations of the significantly regulated gene sets in connection with clinicopathological characteristics and histological examination of tumour tissue from patients, whose adipose tissue was used, will enhance our understanding of how adipose tissue facilitates cancer progression through local mechanisms and how this is influenced by tumour-, location- or patient-specific parameters.

P14.03.08

### ***Screening for putative actionable targets reveals dynamic changes of PD-L1 expression throughout IPN-associated cholangiocarcinogenesis***

A. Charbel<sup>1</sup>, L. Tavernar<sup>1</sup>, T. Albrecht<sup>1</sup>, J. Verheij<sup>2</sup>, E. Roos<sup>2</sup>, M. N. Vogel<sup>3</sup>, B. Köhler<sup>3</sup>, P. Schirmacher<sup>1</sup>, S. Singer<sup>4</sup>, A. Mehrabi<sup>3</sup>, S. Rössler<sup>1</sup>, B. Geoppert<sup>5</sup>

<sup>1</sup>Institute of Pathology, Heidelberg University Hospital, Heidelberg, Germany, <sup>2</sup>Department of Pathology, Amsterdam UMC, University of Amsterdam, Amsterdam, The Netherlands, <sup>3</sup>Heidelberg University Hospital, Heidelberg, Germany, <sup>4</sup>Institute of Pathology, Tübingen University Hospital, Tübingen, Germany, <sup>5</sup>Institute of Pathology, Hospital RKH Kliniken Ludwigsburg, Ludwigsburg, Germany

#### **Background**

Intraductal papillary neoplasms (IPN) have recently emerged as a well-defined group of preinvasive lesions of cholangiocarcinoma (CCA), yet their significance in the intricate multistep model of cholangiocarcinogenesis remains largely unexplored. Programmed death-ligand 1 (PD-L1), an immune inhibitory molecule expressed on both tumour and intra-/peritumoral immune cells, plays a significant role in fostering immune evasion. The focus of this study is to elucidate the dynamic evolution of PD-L1 expression throughout IPN-associated biliary cholangiocarcinogenesis.

## Methods

Intraindividually corresponding high-grade IPN (n = 65), including 54 IPNB, 11 ITPN and their associated invasive CCA (n=46) were selected for TMA construction. Immunohistochemistry and chromogen-in-situ-hybridization were employed to assess the expression of various targetable biomarkers, including p16, p53, c-myc, c-met, EGFR, HER2 and PD-L1. These results were correlated with our previously studied spatiotemporal evolution of the tumour immune microenvironment in IPN-associated cholangiocarcinogenesis.

## Results

PD-L1 was expressed in tumour cells in 6,2% (n = 4) of IPN cases (TPS  $\geq$  1%), compared to 11,9% in corresponding CCA. Higher PD-L1 expression levels were observed by integrating the tumour immune microenvironment (TIME), reaching 21,5% and 50,8% in IPN, as opposed to 11,9% and 42,2% in associated CCA at IC  $\geq$  1% and CPS  $\geq$  1%, respectively. At IC  $\geq$  1%, PD-L1 expression was associated with distinct histomorphological IPN-subtypes and UICC-Stages. PD-L1 expression in IPN-TIME directly correlated with increased total, stromal and intraepithelial CD3+-, CD4+- and CD8+-T lymphocyte densities. In contrast, a drastic shift in PDL1 expression pattern was noted in corresponding CCA, with a remnant correlation with CD8+-cell infiltration. PD-L1 positivity in IPN cells was positively correlated with intraepithelial CD3+-T-cell density, whereas no significant association with immune cell infiltration was shown at invasive stage.

## Conclusion

PD-L1 expression in tumour cells and in the tumour immune microenvironment undergoes dynamic changes throughout IPN-associated cholangiocarcinogenesis.

P14.03.09

## ***Tumor regression grading in neoadjuvantly treated ductal adenocarcinoma of the Pancreas – Proposal of a new grading scheme***

V. Henriques<sup>1</sup>, A.-K. König<sup>2</sup>, T. Hackert<sup>3</sup>, S. Roth<sup>2</sup>, U. Hinz<sup>2</sup>, M. Loos<sup>2</sup>, C. Michalski<sup>2</sup>, S. Peter<sup>1</sup>, T. Longerich<sup>1</sup>

<sup>1</sup>Heidelberg University Hospital, Institut of Pathology Heidelberg, Heidelberg, Germany, <sup>2</sup>Heidelberg University Hospital, Department of General, Visceral and Transplantation Surgery, Heidelberg, Germany, <sup>3</sup>University Medical Center Hamburg-Eppendorf, Department of General, Visceral and Chest Surgery, Hamburg, Germany

## Background

Neoadjuvant therapy (NAT) is emerging as a standard approach for tumour downstaging and increase resectability of ductal adenocarcinoma of the pancreas (PDAC), as 80% of the patients present with advanced and inoperable disease. Pathological assessment of tumour response to NAT has been shown to be prognostically relevant. However, a practical, clinically useful, and internationally endorsed tumor regression grading (TRG) for PDAC remains to be defined. This study evaluated and compared the prognostic value of the three most frequently employed TRG scoring systems: the College of American Pathologist (CAP), the MD Anderson Cancer Center (MDACC), and Evans.

## Methods

A cohort of neoadjuvantly treated patients with PDAC was retrieved from a prospectively collected institutional pancreatic database at the Department of Surgery, University Hospital Heidelberg, Germany. Histopathologic slides of all cases were reviewed by two pathologists and TRG scores were estimated according to the CAP, MDACC and Evans original scoring systems. The TRG Scores were correlated with clinicopathological parameters and with 3- and 5-year overall survival (OS).

## Results

A total of 314 patients with initially inoperable PDAC, who have received a predominantly FOLFIRINOX-based NAT were selected. Seven patients (2%) showed pathologic complete response (pCR). Minimal residual viable tumour/significant tumor regression (CAP Grade 1, MDACC 1 or Evans grade III) was observed in 20% of the cases (65 patients). All TRG systems failed to stratify patients for 3 and 5 year OS. After dichotomization of the cohort in good responders (pCR or minimal residual tumour - Group 1) and poor responders (Group 2), significant OS differences were observed in the univariate analysis. None of the TRG systems analysed was an independent prognostic factor for OS in multivariate analysis.



## Conclusion

NAT allows downstaging of primarily unresectable PDAC and a good treatment response translates in improved OS rates. Currently, the most frequently employed TGR Systems suffer from lack of objectivity, clinical validation and international endorsement. We propose a 2-tiered TRG system using a low cut-off of viable tumor per tumor bed area to improve the identification of a subgroup of patients with favourable prognosis.

P14.03.10

## ***Deciphering Intra-Tumoral Heterogeneity and Metastatic Processes in Pancreatic Ductal Adenocarcinoma Using In Situ Sequencing***

J. Wirth<sup>1</sup>, A. Chernysheva<sup>1</sup>, I. Giray<sup>1</sup>, A. Alkhamas<sup>1</sup>, P. Cheung<sup>2,3</sup>, B. T. Grünwald<sup>2</sup>, B. M. Grüner<sup>2,3</sup>, J. T. Siveke<sup>2,3</sup>, C. Mogler<sup>1,4</sup>, W. Weichert<sup>1,4</sup>, K. Steiger<sup>1,4</sup>

<sup>1</sup>Institut für Pathologie, Technische Universität München, München, Germany, <sup>2</sup>West German Cancer Center, University Hospital Essen, Essen, Germany, <sup>3</sup>German Cancer Consortium (DKTK) partner site Essen, Essen, Germany, <sup>4</sup>German Cancer Consortium (DKTK) partner site München, München, Germany

## Background

Despite progress in clinical research leading to improved survival rates for many cancers, pancreatic ductal adenocarcinoma (PDAC) remains a challenging exception. PDAC is marked by intra-tumoral heterogeneity (ITH), which is one of the main causes of poor patient survival rates. While preclinical research has largely been restricted to primary tumors, most patients diagnosed are late stage and show metastatic disease. Thus, to increase the efficacy of treatments and improve the overall prognosis of PDAC patients, advancing the personalized molecular stratification for the late stage and metastatic disease is imperative. Spatially resolved single-cell transcriptomics (scST) methodologies such as Xenium In Situ (XIS) map individual RNA molecules at subcellular resolution and thus determine the transcriptional state of single cells in a tissue section. Their application to clinical samples promises to improve the understanding of ITH, metastasis, and treatment responses.

## Methods

In collaboration with an expert team, we created a panel of 477 genes to study central pathogenic processes of PDAC. The panel includes marker genes for all major immune cells, cancer-associated fibroblasts (CAFs), “classical” and “basal-like” tumor cells as well as other pathologically relevant processes like epithelial-to-mesenchymal transition, metastasis, and hypoxia. We used this panel to acquire scST datasets of three tissue microarrays (TMAs) comprising a total of about 100 samples from both primary tumors and metastases of 51 PDAC patients. After XIS analysis, TMA sections were stained histologically and thoroughly annotated by pathologists.

## Results

To analyze the data, we established a novel framework to process and visualize XIS data of TMAs, facilitating the efficient integration of pathological annotations with computational analysis. We identified differentially expressed genes between cells of the primary tumor site and the metastasis side, focusing especially on the cancer cells and cells of the tumor microenvironment, including CAFs and different immune cells.

## Conclusion

Eventually, we are planning to use spatially aware analysis algorithms to identify differences in the cellular interaction networks between primary tumors. Findings of these analyses, including spatial distribution patterns, will be validated on a protein level using IHC and assessed for their potential use as markers for patient stratification to improve the effectivity of future PDAC therapy.

P14.03.11

### ***Pancreatic ductal adenocarcinoma (PDAC) has distinct morphological subtypes with different characteristics and prognostic values***

A. Yavas, L. Häberle, I. Esposito

Institut für Pathologie, Universitätsklinikum Düsseldorf, Düsseldorf, Germany

#### **Background**

Recently suggested molecular classifications of PDAC include mainly 2 subtypes: classical and basal. The relationship between molecular subtypes and morphology is still not well characterized. This study aims to classify PDACs based on tumor morphology and investigate the relationship between morphologic subtypes and clinicopathological parameters.

#### **Methods**

A detailed histomorphological analysis of 270 PDACs was performed. WHO 2019 classification was applied: 248 PDAC NOS and 22 PDAC variants (10 adenosquamous, 7 undifferentiated, 5 micropapillary and 3 colloid carcinomas) were identified. PDAC NOS was further classified as conventional, complex, cribriform and papillary according to the presence of more than 40% specific morphological pattern. Immunohistochemistry (IHC) for CK5, CK17, CK19, p40, GATA6 and SMAD4 was performed on tissue microarrays with 573 tumor cores. Clinicopathological information was obtained from institutional records and statistical analysis was performed using GraphPadPrism.

#### **Results**

Thirty-five percent of PDAC NOS cases were classified as conventional, while 40% were complex, 20% papillary and 5% cribriform. 90% of the PDAC NOS cases had a second (or more) additional component, 27% of conventional PDACs were "pure". Notably, 94% of papillary PDAC were characterized by the presence of >0.5 mm large ducts ( $p < 0.0001$ ). Compared to conventional, cribriform and papillary subtypes, adenosquamous, undifferentiated and complex tumors had higher WHO histological grades, more frequent marked pleomorphism and occurrence of single tumor cells ( $p < 0.0001$ ). Undifferentiated and colloid carcinoma had significantly higher TNM stages than conventional and papillary subtypes ( $p = 0.014$ ).

By IHC, the complex subtype demonstrated a basal-like profile with p40, CK5 and CK17 expression similar to that of adenosquamous and undifferentiated carcinomas. Conventional, papillary and cribriform subtypes revealed preserved Gata6 and CK19 and missing CK5, CK17, p40 expression, closer to the classical subtype. Papillary subtype showed a tendency towards longer overall survival (median 23.7 months) than conventional, complex and cribriform subtypes (median 19.2, 14.6 and 15.4 months, respectively) ( $p = 0.21$  ( $p = 0.21$ )).

#### **Conclusion**

These results provide valuable insights into the heterogeneous nature of PDAC. Further analyses are currently being conducted to investigate the association between molecular and morphological subtypes of PDAC.

P14.03.12

### ***Mucinous Cystic Neoplasms of the Pancreas and Liver share a similar DNA methylation profile with mucinous ovarian tumors***

Z. Leoni<sup>1</sup>, T. G. Calina<sup>2</sup>, T. Janik<sup>3</sup>, J. Benhamida<sup>4</sup>, S. Schallenberg<sup>1</sup>, D. Capper<sup>3,5</sup>, D. Horst<sup>1,3</sup>, M. P. Dragomir<sup>1,3,6</sup>

<sup>1</sup>Charité – Universitätsmedizin Berlin, Corporate Member of Freie Universität Berlin, Humboldt-Universität zu Berlin, Institute of Pathology, Berlin, Germany, <sup>2</sup>TGC Ventures UG, Berlin, Germany, <sup>3</sup>German Cancer Consortium (DKTK), Partner Site Berlin, and German Cancer Research Center (DKFZ), Heidelberg, Germany, <sup>4</sup>Memorial Sloan Kettering Cancer Center, Department of Pathology and Laboratory Medicine, New York, United States of America, <sup>5</sup>Charité – Universitätsmedizin Berlin, Corporate Member of Freie Universität Berlin, Humboldt-Universität zu Berlin, Department of Neuropathology, Berlin, Germany, <sup>6</sup>Berlin Institute of Health, Berlin, Germany

#### **Background**

Mucinous cystic neoplasms (MCN) remain one of the most peculiar tumors of hepato-pancreato-biliary pathology. These cystic lesions are characterized by a mucinous epithelium and an ovarian-type stroma, and may progress to invasive carcinoma in ca. 10% of cases. Their origin remains controversial. Several studies have suggested that MCNs may originate from left-sided primordial germ cells arrested during embryogenesis in the dorsal mesentery. Therefore, we

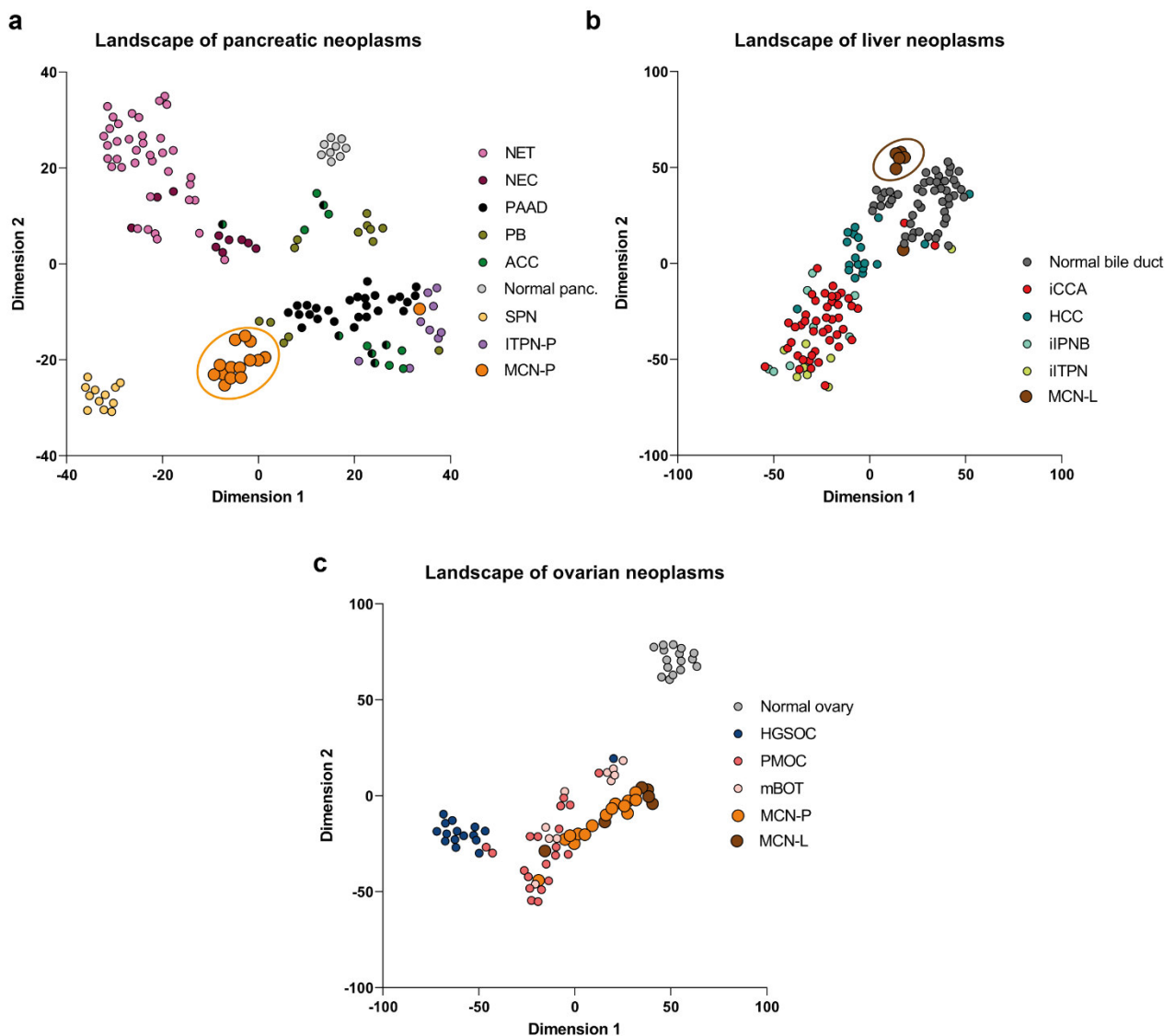
hypothesized that MCNs have a DNA methylation profile similar to mucinous ovarian tumors.

## Methods

We collected 16 MCN of the pancreas (MCN-P) and 6 MCN of the liver (MCN-L) from the archive of the Institute of Pathology, Charité, Berlin. We performed histological and immunohistochemical analyses to confirm the diagnosis and characterize the samples. We performed genome-wide DNA methylation analysis for all samples. We clustered MCN-P DNA methylation profile with 7 different pancreatic tumor types and normal pancreatic tissue (n=145) and MCN-L with 4 different liver tumors and normal bile duct tissue (n=117). Finally, we compared the DNA methylation profile of MCN-P and MCN-L with that of ovarian tumors and normal ovarian stroma (n=136).

## Results

We observed that MCN-P formed a distinct cluster in the landscape of pancreatic tumors, located near pancreatic ductal adenocarcinoma (Figure 1a). Moreover, high-grade MCN-P or with invasive component localized closer to pancreatic ductal adenocarcinomas. Similarly, MCN-L created a separate cluster in the landscape of liver tumors (Figure 1b). Finally, we observed that MCN-P and MCN-L formed a cluster together with mucinous borderline ovarian tumors and mucinous ovarian carcinomas, distinct from high-grade serous ovarian carcinoma or normal ovarian stroma (Figure 1c). In addition, we observed a tendency of low-grade MCNs to co-localize with mucinous borderline tumors and of high-grade MCNs to associate with mucinous ovarian carcinomas.



a. MCN-P in the landscape of pancreatic neoplasms; b. MCN-L in the landscape of liver neoplasms; c. MCN-P and -L in the landscape of ovarian neoplasms.

## Conclusion

We showed a common DNA methylation profile between mucinous cystic neoplasms of the pancreas and the liver with mucinous ovarian tumors suggesting a common origin.

P14.03.13

## ***Lysyl oxidase-like 2-associated immunomodulation in pancreatic ductal adenocarcinoma***

P. Zens<sup>1</sup>, S. April-Monn<sup>1</sup>, J. L. Rohrbach<sup>1</sup>, J. A. Galván<sup>1</sup>, S. Reinhard<sup>1</sup>, A. S. Wenning<sup>2</sup>, B. Gloor<sup>2</sup>, M. D. Berger<sup>3</sup>, M. Wartenberg<sup>1</sup>

<sup>1</sup>Institute of Tissue Medicine and Pathology (ITMP) University of Bern, Bern, Switzerland, <sup>2</sup>Inselspital University Hospital, University of Bern, Department of Visceral Surgery, Bern, Switzerland, <sup>3</sup>Inselspital University Hospital, University of Bern, Department of Medical Oncology, Bern, Switzerland

## Background

Extracellular matrix (ECM) modifying enzyme lysyl oxidase-like 2 (LOXL2) affects the tumor microenvironment (TME) of pancreatic ductal adenocarcinoma (PDAC). Impact of LOXL2 expression with consecutive crosslinking of collagen and elevated matrix stiffness on immune evasion and tumor morphology in PDAC was investigated.

## Methods

LOXL2 mRNA was visualized by applying RNAscope chromogenic probes on a tissue micro array (TMA) cohort, comprising of 117 cases of curatively resected PDAC. Hybridization signal recognition and quantification in tumor front and tumor center TMA spots were automated by digital image analysis (DIA) algorithms (RandomForest Pixel classifiers). Statistical correlation of mRNA signal counts was achieved for the tumor front and tumor center spots separately. Additionally, T-cell infiltrates (immunohistochemistry for CD3, CD4, CD8, CD20) and tumor budding (TB) status (present vs. absent) were analyzed in the respective TMA spots and statistically correlated with LOXL2 mRNA signal counts.

## Results

On successively cut TMA slides analyzed for LOXL2 mRNA, immune cell infiltrates and TB, statistically significant inverse correlations between lymphocyte counts (CD8, CD3, CD4; CD20) and LOXL2 mRNA signal counts were present for the tumor front spots but not the tumor center spots ( $p < 0.001$ ;  $p < 0.001$ ;  $p=0.002$ ;  $p=0.004$ , respectively). Presence of TB was significantly correlated inversely with CD20 and CD8 ( $p=0.002$ ;  $p=0.005$ ) immune cell counts in tumor front but not in tumor center spots. Additionally, presence of TB was positively correlated with LOXL2 mRNA counts in tumor front ( $p=0.003$ ). Together, stroma-modifying enzyme LOXL2 mRNA expression correlated negatively with immune cell infiltrates in PDAC and positively with TB in tumor front but not tumor center TMA spots.

## Conclusion

Implications of cancer-stroma crosstalk in PDAC was highlighted by inverse correlations of LOXL2 mRNA expression with immune cell infiltrates and positive correlation with TB. These findings highlight the complexity of TME biology in PDAC and argue for patient stratification for clinical trials based on stromal features. A combination of stromal-based therapeutic concepts with immunomodulatory and conventional treatment concepts might improve overall survival in a subset of PDAC patients stratified for stromal characteristics.

**Index of authors**  
**(bold = first author)**

Abbas, M.	DGP07.04
Abdouli, A.	<b>P11.01.03</b>
Abedellatif, S.-E.	AG14.05
Abubrig, M.	P11.02.04
Ackermann, M.	AG05.03
Adam, E.	AG11.11, AG11.14, DGP01.04
Adamczyk, M.	DGP15.04
Aeschlimann, L.	<b>DGP09.05</b>
Agaimy, A.	P05.10, P14.01.10
Agrawal, A.	P14.02.12
Aguilera, D.	DGP15.04
Ahmad, W.	<b>P.ComPath.01.06</b> , AG10.08
Ahrens, M.	P05.10
Al Kallaa, M.	<b>AG13.06</b> , AG13.13
Al-Adilee, O.	AG03.03
Al-Ali, H. K.	AG03.04
Alber, M.	AG11.07, P.ComPath.01.01, P.ComPath.01.05
Albers, P.	AG05.02
Albrecht, T.	<b>DGP13.05</b> , P14.01.13, P14.02.03, P14.02.13, P14.03.08
Albuquerque, T.	P13.04
Alinger-Scharinger, B.	AG11.06
Alkhamas, A.	P14.03.10
Allerkamp, D.	AG13.12
Allgäuer, M.	P.ComPath.01.09
Allmang, S.	P14.03.07
Almeida, S. D.	DGP13.04
Ament, C. E.	<b>P14.02.04</b>
Ammerpohl, O.	AG10.06
Anagnostopoulos, I.	AG03.10, AG03.12
Andreev, G.	DGP10.04, <b>P13.08</b>
Andrieux, G.	P04.03
Anokhina, M. M.	AG01.04, <b>P01.02</b>
Anzenhofer, K.	P14.03.05
April-Monn, S.	P14.03.13
Arens, N.	P14.03.01
Arèvalo, L.	P05.02
Armbruster, H.	<b>AG01.09</b>
Arndt, M.	<b>P14.01.03</b>
Arndt, S.	P04.01
Arnold, I.	DGP18.06
Arps, L.	<b>P.VergPath.05</b> , P14.01.01
Arslan, M. D.	<b>AG14.06</b>
Ashraf, A. P. K.	AG05.01
Aupperle-Lellbach, H.	DGP09.04, P.VergPath.02
Aurora, R.	P14.01.05
Aust, D.	P11.01.04
Bachmann, C.	AG03.02
Baenke, F.	P11.01.04
Baerenfaller, K.	P.PersMed.02.07
Baessler, B.	P.ComPath.01.07
Bahlinger, V.	AG01.09, AG05.14
Ballke, S.	P.PersMed.01.03, <b>P.VergPath.04</b>
Balsliemke, M.	P14.03.01
Banek, S.	AG05.05
Banz, Y.	DGP18.06
Barbai, T.	DGP18.02
Baretton, G.	AG09.03
Bargou, R. C.	AG03.01

Barkóczi, B.	DGP18.05
Barrett, J. C.	P.ComPath.02.02
Barta, B. A.	<b>P14.01.12</b>
Bartels, S.	AG01.02
Barth, T.	P.ComPath.02.11, AG03.05, AG07.06, AG07.07
Barth, U.	P04.01, P04.02
Barthélémy, P.	P05.10
Bartsch, D.	AG14.08
Bartsch, J.	P11.02.09, DGP07.05
Basitta, P.	DGP08.04, P05.02
Basturk, O.	<b>AG14.01</b>
Battistella, A.	DGP04.07
Bauer, M.	<b>AG01.10, AG03.04</b> , P03.02
Bauerschlag, D.	AG01.05
Bausch, A.	P11.02.13
Beck, J.	P.ComPath.02.01
Beckers, A.	P.VergPath.01
Beckmann, D.	P14.02.06
Bedke, J.	P05.10
Behr, J.	P10.02
Bein, J.	P.ComPath.01.03
Bekisoglu, A.	P.ComPath.02.04
Belicza, E.	DGP18.03
Benhamida, J.	P14.03.12
Benz, M.	P13.03
Berg, M.	AG05.01
Berger, M. D.	P14.03.13
Bergmann, A. K.	AG12.02
Bergmann, L.	P05.10
Bergmann, L.	P.PersMed.01.07
Bermeitinger, J.	P13.06
Berndt, A.	DGP04.05, P11.02.04, P14.01.05
Bernhardt, M.	<b>AG05.09, P.VergPath.06, P05.05</b>
Berres, M.-L.	P.VergPath.01
Berthold, R.	AG07.05
Bertz, S.	P05.06
Bette, S.	<b>AG07.06</b>
Beutler, C.	DGP09.04
Biral, R.	AG11.03
Biró, A.	DGP18.05
Bisanz, H.	AG10.09
Bischoff, P.	<b>AG10.03</b>
Bisht, S.	AG03.03
Bissinger, M.	P14.03.04
Bisson, T.	AG13.05
Bjelic-Radasic, V.	AG01.08
Bläker, H.	AG10.09
Blattgerste, C.	<b>P13.07</b>
Blind, L.	P14.01.10
Blumenstock, G.	AG09.03
Blüthgen, N.	DGP04.04
Bobe, S.	<b>DGP17.05</b> , P14.02.06
Böck, J.	<b>AG03.10</b>
Bödecker, J.	P13.06
Boehlke, J. M.	AG10.05
Böhm, C.	AG11.07
Bohnenberger, H.	AG10.04
Boleti, E.	P05.10
Bollwein, C.	<b>AG07.04</b> , DGP04.01, P.PersMed.02.01
Bonzheim, I.	AG01.09, P11.02.02
Boor, P.	AG04.05, P04.04, P04.08
Bootsma, S.	P14.01.10

Boovadira Poonacha, J.	AG14.05
Borka, K.	DGP18.05
Boschung, K.	AG11.07
Boxberg, M.	AG06.01, P.PersMed.01.03
Boy, M.	AG03.02
Bozek, K.	DGP06.04
Bozek, K.	P.PersMed.02.05
Branchi, V.	AG14.05
Brändlein, S.	AG03.10
Braren, R.	DGP13.04
Bräsen, J. H.	AG04.04
Braubach, P.	P10.04
Braunschweig, T.	<b>AG09.04</b>
Breitkopf-Heinlein, K.	P14.02.12
Bremmer, F.	<b>AG05.02</b> , AG05.06
Breuhahn, K.	P14.01.13, P14.03.04
Brinkmann, F.	DGP13.05
Brobeil, A.	AG14.08
Bronger, H.	AG01.03
Bronsert, P.	P.ComPath.02.01, P.ComPath.02.10, P.PersMed.02.07, P01.03, P11.02.06, P14.01.09, P14.01.12
Brossart, P.	AG06.02
Brucker, S.	AG01.09
Bruehl, F.	AG03.02
Brune, B.	AG01.08
Brünig, J.	DGP18.06
Brunner, S. M.	AG14.11
Bruns, V.	P13.03
Bucher, P.	P.PersMed.01.06
Buchstab, O.	DGP06.05, P.ComPath.01.01
Buchwaldt, J.	<b>DGP05.04</b>
Budczies, J.	AG06.01
Buhl, E. M.	AG05.12, P04.08
Bülöw, R. D.	P04.04
Bundschuh, R. A.	AG10.01
Buness, A.	AG03.03, AG05.01
Burg, S.	P14.03.01
Burger, I. A.	AG05.07
Burger, M.	P05.06
Burgstaller, G.	P10.02
Büttner, R.	AG10.08, AG11.04, AG11.07, AG11.10, AG14.14, AG14.16, DGP06.04, P.ComPath.01.06, P.ComPath.01.08, P.ComPath.02.04
Bychkov, A.	AG10.08, AG14.16
Cabrita Figueiredo, A. E.	P.PersMed.02.07
Calina, T. G.	P14.03.12
Calvisi, D. F.	P.PersMed.01.08
Campean, V.	P05.06
Cano Garcia, C.	AG05.05
Capper, D.	P14.03.12
Carvalho, R.	<b>P.ComPath.02.04</b>
Castellano, D.	P05.10
Častven, D.	P.VergPath.01
Casuscelli, J.	P05.03
Cattaneo, M.	AG11.08
Chakraborty, S.	P04.03
Chakraborty, S.	AG11.09, AG14.03, DGP04.02, P.VergPath.03, P05.04, P11.01.03, P11.01.11, <b>P11.01.13</b> , P11.02.12
Charbel, A.	DGP13.05, P14.02.03, P14.02.13, <b>P14.03.08</b>
Che, Y.	AG05.02

Chen, J.	AG13.06, AG13.13
Chen, Y.	<b>AG10.05</b> , DGP04.05, P11.02.04
Chernysheva, A.	P14.03.10
Cheung, P.	P14.03.10
Chon, S.-H.	P.ComPath.01.08
Chong, L. Y.	P11.01.01
Christe, L.	AG01.04
Christensen, D.	AG04.04
Chun, F.	AG05.05
Ciernik, L.	DGP06.05
Claesen, M.	P11.01.01
Claus, R.	AG10.01, P13.06
Clement, J. H.	P11.02.04
Cook, L.	DGP07.05
Cosenza Contreras, M.	DGP07.05
Cronauer, M. V.	<b>AG05.04</b> , <b>AG05.13</b> , P05.02
Croner, R. S.	P14.01.03
Csajbók, V.	DGP18.05
Da Silva Mourato Henriques, V.	P14.01.13
Dale, T.	DGP10.05
Danics, K.	DGP18.03
Dannehl, D.	AG01.09
Dasmeh, P.	P.ComPath.01.08
de Barbanson, B.	P11.02.01
de Brot, S.	DGP09.05
De La Torre, C.	P14.01.13
de Ridder, J.	P11.02.01
Dederer, M.	P14.01.05
Deeb, J.	<b>P04.02</b>
Delbridge, C.	AG13.03
Demir, I. E.	P.PersMed.01.05, P.PersMed.02.01, P14.03.06
Deng, H.	<b>DGP16.04</b>
Denkert, C.	AG01.07, AG01.08, AG14.08
Dernbach, G.	AG11.07, P.ComPath.01.05
Deserno, T. M.	AG13.12
Dheenadayalan, R.	P03.04
Diederich, V. J.	<b>AG03.08</b>
Diederichs, M.	P14.03.01
Diedrichs, F.	AG05.11, DGP04.03
Dietmaier, W.	AG11.04, <b>AG11.05</b>
Dietrich, D.	DGP07.04
Dinser, M.	<b>P.ComPath.02.06</b>
Dintner, S.	AG10.01, AG11.04, <b>P11.01.08</b> , P14.01.11
Dippel, J.	DGP06.05, <b>P.ComPath.01.01</b> , <b>P.ComPath.01.05</b>
Dislich, B.	DGP18.06, P.ComPath.02.05
Djudjaj, S.	AG04.05, P04.08
Dohle, F.	AG12.02
Doil, L.	AG12.02
Doll, S.	DGP04.01
Dombrowski, F.	AG11.12, P11.01.06
Dopfer, E.-P.	AG11.14, DGP02.05, <b>P.PersMed.01.07</b>
Döring, C.	AG05.05
dos-Santos-Silva, I.	AG01.10
Dragomir, M. P.	P14.03.12, AG11.07
Dreßler, F. F.	<b>AG05.11</b> , <b>DGP04.03</b> , <b>P.PersMed.02.06</b>
Dressel, N.	P11.01.04
Droste, P.	AG04.05, <b>P04.08</b>
Droste, S.	P01.05, P01.06
Dubach, P.	AG06.03
Duret, D. S.	P14.02.05
Durruthy-Durruthy, R.	AG11.08



Dzubak, P.	AG11.03
Eberle, M.	P13.06
Eberli, D.	AG05.07
Ebert, K.	P14.03.02, P14.03.05
Eckermann, M.	AG05.03
Eckstein, M.	AG01.07, AG05.14, AG14.08, DGP04.06, <b>DGP07.04, DGP07.04,</b>
<b>DGP07.04</b>	
Ehmer, U.	P14.02.01
Eiber, M.	P05.04
Eich, M.-L.	DGP06.04
Eismann, L.	P05.03
Ekici, K.	P13.02
Elakad, O.	AG10.04
Elamin, F.	DGP18.03
Elezkurtaj, S.	<b>DGP04.04</b>
Ellinger, J.	AG05.01
Enderle-Ammour, K.	P.ComPath.02.01
Engel, K. M.	DGP04.05
Engelbrecht, L.	<b>P14.03.06</b>
Engelhardt, S.	P.ComPath.01.07
Engelmann, T.	AG12.02
Engler, T.	AG01.09
Englert, N.	<b>P.ComPath.01.09</b>
Enke, J. S.	<b>AG10.01</b>
Erapaneedi, R.	DGP17.05
Erdlenbruch, B.	AG12.02
Erlenbach-Wuensch, K.	DGP04.07
Escherich, A.	AG11.04
Escudier, B.	P05.10
Eser, S.	P11.01.08
Eslami, S.	P.PersMed.02.03, P13.04
Espadas, G.	DGP07.05
Esposito, I.	DGP17.04, P14.03.11
Evers, M.	<b>AG03.01</b>
Evert, K.	AG10.02, AG14.11
Evert, M.	AG10.02, AG11.08, AG14.07, AG14.08, AG14.09, AG14.11, AG14.15,
P.PersMed.01.08	
Fahrner, M.	<b>DGP02.05, P14.01.09</b>
Farah, J.	P14.03.05
Farfán López, F. J.	<b>P14.01.07</b>
Fassunke, J.	AG11.04, AG11.10, <b>P11.02.05</b>
Fehm, T.	AG01.04, P01.02
Feilen, T.	DGP07.05, P04.07, <b>P05.09</b>
Felder, B.	AG01.08
Fend, F.	AG01.09, AG03.02, AG09.03, AG12.05, AG12.08
Fernandez, A.	AG01.07, AG13.07, P.ComPath.01.07
Ferraro, D. A.	AG05.07
Feucht, J.	P.PersMed.01.06
Feuerhake, F.	AG13.05, AG13.12
Feulner, B.	<b>P.ComPath.01.05</b>
Fichtner, A.	<b>AG05.06</b>
Fiestas Cueto, R.	P.PersMed.02.07
Firmbach, D.	<b>AG13.11, P13.03</b>
Fischer, M.	<b>DGP13.04</b>
Fitzgerald, R.	P.ComPath.01.08
Flechon, A.	P05.10
Flechtenmacher, C.	P14.02.11
Fliedner, F.	<b>P.ComPath.01.03</b>
Flinner, N.	AG13.05, P.ComPath.01.03, P.ComPath.01.04, P.ComPath.02.09
Florian, S.	P.PersMed.02.05

Foersch, S.	AG01.07, AG13.07, <b>DGP19.04</b> , P.ComPath.01.07
Föll, M.	P.PersMed.01.04, P11.02.09, P14.01.12
Forberger, M.	<b>AG10.09, P01.05</b>
Foreman, R.	P.PersMed.01.02
Forestier, G.	AG13.12
Försch, S.	AG14.08, P14.01.06
Förster, S.	AG03.03
Forster, S.	<b>AG03.02</b>
Fraas, A.	P14.01.13
Franitza, M.	P.ComPath.01.08
Franke, S.	AG07.03, DGP08.05, P11.01.05
Franz-Wachtel, M.	P14.01.08
Franzen, J.	DGP04.04
Franzmeier, S.	<b>P11.02.12</b>
Freiberger, S. N.	AG05.07, AG06.03
Freitag, H.	AG12.02, P10.04
Frentsch, M.	AG11.07
Freude, A.	P01.05
Friebe, R.	<b>P04.01</b>
Friedland, F.	AG05.12
Friedrich, C.	AG11.07
Friess, H.	AG14.07, P.PersMed.01.05
Fritsch, A.	P14.01.09
Fritz, R.	AG11.07
Fritzsche, S.	P14.01.13
Froeberg Mathisen, I.	<b>P.ComPath.02.09</b>
Frosina, D.	AG14.01
Frost, N.	AG10.03, AG11.07
Frost Frederiksen, S.	P11.02.09
Fuchs, K.	AG05.01
Fuerte, G.	AG11.08
Fukuoka, J.	AG10.08, AG14.16
Funke, K.	P05.07
Fürstberger, A.	AG03.05
Fusco, F.	AG13.03, <b>DGP13.05</b>
Fusco, S.	P14.01.08
Gaida, M. M.	AG14.03, P14.03.07
Gaisa, N.	AG03.05, AG05.12, AG07.06, AG07.07, AG08.03, AG10.08, P03.04, P05.06, P11.01.07, P11.02.11, P.ComPath.02.03
Gallenmiller, Y.	P11.02.11
Galván, J. A.	P14.03.13
Gan, L.	AG05.12
Ganter, C.	<b>P14.02.06</b>
Gaßler, N.	AG10.05, DGP04.05, P11.02.04
Gebhart, F.	DGP04.07
Geffers, R.	P14.03.02
Gehring, A.	DGP04.07
Geisenberger, C.	<b>P11.02.01</b>
Geister, D.	AG10.09
Genzel, N.	DGP04.04
Geoppert, B.	P14.03.08
Georgiades, M.	AG07.03
Geppert, C. I.	P13.03
Gerber, T.	DGP13.05
Gerckens, M.	<b>P10.02</b>
Gerhard-Hartmann, E.	AG03.10, AG03.12
Geßner, P.	AG10.09
Gharib, M.	P.PersMed.02.03, P13.04
Ghosh, S.	AG11.07
Giammanco, A.	<b>AG14.16</b>
Giedl, J.	P05.06

Giel, A.-S.	P.ComPath.01.08
Gilks, B.	P01.08
Giray, I.	P14.03.10
Girkinger, V.	P.ComPath.02.05
Glamann, L.	<b>P03.02</b>
Glasner, C.	AG01.07, <b>AG13.07</b> , P.ComPath.01.07
Glasz, T.	DGP18.03
Gleitsmann, M.	AG01.08
Gloor, B.	P.ComPath.02.05, P14.03.13
Gockel, I.	P.ComPath.01.08
Goeppert, B.	DGP13.05, P14.01.13, P14.02.03, P14.02.13
Goldmann, T.	AG10.06
Gonçalves, J.	<b>DGP04.02, DGP16.05</b>
Goncharenko, L.	P.PersMed.02.07
Gonzalez-Carmona, M. A.	AG14.05
Göring, W.	P01.02
Götting, I.	AG01.09
Gottlieb, J.	P11.02.07
Götz, M.	DGP13.04
Grabbert, M.	DGP10.04, P05.09, P13.08
Gradhand, E.	AG12.02, AG12.04
Gräler, M.	AG10.05
Gramlich, S.	AG03.12
Grass, A.	<b>AG14.08</b>
Gravis, G.	P05.10
Gress, T.	AG14.08
Gretser, S.	<b>AG12.04</b> , P.ComPath.01.04
Grieser, T.	AG07.06
Grimm, M.-O.	P05.10
Grochowski, P.	AG14.13, <b>P.PersMed.02.04</b>
Groll, T.	<b>DGP09.04</b> , P.PersMed.01.03, P.VergPath.01, P.VergPath.04, P01.04
Größler, F.	AG04.04
Gross-Goupil, M.	P05.10
Grosser, B.	<b>AG14.12</b> , AG14.13
Grote, A.	DGP07.05
Grozdanov, V.	AG14.13
Grün, D.	P14.02.12
Grüner, B. M.	P14.03.10
Grünwald, B. T.	P14.03.10
Grünwald, V.	DGP07.04
Guck, J.	DGP04.07
Guenther, M.	AG14.06
Gür, K.	P14.01.13
Gustav, M.	AG13.07
Gustavson, M.	P.ComPath.02.02
Gütgemann, I.	AG03.03
Guyon, V.	P01.03
Haack, T.	P04.06
Haanen, J.	P05.10
Haas, A.	P13.02
Haase, L.	AG07.06
Häberle, L.	P14.03.11, DGP17.04
Hacker, J.	<b>P14.03.05</b>
Hackert, T.	P14.03.09
Haddouti, E.-M.	AG03.03
Hadnagy, V. S.	<b>AG06.03</b>
Haferkamp, A.	AG05.08
Haffner, I.	<b>AG14.02</b> , P14.03.02
Hagemann, L.	P14.02.06
Hagemeyer, L.	AG12.02
Hahn, H.	AG13.05

Hahn, O.	DGP07.04
Hajduk, E.	<b>P14.01.02</b>
Halloul, Z.	P04.01, P04.02
Hamdorf, M.	<b>DGP08.04</b>
Haneder, S.	<b>P.ComPath.02.02</b>
Hänisch, J.	AG04.04
Hansen, A.	P05.07
Hansen, I.	P11.02.10
Hansen, T.	<b>P01.09, P11.02.10, P14.01.05, P14.02.02, P14.03.01</b>
Hansmann, M.-L.	AG03.07, AG03.08
Hanusch, C.	AG01.08
Hapfelmeier, A.	AG14.03
Harder, C.	<b>DGP06.04</b>
Hardt, J.	AG14.12
Hartkopf, A.	AG01.08, AG01.09
Hartmann, A.	AG05.14, AG13.11, DGP04.06, DGP04.07, DGP07.04, DGP10.05, P05.06, P05.10, P13.03, P14.01.10, P14.02.10
Hartmann, F.	P14.03.05
Hartmann, N.	DGP05.04
Hartmann, W.	AG07.05, DGP04.01
Hartung, S.	P03.04
Hasebauer, J.	AG14.02
Hasenauer, J.	P14.03.02
Hasselblatt, P.	P14.01.09
Hauser, A.	DGP04.04
Heck, C.	P14.03.02
Heemann, U.	AG13.03
Heid, I.	P.VergPath.05
Heidel, C.	AG10.06
Heidenreich, A.	AG05.02, DGP06.04
Heider, D.	P.ComPath.01.08
Heimer, J.	AG05.07
Heine, A.	AG06.02
Heinlein, H.-P.	AG08.03
Heinst, L.	AG07.05
Heinzow, H.	P14.03.01
Heiß, Q.	AG11.09, <b>P11.01.03</b> , P11.01.12, P11.01.13
Hekmat, K.	AG11.07
Heldwein, M.	AG11.07
Helmer, J.	<b>P.ComPath.01.02</b>
Hemmer, H.	P14.02.12
Hemming, E. C.	AG03.07
Hendrich, C.	<b>AG12.02</b>
Henkel, C.	P11.02.09
Hennes, M.	DGP07.05
Hennig, A.	<b>P11.01.04</b>
Hennig, S.	DGP04.04
Henning, M.	AG05.11, DGP04.03
Henriques, V.	<b>P14.03.09</b>
Hense, J.	<b>DGP06.05</b> , P.ComPath.01.01
Herbst, C.	P.ComPath.02.07
Herkens, L.	<b>AG04.05</b>
Hermann, S.	DGP17.05
Hernandez, E.	AG14.01
Herold, S.	AG11.04
Herwig, L.	AG05.05
Hess, J.	DGP06.05
Hesser, J.	P.ComPath.01.09
Heukamp, L. C.	AG11.04
Heusinger-Heß, V.	AG13.06, AG13.13
Heydt, C.	P11.02.05, P11.02.05
Heyer, J.	P11.02.06

Hieber, D.	P.ComPath.02.06
Hildebrand, K.	<b>P13.06</b>
Hiller, G. G. R.	P01.05, P01.06, P01.08, P12.03
Hiller, L.	DGP09.05
Hiller, R.	<b>AG12.01</b>
Hiller, W.	P14.02.02
Hillmer, A.	<b>P.ComPath.01.08</b>
Hinrichs, S.	AG05.11, DGP04.03
Hinz, U.	P14.03.09
Hirsch, B.	DGP04.04
Hirsch, D.	AG11.05, AG11.08, AG14.09, AG14.11, AG14.15
Höbart, J.	P.VergPath.03
Hobisch, L.-M.	<b>AG05.14</b>
Hoeh, B.	AG05.05
Höfener, H.	AG13.05
Hoff, J.	AG10.05
Hoffmann, A.	AG11.02, P.PersMed.01.02
Hoffmann, H.	AG10.02
Hoffmann, M. J.	AG05.12
Hofmann, K.	<b>P14.02.11</b>
Hofmann, R. S.	<b>P14.02.05</b>
Höhn, A. K.	P01.05, P01.06, P01.08
Hollerith, K.	AG13.03
Hollfoth, V.	<b>P14.01.08</b>
Hölscher, F.	DGP08.04, P05.02
Hölzel, M.	AG14.05, DGP07.04
Holzmann, D.	AG06.03
Holzner, P.	P.PersMed.01.04
Hommerding, M.	P05.01
Hommerding, O.	AG05.09, P.VergPath.06, <b>P05.01</b> , P05.05
Hönscheid, P.	P14.01.12
Hoppe, H.	<b>DGP18.06</b>
Hoppe, S.	P.ComPath.01.08
Horn, H.	AG03.11
Horn, L.-C.	AG12.01, P01.05, <b>P01.06</b> , P01.08, P12.03
Horny, K.	AG01.04
Horst, D.	AG05.11, AG10.03, AG11.07, DGP04.03, DGP04.04, P.ComPath.01.01,
P.ComPath.01.05, P.PersMed.02.05, P14.03.12	
Horstmann, J.	AG13.10
Hosni, R.	<b>AG14.05</b>
Hu, Y. L.	AG14.11
Huber, O.	DGP04.05, P11.02.04
Huebner, K.	<b>DGP04.07</b> , DGP10.05, <b>P14.01.10</b>
Hufnagl, M.	<b>P14.03.02</b> , P14.03.05
Hulla, W.	AG10.08, AG14.16, DGP06.04
Hüllner, M.	AG06.03
Hummel, A.	AG11.11
Hummel, M.	DGP04.04
Huober, J.	AG01.08
Huss, R.	<b>P.ComPath.02.07</b>
Hussein, K.	AG12.07, P12.01
Hutarew, G.	<b>AG11.06</b>
laccarino, I.	P03.03
Idzikowski, M.	P14.03.06
Ihle, M.	<b>AG11.10</b> , P11.02.05
Ihringer, R.	P11.01.08
Ikonomi, N.	P.ComPath.02.03
Ilm, K.	AG11.05
Imboden, S.	AG01.04
Immel, A.	AG11.08, AG14.09, AG14.15
Inal, A.	P14.02.03

Isfort, I.	AG07.05
Islam, R.	P05.07
Ivanyi, P.	DGP07.04, P05.10
Iwuajoku, V.	<b>P13.02</b>
Jackermaier, V.	P14.03.05
Jäger, C.	P.PersMed.01.05, P.PersMed.02.01
Jagomast, T.	AG10.06
Jakab, A.	DGP18.03
Jamshidi Idaji, M.	DGP06.05
Janecke, A. R.	P12.02
Janik, T.	P14.03.12
Jank, P.	AG01.08
Janssen, K.-P.	P.VergPath.02
Jechorek, D.	AG07.03, DGP08.05, P11.01.05
Jesinghaus, M.	AG01.07, AG13.07, AG14.03, AG14.08, DGP09.04, P14.01.06
Jessen, A.	P13.07
Joffe, M.	AG01.10
Jöhrens, K.	AG11.05
Jonas, C.	<b>AG11.04</b> , P.ComPath.01.08, P11.02.05
Jonigk, D.	AG05.03, AG05.12, AG10.08, P10.01, P11.01.07, P10.04, P11.02.07
Jud, S.	P01.09
Juhasz-Böss, I.	P01.03
Julius, U.	P04.09
Jung, A.	AG14.06
Jungbluth, A.	AG14.01
Junker, K.	DGP07.04
Jurmeister, P.	AG09.03, P.ComPath.01.05
Kaemmerer, D.	AG10.02
Kahl, K.-H.	P.PersMed.02.02
Kainmüller, D.	DGP04.04
Kalff, J.	AG14.05
Kalmbach, S.	AG03.11
Kaltenbacher, T.	P.VergPath.04
Kammerstetter, F. A.	<b>AG13.03</b>
Kamp, J.-C.	P10.01, P10.04, <b>P11.02.07</b>
Kanaan, M. R.	<b>P14.03.03</b>
Kantelhardt, E.	AG01.10
Kapil, A.	P.ComPath.02.02
Karim, M.	<b>P11.01.06</b>
Karras, F.	<b>DGP08.05, P11.01.05</b> , AG07.03
Karyniotakis, K.	AG04.05
Kasajima, A.	AG10.02, AG13.03, AG14.07, AG14.08
Kather, J. N.	AG01.07, AG13.07, AG14.13, DGP13.05, P.ComPath.01.07
Kazemi, A.	AG13.10, <b>P.PersMed.02.03, P13.04</b>
Keck, J.	P12.02
Kehl, A.	<b>P.VergPath.02</b>
Kehl, M.	AG05.01
Keil, F.	<b>AG14.11</b>
Keilholz, U.	AG11.07
Keller, G.	AG14.03
Kellers, F.	<b>AG01.05</b> , AG01.07, AG11.15, AG13.07, P14.01.06, P14.02.08,
P14.02.09	
Kemter, E.	P04.08
Kenessey, I.	DGP18.02
Kerner, A.	<b>AG11.15</b>
Kers, J.	P04.04
Kestler, H.	P.ComPath.02.03, P.ComPath.02.11
Keyl, J.	<b>P13.05</b>
Keyl, P.	P13.05

Khan, M. Z.	P13.02
Kiechle, M.	AG01.03
Kiefer, F.	DGP17.05, P14.02.06
Kießling, P.	P14.02.12
Kinzler, M. N.	AG12.04, P.ComPath.01.04
Kirfel, J.	AG10.06
Kirschbaum, A.	AG14.08
Kiss, A.	<b>DGP18.02</b> , DGP18.03, DGP18.05
Kittel, D.	AG06.02
Klapper, W.	AG03.05, P03.03
Klare, P.	AG01.08
Klatt, N.	P11.02.06
Klaus, F.-L.	<b>P13.01</b>
Klaus, J.	DGP18.06
Klauschen, F.	AG11.07, DGP06.05, P.ComPath.01.01, P.ComPath.01.05, P01.01,
P05.03, P13.05	
Kleesiek, J.	DGP13.04, P13.05
Klein, I. M.	P14.02.11
Klein, S.	AG10.08, AG14.16, DGP06.04, P.ComPath.02.04
Kleinle, A.	P.PersMed.01.08
Kleinlein, I.	P.PersMed.02.04
Klessinger, T.	<b>P14.03.04</b>
Kling, C.	<b>AG11.09</b> , P11.01.11, P11.01.13
Klingel, K.	AG12.08, P04.05
Klinkhammer, B. M.	P04.08
Kloft, M.	P.ComPath.01.01
Klopfleisch, R.	P.VergPath.05
Klöppel, G.	AG10.02, AG14.07, AG14.08
Kloth, M.	DGP05.04
Kludt, C.	AG10.08
Kluge, J.	P.PersMed.02.05
Klump, D. M.	DGP17.05
Klümper, N.	AG14.05, DGP07.04
Kluth, L.	AG05.05
Knebel, C.	DGP04.01
Kneidinger, N.	P10.02
Knittel, J.	DGP04.07
Koch, C.	<b>P.PersMed.02.01</b>
Koch, I.	AG11.07
Koch, V.	AG13.04
Kocsmár, É.	<b>DGP18.03, DGP18.05</b>
Kocsmar, I.	DGP18.03
Köfler, S.	<b>P.ComPath.02.05</b>
Köhler, B.	P14.03.08, DGP13.05
Kohlmayer, F.	P14.01.01
Kohlross, M.	<b>AG14.03</b>
Kolbe, K.	<b>AG14.02</b>
Koll, F.	<b>AG05.05</b>
Köllermann, J.	AG05.05
Kölzer, V.	DGP15.04
König, A.-K.	P14.03.09
Kontsek, E.	DGP18.05
Konukiewitz, B.	AG01.05, AG11.15, P14.01.06, P14.02.08, P14.02.09
Koppermann, M.-L.	AG01.03, AG11.09, P11.01.03, P11.01.11, <b>P11.01.13</b>
Körber, R.-M.	AG03.03
Körber-Ferl, K.	AG07.03, P11.01.05
Körner, M.	AG06.03
Kössinger, A. L.	P05.09
Kovacs, Z. E.	P01.09
Kraeter, M.	DGP04.07
Kraus, A.	<b>P14.02.09</b>
Kraus, T.	AG11.06

Krauss, P.	P.PersMed.02.02
Kreft, T.	AG05.09, P.VergPath.06, P05.05, <b>P05.08</b>
Kreipe, H.	AG01.02, AG12.07, P11.02.07, P12.01
Kremer, A.	AG05.04, P05.02
Kremer, M.	AG10.02, AG14.07, AG14.08
Kresbach, C.	AG05.02
Kressler, D.	AG11.03
Kretzschmar, T.	DGP04.05
Kriegsmann, J.	P01.09, P11.02.10, P14.01.05, P14.02.02, P14.03.01
Kriegsmann, K.	P11.02.10
Kriegsmann, M.	AG14.08, P11.02.10
Kristiansen, G.	AG03.03, AG03.12, AG05.01, AG05.04, AG05.09, AG05.13, AG06.02, AG14.05, DGP07.04, P.VergPath.06, P05.01, P05.02, P05.05, P05.07, P05.08, DGP08.04
Kröncke, T.	P11.01.08
Krummeich, J.	<b>P11.02.08</b>
Kubankova, M.	DGP04.07
Küffer, S.	AG10.04
Kugler, C.	AG10.06
Kuhn, P.-H.	AG13.03, DGP04.01, DGP13.05
Kühnel, M.	AG10.08, P10.01, P11.02.07
Kulka, J.	DGP18.02
Kulow, F.	<b>P14.01.06</b>
Kumbrink, J.	AG14.06
Kümpers, C.	<b>AG10.06, DGP19.03</b>
Kunft, A.	P.ComPath.01.05
Kuntze, A.	<b>AG07.05</b>
Kunze, P.	P14.02.10
Kuppe, C.	DGP07.04, P14.02.12
Kurircyn, P.	<b>P13.03</b>
Kurowski, K.	P.ComPath.02.01, P.ComPath.02.10, P.PersMed.01.04, P.PersMed.02.07, <b>P01.03</b> , P14.01.12
Kurz, F.	P14.01.07
Kurz, K.	<b>AG03.11</b> , AG03.10, AG03.12
Kuss, S.	<b>P04.09</b>
Kuster, B.	DGP13.05
L'Imperio, V.	AG14.13
Lahmer, T.	AG13.03
Laib, A.	P.ComPath.01.03
Lambrecht, S. J.	<b>AG11.11</b>
Lammert, F.	AG05.12
Lammert, J.	<b>AG01.03</b>
Lan, Y.-C.	<b>P04.04</b>
Lang, S. M.	P11.02.04
Lang-Schwarz, C.	AG13.11, P14.01.10
Lange, F.	AG05.14, P05.10
Lange, S.	<b>AG11.09</b>
Lange-Herr, N.	DGP18.06
Langer, R.	P.ComPath.02.05
Lapa, C.	AG10.01
Laqua, F.	P.ComPath.01.07
Laßmann, S.	AG11.11, AG11.14, DGP01.04, DGP02.05, P.PersMed.01.07
Lau, M. C.	P11.01.01
Laudicella, R.	AG05.07
Le, U.-T.	P.ComPath.02.10
Le Marois, M.	P14.01.13
Lebenatus, A.	AG01.05
Ledderose, C.	P05.03
Ledderose, S.	<b>P05.03</b>
Legnar, M.	P.ComPath.01.09, <b>P.ComPath.02.08</b>
Lehmann, K.-V.	AG05.12
Lehmann, U.	AG01.02



Leibold, J.	P.PersMed.01.06
Leich, E.	AG03.01, AG03.11
Leiner, H.	AG11.12, P11.01.06
Lennerz, V.	DGP04.04
Leoni, Z.	<b>P14.03.12</b>
Leybold, S.	AG05.03
Li, Y.	AG05.01
Li, Y.	AG10.04
Liebeskind, J.	DGP04.04
Liesche-Starnecker, F.	AG10.01, P.ComPath.02.06, P.PersMed.02.02, P.PersMed.02.04
Liesen, A.	<b>P05.07</b>
Lindauer, J.	P11.02.11
Link, T.	AG01.08
Lippert, H.	P14.01.03
Lisiecki, H.	P.PersMed.01.03, <b>P01.04</b>
Litchfield, C.	DGP15.04
Liu, D. H. W.	P.ComPath.02.05
Liu, J.	<b>P.ComPath.01.10</b>
Liznerski, P.	P.ComPath.01.01
Lohmann, C.	AG07.03
Lohner, B.	P14.01.07
Loibl, S.	AG01.08
Lölkes, C.	AG13.13
Longerich, T.	P14.03.09
Loos, M.	P14.03.09
Löprich, L.	P.VergPath.04
Lordick, F.	AG14.02, P14.03.02
Lösch, A.	AG14.11
Lothion-Roy, J.	DGP09.05
Lotz, G.	DGP18.02, DGP18.03, DGP18.05
Lotz, J.	AG13.05
Lübbe, K.	AG01.08
Luber, B.	P14.03.02, P14.03.05
Ludewig, L.	AG10.05
Lueftl, E.	<b>AG11.08</b>
Lukacs-Kornek, V.	AG14.05
Lukic, I.	AG11.08
Lützen, U.	AG01.05
Luzarowski, M.	P14.03.04
Ly, A.	P11.01.01
Ma, Y.	AG10.05, DGP04.05, <b>P11.02.04</b>
Maas, J.	AG09.03
Macek, B.	P14.01.08
Macher-Goeppinger, S.	AG05.08
Macion, A.	AG12.06
Mackedanz, P.	AG05.11, DGP04.03
Mahlberg, R.	P14.03.01
Maier, J.	P14.03.02
Maier, J.	<b>P.ComPath.02.03</b>
Maier-Hein, K.	DGP13.04
Mair, A.	P14.01.11
Mairinger, F.	AG10.08, AG14.16
Maiuthed, A.	DGP04.07
Maj, C.	P.ComPath.01.08
Maldacker, M.	<b>P11.02.06</b>
Malek, N.	P14.01.08
Malinova, A.	P11.02.13
Mann, M.	DGP04.01
Manukyan, A.	P11.01.09
Manuylova, T.	<b>AG12.05</b> , AG12.08
March, C.	P04.01

Marienfeld, R. AG07.06, P.ComPath.02.03, P03.04, P11.02.11  
 Marienfeld, U. P11.02.11  
 Marinoni, I. AG14.07  
 Märkl, B. AG09.03, AG10.01, AG10.02, AG14.07, AG14.08, AG14.12, AG14.13,  
 P.ComPath.02.07, P.PersMed.02.02, P.PersMed.02.04, P11.01.08, P14.01.07, P14.01.11  
 Marnet, N. P14.03.07  
 Marquard, S. **P14.03.07**  
 Marquardt, J. P.VergPath.01  
 Marr, C. **AG03.06**, AG13.04  
 Martignoni, M. AG14.07  
 Martis-Thiele, M. AG11.09, **P11.01.03**, P11.01.13  
 Matek, C. AG13.11, **DGP04.06**, P05.10, P13.03  
 Matiasek, K. P11.02.12  
 Mattern, S. P14.01.08  
 Matthaei, H. AG14.05  
 Matthäus, T. P04.06  
 Matysiak, U. AG11.11, **AG11.14**, DGP01.04, DGP02.05, P.PersMed.01.07  
 Maurer, E. AG14.08  
 Maurer, J. AG05.12  
 Maurus, K. AG03.10, AG03.12  
 Mayer, R. **P.ComPath.01.04**  
 Mayr, D. P01.01  
 Mayr, E. **P11.01.11**, P11.01.03, P11.01.13, DGP04.02, AG11.09, P.VergPath.03  
 Mayr, M. DGP07.04  
 Mayr, T. AG03.03, AG05.04, AG05.13, **P05.02**  
 McAlpine, J. P01.08  
 McCormack, V. AG01.10  
 Meeks, J. DGP07.04  
 Meerdink, E. P13.06  
 Mehrabi, A. DGP13.05, P14.02.11, P14.03.08  
 Meier, N. P.PersMed.01.04  
 Meier, W. P01.02  
 Mellado, B. P05.10  
 Mellert, K. AG07.06, AG07.07  
 Mentzel, T. AG08.03  
 Merhof, D. AG13.05  
 Merkelbach-Bruse, S. AG11.04, AG11.07, AG11.10, AG11.13, P11.02.05  
 Merle, U. P14.02.11  
 Merseburger, A. AG05.11, DGP04.03  
 Merz, A. **P04.03**  
 Messner, C. P.PersMed.02.07  
 Metzger, C. **P14.02.03**  
 Metzger, M. P11.02.06  
 Metzger, M. C. P.ComPath.02.01  
 Metzler, T. **P.VergPath.03**  
 Meyer, F. P04.01, P04.02, P14.01.02, P14.01.03, P14.01.04, P14.03.03  
 Meyer, L. **P.PersMed.01.04**  
 Michalk, I. **P11.01.04**  
 Michalski, C. P14.03.09  
 Michels, S. P.ComPath.01.06  
 Middelhoff, M. P14.01.01  
 Mielewczyk, Z. **P.PersMed.02.02**  
 Miernik, A. AG05.11, DGP04.03  
 Mihalkov, A. P11.01.12  
 Mitchell, S. P.PersMed.01.02  
 Mitchell Barroso, V. **AG14.14**, P.ComPath.02.04  
 Moch, H. AG05.07, DGP15.04  
 Mock, A. DGP06.05  
 Mögele, T. P.PersMed.02.02, **P13.06**  
 Mogler, C. AG01.03, AG14.07, DGP09.04, P.VergPath.01, P01.04, **P13.02**,  
 P14.01.01, P14.02.01, P14.03.10  
 Moguler, C. AG10.02

Mohammadian Roshan, N.	P.PersMed.02.03
Mokry, T.	DGP07.04
Möller, J.	<b>P11.01.07</b>
Möller, P.	AG03.05, AG07.06, AG07.07, P.ComPath.02.03, P.ComPath.02.11,
P03.04, P11.02.11	
Mongan, N.	DGP09.05
Monoranu, C.-M.	P.ComPath.02.06
Montavon, G.	P13.05
Montes-Mojarro, I.	AG01.09
Morkel, M.	DGP04.04
Mortoga, S.	P11.01.06
Moser, E.	AG10.02, <b>AG14.07</b>
Moser, S.	AG13.06
Mrazkova, B.	DGP04.07
Muckenhuber, A.	AG11.09, <b>DGP13.04</b> , P.PersMed.01.05, P.PersMed.02.01, P13.01
Mucsi, Z.	DGP18.05
Muders, M. H.	AG03.03
Muehlematter, U. J.	AG05.07
Mueller, M. D.	AG01.04
Mühlbauer, M.	<b>AG14.09</b> , AG14.11, AG14.15
Mühlberger, K.	P.ComPath.02.05
Mühlberger, M.	AG08.03
Muley, T.	AG14.08
Müller, A.	<b>P12.02, AG12.06</b>
Müller, G.	<b>AG05.03</b>
Müller, J.	<b>P01.08, P12.03</b>
Müller, K.-R.	DGP06.05, P.ComPath.01.01, P.ComPath.01.05, P13.05
Müller, S.	P.VergPath.05
Mümmeler, C.	P10.02
Muti, H. S.	AG14.13
Na, I.-K.	AG11.07
Nádorvári, L. M.	DGP18.02
Nägel, A.	DGP10.04
Nagy, D.	DGP07.04, P.VergPath.06
Nagy, R.	P14.02.10
Naisar, S. M.	P14.03.06
Nakauma-González, A.	DGP07.04
Neemann, J.	AG13.12
Neher, P.	DGP13.04
Nekljudova, V.	AG01.08
Nell, J.	AG07.06
Nenkov, M.	AG10.05, <b>DGP04.05</b> , P11.02.04
Neo, Z. W.	P11.01.01
Neppl, C.	<b>AG01.04</b> , P01.02
Nesic, S.	AG03.03
Nettersheim, D.	AG05.02
Netto, G. J.	DGP06.04
Neubert, L.	P10.01, <b>P10.04</b> , P11.02.07
Neukunft, V.	P01.01
Neumahr, J.	<b>AG07.07</b>
Neumann, K.	AG11.04
Neumann, O.	DGP13.05
Neuß, T.	<b>P11.02.13</b>
Newton, S.	AG11.10
Ng, S.	AG14.05
Ngoc, N.	DGP07.04
Nguyen, H. Q.	<b>AG13.10</b>
Nguyen, T.	P04.04
Nicke, T.	<b>AG13.05</b>
Nickl, V.	P.ComPath.02.06
Niedersüß-Beke, D.	DGP07.04

Niegisch, G.	DGP07.04
Nienhold, R.	<b>DGP15.04</b>
Nimsky, C.	DGP07.05
Nitschkowski, D.	AG10.06
Noetzel-Reiss, E.	AG05.12
Nolden, M.	DGP13.04
Notni, J.	P.PersMed.01.03, P.VergPath.04
Notter, A.	P14.03.05
Novak, V.	AG13.13
Novotny, A.	AG14.03
Nowak, M.	DGP15.04
Nursaitova, A.	DGP04.07
Obermayer, B.	DGP04.04
Ochsenbein, A.	AG03.02
Ócsai, K.	DGP18.05
Oeckl, P.	AG07.07
Oettle, H.	P.PersMed.01.05
Ohm, B.	P.ComPath.02.10
Olbinado, M.	AG13.13
Oliver Metzig, M.	AG11.02, <b>P.PersMed.01.02</b> , P11.02.08
Opitz, F.	DGP17.04
Ormanns, S.	AG14.06
Ortiz-Brüchle, N.	P11.01.07
Örüm, M.	AG01.08
Ott, G.	AG03.05, AG03.10, AG03.11, AG03.12
Ott, K.	AG14.03
Otto, M.	P14.01.05
Otto, R.	P14.01.03
Overkamp, M.	<b>AG12.08</b>
P. L. Gonçalves, J.	AG07.04
Pabst, G.	AG06.03
Paffenholz, P.	AG05.02
Pagenstecher, A.	DGP07.05
Palles, C.	P.ComPath.01.08
Palmisano, R.	DGP04.07, P14.01.10
Paolini, A.	P04.03
Papai, L.	DGP18.03
Papargyriou, A.	DGP10.05
Papić, D.	P.PersMed.02.05
Pappesch, R.	P11.02.05
Park, D.-H.	P10.01
Park-Simon, T.-W.	AG01.02
Parmaksiz, F.	AG05.02
Passlick, B.	P.ComPath.02.10
Patterson, N. H.	P11.01.01
Pauls, S.	AG05.02
Pech, M.	P04.02
Pelusi, N.	AG14.05, DGP08.04
Pelzer, U.	P.PersMed.01.05
Pelzl, L.	AG12.08
Peng, T.	AG13.04
Penzel, R.	P14.02.11
Pereira Lopes Goncalves, J.	P.PersMed.01.03, <b>P.PersMed.02.01</b>
Perner, S.	AG05.11, AG10.06, DGP04.03
Perren, A.	AG14.07
Pesti, A.	DGP18.03, DGP18.05

Peter, S.	P14.03.09
Peters, K.	<b>P11.01.09</b>
Petersen, M.	P04.02
Pfarr, N.	AG01.03, AG11.09, AG11.15, AG14.03, DGP04.01, DGP04.02, DGP09.04, P.VergPath.03, P05.04, P11.01.03, P11.01.11, P11.01.12, P11.01.13, P11.02.12
Pfeffer, T.	P.ComPath.01.09, P14.02.11
Pfeiffer, T.	P14.01.11
Pikki, N.	<b>P.PersMed.02.05</b>
Pilva, P.	P04.04
Pinter, N.	DGP02.05, DGP07.05
Plesch, D.	AG04.04
Ploeger, C.	P14.02.13
Plucinski, E. K.	P10.01, <b>P11.02.07</b>
Plum, P.	P.ComPath.01.08
Polifka, I.	P05.10
Pongratanakul, P.	<b>AG05.02</b>
Poon, P.	AG11.13
Popovic, Z.	P.ComPath.02.08
Poppinga, J.	AG14.08
Port, C.	P11.02.13
Porubsky, S.	AG05.08, P.ComPath.02.08
Poschmann, G.	AG05.02
Poth, T.	P14.02.12
Poxleitner, P.	P.ComPath.02.01
Poyet, C.	AG05.07
Prenißl, N.	<b>P.ComPath.01.01</b>
Press, A.	AG10.05
Preusse, C.	AG12.06
Prey, J.	AG11.12, P11.01.06
Probst, A.	P11.01.08
Prochazka, J.	DGP04.07, P14.02.10
Pryalukhin, A.	AG10.08, AG14.16, DGP06.04
Pryss, R.	P.ComPath.02.06
Pukrop, T.	AG14.09, AG14.11
Pusl, T.	P14.01.11
Puzalkova, A. V.	P14.02.11
Qasem, R.	AG04.04
Quaas, A.	AG10.08, AG11.07, AG14.08, AG14.14, AG14.16, DGP06.04, P.ComPath.01.06, P.ComPath.01.08, P.ComPath.02.04
Quante, M.	AG11.09, AG13.10
Racz, G.	DGP18.03
Rad, R.	P.VergPath.04, P.VergPath.05
Radbruch, H.	DGP04.04
Radke, J.	P11.01.09
Radpour, R.	AG03.02
Raffler, J.	P.ComPath.02.07
Rahbari, N.	P14.02.12
Raimundez, E.	AG14.02, P14.03.02
Raith, D.	P13.06
Ralsler, D. J.	AG14.05
Rambusch, E.	P14.03.01
Randerath, W.	AG11.07
Ranjan, R.	P.PersMed.01.01
Rao, J.	<b>P.PersMed.01.05</b> , P.PersMed.02.01
Rásó, E.	DGP18.02
Rasokat, A.	P.ComPath.01.06
Rasouli-Saravani, A.	P13.04
Rau, T. T.	AG01.04, P01.02
Rausch, S.	DGP07.04
Reck, M.	AG10.03, AG10.06

Redmer, T.	P11.01.09
Reger, M.	AG12.02
Reichert, M.	DGP10.05, P.PersMed.01.01, P.VergPath.05
Reichle, H.	P14.01.08
Reinhard, S.	P14.03.13
Reinisch, M.	AG01.08
Reis, H.	AG05.05
Reitsam, N. G.	AG10.01, AG14.12, <b>AG14.13</b>
Remke, M.	P.PersMed.01.03, <b>P05.04</b>
Rentschler, L.	<b>P14.01.11</b>
Rete, N.	P11.01.12
Reuter-Jessen, K.	AG05.06
Rhiem, K.	AG01.08
Ribback, S.	AG11.12, P11.01.06
Richter, G.	P05.06
Richter, J. W.	AG12.02
Richter, M.	AG12.02
Ridder, D. A.	P14.02.05
Ridwelski, K.	P14.01.02, P14.01.03
Rief, L.	AG01.03
Riehle, C.	P10.04
Riemer Cysar, S.	DGP02.05, AG11.14, P.PersMed.01.07
Riess, H.	P.PersMed.01.05
Riether, C.	AG03.02
Ringelhan, M.	P14.02.01
Rinke, A.	AG14.08
Ripperger, T.	AG12.02
Ritter, M.	DGP07.04
Röcken, C.	AG01.05, AG11.15, P14.01.06, P14.02.08, P14.02.09
Rodler, S.	P05.03
Roehrl, M. H.	<b>DGP13.04</b>
Roessler, S.	DGP13.05, P.VergPath.01, <b>P14.01.13</b> , P14.02.03, P14.02.13
Roessner, A.	AG07.03, DGP08.05, P11.01.05
Rogg, M.	DGP10.04, P04.03, P04.07, P05.09, P13.08
Rogmann, F.	DGP07.04
Rohe, J.	<b>AG05.01</b>
Rohr, K.	P13.07
Rohrbach, J. L.	P14.03.13
Roos, E.	P14.03.08
Röpke, M.	AG07.03
Roßberg, A.	DGP13.05
Rose, M.	AG05.12, P11.01.07
Rosenwald, A.	AG03.01, AG03.05, AG03.10, AG03.11, AG03.12, P14.01.07
Rössle, M.	AG06.03
Rössler, S.	P14.03.08
Rossmann, J.	<b>AG11.02</b> , P11.02.08
Röst, G.	DGP18.03
Roth, B.	<b>AG13.04</b>
Roth, C.	P12.03
Roth, S.	AG03.12
Roth, S.	P14.03.09
Roth, W.	AG01.07, AG05.08, AG11.02, AG13.07, DGP05.04, P.ComPath.01.07,
P11.02.08, P14.02.05, P14.03.07	
Rothweiler, R.	P.ComPath.02.01
Röttele, F.	P14.01.09
Rottenberg, S.	DGP09.05
Rózsa, B.	DGP18.05
Ruane, S.	AG11.07
Ruchhaeberle, E.	AG01.04, P01.02
Rückert, J.-C.	AG11.07
Rudroff, L. M.	<b>DGP17.04</b>
Ruff, L.	AG11.07, P.ComPath.01.01, P.ComPath.01.05

Ruh, P.	AG14.01
Ruland, J.	P.VergPath.03
Rupp, N.	<b>AG05.07</b> , AG06.03
Rüschhoff, J.	DGP15.04, AG05.07
Rushing, E. J.	AG06.03
Saal, J.	DGP07.04
Saar, M.	AG05.03
Sabido, E.	DGP07.05
Saborowski, A.	DGP13.05
Sabtan, D.	AG05.11, DGP04.03
Sade, H.	P.ComPath.02.02
Sagar, S.	P14.02.12
Sahu, A.	AG03.03
Saldanha, O.	P.ComPath.01.07
Sander, R.	P01.02
Sanders, C.	<b>AG06.02</b> , P.VergPath.06
Sandhaus, T.	P11.02.04
Sarikouch, S.	P10.04
Sauerbrei, B.	P11.02.10
Saur, D.	P.VergPath.05
Savini, L.	<b>P11.02.11</b>
Schaadt, N. S.	<b>AG13.12</b>
Schäfer, A.	DGP07.05
Schäfer, H.	<b>AG03.07</b> , AG03.08
Schäfer, J. R.	AG13.05
Schaff, Z.	DGP18.03
Schallenberg, S.	<b>AG11.07</b> , P.ComPath.01.01, P.ComPath.01.05, P14.03.12
Schaller, T.	P.ComPath.02.07, P.PersMed.02.04
Schanze, D.	AG07.03
Schaper, S.	DGP04.04
Scharf, S.	AG03.07, AG03.08
Schatz, U.	AG01.03
Schaumann, N.	<b>AG12.03</b> , AG12.07, P12.01
Scheidereit, E.	P14.02.12
Scheidhauer, K.	AG14.07
Schelbert, S.	<b>AG03.12</b>
Schell, C.	DGP10.04, P04.03, P04.07, P05.09, P13.08
Schenkirsch, G.	P14.01.07
Scherl, C.	P13.07
Scheufele, F.	P14.03.06
Schick, M.	P.ComPath.02.02
Schicktanz, F.	<b>P.PersMed.01.01</b>
Schierle, K.	AG09.04
Schildberg, F.	AG03.03
Schilling, O.	DGP02.05, DGP07.05, P.PersMed.01.04, P.PersMed.02.07, P04.07,
	P05.09, P11.02.06, P11.02.09, P14.01.09, P14.01.12
Schindeldecker, M.	AG05.08, P14.02.05
Schirmacher, P.	DGP13.05, P.ComPath.01.09, P14.01.13, P14.02.03, P14.02.11,
	P14.02.13, P14.03.04, P14.03.08
Schlachtenberger, G.	AG11.07
Schlack, K.	DGP07.04
Schleiß, J.	<b>P14.02.07</b>
Schlegel, J.	P11.02.12
Schlenz, M.	P01.02
Schliemann, M.	DGP13.05
Schlitt, H.-J.	AG14.11
Schlitter, M.	P.PersMed.02.01
Schlotfeldt, M.	AG05.11, DGP04.03
Schmelzeisen, R.	P.ComPath.02.01
Schmid, M.	P05.05
Schmid, M.	DGP15.04

Schmid, N.	P01.04, <b>P.PersMed.01.03</b>
Schmid, S.	P.ComPath.02.10
Schmidt, C.	DGP08.05
Schmidt, M.	DGP04.05, P11.02.04
Schmitt, M.	AG14.08
Schmitz, J.	AG04.04
Schmitz, N.	P04.04
Schmoeckel, E.	AG01.03, P.PersMed.01.03, P01.04
Schnabel, J. A.	AG13.04
Schneider, A.	DGP13.05
Schneider-Stock, R.	DGP04.07, DGP10.05, P14.01.10, P14.02.10
Schobel, J.	P.ComPath.02.06
Schoner, K.	AG12.02
Schorle, H.	DGP08.04, P05.07
Schotte, T.	AG01.09
Schreck, J.	DGP13.05, <b>P14.02.13</b>
Schreier, J.	AG07.03, P11.01.05
Schröder, K.-M.	<b>P.ComPath.02.10</b>
Schröder, L.-J.	P10.01
Schubert, S.	<b>P10.01</b>
Schuerch, C.	AG03.02
Schüffler, P.	DGP13.04, P.ComPath.01.10, <b>P13.02</b> , AG13.10, P.PersMed.02.03, P13.04
Schul, L.	AG13.03
Schuler, M.	P13.05
Schüller, U.	AG05.02
Schult-Hannemann, D.	P14.01.01
Schultheis, A.	AG10.08
Schulz, B.	P11.02.10, P14.02.02
Schulz, G. B.	P05.03
Schulz, S.	<b>AG01.07</b> , AG13.07, <b>P.ComPath.01.07</b>
Schulze, C.	DGP04.05
Schumacher, J.	P.ComPath.01.08
Schürch, C. M.	P.PersMed.01.06
Schürheck, K.	P14.02.02
Schusser, B.	P.VergPath.02
Schustetter, C.	AG13.03
Schwab, C.	DGP07.04, P.ComPath.01.09
Schwab, J. D.	P.ComPath.02.03
Schwamborn, K.	AG07.04, AG11.09, DGP04.02, DGP16.05, P.PersMed.01.03, P.PersMed.02.01, P01.04, P05.04
Schweizer, L.	<b>DGP04.01</b>
Schwen, L. O.	AG13.05
Schwendener, N.	DGP18.06
Schwenke, J.	<b>AG08.03</b>
Schwittlick, U.	DGP09.04
Seeling, C.	AG07.07
Seidel, A.	<b>P10.04</b>
Seidl, D.	DGP15.04
Seidl, M.	AG13.06, AG13.13
Seiler, F.	P11.01.12
Seillier, L.	AG05.12, P11.01.07
Seitz, V.	DGP04.04
Seliger, B.	AG01.10, AG03.04
Sendelhofert, A.	P05.03
Seper, A.	AG14.16, DGP06.04
Seredynska, A.	<b>P.PersMed.02.07</b> , P11.02.06
Shakhtour, J.	<b>P14.01.01</b> , P14.03.06
Shiban, E.	P.PersMed.02.02
Shumilov, A.	P.ComPath.02.02
Siebenhüter, L.	P11.01.08
Siebolts, U.	AG11.10, AG11.13, P11.02.05



Siegenthaler, F. AG01.04  
 Siehr, E. **P01.07**  
 Siemanowski-Hrach, J. **AG11.13**, P11.02.05  
 Siemoneit, J.-H. H. P.ComPath.02.08  
 Sikic, D. AG05.14, DGP04.06  
 Simion, V. P14.03.05  
 Singer, S. DGP13.05, P14.01.08, P14.03.08  
 Sinn, M. P.PersMed.01.05  
 Sipors, E. AG10.02  
 Sipos, É. P11.01.08, P14.01.07, AG10.01, AG14.12  
 Sistic, L. AG14.03  
 Siveke, J. T. P14.03.10  
 Skowron, M. A. AG05.02  
 Slotta-Huspenina, J. AG13.03, AG13.10, AG14.03, DGP18.01, P10.03  
 Sobottka, B. DGP15.04  
 Solbach, C. AG01.08  
 Soltermann, A. **AG11.03**  
 Sommer, F. AG14.12, P14.01.07  
 Soteriu, D. DGP04.07  
 Sotlar, K. AG11.06  
 Spada, F. **AG03.05**, P.ComPath.02.11  
 Spang, R. AG14.11  
 Specht, K. DGP04.01  
 Sprengel, F. AG13.12  
 Staebler, A. AG01.09  
 Standvoss, K. AG11.07  
 Stange, D. E. P11.01.04  
 Stanonik, Ž. P.ComPath.01.10  
 Steege, A. AG01.04  
 Steenbuck, I. D. P11.02.06  
 Stehl, V. AG13.06, **AG13.13**  
 Steiger, K. AG10.02, AG13.03, AG14.07, DGP04.01, DGP09.04, DGP13.04,  
 P.PersMed.01.01, P.PersMed.01.03, P.PersMed.01.05, P.PersMed.02.01, P.VergPath.01, P.VergPath.02,  
 P.VergPath.03, P.VergPath.04, P.VergPath.05, P01.04, P05.04, P13.02, P14.01.01, P14.03.10  
 Stein, K. AG10.06  
 Steiner, D. F. AG14.13  
 Steinmann, S. **P.PersMed.01.08**  
 Stenzel, P. **AG05.08**, P.ComPath.01.07  
 Stenzinger, A. DGP13.05, P14.02.11  
 Stephan, A. AG05.02  
 Steybe, D. P.ComPath.02.01  
 Sticht, C. P14.01.13  
 Stiller, J. P11.02.13  
 Stiller, M. AG10.09  
 Stock, K. DGP18.01, P10.03, AG13.03  
 Stögbauer, F. **AG06.01**, P.PersMed.02.03, P13.02  
 Stöhr, C. P05.10  
 Stöhr, R. AG05.14, **P05.06**  
 Stoll, A. P.ComPath.01.04, P.ComPath.02.09  
 Stoll, V. AG01.05, AG11.15, P14.01.06, P14.02.08, P14.02.09  
 Stolz, T. P14.01.05  
 Straehle, J. P.ComPath.02.01  
 Straub, B. K. DGP13.05, P14.02.05  
 Strauch, M. P04.04  
 Strauß, A. AG05.06  
 Strick, R. DGP04.06  
 Strieth, S. AG06.02  
 Strischewski, D. **P14.01.04**  
 Strissel, P. L. DGP04.06  
 Ströbel, P. AG05.02, AG05.06, AG10.04  
 Strobl, S. AG01.07, AG13.07, P.ComPath.01.07  
 Strodel, J. P10.02

Struckmann, S.	<b>AG01.02</b>
Stühler, K.	AG05.02
Stühmer, T.	AG03.01
Stumpe, M.	AG11.03
Sugiyanto, R.	P14.01.13, P14.02.03
Suhren, J.-T.	AG12.03, <b>AG12.07</b> , <b>P12.01</b>
Sulyok, M.	AG09.03
Surendran, S. A.	AG14.06
Szensny, M.	P11.02.09
Tagscherer, K.	AG05.08, DGP05.04
Tang, Y.	P.PersMed.01.02
Taraz Jamshidi, S.	P.PersMed.02.03
Taubert, H.	AG05.14
Tavernar, L.	P14.03.08
Taylor, B.	P.PersMed.01.02
Terron Kwiatkowski, A.	AG11.09, P11.01.03, <b>P11.01.12</b> , P11.01.13
Tesch, K.	AG01.05
Thalheim, D.	<b>P14.02.10</b>
Thalwaththe Gedara, M.	AG13.06, AG13.13
Theilen, T.	AG12.04
Thiam, P.	<b>P.ComPath.02.11</b>
Thielke, F.	AG13.05
Thielmann, X.	AG05.01
Thieme, R.	P.ComPath.01.08
Thiery, J.	DGP02.05, <b>P14.01.09</b>
Thomann, S.	<b>P14.02.12</b>
Thomas, A.	AG05.08
Tietz, S.	P.ComPath.01.05
Tietze, R.	P14.02.10
Tímár, J.	DGP18.02
Timme-Bronsert, S.	AG11.14, P.PersMed.01.07
Tischler, V.	DGP08.04, P05.01
Titze, U.	P11.02.10, P14.02.02
Tögel, L.	P05.06
Tolkach, Y.	AG10.08, AG14.14, AG14.16, DGP06.04, P.ComPath.01.06,
P.ComPath.02.04	
Toma, M.	AG05.01, AG06.02, AG14.05, DGP07.04, P03.02
Tóth, M.	P14.02.12
Trabulssi, H.	P.VergPath.05
Tran, P. T.	P11.01.01
Trautmann, M.	AG07.05
Trepel, M.	AG10.01, P13.06
Tretiakova, M.	DGP06.04
Triesch, J.	P.ComPath.02.09
Trinks, A.	DGP04.04
Trippel, M.	DGP18.06
Truhn, D.	AG01.07, AG13.07, P.ComPath.01.07
Trummer, M.	AG11.05
Tsaur, I.	AG05.08
Tschurtschenthaler, M.	AG14.08
Tsvetkov, A.	AG14.16
Tulessin, M.	<b>P.VergPath.01</b>
Turzynski, A.	AG13.05
Tzankov, A.	AG11.03
Ugliano, S.	P.PersMed.02.05
Ullmann, D.	AG07.03
Ullmann, J.	AG07.03
Ullmann, S. R.	P11.01.05, <b>AG07.03</b>
Ulrich, C.	DGP13.04
Unger, C.	P01.03

Untch, M.	AG01.08
Ura, A.	<b>AG10.02</b> , AG14.07
Utpatel, K.	AG11.05
Vajkoczy, P.	AG10.03
van Batenburg, V.	<b>P11.02.01</b>
van de Loo, D.	P14.02.06
van den Berg, E.	AG01.10
van den Berg, J.	<b>P11.02.01</b>
van Oudenaarden, A.	P11.02.01
Varkonyi, T.	DGP18.03
Vasaturo, A.	AG11.07
Végyvári, Á.	AG05.11, DGP04.03
Vera Badillo, F.	DGP07.04
Verbeeck, N.	P11.01.01
Verburg, F.	AG01.05
Veress, M.	DGP18.05
Verheij, J.	P14.03.08
Verity-Legg, J.	P11.02.01
Vermeulen, L.	P14.01.10
Vlaški, A.	<b>P01.01</b>
Vogel, A.	DGP13.05, P.ComPath.01.04
Vogel, L.	AG14.07
Vogel, M. N.	P14.03.08
Vogel, U.	P01.07, <b>P03.01, P04.05, P04.06, P11.02.02</b>
Vogl, M.	AG14.09, <b>AG14.15</b>
Vogler, M.	AG12.04
Vogt, B.	P12.03
Vollmer-Kary, B.	P.PersMed.01.04
Volmer, L.-L.	AG01.09
von der Wall, E.	DGP04.04
von Eisenhart-Rothe, R.	DGP04.01
von Hammerstein-Equord, A.	AG10.04
von Hardenberg, S.	AG12.02
von Laffert, M.	AG10.09
von Werder, A.	AG14.07
Vorfelder, L.	<b>P05.10</b>
Vosbeck, K.	<b>AG03.03</b>
Wach, S.	AG05.14
Wachten, D.	AG05.01
Wagener-Ryczek, S.	AG11.10, <b>P11.02.05</b>
Wagner, D.-C.	AG01.07, AG13.07, AG14.08, P.ComPath.01.07, DGP05.04
Wagner, S. J.	AG13.04
Wagner, T.	P14.01.11
Wagner, U.	DGP15.04
Wagner, Y.	AG11.09, P11.01.03, P11.01.12, P11.01.13
Walch, A.	AG14.02, P14.03.02
Waldmüller, S.	P04.06
Walker, M.	AG11.09, DGP04.01, P11.01.03, P11.01.12, P11.01.13
Walz, G.	P04.03
Wang, H.	P05.04
Wang, R.	AG05.12
Wang, Y.	<b>AG10.08</b>
Wanke, R.	P04.08
Wardelmann, E.	AG07.05
Warkotsch, J.	P.ComPath.02.07
Warm, V.	<b>AG09.03</b>
Wartenberg, M.	P14.03.13
Wasilewski, D.	AG10.03
Weber, A.	<b>P.ComPath.02.01, P.ComPath.02.10</b> , P14.01.12
Weber, I.	AG11.11

Wee, F.	P11.01.01
Weichert, W.	AG11.09, AG14.03, DGP04.01, DGP04.02, P.VergPath.04, P11.01.13,
P14.03.10	
Weigel, J.	DGP13.05
Weiler, S. M. E.	P14.03.04
Weingardt-Kocher, S.	P14.02.07
Weinhold, L.	P05.05
Weinmann, A.	P14.02.05
Weirich, G.	AG13.03, <b>DGP18.01</b> , <b>P10.03</b> , P14.03.06
Weis, C.-A.	DGP13.05, P.ComPath.01.09, P.ComPath.02.08, P13.07
Weißinger, S. E.	P14.02.07
Weitz, J.	P11.01.04
Welter, V.	P11.02.05
Wemmert, C.	AG13.12
Wendik, B.	<b>P11.02.09</b>
Wendler, O.	P05.06
Wengenmayr, C.	P.ComPath.02.07
Wenning, A. S.	P14.03.13
Wenzel, M.	P.ComPath.01.08
Wenzel, M.	AG05.05
Werder von, A.	AG10.02
Werle, S. D.	P.ComPath.02.03
Werlein, C.	P10.01, P10.04, P11.02.07
Werner, M.	AG11.11, AG11.14, DGP01.04, DGP02.05, DGP10.04,
P.ComPath.02.01, P.ComPath.02.10, P.PersMed.01.04, P.PersMed.01.07, P.PersMed.02.07, P01.03,	
P04.03, P04.07, P05.09, P11.02.06, P13.08, P14.01.09, P14.01.12	
Werner, T.	<b>DGP07.05</b>
Wess, M.	<b>P04.07</b>
Wessels, M.	<b>P14.02.08</b>
Westermann, P.	P.PersMed.02.07
Westhoff, C. C.	<b>AG01.08</b>
Weydandt, L.	P01.06
Wickenhauser, C.	AG01.10, AG03.04, P03.02
Wieczorek, M.	AG13.06, AG13.13
Wiegeling, A.	P14.01.07
Wiese, D.	AG14.08
Wild, P. J.	AG05.05, P.ComPath.01.03, P.ComPath.01.04, P.ComPath.02.09
Wildfeuer, J.	<b>P03.04</b>
Wildhagen, V. M.	P01.02
Wilfer, A.	AG03.04
Willer, F.	P11.01.06
Wimmers, D.	<b>DGP10.05</b>
Winter, H.	AG14.08
Winterhoff, T.	P.ComPath.01.01, <b>P.ComPath.01.05</b>
Wirges, N.	P.VergPath.05
Wirth, J.	P.VergPath.03, <b>P14.03.10</b>
Wirtz, J.	<b>AG05.12</b>
Wirtz, R.	P14.03.02
Wirtz, T. H.	P.VergPath.01
Witzel, H. R.	P14.02.05, P14.03.07
Wlokka, U.	DGP02.05
Wolf, B.	P01.05, P01.06
Wolf, E.	P11.02.12
Wolf, F.	AG13.07
Wolf, P.	AG05.11, DGP04.03
Wolff, L.	P14.03.05
Wollman, R.	P.PersMed.01.02
Wolter, S.	AG11.11, AG11.14, <b>DGP01.04</b>
Wörtler, K.	DGP04.01
Wührl, M.	<b>P14.02.01</b> , P14.03.06
Wulf, A.-L.	DGP08.04, P05.01
Wulff, R.	P14.01.05

Wullich, B.	AG05.14, DGP04.06, P05.06
Wurzel, P.	AG03.07, AG03.08
Wyler, E.	P11.01.09
Xiao, S.	DGP13.04
Yalcin, F.	<b>P03.03</b>
Yao, S.	<b>AG10.04</b>
Yasser, M.	<b>AG11.12</b> , P11.01.06
Yavas, A.	DGP17.04, <b>P14.03.11</b>
Yeong, J. P. S.	P11.01.01
Yim, W.	P11.01.01
Zachrau, T.	<b>AG04.04</b>
Zahn, M.	P03.04
Zamo, A.	AG03.10, AG03.11
Zander, T.	P.ComPath.02.04
Zech, W.-D.	DGP18.06
Zemankova, R.	P11.01.12
Zens, P.	<b>P14.03.13</b>
Zerbe, N.	AG13.05, P.ComPath.02.04
Zhang, W.	<b>P11.01.01</b>
Zhang, Y.	<b>P.PersMed.01.06</b>
Zhao, Y.	P.ComPath.01.08
Zhou, X.	P.VergPath.06
Zimmer, T.	P14.01.05
Zirngibl, M.	<b>DGP10.04</b>
Zoche, M.	DGP15.04
Zschäbitz, S.	DGP07.04
Zubarev, R.	AG05.11, DGP04.03
Zukowska, M.	P.VergPath.05
Zwingenberger, G.	P14.03.02